

• REVIEW •

# Experimental models to study cholangiocyte biology

Pamela S. Tietz, Xian-Ming Chen, Ai-Yu Gong, Robert C. Huebert, Anatoliy Masyuk, Tatyana Masyuk, Patrick L. Splinter, Nicholas F. LaRusso

Pamela S. Tietz, Xian-Ming Chen, Ai-Yu Gong, Robert C. Huebert, Anatoliy Masyuk, Tatyana Masyuk, Patrick L. Splinter, Nicholas F. LaRusso, Center for Basic Research in Digestive Diseases, Department of Internal Medicine and Biochemistry and Molecular Biology, Mayo Medical School, Clinic and Foundation, Rochester, MN 55905

Supported by grants DK24031 and DK57993 (N. F. LaRusso) from the National Institutes of Health and by the Mayo Foundation.

Correspondence to: Nicholas F. LaRusso, Center for Basic Research in Digestive Diseases, Mayo Medical School, Clinic and Foundation, 200 First Street, SW Rochester, MN 55905, United States. larusso.nicholas@mayo.edu

Telephone: +1-507284-1006 Fax: +1-507284-0762

Received 2002-01-14 Accepted 2002-01-18

## Abstract

**Cholangiocytes-the epithelial cells which line the bile ducts-are increasingly recognized as important transporting epithelia actively involved in the absorption and secretion of water, ions, and solutes. This recognition is due in part to the recent development of new experimental models. New biologic concepts have emerged including the identification and topography of receptors and flux proteins on the apical and/or basolateral membrane which are involved in the molecular mechanisms of ductal bile secretion. Individually isolated and/or perfused bile duct units from livers of rats and mice serve as new, physiologically relevant *in vitro* models to study cholangiocyte transport. Biliary tree dimensions and novel insights into anatomic remodeling of proliferating bile ducts have emerged from three-dimensional reconstruction using CT scanning and sophisticated software. Moreover, new pathologic concepts have arisen regarding the interaction of cholangiocytes with pathogens such as *Cryptosporidium parvum*. These concepts and associated methodologies may provide the framework to develop new therapies for the cholangiopathies, a group of important hepatobiliary diseases in which cholangiocytes are the target cell.**

Tietz PS, Chen XM, Gong AY, Huebert RC, Masyuk A, Masyuk T, Splinter PL, LaRusso NF. Experimental models to study cholangiocyte biology. *World J Gastroenterol* 2002;8(1):1-4

## INTRODUCTIONS

The liver contains two types of epithelia: hepatocytes, accounting for ~65% of the liver cell population; and intrahepatic bile duct cells, or cholangiocytes, the epithelial cells that line the intrahepatic biliary tree and account for ~5% of the liver cell population.

In the past decade, interest in cholangiocyte pathobiology has exploded due to: (i) the development of new experimental techniques that allow hypotheses related to cholangiocyte biology to be directly addressed (Figure 1); (ii) the recognition that cholangiocytes are critically important to normal liver function, especially solute and water transport, cell-cycle phenomena, cell signaling, and interactions with other cells, matrix components, foreign organisms and xenobiotics; and (iii) the appreciation that cholangiocytes

represent the major target of a group of serious genetic and acquired diseases termed the cholangiopathies. In a coordinated series of hypothesis-driven studies, we have explored selective aspects of cellular processing by cholangiocytes focusing on proteins (receptors, channels, exchangers, transporters, junctional proteins, molecular motors, pro/anti-apoptotic molecules) that we hypothesized were likely critically important in cholangiocyte secretion, absorption, intracellular transport, and structural modifications. Thus, we briefly review here a variety of novel *in vivo* and *in vitro* experimental models that have allowed us to expand our understanding of how cholangiocytes function and what happens when disease alters their normal physiology. Several more extensive reviews on cholangiocyte pathobiology are referenced for readers interested in more comprehensive reviews.

## IN VIVO MODELS

The rat biliary tree has been shown to undergo selective proliferation in response to different experimental stimuli such as bile duct ligation (BDL)<sup>[1]</sup>, 70% hepatectomy<sup>[2]</sup>, carbon tetrachloride treatment<sup>[3]</sup>, and feeding of  $\alpha$ -naphthylisothiocyanate (ANIT)<sup>[4,5]</sup>. As best we know, the proliferated cholangiocytes retain a normal cholangiocyte phenotype. The bile duct ligated rat model has been useful in initiating studies on the effect of hormones on bile secretion. Infusion of secretin and somatostatin results in a choleric and cholestatic response, respectively, in the bile duct ligated but not sham-operated rat, due not only to an increased number of cells but an increased expression of the receptors for secretin and somatostatin on individual cholangiocytes<sup>[6-8]</sup>. Much less is known about how the mouse biliary tree responds to hormones. To further explore the regulatory mechanisms of ductal bile secretion, it was necessary to develop additional novel *in vitro* experimental models.

## IN VITRO MODELS

### Freshly Isolated Cells

The development of *in vitro* models of biliary epithelia essentially began with the ability to isolate cholangiocytes of high purity from normal rat, mouse and human liver<sup>[9,10]</sup>. This experimental model allowed direct studies on the effects of hormones on cholangiocytes which demonstrated among other things, that secretin stimulated exocytosis via a cyclic AMP mechanism, and that this effect was blocked by somatostatin<sup>[11]</sup>.

The technique of counter-flow elutriation has allowed refinement of cell isolation techniques from normal or BDL rats<sup>[12,13]</sup> by allowing separation of subpopulations of cholangiocytes which differ in size. Using this model, we have provided evidence that these small, medium and large cholangiocytes originate from different portions of the intrahepatic biliary ductal system. Using molecular and physiological approaches, we have also demonstrated that these subpopulations of cholangiocytes differ in their transport and proliferative capabilities<sup>[12,13]</sup>.

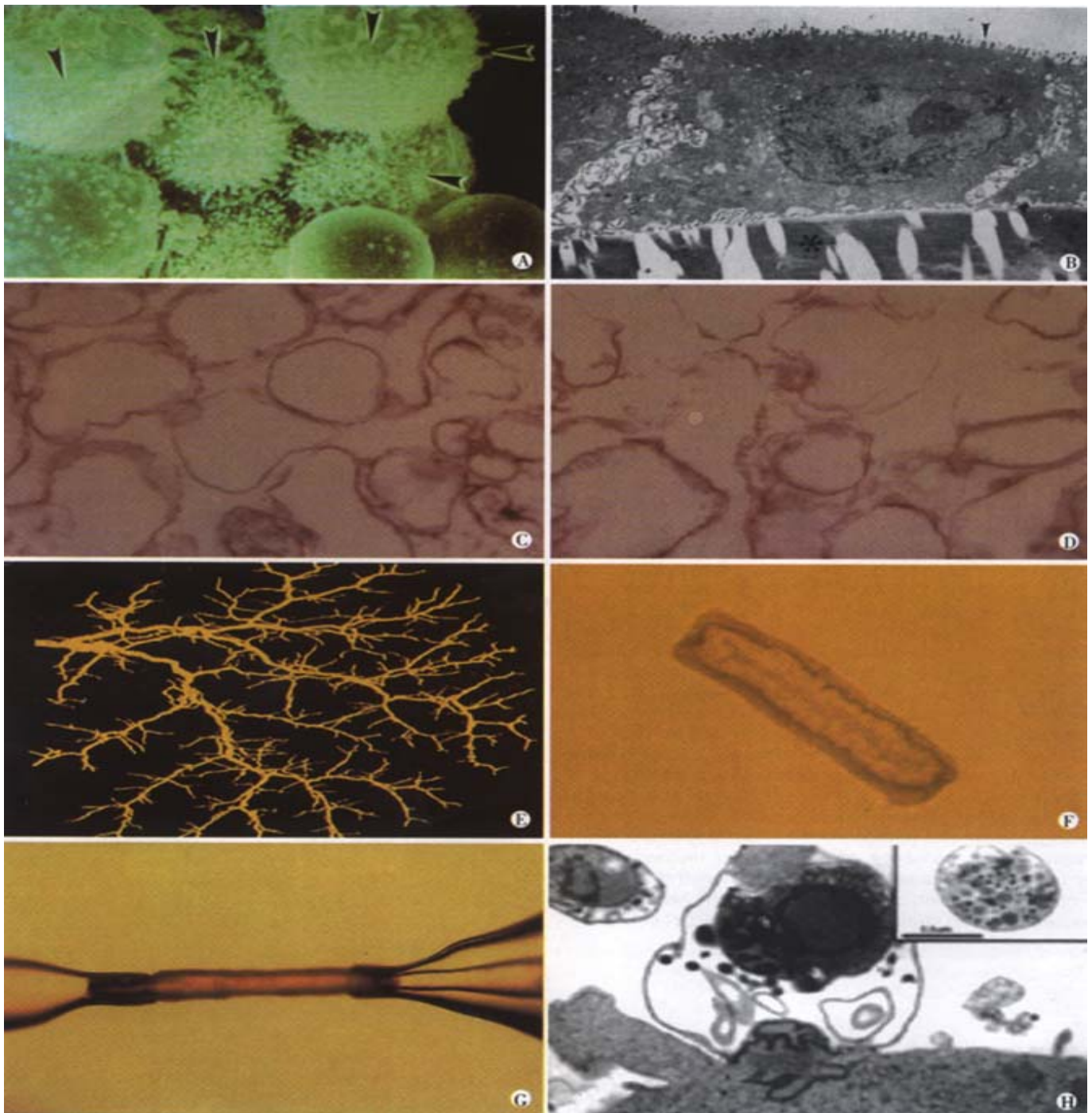


**Figure 1** Experimental *in vitro* models of biliary epithelia.

(a) A scanning electron micrograph of a group of isolated cholangiocytes after separation using immunomagnetic beads. Note that the prominent microvilli (arrowheads) are limited to one side of the cells. Mag = 4,400.

(b) A transmission electron micrograph cross-section of normal rat cholangiocytes in culture demonstrates characteristics of polarized cells with apical microvilli (arrowheads) and numerous basolateral intercellular interdigitations near the collagen coated filter denoted by \*, (Bar = 2 mm, Mag = 7,500).

(c) (d) A transmission electron micrograph of apical (c) and basolateral (d) plasma membrane domains revealed similar homogenous vesiculated membranes of varied shapes and sizes without apparent contamination of other organelles (Bar = 0.5 mm, Mag = 22,500).

(e) A three-dimensional reconstructed image of the intrahepatic biliary tree isolated from normal rat liver.

(f) A light micrograph of an unstained isolated bile duct unit from rat liver. After overnight culture, the two ends seal forming an enclosed unit. A single layer of epithelial cells with a thin outer layer of connective tissue surrounds the lumen.

(g) A microperfused intrahepatic bile duct unit isolated from rat liver, manually dissected and cannulated with micropipettes.

(h) Transmission electron micrograph of *C. parvum* infection of cultured human cholangiocytes. A parasitophorous vacuole contains a developing parasite stage which is intracellular but extracytoplasmic. A macrogamete is shown in the inset, demonstrating development of sexual stages of the parasite. Bar = 1 mm.

### **Cholangiocyte cDNA Library**

A unique cDNA library has been constructed from highly purified cholangiocytes isolated from rats subjected to bile duct ligation for 2 weeks<sup>[14]</sup>. Total cellular RNA was extracted from cholangiocytes and poly(A)+ mRNA isolated. Subsequently, the poly(A)+ mRNA was reverse transcribed and directionally cloned. The cholangiocyte cDNA library allows screening and sequencing of positive clones for numerous molecules yet to be identified.

### **Cultured Cells**

Freshly isolated cells maintained in short-term culture provided the opportunity to perform patch-clamp studies yielding novel insights into the electrophysiology of cholangiocytes<sup>[15]</sup>. Established long-term cultured cholangiocytes can be grown on semi-permeable cell culture filters by which they quickly reach confluence, maintain morphologic polarity and develop adequate transepithelial electrical resistance, making them a prototype for use in transport studies. This model has been utilized to characterize the uptake of glucose and bile acids and to study water transport<sup>[16-19]</sup>.

### **Isolated Organelles**

In order to perform more rigorous transport studies and to generate accurate kinetic transport parameters (i.e., Km and Vmax), we developed techniques for isolating vesicles enriched in either the apical or the basolateral domain of cholangiocytes starting either with whole rat liver or with cholangiocytes in culture<sup>[20,21]</sup>. An initial application of these vesicles was to generate kinetic values for sodium-dependent taurocholate uptake, a process that we demonstrated occurs in apical but not basolateral vesicles<sup>[17]</sup>. This tool allows continued studies to localize and functionally evaluate transport processes in cholangiocytes.

### **Intrahepatic Bile Duct Units**

Experiments using intact intrahepatic bile duct units isolated by mechanical and enzymatic techniques from normal rats to study biliary epithelial transport physiology have been previously described<sup>[22]</sup>. An advantage of this model is that we can not only control the luminal contents (by manipulating components of the perfusate) but we can independently and simultaneously modify the basolateral milieu (by manipulating components of the bathing buffer). With this approach, we were able to detect changes in intraluminal pH and electrolyte concentrations in response to agonists. We could also demonstrate water transport across this epithelial barrier in response to osmotic gradients, the characteristics of which (kinetics, temperature independence and mercury sensitivity) all suggested the presence of water selective channel proteins (i.e., aquaporins) (AQP) on the membranes of cholangiocytes. Using quantitative computer-assisted image analysis to measure expansion and reduction of luminal area as a reflection of water movement, we have demonstrated that water movement across the bile duct units is transcellular and channel-mediated<sup>[13]</sup>.

We have subsequently expanded this model using a microperfusion technique and an epifluorescence detection system<sup>[24]</sup>. With this modification, we have demonstrated the movement of water into (secretion) and out of (absorption) the lumen of the perfused ducts in response to inward and outward osmotic gradients. The calculation of both net water movement (Jv) and osmotic water permeability (Pf) provide evidence that the measured bi-directional fluxes reflect water movement through water channels.

In addition, we have demonstrated that isolated bile duct units actively absorb solutes such as bile acids and glucose, and transport ions such as bicarbonate. We have also shown that luminal perfusion of ATP and other nucleotides activates P2Y

ATP receptors on the apical cholangiocyte plasma membrane and induces increases in  $[Ca^{2+}]_i$  and net ductular alkalization, suggesting that ductal bile secretion is regulated by these signaling molecules<sup>[25]</sup>.

This technique has now been adapted to the mouse in which we can reproducibly isolate and microperfuse intact bile duct units from normal mouse liver with the anticipated application to transgenic or knockout mouse models<sup>[26]</sup>. Transgenic mice continue to be developed in which there is a selective knockout of one or more aquaporin water channels<sup>[27]</sup>. The isolated and perfused bile duct unit model would allow us to test the hypothesis that knockout mice lacking AQP1 and AQP4 water channels or perhaps other naturally expressed aquaporins may have substantially reduced choleretic and cholestatic responses to hormones since the flux of water molecules through these water channels should be absent.

The isolation of intact, polarized intrahepatic bile duct units from both rat and mouse allows the direct study of secretory and absorptive activities of the bile ducts in a way which most closely approximates the normal biliary ductal system.

### **Three-Dimensional Modeling**

Although cholangiocyte functional and morphological heterogeneity likely contributes to the selective involvement of different portions of the biliary tree in the cholangiopathies, our understanding of the nature and mechanisms for normal and abnormal anatomical remodeling of the biliary tree is limited. To better define the heterogeneous nature of the biliary tree, we utilized a computer-aided three-dimensional imaging technique, first described in a study of the normal human biliary tree<sup>[28]</sup>, to perform quantitative anatomical studies of the rat intrahepatic biliary system<sup>[29]</sup>.

Computer generated three-dimensional reconstruction of the intrahepatic biliary tree using microscopic-computed tomography scanning and sophisticated software allowed us to generate key biliary tract dimensions (length, surface area, duct diameter, volume) and branching patterns (distance from the junction of intra- and extrahepatic ducts, number of bile duct branches and branching angles).

In various forms of liver disease, including the cholangiopathies, proliferation of cholangiocytes is a common pathological response<sup>[1, 30, 31]</sup>. The anatomical basis and remodeling process which occurs in response to various stimuli remain unclear. We have since applied the three-dimensional reconstruction of the biliary tree to rats in whom selective cholangiocyte proliferation was induced by ANIT feeding<sup>[4,5]</sup>. The anatomical remodeling and quantitative observations after selective cholangiocyte proliferation suggest that the proliferation process involves sprouting of new side branches. Recently three-dimensional modeling has been applied to generate data for the hepatic artery and portal vein within the same liver (Masyuk, LaRusso unpublished). This descriptive study allowed key findings on the length of vascular segments, diameter of blood vessel segments and volume of the hepatic artery and portal vein, associated with experimentally-induced cholangiocyte proliferation.

Three-dimensional reconstruction will provide complementary data that, at a minimum, will yield structural information on biliary tract architecture and biliary mapping (i.e., which branches of the biliary tree are involved in absorption or secretion, the mechanisms by which ducts proliferate in response to injury, and the impact of these modifications on the peribiliary vasculature.) The significance of these studies relates not only to the intrinsic value of understanding cholangiocyte physiology but also to providing a biologic rationale for why only certain segments of the biliary tree are involved in the individual cholangiopathies. Primary biliary cirrhosis, for example, leads to destruction of interlobular bile ducts, while intrahepatic cholestasis induced by drugs affects principally the cholangiocytes that line small bile ducts<sup>[30, 32, 33]</sup>.

### *In Vitro* Infection Model of Biliary Cryptosporidiosis

Using monolayers of human cholangiocytes derived from normal liver and immortalized by SV40 transformation, we developed an *in vitro* infection model of biliary cryptosporidiosis<sup>[34]</sup>. Cryptosporidiosis is an infectious disease caused by *Cryptosporidium parvum* (*C. parvum*), an emerging parasite which causes self-limited diarrhea in immunocompetent subjects and potentially life-threatening syndromes in immunocompromised individuals, primarily those with acquired immunodeficiency syndrome (AIDS). Despite the magnitude and severity of cryptosporidial infection, the pathogenesis is poorly understood, and there is currently no effective therapy. Using this novel infection model, we found that *C. parvum* sporozoites (derived from oocysts excysted *in vitro*) attach to the apical surface of biliary epithelia, invade the cells, reside in a parasitophorous vacuole, and undergo both sexual and asexual development.

*C. parvum* attachment to cholangiocytes involves interactions between specific glycoproteins on cholangiocytes and *C. parvum* sporozoite lectins while the invasion into cholangiocytes works through actin-dependent membrane spreading mediated by cortactin and RhoGTP-binding proteins<sup>[34-36]</sup>. While *C. parvum* is cytopathic to uninfected cells adjacent to infected cholangiocytes via Fas/FasL-dependent apoptosis, the organism prevents cell death of infected cells by inhibiting apoptosis via activation of NF- $\kappa$ B<sup>[37, 38]</sup>. This model provides a useful system for the development of novel therapeutic strategies for *C. parvum* induced enterology and AIDS-cholangiopathy.

### CONCLUSION

Advances in medical knowledge most often are preceded by advancements in technology and experimental models. Results from experiments using these new models and methods have clarified which flux proteins are expressed in cholangiocytes, their intracellular topography and segmental distribution, what molecules control their cellular compartmentalization, and their physiologic relevance to ductal bile formation. In addition, the information has provided a theoretical framework for development of novel therapeutic strategies for the cholangiopathies, a group of cholestatic genetic/acquired hepatobiliary diseases in which the cholangiocyte is the principal target of diverse destructive processes.

### Abbreviations

|                  |                               |
|------------------|-------------------------------|
| ANIT             | a-naphthylisothiocyanate      |
| AQP              | aquaporin                     |
| BDL              | bile duct ligation            |
| <i>C. parvum</i> | <i>Cryptosporidium parvum</i> |

**Acknowledgement** We greatly appreciate the secretarial assistance of Deb Hintz in preparation of this manuscript.

### REFERENCES

- Alpini G, Phillips JO, LaRusso NF. The biology of biliary epithelia. Edited by Arias IM, Boyer JL, Fausto N, Jakoby WB, Schachter DA, Shafritz DA. The Liver: Biology and Pathobiology. New York: Raven Press 1994:623-653
- LeSage G, Glaser SS, Gubba S, Robertson W, Phinizz J, Lasater J, Rodgers R, Alpini G. Regrowth of the rat biliary tree after 70% partial hepatectomy is coupled to increased secretin-induced ductal secretion. *Gastroenterology* 1996; 111:1633-1644
- LeSage G, Benedetti A, Glaser S, Marucci L, Tretjak Z, Caligiuri A, Rodgers R, Phinizz JL. Acute carbon tetrachloride feeding selectively damages large, but not small, cholangiocytes from normal rat liver. *Hepatology* 1999;29:307-319
- Desmet VJ, Krsulovic B, van Damme B. Histochemical study of rat liver in alpha-naphthylisothiocyanate (ANIT) induced cholestasis. *Am J Pathol* 1968;52:401-421
- Kossor DC, Goldstein RS, Ngo W, DeNicola DB, Leonard TB, Dulik DM, Meunier PC. Biliary epithelial cell proliferation following alpha-naphthylisothiocyanate (ANIT) treatment: relationship to bile duct obstruction. *Fundam Appl Toxicol* 1995;26:51-62
- Alpini G, Ulrich C, Pham LD, Phillips JO, Miller LJ, LaRusso NF. Upregulation of secretin receptor gene expression in rat cholangiocytes after bile duct ligation. *Am J Physiol* 1994;266:G922-G928
- Tietz P, Alpini G, Pham L, LaRusso NF. Somatostatin inhibits secretin-induced ductal hyperchloresis and exocytosis by cholangiocytes. *Am J Physiol* 1995; 269:G110-G118
- Tietz PS, Hadac E, Miller LJ, LaRusso NF. Upregulation of secretin receptors on cholangiocytes after bile duct ligation. *Regul Pept* 2001;297:1-6
- Ishii M, Vroman B, LaRusso NF. Isolation and morphologic characterization of bile duct epithelial cells from normal rat liver. *Gastroenterology* 1989;97:1236-1247
- Vroman B, LaRusso NF. Development and characterization of polarized primary cultures of rat intrahepatic bile duct epithelial cells. *Lab Invest* 1996;74:303-313
- Kato A, Gores GJ, LaRusso NF. Secretin stimulates exocytosis in isolated bile duct epithelial cells by a cyclic AMP-mediated mechanism. *J Biol Chem* 1992; 267:15523-15529
- Alpini G, Roberts S, Kuntz SM, Ueno Y, Gubba S, Podilla PV, LeSage G, LaRusso NF. Morphologic, molecular and functional heterogeneity of cholangiocytes from normal rat liver. *Gastroenterology* 1996;110:1636-1643
- Alpini G, Ulrich C, Roberts S, Phillips JC, Ueno Y, Podila PV, Colegio O, LeSage G, Miller LJ, LaRusso NF. Molecular and functional heterogeneity of cholangiocytes from rat liver after bile duct ligation. *Am J Physiol* 1997;272:G289-G297
- Pham L, Lazaridis K, LaRusso NF, deGroen PC. Development and characterization of a cDNA library prepared from isolated rat cholangiocytes. *Gastroenterology* 1997;112:A1358
- Balan V, Larkin J, Pham L, Vroman B, McNiven MA, LaRusso NF. Identification of Rab3d in intrahepatic bile duct epithelial cells: Implications for exocytosis and bile secretion. *Gastroenterology* 1994;106:A863
- Lazaridis KN, Pham L, Vroman B, DeGroen PC, LaRusso NF. Kinetic and molecular identification of sodium-dependent glucose transporter in normal rat cholangiocytes. *Am J Physiol* 1997;272:G1168-1174
- Lazaridis KN, Pham L, Marinelli RA, Tietz P, deGroen PC, Levine S, Dawson PA, LaRusso NF. Rat cholangiocytes absorb bile acids at their apical domain via the ileal sodium-dependent bile acid transporter. *J Clin Invest* 1997;100:2714-2721
- Lazaridis KN, Tietz PS, Kip S, Dawson P, LaRusso NF. Alternative splicing of the rat sodium/bile acid transporter changes its cellular localization and transport properties. *Proc Natl Acad Sci USA* 2000;97:11092-11097
- Marinelli RA, Pham LD, Tietz PS, LaRusso NF. Expression of aquaporin 4-water channels in rat cholangiocytes. *Hepatology* 2000;31:1313-1317
- Tietz PS, Holman RT, Miller LJ, LaRusso NF. Isolation and characterization of rat cholangiocyte vesicles enriched in apical or basolateral plasma membrane domains. *Biochemistry* 1995;34:15436-15443
- Tietz P, Levine S, Holman R, Fretham C, LaRusso NF. Characterization of apical and basolateral plasma membrane domains derived from cultured rat cholangiocytes. *Anal Biochem* 1997;254:192-199
- Roberts SK, Kuntz SM, Gores GJ, LaRusso NF. Regulation of bicarbonate-dependent ductular bile secretion assessed by luminal micropuncture of isolated rodent intrahepatic bile ducts. *Proc Natl Acad Sci USA* 1993;90:9080-9084
- Cova E, Gong A, Marinelli RA, LaRusso NF. Water movement across rat bile duct units is transcellular and channel-mediated. *Hepatology* 2001;34:456-463
- Masyuk AI, Gong AY, Kip S, Burke MJ, LaRusso NF. Perfused rat intrahepatic bile ducts secrete and absorb water, solute and ions. *Gastroenterology* 2000; 119:1672-1680
- Dranoff JA, Masyuk AI, Kruglov EA, LaRusso NF, Nathanson MH. Polarized expression and function of P2YATP receptors in rat bile duct epithelia. *Am J Physiol* 2001;281:G1059-G1067
- Gong AY, Masyuk AI, Splinter PL, LaRusso NF. Development and initial application of a micropfusion model of intrahepatic mouse bile duct units. *Hepatology* 2000;32(4, Pt2):433A
- Verkman AS, Yang B, Song Y, Manley GT, Ma T. Role of water channels in fluid transport studied by phenotype analysis of aquaporin knockout mice. *Exp Physiol* 2000;85:233S-241S
- Ludwig J, Ritman EL, LaRusso NF, Sheedy PF. Anatomy of the human biliary system studies by quantitative computer-aided three-dimensional imaging techniques. *Hepatology* 1998;27:893-899
- Masyuk TV, Ritman EL, LaRusso NF. Quantitative assessment of the rat intrahepatic biliary system by three-dimensional reconstruction. *Am J Pathol* 2001;158:2079-2088
- LaRusso NF. Morphology, physiology and biochemistry of biliary epithelia. *Toxicol Pathol* 1996;24:84-89
- Thung SN. The development of proliferating ductular structures in liver disease. *Arch Pathol Lab Med* 1990;114:407-411
- Roberts SK, Ludwig J, LaRusso NF. The pathology of biliary epithelia. *Gastroenterology* 1997;112:269-279
- Birnbaum A, Suchy FJ. The intrahepatic cholangiopathies. *Semin Liver Dis* 1998;18:263-269
- Chen XM, Levine SA, Tietz P, Krueger E, McNiven MA, Jefferson DM, Mahle M, LaRusso NF. Cryptosporidium parvum is cytopathic for cultured human biliary epithelia via an apoptotic mechanism. *Hepatology* 1998;28:906-913
- Chen XM, LaRusso NF. Mechanisms of attachment and internalization of Cryptosporidium parvum to biliary and intestinal epithelial cells. *Gastroenterology* 2000;118:368-379
- Chen XM, Huang BQ, Splinter PL, McNiven MA, LaRusso NF. Molecular mechanism of Cryptosporidium parvum invasion of biliary epithelia. *Gastroenterology* 2001;120:A325
- Chen XM, Gores GJ, Paya CV, LaRusso NF. Cryptosporidium parvum induces apoptosis in biliary epithelia by a Fas/Fas ligand-dependent mechanism. *Am J Physiol* 1999;277:G599-608
- Chen XM, Levine SA, Splinter PL, Tietz PS, Ganong AL, Jobin C, Gores GJ, Paya CV, LaRusso NF. Cryptosporidium parvum activates nuclear factor kappa B in biliary epithelia preventing epithelial cell apoptosis. *Gastroenterology* 2001;120:1774-1783

• BASIC RESEARCH •

# Direct effect of croton oil on intestinal epithelial cells and colonic smooth muscle cells

Xin Wang, Mei Lan, Han-Ping Wu, Yong-Quan Shi, Ju Lu, Jie Ding, Kai-Cun Wu, Jian-Ping Jin, Dai Ming Fan

Xin Wang, Mei Lan, Han-Ping Wu, Yong-Quan Shi, Jie Ding, Kai-Cun Wu, Dai Ming Fan, Institute of Digestive Diseases, Xijing Hospital, Fourth Military Medical University, Xi'an 710032, Shaanxi Province, China

Ju Lu, Class EE 87, Department of Electronic Engineering, Tsinghua University, Beijing 100084, China

Jian-Ping Jin, Department of Physiology and Biophysics, Case Western Reserve University School of Medicine, Cleveland, 44106-4970, Ohio, USA

Supported by the National Natural Science Foundation of China, No. 39970901

Correspondence to: Prof. Dai-Ming Fan, Institute of Digestive Disease, Xijing Hospital, Fourth Military Medical University, Xi'an 710033, Shaanxi Province, China. Daimfan@pub.xaonline.com  
Telephone: +86-29-3375221 Fax: +86-29-2539041

Received 2001-08-08 Accepted 2001-10-23

## Abstract

**AIM:** To investigate the direct effect of croton oil (CO) on human intestinal epithelial cell (HIEC) and guinea pig colonic smooth muscle cells *in vitro*.

**METHODS:** Growth curves of HIEC were drawn by MTT colorimetry. The dynamics of cell proliferation was analyzed with flow cytometry, and morphological changes were observed under light and electron microscopy after long-term (6 weeks) treatment with CO. Expression of cyclooxygenase-2 (COX-2) mRNA was detected by dot blot in HIEC treated with CO. Genes related to CO were screened by DD-PCR, and the direct effect of CO on the contractility of isolated guinea pig colonic smooth muscle cells was observed.

**RESULTS:** High concentration (20 - 40 mg · L<sup>-1</sup>) CO inhibited cell growth significantly (1, 3, 5, 7d OD sequence: (20 mg · L<sup>-1</sup>) 0.040±0.003, 0.081±0.012, 0.147±0.022, 0.024±0.016; (40 mg · L<sup>-1</sup>) 0.033±0.044, 0.056±0.012, 0.104±0.010, 0.189±0.006; OD control 0.031±0.008, 0.096±0.012, 0.173±0.009, 0.300±0.016, *P*<0.01), which appeared to be related directly to the dosage. Compared with the control, the fraction number of cells in G1 phase decreased from 0.60 to 0.58, while that in S phase increased from 0.30 to 0.34 and DNA index also increased after 6 weeks of treatment with CO (the dosage was increased gradually from 4 to 40 mg · L<sup>-1</sup>). Light microscopic observation revealed that cells had karyomegaly, less plasma and karyoplasm lopsidedness. Electron microscopy also showed an increase in cell proliferation and in the quantity of abnormal nuclei with pathologic mitosis. Expression of COX-2 mRNA decreased significantly in HIEC treated with CO. Thirteen differential cDNA fragments were cloned from HIEC treated with CO, one of which was 100 percent homologous with human mitochondrial cytochrome C oxidase subunit II. The length of isolated guinea pig colonic smooth muscle cells was significantly shortened after treatment with CO (*P*<0.05).

**CONCLUSION:** At a high CO concentration (>20 mg · L<sup>-1</sup>),

cell growth and proliferation are inhibited in a dosage-dependent manner. Increase in cell proliferation and in malignant conversion of the cellular phenotype is observed in cells cultured chronically with CO. COX-2 mRNA expression decreases significantly, while human mitochondrial cytochrome C oxidase subunit II mRNA expression increases markedly in HIEC treated with CO. CO also has a direct effect on the contractility of Guinea pig colonic smooth muscle cells.

Wang X, Lan M, Wu HP, Shi YQ, Lu J, Ding J, Wu KC, Jin JP, Fan DM. Direct effect of croton oil on intestinal epithelial cells and colonic smooth muscle cells. World J Gastroenterol 2002; 8(1):103-107

## INTRODUCTION

Croton is the fruit of *Croton tiglium* L, which consists of 34%-57% croton oil and 18% proteins. Croton oil (CO) contains crotonoleic acid, crotonic acid, crotonyl alcohol, 16 kinds of crotonyl alcohol bisester and many kinds of crotonyl alcohol trisester. Also contained in the seed of croton are croton, cocarcinogen C-3, crotonoside, isoguanine, β-sitosterol, amino acids and many kinds of enzymes. However, the principal component of croton extract is CO, which possesses multiple drug effects. CO is a stimulant in making inflammatory models, especially in models of skin and mucosal inflammation<sup>[1]</sup>, such as animal models of hemorrhoids, pleuritis, ear edema and uveitis<sup>[2]</sup>. Investigations have shown that allergic contact dermatitis (ACD) induced by CO is not a kind of late pleoergy response, but is mediated by the immune system in skin<sup>[3,4]</sup>. Metalloprotease neutral endopeptidase (NEP) and neuropeptide play an important role in ACD<sup>[5]</sup>. After CO administration to mice for 3 h<sup>[6,7]</sup>, there was no change in the mucosa of stomach and intestine under light microscope, but mucosal epithelial cell inflammation was observed under electron microscopy.

According to the recent, that dehydrocrotonin (DCTN), an extract of CO, had anti-ulcer effect<sup>[8]</sup>, especially in ulcers induced by hypothermia, alcohol and pyloric ligation. This effect was supposed to be related to the increase in the release of prostaglandin E2, the non-specific competitive binding of H2 and M receptors of stomach, the reinforcement of mucosal protective action and the weakening of mucosa-impairing factors. So DCTN has the potential to be a new anti-ulcer drug<sup>[9,10]</sup>.

It was reported that croton extract could not only suppress tumor growth but also promote tumor development. It has been confirmed that t-DCTN, which possesses neither genetic toxicity nor cytotoxicity, has anti-tumor activity and can significantly elongate the survival period of mice with S180 sarcoma and ascites neoplasia<sup>[11,12]</sup>. Recent research showed that 2,3-dihydroxy-labda-8 (17), 12(E), 14-triene, one of the croton extracts, had non-specific cytotoxicity for various tumor cells<sup>[13]</sup>. However, some investigations found that CO could cause skin carcinoma by lipid peroxidation and hydroperoxide production; it could directly bind protein kinase C, stimulating over-proliferation of epidermis, and repeatedly impair skin, which induces skin hyperplasia.

Croton is a strong cathartic; trace of croton can cause severe



diarrhea because of its potent in accelerating gastrointestinal motility. Now, Chinese medicine is the hot spot in the development of new drugs promoting gastrointestinal motility<sup>[14-28]</sup>. However, its mechanism in inducing diarrhea and accelerating gastrointestinal motion is not yet clarified<sup>[29-32]</sup>.

The aim of this research is to observe the effect of CO on intestinal epithelial cells and isolated colonic smooth muscle cells; investigate the effect of CO on biological properties of intestinal epithelia, mRNA differential expression and intestinal smooth muscle cell contraction; and further clarify its molecular mechanism so as to lay the foundation of the development of new drugs promoting gastrointestinal motility.

## MATERIALS AND METHODS

### Cell lines and culture

Human intestinal epithelial cell line (HIEC), presented as a gift by Dr. Ren DQ from Department of Radiation Medicine, Fourth Military Medical University, was grown in RPMI 1640 medium with 100 mL·L<sup>-1</sup> fetal bovine serum. CO dissolved in dimethyl sulfoxide (DMSO) was added into the culture medium when the medium was exchanged<sup>[32]</sup>. The end-concentration of CO was 4 mg·L<sup>-1</sup>; then the concentration increased progressively to 40 mg·L<sup>-1</sup> in 6 weeks.

### Effects of CO on HIEC growth (MTT)

Add HIEC into 96 well plate (200 µL/well); and add CO of different concentrations (4, 20, 40, 80 mg·L<sup>-1</sup>) and control DMSO (0.2, 1, 2, 4 mL·L<sup>-1</sup>) to corresponding groups, with three wells in each group. Put the culture plates into culture cassette, then take out one 96-well plate each time (1, 3, 5, 7 d), add 20 µL MTT solution (5 g·L<sup>-1</sup>) into each well, and resume culturing at 37°C for 4 h. Afterwards, suck and throw away the culture medium from the 96-well plate and add 150 µL DMSO to the plate. Detect OD in each well with photometer (wave length: 490 nm) and draw the growth curve.

### Flow cytometry analysis of HIEC proliferation treated with CO

Harvest HIEC in log phase growth that was treated with CO for 6 weeks. Cell proliferation cycle of HIEC was analyzed with flow cytometry after HIEC was routinely digested, washed twice with PBS and fixed with 700 mL·L<sup>-1</sup> ethanol. DNA index (DI) was calculated with the formula: DI = experimental group cells G0/1 / control cells G0/1. DNA.

Judgment standard of ploidy<sup>[33]</sup>. DI = 0.95-1.05 (DI = 1 ± CV, CV is 0.05): diploid; DI ≠ 1.00, between 0.90-1.10: proximal diploid; DI > 1.10 or DI < 0.9: increased or decreased heteroploid DNA content.

### Morphological changes of HIEC treated with CO

Changes in cell morphology were observed dynamically under inverted microscope. HIEC in log phase growth that was treated with CO for 6 weeks was harvested, and its proliferation cycle was analyzed with flow cytometry after routinely digested, washed twice with PBS, centrifuged for 5 min at 1200-1400 r·min<sup>-1</sup>, fixed with glutaraldehyde for 30 min at 4°C, and prepared into ultrathin section for transmission electron microscopic observation.

### Expression of COX-2 mRNA in HIEC (Dot blot)

Total RNA was extracted from control and experimental cells treated with CO for 6 wk. RNA samples were pointed onto the nitric cellulose membrane, and specific COX-2 oligonucleotide probes were end-labeled. Expression of COX-2 mRNA was detected with dot blot.

### mRNA differential display of HIEC treated with CO (DD-

### PCR)

Gene expressions of HIEC treated with CO for 6 weeks and of control were compared through DD-PCR. Primers were designed according to the literature: 3' end anchor primer H-T<sub>11</sub>C: 5'-AAGCTTTTTTTTTTTC-3', 8 strips of 5' end random primers: H-AP<sub>1</sub>-H-AP<sub>8</sub>. The first chain of cDNA was synthesized by reverse transcription; then with RT products as templates, and PCR was performed with 8 strips of 5' end random primers individually. Products of RT-PCR were run on 60 g·L<sup>-1</sup> urea denaturation polyacrylamide gels until the indicator arrived at the basal part of the gel at 200-300 V for 6-8 h. The gels were stained with modified silver-stain. Differential cDNA fragments were cut, recovered and purified for secondary amplification with PCR, and amplification products were isolated by agarose gel electrophoresis and ligated with pUC-Tm vector after recovery and purification. Recombinant plasmids were transfected into DH5α Escherichia coli and the bacteria were plated and incubated at 37°C overnight. Positive clones were picked out and the plasmids were extracted, followed by restriction enzyme cleavage identification. Further identification of the positive clones included reverse Northern blot and sequencing by automatic sequencer. Homology of the sequences of the differential expression cDNA fragments was searched in Gene Bank Database.

### Direct effect of CO on Guinea pig colonic smooth muscle cells

Guinea pig colonic smooth muscle cells were isolated by modified methods reported by Bitar and Makhoul<sup>[34,35]</sup>. Activity of the smooth muscle cells was detected with trypan blue, and the number of the cells were calculated under invert microscope. The number of smooth muscle cells with vitality must exceed 90% for experiment. CO was dissolved in dimethyl sulfoxide (DMSO) to make 4, 2, and 0.25 g·L<sup>-1</sup> CO solutions. Ten µL CO solutions of different concentrations were added into 200 µL colonic smooth muscle cell suspensions, the end-concentration of CO being 0.14, 0.07, and 0.009 g·L<sup>-1</sup>, respectively. The cells were incubated with CO at 30°C for 30 s and 80 µL of 25 g·L<sup>-1</sup> glutaraldehyde was added to terminate the reaction.

The length change of the smooth muscle cells was detected with micrometer under invert microscope. The average length was calculated from every 50 cells randomly. The contractile response of the smooth muscle cells was measured by the decrease of average length of cells treated with CO compared with that of the control. The formula is:

Percentage of cell contractile change = (average length of experimental cells - average length of control cells) / average length of control cells × 100%.

## RESULTS

### Effect of CO on the growth and cell cycle-phase of HIEC

High dosage (80 mg·L<sup>-1</sup>) CO resulted in the death of all HIEC; moderate dosage (20-40 mg·L<sup>-1</sup>) significantly inhibited cell growth (1, 3, 5, 7 d OD sequence: (20 mg·L<sup>-1</sup>) 0.040 ± 0.003, 0.081 ± 0.012, 0.147 ± 0.022, 0.024 ± 0.016; (40 mg·L<sup>-1</sup>) 0.033 ± 0.044, 0.056 ± 0.012, 0.104 ± 0.010, 0.189 ± 0.006; OD control 0.031 ± 0.008, 0.096 ± 0.012, 0.173 ± 0.009, 0.300 ± 0.016,  $P < 0.01$ ) in a dosage-dependent manner ( $IC_{50}$  is 52 mg·L<sup>-1</sup>); and low dosage (4 mg·L<sup>-1</sup>) had no effect on cell growth ( $P > 0.05$ ). The flow cytometry showed that S phase HIEC quantity significantly increased, G<sub>2</sub>/M phase cell quantity decreased and DI rose to 1.15 after HIEC was treated with CO for 6 weeks.

### Changes of HIEC morphology treated with CO

Morphologic changes of HIEC were dynamically observed under invert microscope in cells incubated with CO. Initially many cells exhibited

sheet shedding, intercellular space increased, toxic granules accumulated in the cytoplasm, and cell growth was significantly delayed. The growth behavior of the cells improved after treatment with CO for 11d. After the dosage of CO was progressively increased to  $40 \text{ mg} \cdot \text{L}^{-1}$  at the 6th week, the following phenomena occurred: fusiform cells significantly increased, cell bodies shrank, the nuclei were enlarged, the cytoplasm was reduced, karyoplasm lopsidedness was developed, and cell growth was accelerated. Under transmission electron microscope, we observed many wide apophyses in cell membrane, abundant microvilli, enlarged nuclei, multiplied nucleoli, and abnormal nuclei with pathologic mitosis (Figure 1).

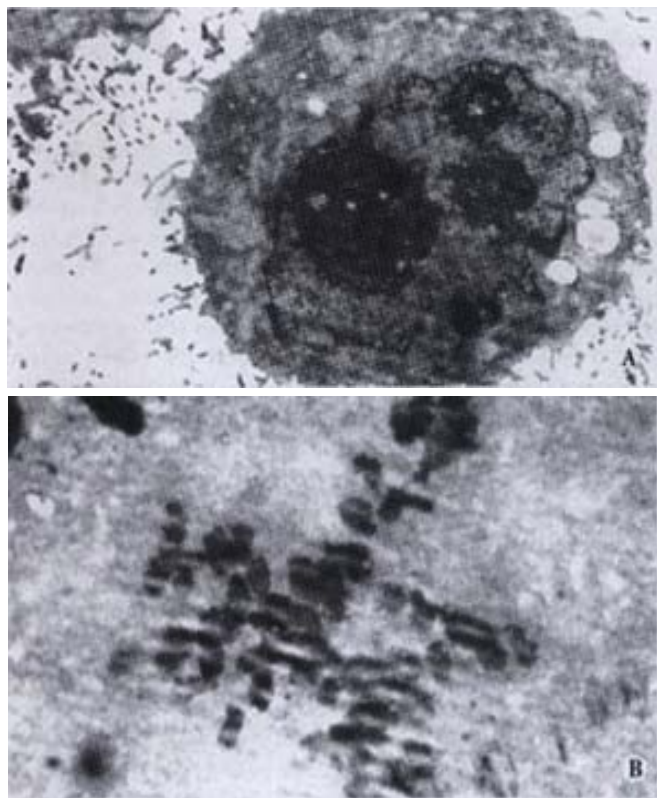


**Figure 1** A: Rich microvilli, enlarged nuclei and increased nucleoli in HIEC treated with CO (left);  
B: Abnormal nuclei with pathologic mitosis in HIEC treated with CO (right).

#### Expression of COX-2 mRNA in HIEC

Expression of COX-2 mRNA was significantly down regulated in HIEC after treated with CO for 6 week (Figure 2).

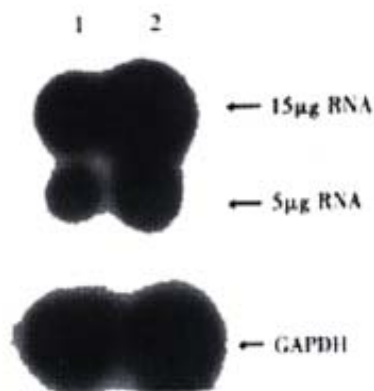


**Figure 2** Expression of COX-2mRNA in HIEC 1:HIEC treated with CO for 6week; 2:Control HIEC

#### DD-PCR

Some cDNA fragments found in HIEC treated with CO were up-regulated, down-regulated, newly born or deleted in comparison of experimental cells with controls (Figure 3). Thirteen different cDNA fragments were successfully cloned; among the 13 positive clones, 2 fragments were significantly up-regulated and 11 down-regulated in HIEC treated with CO, which was confirmed through reverse Northern blot analysis. Sequencing and homology demonstrated that one over-expressed cDNA fragment is 100% homologous with the homeobox gene of mitochondrial cytochrome C oxidase subunit-2 gene.

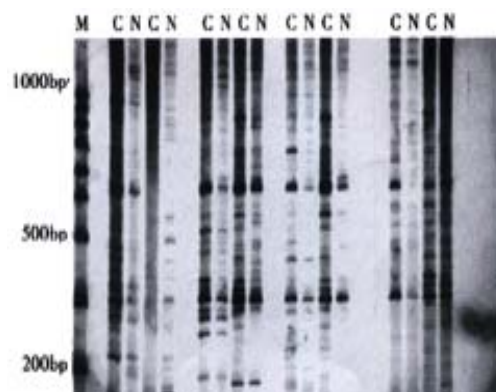


**Figure 3** Differential display of mRNA in HIEC treated with COM: 100bp ladder; C: HIEC treated by CO; N: Normal HIEC

#### Direct effect of CO on guinea pig colonic smooth muscle cells

Free Guinea pig colonic smooth muscle cells appeared in fusiform shape with diverse length. Some of them were relaxed while others were at different phases of contraction (Figure 4). The length of normal guinea pig colonic smooth muscle cells ranged from  $60 \mu\text{m}$  to  $160 \mu\text{m}$ , with an average length being  $(102 \pm 23) \mu\text{m}$ . After incubated with different concentrations of CO ( $0.14$ ,  $0.07$ ,  $0.009 \text{ g} \cdot \text{L}^{-1}$ ), the average length of colonic smooth muscle cells became  $(72 \pm 27) \mu\text{m}$ ,  $(74 \pm 26) \mu\text{m}$  and  $(72 \pm 17) \mu\text{m}$ , respectively, while that of the control cells was  $(104 \pm 22) \mu\text{m}$  (Figure 5). The percentages of decrease in cell length were 29.5%, 28% and 29.6%, respectively, significantly smaller than that of the control ( $P < 0.05$ ).

#### DISCUSSION

Our study showed that<sup>[36]</sup> high dosage of CO could result in the death of HIEC; middle dosage could inhibit cell growth in a dose-dependent manner; low dosage had no effect on cell growth. Meanwhile, after long-term continuous incubation with CO, the cycle from  $G_1$  to S of HIEC was shortened, the quantity of  $G_1$  phase cells was reduced, the quantity of S phase cells was increased, and DI was raised. We found that the principal phenomena of HIEC treated with CO included cell degeneration, necrosis, diminished ability of cells adhesion, and delayed cell growth. As the drug action persisted, degenerated cell quantity decreased and cell proliferation was accelerated. We also observed that HIEC treated with CO proliferated faster than control cells, and abnormal nuclei with pathologic mitosis were observed under electron microscope. These phenomena indicated that the cytotoxicity of high concentration CO might be the major cause for cell growth suppression. CO had the potential effect on promoting cell over-proliferation and increasing the content of heteroploid DNA when HIEC was incubated with CO for a long time.



Figure 4 A: Relaxed colonic smooth muscle cell; B: Contracted colonic smooth muscle cell

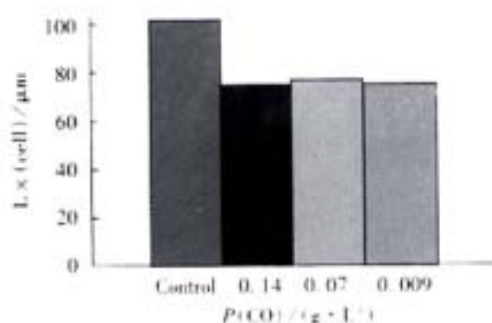


Figure 5 Direct contractile effect of CO on the colonic smooth muscle cells

COX-2 is an isoenzyme of cyclooxygenase discovered recently. Under normal conditions, COX-2 expression was low or non-existent in most tissues and cells in human body, but its expression could be promptly enhanced when cells were stimulated by a variety of factors. Recent studies showed that COX-2 is closely related to the development and progression of many kinds of human tumors, especially gastrointestinal tumors, such as colon cancer and gastric cancer. It has been confirmed that the expression of COX-2 increases more significantly in colon cancer tissues than in normal colonic tissues<sup>[37]</sup>, and its expression is higher in many kinds of gastric cancer cell lines and tissues than in their normal counterparts<sup>[38,39]</sup>. The incidence and mortality of colon cancer were decreased with the long-term intake of non-steroidal anti-inflammatory drugs (NSAIDs), a COX-2 inhibitor, which is effective on familial adenomatous polyposis. These data indicated that COX-2 might play an important role in the pathology of these tumors. The specific mechanism of COX-2 induced tumorigenesis is yet unclear, but it is suspected to be related to the following factors: catalysis of carcinogen synthesis; catalysis of prostaglandin (PGs) synthesis, which can regulate the expression of genes and accelerate DNA synthesis and cell proliferation; inhibition of cell apoptosis; enhancement of adhesion between cells and extracellular matrix; promotion of tumor angiogenesis<sup>[40,41]</sup>; inhibition of immunological response<sup>[42]</sup>. The expression of COX-2 mRNA was detected in HIEC treated with CO for 6 weeks, and the results revealed its significant down-regulation. The relationship between CO-induced tumorigenesis and down-regulation of COX-2 in HIEC remains to be elucidated.

Thirteen differential expression gene fragments were detected in HIEC treated with CO for long time through mRNA differential display. Therefore, these genes may be related to the biological effects of CO on HIEC. One of the genes is human mitochondria cytochrome C oxidase subunit II gene, whose expression is high in CO treated HIEC. Human mitochondria cytochrome C oxidase consists of subunit I, II and III, which contributes substantially to the respiratory function of mitochondrion. In addition, two notably highly expressed genes were separated from Cisplatin-resistant human head and neck squamous epithelium cancer by Higuchi<sup>[43]</sup> through DDRT-PCR, and

one of them is again the human mitochondria cytochrome C oxidase subunit II gene, which is putatively related to Cisplatin-resistance of tumor cells. We have also separated the highly expressed mitochondria cytochrome C oxidase subunit II gene from vincristine-resistant human gastric cancer cell SGC7901/VCR by DDRT-PCR (to be published separately). This suggests that mitochondria cytochrome C oxidase subunit II gene is closely correlated with drug-resistance. We found that CO-resistance of HIEC could be induced by gradually increasing the concentration of CO. However, the mechanism of CO-resistance in HIEC is unclear. As normal intestinal epithelial cells express certain multidrug resistance genes and proteins, such as P-glycoprotein (P-gp) in small intestinal epithelial cell line<sup>[44,45]</sup>, it demands further investigation about whether the CO-resistance is mediated by P-gp or mitochondria cytochrome C oxidase subunit II gene product.

Croton possesses many kinds of drug actions; however, its clinical application is largely limited to treating constipation, while its effect in promoting gastrointestinal motility is neglected. The neglect is not only due to its complexity in components and severe side effects, but also to the ignorance of its molecular mechanism in promoting gastrointestinal motility. Pol<sup>[46]</sup> found that CO could accelerate gastrointestinal movement of mice at 3h after gastric administration. When CO was administrated to dogs<sup>[47]</sup>, it could quickly evoke a rapid complex wave similar to the interdigestive myoelectric complex (IMC) III phase, although its contractile time was shorter its velocity of conduction faster than normal IMC. However, it was not affected by vagus nerve, which showed no relationship with  $\alpha$  and  $\beta$  receptors. IMC cycle shortening induced by CO was the principal cause of diarrhea. Albuquerque made a series of gastrointestinal movement experiments on animals with CO<sup>[48]</sup>. The results showed that CO and its preparations could directly affect intestinal smooth muscles and rat diaphragm muscles and cause them to contract. Other researchers reported<sup>[49,50,51]</sup> that senna could induce diarrhea and accelerate gastrointestinal movement by enhancing the synthesis and release of endogenous prostaglandin  $E_2$  (PGE<sub>2</sub>). Although we do not know whether the gastrointestinal motility enhancement of CO is related to PGE<sub>2</sub>, the significant down-regulation of COX-2 expression in HIEC with long-term treatment of CO indicated that the mechanism of CO promoted motility is different from that induced by senna. Furthermore, our experiment confirmed that the average length of colonic smooth muscle cells was significantly shortened when they were incubated with CO of different concentrations, which showed that CO had a direct contractile effect on colonic smooth muscle cells.

To sum up, the effect of CO on the HIEC growth was in a dose-dependent manner. High dosage of CO could delay cell growth or cause cell death; and low dosage had no effect. A long-term administration with progressively increased CO dosage could promote cell proliferation, increase heteroploid DNA content, and induce malignant conversion of cells. COX-2 expression was significantly down-regulated and mitochondria cytochrome C oxidase subunit-2 gene was significantly up-regulated in HIEC after induced by CO for a long time. At the same time, the expression of many genes



was changed. CO has a direct contractile effect on the colonic smooth muscle cells of guinea pig.

## REFERENCES

- Moon SH, Seo KI, Han WS, Suh DH, Cho KH, Kim JJ, Eun HC. Pathological findings in cumulative irritation induced by SLS and croton oil in hairless mice. *Contact Dermatitis* 2001; 44: 240-245
- Villena C, Vivas JM, Villar AM. Ocular inflammation models by topical application: croton oil induced uveitis. *Curr Eye Res* 1999; 18: 3-9
- Zhang L, Tinkle SS. Chemical activation of innate and specific immunity in contact dermatitis. *J Invest Dermatol* 2000; 115: 168-176
- Kaminski MJ, Mroczkowski TF, Krotoski WA. Dendritic epidermal gamma/delta T cells (DETC) activated in vivo proliferate in vitro in response to Mycobacterium leprae antigens. *Int J Dermatol* 2000; 39: 603-608
- Scholzen TE, Steinhoff M, Bonaccorsi P, Klein R, Amadesi S, Geppetti P, Lu B, Gerard NP, Olerud JE, Luger TA, Bunnett NW, Grady EF, Armstrong CA, Ansel JC. Neutral endopeptidase terminates substance P-induced inflammation in allergic contact dermatitis. *J Immunol* 2001; 166: 1285-1291
- Pol O, Ferrer I, Puig MM. Diarrhea associated with intestinal inflammation increased the potency of Mu and Delta Opioids on the inhibition of gastrointestinal transit in mice. *J Pharmacol Exp Ther* 1994; 270: 386-391
- Pol O, Planas E, Puig MM. Peripheral effects of naloxone in mice with acute diarrhea associated with intestinal inflammation. *J Pharmacol Exp Ther* 1995; 272: 1271-1276
- Hiruma-Lima CA, Spadari Bratfisch RC, Grassi Kassisse DM, Brito AR. Antiulcerogenic mechanisms of dehydrocrotonin, a diterpene lactone obtained from Croton cajucara. *Planta Med* 1999; 65: 325-330
- Hiruma-Lima CA, Gracioso JS, Rodriguez JA, Haun M, Nunes DS, Souza Brito AR. Gastroprotective effect of essential oil from Croton cajucara Benth. (Euphorbiaceae). *J Ethnopharmacol* 2000; 69: 229-234
- Brito AR, Rodriguez JA, Hiruma-Lima CA, Haun M, Nunes DS. Antiulcerogenic activity of trans-dehydrocrotonin from Croton cajucara. *Planta Med* 1998; 64: 126-129
- Grynberg NF, Echevarria A, Lima JE. Anti-tumour activity of two 19-nor-clerodane diterpenes, trans-dehydrocrotonin and trans-crotonin, from Croton cajucara. *Planta Med* 1999; 65: 687-689
- Agner AR, Maciel MA, Pinto AC. Investigation of genotoxic activity of trans-dehydrocrotonin, a clerodane diterpene from Croton cajucara. *Teratog Carcinog Mutagen* 1999; 19: 377-384
- Roengsumran S, Petsom A, Kuptiyanuwat N. Cytotoxic labdane diterpenoids from Croton oblongifolius. *Phytochemistry* 2001; 56: 103-107
- Wang ZH, Lu LS. Effect of Weichangtong on gastrointestinal motility disorders. *Xin Xiaohuabingxue Zazhi* 1997; 5: 448-449
- Zheng TZ, Li W, Qu SY, Ma YM, Ding YH, Wei YL. Effects of Dangshen on isolated gastric muscle strips in rats. *World J Gastroenterol* 1998; 4: 354-356
- Ma XS, Fan XP, Chen Z, Li CW, Xing YS. Effects of rhizoma atracylodes macrocephalae on the contraction of isolated ileum of guinea pig. *Xin Xiaohuabingxue Zazhi* 1996; 4: 603-604
- Li SZ, Tan XH. Effect of Astragalus membranaceus on intestinal blood flow and motility in dogs. *Xin Xiaohuabingxue Zazhi* 1997; 5: 659-660
- Hao Q, Li Y, Yin HT. Comparative effect of different varieties of Bupleurum and Citrus on gastrointestinal motility in mice. *Huaren Xiaohua Zazhi* 1998; 6: 205-207
- Li Y, Sun SY, Zou Z, Chen SN, Wang XY. Influences of 6 formula compositions combined of 8 kinds of Chinese medicinals on gastro intestinal motility in mice. *Huaren Xiaohua Zazhi* 1998; 6: 208-209
- Li HM, Liang H, Tang HQ, Li X. Therapeutic effects of pinaverium bromide in functional constipation and diarrhea in mice. *Huaren Xiaohua Zazhi* 1998; 6: 36-39
- Pang L, Zhou DR. Regulative action of Chinese traditional medicine in gastrointestinal motility. *Huaren Xiaohua Zazhi* 1998; 6: 535-536
- Zhu JZ, Yang GH, Leng ER, Chen DF. Gastrointestinal motility promoting action of traditional Chinese medicine. *Shijie Huaren Xiaohua Zazhi* 1999; 7: 689-690
- Wang J, Hou JY. Effect of granulae Li Wei on gastrointestinal activity. *Shijie Huaren Xiaohua Zazhi* 2000; 8: 377-381
- Shi BJ, Liu HY. Comparison between cisapride and metoclopramide in the treatment of irritable bowel syndrome. *Xin Xiaohuabingxue Zazhi* 1997; 5: 51-52
- Xiang AM, Zhou DD. Traditional Chinese medicine and gastric mucosal barrier. *Huaren Xiaohua Zazhi* 1998; 6: 537-538
- Gao F, Zhang SB, Zhang LY, Liu F, Tong WD, Li FZ. An experiment study of the small intestinal transit injured by contact laxatives. *Shijie Huaren Xiaohua Zazhi* 1999; 7: 659-660
- Lin J, Cai G, Xu JY. A comparison between Zhishi Xiaopiwan and cisapride in treatment of functional dyspepsia. *World J Gastroenterol* 1998; 4: 544-547
- Tian XL, Mourelle M, Li YL, Guarner F, Malagelada JR. The role of Chinese herbal medicines in a rat model of chronic colitis. *World J Gastroenterol* 2000; 6: 40-42
- Zhang HX, Ren P, Huang X, Li Yuan. Regulation of the traditional Chinese medicine on gastrointestinal hormone and motility. *Shijie Huaren Xiaohua Zazhi* 2000; 8
- Zhu JZ, Yang GH, Leng EF, Chen DF. Effects of the traditional Chinese medicine on gastrointestinal motility. *Shijie Huaren Xiaohua Zazhi* 1999; 7: 689-690
- Pang L, Zhou DR. Regulation of the traditional Chinese medicine on gastrointestinal motility. *Huaren Xiaohua Zazhi* 1998; 6: 535
- Wang X, Zhang ZY, Shi YQ, Lan M, Han QL, Wu HP, Jin JP, Fan DM. Preliminary study on protein differential expression of small bowel in BALB/c mice induced by croton oil. *Weichangbingxue He Ganzhangbingxue Zazhi* 2000; 9: 103-106
- Hu CJ, Yang DL, Yin GP, Song XM, Li JS, Cao YC. Quantitative studies of RNA, DNA and proliferation index in Hepatocarcinoma cells. *Xinxiaohua Bingxue Zazhi* 1997; 5: 516
- Ennes HS, McRoberts JA, Hyman PE, Snape WJ. Characterization of colonic circular smooth muscle cells in culture. *Am J Physiol* 1992; 263: G365-G370
- Murthy, Karnam S, Makhlof GM. cGMP-mediated Ca<sup>2+</sup> release from IP<sub>3</sub>-insensitive Ca<sup>2+</sup> stores in smooth muscle. *Am J Physiol* 1998; 274: C1199-C1205
- Mei Lan, Xin Wang, Han Ping Wu, Dai Ming Fan. Effect of croton extract on biological characterization of human intestinal epithelial cells. *Shijie Huaren Xiaohua Zazhi* 2001; 9: 366-373
- Sano H, Kawahito Y, Wilder RL, Hashimoto A, Mukai S, Asai K, Kimura S, Kato H, Kondo M, Hla T. Expression of cyclooxygenase-1 and -2 in human colorectal cancer. *Cancer Res* 1995; 55: 3785-3789
- Li L, Wu KC, Wu HP, Wang X, Nie YZ, Fan DM. Expression and biological activity of COX-2 in human gastric cancer cells. *J Cell Mol Immunol* 2000; 16: 255-259
- Wu KC, Jackson L, Mahida YR. Cyclooxygenase (Cox)-1 and -2 in human gastric mucosa: Constitutive expression by parietal cells and induction of Cox-2 in lamina propria cells proximal to ulcers. *Gastroenterology* 1998; 114: G1365
- Gke M, Kanai M, Lynch Devaney K, Podolsky DK. Rapid mitogen activated protein kinase activation by transforming growth factor  $\alpha$  in wounded rat intestinal epithelial cells. *World J Gastroenterol* 1998; 4: 263
- Sujii M, Kawano S, Tsuji S, Sawaono H, Hori M, DuBois RN. Cyclooxygenase regulates angiogenesis induced by colon cancer cells. *Cell* 1998; 93: 705-716
- Huang M, Stoling M, Sharma S, Mao JT, Zhu L, Miller PW, Wollman J, Herschman H, Dubinett SM. Non-small cell lung cancer cyclooxygenase-2-dependent regulation of cytokine release in lymphocytes and macrophages: up-regulation of interleukin10 and down-regulation of interleukin12 production. *Cancer Res* 1998; 58: 1208-1216
- Higuchi. Up-regulation of human chorionic gonadotropin alpha subunit gene and human mitochondrial cytochrome C oxidase subunit II gene in cis-Diamminedichloroplatinum (II)-resistant human head and neck squamous carcinoma cells. *Hokkaido Igaku Zasshi* 1999; 74: 231-238
- Li M, Hurren R, Zastawny RL, Ling V, Buick RN. Regulation and expression of multidrug resistance (MDR) transcripts in the intestinal epithelium. *Br J Cancer* 1999; 80: 1123-1131
- Edelmann H M, Duchek P, Rosenthal FE, Foger N, Glackin C, Kane SE, Kuchler K. Cmdr1, a chicken P-glycoprotein, confers multidrug resistance and interacts with estradiol. *Biol Chem* 1999; 380: 231-241
- Margarita M, Puig MM, Pol O. Peripheral effects of Opioids in a model of chronic intestinal inflammation in mice. *J Pharmacol Exp Ther* 1998; 287: 1068-1075
- Xu JD, Zhang JJ, Hu GQ. Change of small intestinal electric activity during diarrhea induced by croton oil in dog. *Chin J Appl Physiol* 1991; 7: 139-142
- Albuquerque AA, Sorenson AL, Leal JH. Effects of essential oil of Croton zehntneri, and of anethole and estragole on skeletal muscles. *J Ethnopharmacol* 1995; 49: 41-49
- Qin XM, Li HF, Wang LD. Effects of metoclopramide on gastrointestinal myoelectric activity in rats. *Chin Natl J New Gastroenterol* 1997; 3: 169-170
- Beubler E, Kolllar G. Prostaglandin-mediated action of sennosides. *Pharmacology* 1993; 36(Suppl 1): 85-91
- Nijs G, Witter P, Geboesk K, Lemli J. Influence of rhein anthrone and rhein on small intestine transit rate in rats: evidence of prostaglandin mediation. *Eur J Pharmacol* 1992; 218: 199-203

• BASIC RESEARCH •

# Identification of CD226 ligand on colo205 cell surface

Kai Sun, Bo-Quan Jin, Qi Feng, Yong Zhu, Kun Yang, Xue-Song Liu, Bang-Quan Dong

Kai Sun, Department of Hepatobiliary Surgery, Xijing Hospital, Xi'an 710032, Shaanxi province, China

Bo-Quan Jin, Yong Zhu, Kun Yang, Xue-Song Liu, Bang-Quan Dong, Department of Immunology, The Fourth Military Medical University, Xi'an 710032, Shaanxi province, China

Qi Feng, Department of Hematology, Xijing Hospital; Xi'an 710032, Shaanxi province, China

Supported by the National Nature Science Foundation. No 39700065

Correspondence to: Kai Sun, M.D, Department of Hepatobiliary Surgery, Xijing Hospital, Xi'an 710032, Shaanxi province, China. iamsunkai@263.net

Telephone: +86-029-3242969 Fax: +86-029-3242969

Received 2001-06-11 Accepted 2001-10-16

## Abstract

**AIM:** To confirm the existence of CD226 ligand and its distribution, which is a novel molecule that was cloned in 1996.

**METHODS:** The mRNA was extracted from TPA activated Jurkat cells and used as a template for reverse-transcription. After PCR amplification, the fragment including CD226 extracellular region and the splice donor sequence "ACTTACCTGT" was obtained and cloned into fusion expression vector pIG. The recombinant vector pCD226/Ig was transfected in COS-7 cells by DEAE-Dextran method, the secreting fusion protein was identified by Sandwich ELISA, and was purified by anti-CD226 affinity chromatography. This fusion protein was used as a probe in the investigation of CD226 ligand by immunohistochemistry. Existence of CD226 ligand was further identified by adhesion experiment.

**RESULTS:** Expression of a secreting fusion protein was identified by sandwich ELISA, indicating that both CD226 extracellular domain and IgGFC domain could be recognized respectively by anti-CD226 and anti-IgGFC mAb. About 130µg CD226/Ig fusion protein could be obtained from 100mL COS-7 culture supernatants by anti-CD226 affinity chromatography purification. SDS-PAGE showed that this fusion protein has a molecular mass of 83 ku. It was confirmed by immunohistochemistry that CD226 ligand expressed on the Colo205 cells, but not on Jurkat cell, U937 cell and mixed lymphocyte culture cells. In adhesive assay, resting Jurkat cells did not have significant adhesion to Colo205 cells. In contrast, activated Jurkat cells could bind to colon carcinoma Colo205 cells and this adhesive reaction could be blocked by CD226/Ig fusion protein or anti-CD226 mAb. Immunochemical experiment showed that Colo205 cells could be specifically stained by CD226/Ig, indicating that CD226 ligand exists on the surface of Colo205 cells.

**CONCLUSION:** Existence of CD226 ligand on the surface of Colo205 cells was identified by immunohistochemistry and adhesion blocking experiment. In addition, the secreting CD226/Ig fusion protein prepared in this study will be a potential tool for further investigation of CD226 ligand.

## INTRODUCTION

CD226 was initially reported by Burns in 1985 with a name TLI SA1 (T lineage specific activation antigen 1, TLI SA1)<sup>[1]</sup>, and was renamed PTA1 (platelet and T cell antigen 1, PTA1) in 1989 because of its expression on platelet as well<sup>[2]</sup>. Since 1985, a lot of investigations have been done on CD226 expression, functions and its relationship with diseases<sup>[2-6]</sup>. CD226 was mainly expressed on the activated T cells, NK cells, monocytes, platelets and megakaryocytes lineage<sup>[4-8]</sup>, taking part in signal transduction of T cell activation and differentiation as well as platelet activation and aggregation. CD226 mAb was found to stimulate the activation and aggregation of platelets<sup>[2,3]</sup>, inhibit differentiation of CTL<sup>[2,9]</sup> and T and NK cell mediated cytotoxicity<sup>[7]</sup>. In 1997, PTA1 cDNA was cloned from cDNA library of TPA activated Jurkat cells<sup>[10]</sup>. It belongs to an immunoglobulin super family (IgSF) with a 232aa extracellular region, 25aa transmembrane region and 61aa intracellular region. Interestingly, PTA1 cDNA was almost the same as that of DNAM-1 (DNAX associated molecule-1), a novel molecule cloned by Shibuya in 1996<sup>[7]</sup>. In 2000, PTA1 (DNAM-1) was designated as CD226 on the 7th Workshop and Conference on the Human Leucocyte Differentiation Antigen in Harrogate. CD226 is the only IgSF member whose extracellular region consists of two IgV-like domains.

Almost all the important Ig-superfamily members are highly conserved during molecular evolution<sup>[11-13]</sup>, such as CD2, CD4/CD8 and CD28. Homological analysis showed that CD226 molecules are highly conserved (93%-95%) among human, ape and monkey, suggesting that CD226 may have very important functions<sup>[14]</sup>. It seems that CD226 takes part in the mechanism of platelet function disorders, autoimmune diseases, transplantation, virus infection diseases and tumors<sup>[3,15-20]</sup>, suggesting that CD226 plays an important role in immune system and may have a potential application to clinical diagnosis and treatment. Up to, little is known about CD226 ligand. So, the aim of this study is to make a preliminary research on CD226 ligand.

## MATERIAL AND METHODS

### Materials

pIG vector was a gift kindly presented by Dr. Xu. COS-7, U937, Jurkat, Colo205 cell line and CD226 hybridoma (secreting mAb Leo-A1 against the extracellular domain of CD226) were provided by Prof. Jin. Goat anti-human Ig-SABC immunohistochemistry kit was purchased from Boster Co. Vectors and restrict enzymes were purchased from Huamei Co; Trizol reagent kit was purchased from Gibco Co, and CNBr-Sepharose 4B is a product of Pharmacia Co.

### Design of the primers for semi-nest RT-PCR

Primers were designed according to the sequence of CD226 cDNA: primer 1, 5'-GCAAGCTTCAGAGATGGATTATCCTACT-3' (forward, containing HindIII enzyme site at 5'); primer 2, 5'-GCGGATCCACTTACCTGTAGCCACAAAGAGGGTA TATTGG-3' (reverse, containing BamHI enzyme site and donor splice region "ACTTACCTGT" at 5'); primer 3, 5'-ACTCTAGTCTTTGGTCCTGC-3'. Primer1 and Primer 3 were used to amplify the whole length CD226 cDNA, and primer 1 and primer 2 were used to amplify cDNA encoding CD226 extracellular region (Figure 1).

|                                                       |                 |                 |                   |                   |                   |                   |      |
|-------------------------------------------------------|-----------------|-----------------|-------------------|-------------------|-------------------|-------------------|------|
| 121                                                   | agagcgagca      | gcactcacat      | ctcaagaacc        | P1→               | <u>gcaagcttca</u> | <u>gagatggatt</u> | 180  |
|                                                       | <u>atcctact</u> |                 |                   | agcctttcaa        | acagtttcca        | gagATGgatt        |      |
| 181                                                   | atcctacttt      | actttttggt      | cttcttcatg        | tatacagagc        | tctatgtgaa        | gaggtgcttt        | 240  |
| 241                                                   | ggcatacatc      | agttcccttt      | gccgagaaca        | tgtctctaga        | atgtgtgtat        | ccatcaatgg        | 300  |
| 301                                                   | gcattctaac      | acaggtggag      | tggttcaaga        | tccgggacca        | gcaggattcc        | atagccattt        | 360  |
| 361                                                   | tcagccctac      | tcatggcatg      | gtcataagga        | agccctatgc        | tgagagggtt        | tactttttga        | 420  |
| 421                                                   | attcaacgat      | ggcttccaat      | aacatgactc        | ttttctttcg        | gaatgcctct        | gaagatgatg        | 480  |
| 481                                                   | ttgggtacta      | ttcctgtctt      | ctttacactt        | acccacaggg        | aacttggcag        | aaggtgatac        | 540  |
| 541                                                   | aggtgggtca      | gtcagatagt      | tttgaggcag        | ctgtgccatc        | aaatagccac        | attgtttcgg        | 600  |
| 601                                                   | aacctggaaa      | gaatgtcaca      | ctcacttgte        | agcctcagat        | gacgtggcct        | gtgcaggcag        | 660  |
| 661                                                   | tgaggtggga      | aaagatccag      | ccccgtcaga        | tgcacctctt        | aacttactgc        | aacttgggtc        | 720  |
| 721                                                   | atggcagaaa      | tttcacctcc      | aagttcccaa        | gacaaatagt        | gagcaactgc        | agccacggaa        | 780  |
| 781                                                   | ggtggagctg      | categtcate      | cccgatgtca        | cagtcctcaga       | ctcggggctt        | taccgctgct        | 840  |
| 841                                                   | acttgccaggc     | cagcgcagga      | gaaaacgaaa        | ccttcgtgat        | gagattgact        | gtagccgagg        | 900  |
|                                                       | P3←             | <u>gggttata</u> | <u>tgggagaaac</u> | <u>accgatgtcc</u> | <u>attcacctag</u> | <u>gcg</u>        |      |
| 901                                                   | gtaaaaccga      | taaccaatat      | accctctttg        | tggctggagg        | gacagtltta        | ttgtttgtgt        | 960  |
| 961                                                   | ttgttatctc      | aattaccacc      | atcattgtca        | ttttccttaa        | cagaaggaga        | aggagagaga        | 1020 |
| 1021                                                  | gaagagatct      | atttacagag      | tcttgggata        | cacagaaggc        | acccaataac        | tatagaagtc        | 1080 |
| 1081                                                  | ccatctctac      | cagtcacact      | accaatcaat        | ccatggatga        | tacaagagag        | gatattttatg       | 1140 |
|                                                       |                 | P2←             | <u>cgctcctgg</u>  | <u>ttctgatctc</u> | <u>a</u>          |                   |      |
| 1141                                                  | tcaactatcc      | aaccttctct      | cgcaggacca        | aagacTAGag        | tttaagctta        | ttcttgacat        | 1200 |
| 1201                                                  | gagtgcatta      | gtaatgactc      | ttatgtactc        | atgcattgat        | c                 |                   |      |
| Primer 1 5'GCAAGCTTCAGAGATGGATTATCCTACT3'             |                 |                 |                   |                   |                   |                   |      |
| Primer 2 5'ACTCTAGTCTTTGGTCCTGC3'                     |                 |                 |                   |                   |                   |                   |      |
| Primer 3 5'GCGGATCCACTTACCTGTAGCCACAAAGAGGGTATATTGG3' |                 |                 |                   |                   |                   |                   |      |

**Figure 1** Sequence of CD226 cDNA and primers.

174-923bp: extracellular region of CD226; 174-227bp: signal peptide sequence; 924-998bp: transmembrane region; □labeled sequence: primers; underlined sequence was the splicing donor sequence.

### Reverse transcription-polymerase chain reaction (RT-PCR)

Jurkat cells were cultured at a concentration of  $1 \times 10^6 \text{ L}^{-1}$  with TPA ( $50 \mu\text{g} \cdot \text{L}^{-1}$ ) for 18-30 h at  $37^\circ\text{C}$ , and the total RNA was isolated by Trizol reagent kit. RNA was primed and reverse transcribed into cDNA in a  $20 \mu\text{L}$  reaction volume containing 10U reverse transcriptase,  $10 \mu\text{g}$  RNA,  $10 \times \text{Buffer}$   $2 \mu\text{L}$ ,  $10 \text{mmol} \cdot \text{L}^{-1}$  dNTP complex  $4 \mu\text{L}$ , and primer 3. After incubation at  $42^\circ\text{C}$  for 1 h, the reverse transcription product was PCR amplified by Primer 1 and Primer 3, and then by Primer 1 and Primer 2. The PCR parameters were  $94^\circ\text{C}$  for 1 min,  $60^\circ\text{C}$  for 1 min, and  $72^\circ\text{C}$  for 80 s for 35 cycles.

### Plasmid construction

Expression vector for CD226 extracellular region was prepared as previously described<sup>[21]</sup>. The corresponding PCR fragment was cloned into pUC-19 and M13mp18/19 vector for DNA sequencing. After DNA sequencing, the 793bp fragment encoding CD226 extracellular region and the splice donor sequence "ACTTACCTGT" was subcloned into pIG, a mammalian fusion protein expression vector containing the cytomegalovirus (CMV) promoter, splice acceptor, genomic human IgG1, and SV40 polyadenylation signal. The resulting expression vector pCD226/Ig was identified by PCR and restrict enzyme digestion.

### COS-7 cell Transfection

COS-7 cell transfection was performed by a modified method<sup>[22]</sup>. Briefly, COS-7 cells at 50%-75% confluence were transfected in 7mL glucose Dulbecco's modified Eagle's medium (DMEM) containing  $100 \text{mL} \cdot \text{L}^{-1}$  fetal calf serum (FCS),  $400 \mu\text{g}$  DEAE-dextran/mL,  $100 \mu\text{mol} \cdot \text{L}^{-1}$  chloroquine diphosphate, and  $40 \mu\text{g}$  purified DNA. After 3 h at  $37^\circ\text{C}$ , the transfection mixture was removed and the cells were treated with  $100 \text{g} \cdot \text{L}^{-1}$  dimethyl sulfoxide in PBS for 2 min. Cells were then returned to DMEM supplemented with  $10 \text{mL} \cdot \text{L}^{-1}$  fetal calf serum (FCS) for 4 d to allow CD226/Ig expression.

### Purification and identification of CD226/Ig fusion protein

Leo-A1 affinity chromatography column was prepared as previously described<sup>[23]</sup>. The pCD226/Ig transfected COS-7 supernatant was spined out cell debris for 5 minutes at  $10000 \text{ r} \cdot \text{min}^{-1}$ , filtered through a  $0.45 \mu\text{m}$  filter and then purified by Leo-A1 affinity chromatography. The expression of a secreting fusion protein was identified by sandwich ELISA (anti-CD226 mAb and HRP-conjugated anti-hIg mAb, anti-IL-8 antibody was used as control). SDS-PAGE and Western-blot (polyclonal anti-hIgG antibody) were performed by routine methods.

### Immunohistochemical staining by CD226/Ig

Immunohistochemical experiment was performed by SABC methods. For light microscopy, cytospin preparations of Colo205 cells were incubated with  $3 \text{g} \cdot \text{L}^{-1}$  methanol-hydrogen peroxide solution at  $37^\circ\text{C}$  for 30 min to inactivate endogenous peroxidases. The slides were then blocked in goat serum blocking solution at  $37^\circ\text{C}$  for 30 min. Without washing, the slides were incubated with CD226/Ig fusion protein ( $10 \text{mg} \cdot \text{L}^{-1}$ ) at  $4^\circ\text{C}$ . After overnight incubation, the slides were washed three times with PBS, and incubated with biotin labeled goat anti human IgG for 4 h at room temperature. Finally, the slides were washed, allowed to sit for 2 min, and then reacted with SABC complex and DAB peroxidase substrate solution. Human IgG1 was used instead of CD226/Ig in the control experiment.

### Adhesion assay

In 96 well plate, Colo205 cells with the density of  $0.5 \times 10^5/\text{well}$  were cultured for one day to let cells confluence, and  $3.7 \text{ MBq}$   $^{51}\text{Cr}$  labeled resting or activated Jurkat cells were added with  $1 \times 10^5/\text{well}$  and cultured for 4 h, and non-adhered cells were moved by gently washing, the adhered cells were lysed by  $20 \text{g} \cdot \text{L}^{-1}$  Triton X-100, and Bq was measured. Different concentrations of CD226/Ig fusion protein and anti-CD226 mAb Leo-A1 were used in the adhesion blocking experiment.

## RESULTS

### Construction of pCD226/Ig fusion expression vector

A very low level of CD226 molecules was expressed on resting Jurkat cells, and the expression level could be enhanced by TPA stimulation for 24 h. The CD226 mRNA from Jurkat cells was enriched by TPA stimulating. After retro-transcription, semi-nests PCR amplification, a single band about 800bp has been obtained. This fragment was then ligated into pUC19 and subcloned into M13mp18/19 vector for sequencing. The sequencing data showed that the fragment was 793bp long in total, a HindIII enzyme site could be found at the upstream and the "ACTTACCTGT" donor splicing sequence and a BamHI site could be found at the downstream. The 793 bp fragment was ligated between HindIII and BamHI sites of pIG vector. The recombinant vector pCD226/Ig was identified by restrict enzyme digestion assay and PCR identification (Figure 2).

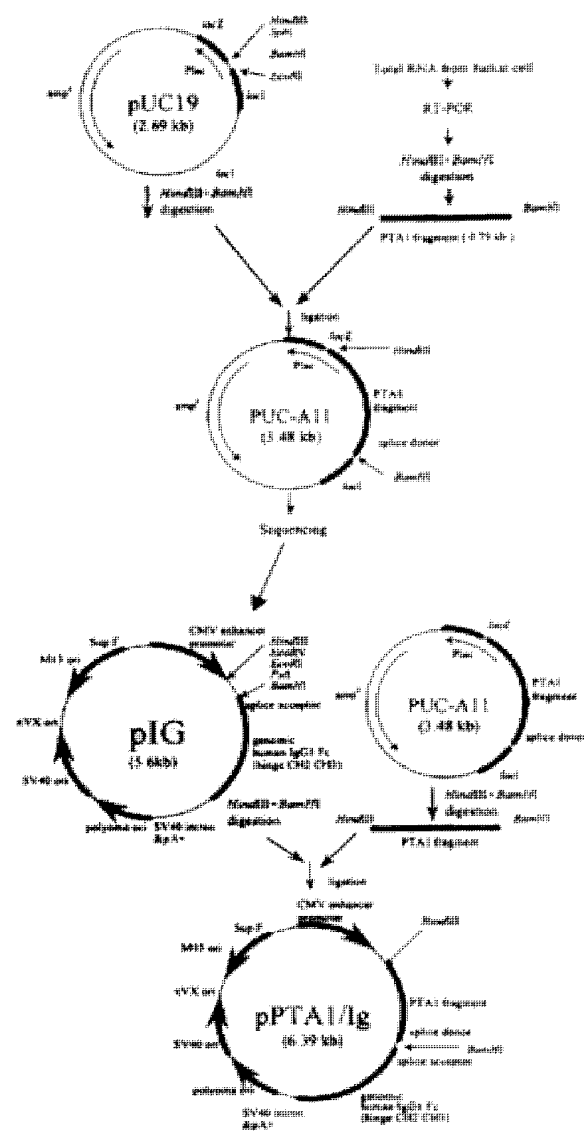


Figure 2 Construction of pCD226/Ig fusion vector.

### Expression, identification and purification of CD226/Ig fusion protein

The pCD226/Ig vector was transiently transfected into COS-7 cells. The optimal conditions was checked before large-scale transfection, and it was found that transfected COS-7 cells cultured in medium with 10ml·L<sup>-1</sup> serum for 96 h could produce CD226/Ig most effectively. The secreted CD226/Ig fusion protein was purified by Leo-A1 affinity chromatography. About 130μg CD226/Ig fusion protein could be obtained from 100mL COS-7 culture supernatants by anti-CD226 affinity chromatography purification. SDS-PAGE showed CD226/Ig fusion protein has a molecular mass of 83 ku (Figure 3) and could be recognized by anti-IgG polyclonal antibody in Western-blot assay (Figure 4). In ELISA assay, CD226/Ig expression could be identified in pCD226/Ig transfected COS-7 supernatant, but a negative result was obtained in pIG vector transfected COS-7 supernatant (Table 1). Both CD226 extracellular domain and Fc domain of the CD226/Ig protein could be recognized respectively by anti-CD226 and anti-hIg Fc mAb, suggesting that CD226/Ig could mimic the nature CD226 molecule and be a potential tool in the research of CD226 ligand and its functions.

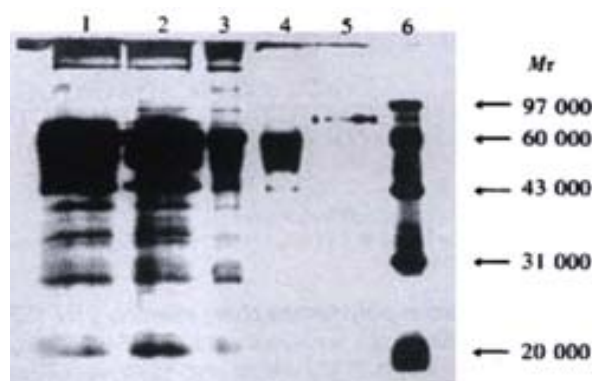


Figure 3 Identification of CD226/Ig fusion protein purified by Leo-A1 Sepharose-4B affinity column.

1. Supernatant of pIG vector transfected COS-7 cells; 2. Supernatant of pCD226/Ig transfected COS-7 cells; 3. Supernatant of pCD226/Ig transfected COS-7 cells after concentrated by ammonium sulfate; 4. Flow through solution of pCD226/Ig transfected COS-7 cells after affinity chromatography; 5. CD226/Ig fusion protein purified by Leo-A1 sepharose-4B affinity column; 6. Marker.



Figure 4 Western-blot result of CD226/Ig by anti-IgG polyclonal antibody Lane 1. Supernatant of pCD226/Ig transfected COS-7 cells; Lane 2. Supernatant of pIG transfected COS-7 cells

Table 1 Identification of CD226/Ig fusion protein expression by sandwich-ELISA

| Coated antibody | Samples tested                        | Conjugated secondary antibody | Results |
|-----------------|---------------------------------------|-------------------------------|---------|
| Anti-CD226      | pCD226/Ig transfected COS supernatant | HRP-GohlgG                    | +++     |
| Anti-CD226      | pIG transfected COS supernatant       | HRP-GohlgG                    | -       |
| Anti-IL-8       | pCD226/Ig transfected COS supernatant | HRP-GohlgG                    | -       |



### Identification of CD226 ligand on Colo205 cells

Immunohistochemical experiment showed that Colo205 cells could be specifically stained by CD226/Ig but not by control protein (hIgG), indicating that CD226 ligand exists on the surface of Colo205 cells (Figure 5). Resting Jurkat cells had a low-level expression of CD226 on cell surface, whereas activated Jurkat cells expressed high level of CD226 after TPA treatment for 24h. In adhesive assay, resting Jurkat cells have a very low level adhesion to Colo205 cells. In contrast, activated Jurkat cells could bind to colon carcinoma Colo205 cells and this adhesive reaction could be blocked by CD226/Ig fusion protein or Leo-A1 mAb but not control Ig and anti-IL-1 mAb, indicating that CD226 takes part in this specific adhesion (Figure 6).



**Figure 5** CD226L expression on Colo205 cells identified by CD226/Ig immunohistochemistry.

A: Colo205 negative control (stained with hIg); B: Colo205 cells were specifically stained by CD226/Ig.

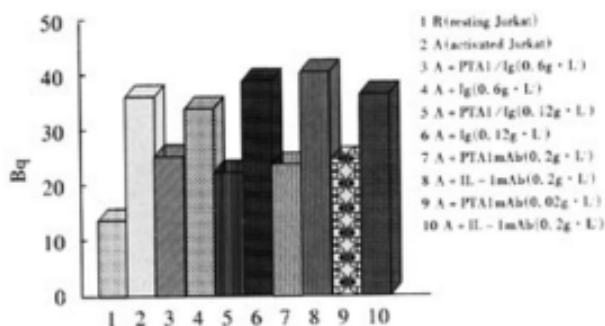


**Figure 6** Adhesion experiments of activated Jurkat cells with Colo205 cells. Density of Colo205 was  $0.5 \times 10^5$  per well. Density of Jurkat was  $1 \times 10^5$  per well. R stand for resting Jurkat cells. A stand for activated Jurkat cells.

### DISCUSSION

CD226 is a 65 ku glycoprotein expressed on the surface of activated T cells, NK cells, and platelets. It is a member of the Ig-superfamily containing 2 Ig-like domains of the V-set and is encoded by a gene on human chromosome 18q22.3<sup>[24]</sup>. Ig-superfamily members play essential roles in many aspects of immune responses by acting as immunoglobulin Fc receptors, cytokine receptors, adhesive molecules and accessory molecules<sup>[11,25-27]</sup>. The main function of Ig-super family concentrated in cell-to-cell recognition and interaction, such as LFA-1/CD2, CD4/MHC, CD28/B7, and many of these Ig-super family members are involved in the T cell activation<sup>[28-32]</sup>. Cross-linking CD226 with antibodies cause the activation of T cells and aggregation of platelets. Previous studies also showed the cross-linking of LFA-1 induced tyrosine phosphorylation of CD226, in which the Fyn protein tyrosine kinase may play a role<sup>[33,34]</sup>. The above results indicate that CD226 mediates cellular adhesion to other cells bearing an unidentified ligand and takes part in signal transduction. Interaction

between ligand and receptor is the basis of immune response. So, identification of CD226L is very important for the further investigation of CD226.

Intercellular adhesive molecules play an important role in the immune response, they provide not only intercellular binding, but also participate in signal transduction, and are closely related with allograft rejection, tolerance, cell differentiation, lymphocyte homing and tumor immunity<sup>[35-39]</sup>. In addition to the specific antigen recognition signal provided by CD3-TCR complex, a lot of other signals are required in the T cells mediated immune response, such as signals provided by CD4/CD8, CD2, LFA-1, CD28<sup>[40-42]</sup>. Our previous results showed that resting T cells expressed low-level of CD226 molecule. When T cells were activated, they expressed high-level CD226 molecules. This finding suggested that CD226 might be closely related to the function of activated T cells. Differentiation of T cell to CTL could be inhibited when Leo-A1 mAb or Leo-A1 F(ab')<sub>2</sub> were added into mixed lymphocyte culture (MLC), and production of LAK cells was also reduced, this action of Loe-A1 was not dependent on Fc of Leo-A1. The inhibiting effect of Loe-A1 only works in the differentiation phase of CTL but not in the cytotoxicity phase, suggesting that the epitope recognized by CD226 is related with the differentiation of CTL<sup>[1,2,7]</sup>. Another mAb DX11 against CD226 (DNAM-1) was reported to significantly inhibit the cytotoxicity of CTL to several tumor cell lines, such as Colo205, PA-1, MCF7<sup>[7]</sup>. Therefore, epitope recognized by DX11 mAb was different from that recognized by Leo-A1 mAb, and these two different epitopes may take part in the differentiation and cytotoxicity of CTL.

Since the mid 1980s, there has been a rapid increase in our knowledge about the specific cell surface molecules mediating cell-cell interaction and adhesion events. This has been largely due to the success of molecular cloning techniques, allowing the isolation of functional cDNA clones that encoding these glycoproteins. Always methods have been successfully used in the cloning of novel cDNA. One of these methods reported by Aruffo and Seed is very effective<sup>[43,44]</sup>. This method is based on the transient expression of cDNA library in cells and specific mAb recognition (capture and panning). Several molecules, such as CD2, CD22, CD28, CD36 and CD58<sup>[43-47]</sup>, have been cloned by this method. So, once a suitable antibody, ligand or cell line has been identified to recognize a cell surface molecule, the cDNA encoding this molecule could be cloned by this method. CD226 molecule or its homologue to be used in the investigation of CD226 ligand should have the following characteristics: easy to obtain, high in purity and natural in motif. So these molecules could be obtained by purification from platelet, preparations of anti-idiotypic mAb or preparations of recombinant CD226 molecule. In this study, we prepared the CD226/Ig fusion protein containing CD226 extracellular region 232aa (including 10 glycosylation sites, 57ku) and IgG Fc region (CH2, CH3 and H region, 26ku), the putative molecule weight is consistent with that identified in SDS-PAGE and Western-blot. CD226/Ig fusion protein is expressed in secreting form that was detected by Sandwich-ELISA, its two different domains could be recognized by anti-CD226 mAb and anti-hIg Fc mAb, respectively, but could not be recognized by other mAb, suggesting CD226/Ig can mimic the nature of CD226 molecule and can be used in the research of CD226 ligand. Ig fusion proteins have many advantages such as easy to purify, easy to label and easy to detect, and thus were widely used in ligand identification<sup>[48-53]</sup>, and disease protection<sup>[54-56]</sup>. These advantages make it more convenient to further clone CD226 ligand.

Immunohistochemical research suggested that CD226 ligand was expressed on Colo205 cells and this result was also supported by adhesion-blocking experiment. It was shown that resting Jurkat cells expressed very low level of CD226 molecules, but activated Jurkat cells expressed high-level CD226 molecules after TPA activation for 24

h, and the expression of CD226 was regulated by cytokines, such as TGF- $\beta$ , TNF- $\alpha$  and IL-2<sup>[57]</sup>. In the experiment about adhesion, activated Jurkat cells could bind to colon carcinoma Colo205 cells and this adhesion reaction could be blocked by CD226/Ig fusion protein or Leo-A1 mAb but not by control Ig and anti-IL-1 mAb, indicating that CD226 ligand exist in Colo205 cells and takes part in this specific adhesion.

When T cells were activated, they expressed high-level CD226 molecules. Interestingly, CD226 ligand seemed to express on the surface of tumor cells. Activated T cells not only need the specific antigen recognition by TCR, but also the engagement of accessory molecules on T cells by their respective ligands expressed on the target cells.<sup>[38,39,58,59]</sup> More researches need to be done to reveal their relationship and what signal have CD226 transduced during immune response against tumors. The above results made a solid foundation for further cloning of CD226 ligand and is helpful for thorough investigations on CD226L structure and function.

**ACKNOWLEDGMENT** Dr. Xu and Dr. Lan for their valuable technical advice and assistance.

## REFERENCES

- Burns GF, Triglia T, Werkmeister JA, Begley CG, Boyd AW. TLISA, a human T lineage-specific activation antigen involved in the differentiation of cytotoxic T lymphocytes and anomalous killer cells from their precursors. *J Exp Med* 1985; 161: 1063-1078
- Scott JL, Dunn SM, Jin B, Hillam AJ, Walton S, Berndt MC, Murray AW, Krissansen GW, Burns GF. Characterization of a novel membrane glycoprotein involved in platelet activation. *J Biol Chem* 1989; 264: 13475-13482
- Zuzel M, Walton S, Burns GF, Berndt MC, Cawley JC. A monoclonal antibody to a 67 kD cell membrane glycoprotein directly induces persistent platelet aggregation independently of granule secretion. *Br J Haematol* 1991;79:466-473
- Sun Chen, Jin Boquan, Liu Xuesong, Yang Kun, Zhang Tingting, Dong Bangquan, Li Jiazeng, Wu huaizhu, Peng Lin, Bao Chengxin, Wu Wenjie. PTA1 monoclonal antibody induce human platelet aggregation and intra-cytoplasmic Ca<sup>2+</sup> elevation. *Zhonghua Xueye Zazhi* 1998;19:133-137
- Li Demin, Jin Boquan, Su Li, Jia Wei, Sun Kai, Liu Xuesong, Zhang Tingting. Distribution and function of murine platelets and T cell activation antigen 1. *Zhonghua Weishengwu Xuehemiao Yixue Zhazhi* 1999;19:232-235
- Sun Kai, Feng Qi, Jin Boquan. Platelet and T cell antigen 1 (PTA1). *Zhonghua Wei Sheng Wu Xue He Mian Yi Xue Zha Zhi* 1999;19:261-264
- Shibuya A, Campbell D, Hannum C, Yssel H, Franz Bacon K, McClanahan T, Kitamura T, Nicholl J, Sutherland GR, Lanier LL, Phillips JH. DNAM-1, A Novel Adhesion Molecule Involved in the Cytolytic Function of T Lymphocytes. *Immunity* 1998; 4: 573-581
- Slupsky JR, Cawley JC, Kaplan C, Zuzel M. Analysis of CD9, CD32 and p67 signalling: use of degranulated platelets indicates direct involvement of CD9 and p67 in integrin activation. *Br J Haematol* 1997;96:275-286
- Chen LK, Bensussan A, Burns GF, Tourvieille B, Soulie A, Sasportes M. Allospecific proliferative human T-cell clones acquire the cytotoxic effector function after three months in culture, in IL-2 conditioned medium. *Hum Immunol* 1986;17:30-36
- Sherrington PD, Scott JL, Jin B, Simmons D, Dorahy DJ, Lloyd J, Brien JH, Aebersold RH, Adamson J, Zuzel M, Burns GF. TLISA (PTA1) activation antigen implicated in T cell differentiation and platelet activation is a member of the regulation of expression. *J Biol Chem* 1997; 272: 21735-21744
- Halaby DM, Mornon JP. The immunoglobulin superfamily: an insight on its tissular, species, and functional diversity. *J Mol Evol* 1998; 46:389-400
- Hawke NA, Yoder JA, Litman GW. Expanding our understanding of immunoglobulin, T-cell antigen receptor, and novel immune-type receptor genes: a subset of the immunoglobulin gene superfamily. *Immunogenetics* 1999;50:124-133
- Ioerger TR, Du C, Linthicum DS. Conservation of cys-cys trp structural triads and their geometry in the protein domains of immunoglobulin superfamily members. *Mol Immunol* 1999;36:373-386
- Tian Fang, Li Demin, Xia Haibin, Liu Xuesong, Jia Wei, Sun Chen, Sun Kai, Jin Boquan. Isolation of cDNAs Encoding Gibbon and Monkey Platelet and T Cell Activation Antigen 1(PTA1). *DNA Sequence* 1999; 10: 155-161
- Huang Chuanshu, Jin Boquan, Wang Meixian, Li Enshan. Study on the activated antigen expression on the lymphocytes and lymphoblasts from HFRS patients. *Shanghai Mian Yi Xue Zha Zhi* 1991;11:94-96
- Su Min, Niu Shumiao, Tian Dongping, Li Jian, Li Hengli, Guo Shangwen, Shi Bingyin. The clinical significance of aberrant HLA-DR antigen expression on thyrocytes. *Zhonghua Bing Li Xue Za Zhi* 1994;23:34-36
- Tabata H, Hara M, Kitani A, Hirose T, Norioka K, Harigai M, Suzuki K, Kawakami M, Kawagoe M, Nakamura H. Hirose-T Expression of TLISA1 on T cells from patients with rheumatoid arthritis and systemic lupus erythematosus. *Clin Immunol Immunopathol* 1989;52:366-375
- Miller FW, Love LA, Barbieri SA, Balow JE, Plotz PH. Lymphocyte activation markers in idiopathic myositis: changes with disease activity and differences among clinical and autoantibody subgroups. *Clin Exp Immunol* 1990; 81:373-379
- Huang Chuanshu, Jin Boquan, Wang Meixian, Li Enshan, Sun Chen. Hemorrhagic fever with renal syndrome: relationship between pathogenesis and cellular immunity. *J Infect Dis* 1994;169:868-870
- Loertscher R, Forbes RD, Halabi G, Lavery P, Quinn T. Expression of early and late activation markers on peripheral blood T lymphocytes does not reliably reflect immune events in transplanted hearts. *Clin Transplant* 1994;8:230-238
- Sun Kai, Jin Boquan, Sun Chen, Tian Fang, Zhu Yong, Yang Kun, Liu Xuesong. Construction and expression of a novel human platelet/T cell activation antigen 1(PTA1) fusion protein in COS-7 cells. *Xi Bao Yu Fen Zi Mian Yi Xue Zha Zhi* 1998;14:1-4
- Lena Serghides, Ian Crandall, Eric Hull, and Kevin C. Kain. The Plasmodium falciparum-CD36 Interaction Is Modified by a Single Amino Acid Substitution in CD36. *Blood* 1998;92:1814-1819
- Sun Kai, Jin Boquan, Sun Chen, Zhu Yong, Jia Wei, Yang Kun, Liu Chenggang. Purification of PTA1/Ig fusion protein by affinity chromatography for PTA1. *Xi Bao Yu Fen Zi Mian Yi Xue Zha Zhi* 1998;14: 113-116
- Callen DF, Baker E, Eyre HJ, Chernos JE, Bell JA, Sutherland GR. Reassessment of two apparent deletions of chromosome 16p to an ins (11;16) and a t(1;16) by chromosome painting. *Ann Genet* 1990;33:219-221
- Hawke NA, Yoder JA, Litman GW. Expanding our understanding of immunoglobulin, T-cell antigen receptor, and novel immune-type receptor genes: a subset of the immunoglobulin gene superfamily. *Immunogenetics* 1999;50:124-133
- Linsley PS, Peach R, Gladstone P, Bajorath J. Extending the B7 (CD80) gene family. *Protein Sci* 1994;3:1341-1343
- Taheri M, Saragovi U, Fuks A, Makkerh J, Mort J, Stanners CP. Self recognition in the Ig superfamily. Identification of precise subdomains in carcinoembryonic antigen required for intercellular adhesion. *J Biol Chem* 2000;275:26935-26943
- Bierer BE, Sleckman BP, Ratnoffsky SE, Burakoff SJ. The biologic roles of CD2, CD4, and CD8 in T-cell activation. *Annu Rev Immunol* 1989; 7:579-599
- Kupfer A, Singer SJ. Cell biology of cytotoxic and helper T cell functions: immunofluorescence microscopic studies of single cells and cell couples. *Annu Rev Immunol* 1989;7:309-337
- Springer TA, Dustin ML, Kishimoto TK, Marlin SD. The lymphocyte function-associated LFA-1, CD2, and LFA-3 molecules: cell adhesion receptors of the immune system. *Annu Rev Immunol* 1987;5:223-252
- Dustin ML, Sanders ME, Shaw S, Springer TA. Purified lymphocyte function-associated antigen 3 binds to CD2 and mediates T lymphocyte adhesion. *J Exp Med* 1987;165:677-692
- Kishimoto TK, O'Connor K, Lee A, Roberts TM, Springer TA. Cloning of the beta subunit of the leukocyte adhesion proteins: homology to an extracellular matrix receptor defines a novel supergene family. *Cell* 1987;48:681-690
- Shibuya K, Lanier LL, Phillips JH, Ochs HD, Shimizu K, Nakayama E, Nakauchi H, Shibuya A. Physical and functional association of LFA-1 with DNAM-1 adhesion molecule. *Immunity* 1999;11:615-623
- Shibuya A, Lanier LL, Phillips JH. Protein kinase C is involved in the regulation of both signaling and adhesion mediated by DNAM-1 receptor. *J Immunol* 1998;161:1671-1676
- Isobe M, Suzuki J, Yamazaki S, Yazaki Y, Horie S, Okubo Y, Maemura K, Yazaki Y, Sekiguchi M. Regulation by differential development of Th1 and Th2 cells in peripheral tolerance to cardiac allograft induced by blocking ICAM-1/LFA-1 adhesion. *Circulation* 1997;96:2247-2253
- Gunji Y, Nakamura M, Hagiwara T, Hayakawa K, Matsushita H,

- Osawa H, Nagayoshi K, Nakauchi H, Yanagisawa M, Miura Y. Expression and function of adhesion molecules on human hematopoietic stem cells: CD34+ LFA-1- cells are more primitive than CD34+ LFA-1+ cells. *Blood* 1992;80:429-436
- 37 Hogg N, Landis RC. Adhesion molecules in cell interactions. *Curr Opin Immunol* 1993;5:383-390
- 38 Springer TA. Adhesion receptors of the immune system. *Nature* 1990;346:425-434
- 39 Phillips JH, McKinney L, Azuma M, Spits H, Lanier LL. A novel beta 4, alpha 6 integrin-associated epithelial cell antigen involved in natural killer cell and antigen-specific cytotoxic T lymphocyte cytotoxicity. *J Exp Med* 1991;174:1571-1581
- 40 Adler B, Ashkar S, Cantor H, Weber GF. Costimulation by extracellular matrix proteins determines the response to TCR ligation. *Cell Immunol* 2001;210:30-40
- 41 Park WR, Park CS, Tomura M, Ahn HJ, Nakahira Y, Iwasaki M, Gao P, Abe R, Hamaoka T, Fujiwara H. CD28 costimulation is required not only to induce IL-12 receptor but also to render janus kinases/STAT4 responsive to IL-12 stimulation in TCR-triggered T cells. *Eur J Immunol* 2001;31:1456-1464
- 42 Clavreul A, Fisson S, D'hellencourt CL, Couez D. Interrelationship between CD3 and CD28 pathways in a murine T cell thymoma. *Mol Immunol* 2000;37:571-577
- 43 Aruffo A, Seed B. Molecular cloning of a CD28 cDNA by a high-efficiency COS cell expression system. *Proc Natl Acad Sci U S A* 1987;84:8573-8577
- 44 Seed B, Aruffo A. Molecular cloning of the CD2 antigen, the T-cell erythrocyte receptor, by a rapid immunoselection procedure. *Proc Natl Acad Sci U S A* 1987;84:3365-3369
- 45 Sewell WA, Brown MH, Dunne J, Owen MJ, Crumpton MJ. Molecular cloning of the human T-lymphocyte surface CD2 (T11) antigen. *Proc Natl Acad Sci U S A* 1986;83:8718-8722
- 46 Wilson GL, Fox CH, Fauci AS, Kehrl JH. cDNA cloning of the B cell membrane protein CD22: a mediator of B-B cell interactions. *J Exp Med* 1991;173:137-146
- 47 Wyler B, Daviet L, Bortkiewicz H, Bordet JC, McGregor JL. Cloning of the cDNA encoding human platelet CD36: comparison to PCR amplified fragments of monocyte, endothelial and HEL cells. *Thromb Haemost* 1993;70:500-505
- 48 Ianelli CJ, Edson CM, Thorley-Lawson DA. A ligand for human CD48 on epithelial cells. *J Immunol* 1997;159:3910-3920
- 49 Koopman G, Keehnen RM, Lindhout E, Zhou DF, de Groot C, Pals ST. Germinal center B cells rescued from apoptosis by CD40 ligation or attachment to follicular dendritic cells, but not by engagement of surface immunoglobulin or adhesion receptors, become resistant to CD95-induced apoptosis. *Eur J Immunol* 1997;27:1-7
- 50 Piepkorn M, Hovingh P, Bennett KL, Aruffo A, Linker A. Chondroitin sulphate composition and structure in alternatively spliced CD44 fusion proteins. *Biochem J* 1997;327:499-506
- 51 Lee JW, Gersuk GM, Kiener PA, Beckham C, Ledbetter JA, Deeg HJ. HLA-DR-triggered inhibition of hemopoiesis involves Fas/Fas ligand interactions and is prevented by c-kit ligand. *J Immunol* 1997;159:3211-3219
- 52 Zollner O, Lenter MC, Blanks JE, Borges E, Steegmaier M, Zerwes HG, Vestweber D. L-selectin from human, but not from mouse neutrophils binds directly to E-selectin. *J Cell Biol* 1997;136:707-716
- 53 Mannori G, Santoro D, Carter L, Corless C, Nelson RM, Bevilacqua MP. Inhibition of colon carcinoma cell lung colony formation by a soluble form of E-selectin. *Am J Pathol* 1997;151:233-243
- 54 Dmitrieva N, Shelton D, Rice AS, McMahon SB. The role of nerve growth factor in a model of visceral inflammation. *Neuroscience* 1997;78:449-459
- 55 Kirk AD, Harlan DM, Armstrong NN, Davis TA, Dong Y, Gray GS, Hong X, Thomas D, Fechner JH Jr, Knechtle SJ. CTLA4-Ig and anti-CD40 ligand prevent renal allograft rejection in primates. *Proc Natl Acad Sci U S A* 1997;94:8789-8794
- 56 Moreland LW, Baumgartner SW, Schiff MH, Tindall EA, Fleischmann RM, Weaver AL, Ettlinger RE, Cohen S, Koopman WJ, Mohler K, Widmer MB, Bloch CM. Treatment of rheumatoid arthritis with a recombinant human tumor necrosis factor receptor (p75)-Fc fusion protein. *N Engl J Med* 1997;337:141-147
- 57 Jin Boquan, Scott JL, Vadas MA, Burns GF. TGF beta down-regulates TLiSA1 expression and inhibits the differentiation of precursor lymphocytes into CTL and LAK cells. *Immunology* 1989;66:570-576
- 58 O'Rourke AM, Mescher MF. Cytotoxic T-lymphocyte activation involves a cascade of signalling and adhesion events. *Nature* 1992;358:253-255
- 59 Rodrigues M, Nussenzweig RS, Romero P, Zavala F. The *in vivo* cytotoxic activity of CD8+ T cell clones correlates with their levels of expression of adhesion molecules. *J Exp Med* 1992;175:895-905

Edited by Ma JY

• BASIC RESEARCH •

# Effect of manganese on heat stress protein synthesis of new-born rats

Ben-Yan Zhang, Sheng Chen, Fang-Li Ye, Chang-Cai Zhu, He-Xi Zhang, Rui-Bo Wang, Cheng-Fen Xiao, Tang-Chun Wu, Guo-Gao Zhang

Ben-Yan Zhang, Fang-Li Ye, Chang-Cai Zhu, Department of Preventive Medicine, College of Medicine, Wuhan University of Science and Technology, Wuhan 430080. Hubei Province, China  
Sheng Chen, Rui-Bo Wang, Cheng-Fen Xiao, Tang-Chun Wu, Guo-Gao Zhang, Department of Labor Hygiene, Wuhan Tongji Medical University, Wuhan 430030, Hubei Province, China  
He-Xi Zhang, Department of Preventive Medicine, Xinxiang Medical College, Xinxiang 453002, Henan Province, China  
Supported by Natural Science Foundation of Metallurgical Industry Ministry. No. (1996) 254-21

Correspondence to: Ben-Yan Zhang, Department of Preventive Medicine, College of Medicine, Wuhan University of Science and Technology, 205 Yejin Road Wuhan 430080. Hubei Province, P.R.China.  
zhangbe7020@sina.com

Telephone: +86-27-86831703 / 86830745

Received 2001-06-02 Accepted 2001-10-26

## Abstract

**AIM:** To study the effect of manganese (Mn) on heat stress protein 70 (HSP70) synthesis in the brain and liver of new-born rats whose mother-rats were exposed to Mn.

**METHODS:** 32 female rats were randomly divided into four groups. One group was administrated with physiological saline only as control group, the other three groups were administrated with 7.5, 15 and 30 mg·kg<sup>-1</sup> manganese chloride (MnCl<sub>2</sub>) by intraperitoneal injection every two days for two weeks. After delivery, the mother-rats received MnCl<sub>2</sub> unceasingly for a week with the same method. Then the contents of Mn, Zn, Cu and Fe in the livers of the new-born rats were determined by atomic absorption spectroscopy; The level of HSP70 in the brains and the livers of the new-born rats as detected by Western-dot-blotting, and the SOD activities were measured simultaneously.

**RESULTS:** The contents of Mn in the livers of new-born rats of the experimental groups (respective 1.38±0.18, 2.73±0.65, 3.44±0.89 μg·g<sup>-1</sup>) were significantly increased compared with the control group (0.88±0.18 μg·g<sup>-1</sup>; *P*<0.01); The contents of Fe in the livers of new-born rats of 15 and 30 mg·kg<sup>-1</sup> experimental groups (426±125, 572±175 μg·g<sup>-1</sup>, respectively) were significantly increased compared with the control group (286±42 μg·g<sup>-1</sup>; *P*<0.05); the levels of Zn in the livers of the new-born rats of three experimental groups (254±49, 263±47, 213±28 μg·g<sup>-1</sup>, respectively) were lower than those of the control group (335±50 μg·g<sup>-1</sup>; respective *P*<0.05, *P*<0.01); and the levels of Cu showed no significant difference among the four groups (three experimental groups: 75±21, 68±241 and 78±18 μg·g<sup>-1</sup>; control group: 83±9 μg·g<sup>-1</sup>; *P*>0.05). There was a significant increase in the levels of HSP70 in the brains of new-born rats of the 30 mg·kg<sup>-1</sup> group (19.5×10<sup>3</sup>±1.3×10<sup>3</sup> A; control group: 14.3×10<sup>3</sup>±1.4×10<sup>3</sup> A; *P*<0.01), and the levels of HSP70 in the livers of new-born rats of three experimental groups (respective 19.6×10<sup>3</sup>±3.9×10<sup>3</sup> A, 18.5×10<sup>3</sup>±3.8×10<sup>3</sup> A, 22.4×10<sup>3</sup>±1.9×10<sup>3</sup> A) also increased

than control group (13.3×10<sup>3</sup>±1.0×10<sup>3</sup> A; *P*<0.01), but the SOD activities showed no significant difference among brains of the four groups (experimental groups: 5.04±0.43, 4.83±0.48, 4.60±0.84 ku·g<sup>-1</sup>; control group: 4.91±0.37 ku·g<sup>-1</sup>; *P*>0.05). The SOD activities in the livers of 15 mg·kg<sup>-1</sup> group (5.41±0.44 ku·g<sup>-1</sup>) was lower than the control group (5.95±0.36 ku·g<sup>-1</sup>; *P*<0.05).

**CONCLUSION:** While mother-rats were exposed to manganese, the metabolisms of Mn, Zn and Fe of new-born rats in the livers were influenced and were situated in a stress status, thus HSP70 syntheses is induced in the brains and livers of new-born rats, but the mechanism of this effect in the developmental toxicity of Mn remains to be further studied.

Zhang BY, Chen S, Ye FL, Zhu CC, Zhang HX, Wang RB, Xiao CF, Wu TC, Zhang GG. Effect of manganese on heat stress protein synthesis of new-born rats. *World J Gastroenterol* 2002;8(1):114-118

## INTRODUCTION

Manganese (Mn) has bi-directional effect on the mammal<sup>[1-3]</sup>, both deficient and excess intake of Mn result in altered enzymatic reactions and brain function because of its essential element nutrition<sup>[4]</sup> and neurotoxic effect. With exposure to higher concentrations is harmful to health<sup>[5,6]</sup>. Excessive manganese has been associated with neurobehavioral deficits and neurological and/or neuropsychiatric illness<sup>[7]</sup>. As a nervous toxicant, Mn damages central nervous system, and has procreant toxicity. Mn also could transplacenta to embryo and affects growth of offspring<sup>[8,9]</sup>. Thus, excessive manganese also is an embryotoxicant and fetotoxicant in mammals<sup>[10]</sup>, but the mechanism of this effect has not been elucidated yet. It is well known that heat stress / shock proteins (Hsps) are induced by a series of occupational factors and their main biological action is to participate in thermotolerance and toxicant tolerance. Hsps participate in protein synthesis, folding, assemblage and intracellular protein transport as the molecular chaperones<sup>[11,12]</sup>. It has not been reported whether these functions are relative with toxicity of Mn. The HSP70 levels and the SOD activities of the brains and livers and the trace-element contents of the livers were measured in the new-born rats after their mother-rats were exposed to the manganese.

## MATERIALS AND METHODS

### Animal Treatment

Thirty-two healthy Wistar female rats that weigh 200~240g (obtained from center of experimental animal of Tongji Medical University) were randomly divided into four groups. Except one group as control, the other three groups were treated with Manganese chloride tetrahydrate (MnCl<sub>2</sub>·H<sub>2</sub>O<sub>2</sub>). By mean of single intraperitoneal injection administration every two days for two weeks, the doses were 7.5, 15 and 30 mg·kg<sup>-1</sup> respectively. The control group was similarly injected physiological saline. Then the rats (1 ♂ : 1 ♀) were housed together. The next morning gestation was defined as d 0 when sperms were founded in the vaginal smear. After



pregnancy, the mother-rats were treated with  $\text{MnCl}_2$  at the same concentration of before, then harvested at time points up to a week with the same method as before. These female rats received  $\text{MnCl}_2$  11 times. The newborn rats were killed by cervical dislocation in 24 h. The brain and liver of the newborn rats was reserved in  $-20^\circ\text{C}$  immediately.

### Determination of trace elements

The reserved livers were put into roaster for 2 h at  $105^\circ\text{C}$  and reserved into desicator. Drying sample accurately Weighed up 0.0500~0.1000g was put into conical flask and added 2 mL nitric acid (G.R), 0.5 mL perchloric acid (G.R) and digested to dry approximately. After cooling, the digestive sample was dissolved with redistilled water that was distilled for 4 times, the sample was put into 10 mL test tube and fixed volume to 5 mL. Trace elements were measured with atomic absorption spectroscopy (Spectr AA-40 atomic absorption apparatus, VARIAN corp., USA). Mn was measured with graphite stove atomic absorption spectroscopy analysis, and adopted flame atomic absorption spectroscopy to mensurate Cu, Zn and Fe.

### Brains and livers homogenate

Prepared homogenates of the brains and livers were done as described by routine technique. Mensurated contents of the protein of the brains and livers as Lowry.

### Detection of SOD activities

Taking equal quality proteins of the brains and livers to determine SOD activities in the brains and livers with SOD kits supplied by Nanjing Jiancheng Bioengineering Graduate Institute.

### Determination of HSP70

Equal amount proteins of the brains and livers was taken to determine the HSP70 levels in the brains and livers with Western-dot-blotting<sup>[13]</sup>. After Western blotting, HSP70 was detected using anti-HSP70 rabbit polyclonal antibodies (provided by Lab of Cell & Developmental Genetics, University Laval, Canada) and anti-rabbit

horseradish peroxidase-conjugated secondary antibodies (Sigma), and visualized using 3-3'-diaminobenzidine (DAB). The results were quantified by a densitometry (CS-930, Japan).

### Statistic analysis

The results were analyzed with SAS programs in IBM-PC.

## RESULTS

### Effect of Mn on female rat Reproduction

After female rats exposed to Mn, their gestation periods had no significant difference from the control group ( $P>0.05$ ). The parturition indexes seem to reduce along with manganic dosage increment, but the difference is not significant compared with control group ( $P>0.05$ ) yet. Average of fetiferous quality of puerperal female rats seem to reduce in 7.5 and  $15\text{mg}\cdot\text{kg}^{-1}$  groups, but the differences are not significant compared with control group ( $P>0.05$ ) yet. However,  $30\text{mg}\cdot\text{kg}^{-1}$  group significantly reduced compared with control group ( $P<0.01$ ). Average of fetiferous quality of pregnant female rats in 15 and  $30\text{mg}\cdot\text{kg}^{-1}$  groups significantly reduced compared with the control group ( $P<0.05$ ,  $P<0.01$ ). The viability index of 1-day-old filial rats in  $30\text{mg}\cdot\text{kg}^{-1}$  group significantly reduced compared with the control group ( $P<0.01$ ). The newborn rats' weight and height showed no significant difference among four groups ( $P>0.05$ , Table 1).

### Effect of Mn on traceelements in newborn rats

The manganese contents of the new-born rats' livers in three experimental groups significantly increased compared with control group ( $P<0.01$ ), and there was a dose-dependent increase in these groups. The levels of zinc in the new-born rats' livers in three experimental groups were lower than those of control group too ( $P<0.05$ ,  $P<0.01$ , respectively). The iron contents of the new-born rats' livers in 15 and  $30\text{mg}\cdot\text{kg}^{-1}$  experimental groups were higher than control group ( $P<0.05$ ,  $P<0.01$ , respectively), but the copper levels of the newborn rats' livers showed no significant difference among four rroups ( $P>0.05$ , Table 2).

**Table 1** Effect of Mn on reproduction in female rats

| Mn<br>( $\text{mg}\cdot\text{kg}^{-1}$ ) | Gestation<br>(d) | Puerpera<br>female<br>rats<br>(n) | Paturition<br>index<br>(%) | Tatol<br>Filial<br>rats<br>(n) | puerperal<br>female rats<br>Fetiferous<br>quality<br>(n) | pregnant<br>female rats<br>fetiferous<br>quality<br>(n) | Livabilit<br>of d 1<br>filial rats<br>(%) | Newborn<br>rats' mass<br>(g) | Newborn<br>rats' height<br>(cm) |
|------------------------------------------|------------------|-----------------------------------|----------------------------|--------------------------------|----------------------------------------------------------|---------------------------------------------------------|-------------------------------------------|------------------------------|---------------------------------|
|                                          |                  |                                   |                            |                                |                                                          |                                                         |                                           |                              |                                 |
| control                                  | 21.3±0.8         | 7                                 | 87.5                       | 68                             | 9.7±2.1                                                  | 8.5±3.9*                                                | 98.5                                      | 5.89±0.49                    | 5.2±0.25                        |
| 7.5                                      | 21.8±1.2         | 6                                 | 75.0                       | 41                             | 6.8±3.1                                                  | 5.1±4.1                                                 | 95.1                                      | 5.47±0.54                    | 5.1±0.36                        |
| 15                                       | 22.2±0.8         | 5                                 | 62.5                       | 33                             | 6.6±2.7                                                  | 4.1±3.9*                                                | 87.9                                      | 5.38±0.53                    | 4.98±0.35                       |
| 30                                       | 22.7±1.5         | 3                                 | 37.5                       | 15                             | 5.0±2.6*                                                 | 1.8±2.9*                                                | 73.3*                                     | 5.13±0.51                    | 4.87±0.38                       |

\* $P<0.05$ ,  $P<0.01$ , vs control.

### Effect of Mn on SOD activities in newborn rats

Although the SOD activities of the newborn rat' brains seem to reduce in 15,  $30\text{mg}\cdot\text{kg}^{-1}$  groups and increase in  $7.5\text{mg}\cdot\text{kg}^{-1}$  group, but no significant difference showed among all the four groups ( $P>0.05$ ). The

SOD activities of the newborn rat' livers were lower in  $15\text{mg}\cdot\text{kg}^{-1}$  group than control group ( $P<0.05$ ), but showed no significant difference among 7.5,  $30\text{mg}\cdot\text{kg}^{-1}$  and control groups ( $P>0.05$ , Table 3).

**Table 2** Effect of Mn on traceelements in newborn rats' livers ( $\bar{x}\pm s$ ,  $\mu\text{g}\cdot\text{g}^{-1}$ )

| Mn ( $\text{mg}\cdot\text{kg}^{-1}$ ) | Filialrats (n) | Mn         | Cu    | Zn      | Fe       |
|---------------------------------------|----------------|------------|-------|---------|----------|
| control                               | 5              | 0.88±0.18  | 83±9  | 335±50  | 286±42   |
| 7.5                                   | 5              | 1.38±0.18* | 75±21 | 254±50* | 271±88   |
| 15                                    | 7              | 2.73±0.65* | 68±24 | 263±47* | 426±125* |
| 30                                    | 5              | 3.44±0.89* | 78±18 | 213±28* | 572±175* |

\* $P<0.05$ ,  $P<0.01$ , vs control.

**Table 3** Effect of Mn on SOD and HSP70 in brains and livers ( $\bar{x} \pm s$ )

| Mn (mg·kg <sup>-1</sup> ) | Filial Rats (n) | Brain                    |                          | Liver                    |                          |
|---------------------------|-----------------|--------------------------|--------------------------|--------------------------|--------------------------|
|                           |                 | SOD / ku·g <sup>-1</sup> | HSP70/×10 <sup>3</sup> A | SOD / ku·g <sup>-1</sup> | HSP70/×10 <sup>3</sup> A |
| control                   | 8               | 4.91±0.37                | 14.3±1.4                 | 5.95±0.36                | 13.4± 1.0                |
| 7.5                       | 9               | 5.04±0.43                | 16.0±1.8                 | 5.96±0.41                | 19.6±3.9 <sup>b</sup>    |
| 15                        | 7               | 4.83±0.48                | 14.4±1.4                 | 5.41±0.44 <sup>a</sup>   | 18.5±3.8 <sup>b</sup>    |
| 30                        | 6               | 4.60±0.84                | 19.5±1.3 <sup>b</sup>    | 5.87±0.68                | 22.4±1.9 <sup>b</sup>    |

<sup>a</sup>P<0.05, <sup>b</sup>P<0.01, vs control**Effect of Mn on HSP70 synthesis in newborn rats**

The level of HSP70 in the brain showed no significant difference among 7.5, 15mg·kg<sup>-1</sup> and control groups ( $P>0.05$ ), but showed significantly increased between 30mg·kg<sup>-1</sup> and control groups ( $P<0.01$ ). The level of HSP70 in the livers significantly increased in three experimental groups to be compared with control group ( $P<0.01$ , Table 3).

**DISCUSSION**

The fetiferous quality reduces after female rats are imbued with Mn; parturition index also tended to reduce along with the manganese dosage increase, and livability of d 1 old filial rats significantly reduced along with the manganese dosage increase. The fact illustrates that manganese influences female rats' reproductive function. Manganese could transplacenta to enter filial central nervous system<sup>[15]</sup>. Yang BN reported that the new-born rats' manganese contents of the brain were significantly higher than those of control group with inductance coupling plasmic emanant spectroscopy after mother-rats exposed to by manganese<sup>[16]</sup>. This study determined that the new-born rats' manganese contents of the livers are significantly higher than control group with atomic absorption spectroscopy after mother-rats exposed to manganese, and have a dose-effect relationship. The results show that the manganese could be transferred to the embryo by placental barrier and accumulate in filial rat's brains and livers after mother-rats to be exposed by manganese in gestation. It has not been reported that the effect of Mn on other microelements in the newborn rats' liver of intoxicated mother-rats. This study also detected that the levels of Zn in the new-born rats' livers of three experimental groups were lower than those of control group, and the iron contents in the new-born rats' livers of and 30mg·kg<sup>-1</sup> treated groups were higher than the control group, but the copper levels showed no significant difference among four groups. It was obvious that the zinc and iron metabolism were disturbed in the livers of new-born rats after mother-rats exposed to manganese. Zn is an essential microelement and has much to do with many enzymatic bioactivities. Zn is very important to maintain normal body growth and reproductive function. While the body zinc deficiency, the hormone syntheses reduce and their activities decrease, which, therefore, result in serious obstruction of the growth, children's testicles agenesis, reducing spermic quantity, weakening spermic activity, agenesis of the immune apparatus in the thymus gland etc and immune estate. While serum zinc contents descend, it is degressive that the levels of neuropeptide somatostatin and arginine-vasopressin have much to do with capability of the learning and memory in rats' hippocampi, and make the rats' capability of learning and memory clearly decline<sup>[17]</sup>. When filial rats lack the zinc during the lactation and weaning stage, the brain weight, the hippocampal weight, the serum and hippocampal zinc concentrations are significantly lowered, and proportion of induced long-term potentiation (LTP) is zero and proportion of active avoidance response decreased profoundly<sup>[18]</sup>. Cognition is a field of thought processes by which an individual processes information through skills of perception, thinking, memory, learning and attention. Zinc deficiency may affect cognitive development by alterations in attention, activity, neuropsychological behavior and motor development. The exact mechanisms are not clear but it appears that zinc is essential for neurogenesis, neuronal migration, synaptogenesis<sup>[19]</sup>. Excessive manganese arising zinc deficiency could interfere with

neurotransmission and subsequent neuropsychological behavior.

This study determined zinc decrease in newborn rats' livers after mother-rats were administrated by manganese, it tallies with the phenomenon that as we observed, filial rats' neurobehavior functions deferred and the capability of learning and memory weakened<sup>[20]</sup>. The result enlightens that the effect of Mn on filial rats' developmental toxicity might be responsible for the manganese which leads to the zinc deficiency in the brain and liver. A new pathway is suggested in the manganese mechanism research on filial rats' neurotoxicity. Fe is also an essential microelement and has important physiologic function. The study also discovered that newborn rats' irons to heighten in the livers after mother-rats were imbued by manganese. The most actions are antagonistic between Fe and Zn. It is uncertain that whether the manganese cumulated in the liver to arise the zinc decreases and results in heightening Fe antagonistically. So, the reason needs further study.

Mn has an especial affinity with the mitochondrial and can largely cumulate in the cells that contain plentiful mitochondrial, so the manganese content is highest in the liver and the content is higher in the spleen, the kidney and brain<sup>[21]</sup>. The manganese mainly damages extrapyramidal system on central nervous system, which is related to specifically organization and the neurons distribution in the substantia nigra and corpus striatum. Many melanin neurons and aminergic neurons are distributed in the dense area of substantia nigra. They have a speciality that collect and cumulate the amine and metal elements, such as manganese etc. Superfluous manganese on one hand activate the cytochrome oxidase P-450 to engender the free radicals to deplete the sulthydyls and impair cellular resistivity, Mn on the other hand can also produce plentiful free radicals to damage mitochondrial, and to disturb energy metabolism, then mediate the toxicity of excitability amino acids and result in increasing intracellular calcium, activating the calcium-dependent protease, nuclease, phosphatase and promoting the cellular recessive denaturalization. The increase of calcium ions again, promotes the production of free radicals as result, forms a vicious circle. Therefore, cumulative manganese may destroy the protective barrier of the melanin neurons and constantly releases to beget continual toxicity in the extrapyramidal system). The free radicals play very important role in manganese neurotoxicity. SOD is a important enzyme among enzymes system that eliminates free radicals. The manganese is able to inhibit SOD by forming free radicals. In our study only the SOD activities of livers in 15mg·kg<sup>-1</sup> group were lower than the control group. Although it inclined depression that the SOD activities of the livers in 7.5 and 30mg·kg<sup>-1</sup> groups and of the brains in the three experimental groups, the differences were not significant to be compared with control group. This causation may be that SOD have a insensitivity on free radicals by the manganese toxicity, also may have other cause to be elucidated. The body was situated in a toxicant stress status and oxidative stress after the manganese was accumulated in the filial rat's brain and liver<sup>[22]</sup>. When body was situated in a toxicant stress / oxidative stress status, heat stress protein is markedly elevated *in vivo* on response of toxicant stress / oxidative stress.<sup>[23-26]</sup> The stress response is a common physiological response from the prokaryotes to the human. It is the character of various stress responses that Hsps syntheses appear as increase or grow out of nothing in the cells. Hsps are a kind proteins that have protective function as quite conservation in the evolution. Hsps could respond stress responses by some injurious environmental factors, such as Pb<sup>[27]</sup>, Cd<sup>[28]</sup>, Hg<sup>[29]</sup>, As<sup>[30,31]</sup>, benzene<sup>[32,33]</sup>, CO<sup>[34]</sup>, ischemia<sup>[35]</sup>, psychological tension<sup>[36]</sup> etc. Hsps have been proposed as

general markers of cellular aggression and their use for environmental monitoring is often suggested<sup>[37]</sup>. Hsps endow with resumptive capability of the cells or biology from various stress responses and protect them to keep from the damages of these factors<sup>[38-46]</sup>. The primary signification of Hsps is to keep protect the cells from suffering from ill conditions of high temperature, low oxygen, heavy metal and illness etc<sup>[47-54]</sup>. Therefore it is obvious that thermotolerance was formed, in other words, after the cells or organisms were exposed to subthermal death point, the livability significantly increases on the thermal death point. HSP70 exerts main action in the form of stress tolerance. HSP70 has important protective function in intracellular hereditary substance DNA, the process of biologic growth, development, differentiation and regulation<sup>[55-57]</sup>. HSP70 connects with many internal bioactive substances and take part in many biochemical processes. It is principal that HSP70 promote protein synthesis, folding, assemblage, transportation and take part in the elimination of metamorphic proteins as molecular chaperones under non-stress conditions<sup>[58-62]</sup>. These important functions may have to do with the function of the thermotolerance and poison tolerance. When cells experience thermal or toxicant stress, Hsps take on a new role, conserved from poison to humans, of protecting cells from the detrimental effects of stress. This role takes on added significance for the embryo in which the developmental program must be read linearly, with little opportunity to cycle backward to complete a missed segment of the program. Thereby Hsps will afford protection to the human embryo/fetus exposed to thermal/toxicant stress<sup>[63-65]</sup>.

This study showed that some HSP70 were synthesized in normal newborn rats' brains and livers. The HSP70 contents of the newborn rats' brains in Low and medium dosage groups had a few increase, but the differences were not significant compared with control group. The HSP70 contents in the newborn rats' brains of high manganese dosage group significantly increased. The HSP70 contents all significantly increased in the newborn rats' livers of three experimental groups to be compared with control group. These results indicated that HSP70 had a certain degree role in normal growth and the manganese had effect on HSP70 syntheses in the newborn rats' brains and livers. However the HSP70 syntheses were low in very few newborn rats' brains and livers of experimental groups too. It remains to be elucidated that HSP70 synthesis is related to manganese toxicity in the pathology, clinic, susceptibility of manganese poisoning and other biochemical variety.

Through contrast affected degree of HSP70 syntheses in newborn rats' brain and livers, induction of HSP70 is sensitive in the liver than in the brain. The reason may have to do with manganese accumulation that is higher in the liver than in the brain in the newborn rats. Recently some researcher explore HSP70 to relate to the fetation from the point of the development and had acquired many interesting results. They considered stress response to have diploid effects. On the one hand protect embryonic growth, on the other hand disturb as well as embryonic growth. Final procreant consequence mainly depend on the intensity and duration in the stress response whether to exceed self regulative level in intracellular HSP70 synthesis and also relate to injured period in fetation. Many results all had proved that HSP70 could influence embryonic growth *in vivo* and *in vitro*. HSP70 maybe is a biomaker as screening developmental toxicant<sup>[66]</sup>, and excessive manganese may be considered a developmental toxicant.. Moreover, the stress status also leads to disorder of digestive system, for instance, gastrointestinal motility disorders<sup>[67,68]</sup>, vasoactive intestinal peptide (VIP), neuropeptide Y (NPY) of colonic mucosa was increased<sup>[69]</sup>, platelet derived growth factor (PDGF)<sup>[70]</sup>, and tissue inhibitor of metalloproteinase 1 (TIMP-1) are increased<sup>[71]</sup>, and heme oxygenase-1 (HO-1) mRNA and protein were highly induced and HO enzyme activity was higher after hemorrhagic shock and resuscitation (HR)<sup>[72]</sup>. Besides accelerates HSP70 synthesis *in vivo*, The manganese could induce the nitric oxide synthase (NOS) yet. The NOS begets increasing the synthesis of nitric oxide (NO). Superfluous NO could mediate neurotoxicity of excitative amino acid as a cytotoxicity molecule and could damage central nervous system in budding filial generation<sup>[73]</sup><sup>[28]</sup>, whereas, HSP70 could diminish the liver damage

by NO. Re-induction of HSP70 expression by stress effect re-established resistance to NO toxicity<sup>[74]</sup>.

Our study demonstrates that the excessive manganese cumulated largely filial rat's brain and liver by way of placenta after mother-rats exposed to manganese, and disturbed the microelement metabolisms of the l manganese, zinc and iron *in vivo* and injured the growth on the offspring. On the other hand the body was situated in a stress status and the embryo and filial generation growth were damaged by the inducement of HSP70 synthesis in the brain and liver. The mechanism of this effect in the developmental toxicity of Mn remains to be further researched.

## REFERENCES

- Greger JL. Nutrition versus toxicology of manganese in humans: evaluation of potential biomarkers. *Neurotoxicology* 1999;20:205-212
- Greger JL. Dietary standards for manganese: overlap between nutritional and toxicological studies. *J Nutr* 1998;128(2 Suppl):368-371
- Kafritsa Y, Fell J, Long S, Bynevelt M, Taylor W, Milla P. Long-term outcome of brain manganese deposition in patients on home parenteral nutrition. *Arch Dis Child* 1998;79:263-265
- Amemiya T. The eye and nutrition. *Jpn J Ophthalmol* 2000;44:320-329
- Chua AC, Morgan EH. Effects of iron deficiency and iron overload on manganese uptake and deposition in the brain and other organs of the rat. *Biol Trace Elem Res* 1996;55:39-54
- Verity MA. Manganese neurotoxicity: a mechanistic hypothesis. *Neurotoxicology* 1999;20:489-497
- Mergler D, Baldwin M, Belanger S, Larribe F, Beuter A, Bowler R, Panisset M, Edwards R, de Geoffroy A, Sassine MP, Hudnell K. Manganese neurotoxicity, a continuum of dysfunction: results from a community based study. *Neurotoxicology* 1999;20:327-342
- Zhang D, He X, Zhang W, Tan J. Effect of manganese on the growth and development of rat offspring. *Wei Sheng Yan Jiu* 1998;27:237-240
- Spencer A. Whole blood manganese levels in pregnancy and the neonate. *Nutrition* 1999; 15:731-734
- Olomina MT, Domingo JL, Llobet JM, Corbella J. Effect of day of exposure on the developmental toxicity of manganese in mice. *Vet Hum Toxicol* 1996;38:7-9
- Zhang GG, He HZ, Wu TC. Heat Stress Proteins and It Expectation of Application Study in Occupational Medicine. *Zhonghua Laodong Weisheng Zhiyebing Zazhi* 1998; 17: 67-71
- Wu TC, Yuan Y, Bi YY, He HZ, Zhang GG. Plasma free amino acid in workers working under different stress conditions. *J Occupa Health* 1998; 40: 203-206
- He XS, Pan QP, Wu TC, Yuan Y, Tang PT, He HZ. Determine Chief Heat Stress Proteins with Western Blot Doting. *Zhonghua Laodong Weisheng Zhiyebing Zazhi* 1996; 13: 376-378
- Krachler M, Rossipal E, Micetic-Turk D. Trace element transfer from the mother to the newborn—investigations on triplets of colostrum, maternal and umbilical cord sera. *Eur J Clin Nutr* 1999;53:486-494
- Brenneman KA, Cattley RC, Ali SF, Dorman DC. Manganese-induced developmental neurotoxicity in the CD rat: is oxidative damage a mechanism of action. *Neurotoxicology* 1999;20:477-487
- Yang BL, Zang DX, Tan JF, Ke MH, Wu xj, Song SH, Xet. Effect of Mn on manganese, zinc, copper and iron of filial rats' brains during pregnancy of maternal rats. *Weisheng Dulixue Zazhi* 1997; 11: 101-103
- Li JS, Xu PX, Ren HM, Hu HT, Ling FD. changes of the somatostatin and arginine vasopressin contents of the rat hippocampus in zinc deficiency. *Acta Nutrimeta Sinica* 1998; 21: 21-24
- Kong X, Ren R, Liu L. Effects of zinc deficiency in fodder on brain development, learning and memory in rats. *Zhonghua Yu Fang Yi Xue Za Zhi* 1997;31:295-298
- Bhatnagar S, Taneja S. Zinc and cognitive development. *Br J Nutr* 2001;85(Suppl 2):139-145
- Zhang BY, Zhu ZC, Ye FL, Xiao BS, Xu T. Effect of manganese on neurobehavioral function of offsprings of intoxicated rat. *Zhongguo zhiye Yixue* 1999;26:5-7
- He FS. Manganese and manganic compounds. In: He FS. Chinese occupational medicine. Beijing: *People's Medical Publishing House*. 1999; 241-247
- Jauniaux E, Watson AL, Hempstock J, Bao YP, Skepper JN, Burton GJ. Onset of maternal arterial blood flow and placental oxidative stress. A possible factor in human early pregnancy failure. *Am J Pathol* 2000;157:2111-2122
- Lin KC, Krieg RJ Jr, Saborio P, Chan JC. Increased heat shock protein-70 in unilateral ureteral obstruction in rats. *Mol Genet Metab* 1998;65:303-310
- Wong HR, Menendez IY, Ryan MA, Denenberg AG, Wispe JR. Increased expression of heat shock protein-70 protects A549 cells against hyperoxia. *Am J Physiol* 1998;275(4 Pt 1):L836-841

- 25 Sugaya K, Chou S, Xu SJ, McKinney M. Indicators of glial activation and brain oxidative stress after intraventricular infusion of endotoxin. *Brain Res Mol Brain Res* 1998;58:1-9
- 26 Singh AK, Lakhota SC. Tissue-specific variations in the induction of Hsp70 and Hsp64 by heat shock in insects. *Cell Stress Chaperones* 2000; 5:90-97
- 27 Ait-Aissa S, Porcher J, Arrigo A, Lambre C. Activation of the hsp70 promoter by environmental inorganic and organic chemicals: relationships with cytotoxicity and lipophilicity. *Toxicology* 2000;145:147-157
- 28 Damelin LH, Vokes S, Whitcutt JM, Damelin SB, Alexander JJ. Hormesis: a stress response in cells exposed to low levels of heavy metals. *Hum Exp Toxicol* 2000;19:420-430
- 29 Goering PL, Fisher BR, Noren BT, Papaconstantinou A, Rojko JL, Marler RJ. Mercury induces regional and cell-specific stress protein expression in rat kidney. *Toxicol Sci* 2000;53:447-457
- 30 Sok J, Calton M, Lu J, Lichtlen P, Clark SC, Ron D. Arsenite-inducible RNA -associated (AIRAP) protects cells from arsenite toxicity. *Cell Stress Chaperones* 2001; 6:6-15
- 31 Ibrahim EC, Morange M, Dausset J, Carosella ED, Paul P. Heat shock and arsenite induce expression of the nonclassical class I histocompatibility HLA-G gene in tumor cell lines. *Cell Stress Chaperones* 2000;5:207-218
- 32 Vojdani A, Lapp CW. Interferon-induced proteins are elevated in blood samples of patients with chemically or virally induced chronic fatigue syndrome. *Immunopharmacol Immunotoxicol* 1999;21:175-202
- 33 Wu TC, Yuan Y, Wu Y, He HZ, Zhang GG, Tanguay RM. Presence of antibodies to heat stress proteins and its potential significance in workers exposed to benzene and patients with benzene-poisoning. *Cell Stress Chaperones* 1998;3:161-167
- 34 Wu TC, Tanguay RM, Wu Y, He HZ, Xu DG, Feng JD, Shi WX, Zhang GG. Presence of antibodies to heat stress proteins and its possible significance in workers exposed to high temperature and carbon monoxide. *Biomedical and Environmental Science* 1996;9:370-379
- 35 Kumar Y, Tatu U. Induced hsp70 is in small, cytoplasmic complexes in a cell culture model of renal ischemia: a comparative study with heat shock. *Cell Stress Chaperones* 2000;5:314-327
- 36 Wu TC, Xiong YL, Chen S, Leng ST, Hai T, Tanguay RM. Biochemical changes of plasma in paratroops after parachuting: a preliminary investigation. *Space medicine & medical engineering* 1999; 12:235-239
- 37 Mun HS, Aosai F, Norose K, Chen M, Hata H, Tagawa YI, Iwakura Y, Byun DS, Yano A. Toxoplasma gondii Hsp70 as a danger signal in toxoplasma gondii-infected mice. *Cell Stress Chaperones* 2000;5:328-335
- 38 Wagner M, Hermanns I, Bittinger F, Kirkpatrick CJ. Induction of stress proteins in human endothelial cells by heavy metal ions and heat shock. *Am J Physiol* 1999;277(5 Pt 1):L1026-1033
- 39 Weber H, Wagner AC, Jonas L, Merkord J, Hofken T, Nizze H, Leitzmann P, Goke B, Schuff-Werner P. Heat shock response is associated with protection against acute interstitial pancreatitis in rats. *Dig Dis Sci* 2000;45:2252-2264
- 40 Matranga V, Toia G, Bonaventura R, Muller WE. Cellular and biochemical responses to environmental and experimentally induced stress in sea urchin coelomocytes. *Cell Stress Chaperones* 2000;5:113-120
- 41 Hamel L, Kenney M, Jayyosi Z, Ardati A, Clark K, Spada A, Zilberstein A, Perrone M, Kaplow J, Merkel L, Rojas C. Induction of heat shock protein 70 by herbimycin A and cyclopentenone prostaglandins in smooth muscle cells. *Cell Stress Chaperones* 2000;5:121-131
- 42 Volloch V, Gabai VL, Rits S, Force T, Sherman MY. HSP72 can protect cells from heat-induced apoptosis by accelerating the inactivation of stress kinase JNK. *Cell Stress Chaperones* 2000;5:139-147
- 43 Locke M, Atance J. The myocardial heat shock response following sodium salicylate treatment. *Cell Stress Chaperones* 2000;5:359-368
- 44 He H, Chen C, Xie Y, Asea A, Calderwood SK. HSP70 and heat shock factor 1 cooperate to repress Ras-induced transcriptional activation of the c-fos gene. *Cell Stress Chaperones* 2000;5:406-411
- 45 Hightower LE, Brown, Renfro JL, Perdrizet GA, Rewinski M, Guidon PT Jr, Mistry T, House SD. Tissue-level cytoprotection. *Cell Stress Chaperones* 2000;5:412-414
- 46 Basu S, Srivastava PK. Heat shock proteins: the fountainhead of innate and adaptive immune responses. *Cell Stress Chaperones* 2000;5:443-451
- 47 Multhoff G, Mizzen L, Winchester CC, Milner CM, Wenk S, Eissner G, Kampinga HH, Laumbacher B, Johnson J. Heat shock protein 70 (Hsp70) stimulates proliferation and cytolytic activity of natural killer cells. *Exp Hematol* 1999;27:1627-1636
- 48 Hantschel M, Pfister K, Jordan A, Scholz R, Andreesen R, Schmitz G, Schmetzer H, Hiddemann W, Multhoff G. Hsp70 plasma membrane expression on primary tumor biopsy material and bone marrow of leukemic patients. *Cell Stress Chaperones* 2000;5:438-442
- 49 van Eden W, Wendling U, Paul L, Prakken B, van Kooten P, van der Zee R. Arthritis protective regulatory potential of self-heat shock protein cross-reactive T cells. *Cell Stress Chaperones* 2000;5:452-457
- 50 Ostberg JR, Patel R, Repasky EA. Regulation of immune activity by mild (fever-range) whole body hyperthermia: effects on epidermal Langerhans cells. *Cell Stress Chaperones* 2000;5:458-461
- 51 Hasday JD, Singh IS. Fever and the heat shock response: distinct, partially overlapping processes. *Cell Stress Chaperones* 2000;5:471-480
- 52 Samali A, Robertson JD, Peterson E, Manero F, van Zeijl L, Paul C, Cotgreave IA, Arrigo AP, Orrenius S. Hsp27 protects mitochondria of thermotolerant cells against apoptotic stimuli. *Cell Stress Chaperones* 2001;6:49-58
- 53 Ip SP, Che CT, Kong YC, Ko KM. Effects of schisandrin B pretreatment on tumor necrosis factor-alpha induced apoptosis and Hsp70 expression in mouse liver. *Cell Stress Chaperones* 2001;6:44-48
- 54 Wu TC, Chen S, Xiao CF, Wang CL, Pan Q, Wang ZZ, Xie MX, Mao ZC, Wu Y, Tanguay RM. Presence of antibody against the inducible Hsp71 in patients with acute heat-induced illness. *Cell Stress Chaperones* 2001;6:113-120
- 55 Kozawa O, Matsuno H, Niwa M, Hatakeyama D, Kato K, Uematsu T. AlphaB-crystallin, a low-molecular-weight heat shock protein, acts as a regulator of platelet function. *Cell Stress Chaperones* 2001;6:21-28
- 56 Loones MT, Chang Y, Morange M. The distribution of heat shock proteins in the nervous system of the unstressed mouse embryo suggests a role in neuronal and non-neuronal differentiation. *Cell Stress Chaperones* 2000;5:291-305
- 57 Constitutive expression of heat shock proteins Hsp90, Hsc70, Hsp70 and Hsp60 in neural and non-neural tissues of the rat during postnatal development. *Cell Stress Chaperones* 1998;3:188-199
- 58 Kimmins S, MacRae TH. Maturation of steroid receptors: an example of functional cooperation among molecular chaperones and their associated proteins. *Cell Stress Chaperones* 2000;5:76-86
- 59 Fernando P, Heikkila JJ. Functional characterization of Xenopus small heat shock protein, Hsp30C: the carboxyl end is required for stability and chaperone activity. *Cell Stress Chaperones* 2000;5:148-159
- 60 Asea A, Kabingu E, Stevenson MA, Calderwood SK. HSP70 peptidomimetic and peptide-negative preparations act as chaperokines. *Cell Stress Chaperones* 2000;5:425-431
- 61 Kedzierska S, Jezierski G, Taylor A. DnaK/DnaJ chaperone system reactivates endogenous E. coli thermostable FBP aldolase *in vivo* and *in vitro*; the effect is enhanced by GroE heat shock proteins. *Cell Stress Chaperones* 2001;6:29-37
- 62 Locke M. Heat shock transcription factor activation and hsp72 accumulation in aged skeletal muscle. *Cell Stress Chaperones* 2000;5:45-51
- 63 Mirkes PE. Molecular/cellular biology of the heat stress response and its role in agent-induced teratogenesis. *Mutat Res* 1997;396:163-173
- 64 Lang L, Miskovic D, Lo M, Heikkila JJ. Stress-induced, tissue-specific enrichment of hsp70 mRNA accumulation in Xenopus laevis embryos. *Cell Stress Chaperones* 2000;5:36-44
- 65 Martin CC, Tang P, Barnardo G, Krone PH. Expression of the chaperonin 10 gene during zebrafish development. *Cell Stress Chaperones* 2001;6:38-43
- 66 Todd MD, Lin X, Stankowski LF Jr, Desai M, Wolfgang GH. Chiron Corporation, Emeryville, CA. Toxicity Screening of a Combinatorial Library: Correlation of Cytotoxicity and Gene Induction to Compound Structure. *J Biomol Screen* 1999;4:259-268
- 67 Wood JD. Enteric nervous system in pathogenesis of gastrointestinal motility disorders. *Chin Natl J New Gastroenterol* 1996;2(Suppl 1):26-31
- 68 Schmelz M, Schmid VJ, Parrish AR. Selective disruption of cadherin/catenin complexes by oxidative stress in precision-cut mouse liver slices. *Toxicol Sci* 2001;61:389-394
- 69 Chen ZY, Yan MX, Xiang BK, Zhan HW. Alterations of gut hormones of blood and colonic mucosa in rats with chronic stress. *Shijie Huaren Xiaohua Zazhi* 2001;9:59-61
- 70 Lin H, LO M, Zhang YX, Wang BY, Fu BY. Induction of a rat model of alcoholic liver diseases. *Shijie Huaren Xiaohua Zazhi* 2001;9:24-28
- 71 Lo XH, Xie YH, Fu BY, Liu CR, Wang BY. Dynamic expression of tissue inhibitor of metallo- proteinase1 in alcoholic liver disease in rats. *Shijie Huaren Xiaohua Zazhi* 2001;9:29-33
- 72 Hoetzel A, Vagts DA, Loop T, Humar M, Bauer M, Pahl HL, Geiger KK, Pannen BH. Effect of nitric oxide on shock-induced hepatic heme oxygenase-1 expression in the rat. *Hepatology* 2001;33:925-937
- 73 Zhang BY, Zhu ZC, Ye FL, Fan YH. Effect of manganese on activity of nitric oxide synthase of filial rat's brain. *Weisheng Dulixue Zazhi* 1999;13:255-257
- 74 Burkart V, Liu H, Bellmann K, Wissing D, Jaattela M, Cavallo MG, Pozzilli P, Briviba K, Kolb H. Natural resistance of human beta cells toward nitric oxide is mediated by heat shock protein 70. *J Biol Chem* 2000;275:19521-19528



• BASIC RESEARCH •

# Severe biliary complications after hepatic artery embolization

Xiao-Qiang Huang, Zhi-Qiang Huang, Wei-Dong Duan, Nin-Xing Zhou, Yu-Quan Feng

Xiao-Qiang Huang, Zhi-Qiang Huang, Wei-Dong Duan, Nin-Xing Zhou, Yu-Quan Feng, Department of Hepatobiliary Surgery, General Hospital of PLA, Beijing 100853, China

Correspondence to: Xiao-Qiang Huang, The General Hospital of PLA, 28 Fuxing Road, Beijing 100853, China. huangxq@ht.rol.cn.net  
Telephone: +86-10-66937343

Received 2001-07-12 Accepted 2001-10-12

## Abstract

**AIM:** To study the mechanism and treatment of severe biliary complications arising from hepatic artery embolization (HAE).

**METHODS:** Of seven cases of intra- and extrahepatic biliary damage resulting from hepatic artery embolization reported since 1987, 6 patients suffered from hepatic haemangioma, the other case was due to injection of TH compound into the hepatic artery during operation. The hepatic artery was injected with ethanol so as to evaluate the liver damage in experimental rats.

**RESULTS:** All the cases were found to have destructive damage of intra- and extrahepatic bile duct at the hilum with biliary hepatocirrhosis. Experimental results revealed necrosis of the liver parenchyma, especially around the portal tract and obliteration of intrahepatic bile duct.

**CONCLUSIONS:** To prevent the severe biliary complications of HAE, the use of HAE for hepatic haemangioma which was widely practiced in China, should be re-evaluated. Hepatic arterial embolization of hepatic haemangioma may result in severe destructive biliary damages and its indiscriminate use should be prohibited.

Huang XQ, Huang ZQ, Duan WD, Zhou NX, Feng YQ. Severe biliary complications after hepatic artery embolization. *World J Gastroenterol* 2002;8(1):119-123

## INTRODUCTION

Hepatic artery embolization (HAE) has been used for the treatment of malignant tumors of the liver. At present, in Chinese literatures, HAE has been widely used for liver cancer therapy<sup>[1-6]</sup>. Recent reports showed that the method has been advocated for the treatment of liver benign tumors especially in hepatic hemangioma<sup>[7-15]</sup>. However, the value of HAE as well as the pitfalls of this form of treatment in hepatic hemangioma have not been fully evaluated. Some basic differences of hepatic hemodynamics between hepatic hemangioma and hepatic cell carcinoma<sup>[16]</sup>, may in turn affect the result of treatment. Severe complications after HAE for hepatic hemangioma had rarely been mentioned in the literature, therefore, such kind of non-operative treatment may be taken as an "innocuous" procedure and it has been used indiscriminately. Little attention to the biliary complications of HAE has been paid and the treatment of the biliary complication is a very knotty problem<sup>[17]</sup>. We have treated 7 consecutive cases of severe destructive damages of the bile duct resulting from HAE from February 1987 to September 1999. In addition, damage of bile duct after HAE has been testified by a series

of animal experiments. This report reviews our experience in the treatment of severe biliary complications of HAE and the results of animal experiment.

## MATERIALS AND METHODS

### Animal experiment

Male and female Wistar rats (220g-280g) purchased from the Laboratory Animal Unit of the General Hospital of PLA, Beijing. All animals were reared on a standard laboratory diet, and tap water. They were kept in a room where the temperature (20°C±2°C), humidity (65%-70%), and day : night cycle (12:12 light:dark) were controlled.

### Hepatic artery embolization

Ethanol (100%) was selected as the embolizing agent for the study. Hepatic artery embolization was performed under inhalant anesthesia. Branches of the abdominal aorta, and the branches from coeliac artery to spleen, stomach and duodenum were temporarily ligated. Ethanol (100%) with small amount of methylene blue was injected into the abdominal aorta with syringe, 0.2 milliliter ethanol for each rat. After the injection, the ligated arteries were loosened.

The animals lost appetite and 3/20 had obstructive jaundice after the operation. The rats were randomly divided into two groups, ten rats for each group.

Ten rats were killed 3 days (group A) after the embolization, the others were killed after 7 days (group B). Blood samples of Group A, Group B and control (abdominal operation but without ethanol injection) were collected for liver function test including glutamic pyruvic transaminase (GPT), glutamic oxaloacetic transaminase (GOT), bilirubin, alkaline phosphatase (ALP) and total bile acid (TBA). At the same time, the liver was removed and fixed in 10% formalin solution and embedded in paraffin. The specimens were sectioned and stained with hematoxylin-eosin (H&E).

### Statistical analysis

The results were expressed as mean ±S.E. ( $\bar{x} \pm S\bar{e}$ ).

## RESULTS

### Liver function changes

Changes of liver function differed among rats with or without jaundice after the embolization. GPT, GOT, ALP and TBA were significantly increased after HAE on the 3rd day and 7th day when compared with the control group, these changes seemed to be recovered on the 7th day (Table 1).

**Table 1** Liver function changes ( $\bar{x} \pm S\bar{e}$ )

|         | GPT(U/L) | GOT(U/L) | TB(μmol/L) | DB(μmol/L) | ALP(U/L) | TBA(μmol/L) |
|---------|----------|----------|------------|------------|----------|-------------|
| Control | 30±8     | 63±6     | 10±9       | 5±5        | 146±115  | 6±2         |
| Group A | 245±191  | 443±382  | 129±213    | 61±99      | 104±11   | 161±249     |
| Group B | 55±67    | 233±266  | 5±2        | 3±1        | 243±174  | 48±36       |

GPT=glutamic pyruvic transaminase, GOT= glutamic oxaloacetic transaminase, TB= total bilirubin, DB= direct bilirubin, ALP= alkaline phosphatase, TBA= total bile acid.

### Pathological changes

Small yellowish necrosis patches can be seen by naked eyes in some lobes of the liver of groups A and B. There were small local necrotic areas in the liver parenchyma of groups A and B, the control group showed no liver necrosis. Most of the necrosis was located near the portal triad, the necrotic areas showed eosinophilic staining. The damaged areas presented coagulation necrosis of hepatocytes, where the hepatocytes showed uniformly eosinophilic, the liver cell plate was still visible but the hepatic cell nuclei disappeared. There was a clear borderline around the necrotic areas after the 7<sup>th</sup> day with infiltration of inflammatory cells. Most of the portal veinules remained normal, but the wall of the surviving artery was thickened and bile duct disappeared from the portal tract. Proliferation of small bile ducts was easily seen outside the necrotic areas (Figure 1). Obliteration of the bile duct with impairment of biliary drainage was responsible for the above findings.

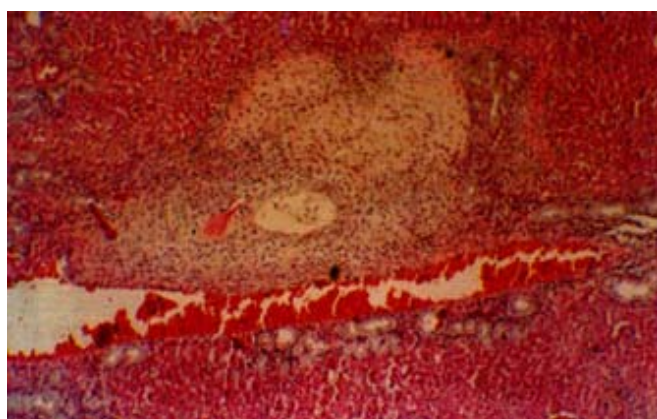


**Figure 1** Liver necrosis after HAE in rats. The necrotic area is seen near the portal triad. HE×100

The above findings showed that the liver damage of HAE could be reproduced in animal experiment. Injecting ethanol through hepatic artery can certainly result in local necrosis of the liver, especially the biliary tract in the portal triads of the liver. Necrosis of portal triads or liver parenchyma will lead to biliary abscess formation and fibrosis of the liver.

## CASE REPORTS

### Case 1

A 55-year-old male was found to have a 4cm×4.5cm hemangioma in the right lobe of the liver during a routine physical examination in March 1989. He was advised to have his liver thrombosed. HAE with iodized oil 10ml and sodium morrhuate 4ml were injected with Seldinger technique. He felt severe abdominal pain at once after the injection. Pain was not relieved until 5 days after the embolization. Intense vomiting appeared 20 min after the embolization, and persisted for 4 days. Obstructive jaundice appeared after 20 days. Percutaneous transhepatic cholangiogram (PTC) showed changes of the right and left hepatic duct. Occlusion of extrahepatic bile duct was noted in July 1989. Ultrasound showed dilatation of the gallbladder and fluid accumulated around the gallbladder. Gallbladder necrosis with segmental bile duct necrosis were confirmed at operation on July 29, 1989. Cholecystectomy, partial hepatic bile duct excision and choledochocholedochostomy with T-tube stenting were performed. Serum icterus index descended from 90U to 20U with T-tube kept in place for two years. He was admitted to the General Hospital of PLA, Beijing, because of biliary cirrhosis, portal hypertension, enlarged spleen and ascites in 1994. Due to severe hepatocirrhosis, atrophy of the right lobe of the liver and portal hypertension, reconstructive biliary operation was deemed to be unsafe unless the portal pressure has been lowered down. So he was to under go staged

operation, the first operation consisted of splenectomy and splenicocaval shunt on June 9, 1994. Hepatocholedochojejunostomy was performed 6 months afterwards. The patient remained well without jaundice since the last operation.

### Case 2

A 55-year-old female was found to have a large mass (5cm×6cm) in the right lobe of liver in June 1996, but she experienced no remarkable symptoms. Nevertheless, HAE was performed with ethanol (100%) following doctor's advice. The patient suffered from irregular fever and epigastric pain after the HAE. Ultrasound showed liver abscess formation two months later. She was still febrile and appeared toxic in spite of drainage of bile containing pus by a percutaneous catheter. Laparotomy and liver abscess drainage were performed three months later. But jaundice reappeared 4 months after the operation. Computed tomography scan showed left hepatic duct dilatation, and infective necrotic lesion of unhomogenous density in the right lobe of the liver. Fistulography through the right liver drainage tube showed abnormal communication between the drainage tract and the extrahepatic bile duct, as well as a duodenal fistula. Hepatectomy, hepatocholedocho-jejunostomy and U-tube stenting were performed 4 months later in April 1997. Jaundice disappeared after the operation. The stenting tube was maintained for one and half years. She recovered after withdrawal of the tube.

### Case 3

A 62-year-old woman was found to have an asymptomatic hemangioma (10cm×9cm) in the right liver by ultrasound in December 1994. HAE was advised and performed with iodized oil and sodium morrhuate. Persisted epigastric pain followed the procedure. Ultrasound and CT showed cystic lesions (5.6cm×6.1cm) in the left lobe of the liver 2 months later (Figure 2). The patient had had repeated attacks of high fever with chills, and antibiotics administration was not effective. She was admitted with the diagnosis of biliary multi-abscesses of the liver. A transcatheter catheter was placed with drainage of about 180-200 mL bile each day. The last operation was performed in June 1996. A large amount of bile stained necrotic tissue along the portal tract on both sides of the liver was removed. During the operation, the normal intrahepatic ducts were found destroyed. The right and left liver parenchyma was atrophied while the caudate lobe became hypertrophied. A fibrous stricture band was present around the common hepatic duct. The stricture band was removed and U-tube stents were placed during the operation. Jaundice disappeared 2 years after the operation.

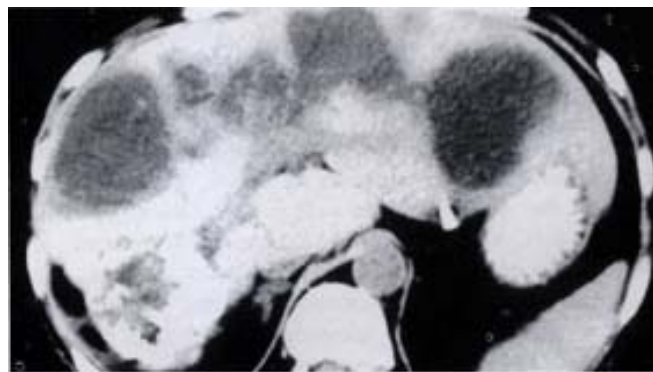


**Figure 2** Biliary abscess of liver after HAE. CT shows multi-abscess along portal tract.

### Case 4

A 24-year-old female was diagnosed having a space occupying lesion in the right liver. She was operated upon in 1987. Multiple nodular lesions were found in her right liver, which were supposed to be

metastatic nodules. A nodule was taken for pathological sections, and the hepatic artery was ligated and methacrylate (TH glue) was injected through distal end of the hepatic artery during operation. The postoperative course was very stormy. She developed continued abdominal pain with high fever and jaundice after the operation. The abdominal X-ray showed that the branches of the left, and right hepatic artery and gastroduodenal artery were embolized. However, the tissues from the right lobe of the liver was inflammatory in nature pathologically. Seven months later, she was admitted to the General Hospital of PLA, and PTC showed that stricture of hilar bile duct and the left hepatic duct with diffuse fibrosis in the perihilar region and necrosis of the right liver and the gallbladder. GI examination revealed an internal fistula between the first portion of duodenum and hepatic hilum. The operation undertaken was very difficult. However, the intestinal fistula was repaired, anastomosis of the dilated segment III bile duct and a long Roux-en-Y jejunal loop was created with a U-tube stent. The tube was removed 11/2 years later. The patient recovered from the operation. She delivered a child two years later, but eventually, the patient died of hepatocellular carcinoma 5 years after the operation.

### Case 5

A 60-year-old male was found to have a hepatic hemangioma (5cm×5cm) in 1994. CT examination in 1998 showed an increase in the size of the tumor. HAE was advised and performed with iodized oil, steel wire ring and pingyangmycinum in July 1998. Persistent epigastric pain occurred for 3 days after the procedure, followed by jaundice and fever with gray colored stool 20 days later. This condition was aggravated 4 months later. The patient when seen was suffering from continual high fever and deep jaundice and was admitted to the hospital in January 1999. Diagnoses of hepatic abscesses and gallbladder necrosis after the embolization were made. ERCP showed extensive hepatic bile duct stricture (Figure 3), which was thought to be not amenable to surgery. The patient was treated conservatively.



**Figure 3** Intrahepatic bile duct stricture after HAE. ERCP shows biliary stricture.

### Case 6

A 43-year-old female was found to have a liver hemangioma in October 1998. HAE was performed which was complicated by severe abdominal pain and repeated vomiting for a week, and jaundice occurred 3 months later. Antibiotic therapy was effective. The patient was admitted with the diagnosis of obstructive jaundice in September 1999. MRI showed gallbladder necrosis perforation and with fluid collection around it (Figure 4). Intrahepatic bile ducts were dilated. A hemangioma (3cm×3.5cm) in the right lobe of the liver was still seen. The gallbladder was found to be necrotic, and the abscess cavity communicated with the common bile duct as seen at operation. Cholecystectomy, and T tube stenting were performed. Jaundice disappeared after the operation.



**Figure 4** MRI showed fluid around the gallbladder.

### Case 7

A 43-year-old man was found to have a hemangioma of the right liver during physical examination in June 1993. HAE was advised and was performed using iodized oil and sodium morrhuate. Serious epigastric pain occurred immediately after the embolization. Jaundice appeared in July 1995. He was then operated upon, three coagulated blood coagula were taken out during choledochostomy. The patient was reoperated in June 1996. Choledochenterostomy and drainage of the III segmental duct were performed in January 1998. An external bile fistula was formed and biliary drainage of 300 mL was given each day but jaundice did not subside. The patient was admitted for operation in September 1999, marked biliary cirrhosis and atrophy of right lobe were found at operation. Cholangioenterostomy of the dilated III segmental duct and T tube stenting were performed. Jaundice subsided very slowly after the operation.

## DISCUSSION

### *Blood supply of the hepatic duct and mechanism of bile duct injury in HAE*

Branches of intrahepatic bile duct, artery and portal vein come together in the same Glisson sheath in the portal tract. Arterioles from the hepatic artery form a dense capillary network around the bile duct, which is the so-called peribiliary plexus. Therefore, only a small portion of hepatic arterial blood directly enters the sinusoids. The blood supply of the bile duct and structure of portal tract comes completely from hepatic artery. Hence, the intrahepatic bile duct receives unique nutrient blood supply from the hepatic artery in contrast to the double blood supply of hepatic cell<sup>[18-25]</sup>. Therefore, damages of the biliary system are more severe than the liver cell in hepatic arterial embolization. Clinically, continuous hepatic artery infusion of FUDR is expected to cause development of permanent stricture of the biliary system<sup>[26]</sup>. The complication was thought to be the result of regional drug toxicity and biliary vascular embolism. The end result is sclerosing cholangitis and diffuse fibrosis as well as scarring of biliary tree. Stapleton *et al*<sup>[27]</sup> in the study of the blood supply of the right and left hepatic ducts found that the peribiliary plexus of the caudate lobe has bilateral artery blood supply. This may be the reason for atrophy of right and left lobes but accompanied with hypertrophy of the caudate lobe after HAE injury which was consistently found in the cases in this report.

Hemangioma occurs more frequently in the right liver lobe and stricture of hilar hepatic duct was found in the HAE of right lobe lesions as shown in this report. This is explained by the finding that hilar bile duct blood supply chiefly derived from right hepatic and cystic arteries<sup>[28-30]</sup>.

Sodium morrhuate is commonly used as a vascular sclerosing agent<sup>[31-33]</sup>, but it is a strong irritant, it can cause local tissue necrosis and inflammation as well as complete occlusion of large blood

vessels in the injecting area. It was used for sclerosing therapy of varicosity vein and it is scarcely used for HAE. Four cases in this report used sodium morrhuate as the sclerosent, resulting in liver necrosis and abscess formation. We are of the opinion that the use of sclerosing drug as an embolizing agent in HAE is very dangerous.

Ethanol caused protein coagulation and damage of vascular endothelium which causes thrombosis and obstruction of blood vessel<sup>[34-36]</sup>. In this report, one case received ethanol as the embolizing agent. Animal experiment demonstrated that ethanol causes intrahepatic biliary obliteration and acute liver focal necrosis in the rat model.

### Surgical treatment

Cases in this report have the following characteristics of: ① 6/7 cases were hepatic hemangiomas and strong destructive embolizing agents were employed; ②clinically, all patients presented persistent abdominal pain following the procedure; ③all resulted in extensive hepatic necrosis and damage of the biliary tree, hepatic biliary abscesses developed after the embolization; ④ damage of the intra- and extra-hepatic biliary system was destructive, it was difficult to rehabilitate the patients and a prolonged hospitalization is needed.

Treatment of the complications after HAE: Liver parenchyma necrosis was distributed along the portal tract after the HAE. Because of the disruptive effect of sclerosing agent on the biliary tract and the focal necrosis liver cells, some of the liver cells near the foci of necrosis are still secreting bile, the end result is biliary abscess forming in the necrosed area. The bile duct in its entire course may be completely destroyed. The damaged hepatic lobe will eventually be atrophied. Necrosis and fibrous stricture often consequently involve the hepatic duct bifurcation as well as the left hepatic duct, which results in obstructive jaundice in the end. In late cases, when complicated with biliary cirrhosis and portal hypertension, restorative biliary surgery is very difficult. Under such conditions, it is our experience that the treatment needs to be divided into several steps. The first step is the drainage of bile collection and removal of necrotic tissue to control the infection. First step of treatment is to improve patients'ä general status as well as the local condition by maintaining biliary drainage. Treatment of the second step is hepatotomy and necrotic tissue elimination. If biliary stricture is of perihilar type, operation to relieve hilar bile duct stricture and Roux-en-Y hepatocholecho-jejuno-stomy and place U tubes for stenting are necessary<sup>[37-41]</sup>. If patients are complicated with biliary cirrhosis and portal hypertension, preliminary operation of portal pressure decompression, for example spleno-renal shunt is often needed before the difficult biliary restoration operation is attempted<sup>[42]</sup>. If bile ducts were badly damaged, bilateral biliary drainage with U tubes is a better alternative.

To prevent severe biliary complications of HAE, the use of HAE for hepatic hemangioma should be re-evaluated and the indiscriminate use of sclerosing agents in HAE should be prohibited.

### REFERENCES

- Jia YC, Tian JM, Wang ZT, Chen D, Ye H, Liu Q, Yang JJ, Sun F, Lin L, Lu JP, Wang F, Cheng HY. A retrospective review on interventional treatment of 10000 cases of liver cancer. *Huaren Xiaohua Zazhi* 1998;6:2-3
- Ji XL, Liu YX, Wang YH, Zhao H. Histopathological study of hepatocellular carcinoma after transcatheter hepatic arterial

- embolization. *China Natl J New Gastroenterol* 1996;2:79-81
- Zheng CS, Feng GS, Zhou RM, Liang B, Liang HM, Zhen J, Yu JM, Liu H. Hepatic arterial infusion chemotherapy and embolization in the treatment of primary hepatic carcinoma. *China Natl J New Gastroenterol* 1997;3:104-107
- Fan J, Ten GJ, He SC, Guo JH, Yang DP, Weng GY. Arterial chemoembolization for hepatocellular carcinoma. *World J Gastroenterol* 1998;4:33-37
- Cheng XM, Luo PF, Shao PJ, Zhou ZJ, Ma Z. Analysis of the Cause of Death after Chemoembolization for Liver Cancer. *Jieru Yixue Zazhi* 1997;2: 11-13
- Huang FG, Li Y, Xie XD. Side effects and complications of hepatic arterial infusion and embolization of liver carcinoma in aged patients and its management. *World J Gastroenterol* 1998;4:67-68
- Li GW, Zhao ZR, Li BS, Liu XG, Wang ZL, Liu QF. Source of blood supply of liver cavernous hemangioma and sclerosis and embolization treatment. *China Natl J New Gastroenterol* 1997;3: 147-149
- Xie ZG, Wang ZD. Blood supply of hepatic cavernous haemangioma and interventional treatment. *Xinxiaohuabingxue Zazhi* 1996; 4:46-48
- Li Y, Li S. An experiment study of sodium morrhuate as an agent for arterial embolization. *Zhonghua Fangshe Zazhi* 1987;21:357-360
- Jiang XX. Hepatic artery embolization in treatment of huge cavernous hemangioma. *Zhonghua Fangshe Zazhi* 1992; 26:88-90
- Yan XF, He JG, Song HZ, Zhao CZ. Interventional therapy of hepatic cavernous hemangioma. *Zhonghua Waikexue Zazhi* 1994;32: 563-564
- Panis Y, Fagniez PL, Cherqui D, Roche A, Schaaill JC, Jaeck D. Successful arterial embolization of giant liver hemangioma. Report of a case with five-year computed tomography follow-up. *HPB-Surg* 1993; 7:141-146
- Li GW, Zhao ZR, Li BS, Liu XG, Wang ZL, Liu QF. Embolization therapy and its mechanism of cavernous hemangioma of liver. *Shanxi Yixue Zaizhi* 1993; 22:515-517
- Li IQ, Li JL, Wu S, Liang ST, Liao QH. Fifteen cases lipidol embolization treatment of hepatic cavernous haemangioma. *Zhonghua Shiyianwaikexue Zazhi* 1994; 14:1-3
- Li GW, Liu XG, Li BS, Wang ZL, Le XB, Wang Y, Liu QF, Gao H. Study of sclerosing treatment of liver haemangioma. *Zhonghua Shiyianwaikexue Zazhi* 1992;9:1-3
- Zhou Runsu, Qiao Hongqing, Deng Jinglan, Huo JP, Ma XR. Analysis of radioimage of hepatic artery perfusion in patients with hepatic space-occupying lesions. *Zhongguo Zhongliu Linchuang* 1995; 22:381-383
- Huang XQ, Huang ZQ, Duan WD, Zhou NX, Feng YQ. Destructive damage of bile duct of hepatic artery embolization in treatment of hepatic cavernous haemangioma. *Junyijingxiu xueyan Xuebao* 2000; 21:88-91
- Jing JG, Wang CL, Han MJ, Yang MW. The experimental study of local blood flow and pathologic changes after embolization of portal vein branch with two kinds of embolic materials. *Zhongguo Yikedaxue Xuebao* 1995;24:602-604
- Wang X, Zhong YX, Zhang LL, Huang YX, Wen QS, Chu YK, Zhang HX, Wang QL. Effect of IL-8 and ET-1 on secondary liver injury by hepatic arterial embolization in rabbits. *Shijie Huaren Xiaohua Zazhi* 2000;8:413-416
- Motta PM. The three-dimensional microanatomy of the liver. *Arch Histol Jap* 1984;47:1-30
- Huang XQ. Changes of liver microcirculation in cirrhosis and biliary obstruction. *Guowaiyixue Waikexue Fence* 1986;6:321-323
- Huang XQ, Yang KZ, Huang ZQ, Ying GQ, Wang BZ. An experiment study of liver microcirculation after ligation bile duct. *Zhonghua Shiyianwaikexue Zazhi* 1987; 4:151-154
- Compagno J, Grisham JW, Louis St. Scanning electron microscopy of extrahepatic biliary obstruction. *Arch Pathol* 1974;97: 348-351
- Bosch J, Enriquez R, Groszmann RJ, Storer EH. Chronic bile duct ligation in the dog: Hemodynamic characterization of a portal hypertensive model. *Hepatology* 1983;3:1002-1007
- Jones AL, Schmuker DL. Current concepts of liver structure as related to function. *Gastroenterology* 1977;73:833-851
- Margaret K M, Hector B, Blayney D W, Cecchi G, Goldberg D A, Leong L A, Margolin K A, Terz J J. Sclerosing cholangitis after continuous hepatic artery infusion of FUDR. *Ann Surg* 1985; 202: 176-181
- Stapleton GN, Hickman R, Jerblanche J. Blood supply of the right and left hepatic ducts. *Br J Surg* 1998;85:202-207
- Zheng JF, Sun FL, Yu XF, Dou YC. Transhepatic arterial



- chemoembolization using lipiodol and ischemic injury to the gallbladder. *Linchuang Waike Zazhi* 1998; 6: 270-271
- 29 Wang X, Huang YX, Wen QS, Cu YK, Li DY, Zhang HX, Zhang JZ, Wang YD. Experimental study on gastric mucosal injury by hepatic arterial embolization in rabbits. *Huaren Xiaohua Zazhi* 1998; 6:997-999
  - 30 Chen WJ, Ying DJ, Liu ZJ, Liu ZJ, He ZP. Analysis of the arterial supply of the extrahepatic bile ducts and its clinical significance. *Clinical Anatomy* 1999;12:245-249
  - 31 Zhang TL, Cheng HH, Hou KY, Yan NS. Necrosis of the gastric wall after alpha-cyanoacrylate embolization of gastric coronary vein. *Beijing Yikedaxue Xuebao* 1996; 28:452-453
  - 32 Jing YC, Yang ZD, Ding HY, Ma FC. Pathological changes of perivascular tissues after gastric and hepatic vascular embolization with medical TH tissue adhesive in rabbits. *Linchuang Yushiyang Binglixue Zazhi* 1997; 13: 51-52
  - 33 Lu MD, Chen JW, Xie XY, Liang LJ, Huang JF. Portal vein embolization by fine needle ethanol injection: experimental and clinical studies. *World J Gastroenterol* 1999;5:506-510
  - 34 Lu MD, Yin YY, Ren W. A study of portal vein embolization with absolute ethanol injection in cirrhotic rats. *World J Gastroenterol* 1998; 4:415-417
  - 35 Lu MD, Liang LJ, Peng BG, Ren W. Study of portal vein embolization with ethanol injection in cirrhotic rats. *Zhonghua Shiyian Waike Zazhi* 1998; 15: 75-76
  - 36 Lu MD, Chen JW, Xie XY, Liang LJ, Huang JF. Portal vein embolization by fine needle ethanol injection: experimental and clinical studies. *World J Gastroenterol* 1999;5:506-510
  - 37 Liu YX, Huang ZQ, Zhou YB, Chai ZJ, Qiang GX, Chi YB, Han BL, He ZP, Zhang QZ, Tu JM. Surgical treatment of injury bile duct strictures. *Puwai Linchuang* 1986;234-237
  - 38 Huang ZQ. New development of biliary surgery in China. *World J Gastroenterol* 2000;6:187-192
  - 39 Wang J, Liu YU, Huang ZQ, Feng YQ, Zhou NX, Gu WQ, Duan YP, Huang XQ, Zhang WZ. Surgical treatment of 42 cases of traumatic strictures of bile duct. *Gandanyipi Waike Zazhi* 1995; 1:81-84
  - 40 Huang ZQ. Surgical treatment of biliary obstruction in posterior segment of the right lobe. *Zhonghua Waike Zazhi* 1988;26: 593-597
  - 41 Huang XQ, He ZP, Zhou YB, Zhong JC, Guo ZY, Feng YQ. Repair biliary stricture used mucous segments with blood supply. *Zhonghua Waike Zazhi* 1986; 24:523-526
  - 42 Huang ZQ, Zai JX, Han BL, Qian GX. Surgical treatment of bile duct strictures with portal hypertension. *Zhonghua Waike Zazhi* 1979;17:351-356

Edited by Ma JY

• BASIC RESEARCH •

# Lipopolysaccharide induced synthesis of CD14 proteins and its gene expression in hepatocytes during endotoxemia

Sheng-Wei Li, Jian-Ping Gong, Chuan-Xin Wu, Yu-Jun Shi, Chang-An Liu

Sheng-Wei Li, Jian-Ping Gong, Chuan-Xin Wu, Yu-Jun Shi, Chang-An Liu, Department of General Surgery, The Second College of Clinical Medicine & the Second Affiliated Hospital of Chongqing University of Medical Sciences, Chongqing 400010, China

Supported by the National Natural Science Foundation of China (No. 39970719)

Correspondence to: Sheng-Wen Li, Department of General Surgery, The Second College of Clinical Medicine & the Second Affiliated Hospital of Chongqing Medical University, 74 Linjiang Road, Central District, Chongqing 400010, China. lswgg@163.com

Telephone: +86-23-63849075-2100

Received 2001-08-23 Accepted 2001-09-05

## Abstract

**AIM:** To observe synthesis of CD14 protein and expression of CD14 mRNA in hepatic tissue and hepatocytes of rats during endotoxemia.

**METHODS:** The endotoxemia model of Wistar rat was established by injection of a dose of lipopolysaccharide (LPS) ( $5\text{mg}\cdot\text{kg}^{-1}$ , *Escherichia coli* O111:B4) via the tail vein, and then the rats were sacrificed after 3, 6, 12 and 24 h in batches. Hepatocytes were isolated from normal and LPS-injected rats by in situ collagenase perfusion technique and were collected to measure the expression of CD14 mRNA and synthesis of CD14 protein by reverse transcript-polymerase chain reaction (RT-PCR) or Western blot analysis. The binding of fluorescein isothiocyanate (FITC)-CD14 polyclonal antibody to isolated hepatocytes was also assessed by flow cytometric analysis (FCM).

**RESULTS:** In the rats with endotoxemia, the expressions of CD14 mRNA in hepatic tissue and isolated hepatocytes were stronger at 3, 6, and 12 h than that in control rats ( $3.48\pm 0.15$ ,  $5.89\pm 0.62$ ,  $4.33\pm 0.18$ , vs  $1.35\pm 0.14$  in hepatic tissue,  $P<0.01$ ;  $4.12\pm 0.17$ ,  $6.24\pm 0.64$ ,  $4.35\pm 0.18$ , vs  $1.87\pm 0.15$  in hepatocytes,  $P<0.01$ ). The synthesis of CD14 protein in hepatic tissue and isolated hepatocytes increases also obviously in 6 and 12 h when compared to that in control rats ( $13.27\pm 1.27$ ,  $17.32\pm 1.35$ ,  $11.42\pm 1.20$ , vs  $7.34\pm 0.72$  in hepatic tissue,  $P<0.01$ ;  $14.68\pm 1.30$ ,  $17.95\pm 1.34$ ,  $11.65\pm 1.19$ , vs  $7.91\pm 0.70$  in hepatocytes,  $P<0.01$ ). FCM showed that mean fluorescence intensity (MFI) and numbers of FITC-CD14 positive cells in the rats with endotoxemia increased obviously at 3, 6, 12 and 24 h when compared with normal control group (43.4%, 70.2%, 91.4%, 32.6% vs 4.5%,  $P<0.01$ ).

**CONCLUSION:** LPS can markedly promote the synthesis of CD14 protein and up-regulate the expression of CD14 mRNA in isolated hepatocytes and hepatic tissue. Liver might be a main source for soluble CD14 production during endotoxemia.

Li SW, Gong JP, Wu CX, Shi YJ, Liu CA. Lipopolysaccharide induced synthesis

of CD14 proteins and its gene expression in hepatocytes during endotoxemia. *World J Gastroenterol* 2002;8(1):124-127

## INTRODUCTION

CD14 is a glycosylphosphatidylinositol-anchored lipopolysaccharide (LPS) receptor, and first reported to be a differentiation marker expressed on the surface of macrophages, neutrophils and other myeloid lineage cells<sup>[1,2]</sup>. Recent works have shown that the CD14 antigen is expressed in many types of cell and tissues<sup>[3-8]</sup>. But it is not yet clear whether hepatocytes can express CD14 protein and gene. Hepatocytes are the major source of most acute-phase proteins. If in fact soluble CD14 (sCD14) is an acute-phase protein, then hepatocytes might be expected to express CD14, which is upregulated during endotoxemia<sup>[9-11]</sup>. Furthermore, hepatocytes isolated from endotoxemic animals exhibit markedly enhanced responses to LPS, raising the possibility that these cells may express CD14<sup>[3,4,12-14]</sup>. To determine whether hepatocytes express CD14, our experiments were to observe the synthesis of CD14 protein and expression of CD14 mRNA in hepatocytes and hepatic tissue of rats during endotoxemia and to verify hepatocytes as a main source for soluble CD14 (sCD14) production.

## MATERIALS AND METHODS

### Reagents

LPS (*Escherichia coli* O111:B4) and type IV of collagenase were purchased from Sigma Chemical Company (St. Louis, Mo.). An anti-CD14 polyclonal antibody was purchased from Santa Cruz Biotechnology (Santa Cruz, Calif.). SP Reagent boxes and fluorescein isothiocyanate (FITC)-IgG were purchased from Zhongshan Biotechnology Company (Beijing, China).

### Animals

Male Wistar rats, which were pathogen-free and weighed approximately 250 g each, were purchased from the Animal Center of Chongqing University of Medical Science. The rats were exposed each day 12 h of light and darkness. Rodent chow and water were provided ad libitum. Experimental protocols were approved by the Institutional Care and Use Committee of the Chongqing university of Medical Science.

### The endotoxemia model of animals

The acute endotoxemia model of Wistar rat was established as described by Li SW, *et al*<sup>[4]</sup>. In brief, animals were injected with a dose of LPS ( $5\text{mg}\cdot\text{kg}^{-1}$ , *Escherichia coli* O111:B4) via the tail vein, and then the rats were sacrificed at 3, 6, 12 and 24 h respectively. There were six rats at each time point, and other six animals were used as controls (0 h).

### Hepatocyte Isolation

Hepatocytes were isolated from normal and LPS-injected rats by an in situ collagenase perfusion technique, modified as described previously<sup>[15, 16]</sup>. In brief, livers were removed after a portal vein

perfusion with Hanks' balanced salt solution (HBSS) and the homogenate was digested in a solution of  $0.5\text{g}\cdot\text{L}^{-1}$  collagenase. Hepatocytes were separated from the nonparenchymal cells by two cycles of differential centrifugation ( $50\text{g}$  for 2 min) and further purified over a 30% Percoll gradient. Hepatocyte purity exceeded 90% as assessed by light microscopy, and viability was typically greater than 95% as determined by trypan blue exclusion assay.

### RNA Isolation and Complementary DNA Synthesis

Total RNA was isolated from rat liver tissue and hepatocytes by using the TRIZOL Reagent (Life Technologies, USA). The quality of RNA was controlled by the intactness of ribosomal RNA bands. A total of  $0.5\text{mg}$  of each intact total RNA samples was reverse-transcribed to complementary DNA (cDNA) by using the reverse transcription-polymerase chain reaction (RT-PCR) kit (Roche, USA). cDNA was stored at  $-70^{\circ}\text{C}$  until polymerase chain reaction (PCR) analysis.

### Determination of CD14 mRNA by RT-PCR

The PCR primers used were CD14: sense ( $5'$ -CTCAACCTAGAGCCGTTTCT- $3'$ ), anti-sense ( $5'$ -CAGGATTGTCAGACAGGTCT- $3'$ );  $\beta$ -actin: sense ( $5'$ -ACCACAG-CTGAGAGGGAAATCG- $3'$ ), anti-sense ( $5'$ -AGAGGTCTTTACGGATGTCAACG- $3'$ ). The sizes of the amplified PCR products were 267 bp for CD14 and 281 bp for  $\beta$ -actin. The conditions for amplification were as follows: denaturation at  $93^{\circ}\text{C}$  for 1 min, annealing at  $57^{\circ}\text{C}$  for 1 min, and extension at  $70^{\circ}\text{C}$  for 2 min for 30 cycles. The PCR products were electrophoresed in  $20\text{g}\cdot\text{L}^{-1}$  agarose gels, and the gels were ethidium bromide stained and video photographed on an ultraviolet transilluminator, and the results were showed with the relative absorbance (Ar: relative optical density, ROD).

### Western blot analysis of CD14 protein

Cultured hepatocytes were washed twice with phosphate-buffered saline (PBS), pelleted by centrifugation. Cell pellets were resuspended in 50  $\mu\text{l}$  of lysis buffer containing 20  $\text{mmol}\cdot\text{L}^{-1}$  HEPES (pH 7.9), 25% glycerol,  $0.42\text{ mmol}\cdot\text{L}^{-1}$  NaCl,  $15\text{ mmol}\cdot\text{L}^{-1}$   $\text{MgCl}_2$ ,  $0.2\text{ mmol}\cdot\text{L}^{-1}$  EDTA,  $0.5\text{ mmol}\cdot\text{L}^{-1}$  phenylmethylsulfonyl fluoride (PMSF) and  $0.5\text{ mmol}\cdot\text{L}^{-1}$  dithiothreitol (DTT). After three freeze-thaw cycles, cell lysates were centrifuged at  $12000\text{g}$  for 30 min, and the supernatant was saved. The liver tissue was homogenized with homogenizer before the freeze-thaw lysis, as described above for cultured hepatocytes. For Western blot analysis, samples (20  $\mu\text{g}$  per lane) were separated on an SDS- $100\text{g}\cdot\text{L}^{-1}$  polyacrylamide gel and transferred to nitrocellulose membrane. The membrane was sequentially blocked in PBS-Tween ( $1\text{g}\cdot\text{L}^{-1}$ ) containing  $50\text{ml}\cdot\text{L}^{-1}$  milk and then incubated with 5  $\mu\text{g}$  of anti-rat CD14 polyclonal antibody per mL, washed three times, and further incubated with a goat anti-rabbit immunoglobulin G horseradish peroxidase-conjugated secondary antibody. Blocking and antibody incubations each lasted 1 h at room temperature. After several washes, the membrane was developed with DAB reagent, and the results were showed with relative absorbance Ar (relative optical density, ROD).

### Flow cytometric analysis (FCM)

Expression of CD14 protein in hepatocytes was examined by FCM. In brief, hepatocytes were incubated with the anti-CD14 polyclonal antibody ( $0.1\text{mg}\cdot\text{L}^{-1}$ ) after washing, cells were incubated with goat anti-rabbit immunoglobulin G labeled with FITC, after being washed three times, and 10000 cells were analyzed by flow cytometry (Coulter, USA).

### Statistical Analysis

All results were expressed as  $\bar{x}\pm s$ . Statistical difference between means were determined by using Student's *t* test. A *P* value of  $<0.01$  was considered significant.

## RESULTS

### Expression of CD14 mRNA in liver tissue and hepatocytes

We postulated that hepatocytes and hepatic tissue could express CD14 gene which could be upregulated during endotoxemia. Rats were injected with LPS and total RNA was extracted from freshly isolated and purified hepatocytes and hepatic tissue at different time points indicated. RT-PCR analysis showed that hepatocytes and liver tissue from controls had low but detectable levels of CD14 mRNA. LPS treatment showed steady-state CD14 mRNA levels in hepatocytes, inducing a threefold elevation by as early as 3 h after LPS treatment. The levels increased with times, reaching a maximum of six-fold by 6 h after treatment, and subsequently declined to near baseline levels by 24 h. We also examined the CD14 mRNA levels in RNA isolated from hepatic tissue during endotoxemia and found that the pattern of CD14 mRNA induction by LPS was similar to that of the isolated hepatocytes, indicating that the upregulation of CD14 mRNA was not likely to be simply a consequence of the hepatocyte isolation procedure (Figure 1).

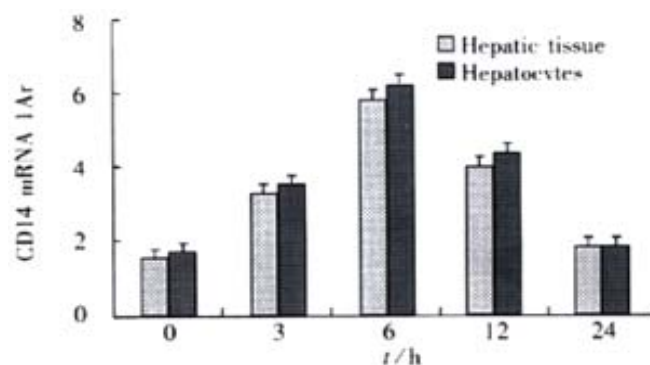


Figure 1 Expression of CD14 mRNA in hepatic tissue and hepatocytes  $P<0.01$ , vs 0 h.

### CD14 protein expression in hepatocytes and hepatic tissue

To determine if the upregulation of CD14 expression could also be appreciated in protein levels, Western blot analysis was performed on both hepatocytes and hepatic tissue sample from LPS-treated animals or control animals. In hepatocytes extracts, increases of CD14 protein were seen 6 h after LPS treatment, peaked at 12 h, and declined thereafter. A similar increase of CD14 protein in hepatic tissue was observed. there were significantly different when compared with control animals ( $P<0.01$ , Figure 2).

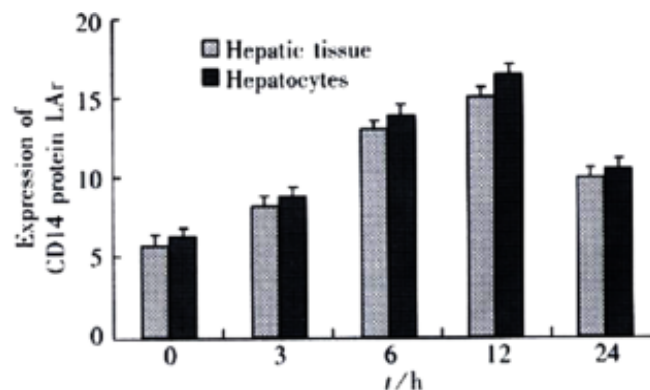


Figure 2 Expression of CD14 protein in hepatic tissue and hepatocytes  $P<0.01$ , vs 0 h

### Binding of FITC to Hepatocytes

To confirm the expression of CD14 on hepatocytes, we also examined the binding of FITC to the cells. FITC-CD14 positive cells were 4.5% in rats of normal group. But in rats with endotoxemia, the mean fluorescence intensity (MFI) increased, the numbers of FITC-CD14 positive cells were 43.4%, 70.2%, 91.4%, and 32.6%, respectively in 3, 6, 12 and 24 h after stimulation of LPS. There was significant difference when compared to normal group animals ( $P < 0.01$ , Figure 3).

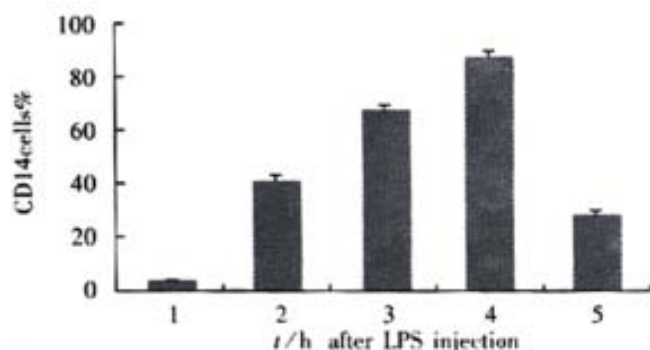


Figure 3 Percentage of CD14 positive cells  $P < 0.01$ , vs 0 h.

### DISCUSSION

CD14 was first described as a myeloid differentiation antigen in 1980<sup>[1]</sup>. It is a 55-kDa glycoprotein with multiple leucine-rich repeats and is encoded on chromosome (5q) together with growth factors, such as granulocyte macrophage colony stimulating factor. CD14 has been identified as a receptor for complexes of LPS and LPS-binding protein but it also binds other bacterial products<sup>[17-22]</sup>. The LPS-binding region within the CD14 molecule is remarkably conserved across species with a high degree of gene sequence homology, and it has therefore been suggested that CD14 is a pattern recognition receptor<sup>[17,23-25]</sup>. CD14 as a key LPS signaling molecule was reported to be expressed mainly in the monocyte-macrophages system<sup>[1,26-29]</sup>. Recent works have shown that the CD14 antigen is expressed in many types of cells and tissues<sup>[5-8,12]</sup>. But it is not yet clear whether hepatocytes express CD14. Although shedding from leukocytes has been proposed as the major source of sCD14 in blood, it is likely that other sources exist<sup>[3,5,30-32]</sup>. Some reports suggested that sCD14 behaves like other acute-phase proteins<sup>[9-11,33-36]</sup>. Hepatocytes are the major source of most acute-phase proteins. So we think if sCD14 is an acute-phase protein, then hepatocytes might be expected to express CD14 gene and synthesize CD14 protein, which is upregulated during endotoxemia<sup>[37-40]</sup>.

To determine whether hepatocytes synthesize CD14 protein and express CD14 gene, we measured steady-state CD14 protein and its mRNA both *in vivo* and *in vitro*. We found that: ① isolated hepatocytes and liver tissue could synthesize basal levels of CD14 protein and express basal levels of CD14 gene and that synthesis and expression of CD14 were markedly upregulated by LPS during endotoxemia; these results are in agreement with previous report<sup>[41,42]</sup>; ② synthesis of CD14 protein and expression of CD14 mRNA in both Hepatocytes and liver tissue indicated that such synthesis and expression were not likely to be simple a consequence of hepatocyte isolation procedure; ③ in liver, besides hepatocytes, nonparenchymal cells such as Kupffer cells, endothelial cells, neutrophils and other cells can also express CD14 gene and synthesize CD14 protein<sup>[4,43-47]</sup>, but the fact that both isolated hepatocytes and hepatic tissue expressed CD14 protein and its mRNA indicated that the nonparenchymal cells could hardly have any effect on such expression in liver tissue.

Although we do not provide direct evidence here that sCD14 in plasma originates from hepatocytes during endotoxemia, our results showed that there was the possibility that the liver is an important source for sCD14 during endotoxemia. Pan *et al*<sup>[5]</sup> found that the liver is one of the major organs for the production of soluble CD14. Liu *et al*<sup>[41,42]</sup> reported also that CD14 transcription rates were significantly increased in hepatocytes from LPS-treated rat, indicating that the upregulation in CD14 mRNA levels observed in rats hepatocytes after LPS treatment was dependent, in part, on increased transcription, and their observations supported the idea that sCD14 would be an acute-phase protein and hepatocytes might be a source for circulating sCD14 production<sup>[3,4,8,48-52]</sup>. Our data indicate that hepatocytes from LPS-stimulated rats express higher amounts of CD14 gene and CD14 protein, and may release more sCD14. Further investigation of the expression of CD14 in hepatocytes is actively ongoing in our laboratory.

In summary, our *in vitro* and *in vivo* data indicate that hepatocytes can synthesize CD14 protein and express CD14 mRNA and their synthesis and expression are upregulated effectively by LPS during endotoxemia. Liver is a main source for sCD14 production during sepsis or endotoxemia.

### REFERENCES

- 1 Lichtman SN, Wang J, Lemasters JJ. LPS receptor CD14 participates in release of TNF-alpha in RAW 264.7 and peritoneal cells but not in kupffer cells. *Am J Physiol* 1998;275:G39-46
- 2 Fearn C, Ulevitch RJ. Effect of recombinant interleukin-1beta on murine CD14 gene expression *in vivo*. *Shock* 1998;9:157-163
- 3 Su GL, Dorko K, Strom SC, Nussler AK, Wang SC. CD14 expression and production by human hepatocytes. *J Hepatol* 1999;31:435-442
- 4 Li SW, Wu CX, ShiYJ, Liu CA. Lipopolysaccharide upregulates expression of CD14 gene and CD14 proteins of hepatocytes in rats. *Zhonghua Ganzangbing Zazhi* 2001;9:103-104
- 5 Pan Z, Zhou L, Hetherington CJ, Zhang DE. Hepatocytes contribute to soluble CD14 production, and CD14 expression is differentially regulated in hepatocytes and monocytes. *J Biol Chem* 2000;275:36430-36435
- 6 Ahmed AF, Nio M, Ohtani H, Nagura H, Ohi R. In situ CD14 expression in biliary atresia: comparison between early and late stages. *J Pediatr Surg* 2001;36:240-243
- 7 Furusako S, Takahashi T, Mori S, Takahashi Y, Tsuda T, Namba M, Mochizuki H. Protection of mice from LPS-induced shock by CD14 antisense oligonucleotide. *Acta Med Okayama* 2001;55:105-115
- 8 Jersmann HP, Hii CS, Hodge GL, Ferrante A. Synthesis and surface expression of CD14 by human endothelial cells. *Infect Immun* 2001;69:479-485
- 9 Patino R, Ibarra J, Rodriguez A, Yague MR, Pintor E, Fernandez-Cruz A, Figueredo A. Circulating monocytes in patients with diabetes mellitus, arterial disease, and increased CD14 expression. *Am J Cardiol* 2000;85:1288-1291
- 10 Choi YH, Lee WH, Lee Y, Kim JK, Lee SY, Park JE. Correlation between monocyte and T-lymphocyte activation markers in patients with acute coronary syndrome. *Jpn Heart J* 2000;41:605-615
- 11 Gluck T, Silver J, Epstein M, Cao P, Farber B, Goyert SM. Parameters influencing membrane cd14 expression and soluble cd14 levels in sepsis. *Eur J Med Res* 2001;6:351-358
- 12 Nanbo A, Nishimura H, Muta T, Nagasawa S. Lipopolysaccharide stimulates HepG2 human hepatoma cells in the presence of lipopolysaccharide-binding protein via CD14. *Eur J Biochem* 1999;260:183-191
- 13 Fang WH, Yao YM, Shi ZG, Yu Y, Wu Y, Lu LR, Sheng ZY. Significance of the expressions of lipopolysaccharide binding protein mRNA and lipopolysaccharide receptor CD14 mRNA in the liver of burned rat. *Zhonghua Shaoshang Zazhi* 2000;16:157-160
- 14 Jiang JX, Xie GQ, Chen YH, Liu DW, Zhou JH, Zhu PF, Wang ZG, Zhang HJ. Expression of scavenger receptor and CD14 on Kupffer cells and its relationship with endotoxin-induced hepatic injury. *Zhonghua Chuangshang Zazhi* 2000;16:478-481
- 15 Gong JP, Xu MQ, Li K. Expression of CD14 in Kupffer's cells induced by Lipopolysaccharide. *Di-San Junyi Daxue Xuebao* 2001;23:425-428
- 16 Gong JP, Hun BL. Isolation, culture and identification of live cells. *Shijie Huaren Xiaohua Zazhi* 1999;7:417-419
- 17 Bernardo J, Billingslea AM, Blumenthal RL, Seetoo KF, Simons ER, Fenton MJ. Differential responses of human mononuclear phagocytes to mycobacterial lipopolysaccharides: role of CD14 and the mannose

- receptor. *Infect Immun* 1998;66:28-35
- 18 Means TK, Lien E, Yoshimura A, Wang S, Golenbock DT, Fenton MJ. The CD14 ligands lipoarabinomannan and lipopolysaccharide differ in their requirement for Toll-like receptors. *J Immunol* 1999;163:6748-6755
  - 19 Hetherington CJ, Kingsley PD, Crocicchio F, Zhang P, Rabin MS, Palis J, Zhang DE. Characterization of human endotoxin lipopolysaccharide receptor CD14 expression in transgenic mice. *J Immunol* 1999;162:503-509
  - 20 Fang WH, Yao YM, Shi ZG, Yu Y, Wu Y, Lu LR, Chang GY, Sheng ZY. Gene expression of lipopolysaccharide receptor CD14 and tumor necrosis factor- $\alpha$  in rats after thermal injury. *Zhonghua Waike Zazhi* 1999;37:271-273
  - 21 Ben DF, Huan JN, Yang Y, Wang L, Chen YL, Xia ZF. Increased expression of peritoneal macrophage CD14 in severely burned mice. *Zhonghua Shaoshang Zazhi* 2000;16:96-99
  - 22 Peng Z, Zhang ZX, Xu YJ. Expressions of CD11c, CD14 and TGF- $\beta$ 1 mRNA in alveolar macrophages in chronic bronchitis. *Zhonghua Weishengwuxue He Mianyixue Zazhi* 2000;20:408-410
  - 23 Gong JP, Hum BL. Role of CD14 in activation of Kupffer cell induced by lipopolysaccharide. *Shijie Huaren Xiaohua Zazhi* 1999;7:875-877
  - 24 Su GL, Rahemtulla A, Thomas P, Klein RD, Wang SC, Nanji AA. CD14 and lipopolysaccharide binding protein expression in a rat model of alcoholic liver disease. *Am J Pathol* 1998;152:841-849
  - 25 Heumann D, Adachi Y, Le Roy D, Ohno N, Yadomae T, Glauser MP, Calandra T. Role of plasma, lipopolysaccharide-binding protein, and CD14 in response of mouse peritoneal exudate macrophages to endotoxin. *Infect Immun* 2001;69:378-385
  - 26 Devitt A, Moffatt OD, Raykundalia C, Capra JD, Simmons DL, Gregory CD. Department of Immunology, University of Birmingham Medical School, UK. Human CD14 mediates recognition and phagocytosis of apoptotic cells. *Nature* 1998;392:442-443
  - 27 Peppelenbosch MP, DeSmedt M, ten Hove T, van Deventer SJ, Grooten J. Lipopolysaccharide regulates macrophage fluid phase pinocytosis via CD14-dependent and CD14-independent pathways. *Blood* 1999;93:4011-4018
  - 28 Liu S, Morris SM Jr, Nie S, Shapiro RA, Billiar TR. cAMP induces CD14 expression in murine macrophages via increased transcription. *J Leukoc Biol* 2000;67:894-901
  - 29 Stelter F, Witt S, Furl B, Jack RS, Hartung T, Schutt C. Different efficacy of soluble CD14 treatment in high- and low-dose LPS models. *Eur J Clin Invest* 1998;28:205-213
  - 30 Hiki N, Berger D, Prigl C, Boelke E, Wiedeck H, Seidelmann M, Staib L, Kaminishi M, Oohara T, Beger HG. Endotoxin binding and elimination by monocytes: secretion of soluble CD14 represents an inducible mechanism counteracting reduced expression of membrane CD14 in patients with sepsis and in a patient with paroxysmal nocturnal hemoglobinuria. *Infect Immun* 1998;66:1135-1141
  - 31 Hiki N, Berger D, Dentener MA, Mimura Y, Buurman WA, Prigl C, Seidelmann M, Tsuji E, Kaminishi M, Beger HG. Changes in endotoxin-binding proteins during major elective surgery: important role for soluble CD14 in regulation of biological activity of systemic endotoxin. *Clin Diagn Lab Immunol* 1999;6:844-850
  - 32 Bessler H, Komlos L, Punsky I, Ntambi JA, Bergman M, Straussberg R, Sirota L. CD14 receptor expression and lipopolysaccharide-induced cytokine production in preterm and term neonates. *Biol Neonate* 2001;80:186-192
  - 33 Wang SC, Klein RD, Wahl WL, Alarcon WH, Garg RJ, Remick DG, Su GL. Tissue coexpression of LBP and CD14 mRNA in a mouse model of sepsis. *J Surg Res* 1998;76:67-73
  - 34 Imai K, Takeshita A, Hanazawa S. Transforming growth factor-beta inhibits lipopolysaccharide-stimulated expression of inflammatory cytokines in mouse macrophages through downregulation of activation protein 1 and CD14 receptor expression. *Infect Immun* 2000;68:2418-2423
  - 35 Liu S, Salyapongse AN, Geller DA, Vodovotz Y, Billiar TR. Hepatocyte toll-like receptor 2 expression *in vivo* and *in vitro*: role of cytokines in induction of rat TLR2 gene expression by lipopolysaccharide. *Shock* 2000;14:361-365
  - 36 Hiki N, Berger D, Mimura Y, Frick J, Dentener MA, Buurman WA, Seidelmann M, Kaminishi M, Beger HG. Release of endotoxin-binding proteins during major elective surgery: role of soluble CD14 in phagocytic activation. *World J Surg* 2000;24:499-506
  - 37 van Oosten M, van de Bilt E, van Berkel TJ, Kuiper J. New scavenger receptor-like receptors for the binding of lipopolysaccharide to liver endothelial and Kupffer cells. *Infect Immun* 1998;66:5107-5112
  - 38 Kono H, Wheeler MD, Rusyn I, Lin M, Seabra V, Rivera CA, Bradford BU, Forman DT, Thurman RG. Gender differences in early alcohol-induced liver injury: role of CD14, NF-kappaB, and TNF-alpha. *Am J Physiol Gastrointest Liver Physiol* 2000;278:G652-661
  - 39 Jiang S, Naito M, Kaizu C, Kuwata K, Hasegawa G, Mukaida N, Shultz LD. Lipopolysaccharide-induced cytokine and receptor expression and neutrophil infiltration in the liver of osteopetrosis (op/op) mutant mice. *Liver* 2000;20:465-474
  - 40 Jiang J, Xie G, Chen Y, Liu D, Qiu J, Zhou J, Zhu P, Wang Z. Intrahepatic expression of scavenger receptor and CD14 and their relationship with local inflammatory responses in endotoxemia in mice. *Shock* 2001;16:75-80
  - 41 Liu S, Khemlani LS, Shapiro RA, Johnson ML, Liu K, Geller DA, Watkins SC, Goyert SM, Billiar TR. Protein Expression of CD14 by hepatocytes: upregulation by cytokines during endotoxemia. *Infect Immun* 1998;66:5089-5098
  - 42 Liu S, Shapiro RA, Nie S, Zhu D, Vodovotz Y, Billiar TR. Characterization of rat CD14 promoter and its regulation by transcription factors AP1 and Sp family proteins in hepatocytes. *Gene* 2000;250:137-147
  - 43 Netea MG, Kullberg BJ, van der Meer JW. Lipopolysaccharide-induced production of tumour necrosis factor and interleukin-1 is differentially regulated at the receptor level: the role of CD14-dependent and CD14-independent pathways. *Immunology* 1998;94:340-344
  - 44 Toshima K, Mochida S, Ishikawa K, Matsui A, Arai M, Ogata I, Fujiwara K. Contribution of CD14 to endotoxin-induced liver injury may depend on types of macrophage activation in rats. *Biochem Biophys Res Commun* 1998;246:731-735
  - 45 Lukkari TA, Jarvelainen HA, Oinonen T, Kettunen E, Lindros KO. Short-term ethanol exposure increases the expression of Kupffer cell CD14 receptor and lipopolysaccharide binding protein in rat liver. *Alcohol Alcohol* 1999;34:311-319
  - 46 Yin M, Ikejima K, Wheeler MD, Bradford BU, Seabra V, Forman DT, Sato N, Thurman RG. Estrogen is involved in early alcohol-induced liver injury in a rat enteral feeding model. *Hepatology* 2000;31:117-123
  - 47 Song PI, Abraham TA, Park Y, Zivony AS, Harten B, Edelhauser HF, Ward SL, Armstrong CA, Ansel JC. The Expression of Functional LPS Receptor Proteins CD14 And Toll-Like Receptor 4 in Human Corneal Cells. *Invest Ophthalmol Vis Sci* 2001;42:2867-2877
  - 48 Su GL, Rahemtulla A, Thomas P, Klein RD, Wang SC, Nanji AA. CD14 and lipopolysaccharide binding protein expression in a rat model of alcoholic liver disease. *Am J Pathol* 1998;152:841-849
  - 49 Fang W, Yao Y, Shi Z. The effect of bactericidal/permeability-increasing protein on lipopolysaccharide-binding protein and lipopolysaccharide receptor CD14 mRNA expression in rats after thermal injury. *Zhonghua Yi Xue Za Zhi* 1999;79:289-291
  - 50 Wang F, Wang LY, Wright D, Parmely MJ. Redox imbalance differentially inhibits lipopolysaccharide-induced macrophage activation in the mouse liver. *Infect Immun* 1999;67:5409-5416
  - 51 Jarvelainen HA, Orpana A, Perola M, Savolainen VT, Karhunen PJ, Lindros KO. Promoter polymorphism of the CD14 endotoxin receptor gene as a risk factor for alcoholic liver disease. *Hepatology* 2001;33:1148-1153
  - 52 Urbaschek R, McCuskey RS, Rudi V, Becker KP, Stickel F, Urbaschek B, Seitz HK. Endotoxin, endotoxin-neutralizing-capacity, sCD14, sICAM-1, and cytokines in patients with various degrees of alcoholic liver disease. *Alcohol Clin Exp Res* 2001;25:261-268



• BASIC RESEARCH •

# Multivariate regression analysis on early mortality after orthotopic liver transplantation

Ye-Ben Qian, Gui-Hua Cheng, Jie-Fu Huang

Ye-Ben Qian, Department of hepatic biliary surgery, first affiliated hospital An Hui Medical University, HeFei 230022, Anhui Province, China

Gui-Hua Cheng, Jie-Fu Huang, Organ transplantation center, first affiliated hospital, Sun Yat-Sen University of Medical Sciences, GuangZhou 510089 Guangdong Province China

Supported by clinic major project foundation of minister of health, No. 97040230

Correspondence to: Dr Ye-Ben Qian, Department of hepatic biliary surgery, first affiliated hospital An Hui Medical University, HeFei 230022, Anhui Province, China. ayqianyb@163.net  
Telephone: +86-551-5129029

Received 2001-05-30 Accepted 2001-10-26

## Abstract

**AIM: To identify the risk factors relating to early mortality after orthotopic liver transplantation.**

**METHODS: Clinical data of 37 adult patients undergoing liver transplantation were retrospectively collected and divided into two groups: the survived group (survival time  $\geq 30$  d) and the death group (survival time  $< 30$  d). The relationship between multivariate risk factors and early mortality after orthotopic liver transplantation were analyzed by stepwise logistic regression.**

**RESULTS: The survival rate was 73%. Early mortality rate was 27%. APACHE III, preoperative serum creatinine level and intraoperative bleeding quantity had a significant independent association with early mortality. ( $R=0.1841$ ,  $0.2056$  and  $0.3738$ ).**

**CONCLUSION: APACHE III, preoperative serum creatinine level and intraoperative bleeding quantity are significant risk factors relating to early mortality after orthotopic liver transplantation. To improve the recipient's preoperative critical condition and renal function and to reduce intraoperative bleeding quantity could lower the early mortality after orthotopic liver transplantation.**

Qian YB, Cheng GH, Huang JF. Multivariate regression analysis on early mortality after orthotopic liver transplantation. *World J Gastroenterol* 2002;8(1):128-130

## INTRODUCTION

In recent years, the success rates of orthotopic liver transplantation (OLT) have improved markedly as a result of rapid advances in immunosuppressions, surgical and preservation techniques. One-year survival rate after liver transplantation exceeds 80%. Orthotopic liver transplantation, as an accepted treatment for end-stage liver disease, has been widely performed in the world<sup>[1-5]</sup>. In our country, the early mortality after OLT remains relatively high and current studies have focused on the improvement of survival rate after liver transplantation<sup>[6,7]</sup>. Clinical data of 37 adult patients undergoing liver transplantation were retrospectively collected in our study. The significant risk factors relating to early mortality after OLT were analyzed and determined, which may contribute to the selection of candidate and improvement of survival in patients with liver

transplantation.

## MATERIALS AND METHODS

### Materials

Thirty-seven adult patients undergoing OLT procedures at our transplantation center from September 1993 to January 2000 were studied. The study population consisted of 32 men and 5 women with a mean age of 39.8 (range 17-64) years. The grafts were obtained from donors. Indications for liver transplantation were end-stage liver cirrhosis ( $n=9$ ), fulminant hepatic failure ( $n=8$ ), primary liver cancer ( $n=14$ ), primary sclerosing cholangitis ( $n=2$ ), Willson's disease ( $n=1$ ), polycystic liver and kidney ( $n=1$ ), hepatoma ( $n=1$ ), and cholangiocarcinoma ( $n=1$ ).

### Multiple risk factors

Thirty-seven patients were divided into two groups: survival group (survival time  $\geq 30$  d) and death group (Survival time  $< 30$  d). There were different possible risk factors relating to early mortality after liver transplantation including preoperative, intraoperative and postoperative ones. Preoperative information consisted of age, APACHE III, hepatoencephalopathy, previous abdominal surgery, serum albumin, prothrombin time (PT), serum creatinine level (Cr), serum Aspartate transaminase (AST), white blood cells counts (WBC), platelet counts (PLC) and mismatch ABO group. Intraoperative information included heat ischemic time, cold ischemic time, anhepatic time and bleeding quantity. Postoperative information included rate of acute rejection and postoperative complications rate (including biliary leakage, cytomegalovirus (CMV) infection, hepatic artery thrombosis, hydrothorax and myocardial infarction, etc).

### Statistical methods

Experimental data were presented as  $\bar{x} \pm s$  and frequency. For continuous data, independent 2-tailed t tests were used to determine whether there were significant differences between the two groups. Pearson's Chi-square statistics were used to test differences in all frequencies. Data with significant difference were entered into a stepwise logistic regression analysis. And all of the statistical calculations were performed using the SPSS (version: 9.0, Chicago, USA).

## RESULTS

Twenty-seven of the 37 adult patients survived more than one month after liver transplantation. Early survival rate was 73% while early mortality was 27%. The other 10 patients died postoperatively within 30 d and the major cause for their death were disseminated intravascular coagulation (DIC  $n=2$ ), myocardial infarction ( $n=2$ ), acute renal failure ( $n=2$ ), hepatic artery thrombosis ( $n=1$ ), cerebral bleeding ( $n=1$ ) and adult respiratory distress syndrome (ARDS) ( $n=1$ ).

Comparison between the survival group and the death group showed significant differences only in terms of age, APACHE III, serum creatinine level, PT, was PLC and intraoperative bleeding quantity, ( $P < 0.05$ , Table 1). The stepwise logistic regression were used to create the best statistical model relating to early mortality after transplantation. The factors that had significant independent

associations with early mortality after the stepwise procedure were APACHE III, serum creatinine level and intraoperative bleeding quantity, with regression coefficients of 0.1841, 0.2056 and 0.3738, respectively (Table 2).

**Table 1** Risk factors relating to early mortality after liver transplantation

| Risk factors                                   | Survival group<br>(n=27) | Death group<br>(n=10) | P value |
|------------------------------------------------|--------------------------|-----------------------|---------|
| Age(yrs)                                       | 38.3±2.5                 | 47.8±2.2              | 0.0000  |
| Previous abdominal surgery                     | 11% (3/27)               | 30% (3/10)            | 0.3130  |
| APACHE III (score)                             | 40.5±6.7                 | 63.4±12.9             | 0.0000  |
| Hepatoencephalopathy                           | 15% (4/27)               | 40% (4/10)            | 0.1712  |
| Serum creatinine level (μmol·L <sup>-1</sup> ) | 82.2±10.8                | 132.8±33.2            | 0.0000  |
| AST (nkat·L <sup>-1</sup> )                    | 97.9±18.6                | 125.8±80.5            | 0.0951  |
| Albumin (g·L <sup>-1</sup> )                   | 36.9±1.7                 | 32.7±2.9              | 0.0000  |
| TB (imol·L <sup>-1</sup> )                     | 298.3±67.9               | 314.9±87.1            | 0.5447  |
| PT /s                                          | 22.5±3.2                 | 25.5±3.7              | 0.0175  |
| WBC/ (×10 <sup>9</sup> ·L <sup>-1</sup> )      | 7.3±1.2                  | 6.8±1.1               | 0.2351  |
| PLC / (×10 <sup>9</sup> ·L <sup>-1</sup> )     | 129.5±17.5               | 53.4±12.3             | 0.0000  |
| Dismatch ABO group                             | 7.3% (2/27)              | 30% (3/10)            | 0.1102  |
| Heat ischemic time /min                        | 3.8±0.1                  | 3.9±0.3               | 0.1478  |
| Cold ischemic time /s                          | 464.9±26.9               | 471.2±46.3            | 0.6104  |
| Anhepatic time/s                               | 87.5±4.9                 | 90.3±10.5             | 0.2704  |
| Intraoperative bleeding quantity /ml           | 5615.1±1003.7            | 12263.6±3606.1        | 0.0000  |
| Rate of acute rejection                        | 18% (5/27)               | 20% (2/10)            | 1.0000  |
| Rate of postoperative complications            | 59% (16/27)              | 70% (7/10)            | 0.709   |

**Table 2** Stepwise logistic regression analysis

| Variable                         | B      | SE     | Wald   | df | Sig    | R      |
|----------------------------------|--------|--------|--------|----|--------|--------|
| APACHE III                       | 0.340  | 0.0141 | 5.8481 | 1  | 0.0156 | 0.1841 |
| Serum creatinine level (Cr)      | 3.6542 | 1.4013 | 6.8002 | 1  | 0.0091 | 0.2056 |
| Intraoperative bleeding quantity | 2.0194 | 0.7516 | 7.2182 | 1  | 0.0020 | 0.3738 |

## DISCUSSION

Orthotopic liver transplantation is a treatment for end-stage liver disease. Early mortality was below 10%<sup>[8,9]</sup>, which remains high in our country. The serious preoperative condition of recipient and the late timing for operation may account for this result<sup>[10,11]</sup>. A number of investigators have examined the factors associated with outcome after liver transplantation including PT, APACHE III and so on<sup>[12-16]</sup>. In our study, 10 of 37 patients died postoperatively, with an early mortality of 27%. After analyzed with stepwise logistic regression, APACHE III, preoperative serum creatinine level (Cr) and intraoperative bleeding quantity showed significant associations with early mortality after liver transplantation.

While APACHE III score is a best predictor of mortality<sup>[17,18,19]</sup>, APACHE III that results from the addition of 3 groups of variables (acute physiology, age and chronic health) consists of multiple organ function evolution, including heart, lung, liver, kidney, brain, etc. It is more accurate than APACHE III. And now it has been widely used to evaluate the severely ill in patients' condition and to predict the mortality of patients<sup>[20,21]</sup>. In our study, the APACHE III score was 40.5±6.7 and 63.4±12.9 in the survival group and the death group respectively. There was a statistical difference between the two groups in APACHE III score,  $P < 0.001$ . The stepwise logistic regression analysis showed a significant independent association with early mortality after transplantation, with a regression coefficient of 0.1841. As one of the main risk factors, it can act as a reference index of the selection of recipient and timing for operation. However because it is not specific to liver function, it needs combination with other indexes when used to predict outcome of OLT.

Renal dysfunction is a common dangerous complication in patients with end-stage liver disease. It results from acute tubular necrosis and caused by hepatorenal syndrome<sup>[22-25]</sup>. Gunning<sup>[26]</sup> reported a significant decrease of 43% in glomerular filtration rate (GFR) during transplantation in patients with normal renal function. Both high preoperative serum creatinine level and intraoperative venovenous bypass can lead to renal hemodynamic instability during operation<sup>[27,28,29]</sup>. The postoperative nephrotoxic immunosuppressions can also contribute to the irreversible renal insufficiency, leading to renal failure after liver transplantation<sup>[30,31]</sup>. In our study, 2 of 10

patients died of renal failure, who were all along with high preoperative serum creatinine level and hepatorenal syndrome before transplantation. A significant difference was found between the survival group and the death group was shown in serum creatinine level ( $P < 0.001$ ), with a mean of 82±11 and 133±33, respectively. The stepwise logistic regression analysis, it also showed a statistical independent association with early mortality after liver transplantation, with a regression coefficient of 0.2056. It is also a main risk factor which predicts early mortality after OLT. It is very important to correct renal malfunction before transplantation. How to prevent and treat renal failure Kuse<sup>[32]</sup> reported that Urotilatin can treat acute renal failure following OLT. Gonwa and the other investigators<sup>[33-36]</sup> reported that renal failure need dialysis. Our principles were to avoid using nephrotoxic treatments and drugs, to maintain stable hemodynamically and monitor central venous pressure, to use small dose of Dopamine (2-5 μg·kg<sup>-1</sup>·min<sup>-1</sup>) and Procaine to dilate renal artery and protect renal function, to use diuretics appropriately, to perform hemodialysis properly performed if needed, and not to use Alprostadil (PGE<sub>1</sub>)<sup>[37]</sup>.

Intraoperative bleeding quantity is the third important risk factor relating to early mortality after liver transplantation<sup>[38]</sup>. If it exceeded 1000ml, mortality was very high. The intraoperative bleeding quantity of the death group was more than that of the survival group statistically ( $P < 0.05$ ), with a mean of 12264±3606mL and 5615±1004mL respectively. Logistic regression analysis showed a significant relationship between intraoperative bleeding quantity and early mortality after transplantation, with a regression coefficient of 0.3738. Severe bleeding and a large amount of transfusion during operation may lead to hemodynamic instability and DIC. And long-term hypoplasia may accelerate preoperative renal insufficiency, leading to irreversible renal failure, and increasing the early mortality after operation<sup>[39,40]</sup>. Intraoperative severe bleeding may due to previous upper abdominal surgery, abdominal extensive adhesions, portal hypertension, splenic hyperfunction, severe coagulation disorders, etc.<sup>[41-44]</sup> In our study, there was no significant difference between the two groups with previous surgical histories. But it should be emphasized that some of our findings might be accidental because of insufficient cases involved in the study. We should pay attention to these patients with previous surgical histories. In these patients, severe bleeding and coagulation disorders may occur during operation because of abdominal extensive adhesions and difficulties in sequestration and ligation, consequently DIC and acute renal failure may follow. In our centre, 2 patients developed DIC.

The other risk factors showed no significant associations with early mortality after liver transplantation. But some of the factors did influence the outcome of the recipients and should be considered carefully, including mismatch ABO group, heat ischemic time, cold ischemic time, rate of acute rejection, rate of postoperative complications, etc.<sup>[45-51]</sup>. Except emergent cases, the recipients and the donors were matched in ABO group at our center. Heat ischemic time and cold ischemic time were also limited strictly within 5 min and 12 h respectively during operation. After transplantation, ultrasonography B, chest X-ray examination, CMV detection and liver biopsy were performed periodically. Acute rejection and other postoperative complications were diagnosed and treated earlier. In patients diagnosed as having acute rejection, a large dose of methylprednisolone and FK506 were administered with a treatment rate of 100%. Therefore, these risk factors showed no significant value in statistical analysis in our study.

## REFERENCES

- Starzl TE, Demetris AJ. Liver transplantation: a 31-year perspective. *Curr Probl Surg* 1990; 27:55-106
- Bismuth H, Farges O, Castaing D, Samuel D, Adam R, Johann M, Azoulay D, Feray C, Astarciglu I, Saliba F. Evaluation of results of liver transplantation: Experience based on a series of 1052 transplantation. *Presse Med* 1995; 24:1106-1110

- 3 Parrilla P, Sanchez-Bueno F, Figueras J, Jaurrieta E, Mir J, Margarit C, Lazaro J, Herrera L, Gomez-Fleitas M, Varo E, Vicente E, Robles R, Ramirez P. Analysis of the complications of the piggy-back technique in 1,112 liver transplants. *Transplantation* 1999; 67: 1214-1217
- 4 Ryckman FC, Alonso MH, Bucuvalas JC, Balistreri WF. Long-term survival after liver transplantation. *J Pediatr Surg* 1999; 34: 849-850
- 5 Goss JA, Shackleton C, Farmer D, Amout W, Seu P, Markowitz J, Martin P. Orthotopic liver transplantation for primary sclerosing cholangitis-a 12 year, single-center experience. *Ann Surg* 1997; 225: 472-481
- 6 Xia SuiSheng. Current status of liver transplantation in China. *Shijie Huaren Xiaohua Zazhi* 1999;7:645-646
- 7 Huang Jiefu. Organ transplantation in china: current status and strategy. *ZhongHua Waike Zazhi* 1999; 37:535-537
- 8 Doyle HR, Marino IR, Jabbour N,Zetti G, McMichael J, Mitchell S, Fung J, Starzl TE. Early death or retransplantation in adults after orthotopic liver transplantation. *Transplantation* 1994; 57:1028-1036
- 9 Deschenes M, Belle SH, Krom RA, Zetterman RK, Lake JR. Early allograft dysfunction after liver transplantation. *Transplantation* 1998; 66: 302-310
- 10 Chung SW, Kirkpatrick AW, Kim HL, Scudamore CH, Yoshida EM. Correlation between physiological assessment and outcome after liver transplantation. *Am J Surg* 2000; 179: 396-399
- 11 Spanier TB, Klein RD, Nasraway SA, Rand WM, Rohrer RJ, Freeman RB, Schwaitzberg SD. Multiple organ failure after liver transplantation. *Crit Care Med* 1995; 23: 466-473
- 12 Baliga P, Merion RM, Turcotte JG, Ham JM, Henley KS, Lucey MR, Schork A, Yushyr R, Campbell DA Preoperative risk factor assessment in liver transplantation. *Surgery* 1992; 112:704-711
- 13 Cillo U, Tedeschi U, Carraro P, Burra P, Varagnolo M, Ambrosino G, Cionfoli M, Brolese A,Borin L, Zanus G. Early predictive markers of irreversible graft dysfunction After liver transplantation. *Transplant Proc* 1994; 26: 3599-3601
- 14 Bein T, Frhlich D, Pmsl J, Forst H, Pratschke E. The predictive value of four scoring systems in liver transplant recipients. *Intensive Care Med* 1995; 21: 32-37
- 15 Clavien PA, Camargo CA, Croxford R, Langer B, Levy GA, Greig PD. Definition and classification of negative outcomes in solid organ transplantation. Application in liver transplantation. *Ann Surg* 1994; 220: 109-120
- 16 Ricci P, Therneau TM, Malinchoc M, Benson JT, Petz JL, Klintmalm GB, Crippin JS. A prognostic Model for the outcome of liver transplantation in patients with cholestatic liver disease. *Hepatology* 1997; 25: 672-677
- 17 Angus DC, Clermont G, Kramer DJ, Linde-Zwirble WT, Pinsky MR. Short-term and long-term outcome prediction with the Acute Physiology and Chronic Health Evaluation II system after orthotopic liver transplantation. *Crit Care Med* 2000; 28:150-156
- 18 Sawyer RG, Durbin CG, Rosenlof LK, Pruett TL. Comparison of APACHE II scoring in liver and kidney transplant recipients versus trauma and general surgical patients in a single intensive-care unit. *Clin Transplant* 1995;9:401-405
- 19 Bein T, Forst H, Pratschke E. Apache-II-scoring in the liver transplant recipient. *Intensive Care Med* 1992; 18:60-61
- 20 Knaus WA, Wagner DP, Draper EA, Zimmerman JE, Bergner M, Bastos PG, Sirio CA, Murphy D, Tedlotring MS, Damiano A MS, Harrell. The APACHE c6 prognostic system risk prediction of hospital mortality for critically hospitalized adults. *Chest* 1991; 100:1619-1636
- 21 Bernal W, Wendon J, Rela M, Heaton N, Williams R. Use and outcome of liver transplantation in acetaminophen-induced acute liver failure. *Hepatology* 1998; 27:1050-1055
- 22 Fraley DS, Burr R, Bernardini J, Angus D, Kramer DJ, Johnson JP. Impact of acute renal failure on mortality in end-stage liver disease with or without transplantation. *Kidney Int* 1998; 54:518-522
- 23 Alvares-da-Silva MR, Waechter FL, Francisconi CF, Barros E, Thome F, Traiber C, Fonseca DL, Zingani JM,Sampaio JA, Pinto RD, Pereira-Lima L. Risk factors for postoperative acute renal failure at a new orthotopicliver transplantation program. *Transplant Proc* 1999; 31: 3050-3052
- 24 Palapattu GS, Barbaric Z, Rajfer J.Acute bilateral renal cortical necrosis as a cause of postoperative renal failure. *Urology* 2001; 58:281
- 25 Kes P. Hepatorenal syndrome: new perspectives in pathophysiology and management. *Acta Med Croatica* 2000; 54:165-173
- 26 Gunning TC, Brown MR, Swygert TH, et al. Perioperative renal function in patients undergoing orthotopic liver transplantation. *Transplantation* 1991; 51: 422-427
- 27 Lafayette RA, Paré G, Schmid CH, King AJ, Rohrer RJ, Nasraway SA. Pretransplant renal dysfunction predicts poorer outcome in liver transplantation. *Clin Nephrol* 1997; 48:159-164
- 28 Thomas G, Kelly D, Norris S, Crosby O, Hegarty J, Crowley K, McEntee G, Traynor O, Watson A, Keogh B Acute renal failure in orthotopic liver transplantation. *Ir J Med Sci* 1996; 165:271-273
- 29 Pascual E, Gomez-Arnau J, Pensado A, de la Quintana B, Carrera A, Arribas MJ, Garcia-Guiral M, Cuervas- Mons V. Incidence and risk factors of early acute renal failure in liver transplant patients. *Transplant Proc* 1993; 25:1837
- 30 Platz KP, Mueller AR, Blumhardt G, Bachmann S, Bechstein WO, Kahl A, Neuhaus P. Nephrotoxicity following orthotopic liver transplantation. A comparison between cyclosporine and FK506. *Transplantation* 1994; 58:170-178
- 31 Van Buren D, Payne J, Geevarghese S, MacDonell R, Chapman W, Wright JK, Helderma JH, Richie R, Pinson CW. Renal function in primary liver transplant recipients receiving neoral (cyclosporine) versus prograf (tacrolimus). *Transplant Proc* 1998; 30:1401-1402
- 32 Kuse ER, Meyer M, Constantin R, Oldhafer K, Schlitt HJ, Schulz-Knappe P, Uberbacher HJ, Pichlmayr R, Forssmann WG. Urodelatin (INN: ularitide). A new peptide in the treatment of acute kidney failure following liver transplantation. *Anaesthesist* 1996; 45:351-358
- 33 Gonwa TA, Mai ML, Melton LB, Hays SR, Goldstein RM, Levy MF, Klintmalm GB.Renal replacement therapy and orthotopic liver transplantation: the role of continuous veno-venous hemodialysis. *Transplantation* 2001; 71:1424-1428
- 34 L'htkes P, Lutz J, Loock J, Daul A, Broelsch C, Philipp T, Heemann U. Continuous venovenous hemodialysis treatment in critically ill patients after liver transplantation. *Kidney Int Suppl* 1999;72:S71-74
- 35 Richardson D. Dialysis in non-renal organ (liver) transplantation. *Nephron* 2001;88:296-306
- 36 Morales JM. Management and prevention of acute renal failure in solid organ transplantation. *Ren Fail* 1996; 18:481-488
- 37 Manasia AR, Leibowitz AB, Miller CM, Silverstein JH, Schwartz M, Delguidice R, Vallabhajosula S, Oropello JM, Benjamin E. Postoperative intravenous infusion of alprostadil (PGE1) does not improve renal function in hepatic transplant recipients. *J Am Coll Surg* 1996; 182:347-352
- 38 Nasraway SA, Klein RD, Spanier TB, Rohrer RJ, Freeman RB, Rand WM, Benotti PN. Hemodynamic correlates of outcome in patients undergoing orthotopic liver transplantation. Evidence for early post-operative myocardial depression. *Chest* 1995;107:218-224
- 39 Bilbao I, Charco R, Balsells J, Lazaro JL, Hidalgo E, Llopart L, Murio E, Margarit C. Risk factors for acute renal failure requiring dialysis after liver transplantation. *Clin Transplant* 1998; 12:123-129
- 40 Bartosh SM, Alonso EM, Whittington PF. Renal outcomes in pediatric liver transplantation. *Clin Transplant* 1997; 11:354-360
- 41 Cacciarelli TV, Esquivel CO, Moore DH, Cox KL, Berquist WE, Concepcion W, Hammer GB, So SKS.Factors affecting survival after liver transplantation in Infants. *Transplantation* 1997;64:242-248
- 42 Neuberger J, Gunson B, Komolmit P, Davies MH, Christensen E. Pretransplant prediction of prognosis after liver Transplantation in primary sclerosing cholangitis using a Cox regression model. *Hepatology* 1999;29:1375-1379
- 43 Gonzalez FX, Rimola A, Grande L, Antolin M, Garcia-Valdecasas JC, Fuster J, Lacy AM,Cugat E, Visa J, Rodes J. Predictiver factors of early postoperative graft function in human liver transplantation. *Hepatology* 1994;20:565-573
- 44 Wong T, Devlin J, Roland N, Heaton N, Williams R. Clinical characteristics affecting the outcome of liver transplantation. *Transplantation* 1997;64878-64888
- 45 Lo CM, Shaked A, Busuttil RW. Risk factors liver transplantation across the ABO barrier. *Transplantation* 1994; 58: 543-548
- 46 Figuras J, Busquets J, Grande L, Jaurrieta E, Perez-Ferreiroa J, Mir J, Margarit G, Loper P, Vazquez J, Casanova D, Bernardos A, De-Vicente E, Parrilla P, Ramon JM, Bou R. The deleterious effect of donor hight plasma sodium and extended preservation in liver transplantation. A multivariate analysis. *Transplantation* 1996;61:410-413
- 47 Chavez-Cartaya R, Rasmussa A, Tokat Y, Jamieson NV. Effect of preservation time on early graft function And outcome of orthotopic liver transplants. *Transplant Proc* 1995;27:724
- 48 Strasberg SM, Howard TK, Molmenti EP, Hretl M. Selecting the door live, risk factors for poor function after orthotopic liver transplantation. *Hepatology* 1994;20:829-838
- 49 Garcia S, Roque J, Ruza F, Gonzalez M, Madero R, Alvarado F, Herruzo R. Infection and associated risk factors in the immediate postoperative period of pediatric liver transplantation: a study of 176 transplants. *Clin Transplant* 1998; 12:190-197
- 50 Doyle HR, Morelli F, Mc Michael J. Hepatic retransplantation: an analysis of risk factor associated with outcome. *Transplantation* 1996; 61: 1499-1505
- 51 Goss JA, Shackleton CR, McDiarmid SV. Long-term results of pediatric liver transplantation. An analysis of 569 transplants. *Ann Surg* 1998; 228:411-420

• REVIEW •

# The management of patients with the short bowel syndrome

Cameron F. E. Platell, Jane Coster, Rosalie D. McCauley, John C. Hall

Cameron F. E. Platell, Jane Coster, Rosalie D. McCauley, John C. Hall, Department of Surgery, The University of Western Australia, Perth, Australia

Correspondence to: Dr. Cameron Platell, University Department of Surgery, Fremantle Hospital. cplatell@cyllene.uwa.edu.au

Telephone: +8-9-431 2500 Fax: +8-9-431 2623

Received 2001-10-21 Accepted 2001-11-25

## Abstract

**The surgeon is invariably the primary specialist involved in managing patients with short bowel syndrome. Because of this they will play an important role in co-ordinating the management of these patients. The principal aims at the initial surgery are to preserve life, then to preserve gut length, and maintain its continuity. In the immediate postoperative period, there needs to be a balance between keeping the patient alive through the use of TPN and antisecretory agents and promoting gut adaptation with the use of oral nutrition. If the gut fails to adapt during this period, then the patient may require therapy with more specific agents to promote gut adaptation such as growth factors and glutamine. If following this, the patient still has a short gut syndrome, then the principal options remain either long term TPN, or intestinal transplantation which remains a difficult and challenging procedure with a high mortality and morbidity due to rejection.**

Platell CFE, Coster J, McCauley RD, Hall JC. The management of patients with the short bowel syndrome. *World J Gastroenterol* 2002;8(1):13-20

## INTRODUCTIONS

A remarkable feature of the gastrointestinal tract is how little of it we require in order to maintain a normal nutritional state. Nonetheless, there is a small group of patients who, following extensive loss of principally the small intestine, are unable to maintain their nutrition by oral intake alone. These patients are defined as having the short bowel syndrome.

The pathophysiological consequences of loss of the bowel is dependent upon two important points. Firstly, the extent and site of the intestinal resection, and secondly, the adaptability of the remaining intestine. In general, we need 50 to 70 cm (i.e. around 1 cm/kg weight) of healthy jejunum or ileum in continuity with a section of the colon in order to avoid developing the short bowel syndrome. This is remarkable considering that the normal human small intestine ranges from about 3 to 5 metres in length. Some have defined short bowel syndrome as the loss of 70% or more of the length of the small intestine<sup>[1]</sup>. But length is not everything, and if the remaining bowel is involved with the underlying disease process (e.g. Crohn's disease or ischaemia) then its capacity to adapt will be limited. The minimum amount of small intestinal absorptive area required to sustain life varies from individual

to individual. Survival on an oral diet alone may occur in patients with as little as 15 cm of residual jejunum.

This review addresses the medical and surgical management of patients with short bowel syndrome. Particular emphasis is placed on the conduct of the initial surgical procedure and the therapies that may either constitute definitive methods of treatment or serve as useful adjuncts to other forms of surgery. The latter consisting of autologous gastrointestinal reconstruction and small bowel transplantation.

## INITIAL SURGICAL PROCEDURE

The causes of short bowel syndrome differ between adults and children. In adults, it most often results after surgery for Crohn's disease or mesenteric infarction. Whilst in infants, the causes more commonly include necrotizing enterocolitis, gastroschisis, atresia, and volvulus<sup>[2-4]</sup>.

It goes without saying that it is important to preserve as much of the small and large intestine as possible at the initial surgery. However, the subsequent patient progress will depend on not only the length of gut removed, but on whether the patient has a primary anastomosis or a stoma. Nightingale<sup>[5]</sup> has classified patients with short bowel syndrome into two groups: those with a primary jejunocolic anastomosis, and those with a jejunostomy. The latter have major problems with losses of water, sodium, and divalent cations such as magnesium; whereas, patients with a jejunocolic anastomosis rarely have problems with their fluid and electrolyte balance. Maintaining colonic continuity serves to decrease gastric emptying and decreases energy/carbohydrate losses. Nonetheless, if a surgeon is concerned regarding the risk of performing a primary anastomosis for fear of an anastomotic dehiscence, then it is safer to consider a primary stoma with reconstruction delayed for 2-3 mo. Although this can create its own problems of leaving *in situ* a segment of excluded gut. Careful consideration should be given to the siting of stomas. It may be advantageous to have an end stoma in close proximity to a mucus fistula.

Preservation of colonic length is not only important for the absorption of fluid and electrolytes, as has been discussed, but it also has nutritional advantages. Patients with the short bowel syndrome have malabsorption of carbohydrates, even after the ingestion of small amounts of otherwise easily absorbed carbohydrates, and this causes a spill-over of the ingested carbohydrates into the residual colon where it undergoes bacterial fermentation<sup>[6]</sup>.

Jeppesen and Mortensen<sup>[7]</sup> have noted that colonic digestion can salvage up to 3-4 MJ/d<sup>-1</sup> in patients with the short bowel syndrome, which is about 50% of the daily requirements. They observed that preservation of more than one-half of colonic function is unusual in patients who require parenteral nutrition and have more than 100 cm of residual small bowel. This data reinforces the concept of the colon as an energy-salvaging organ.

Excluded gut may act as a reservoir for bacterial translocation and recurrent sepsis<sup>[8]</sup>. Defunctioned gut is

associated with mucosal atrophy and bacterial overgrowth that predispose to bacterial translocation. Reynolds *et al*<sup>[8]</sup>, reported a case where a patient with excluded bowel suffered episodes of clinical deterioration, fever and rigors without isolation of bacteria from blood cultures. It is possible that these episodes may have been the result of migration of viable bacteria from the excluded gut lumen into the mesenteric lymph system and peritoneum. In this situation pathogenic organisms cannot be cultured from the blood but may be isolated from the peripheral lymph nodes. Schafer *et al*<sup>[9]</sup>, reviewed the progress of newborns who had stomas created during surgery for a mechanical ileus or intrauterine perforation of the small bowel. To avoid non-use of the distal bowel, they used a roller pump to pass the effluent from the end enterostomy into the distal bowel through the mucus fistula. They reported that this enabled subsequent re-anastomosis to be performed under optimum bowel conditions. Al-Harbi *et al*<sup>[10]</sup>, described a similar experience in six neonates (gestational ages of 27-38 wk, birth mass of 533-3400g). Mass gain during refeeding ranged from 5 to 25g·kg<sup>-1</sup>·d<sup>-1</sup> with the refeeding lasting for 16-169 d. It was concluded that this technique lessens the need for parenteral nutrition and electrolyte supplementation prior to reanastomosis.

## NATURAL HISTORY OF GUT ADAPTATION

Intestinal failure associated with the short bowel syndrome

may be either transient or permanent. Most patients require nutritional support until their gut has undergone sufficient adaptation to allow survival on an oral diet. Results from animal studies have shown that structural adaptation of the remnant bowel involves both an increase in villous height and mucosal surface area, and an increase in bowel luminal circumference and wall thickness. Functional adaptation is characterised by an increase in rate of absorption of nutrients. This is postulated to be the result of structural change, a slowing of transit rate and/or alterations in intracellular molecular events such as increased transport and/or enzyme activity.

The intestinal mucosa produces several peptides that have a trophic effect upon the intestine (Table 1). Following small bowel resection the rate of secretion of these peptides increases in an attempt to compensate for the missing tissue. Recently, Nightingale<sup>[17]</sup> has discussed the role of one of these peptides, glucagon-like peptide-2 (GLP-2), in intestinal adaptation. L cells, located in the ileum and jejunum, secrete GLP-2. Nightingale noted that, in patients without an ileum, intake of a meal does not alter plasma GLP-2 concentration and that remnant jejunum of these patients does not adapt<sup>[18,19]</sup>. In contrast, intake of a meal induces an increase in plasma GLP-2 concentrations in ileal resected patients with a retained colon and remnant jejunum of these patients does adapt<sup>[20,21]</sup>. Collectively, these pieces of information suggest GLP-2 may be useful in adjunctive therapy for short bowel syndrome.

**Table 1** The effect of small bowel resection on intestinal peptides that are known regulate intestinal growth

| Factor                               | Source                                                         | Effect of Small Bowel Resection on Factor                                                                                                                                                                                                                                                           |
|--------------------------------------|----------------------------------------------------------------|-----------------------------------------------------------------------------------------------------------------------------------------------------------------------------------------------------------------------------------------------------------------------------------------------------|
| Epidermal Growth                     | Salivary glands and Brunner's glands in the jejunum            | EGF levels are increased in saliva and diminished in urine 3 d after resection in mice <sup>[11]</sup> .                                                                                                                                                                                            |
| Factor (EGF)                         |                                                                |                                                                                                                                                                                                                                                                                                     |
| Enteroglucagon                       | L cells of ileum and colon                                     | 12 d after a 75% small bowel resection there was a significant increase in concentration of enteroglucagon in the plasma of rats <sup>[12]</sup> .                                                                                                                                                  |
| Glucagon-like Peptide 2 (GLP-2)      | L cells of ileum and colon                                     | There is an increase in expression of GLP-2 mRNA in the ileum of rats after small bowel resection <sup>[13]</sup> .<br><br>There is a decrease in expression of dipeptidyl peptidase IV mRNA, the enzyme that inactivates GLP-2, in the ileum of rats after small bowel resection <sup>[14]</sup> . |
| Insulin-like Growth factor-I (IGF-1) | Cells of the small intestine                                   | 80% small bowel resection led to a 183% and 249% increase in IGF-1 mRNA in the jejunum and ileum respectively of rats <sup>[15]</sup> .                                                                                                                                                             |
| Peptide tyrosine tyrosine (PYY)      | L cells of ileum                                               | After 70% resection in rats the concentration of PYY in plasma was elevated for at least 2 wk and there was a four and six-fold increase in PYY mRNA in ileum and colon at six hours after resection <sup>[14]</sup> .                                                                              |
| Neurotensin                          | Gut mucosal endocrine cells (N cells) in the jejunum and ileum | 50% resection of the distal intestine in dogs was associated with a transient increase in neurotensin <sup>[16]</sup> .                                                                                                                                                                             |

## INITIAL SUPPORTIVE MANAGEMENT

The aim of supportive care of patients is to maintain nutritional state and promote gut adaptation.

### Parenteral nutrition

An important historical use of parenteral nutrition was in keeping patients with short bowel syndrome alive both in the short and long term. The decision to commence parenteral therapy is based on a number of issues. These include, the extensive loss of gut where the clinician believes the patient will be unable to maintain their own nutrition, or where in the post operative period, the patient is unable to maintain their weight and plasma albumin concentration via oral intake alone. Once parenteral nutrition is commenced, for most patient, there follows a period of gradual transition to enteral nutrition and diet therapy.

The use of parenteral nutrition is associated with a number of side effects. Parenteral nutrition has been found to cause intestinal atrophy in humans and animals<sup>[22-24]</sup> and long-term parenteral nutrition is associated with complications that

include recurring central venous line sepsis, high costs (Aus \$ 150·d<sup>-1</sup>), high mortality (20% in children, mainly due to liver dysfunction) and poor quality of life.

In children with short-bowel syndrome receiving long-term parenteral nutrition, hepatic dysfunction is a major problem. Its aetiology is multifactorial and includes alterations in gut motility which lead to intraluminal stasis which is thought to be a major etiologic factor for bacterial overgrowth and subsequent cholestasis, especially when the ileocecal valve is absent. Sondheimer *et al*<sup>[25]</sup>, reported that 67% of neonates with short bowel syndrome which were nourished by parenteral nutrition developed cholestasis. This progressed to liver failure in 17% of the neonates. As cholestasis developed shortly after the first infection in 90 % of infants<sup>[25]</sup> it seems sepsis may sensitize the liver to cholestatic injury. In spite of the problems associated with parenteral nutrition, Suita *et al*<sup>[26]</sup>, have commented that advances in parenteral nutrition have meant that infants with a small bowel measuring only 20 cm either with or without an ileocecal valve can survive. However, patients do best in the presence of an ileocecal valve and an intact colon<sup>[27]</sup>.



### Medical Therapy

High-volume output from a jejunostomy requires restriction of oral fluids, a high-energy iso-osmolar diet with added salt, and the use of drugs that reduce motility (loperamide, codeine phosphate) and secretions (proton pump inhibitors, octreotide). Nightingale<sup>[5]</sup> has stressed that patients who have less than 100 cm of jejunum *in situ* and a stomal output in excess of their oral intake have the most to gain from the use of antisecretory drugs. This is because they usually lose more from the jejunostomy than they take in orally ('secretors') and are more likely to require long-term parenteral therapy. Yet Octreotide reduces nutrient transport in the small intestine, reduces the number of functional nutrient carriers, and is in general detrimental to gut adaptation. Hence its use in all patients with short bowel syndrome is not indicated.

Gastric hyperacidity is a frequently observed change which occurs transiently in the postoperative period following a massive bowel resection. Unless it is controlled with either proton pump inhibitors or H2 receptor blockers, it may result in extensive gastric or duodenal ulceration.

### Enteral nutrition

Enteral nutrition is a key element in promoting the intestinal

hyperplasia which is characteristic of gut adaptation. It does this by several mechanisms. Enteral nutrition provides epithelial work and stimulates the release of pancreatico-biliary secretions that are known to maintain the structure and function of the intestine. Food within the intestine also stimulates the release of various regulatory peptides from the intestine and can deliver specific nutrients to the cells of the intestinal mucosa.

There are a number of specific gut nutrients that are important in adaptation (Table 2). These nutrients promote intestinal structure and function by providing cells of the intestinal mucosa with substrates for the synthesis of essential molecules or by providing energy. For example, polyamines, small molecules that are essential for cell growth and regulation of the cell cycle, are synthesised from ornithine. Whereas, fermentable fibres and their products (i.e. short chain fatty acids) are important fuels for enterocytes. Glutamine is another important gut nutrient that promotes intestinal adaptation. This amino acid is the main fuel of enterocytes and also is a substrate for the synthesis of nucleic acids<sup>[34]</sup>. The information presented in Table 2 indicate that supplements of glutamine only promote adaptation in parenterally-fed animals. This suggests that supplements of glutamine can only enhance intestinal adaptation in the absence of epithelial work.

**Table 2** Nutrients that regulate gut adaptation

| Nutrient                                  | Effect on Intestinal Adaptation                                                                                                                                                                                                                                                                                                                                                                                                                                                                                                                                                                                                                                                                                                                                                                                                             |
|-------------------------------------------|---------------------------------------------------------------------------------------------------------------------------------------------------------------------------------------------------------------------------------------------------------------------------------------------------------------------------------------------------------------------------------------------------------------------------------------------------------------------------------------------------------------------------------------------------------------------------------------------------------------------------------------------------------------------------------------------------------------------------------------------------------------------------------------------------------------------------------------------|
| Soluble fibre and short chain fatty acids | SCFA-supplemented parenteral nutrition led to an increase in ileal uptake of D-glucose in rats with an 80% small bowel resection <sup>[28]</sup> .                                                                                                                                                                                                                                                                                                                                                                                                                                                                                                                                                                                                                                                                                          |
| Triglycerides                             | A 2% pectin-enriched elemental diet led to a significant increase in intestinal weight, mucosal protein content, and mucosal DNA content in rats with an 80% small bowel resection <sup>[29]</sup> .<br>Rats fed with an elemental diet containing 60% long chain triglycerides after a 60% resection had a greater intestinal adaptation than rats fed a diet containing 17% long chain triglycerides <sup>[30]</sup> .                                                                                                                                                                                                                                                                                                                                                                                                                    |
| Ornithine<br>$\alpha$ -ketoglutarate      | Enteral supplements of ornithine 2g.kg <sup>-1</sup> .d <sup>-1</sup> significantly increased jejunal crypt depth ratio and significantly increased glutamine concentration in anterior tibialis muscle <sup>[31]</sup> .<br>Enteral supplements of ornithine 1g.kg <sup>-1</sup> .d <sup>-1</sup> significantly increased ileal villus height and expression of ornithine decarboxylase mRNA in the ileum <sup>[32]</sup> .                                                                                                                                                                                                                                                                                                                                                                                                                |
| Glutamine                                 | In rats with an 85% small bowel resection, feeding a 2% glutamine-enriched TPN solution, enhanced intestinal adaptation as assessed by mucosal villus height, and mucosal DNA content <sup>[33]</sup> .<br>A glutamine-enriched diet enhanced ileal hyperplasia in rats with an 80% small bowel resection <sup>[34]</sup> .<br>In rats with a 70% small bowel resection, feeding a 5% glutamine-enriched rats chow diet inhibited intestinal adaptation as assessed by duodenal protein content and ileal DNA content <sup>[35]</sup> .<br>A 2% glutamine-enriched elemental diet did not alter markers of intestinal adaptation in rats with a massive small bowel resection <sup>[36]</sup> .<br>A 4% glutamine-enriched oral diet did not significantly alter intestinal adaptation after intestinal resection in rats <sup>[37]</sup> . |

There are a number specific gut peptides which mediate the trophic effect of gut nutrients. Glucagon-like peptide-2, which is released by the intestinal L cells, plays a role in the trophic effect of short chain fatty acids (SCFA) on intestinal adaptation. Treatment of rats with SCFA leads to an increase in expression of proglucagon mRNA, a precursor of GLP-2, in the L-cells<sup>[28,39]</sup>. Furthermore, Vanderhoof *et al*<sup>[30]</sup> speculated that slower absorption of long chain triglycerides allows them to stimulate release of intestinal regulatory peptides, such as GLP-2 and PYY, from L-cells in the ileum. There also may be links between glutamine and PYY as a glutamine-enriched oral diet led to an increase in concentration of PYY in the portal blood after small bowel resection in a rat model<sup>[40]</sup>.

Epithelial work is important for gut adaptation. Clarke<sup>[41]</sup> used a rat model to examine the effect of epithelial work on the structure of the intestine. Isotonic solutions of either glucose, galactose, sodium chloride, *D*-methyl *D*-glucoside, or *D*-mannose were infused into surgically prepared sacs of upper small intestine in rats which fed normally via the gut-in-continuity. Treatment with the glucose, a nutrient and galactose and  $\alpha$ -methyl *D*-glucoside, molecules with no nutritional value, led to an increase in villus height. In

addition, treatment with sodium chloride, a molecule that is absorbed by the intestinal mucosa, also led to an increase in villus height.

Age may influence intestinal adaptation as pediatric patients undergo better bowel adaptation than adults. Wasa *et al*<sup>[42]</sup> reviewed 12 pediatric and 18 adult patients with short bowel syndrome from Osaka University Hospital. The length of the residual small intestine ranged from 0 to 75 cm (mean 47 cm) in pediatric patients and from 0 to 150 cm (mean 47 cm) in adult patients. Eight pediatric patients (67%) and 4 adult patients (22%) were weaned from TPN. None of the adult patients with residual small intestinal length less than 40 cm could achieve complete intestinal adaptation.

A number of specific oral nutritional regimens have been evaluated to assess their ability to promote gut adaptation. The provision of oral medium-chain triglycerides increases the absorption of energy in patients with short bowel syndrome who have a functioning colon<sup>[43]</sup>. Short-chain fatty acids are readily absorbed across the colonic mucosa, whereas long-chain fatty acids are not absorbed by the colon. Hence, patients with a short bowel syndrome and a functioning colon are able to absorb both short-chain and medium-chain C8-C10

triglycerides. Part of their efficacy in this role relates to the fact that both of these types of fat are water-soluble. Manipulation of the dietary fat intake has little appreciable advantage in patients without a functioning colon<sup>[44]</sup>. Sales *et al*<sup>[45]</sup> reported on four patients, aged 40 - 65 years, with on average 54.5 cm of remaining bowel, who were managed with a progressive step diet. It involved the administration of pectin (Step 1), the use of medium-chain triacylglycerols and complex, nonfermentable sugars (Step 2); coconut oil (47% medium - chain triacylglycerols) and simple sugars (Step 3); and finally long-chain triacylglycerols and lactose (Step 4). Total parenteral nutrition was interrupted at steps 3 or 4 when the energy content of the diet reached 150% of the patient's resting energy expenditure, if serum albumin and weight were stable, or if there were no alterations in frequency, amount and consistency of the stool.

### IRREVERSIBLE SMALL BOWEL FAILURE

From studies of patients on long-term parenteral nutrition, it seems that there are between two and three patients per million of population per year who develop irreversible small bowel failure<sup>[46]</sup>. Messing *et al*<sup>[47]</sup> assessed prognostic factors in 124 consecutive adults with non-malignant short bowel syndrome. Survival and parenteral nutrition-dependence probabilities were 86% and 49% at 2 years, and 75% and 45% at 5 years. In multivariate analysis, survival was related negatively to end-enterostomy, to small bowel length of <50 cm, and to arterial infarction as a cause of short bowel syndrome, but not to parenteral nutrition dependence. The latter was related negatively to post-duodenal small bowel lengths of <50 and 50-99 cm and to absence of terminal ileum and/or colon in continuity. Cutoff values of small bowel lengths separating transient and permanent intestinal failure were 100, 65, and 30 cm in end-enterostomy, jejunocolic, and jejunoileocolic type of anastomosis. In adult short bowel

syndrome patients, small bowel length of <100 cm is highly predictive of permanent intestinal failure. Presence of terminal ileum and/or colon in continuity enhances both weaning off parenteral nutrition and survival probabilities. After 2 years of parenteral nutrition, probability of permanent intestinal failure is 94%. These rates may lead to selection of other treatments, especially intestinal transplantation, instead of parenteral nutrition, for permanent intestinal failure caused by short bowel syndrome.

Gambarara *et al*<sup>[48]</sup> have accumulated data that suggests that rather than depending on the length of intestine remaining or the presence of the ileocecal valve, the prognosis of patients with the extreme-short-bowel syndrome depends on recurrent sepsis and early onset liver impairment. In addition, their case review shows that the extreme-short-bowel syndrome is not necessarily an indication for bowel transplantation.

Patients with short bowel syndrome frequently develop other clinical problems which may require therapy. These include, hyperphagia, hyponatremia and hypochloremia, metabolic acidosis, including D-lactic acidosis, cholelithiasis and urolithiasis, gastro-esophageal reflux, dystrophy and symptoms caused by secondary dilatation of the lengthened bowel loops: a protruding abdomen, enteral stasis, leading to constipation or diarrhoea with bacterial overgrowth<sup>[49]</sup>.

### ADAPTATION

The main long term aim of therapy of short bowel syndrome is to promote intestinal adaptation to allow transition to an oral diet. Such management has focused on the use of preferred gut nutrients such as glutamine, and the use of either specific (e.g. intestinal growth factor IGF-1) or general growth factors (e.g. growth hormone). These treatments have followed from the knowledge that both nutrient and growth factor related events drive intestinal adaptation.

**Table 3** Molecules that regulate intestinal adaptation

| Molecule                         | Effect on Intestinal Adaptation                                                                                                                                                                                                                                                                                                                                                                                                                                                                                                                                                                                                                                                                                                                                                                                                                                                                                                                                                                                                                                                                                        |
|----------------------------------|------------------------------------------------------------------------------------------------------------------------------------------------------------------------------------------------------------------------------------------------------------------------------------------------------------------------------------------------------------------------------------------------------------------------------------------------------------------------------------------------------------------------------------------------------------------------------------------------------------------------------------------------------------------------------------------------------------------------------------------------------------------------------------------------------------------------------------------------------------------------------------------------------------------------------------------------------------------------------------------------------------------------------------------------------------------------------------------------------------------------|
| Glucagon-Like Peptide 2          | Treatment of rats with a 75% mid small bowel resection with twice daily injections of 0.1 µg per gram of bodyweight for 21 d induced led to mucosal hyperplasia in the proximal jejunum but not in the terminal ileum and a significant increase in intestinal absorptive capacity <sup>[50]</sup> .                                                                                                                                                                                                                                                                                                                                                                                                                                                                                                                                                                                                                                                                                                                                                                                                                   |
| Interleukin-11                   | Treatment of rats with a 90% small bowel resection with twice daily injections of 125 mg·g <sup>-1</sup> IL-11 significantly increased villus height and crypt cell mitotic rates <sup>[51]</sup> .                                                                                                                                                                                                                                                                                                                                                                                                                                                                                                                                                                                                                                                                                                                                                                                                                                                                                                                    |
| Keratinocyte Growth Factor (KGF) | Treatment of rats with a 75% small bowel resection with 3 mg·kg <sup>-1</sup> ·d <sup>-1</sup> of KGF enhanced intestinal adaptation as assessed by mucosal cellularity, and biochemical activity in duodenal, jejunal and ileal segments <sup>[52]</sup> .                                                                                                                                                                                                                                                                                                                                                                                                                                                                                                                                                                                                                                                                                                                                                                                                                                                            |
| Transforming factor-α            | Treatment of mice with a 50% small bowel resection with intraperitoneal TGF-α enhanced intestinal adaptation <sup>[53]</sup> .                                                                                                                                                                                                                                                                                                                                                                                                                                                                                                                                                                                                                                                                                                                                                                                                                                                                                                                                                                                         |
| Growth Hormone                   | Treatment of rats with a 75% small intestinal resection with 0.1 mg·kg <sup>-1</sup> ·d <sup>-1</sup> for 28 d enhanced ileal adaptation as assessed by ileal mucosal height. Treatment with growth hormone did not alter ileal mucosal DNA content or ileal mucosal IGF-1 content <sup>[54]</sup> .<br>Treatment of rats with an 80% jejunoileal resection with synthetic rat GH for up to 14 d did not enhance ileal adaptation <sup>[55]</sup> .<br>Treatment of an infant with only 25 cm of jejunum and 2 cm of ileum, with an ileocecal valve, with a 4-week course of 0.5 U/kg of GH allowing weaning from TPN <sup>[56]</sup> .<br>Ten patients with short bowel syndrome were treated with daily subcutaneous doses of recombinant human GH (rhGH) of 0.024 mg·kg <sup>-1</sup> ·d <sup>-1</sup> or a placebo for 8 wk in a crossover clinical trial that included a wash-out period of at least 12 wk. Low-dose rhGH doubled serum levels of IGF-1 and increased body weight and lean body mass; but there were no significant changes in absorptive capacity of water, energy, or protein <sup>[57]</sup> . |
| Insulin-like Growth Factor-1     | Treatment of rats with 70% and 80% jejuno-ileal resection with IGF-1 or analogues significantly attenuated malabsorption of fat and increased weight of stomach and proximal small bowel <sup>[58]</sup> .<br>Gastrostomy-fed rats underwent 80% jejuno-ileal resection followed by infusion of 2.4 mg·kg <sup>-1</sup> ·d <sup>-1</sup> IGF-1 for 7 d. IGF-1 infusion led to a modest increase in ileal but not jejunal growth <sup>[59]</sup> .<br>Treatment of TPN-fed rats for 7 d with IGF-1 after a 60% jejunoileal resection led to an increase in jejunal mass, enterocyte proliferation and migration rates yet had minimal effect on colonic structure <sup>[59]</sup> .                                                                                                                                                                                                                                                                                                                                                                                                                                     |
| Epidermal Growth Factor (EGF)    | Treatment of rabbits with 2/3 proximal resection with oral EGF (40 µg·kg <sup>-1</sup> ·d <sup>-1</sup> ) for 5 d led to an increase in maltase specific activity and a 3-4 fold increase in glucose transport and phlorizin binding <sup>[60]</sup> .<br>Treatment of rabbits with a 50%-60% small bowel resection with 0.3 µg·kg <sup>-1</sup> ·h <sup>-1</sup> for 7 d led to a fourfold increase in mucosal dryweight at 3 wk post-resection <sup>[61]</sup> .<br>Treatment of rats with a 75% small bowel resection with 6.25 µg·kg <sup>-1</sup> ·h <sup>-1</sup> of EGF increased mucosal thickness at 28 d post-resection <sup>[62]</sup> .                                                                                                                                                                                                                                                                                                                                                                                                                                                                    |
| Neurotensin                      | Treatment of rats with a 75% small bowel resection with 600 µg·kg <sup>-1</sup> ·d <sup>-1</sup> led to an increase in the rate of mucosal proliferation <sup>[63]</sup> .                                                                                                                                                                                                                                                                                                                                                                                                                                                                                                                                                                                                                                                                                                                                                                                                                                                                                                                                             |

It makes sense to combine the administration of growth factors with an abundant supply of appropriate nutrients. Such approaches have worked well in animal models. Table 3 presents the results of studies that have evaluated the effect of cytokines and growth factors on intestinal adaptation. Clearly, there are a number of agents that can enhance adaptation. However, the effect of these agents is influenced by factors such as nutrition regimen and type of surgery. For example, Ziegler *et al.*<sup>[15]</sup>, found that treatment of gastrostomy-fed rats with 2.4mg·kg<sup>-1</sup>·d<sup>-1</sup> IGF-1 for 7 d after 80% jejuno-ileal resection led to a modest increase in ileal but not jejunal growth. In contrast, treatment of TPN-fed rats for 7 d with IGF-1 after a 60% jejunoileal resection and cecectomy did not alter colonic structure<sup>[59]</sup>. The effect of treatment with other combinations on intestinal adaptation has yielded less equivocal results. Ziegler *et al.*<sup>[34]</sup>, used a rat model to examine the effect of glutamine and IGF-1 on intestinal adaptation in rats. Treatment with a glutamine-enriched diet or daily injections of IGF-1 enhanced ileal hyperplasia. More importantly, treatment with glutamine and IGF-1 synergistically increased ileal weight and protein content. Fiore *et al.*<sup>[64]</sup>, examined the effect of treatment with IL-11 and EGF on intestinal adaptation in rats after 85% small bowel resection. The animals were treated with either 0.10µg·g<sup>-1</sup> EGF, 125µg·kg<sup>-1</sup>

IL-11, or 0.10µg·g<sup>-1</sup> EGF and 125µg·kg<sup>-1</sup> IL-11 for 8 d. Rats which received EGF and IL-11 had the most number of proliferating cells in the mucosal crypts.

The results in humans have been less convincing. In 1995, Byrne *et al.*<sup>[65]</sup>, published the results of their investigation of the effect of GH, glutamine and a high complex carbohydrate/low fat diet on 47 patients with short bowel syndrome who had been dependent on TPN for many years. All patients were treated in hospital over a 4 week period. This treatment enabled 40% of patients to be weaned off TPN at one-year follow-up (Table 4). A number of these patients had small bowel length to weight ratios of a little as 0.5cm·kg<sup>-1</sup>. Subsequent studies have been unable to reproduce these results<sup>[66-68]</sup>. The data presented in Table 4 indicates that there was little difference in the type of patients involved in each of the three clinical studies, nor were there large differences in treatment regimens. However, the patients involved in the study by Byrne *et al.*<sup>[65]</sup>, were treated as inpatients whereas the other patients were all treated as outpatients. It is possible that this may have affected the results as outpatients may have been less compliant. Scolapio *et al.*<sup>[67]</sup>, considered this issue and believed that the patients involved in their study did comply with the treatment regimen. These conflicting data emphasise the need for further studies to evaluate the effect of trophic agents on intestinal adaptation.

**Table 4** The effect of glutamine, growth hormone, and a modified diet on patients with short-bowel syndrome

| Authors                                                            | Design of Study                                                                                               | Treatment                                                                                                                                                                                                                                                                                 | Number and Type of Patients                                                          | Average Length of Remnant Bowel 43                                                                   | Results                                                                                                                                                                                                                                                                                                                                                                                                                                                                                      |
|--------------------------------------------------------------------|---------------------------------------------------------------------------------------------------------------|-------------------------------------------------------------------------------------------------------------------------------------------------------------------------------------------------------------------------------------------------------------------------------------------|--------------------------------------------------------------------------------------|------------------------------------------------------------------------------------------------------|----------------------------------------------------------------------------------------------------------------------------------------------------------------------------------------------------------------------------------------------------------------------------------------------------------------------------------------------------------------------------------------------------------------------------------------------------------------------------------------------|
| Byrne <i>et al.</i> <sup>[65]</sup>                                | Uncontrolled study. Patients admitted to hospital and treated for 21d.                                        | GH 0.11mg·kg <sup>-1</sup> ·d <sup>-1</sup> , glutamine 0.16g·kg <sup>-1</sup> ·d <sup>-1</sup> <sup>158</sup> by the parenteral route with up to 30g·d <sup>-1</sup> by the enteral route, and a diet containing 60% of total calories as carbohydrate, 20% as fat and 20% from protein. | 47 patients that were chronically dependent on parenteral nutrition                  | patients with a colonic remnant had (50±7)cm <sup>[4]</sup> , patients with no colon had (102±24)cm. | At the end of the study 57% of the patients no longer needed TPN, 30% had reduced TPN requirements, and 6% required approximately the same amount of TPN as they did at the start of the study. One year later 40% of the patients no longer needed TPN, 40% had reduced TPN requirements, and 20% required approximately the same amount of TPN as they did at the start of the study.                                                                                                      |
| Scolapio <sup>[66]</sup><br>Scolapio <i>et al.</i> <sup>[67]</sup> | Double-blind, placebo controlled, randomized crossover study. Patients were treated for 21d as out-patients.  | GH 0.14mg·kg <sup>-1</sup> ·d <sup>-1</sup> , glutamine 0.63g·kg <sup>-1</sup> ·d <sup>-1</sup> by oral route, and a diet containing 60% total calories as carbohydrate, 20% as fat and 20% as protein.                                                                                   | 8 patients that were dependent on parenteral nutrition for an average of 12.9 years. | 71 cm <sup>2</sup> patients had colonic continuity.                                                  | Treatment led to a significant increase in bodyweight and lean body mass, a significant decrease in percent body fat and induced peripheral edema. All parameters returned to baseline levels within 14 d of stopping treatment. Treatment had no significant effect on intestinal villus height or crypt depth. No significant effect of treatment on absorption of energy, carbohydrate, nitrogen, wet weight, sodium, potassium, calcium or magnesium. Treatment induced adverse effects. |
| Szkudlarek <i>et al.</i> <sup>[68]</sup>                           | Double-blind, placebo controlled, randomized crossover study. Patients were treated for 28 d as out-patients. | GH 0.14mg·kg <sup>-1</sup> ·d <sup>-1</sup> , glutamine 30g·d <sup>-1</sup> by oral route and glutamine-enriched parenteral nutrition (17% of nitrogen as glutamine).                                                                                                                     | 8 patients that were dependent on parenteral nutrition for an average of 7 years.    | 104 cm. 4 patients had colonic continuity.                                                           |                                                                                                                                                                                                                                                                                                                                                                                                                                                                                              |

## SURGICAL MANAGEMENT

### Non-Transplant Procedures - Autologous Gastrointestinal Reconstruction

Only a few patients with short bowel syndrome are candidates for non-transplant procedures. Surgery in the form of autologous gastrointestinal reconstruction is designed to redistribute the patient's own residual absorptive bowel to enhance adaptation and, possibly, to increase the absorptive mucosal surface by neomucosal growth. The majority of such reconstructions have been performed on paediatric patients. Intestinal lengthening, as described by Bianchi, is the most commonly used method of gastrointestinal reconstruction for the therapy of short bowel syndrome. It divides the bowel in two longitudinal halves based on the bifurcated mesenteric blood supply, then reconnects the two halves in series with the rest of the small intestine.

Bianchi<sup>[69]</sup> has recently reviewed his 16-year experience of longitudinal intestinal lengthening procedures for 20 neonates and infants with short-bowel syndrome that included a dysfunctional dilated jejunum. There was no operative

mortality and the long-term survival was 45%. Survivors had >40 cm residual jejunum and a greater number also retained their ileocaecal valve and a longer colonic length. Death was commonly due to end-stage liver failure. Weber<sup>[54]</sup> reviewed the outcome of 16 infants and children who had this procedure performed, with a resultant increase in the length of their bowel by 22%-85% (mean 42%). There were marked improvements in stool counts, intestinal transit time, intestinal clearance of barium, D-xylose absorption, and fat absorption. Fourteen of the 16 patients (88%) no longer required parenteral nutrition.

### Small Bowel Transplantation

Intestinal transplantation, either alone or in combination with the liver, may eventually emerge as the preferred therapy for patients with permanent intestinal failure. However, in comparison with solid organ transplantations, such as the kidney and the liver, there has been slower progression from experimentation towards routine clinical practice. The first intestinal transplant was performed in Boston in 1964. It

involved the transfer of an ileal segment from the patients mother, but the recipient died 12 hours after surgery. In New York in 1970, a 170 cm jejunoileal segment was transplanted from an identical sister and the recipient lived for 79 d and was able to eat for 6 wk. At Kiel University in 1988, an intestinal transplant from an identical sister resulted in a survival for 4 years<sup>[70]</sup>.

The high level of immune surveillance within the small intestine means that large number of 'passenger' immunocytes and dendritic cells are transplanted along with the intestinal tissue. This increases the risk of acute rejection, which leads to the use of high doses of immunosuppressive agents and a greater incidence of side effects. In addition, the immunocompromised recipient is vulnerable to infections such as cytomegalovirus enteritis. In fact, recipients can die of side effects in the presence of a functioning graft<sup>[71]</sup>. Improved results are only expected with newer immunosuppressive agents, better antiviral prophylaxis and treatment, and improved preservation and surgical techniques<sup>[72]</sup>.

Grant<sup>[73]</sup> has recently reviewed the world experience in which 33 intestinal transplant programs provided data on 273 transplants in 260 patients. These patients received their transplants before March 1997. Only one-thirds of the recipients were adults and the commonest indication for transplantation was the short bowel syndrome. Many of the transplants involved other organs - intestine plus liver (48%); multi-viscera (11%). The one year graft survival for isolated intestinal transplants performed after early 1995 was 55% (the patient survival was 69%). Overall, 77% of the survivors were being sustained on oral nutrition and had no requirement for parenteral nutrition. The overall three-year survival has been about 40%, which is comparable with the results of lung transplantation.

Organ retrieval from a living donor can be performed safely for small bowel transplantation. However, further study of the management of rejection as well as viral infection is necessary for both living and non-living-related small bowel transplantation<sup>[74]</sup>. Endoscopic surveillance may be useful to detect early allograft rejection<sup>[75]</sup>. It has been suggested that a lower severity of graft rejection in combined liver-small bowel transplantation improves functional results of intestinal transplantation in children without additional mortality or morbidity<sup>[76]</sup>.

Goulet *et al*<sup>[77]</sup>, have stressed that, because parenteral nutrition is generally well tolerated, even for long periods, each indication for transplantation must be weighed carefully in terms of risk and quality of life. In this regard, it is of interest that a T cell lymphoma has been reported in the intestinal graft of a multivisceral organ recipient<sup>[78]</sup>. It may have special significance because the lymphoproliferative disorders that are usually observed after transplantation are invariably of B cell origin. Furthermore, Crohn's disease in the recipient can recur in the intestinal transplant<sup>[79]</sup>.

Kato *et al*<sup>[80]</sup>, have used a rodent model to demonstrate that EGF augments both the structural and functional adaptation of intestinal grafts. Recipient Lewis rats underwent resection of the distal 80% of the small bowel followed by the insertion of a 20 cm isograft. EGF (30 µg·kg<sup>-1</sup>·d<sup>-1</sup>), or a control, was infused intraperitoneally for 3 d immediately after surgery. After 7 d, the graft was isolated for morphologic studies and was used for analysis of glucose and water absorption and the expression of sodium glucose cotransporter 1. These were used as indicators of functional adaptation. After seven days, the EGF-treated group exhibited significantly increased mucosal villous height, crypt cell proliferation, glucose and water absorption, and expression of sodium glucose co-transporter 1 protein

compared to the control group.

### Other Surgical Techniques

A variety of surgical techniques have been devised to promote oral absorption of nutrients and delay emptying. These include a reversed intestinal segments, artificial intestinal valves, and recirculating loops. None of these procedures has been associated with significant clinical success. Thompson *et al*<sup>[81]</sup>, studied 48 adults and 112 children with short-bowel syndrome. The eventual outcome was that 44% adapted and survived on enteral nutrition alone, 28% required long-term parenteral nutrition, and 28% underwent surgery. Thirteen of 15 patients with adequate intestinal length (>120 cm in adults), but dilated dysfunctional bowel, were improved by either stricturoplasty or tapering. However, the patients who received an artificial valve (*n*= 2) or a reversed segment (*n*= 1) did poorly and required further surgery for revision or reversal. In general, success is lowest for procedures designed to prolong intestinal transit time; thus, these procedures should be used only in carefully selected patients<sup>[82]</sup>.

This is in contrast with the experience of Panis *et al*<sup>[83]</sup>, who reported their experience with segmental reversal of the small bowel. Eight patients with short bowel syndrome underwent, at the time of intestinal continuity restoration, a segmental reversal of the distal (*n*= 7) or proximal (*n*= 1) small bowel. The median length of the remnant small bowel was 40 cm (range, 25-70cm), including a median length of reversed segment of 12 cm (range, 8-15 cm). Parenteral nutrition cessation was obtained in 3 of 5 patients at 1 years and in 3 of 3 patients at 4 years. Segmental reversal of the small bowel could be proposed as an alternative to intestinal transplantation in patients with short bowel syndrome before the possible occurrence of parenteral nutrition-related complications.

### COORDINATED INTERDISCIPLINARY MANAGEMENT

There have been proposals to develop multidisciplinary teams to care for patients with the short bowel syndrome. The key issues are the maintenance of optimum growth and development in infants and children, the promotion of intestinal adaptation, and the safe progression towards an oral diet. Koehler *et al*<sup>[84]</sup>, evaluated the effect of co-ordinated interdisciplinary team management of children with intestinal failure on nutritional outcome measures. Using an established registry, the authors conducted a comprehensive evaluation of patient data including anthropometric measures, organ system function, and mode of nutrition support. Linear growth velocity of neither pre- nor post-pubescent patients significantly improved during the 2-year study period of interdisciplinary team management.

When innovative, not yet fully proven therapies are introduced, physicians may have neither experience nor sufficient data in the medical literature to assist in their decision. When multiple physicians caring for a single patient have reached different conclusions regarding this new therapy, the potential for disagreement exists that could give rise to ethical issues as well as cause confusion to the patient. To explore these topics, Cooper *et al*<sup>[85]</sup>, investigated the attitudes of specialists to therapies for short bowel syndrome. A forced choice questionnaire was distributed to clinicians in neonatology and pediatric gastroenterology. Significant differences were noted among specialists as to whom would be involved in discussions of therapeutic options with patients about short bowel syndrome. Differences also were noted in the willingness of specialists to discuss and recommend therapies, in the perceived survival and quality of life by various specialists after transplant and palliative surgery, and in the local availability of various options. The neonatologists

and gastroenterologists at the same institution disagreed on responses in 34% of the questions with only 1 of the 25 pairs in full agreement. There is the potential for much patient confusion when counselling physicians recommend different options. Colleagues as individuals and specialists as groups should talk to each other before individual discussions with families to ensure that there is a clear understanding of differing beliefs.

## REFERENCES

- Coran AG, Spivak D, Teitelbaum DH. An analysis of the morbidity and mortality of short-bowel syndrome in the pediatric age group. *Eur J Ped Surg* 1999;9:228-230
- Vennarecci G, Kato T, Misiakos EP, Neto AB, Verzaro R, Pinna A, Nery J, Khan F, Thompson JF, Tzakis AG. Intestinal transplantation for short gut syndrome attributable to necrotizing enterocolitis. *Pediatrics* 2000; 105:E25
- Ramsden WH, Arthur RJ, Martinez D. Gastroschisis: a radiological and clinical review. *Ped Radiol* 1997;27:166-169
- Horwitz JR, Lally KP, Cheu HW, Vazquez WD, Grosfeld JL, Ziegler MM. Complications after surgical intervention for necrotizing enterocolitis: a multicenter review. *J Ped Surg* 1995;30:994-998
- Nightingale JM. Management of patients with a short bowel. *Nutrition* 1999;15:633-637
- Olesen M, Gudmand-Hoyer E, Holst JJ, Jorgensen S. Importance of colonic bacterial fermentation in short bowel patients: small intestinal malabsorption of easily digestible carbohydrate. *Dig Dis Sci* 1999;44: 1914-1923
- Jeppesen PB, Mortensen PB. Significance of a preserved colon for parenteral energy requirements in patients receiving home parenteral nutrition. *Scan J Gastroenterol* 1998;33:1175-1179
- Reynolds N, Zentler-Munro P, Cuschieri A, Pennington CR. Potential hazards of excluded bowel and use of parenteral nutrition: a case report. *Nutrition* 1997;13:971-974
- Schafer K, Zachariou Z, Loffler W, Daum R. Continuous extracorporeal stool-transport system: a new and economical procedure for transitory short-bowel syndrome in prematures and newborns. *Ped Surg Int* 1997; 12:73-75
- Al-Harbi K, Walton JM, Gardner V, Chessell L, Fitzgerald PG. Mucous fistula refeeding in neonates with short bowel syndrome. *J Ped Surg* 1999; 34:1100-1103
- Shin CE, Helmrath MA, Falcone RA, Fox JW, Duane KR, Erwin CR, Warner BW. Epidermal growth factor augments adaptation following small bowel resection: optimal dosage, route, and timing of administration. *J Surg Res* 1998;77:11-16
- Sagor GR, Al-Mukhtar MY, Ghatti MA, Wright NA, Bloom SR. The effect of altered luminal nutrition on cellular proliferation and concentrations of enteroglucagon and gastrin after small bowel resection. *Br J Surg* 1982; 69:14-18
- Fuller PJ, Beveridge DJ, Taylor RG. Ileal proglucagon gene expression in the rat: characterization in intestinal adaptation using in situ hybridisation. *Gastroenterology* 1993;104:459-466
- Dunphy JL, Justice FA, Taylor RG, Fuller PJ. mRNA levels of dipeptidyl peptidase IV decrease during intestinal adaptation. *J Surg Res* 1999;87: 130-133
- Ziegler TR, Mantell MP, Chow JC, Rombeau JL, Smith RJ. Intestinal adaptation after extensive small bowel resection: differential change in growth and insulin-like growth factor system messenger ribonucleic acids in jejunum and ileum. *Endocrinology* 1998;139:3119-3126
- Thompson JS, Quigley EM, Adrian TE. Factors affecting outcome following proximal and distal intestinal resection in the dog: an examination of the relative roles of mucosal adaptation, motility, luminal factors, and enteric peptides. *Dig Dis Sci* 1999;44:63-74
- Nightingale J. Short bowel, short answer. *Gut* 1999;45:478-479
- Jeppesen PB, Hartmann B, Hansen BS, Thulesen J, Holst JJ, Mortensen PB. Impaired meal stimulated glucagon-like peptide 2 response in ileal resected short bowel patients with intestinal failure. *Gut* 1999;45: 559-563
- De Francesco A, Malfi G, Delsedime L. Histological findings regarding jejunal mucosa in short bowel syndrome. Measurement by calcium absorption. *Dig Dis Sci* 1989;34:709-715
- Jeppesen PB, Hartmann B, Thulesen J, Hansen BS, Holst JJ, Poulsen SS, Mortensen PB. Elevated plasma glucagon-like peptide 1 and 2 concentrations in ileum resected short bowel patients with a preserved colon. *Gut* 2000;47:370-376
- Dowling RH, Booth CC. Functional compensation after small bowel resection in man: Demonstration by direct measurement. *Lancet* 1966;ii:146-147
- Platell C, McCauley R, McCulloch R, Hall J. The influence of parenteral glutamine and branched-chain amino acids on total parenteral nutrition-induced atrophy of the gut. *JPEN* 1993;17: 348-354
- Buchman AL, Moukarzel AA, Ament ME, Eckhart C, Bhuta S, Mestecky J, Hollander D. Effects of total parenteral nutrition on intestinal morphology and function in humans. *Trans Proc* 1994; 26:1457
- Pironi L, Paganelli GM, Miglioli M, Biasco G, Santucci R, Ruggeri E, Di-Febo G, Barbara L. Morphologic and cytoproliferative patterns of duodenal mucosa in two patients after long-term parenteral nutrition: changes with oral feeding and relation to intestinal resection. *JPEN* 1994;18:351-354
- Sondheimer JM, Asturias E, Cadnapaphornchai M. Infection and cholestasis in neonates with intestinal resection and long-term parenteral nutrition. *J Ped Gastroenterol Nut* 1998;27:131-137
- Suita S, Masumoto K, Yamanouchi T, Nagano M, Nakamura M. Complications in neonates with short bowel syndrome and long-term parenteral nutrition. *JPEN* 1999;23:S106-S109
- Mayr JM, Schober PH, Weissensteiner U, Hollwarth ME. Morbidity and mortality of the short-bowel syndrome. *Eur J Ped Surg* 1999;9: 231-235
- Tappenden KA, McBurney MI. Systemic short-chain fatty acids rapidly alter gastrointestinal structure, function, and expression of early response genes. *Dig Dis Sci* 1998;43:1526-1536
- Korunda MJ, Rolandelli RH, Settle RG, Saul SH, Rombeau JL. The effect of a pectin supplemented elemental diet on intestinal adaptation to massive small bowel resection. *JPEN* 1986;10:343-350
- Vanderhoof JA, Grandjean CJ, Kaufman SS, Burkley KT, Antonson DL. Effect of high percentage medium-chain triglyceride diet on mucosal adaptation following massive bowel resection in rats. *JPEN* 1984;8:685-689
- Dumas F, De Bandt JP, Colomb V, Le Boucher J, Coudray-Lucas C, Lavie S, Brousse N, Riccour C, Cynober L, Goulet O. Enteral ornithine  $\alpha$ -ketoglutarate enhances intestinal adaptation after small bowel resection in rats. *Metabolism* 1998;47:1366-1371
- Czernichow B, Nsi-Envo E, Galluser M, Gosse F, Raul F. Enteral supplementation with ornithine  $\alpha$ -ketoglutarate improves the early adaptive response to resection. *Gut* 1997;40:67-72
- Tamada H, Nezu R, Matsuo Y, Imamura I, Takagi Y, Okada A. Alanine glutamine-enriched total parenteral nutrition restores intestinal adaptation after either proximal or distal massive resection in rats. *JPEN* 1993;17:236-242
- Ziegler TR, Mantell MP, Chow JC, Rombeau JL, Smith RJ. Gut adaptation and the insulin-like growth factor system: regulation by glutamine and IGF-I administration. *Am J Physiol* 1996;271:G866-G875
- Vanderhoof JA, Blackwood DJ, Mommadpour H, Park JH. Effects of oral supplementation of glutamine on small intestinal mucosa following resection. *J Am Coll Nutr* 1992;11:223-227
- Michail S, Mohammadpour H, Park JH, Vanderhoof JA. Effect of glutamine-supplemented elemental diet on mucosal adaptation after small bowel resection in rats. *J Pediatr Gastroenterol Nutr* 1995; 21:394-398
- Wiren ME, Permert J, Skulman SP, Wang F, Larsson J. No differences in mucosal adaptive growth one week after intestinal resection in rats given enteral glutamine supplementation or deprived of glutamine. *Eur J Surg* 1996;162:489-498
- McCauley R, Kong SE, Hall JC. Glutamine and nucleotide metabolism within enterocytes. *JPEN* 1998;22:105-111
- Reimer RA, McBurney MI. Dietary fiber modulates intestinal proglucagon messenger ribonucleic acid and postprandial secretion of glucagon-like peptide-1 and insulin in rats. *Endocrinology* 1996; 137:3948-3956
- Wiren M, Adrian TE, Arnelo U, Permert J, Staab P, Larsson J. Early gastrointestinal regulatory peptide response to intestinal resection in rats is stimulated by enteral glutamine supplementation. *Dig Surg* 2000;16:197-203
- Clarke RM. 'Luminal nutrition' versus 'functional work-load' as controllers of mucosal morphology and epithelial replacement in the rat small intestine. *Digestion* 1977;15:411-424
- Wasa M, Takagi Y, Sando K, Harada T, Okada A. Long-term outcome of short bowel syndrome in adult and pediatric patients. *JPEN* 1999;23:S110-S112
- Jeppesen PB, Mortensen PB. Colonic digestion and absorption of energy from carbohydrates and medium-chain fat in small bowel failure. *JPEN* 1999;23:S101-S105
- Jeppesen PB, Mortensen PB. The influence of a preserved colon on the absorption of medium chain fat in patients with small bowel resection. *Gut* 1998;43:478-483



- 45 Sales TR, Torres HO, Couto CM, Carvalho EB. Intestinal adaptation in short bowel syndrome without tube feeding or home parenteral nutrition: report of four consecutive cases. *Nutrition* 1998;14:508-512
- 46 Hakim NS, Papalois VE. Small bowel transplantation. *Int Surgery* 1999;84:313-317
- 47 Messing B, Crenn P, Beau P, Boutron-Ruault MC, Rambaud JC, Matuchansky C. Long-term survival and parenteral nutrition dependence in adult patients with the short bowel syndrome. *Gastroenterology* 1999;117:1043-50
- 48 Gambarara M, Ferretti F, Bagolan P, Papadatou B, Rivosecchi M, Lucchetti MC, Nahom A, Castro M. Ultra-short-bowel syndrome is not an absolute indication to small-bowel transplantation in childhood. *Eur J Ped Surg* 1999;9:267-270
- 49 Waag KL, Hosie S, Wessel L. What do children look like after longitudinal intestinal lengthening. *Eur J Ped Surg* 1999;9:260-262
- 50 Scott RB, Kirk D, MacNaughton WK. GLP-2 augments the adaptive response to massive intestinal resection in the rat. *Am J Physiol* 1998;275:G911-G921
- 51 Liu Q, Du XX, Schindel DT, Yang ZX, Rescorla FJ, Willaims DA, Grossfeld JL. Trophic effects of interleukin-11 in rats with experimental short bowel. *J Pediatr Surg* 1996;31:1047-1050
- 52 Johnson WF, DiPalma CR, Ziegler TR, Scully S, Farrell CL. Ketatinocyte growth factor enhances early gut adaptation in a rat model of short bowel syndrome. *Vet Surg* 2000;29:17-27
- 53 Falcone RA, Stern LE, Kemp CJ, Erwin CR, Warner BW. Intestinal adaptation occurs independent of transforming growth factor alpha. *J Pediatr Surg* 2000;35:365-370
- 54 Shulman DI, Hu CS, Duckett G, Lavalee-Grey M. Effects of short-term growth hormone therapy in rats undergoing 75% small intestinal resection. *J Pediatr Gastroenterol* 1992;14:3-11
- 55 Ljungmann K, Grfte T, Kissmeyer-Nielsen P, Flyvbjerg A, Vilstrup H, Tygstrup N, Laurberg S. GH decrease hepatic amino acid degradation after small bowel resection in rats without enhancing bowel adaptation. *Am J Physiol* 2000;279:G700-G706
- 56 Velasco B, Lassaletta L, Gracia R, Tovar JA. Intestinal lengthening and growth hormone in extreme short bowel syndrome: a case report. *J Ped Surg* 1999;34:1423-1424
- 57 Ellegard L, Bosaeus I, Nordgren S, Bengtsson BA. Low-dose recombinanthuman growth hormone increases body weight and lean body mass in patients with short bowel syndrome. *Ann Surg* 1997;225:88-96
- 58 Lemmey AB, Ballard FJ, Martin AA, Tomas FM, Howarth GS, Read LC. Treatment with IGF-1 peptides improves function of the remnant gut following small bowel resection in rats. *Growth Factors* 1994;10:243-252
- 59 Gillingham MB, Dahly EM, Carey HV, Clark MD, Kritsch KR, Ney DM. Differential jejunal and colonic adaptation due to resection and IGF-I in parenterally fed rats. *Am J Physiol* 2000;278:G700-G709
- 60 O'Loughlin E, Winter M, Shun A, Hardin JA, Gall DG. Structural and functional adaptation following jejunal resection in rabbits: effect of epidermal growth factor. *Gastroenterology* 1994;107:87-93
- 61 Swaniker F, Gou W, Diamond J, Fonkalsrud EW. Delayed effects of epidermal growth factor after extensive small bowel resection. *J Pediatr Surg* 1996;31:56-59
- 62 Chaet MS, Arya G, Ziegler MM, Warner BW. Epidermal growth factor enhances intestinal adaptation after massive small bowel resection. *J Pediatr Surg* 1994;29:1035-1038
- 63 Mata A, Gomez de Segura IA, Largo C, Codesal J, De Miguel E. Neurotensin increases intestinal adaptation and reduces enteroglucagon immunoreactivity after large bowel resection in rats. *Eur J Surg* 1997;163:387-393
- 64 Fiore NF, Ledniczky G, Liu Q, Orazi A, Du X, Williams DA, Grosfeld JL. Comparison of interleukin 11 and epidermal growth factor on residual intestine after massive small bowel resection. *J Pediatr Surg* 1998;33:24-29
- 65 Byrne TA, Persinger RL, Younf LS, Ziegler TR, Wilmore DW. A new treatment for patients with short-bowel syndrome. Growth hormone, glutamine, and a modified diet. *Ann Surg* 1995;222:243-255
- 66 Scolapio JS. Effect of growth hormone, glutamine, and diet on body composition in short bowel syndrome: a randomized, controlled study. *JPEN* 1999;23:309-312
- 67 Scolapio JS, Camilleri M, Fleming CR, Oenning LV, Burton DD, Sebo TJ, Batts KP, Kelly DG. Effect of growth hormone, glutamine, and diet on adaptation in short-bowel syndrome: A randomized, controlled study. *Gastroenterology* 1997;113:1074-1081
- 68 Szkudlarek J, Jeppesen PB, Mortensen PB. Effect of high dose growth hormone with glutamine and no change of diet on intestinal absorption in short bowel patients: a randomised, double blind, crossover, placebo controlled study. *Gut* 2000;47:199-205
- 69 Bianchi A. Experience with longitudinal intestinal lengthening and tailoring. *Eur J Ped Surg* 1999;9:256-259
- 70 Margreiter R. Living-donor pancreas and small-bowel transplantation. *Lan Arch Surg* 1999;384:544-549
- 71 Novelli M, Muesan P, Mieli-Vergani G, Dhawan A, Rela M, Heaton ND. Oral absorption of tacrolimus in children with intestinal failure due to short or absent small bowel. *Transplant Int* 1999;12:463-465
- 72 Makisalo H, Ericzon BG. Intestinal transplantation. *Ann Chir Gyn* 1997;86:155-162
- 73 Grant D. Intestinal transplantation: 1997 report of the international registry. Intestinal Transplant Registry. *Transplantation* 1999;67:1061-1064
- 74 Morel P, Kadry Z, Charbonnet P, Bednarkiewicz M, Faidutti B. Paediatric living related intestinal transplantation between two monozygotic twins: a 1-year follow-up. *Lancet* 2000;355:723-724
- 75 Kato T, O'Brien CB, Nishida S, Hoppe H, Gasser M, Berho M, Rodriguez MJ, Ruiz P, Tzakis AG. The first case report of the use of a zoom videoendoscope for the evaluation of small bowel graft mucosa in a human after intestinal transplantation. *Gastrointest. Endoscopy* 1999;50:257-261
- 76 Jan D, Michel JL, Goulet O, Sarnacki S, Lacaille F, Damotte D, Cezard JP, Aigrain Y, Brousse N, Peuchmaur M, Rengeval A, Colomb V, Jouviet P, Ricour C, Revillon Y. Up-to-date evolution of small bowel transplantation in children with intestinal failure. *J Ped Surg* 1999;34:841-843
- 77 Goulet O, Jan D, Lacaille F, Colomb V, Michel JL, Damotte D, Jouviet P, Brousse N, Faure C, Cezard JP, Sarnacki S, Peuchmaur M, Hubert P, Ricour C, Revillon Y. Intestinal transplantation in children: preliminary experience in Paris. *JPEN* 1999;23:S121-S125
- 78 Berho M, Viciana A, Weppler D, Romero R, Tzakis A, Ruiz P. T cell lymphoma involving the graft of a multivisceral organ recipient. *Transplantation* 1999;68:1135-1139
- 79 Sustento-Reodica N, Ruiz P, Rogers A, Viciana AL, Conn HO, Tzakis AG. Recurrent Crohn's disease in transplanted bowel. *Lancet* 1997;349:688-691
- 80 Kato Y, Hamada Y, Ito S, Okumura T, Hioki K. Epidermal growth factor stimulates the recovery of glucose absorption after small bowel transplantation. *J Surg Res* 1998;80:315-319
- 81 Thompson JS, Langnas AN. Surgical approaches to improving intestinal function in the short-bowel syndrome. *Arch Surg* 1999;134:706-709
- 82 Thompson JS, Langnas AN, Pinch LW, Kaufman S, Quigley EM, Vanderhoof JA. Surgical approach to short-bowel syndrome. Experience in a population of 160 patients. *Ann Surg* 1995;222:600-605
- 83 Panis Y, Messing B, Rivet P, Coffin B, Hautefeuille P, Matuchansky C, Rambaud JC, Valleur P. Segmental reversal of the small bowel as an alternative to intestinal transplantation in patients with short bowel syndrome. *Ann Surg* 1997;225:401-407
- 84 Koehler AN, Yaworski JA, Gardner M, Kocoshis S, Reyes J, Barksdale EM Jr. Coordinated interdisciplinary management of pediatric intestinal failure: a 2-year review. *J Ped Surg* 2000;35:380-385
- 85 Cooper TR, Garcia-Prats JA, Brody BA. Managing disagreements in the management of short bowel and hypoplastic left heart syndrome. *Pediatrics* 1999;104:48

• BASIC RESEARCH •

# Relationship between cytokine mRNA expression and organ damage following cecal ligation and puncture

Rong-Qian Wu, Ying-Xin XU, Xu-Hua Song, Li-Jun Chen, Xian-Jun Meng

Rong-Qian Wu, Ying-Xin XU, Xu-Hua Song, Li-Jun Chen, Xian-Jun Meng, Institute of Surgical Research, Chinese PLA General Hospital, Beijing 100853, China

Supported by the National Natural Science Foundation of China, No. 39870796

Correspondence to: Dr. Rong-Qian Wu, Institute of surgical Research, General Hospital of PLA, Beijing 100853, China

Received 2001-04-21 Accepted 2001-08-15

## Abstract

**AIM:** To investigate the role of cytokine gene expression in organ damage at different tissue sites during sepsis.

**METHODS:** Male NIH mice were subjected to cecal ligation and puncture (CLP) or sham operation (Sham). Pro-inflammatory cytokine (TNF $\alpha$ , IL-1 $\beta$  and IL-6) and anti-inflammatory cytokine (IL-4) gene expression in the liver and lung tissue were assessed by RT-PCR. The permeability of microvascular and water content in the lungs and liver were also examined.

**RESULTS:** Significant increase in TNF $\alpha$ , IL-1 $\beta$  and IL-6 gene expression was observed at 3 and 12 h after CLP both in the liver and lungs ( $P < 0.01$ ). The level of IL-4 gene expression was not changed after CLP in the lungs, but increased at 12 h after CLP ( $P < 0.01$ ) in the liver tissue. Both the liver and lungs showed a significant increase in microcirculatory permeability at 12 h after CLP ( $P < 0.01$ ), and the increase in the lungs was higher than that in the liver. The water mass fractions in the liver ( $P < 0.05$ ) and lungs ( $P < 0.01$ ) were increased after CLP, and the increase in the lungs happened earlier and more severely than that in the liver.

**CONCLUSION:** The inflammatory response in the liver and lungs was different during sepsis. At the early stage of sepsis, pro-inflammatory reaction dominates both in the liver and lungs. But at the later stage of sepsis, induction of compensatory anti-inflammatory response was seen in the liver but not in the lungs. This difference *in situ* activity may contribute to the different vulnerability of organ damage during sepsis. The strategy of systemic administration of anti-inflammatory drugs to sepsis should be reconsidered.

Wu RQ, Xu YX, Song XH, Chen LJ, Meng XJ. Relationship between cytokine mRNA expression and organ damage following cecal ligation and puncture. *World J Gastroenterol* 2002;8(1):131-134

## INTRODUCTION

Despite modern techniques of resuscitation and intensive care and an ever-increasing number of powerful and effective antibiotics, sepsis remains a major cause of death in the critically ill<sup>[1]</sup>, including severe trauma, burns, hemorrhage, major operations<sup>[2]</sup>, etc. Sepsis-related mortality frequently results from multiple organ dysfunction syndrome,

which is characterized by impaired pulmonary function, hepatic failure, cardiac dysfunction, acute renal failure, and disseminated intravascular coagulation<sup>[3,4]</sup>. The physiologic derangements of MODS are believed to result from the excessive activation of the systemic inflammatory response by infection, ischemia, injury, or immunologic activation<sup>[5,6]</sup>.

Post-sepsis MODS is now believed to be caused by an overexpression of host defenses<sup>[7]</sup>. Mediators such as TNF $\alpha$ , IL- $\beta$  and other cytokines are acknowledged to be pivotal early effectors. There is evidence that the development of tissue damage in sepsis is closely related to the release of an ever-increasing number of cytokines and accumulation of neutrophils at the sites of infection or injury<sup>[8,9]</sup>. Though there were many studies on the role of cytokines in sepsis. Most studies detect only circulating mediators, not mediators bound to cells or receptors<sup>[10,11]</sup>. Analyses of serum levels are troublesome to interpret. They may underestimate the effective amount of mediator acting at a cellular level. Bioassays, which measure the functional activity of cytokines, often lack specificity and may over-report amounts.

Polymicrobial sepsis induced by cecal ligation and puncture (CLP) is a model of sepsis which reproduces many of the inflammatory and pathological sequelae that are observed clinically<sup>[12]</sup>. Following CLP, animals develop bacteremia, hypothermia, hypotension, and damage to multiple organ systems<sup>[13]</sup>. The present study was designed to observe the gene expression of cytokines in hepatic and pulmonary tissues with CLP model, in order to investigate the role of cytokines in organ damage during sepsis.

## MATERIALS AND METHODS

### *Animal model and experimental groups*

NIH mice were obtained from the animal center of the general hospital of Chinese PLA. The mice were randomly divided into two groups: CLP group and sham group. Sepsis was induced by cecal ligation and puncture (CLP). The mice were anesthetized, and the cecum was ligated below the ileocecal junction; and intestinal continuity was maintained. The cecum was punctured twice with a 20-gauge needle and a small amount of cecal contents was expressed through the punctures. The incision was closed and 1 ml of normal saline was administered subcutaneously. Sham-operated mice underwent the same surgical procedure, but without CLP. The mice were sacrificed at 3 or 12 h after the procedure.

### *Preparation of RNA*

Total RNA was extracted from liver and lung tissues according to the guanidinium isothiocyanate single-step methods. The RNA concentration of each sample was estimated by measuring the absorbance at 260 nm.

### *Reverse transcription and PCR*

Total RNA from experimental samples was used to synthesize cDNA using AMV reverse transcriptase.  $\beta$ -actin and  $\beta_2$ -MG were used as

internal control primers. The primers for the cytokines and control were as follows:  $\beta$ -actin (478bp): 5'AGG GAA ATC GTG CGT GAC ATC AAA 3', 5'ACT CAT CGT ACT CCT GCT TGC TGA 3';  $\beta_2$ -MG (300bp): 5'GGC TCG CTC GGT GAC CCT AGT CTT T 3', 5'TCT GCA GGC GTA TGT ATC AGT CTC A 3'; TNF- $\alpha$  (349bp): 5'TTC TGT CCC TTT CAC TCA CTG G3', 5'TTG GTG GTT TGC TAC GAC GTG G 3'; IL-1 $\beta$  (441bp): 5'ATT AGA CAG CTG CAC TAC AGG CTC 3', 5'AGA TTC CAT GGT GAA GTC AAT TAT 3'; IL-6 (156bp): 5'TGG AGT CAC AGA AGG AGT GGC TAA G 3', 5'TCT GAC CAC AGT GAG GAA TGT CCA C 3'; IL-4 (181bp): 5'CGA AGA ACA CCA CAG AGA GTG AGC T 3', 5'GAC TCA TTC ATG GTG CAG CTT ATC G 3'. PCR was performed in a 25 $\mu$ L reaction volume. A hot start was applied for 5min at 95°C. The amplification cycle (denaturation step at 94°C for 30s, an annealing step at 55°C for 30s and an extension step at 72°C for 90s) was repeated 30 times and followed by a final extension for 10 min at 72°C. Amplified products were separated by electrophoresis in ethidium bromide-stained 15g·L<sup>-1</sup> agarose gel and visualized with UV illumination. The bands representing reaction product on the film were scanned by densitometry. A normalization quotient (Q) was calculated between the integrated optical density values (IOD) for the adhesion molecules and the  $\beta$ -actin or  $\beta_2$ -MG bands ( $Q = \text{IOD adhesion molecules band} / \text{internal control band}$ ). The level of adhesion molecules mRNA were expressed as the quotient of the integrated values for the adhesion molecules and the  $\beta$ -actin or  $\beta_2$ -MG bands.

#### Microvascular permeability in the liver and lungs

Evans blue (15g·L<sup>-1</sup>) was injected intravenously in concentrations of 10 $\mu$ L·g<sup>-1</sup> 0.1ml/10g. The liver and lung tissues were excised and weighed. To each sample of tissues, 4.0mL formamide was added and incubated at 56°C for 72 h. If necessary, the incubation time was prolonged, until the blue color of the samples completely disappeared. After filtration with glass filter, the absorbance of the filtrate was measured at 620nm in a Beckman spectrophotometer. The total amount of dye can be calculated by means of a standard calibration curve. The permeability of microvascular in the liver and lungs was shown as the  $\mu$ g of Evans blue in every mg tissues.

#### Water mass fractions in the liver and lungs

Water mass fractions were used as a parameter of organ water accumulation after CLP. The liver and lung tissues were removed in a humidity chamber and the wet mass was measured immediately. The tissues were dried at 70°C to a constant mass for the determination of dry mass. Organ edema was determined by calculating tissue water content according to the following formula: Water mass fractions (%) = (1-dry mass / wet mass) × 100%.

#### Statistics

All data were reported as  $\bar{x} \pm s$ . Data were analyzed by *t* test for comparisons between two groups.  $P < 0.05$  was accepted as the level of significance.

### RESULTS

#### Cytokine mRNA expression in the liver and lungs

Significant increase in TNF $\alpha$ , IL-1 $\beta$  and IL-6 gene expression was observed at 3 and 12 h after CLP both in the liver and lungs. But the level of IL-4 gene expression was not changed after CLP in the lungs, while it was increased at 12 h after CLP (Figure 1, 2) in the liver tissue.

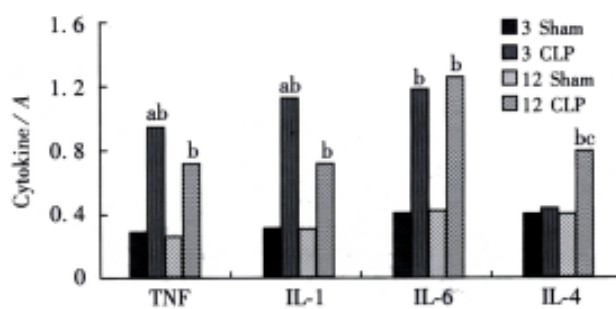


Figure 1 The cytokines gene expression in the liver <sup>a</sup> $P < 0.01$ , vs CLP 12h group, <sup>b</sup> $P < 0.01$ , vs sham group, <sup>c</sup> $P < 0.01$ , vs CLP 3h group

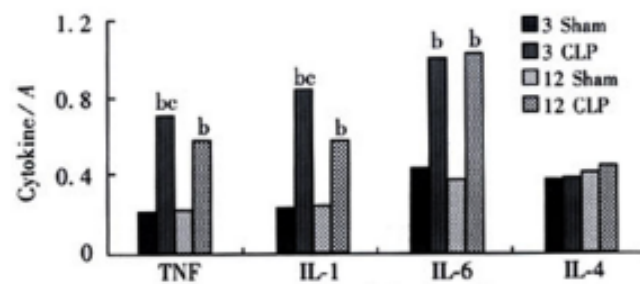


Figure 2 The cytokines gene expression in the lungs <sup>b</sup> $P < 0.01$ , vs sham group, <sup>c</sup> $P < 0.05$ , vs CLP 12h group

#### Microvascular permeability in the liver and lungs

Both the liver and lungs showed a significant increase in microcirculatory permeability at 12 h after CLP, and the increase in the lungs was higher than that in the liver (Figure 3).

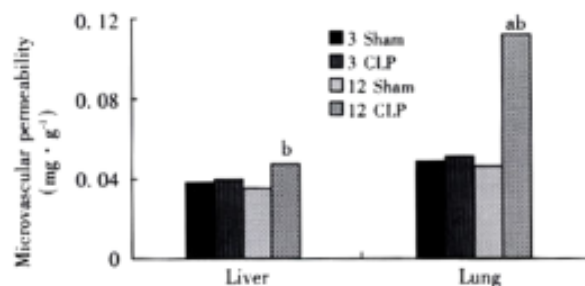


Figure 3 Microvascular permeability in the liver and lungs <sup>a</sup> $P < 0.01$ , vs CLP 3h group, <sup>b</sup> $P < 0.01$ , vs sham group.

#### Water mass fractions in the liver and lungs

The water mass fractions in the liver and lungs were increased after CLP, and the increase in the lungs happened earlier and more severely than that in the liver (Figure 4).

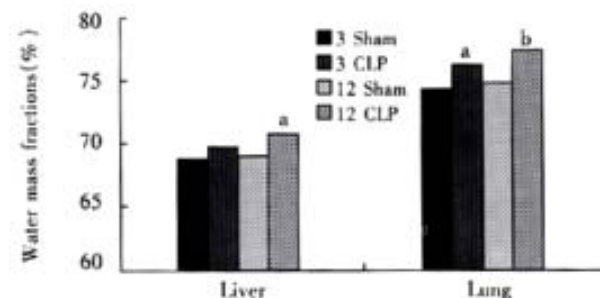


Figure 4 Water mass fractions in the liver and lungs <sup>a</sup> $P < 0.05$ , vs sham group, <sup>b</sup> $P < 0.01$ , vs sham group

## DISCUSSION

SIRS affects all aspects of systemic homeostasis. It is arbitrary, but convenient, to consider its effects from the perspective of the dysfunction of certain key organ systems. It must be recognized, however, that there is no defining combination of systems or temporal sequence of physiologic deterioration that characterizes the syndrome<sup>[14]</sup>. A systematic review of 30 descriptions of MODS published between 1969 and 1993 revealed that respiratory system is the most commonly cited organ system<sup>[15,16]</sup>. The liver with its rich supply of blood and sinusoid is directly exposed to bacteria and endotoxins drained from the GI tract<sup>[17-19]</sup>. Previous works have proclaimed that liver is the most susceptible and vulnerable organ during sepsis and multiple organ failure<sup>[20]</sup>. So in this study, we chose the liver and lungs as the samples to study the role of local cytokine gene expression in organ damage.

Cytokines are polypeptides or glycoproteins of low molecular weight. Most cytokines are not stored as preformed molecules, hence their production requires new gene transcription and translation. Unlike mediators derived from the classical endocrine system, cytokines are produced. The production of cytokines at various tissue sites depends, in part, on the proximity of the site to the injurious stimulus. A lot of cells such as macrophage<sup>[21]</sup> and endothelial cells<sup>[22]</sup> can produce cytokines. Cytokines act predominantly as paracrine and autocrine messengers, not endocrine mediators. Thus, cytokines may exert their major effects locally, within organs and tissues. Assays of circulating cytokine concentrations may be misleading because they do not detect cytokines bound to soluble receptors<sup>[23]</sup>. These assays may also fail to detect cytokines when inhibitors or receptor antagonists are present<sup>[24]</sup>. Therefore investigations in this area require more precise determination of the temporal sequencing and tissue-specific expression of cytokines.

In this study we assessed the gene expression of pro-inflammatory and anti-inflammatory cytokines in the hepatic and pulmonary tissues. Pro-inflammatory cytokines such as TNF $\alpha$ , and IL-1 $\beta$  are known to play predominant roles in the normal inflammatory response. But exaggerated endogenous production is likely responsible for the complications associated with sepsis as tissue injury and ultimate organ failure<sup>[25]</sup>. These pro-inflammatory cytokines result in the production of secondary mediators (including nitric oxide, arachidonic acid metabolites, bradykinin, and histamine) which in turn activate neutrophils and endothelial cells to perpetuate tissue injury<sup>[26, 27]</sup>. But attempts to modulate the biological activity of cytokines with monoclonal antibodies against endotoxin, TNF $\alpha$ , IL-1 have not been successful in improving outcome in several clinical series. Recently, evidence is accumulating that in response to the original inciting event (the inflammatory response), the body also mounts an anti-inflammatory response. Agents that have been identified so far as participating in this anti-inflammatory response include interleukins-4, -10, -11 and -13; transforming growth factor- $\alpha$ ; colony-stimulating factors; soluble receptors to tumor necrosis factor and receptor antagonists to IL-1<sup>[28]</sup>. Because most of these mediators have been discovered recently, we know very little about their actions, and even less about their effects on the pro-inflammatory cascade. However, it had already been shown that some of these mediators, especially some of these interleukins, have a profound effect on monocyte function, including antigen presenting activity<sup>[29]</sup>. They also inhibit T- and B-lymphocyte activity, including antigen-specific T-lymphocyte proliferation. The result is immune suppression, which can sometimes be profound. Of great interest is the fact that these mediators can down-regulate their own synthesis, thereby providing a mechanism through which homeostasis can be restored. Results in this study showed that the conditions of inflammatory reaction in the liver and lungs were different during

sepsis. At the early stage of sepsis, the power of pro-inflammatory reaction was stronger than that of anti-inflammatory reaction both in the liver and lungs. But at the later stage of sepsis, compensatory anti-inflammatory response was found in the liver but not in the lungs.

The consensus of the concept of systemic inflammatory responses has brought about a promising approach in the treatment of SIRS/MODS<sup>[30]</sup> - anti-inflammatory instead of anti-infection<sup>[31,32]</sup>. Various approaches aimed to interrupt the cascade of host inflammatory responses have been tested<sup>[33]</sup>. These include interventions targeted at the inflammation effector cells as monoclonal antibodies or receptor antagonist to pro-inflammatory cytokines<sup>[34,35]</sup>. However, many of these seemingly effective measures in experimental study failed when moved from the laboratory bench to clinical ward<sup>[36,37]</sup>. As results showed in this study that the conditions of inflammatory reaction in the liver and lungs were different during sepsis, it is postulated that in the strategy of anti-inflammatory interventions such as monoclonal antibodies against endotoxin and TNF $\alpha$ , in addition to timing, organ targeting may also be considered.

## REFERENCES

- Memmini G, Buggiani B, Ciulli L, Cavallini MR, Turini M, Pierini A, Bianchi F, Moggi C. Study on 480 hospitalized febrile children: evaluation of the septic risk and results of the antibiotic and corticosteroid combined therapy. *Pediatr Med Chir* 1999; 21:119-123
- D'Amico D, Cillo U. Impact of severe infections on the outcome of major liver surgery: a pathophysiologic and clinical analysis. *J Chemother* 1999; 11:513-517
- Jarrar D, Chaudry IH, Wang P. Organ dysfunction following hemorrhage and sepsis: mechanisms and therapeutic approaches. *Int J Mol Med* 1999; 4:575-583
- Crouser ED, Julian MW, Weinstein DM, Fahy RJ, Bauer JA. Endotoxin-induced ileal mucosal injury and nitric oxide dysregulation are temporally dissociated. *Am J Respir Crit Care Med* 2000; 161:1705-1712
- Brun-Buisson C. The epidemiology of the systemic inflammatory response. *Intensive Care Med* 2000; 26 Suppl 1(-EM-):S64-74
- Qin RY, Zou SQ, Wu ZD, Qiu FZ. Influence of splanchnic vascular infusion on the content of endotoxins in plasma and the translocation of intestinal bacteria in rats with acute hemorrhage necrosis pancreatitis. *World J Gastroenterol* 2000; 6:577-580
- Vincent JL. Update on sepsis: pathophysiology and treatment. *Acta Clin Belg* 2000; 55:79-87
- Terregino CA, Lopez BL, Karras DJ, Killian AJ, Arnold GK. Endogenous mediators in emergency department patients with presumed sepsis: are levels associated with progression to severe sepsis and death? *Ann Emerg Med* 2000; 35:26-34
- Todoroki H, Nakamura S, Higure A, Okamoto K, Takeda S, Nagata N, Itoh H, Ohsato K. Neutrophils express tissue factor in a monkey model of sepsis. *Surgery* 2000; 127:209-216
- Presneill JJ, Waring PM, Layton JE, Maher DW, Cebon J, Harley NS, Wilson JW, Cade JF. Plasma granulocyte colony-stimulating factor and granulocyte - macrophage colony - stimulating factor levels in critical illness including sepsis and septic shock: relation to disease severity, multiple organ dysfunction, and mortality. *Crit Care Med* 2000; 28:2344-2354
- Paterson RL, Webster NR. Sepsis and the systemic inflammatory response syndrome. *J R Coll Surg Edinb* 2000; 45:178-182
- Salkowski CA, Detore G, Franks A, Falk MC, Vogel S. Pulmonary and hepatic gene expression following cecal ligation and puncture: monophosphoryl lipid A prophylaxis attenuates sepsis-induced cytokine and chemokine expression and neutrophil infiltration. *Infect Immun* 1998; 66: 3569-3578
- Matsukawa A, Hogaboam CM, Lukacs NW, Lincoln PM, Evanoff HL, Kunkel SL. Pivotal role of the CC chemokine, macrophage-derived chemokine, in the innate immune response. *J Immunol* 2000; 164: 5362-5368
- Zhang WZ, Han TQ, Tang YQ, Zhang SD. Rapid detection of sepsis complicating acute necrotizing pancreatitis using polymerase chain reaction. *World J Gastroenterol* 2001; 7:289-292
- Somogyi-Zalud E, Zhong Z, Lynn J, Dawson NV, Hamel MB, Desbiens NA. Dying with acute respiratory failure or multiple organ system failure with sepsis. *J Am Geriatr Soc* 2000; 48(5 Suppl):S140-145
- Medoff BD, Harris RS, Kesselman H, Venegas J, Amato MB, Hess D. Use of recruitment maneuvers and high-positive end-expiratory pressure in a patient with acute respiratory distress syndrome. *Crit Care Med* 2000; 28:

- 1210-1216
- 17 Fu WL, Xiao GX, Yue XL, Hua C, Lei MP. Tracing method study of bacterial translocation *in vivo*. *World J Gastroenterol* 2000;6:153-155
- 18 Koo DJ, Chaudry IH, Wang P. Mechanism of hepatocellular dysfunction during sepsis: the role of gut-derived norepinephrine. *Int J Mol Med* 2000; 5:457-465
- 19 Gong JP, Han BL. Effect of CD14 in LPS mediating inactivation of Kupffer cells. *Shijie Huaren Xiaohua Zazhi* 1999;7:875-877
- 20 Wu RQ, Xu YX, Song XH, Chen LJ, Meng XJ. Adhesion molecule and proinflammatory cytokine gene expression in hepatic sinusoidal endothelial cells following cecal ligation and puncture. *World J Gastroenterol* 2001; 7: 128-130
- 21 Ebong S, Call D, Nemzek J, Bolgos G, Newcomb D, Remick D. Immunopathologic alterations in murine models of sepsis of increasing severity. *Infect Immun* 1999; 67:6603-6610
- 22 Marie C, Muret J, Fitting C, Payen D, Cavaillon JM. Interleukin-1 receptor antagonist production during infectious and noninfectious systemic inflammatory response syndrome. *Crit Care Med* 2000; 28:2277-2282
- 23 Zhang GQ, Yu H, Zhou XQ, Liao D, Xie Q, Wang B. TNF- $\alpha$  induced apoptosis and necrosis of mice hepatocytes. *Shijie Huaren Xiaohua Zazhi* 2000; 8: 303-306
- 24 Bulger EM; Maier RV. Lipid mediators in the pathophysiology of critical illness. *Crit Care Med* 2000; 28(4 Suppl):N27-36
- 25 Yu PW, Xiao GX, Fu WL, Yuan JC, Zhou LX, Qin XJ. Pathogenetic effects of platelet activating factor on enterogenic endotoxemia after burn. *World J Gastroenterol* 2000;6:451-453
- 26 Takahashi Y, Katayose D, Shindoh C. Interleukin-13 prevents diaphragm muscle deterioration in a septic animal model. *Tohoku J Exp Med* 1999; 189:191-202
- 27 Matsukawa A, Hogaboam CM, Lukacs NW, Lincoln PM, Evanoff HL, Strieter RM, Kunkel SL. Expression and contribution of endogenous IL-13 in an experimental model of sepsis. *J Immunol* 2000; 164:2738-2744
- 28 Bernard GR. Research in sepsis and acute respiratory distress syndrome: are we changing course? *Crit Care Med* 1999; 27: 434-436
- 29 Ishikawa K, Tanaka H, Nakamori Y, Hosotsubo H, Ogura H, Nishino M, Shimazu T, Sugimoto H. Difference in the responses after administration of granulocyte colony-stimulating factor in septic patients with relative neutropenia. *J Trauma* 2000; 48:814-824
- 30 Faist E, Kim C. Therapeutic immunomodulatory approaches for the control of systemic inflammatory response syndrome and the prevention of sepsis. *New Horiz* 1998; 6: S97-S102
- 31 Suputtamongkol Y, Intaranongpai S, Smith MD, Angus B, Chaowagul W, Permpikul C, Simpson JA, Leelarasamee A, Curtis L, White NJ. A double-blind placebo-controlled study of an infusion of lexipafant (Platelet-activating factor receptor antagonist) in patients with severe sepsis. *Antimicrob Agents Chemother* 2000; 44:693-696
- 32 Abraham E. Why immunomodulatory therapies have not worked in sepsis. *Intensive Care Med* 1999; 25: 556-566
- 33 Deitch EA, Goodman ER. Prevention of multiple organ failure. *Surg Clin North Am* 1999; 79:1471-1488
- 34 Lazon V, Barke RA. Gram-negative bacterial sepsis and the sepsis syndrome. *Urol Clin North Am* 1999; 26:687-699
- 35 Nasraway SA. Sepsis research: we must change course. *Crit Care Med* 1999; 27: 427-430

Edited by Ma JY



• BASIC RESEARCH •

# Construction of HCV-core gene vector and its expression in cholangiocarcinoma

Xiao-Fang Liu, Sheng-Quan Zou, Fa-Zu Qiu

Xiao-Fang Liu, Sheng-Quan Zou, Fa-Zu Qiu, Department of General Surgery of Tongji Hospital, Wuhan 430030, Hubei Province, China  
Correspondence to: Dr.Xiao-Fang Liu, Department of Genneral Surgery of Tongji Hospital, 1095 Jiefang Road, Wuhan 430030, Hubei Province, China. Liu634@263.net

Telephone: +86-27-83662134

Received 2001-04-21 Accepted 2001-08-15

## Abstract

**AIM:** To establish an experimental model for exploring the role of hepatitis C virus (HCV) in the development of cholangiocarcinoma.

**METHODS:** Recombinant plasmid of HCV-core gene was constructed with molecular cloning technique and transfected into QBC939 cells with lipofection. After it was selected with G418, resistant colonies were obtained. The colonies were analysed by immunocytochemistry and Western blotting. The morphology was observed under transmission electron microscope(TEM) and microscope.

**RESULTS:** The recombinant plasmid was proved to carry the target gene by PCR and restriction enzymed mapping. Moreover, it could express HCV-C protein efficiently in QBC939 cells. The HCV-like particles were found in the cytoplasm by electron microscope, which were spherical with a diameter of 50nm-80nm possessing outer membrane. The transfected cells had lower differentiation and higher malignant degree under microscope.

**CONCLUSION:** Because HCV-core gene could express steadily in cholangiocarcinoma cells, the transfected tumor cells(QBC939-HCVC) could be used to study the effect of HCV in the development of cholangiocarcinoma.

Liu XF, Zou SQ, Qiu FZ. Construction of HCV-core gene vector and its expression in cholangiocarcinoma. *World J Gastroenterol* 2002;8(1):135-138

## INTRODUCTION

Cholangiocarcinoma is the second cancer of hepatobiliary system. The incidence and mortality of cholangiocarcinoma are increasing yearly. There are 3000 new patients in America each year. Recent reports showing the expression of HCV RNA and HCV antigens in cholangiocarcinoma<sup>[1-8]</sup>, have provided new insights into the pathogenesis of cholangiocarcinoma. Hepatitis C virus(HCV) is recognized as a kind of serious infectious source to harm the health of the humans. It could lead to cancer<sup>[9-17]</sup>. Moreover, its core protein could act as a transcriptional regulator of various viral and cellular promoters to potentially disrupt normal cellular functions<sup>[18-21]</sup>. Thus, the function of core protein is important for carcinogenesis. We constructed the recombinant plasmid of HCV core gene with molecular cloning technique and transfected into cholangiocarcinoma cells with lipofection, and established an experimental model for exploring the role of HCV in the development of cholangiocarcinoma.

## MATERIALS AND METHODS

### Materials

Plasmids and bacterium strain PBK-HCV encompassing the core and envelope genomic regions of HCV, containing 330nt - 2020nt of HCV II strain, was provided as a gift by Dr.Chen (Institute of Infectious Disease, Zhejiang University), whose restriction sites were *Pst*I and *Eco*RI. The prokaryotic expressing vector of PBK-CMV containing MCS(multiple cloning site), the neomycin- and kanamycin-resistance gene, SV40 poly(A), was purchased from Stratagene Co. *E.coli* JM109 was obtained from the collection kept in our research group.

**Cells** The QBC939 cells(a cholangiocarcinoma cell line) were a generous gift from Dr. Wang Shuguang(Third Military Medical University, China). QBC939 cells were cultured in RPMI 1640 supplemented with 100mL·L<sup>-1</sup> FBS and incubated at 37°C in a 50mL·L<sup>-1</sup> CO<sub>2</sub> atmosphere.

**Reagents** Restriction enzymes(*Sal*I and *Bam*H I), Taq DNA polymerase, T<sub>4</sub> DNA ligase, were purchased from Hua Mei Co. Lipofection was provided by Boehringer Mannheim Co. Mouse anti-HCV C protein monoclonal antibody was purchased from Chemicon Co. House anti-mouse IgG(mouse)-AP, NBT/BICP were purchased from Zhong Shan Co. Biotinylated-conjugated sheep anti-mouse IgG was purchased from Boster Co.

**PCR primers** Two primers were designed according to the sequence of HCV core genomic regions and synthesized by the Shanghai GeneCore Bio Technologies Co. Primer 1: 5'-CTCGTCGACCATGAGCACAAATCCTAA-3'; Primer 2: 5'-CTCGGATCCTAAGCGGAAGC-TGGGATG-3'. Primer 1 was 5' primer containing *Sal*I site and Primer 2 was 5' primer containing *Bam*HI site.

### Methods

**PCR amplification** PCR amplification was done using the PBK-HCV as a template and primers 1 and 2 as primers. The reaction was performed according to the parameters of 94°C 3min, 94°C 1min, 55°C 30s and 72°C 1min for 35 cycles. Then it was extended 10min at 72°C. The amplified fragment (approx 600bp) was analyzed by 9 g·L<sup>-1</sup> agarose-gel electrophoresis. The product was purified and used for DNA recombination.

**DNA recombination** DNA recombination was performed according to the methods described in reference<sup>[22]</sup>. A 0.6kb fragment, containing HCV core gene, was obtained from the PCR product after digestion with *Sal*I and *Bam*HI. The fragment was recombined into plasmid PBK-CMV and the resulted recombinant plasmid was designated as PBK-HCVC (Figure 1).

**Transfection of cells** Transfection was performed with lipofection. The constructed vector and control plasmid were used to transfect QBC939 cells in culture. Seven-two h after transfection, they were selected with G418. Then the cells were harvested and used for the detections.

**Immunocytochemistry for HCV core protein** Detection of HCV core protein expression was performed using a mouse anti-HCV core protein monoclonal antibody(1 : 50) on cell sections of transfected QBC939 and control plasmid.

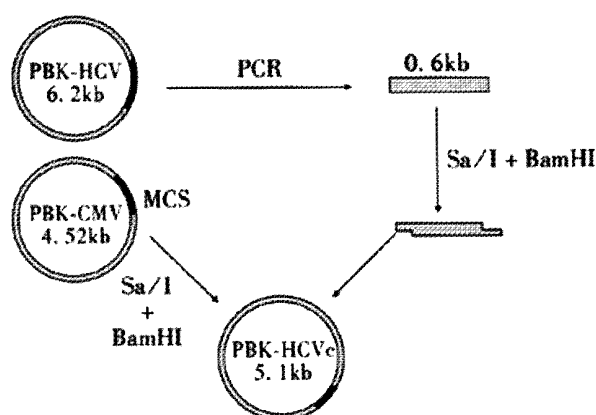


Figure 1 Construction of plasmid PBK-HCVC.

**Western blotting** Detection of HCV core protein by immunoblotting was performed. Briefly, cells ( $1 \times 10^6$ ) were scraped, centrifuged briefly, and lysed for 30 min on ice in  $50 \text{ mmol} \cdot \text{L}^{-1}$  Tris-Cl (pH 7.5),  $150 \text{ mmol} \cdot \text{L}^{-1}$  NaCl,  $0.2 \text{ mmol} \cdot \text{L}^{-1}$  EDTA,  $1 \text{ mmol} \cdot \text{L}^{-1}$  PMSF and  $10 \text{ g} \cdot \text{L}^{-1}$  NP-40. The samples were cleared by centrifugation ( $14000 \text{ r} \cdot \text{min}^{-1}$ , 30 min,  $4^\circ \text{C}$ ), and assessed for protein concentration. SDS-PAGE was performed, and proteins were electroblotted onto nitrocellulose membranes. After 1 h incubation in blocking solution, the membrane was exposed to the primary antibody 2 h at  $4^\circ \text{C}$ . After washing in PBS, the secondary AP-labeled antibody was added for 2 h at room temperature. The proteins were visualized with NBT-BICP.

**Transmission electron microscope** A pellet of the transfected cells was fixed in  $2.5 \text{ g} \cdot \text{L}^{-1}$  glutaraldehyde, postfixed with  $10 \text{ g} \cdot \text{L}^{-1}$  osmium tetroxide, treated with  $20 \text{ g} \cdot \text{L}^{-1}$  uranyl acetate, dehydrated in ethanol, infiltrated with propylene oxide, and embedded in Epon mixture. Ultrathin sections were observed under Opton EM 10C (German).

**Microscope** After selected with G418, the cell sections were stained with HE. The cell sections were observed under microscope.

## RESULTS

### Identification of reconstructed plasmid by PCR and restriction enzymes

The reconstructed plasmid was amplified by PCR, using the PBK-HCVC as a template and primers 1 and 2 as primers, the reaction was performed according to the same parameters. PCR product was approx 600 bp (Figure 2). Then it was identified by the digestion with restriction enzymes (*SmaI* and *BamHI*). Fragments of 4500 bp and 600 bp were produced from the digestion. It was proved to carry the target gene (Figure 3).

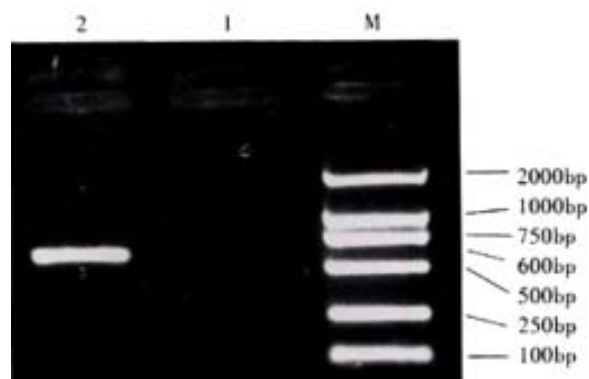


Figure 2 Electrophoretic analysis of PCR product.  
M: Marker DL2000; 1: Negative control; 2: PCR product

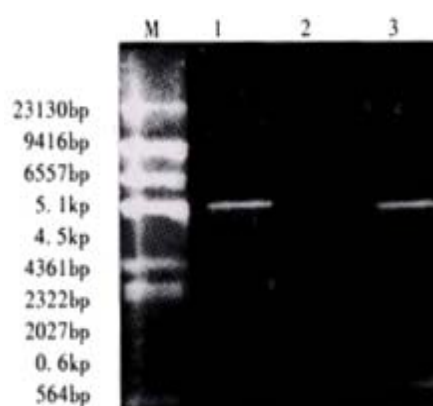


Figure 3 The restriction mapping of PBK-HCVC  
M: Maker;  $\phi$  DNA/Hindc6; 1: PBK-CMV; 2: PBK-HCVC; 3: PBK-HCVC restricted by *SmaI* and *BamHI*

### Expression of the HCV core protein

Cell sections of transfected with PBK-HCVC and control plasmid (PBK-CMV) were stained for HCV core protein. Staining for HCV core protein was seen in the PBK-HCVC transfected QBC939 cells. Positive staining was located to the cytoplasm (Figure 4).

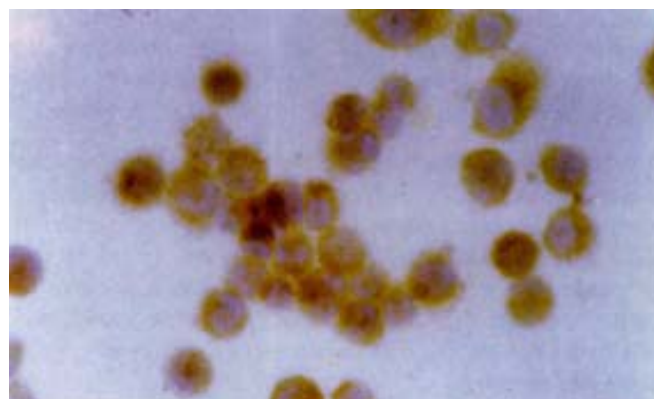


Figure 4 Detection of expressed HCV C antigen by immunocytochemistry.  $\times 200$

The expressed products in the supernatant which were transfected with PBK-HCVC and control plasmid (PBK-CMV) were identified by Western blotting. A approx 21 ku band, similar to the size of HCV core protein, was observed in the supernatant of transfection with PBK-HCVC (Figure 5). These results showed that the QBC939 cells transfected with PBK-HCVC could express HCV core protein.

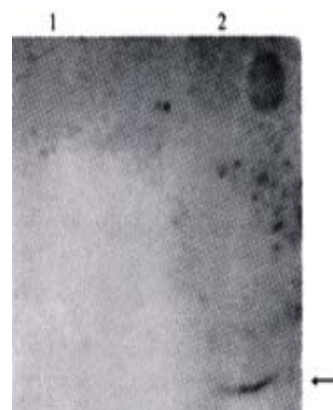
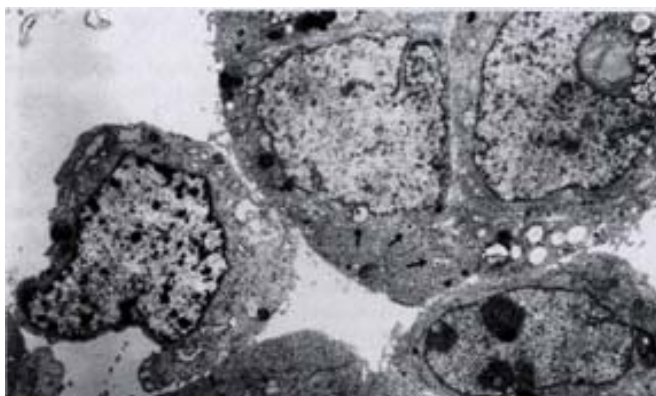


Figure 5 Western blotting detection of the expressed HCV-C protein  
1: Transfected QBC939 cells with PBK-CMV; 2: Transfected QBC939 cells with PBK-HCVC



**Figure 6** Morphology of QBC939-HCVC cells by TEM.  $\times 6500$

### ***The morphologic alteration of the transfected cells***

On day 15 after QBC939 cells were transfected with PBK-HCVC, the HCV-like particles were found in the cytoplasm under TEM, which were spherical with a diameter of 50nm-80nm possessing outer membrane (Figures 6,7). The structures were absent in the negative control. The results suggested that the recombinant plasmid could express HCV core protein efficiently in cholangiocarcinoma cell lines. The splits of nuclei were increased significantly in transfected QBC939 cells with PBK-HCVC than PBK-CMV and QBC939 cells (Figure 8). It suggested that the extent of the differentiation was reduced and malignant degree was enhanced after QBC939 cells were transfected with PBK-HCVC.

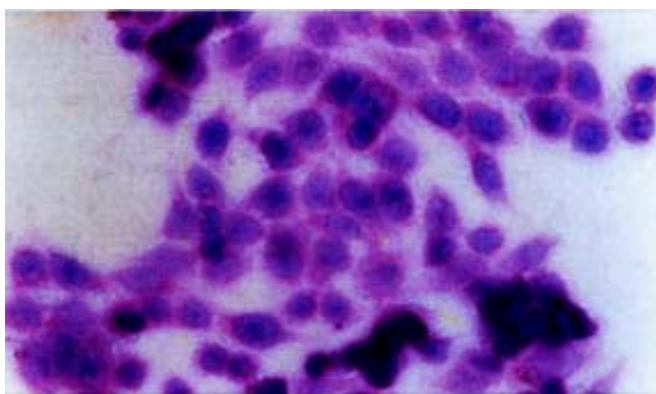


**Figure 8** The morphologic alteration of the transfected cells HE.  $\times 200$

## **DISCUSSION**

The pathogenesis of cholangiocarcinoma is not clear. Cholelithiasis, cystic dilation of the biliary system, ulcerative colitis and primary sclerosing cholangitis are thought to be the risk factors for cholangiocarcinoma. Recently, laboratory and epidemiological studies found and epidemic found the infection of HCV was related to the development of cholangiocarcinoma [1-8,23-25]. But the mechanism of how they are related has not been studied deeply. HCV infection is an important cause of morbidity and mortality worldwide, causing a spectrum of liver diseases ranging from an asymptomatic carrier state to end-stage liver disease. The most important feature of persistent HCV infection is the development of chronic hepatitis in half of the infected individuals and the potential for disease progression to hepatocellular carcinoma. In our country there are 30-40 million of HCV-carriers patients [26-28].

HCV are hepatotropic viruses. Viral replication and cellular injury are largely confined to the liver. Recent studies, however, have suggested that HCV may replicate in tissues other than in hepatocyte only. Many scholars have reported the presence of HCV RNA and

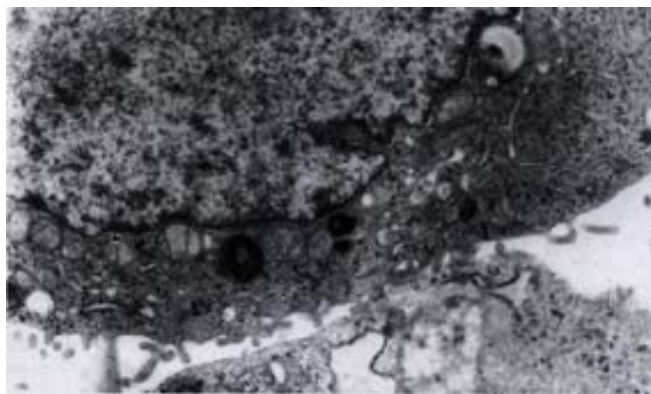


**Figure 7** Morphology of QBC939-HCVC cells by TEM.  $\times 60\ 000$

HCV-antigens in lymph nodes, pancreas, ovary, kidney, heart and bile duct epithelial cells [29-35]. The infection of HCV could lead to bile duct damage and loss. Moreover, bile duct injury is more commonly associated with HCV than either HBV or autoimmune hepatitis, which is the characteristic histologic feature of HCV. The bile duct damage and loss are defined as variable epithelial, steatosis, lymphocytic infiltration of bile ducts [36-38]. The more injury of HCV infection in bile duct provides new evidence that bile duct epithelial cells could be an important reservoir of HCV and might lead to the pathogenesis of cholangiocarcinoma. An HCV genome contains a linear, positive-strand RNA molecule of 9500 nucleotides encoding a single polypeptide precursor of 3000 amino acids. The polypeptide is cleaved by viral proteases to generate three putative structural proteins (C, E1 and E2) and at least six nonstructural proteins (NS2, NS3, NS4A, NS4B, NS5A and NS5B) [39,40]. The genomic region encoding the putative C protein is also called core protein. The HCV core protein could act as a transcriptional regulator of various viral and cellular promoters to potentially disrupt normal cellular functions [18-21]. The core protein may cooperate with ras oncogene and transform primary rat embryo fibroblasts to a tumorigenic phenotype [41]. It may also cause anti-apoptosis by reversion of tumor suppressor gene-p53 and activation of NF- $\kappa$ B and implicate a mechanism by which HCV may evade the host immune surveillance leading to viral persistence and possibly to carcinogenesis [42-51]. Thus, the HCV core protein plays a major role in the malignant transformation of cells. It is important to explore the role of HCV in the development of cholangiocarcinoma by establishing an experimental model which expresses efficiently HCV core protein in cholangiocarcinoma cell lines.

In our study, recombinant plasmid of HCV-core gene was constructed with molecular cloning technique, it was identified by restriction enzymes. Then it was transfected into QBC939 cells with lipofection. After it was selected with G418 made by the presence of the neomycin and kanamycin resistance gene, resistant colonies were obtained. The colonies were analysed by immunocytochemistry and Western blotting. The results suggest that the recombinant plasmid was proved to carry the target gene by PCR and restricted enzyme map, and it could express HCV core protein efficiently in QBC939 cells. The morphology was observed under transmission electron microscopy (TEM), and the HCV-like particles in the cytoplasm, were found spherical with a diameter of 50nm-80nm possessing outer membranes. Moreover, we also found that the splits of nuclei were increased in transfected QBC939 cells with PBK-HCVC, and the extent of differentiation was reduced. It suggested that the malignant degree was enhanced after QBC939 cells were transfected with PBK-HCVC. Because HCV-core gene could express steadily in cholangiocarcinoma cells, the transfected tumor cells (QBC939-HCVC) could be used to study the effect of HCV in the development of cholangiocarcinoma.

## REFERENCES

- Tomimatsu M, Ishiguro N, Tanai M, Okuda H, Saito A, Obata H, Yamamoto M, Takasaki K, Nakano M. Hepatitis C virus antibody in patients with primary liver cancer (hepatocellular carcinoma, cholangiocarcinoma and hepatocellular-cholangiocarcinoma) in Japan. *Cancer* 1993;72:683-688
- Zhang HZ, Tang YB, Lu XY. Detection of hepatitis B virus DNA and hepatitis C virus RNA in human hepatocellular carcinoma by polymerase chain reaction. *Zhonghua Binglixue Zazhi* 1996;25:70-726
- Yin FZ, Chen BF, Xu CS. HCV RNA sequences in cholangiocarcinoma tissues. *Zhonghua Shiyao Waikao Zazhi* 1998;15:109-110
- Chen RF, Zou SQ, Zhao XP. The expression of hepatitis C virus gene in hilar cholangiocarcinoma and implication. *Zhonghua Shiyao Waikao Zazhi* 2000;17:223-224
- Lu HY, Michele Q Ye, Swan N Thung, Dash S, Gerber MA. Detection of hepatitis C virus RNA sequences in cholangiocarcinomas in Chinese and American patients. *Chin Med J* 2000;113:1138-1141
- Chen MY, Huang ZQ, Chen LZ, Gao YB, Peng RY, Wang DW. Detection of hepatitis C virus NS5 protein and genome in Chinese carcinoma of the extrahepatic bile duct and its significance. *World J Gastroenterol* 2000;6:800-804
- Zhai SH, Liu JB, Liu YM, Zhang LL, Du ZP. Expression of HBsAg, HCV-Ag and AFP in liver cirrhosis and hepatocarcinoma. *Shijie Huaren Xiaohua Zazhi* 2000;8:524-527
- Wang WL, Wang CJ, Wang BF. Significance of HCV gene and its antigen expression in human primary intrahepatic cholangiocarcinoma. *Shijie Huaren Xiaohua Zazhi* 2001;9:542-545
- Hiramatsu N, Hayashi N, Haruna Y, Kasahara A, Fusamoto H, Mori C, Fuke I, Okayama H, Kamada T. Immunohistochemical detection of hepatitis C virus-infected hepatocytes in chronic liver disease with monoclonal antibodies to core, envelope and NS3 regions of the hepatitis C virus genome. *Hepatology* 1992;16:306-311
- Yan XB, Wu WY, Wei L. Clinical features of infection with different genotypes of hepatitis C virus. *Huaren Xiaohua Zazhi* 1998;6:653-655
- Zhang LF, Peng WW, Yao JL, Tang YH. Immunohistochemical detection of HCV infection in patients with hepatocellular carcinoma and other liver diseases. *World J Gastroenterol* 1998;4:64-65
- Sorensen HT, Friis S, Olsen JH, Thulstrup AM, Mellemkjaer L, Linet M, Trichopoulos D, Vilstrup H, Olsen J. Risk of liver and other types of cancer in patients with cirrhosis: a nationwide cohort study in Denmark. *Hepatology* 1998;28:921-925
- Yang JM, Wang RQ, Bu BG, Zhou ZC, Fang DC and Luo YH. Effect of HCV infection on expression of several cancer-associated gene products in HCC. *World J Gastroenterol* 1999;5:25-27
- Feng DY, Chen RX, Peng Y, Zheng H, Yan YH. Effect of HCV NS3 protein on p53 protein expression in hepatocarcinogenesis. *World J Gastroenterol* 1999;5:45-46
- Huang F, Zhao GZ, Li Y. HCV genotypes in hepatitis C patients and their clinical significances. *World J Gastroenterol* 1999;5:547-549
- Casemann WH. Clinical characteristics and outcome of a cohort of 101 patients with hepatocellular carcinoma. *World J Gastroenterol* 2001;7:208-215
- Tang ZY. Hepatocellular Carcinoma Cause, Treatment and Metastasis. *World J Gastroenterol* 2001;7:445-454
- Liu QY, Tackney C, Bhat RA, Prince AM, Zhang P. Regulated processing of hepatitis C virus core protein is linked to subcellular localization. *J Virol* 1997;71:657-662
- Dai YM, Shou ZP, Ni CR, Wang NJ, Zhang SP. Localization of HCV RNA and capsid protein in human hepatocellular carcinoma. *World J Gastroenterol* 2000;6:136-137
- Liu LH, Xiao WH, Liu WW. Effect of deoxycytidine on the P16 tumor suppressor gene in hepatocellular carcinoma cell line HepG2. *World J Gastroenterol* 2001;7:131-135
- Ray RB, Meyer K, Ray R. Hepatitis C virus core protein promotes immortalization of primary human hepatocytes. *Virology* 2000;271:197-204
- Sambrook J, Fritsch EF, Maniatis T (Translated by Jin DY, Liang MF). Molecular Cloning: A Laboratory Manual (2nd Ed). Beijing: Science Press 1996:672-898
- Yamamoto M, Takasaki K, Nakanom M. Minute nodular intrahepatic cholangiocarcinoma. *Cancer* 1998;82:2145-2149
- Suriawinata A, Ivanov K, Haim MB, Schwartz ME. A 67-year-old man with hepatitis C virus infection and a liver tumor. *Semi In Liver Dis* 2000;20:227-231
- Kobayashi M, Ikeda K, Saitoh S, Suzuki F, Tsubota A, Arase Y, Murashima N, Chayama K, Kumada H. Incidence of primary cholangiocellular carcinoma of the liver in Japanese with HCV-related cirrhosis. *Cancer* 2000;88:2471-2477
- Zhang SL, Liang XS, Lin SM, Peng Chao Qiu. Relation between viremia level and liver disease in patients with chronic HCV infection. *China Natl J New Gastroenterol* 1996;2:115-117
- Assy N, Minuk GY. A comparison between previous and present histologic assessments of chronic hepatitis C viral infections in humans. *World J Gastroenterol* 1999;5:107-110
- Li LF, Zhou Y, Xia S, Zhao LL, Wang ZX, Wang CQ. The epidemiologic feature of HCV prevalence in Fujian. *World J Gastroenterol* 2000;6:80
- Shimizu YK, Iwamoto A, Hijikata M, Purcell RH, Yoshikura H. Evidence of *in vitro* replication of hepatitis C virus genome in a human T-cell line. *Proc Natl Acad Sci USA* 1993;89:5477
- Moldvay J, Deny D, Pol S, Brechot C, Lamas E. Detection of hepatitis C virus RNA in peripheral blood mononuclear cells of infected patients by *in situ* hybridization. *Blood* 1994;38:269
- Zhou P, Cai Q, Chen YC, Zhang MS, Guan J, Li XJ. Hepatitis C virus RNA detection in serum and peripheral blood mononuclear cells of patients with hepatitis C. *China Natl J New Gastroenterol* 1997;3:108-110
- Kato N, Nakazawa T, Mizutani T, Shimotohno K. Susceptibility of human T-lymphotropic virus type I infected cell line MT-2 to hepatitis C virus infection. *Biochem Bio Res Commun* 1995;26:863-869
- Fan XG, Tang FQ, Ou ZM, Zhang JX, Liu GC, Hu GL. Lymphoproliferative response to hepatitis C virus (HCV) antigens in patients with chronic HCV infection. *Shijie Huaren Xiaohua Zazhi* 1999;7:1038-1040
- Yan FM, Chen AS, Hao F, Zhao XP, Gu CH, Zhao LB, Yang DL, Hao LJ. Hepatitis C virus may infect extrahepatic tissues in patients with hepatitis C. *World J Gastroenterol* 2000;6:805-811
- Cheng JL, Tong WB, Liu BL, Zhang Y, Yan Z, Feng BF. Hepatitis C virus in human B lymphocytes transformed by Epstein-Barr virus *in vitro* by *in situ* reverse transcriptase-polymerase chain reaction. *World J Gastroenterol* 2001;7:370-375
- Bach N, Thung SN, Schaffner F. The histological features of chronic hepatitis C and autoimmune chronic hepatitis: A comparative analysis. *Hepatology* 1992;15:572-577
- Goldin RD, Patel NK, Thomas HE. Hepatitis C and bile duct loss. *J Clin Pathol*, 1996;49: 836-838
- Giannini E, Ceppa P, Botta F, Fasoli A, Romagnoli P, Cresta E. Steatosis and bile duct damage in chronic hepatitis C: distribution and relationships in a group of Northern Italian patients. *Liver* 1999;19:432-437
- Zhang SZ, Liang JJ, Qi ZT, Hu YP. Cloning of the non-structural gene 3 of hepatitis C virus and its inducible expression in cultured cells. *World J Gastroenterol* 1999;5:125-127
- Jiang RL, Lu QS, Luo KX. Cloning and expression of core gene cDNA of Chinese hepatitis C virus in cosmid pTM3. *World J Gastroenterol* 2000;6:220-222
- Ray RB, Lagging LM, Meyer K, Ray R. Hepatitis C virus core protein cooperates with ras and transforms primary rat embryo fibroblasts to tumorigenic phenotype. *J Virol* 1996;70:4438-4443
- Xiao WH, Liu WW, Lu YY, Li Z. Mutation of p53 tumor suppressor gene in hepatocellular carcinoma. *Xin Xiaohuabingxue Zazhi* 1997;5:573-574
- Wei HS, Li DG, Lu HM. Hepatic cell apoptosis and fas gene. *Shijie Huaren Xiaohua Zazhi* 1999;7:531-532
- Li J, Chen YF, Wang WL, Lin SG. Translocated expression of HCV core protein inhibits apoptosis in the tissue of hepatocellular carcinoma. *Shijie Huaren Xiaohua Zazhi* 1999;7:579-582
- Si XH, Yang LJ. Extraction and purification of TGF $\alpha$  and its effect on the induction of apoptosis of hepatocytes. *World J Gastroenterol* 2001;7:527-531
- Ray RB, Meyer K, Ray R. Suppression of apoptotic cell death by hepatitis C virus core protein. *Virology* 1996;226:176-182
- Marusawa H, Hijikata M, Chiba J, et al. Hepatitis C virus core protein inhibits Fas- and Tumor Necrosis Factor Alpha-mediated apoptosis via NF- $\kappa$ B activation. *J Virol* 1999;73:4713-4720
- Ray RB, Meyer K, Steele R, Shrivastava A, Aggarwal BB, Ray R. Inhibition of tumor necrosis factor (TNF- $\alpha$ )-mediated apoptosis by hepatitis C virus core protein. *J BioChem* 1998;273:2256-2259
- Tai DI, Tsai SL, Chen YM, Chuang YL, Peng CY, Sheen IS, Yeh CT, Chang KS, Huang SN, Kuo GC, Liaw YF. Activation of nuclear factor  $\kappa$ B in hepatitis C virus infection: Implication for pathogenesis and hepatocarcinogenesis. *Hepatology* 2000;31:656-664
- Hiramatsu N, Hayashi N, Katayama K, Mochizuki K, Kawanishi Y, Kashara A, Fusamoto H, Kamada T. Immunohistochemical detection of Fas antigen in liver tissue of patients with chronic hepatitis C. *Hepatology* 1994;19:1354-1359
- Yen TS. Nuclear factor  $\kappa$ B and hepatitis C-Is there a connection. *Hepatology* 2000;31:785-787



• BASIC RESEARCH •

# CCK8 inhibits expression of TNF- $\alpha$ in the spleen of endotoxic shock rats and signal transduction mechanism of p38 MAPK

Ai-Hong Meng, Yi-Ling Ling, Xiao-Peng Zhang, Xiao-Yun Zhao, Jun-Lan Zhang

Ai-Hong Meng, Yi-Ling Ling, Xiao-Yun Zhao, Jun-Lan Zhang, Department of Pathophysiology, Hebei Medical University, Shijiazhuang 050017, Hebei Province, China

Xiao-Peng Zhang, Department of Chest Surgery of Hebei Provincial People's Hospital, Shijiazhuang, 050000, China

Supported by the Health Committee of Hebei Province (No.2k002), project supported by Science and Technology Department of Hebei Province (01276410D) and project supported by Natural Science Foundation of Hebei Province (No.302490). The paper published on *World J Gastroenterol*, 2001; 7 (5): 667-671 is key project supported by the Health Committee of Hebei Province (No.2k002), project supported by Science and Technology Department of Hebei Province (01276410D) and project supported by Natural Science Foundation of Hebei Province (No.302490)

Correspondence to: Professor Yi-Ling Ling, Department of Pathophysiology, Hebei Medical University, Shijiazhuang 050017, Hebei Province, China. LingYL20@sina.com.cn

Telephone: +86-311-6052263

Received 2001-10-21 Accepted 2001-12-08

## Abstract

**AIM:** To study the effect of sulfated cholecystokinin-octapeptide (CCK-8) on systemic hypotension, gene and protein expression of TNF- $\alpha$  in spleen of lipopolysaccharide (LPS) induced endotoxic shock (ES) rats, and further investigate the signal transduction mechanism of p38 mitogen-activated protein kinase (MAPK).

**METHODS:** The changes of blood pressure were observed using physiological record instrument in four groups of rats: LPS (8 mg·kg<sup>-1</sup>, iv), CCK-8 (40  $\mu$ g·kg<sup>-1</sup>, iv) pretreatment 10 min before LPS (8 mg·kg<sup>-1</sup>), CCK-8 (40  $\mu$ g·kg<sup>-1</sup>, iv) or normal saline (control) group. The content of TNF- $\alpha$  in the spleen was assayed 2 h after LPS administration using ELISA kit and the expression of TNF- $\alpha$  mRNA was examined 30 min, 2 h and 6 h after LPS administration by reverse transcribed polymerase chain reaction (RT-PCR). Activation of p38 MAPK was detected with Western blot 30 min after LPS administration.

**RESULTS:** CCK-8 reversed LPS-induced decrease of mean arterial pressure (MAP) in rats. The content of TNF- $\alpha$  in the spleen was (282 $\pm$ 30) ng·L<sup>-1</sup> in control group, while it increased to (941 $\pm$ 149) ng·L<sup>-1</sup> in LPS group,  $P < 0.01$ . CCK-8 significantly inhibited the LPS-induced increase of TNF- $\alpha$  content in spleen. It decreased to (462 $\pm$ 87) ng·L<sup>-1</sup> in CCK-8+LPS group,  $P < 0.01$ . The expression of TNF- $\alpha$  mRNA 30 min and 2 h after treatment was stronger in LPS group, while it was lowered after CCK-8 pretreatment. The p38 MAPK expression increased significantly in LPS group (5.84 times of control) and CCK-8 increased the activation of p38 MAPK in ES rats (10.74 times of control).

**CONCLUSION:** CCK-8 reverses the decrease of MAP in ES rats and has inhibitory effect on the gene and protein expression of TNF- $\alpha$  in spleen, and p38 MAPK may be involved in its signal transduction mechanisms.

Meng AH, Ling YL, Zhang XP, Zhao XY, Zhang JL. CCK-8 inhibits expression of TNF- $\alpha$  in the spleen of endotoxic shock rats and signal transduction mechanism of p38 MAPK. *World J Gastroenterol* 2002;8(1):139-143

## INTRODUCTION

Lipopolysaccharide (LPS), main component of Gram-negative bacterial endotoxin<sup>[1]</sup>, is the leading cause of sepsis or endotoxic shock (ES), and when administered experimentally to animals, mimics the same inflammatory response. LPS exerts its effects through cytokines<sup>[2]</sup>. The pathophysiological changes seen in sepsis are often not due to the infectious organism itself but instead to the uncontrolled production of pro-inflammatory cytokines, including tumor necrosis factor (TNF)- $\alpha$ <sup>[3]</sup>. TNF- $\alpha$ , which is produced by LPS-activated target cells, is thought to be LPS's primary mediator<sup>[4]</sup>. TNF is known to have cytotoxic and cytostatic effects on certain tumor cells, and with a pivotal role in inflammatory reactions and regulation of immunological response<sup>[5,6]</sup>. TNF- $\alpha$  was mainly produced in the early stage of endotoxemia, and decreased obviously from 6 h to 9 h after challenge<sup>[7]</sup>. Specific intracellular signaling pathways that modulate cytokine gene expression probably exist in target cells and may represent novel targets for tomorrow's antisepsis therapies<sup>[8]</sup>. Mitogen-activated protein kinases (MAPKs) are members of discrete signaling cascades that form focal points for diverse extracellular stimuli and function to regulate fundamental cellular processes<sup>[9]</sup>. The p38 MAPK, one class of MAPK family, is involved in intracellular signals that regulate a variety of cellular responses during inflammation<sup>[10]</sup>.

CCK-8 possessed both excitatory and inhibitory action on contractile activity of different regions of stomach in guinea pigs<sup>[11]</sup>. In the spleen, CCK-8 is formed in high abundance in the white pulp where it appears to surround cell clusters. CCK-8 is a chemoattractant for human monocytes and rat macrophages, enhances human eosinophil chemotaxis induced by PAF and LTB<sub>4</sub> in allergic patients. Our previous study demonstrated that CCK-8 could protect animals from LPS-induced ES and the protective effect of CCK-8 may be related to its modulation of cytokines<sup>[12-14]</sup>. Spleen, one of the targets stimulated by LPS, is an important immunological organ. In this study, we examined the expression of TNF- $\alpha$  with reverse transcribed polymerase chain reaction (RT-PCR) and enzyme linked immunoabsorbant assay (ELISA) in spleen and further investigated the mechanism involving p38 MAPK.

## MATERIAL AND METHODS

### Material

CCK-8 (sulfated), LPS (*E.coli* LPS, serotype 0111:B4), leupeptin, pepstatin A and Triton X-100 were all purchased from Sigma, and aprotinin from Boehringer. The ELISA kit was purchased from Medsystem (Austria) for assay of TNF- $\alpha$ . Total RNA isolation system and access RT-PCR system were purchased from Promega (USA). Monoclonal anti-p38 MAPK (diphosphorylated p38) was purchased from Sigma (USA). All other reagents used were of analytic grade. Healthy male Sprague-Dawley rats ( $n=52$ , weighing 150 g-200 g BW) were obtained from Experimental Animal Center of Hebei Province.



## Methods

The rats were randomly assigned to four groups and injected different agents via caudal vein. A bolus dose ( $8 \text{ mg} \cdot \text{kg}^{-1}$ ,  $5 \text{ g} \cdot \text{L}^{-1}$ ) of LPS was injected to group receiving LPS and a bolus dose ( $40 \mu\text{g} \cdot \text{kg}^{-1}$ ,  $0.05 \text{ g} \cdot \text{L}^{-1}$ ) of CCK-8 was given to the group of CCK-8+LPS 10 min before injection of LPS. Saline or CCK-8 ( $40 \mu\text{g} \cdot \text{kg}^{-1}$ ) was administered separately to the control or CCK-8 group. Catheter was inserted into femoral artery and Mean arterial pressure (MAP) was detected using physiological record instrument (RM-6000, Japan). The agents were injected through caudal vein after the MAP became steady. Animals were sacrificed at 30 min, 2 h or 6 h after treatment, spleen was rapidly excised, rinsed of blood. The samples were stored at  $-80^\circ\text{C}$ . The samples collected at different time points were for the assay of TNF- $\alpha$  mRNA using RT-PCR, samples collected at 2 h were for the assay of TNF- $\alpha$  protein by ELISA and at 30 min for the expression of p38 MAPK by Western blot.

## TNF- $\alpha$ dection by ELISA

Frozen tissue samples were weighed and placed in homogenization buffer ( $4^\circ\text{C}$ ) at a ratio of 100 mg per milliliter of buffer. Buffer contained a protease-inhibitor cocktail including  $1 \text{ mmol} \cdot \text{L}^{-1}$  phenylmethylsulfonyl fluoride (PMSF),  $1 \text{ mg} \cdot \text{L}^{-1}$  pepstatin A,  $1 \text{ mg} \cdot \text{L}^{-1}$  aprotinin, and  $1 \text{ mg} \cdot \text{L}^{-1}$  leupeptin in phosphate-buffered saline solution, pH 7.2, containing  $5 \text{ g} \cdot \text{L}^{-1}$  Triton X-100. Samples were homogenized and centrifuged at  $18\,000 \text{ r} \cdot \text{min}^{-1}$ ,  $4^\circ\text{C}$ . Tissue supernatants were analyzed for TNF- $\alpha$  using ELISA kit.

## Analysis of TNF- $\alpha$ mRNA by RT-PCR

Total RNA was extracted from spleen tissues. The concentration of RNA was determined from absorption at 260 nm. The primers for TNF- $\alpha$  and  $\beta$ -actin were as follows:  $\beta$ -actin (420bp), 5'-GAGACCTTC AACACCCAGCC-3', 5'-TCGGGGCATCGG AACCGCTCA-3'; TNF- $\alpha$  (468bp), 5'-GGATCATCTTCT CAAAACTCG-3', 5'-TCACAGAGCAATGACTCCAAA-3'. Polymerase chain reactions were performed in a  $50 \mu\text{L}$  reaction volume. RT-PCR reaction was run in the following procedures:  $48^\circ\text{C}$  for 45 min, 1 circle;  $94^\circ\text{C}$  for 2 min, 1 circle;  $94^\circ\text{C}$  for 30 s,  $57^\circ\text{C}$  for 30 s,  $68^\circ\text{C}$  for 1 min, 30 circles;  $68^\circ\text{C}$  for 7 min, 1 circle. Six  $\mu\text{L}$  PCR product was placed on to  $15 \text{ g} \cdot \text{L}^{-1}$  agarose gel and observed by EB staining using Gel-Pro analyzer.

## Detection of p38 MAPK expression by Western blot

Spleen was rapidly excised 30 min after agents administration. Tissues were homogenized with PBS (pH 7.2) and centrifuged at  $4^\circ\text{C}$ ,  $18\,000 \text{ r} \cdot \text{min}^{-1}$  for 10 min. Protein contents were detected in supernatants by coomassie brilliant blue (CBB). Sample loading buffer was added, and each sample was boiled for 8 min prior to loading equal content of protein onto a  $12 \text{ g} \cdot \text{L}^{-1}$  SDS-polyacrylamide gels, transferred to polyvinylidene fluoride (PVDF) membranes, and incubated with phospho-specific anti-p38 MAPK. Being washed three times in T-PBS, membranes were incubated in horseradish peroxidase-linked secondary antibody for 1 h at room temperature. Membranes were again washed three times with T-PBS and stained with diaminobenzidine (DAB).

## Statistical analysis

Data were reported as  $\bar{x} \pm s$ . Statistical differences between values from different groups were determined by one way ANOVA and Newman-Keuls  $q$  test. Significance was set at  $P < 0.05$ . Gel-Pro Analyzer was used to analyze the PCR and Western results.

## RESULTS

### Changes of MAP

There was no significant difference between groups before treatment. LPS administration resulted in a significant sustained decrease in MAP during the period of 2 h, decreased to  $(7.82 \pm 0.43) \text{ kPa}$  30 min after LPS administration and restored to  $(9.33 \pm 0.63) \text{ kPa}$  by pretreatment with CCK-8 (Figure 1).

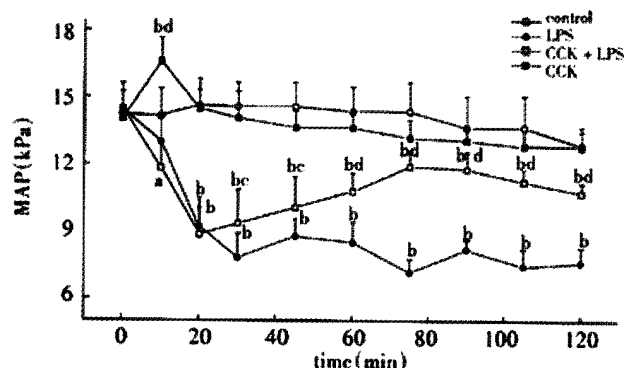


**Figure 1** Mean arterial pressure (MAP) of animals injected normal saline, LPS, CCK+LPS and CCK,  $n=6$ . <sup>a</sup> $P < 0.05$ , <sup>b</sup> $P < 0.01$ , vs Control, <sup>c</sup> $P < 0.05$ , <sup>d</sup> $P < 0.01$ , vs LPS.

### TNF- $\alpha$ content in spleen 2 h after LPS

Spleen TNF- $\alpha$  content became significantly higher 2 h after administration of LPS as compared to the control animals ( $941 \pm 149 \text{ ng} \cdot \text{L}^{-1}$  vs  $(282 \pm 30) \text{ ng} \cdot \text{L}^{-1}$ ,  $P < 0.01$ ), while CCK-8 significantly inhibited the LPS induced increase of TNF- $\alpha$  ( $462 \pm 87 \text{ ng} \cdot \text{L}^{-1}$ ,  $P < 0.01$ ). No significant changes were noted in TNF- $\alpha$  content following CCK-8 administration compared with normal saline administration (Figure 2).

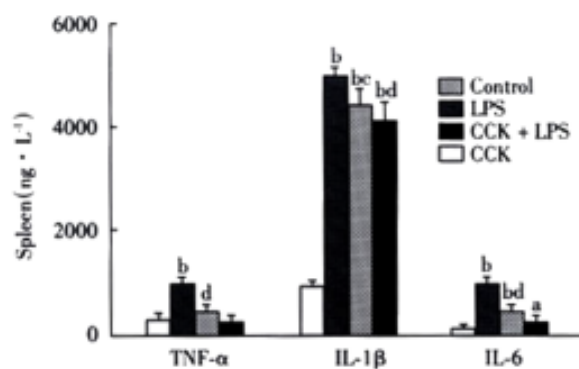


**Figure 2** Effects of CCK on TNF- $\alpha$ , IL-1 $\beta$  and IL-6 2 h (TNF- $\alpha$ ) or 6 h (IL-1 $\beta$  and IL-6) following LPS administration.  $n=6$ . <sup>a</sup> $P < 0.05$ , <sup>b</sup> $P < 0.01$ , vs Control; <sup>c</sup> $P < 0.05$ , <sup>d</sup> $P < 0.01$ , vs LPS.

### RT-PCR detection of TNF- $\alpha$

TNF- $\alpha$  mRNA in spleen was detected by RT-PCR analysis. The results showed that the spleen of rats 30 min and 2 h after LPS administration expressed the gene coding for TNF- $\alpha$  because RT-PCR generated a DNA fragment corresponding to the predicted length, 468bp, of the TNF- $\alpha$  amplification product. The expression of TNF- $\alpha$  decreased in CCK-8+LPS group compared with LPS group. The ratios of  $\beta$ -actin at 30 min and 2 h were  $(85 \pm 8)\%$  and  $(57 \pm 7)\%$  in LPS group, while it decreased to  $(30 \pm 6)\%$  and  $(16 \pm 2)\%$  respectively in CCK-8+LPS group. The TNF- $\alpha$  amplification product was not detected 6 h after agents administration. In each tissue sample, all  $\beta$ -actin amplification products were of 420bp length (Figure 3).

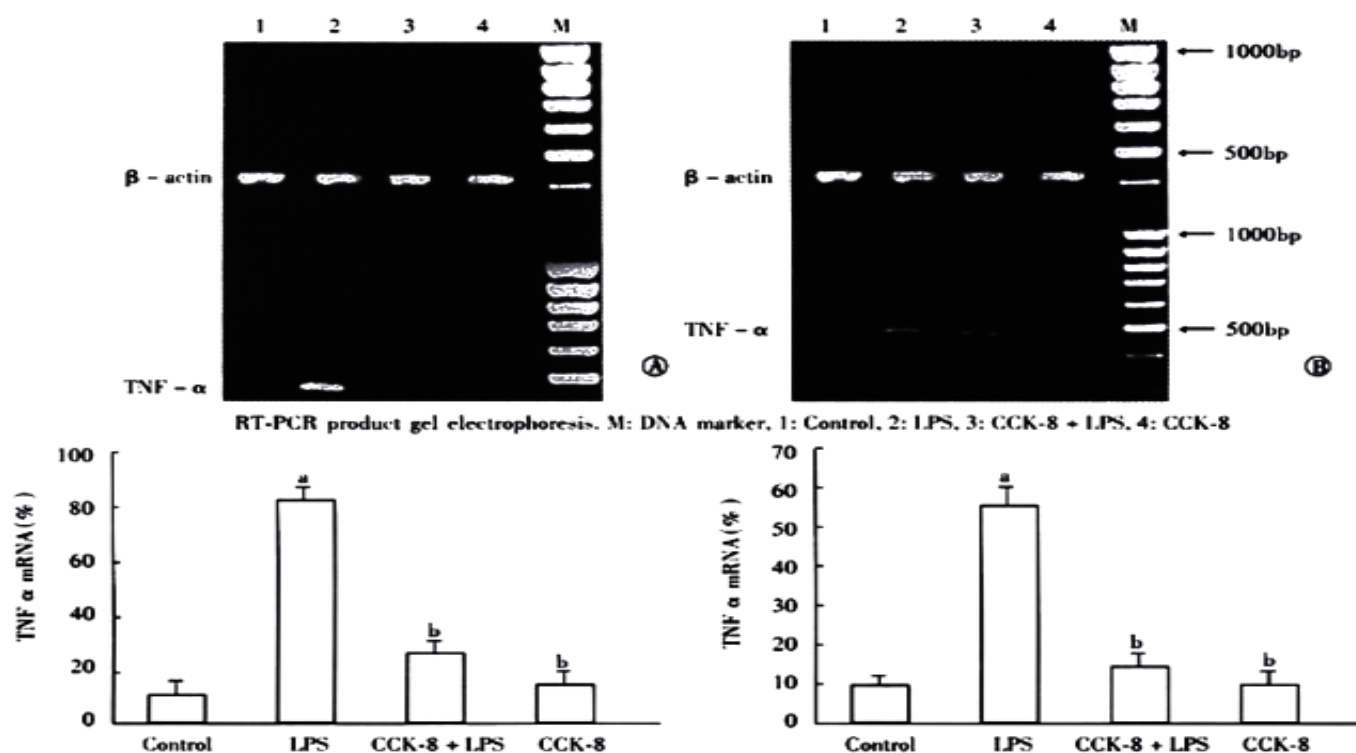


**Figure 3** Effect of CCK-8 on LPS-induced TNF- $\alpha$  mRNA expression. Total RNA from the rat spleen was extracted at 30 min(A) or 2h(B) after LPS administration.  $n=3$ . <sup>a</sup> $P<0.01$  vs Control; <sup>b</sup> $P<0.01$  vs LPS.

#### Analysis of p38 MAPK expression by Western blot

Significant phosphorylation of p38 MAPK was observed in the spleen of rats 30 min after LPS administration, the densitometry units (DU) of LPS group is 5.84 times that of control. CCK-8 can enhance LPS-induced phosphorylation of p38 MAPK significantly, the DU of CCK-8+LPS group is 10.74 times that of control. Phosphorylation of p38 MAPK was also observed in control and CCK-8 groups (4.64 times of control)(Figure 4).

#### DISCUSSION

Although macrophages are the main secretors of TNF- $\alpha$ , other spleen cells, such as lymphocytes, may secrete low amounts of TNF- $\alpha$  and may influence macrophage ability to generate and secrete the cytokine<sup>[15]</sup>. This has led to the suggestion that spleen is an important organ in the production of TNF- $\alpha$  following LPS administration, releasing the cytokines into the circulation, thereby contributing to the elevated serum level of the cytokine. Numerous TNF- $\alpha$  and IL-1 $\beta$  mRNA positive cells were observed using *in situ* hybridization in the marginal zone and in the red pulp of the spleen in rats after LPS injections, whereas sections from saline-treated animals showed minimal cytokine mRNA expression<sup>[16]</sup>. LPS resulted in a greater increase in circulating levels of TNF- $\alpha$  which peaked at 90 min and decreased at 150 min after LPS administration<sup>[17]</sup>. We found that CCK-8 significantly inhibits LPS-induced increase of TNF- $\alpha$  in spleen, which agreed with the results we obtained before<sup>[14]</sup>. While Cunningham *et al*<sup>[18]</sup> reported that CCK-8 stimulated production of TNF- $\alpha$ , IL-1 $\beta$  and IL-6 by monocytes, but was considerably less than LPS response. Later studies<sup>[19]</sup> suggest that the increase of cytokines induced by CCK-8 may be due to the detection of endotoxin/LPS in medium.

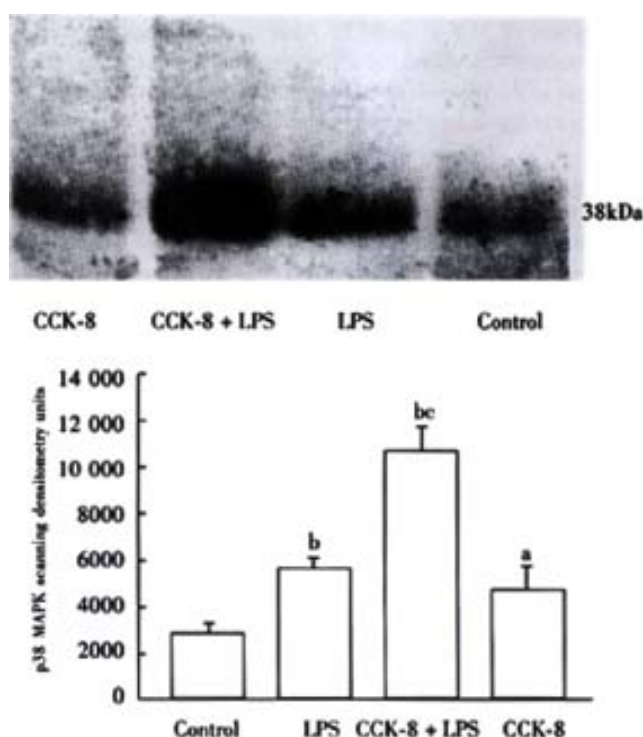


**Figure 4** CCK-8 increases p38 MAPK activation induced by LPS in spleen. <sup>a</sup> $P<0.05$ , <sup>b</sup> $P<0.01$  vs Control; <sup>c</sup> $P<0.01$  vs LPS.

Despite convincing data indicating the protective function of

CCK-8 to organism in ES, the precise mechanism remains elusive. Our previous studies showed that CCK can protect pulmonary arterial endothelium against detrimental effects by LPS or TNF- $\alpha$ <sup>[20,21]</sup>. The anti-inflammatory effect of CCK-8 shown in this study may mediate the cell protective function of CCK-8 in ES. The p38 MAPK pathway may be involved. Members of the MAPK cascade are considered to play key roles in signal transduction pathways activated by a wide range of stimuli<sup>[22]</sup>. CCK is known to activate MAPK signaling pathways<sup>[23]</sup>. Activated MAPK then transduces into the nucleus and phosphorylates the ternary complex factor TCF which activates the expression of immediate-early genes, such as c-fos and egr-1<sup>[24]</sup>. The three best characterized members of this growing family of serine/threonine kinases are extracellular signal regulated kinase (ERK), c-jun N-terminal kinase (JNK) and p38. While ERK responds vigorously to growth factors and certain hormones, JNK and p38 are rather activated by stress stimuli and are widely believed to be part of the cellular stress response machinery<sup>[22,25]</sup>. The p38 MAPK is associated with immune cell activation, because this kinase is activated by a variety of inflammatory mediators. Challenge of neutrophils with LPS leads to activation of p38 but with slower kinetics than G-protein-coupled chemoattractant receptors<sup>[26]</sup>. CCK-A and CCK-B receptors are G-protein-coupled<sup>[27]</sup>. p38 is expressed in the pancreas and rapidly activated by CCK receptor agonist, cerulein<sup>[28,29]</sup>. p38 inhibition aggravated cerulein pancreatitis, indicating that p38 activation may support protection of the pancreas against damage through hyperstimulation stress. CCK activated p38 MAPK and increased the phosphorylation of HSP27<sup>[30]</sup>. The p38-MAPK/HSP27 pathway may be important for organ protection in the pancreas. Other studies indicate that p38 activation can indeed be protective<sup>[14]</sup>. Sodium salicylate (NaSal) significantly reduced TNF- $\alpha$  production in LPS-stimulated macrophages. LPS-stimulated activation of ERK and SAPK/JNK was inhibited by NaSal pretreatment. NaSal treatment of macrophages activated p38 MAPK independent of LPS stimulation<sup>[8]</sup>. Our data have raised the question of how the increase in p38 MAPK activity, a potent intermediate signal transducer involved in the production of TNF- $\alpha$  after LPS administration, could be associated with decreased production of TNF- $\alpha$ , detected by ELISA and RT-PCR analysis in the presence of CCK-8. LPS-induced production of TNF- $\alpha$  is regulated mainly, but not exclusively, through the p38 MAPK pathway<sup>[31]</sup>. TNF- $\alpha$  expression in T cells is regulated by several distinct MAPK pathways that functionally cooperate and are critical for transcriptional as well as for posttranscriptional processes<sup>[32]</sup>. Carbon oxide inhibited the LPS-induced production of TNF- $\alpha$  in mice, which was mediated by p38 MAPK activation<sup>[3]</sup>. Perhaps a delicate balance exists in the actions of p38, in that subtle cellular activation, as with LPS alone, is stimulatory for TNF- $\alpha$  synthesis, whereas hyperstimulation, as seen in spleen treated with CCK-8 and LPS, becomes inhibitory and thus results in downregulation of TNF- $\alpha$ . This modulation by CCK-8 of LPS-induced production of TNF- $\alpha$  exemplifies accumulating evidence emphasizing the complexity of the molecular regulation of TNF- $\alpha$  expression.

The results of the present study show that administration of CCK-8 prevents LPS-induced decrease of MAP and attenuates LPS-induced increase of TNF- $\alpha$  gene and protein expression in spleen. The different activation of p38 MAPK by LPS or CCK-8 may be involved in their effect on TNF- $\alpha$  production. CCK-8, therefore, might be used therapeutically to treat septic shock syndrome and other inflammatory disease states.

## REFERENCES

- Fan K. Regulatory effects of lipopolysaccharide in murine macrophage proliferation. *World J Gastroenterol* 1998; 4:137-139
- Turrin NP, Gayle D, Ilyin SE, Flynn MC, Langhans W, Schwartz GJ, Plata-Salaman CR. Pro-inflammatory and anti-inflammatory cytokine mRNA induction in the periphery and brain following intraperitoneal administration of bacterial lipopolysaccharide. *Brain Res Bull* 2001; 54: 443-453
- Ottervein LE, Bach FH, Alam J, Soares, Lu HT, Wysk M, Davis RJ, Flavell RA, Choi AMK. Carbon monoxide has anti-inflammatory effects involving the mitogen-activated protein kinase pathway. *Nat Med* 2000; 6:422-428
- Yamakawa T, Eguchi S, Matsumoto T, Yamakawa Y, Numaguchi K, Miyata I, Reynolds CM, Motley ED, Inagami T. Intracellular signaling in rat cultured vascular smooth muscle cells: roles of nuclear factor-kappaB and p38 mitogen-activated protein kinase on tumor necrosis factor-alpha production. *Endocrinology* 1999; 140: 3562-3572
- Bai XY, Jia XH, Cheng LZ, Gu YD. Influence of IFN $\alpha$ -2b and BCG on the release of TNF and IL-1 by Kupffer cells in rats with hepatoma. *World J Gastroenterol* 2001; 7:419-421
- Wu RQ, Xu YX, Song XH, Chen LJ and Meng XJ. Adhesion molecule and proinflammatory cytokine gene expression in hepatic sinusoidal endothelial cells following cecal ligation and puncture. *World J Gastroenterol* 2001; 7:128-130
- Zang GQ, Zhou XQ, Yu H, Xie Q, Zhao QM, Wang B, Guo Q, Xiang YQ and Liao D. Effect of hepatocyte apoptosis induced by TNF- $\alpha$  on acute severe hepatitis in mouse models. *World J Gastroenterol* 2000; 6: 688-692
- Vittimberga FJ, McDade TP, Perugini RA, Callery MP. Sodium salicylate inhibits macrophage TNF- $\alpha$  production and alters MAPK activation. *J Surg Res* 1999; 84:143-149
- Browning DD, Windes ND, Ye RD. Activation of p38 mitogen-activated protein kinase by lipopolysaccharide in human neutrophils requires nitric oxide-dependent cGMP accumulation. *J Biol Chem* 1999; 274:537-542
- Ohashi N, Matsumori A, Furukawa Y, Ono K, Okada M, Iwasaki A, Miyamoto T, Nakano A, Sasayama S. Role of p38 mitogen-activated protein kinase in neointimal hyperplasia after vascular injury. *Arterioscler Thromb Vasc Biol* 2000; 20:2521-2526
- Li W, Zheng TZ and Qu SY. Effect of cholecystokinin and secretin on contractile activity of isolated gastric muscle strips in guinea pigs. *World J Gastroenterol* 2000; 6:93-95
- Ling YL, Huang SS, Wang LF, Zhang JL, Wan M and Hao RL. Cholecystokinin-octapeptide (CCK-8) reverses experimental endotoxin shock. *Acta Physiol Sin* 1996; 48: 390-394
- Ling YL, Huang SS, Zhang JL, Wan M, Hao RL. Effect of cholecystokinin on SOD, MDA contents and phagocyte chemiluminescence of reversing endotoxin shock rat. *Zhongguo Bingli Shengli Zazhi* 1997; 13: 483-486
- Ling YL, Meng AH, Zhao XY, Shan BE, Zhang JL and Zhang XP. Effect of cholecystokinin on cytokines during endotoxic shock in rats. *World J Gastroenterol* 2001; 7:667-671
- Lahat N, Rahat MA, Brod V, Cohen S, Weber G, Kinarty A, Bitterman H. Abdominal surgery reduces the ability of rat spleen cells to synthesize and secrete active tumor necrosis factor-alpha (TNF- $\alpha$ ) by a multilevel regulation. *Clin Exp Immunol* 1999; 115: 19-25
- Meltzer JC, Sanders V, Grimm PC, Stern E, Rivier C, Lee S, Rennie SL, Gietz RD, Hole AK, Watson PH, Greenberg AH, Nance DM. Production of digoxigenin-labelled RNA probes and the detection of cytokine mRNA in rat spleen and brain by in situ hybridization. *Brain Res Brain Res Protoc* 1998; 2: 339-351
- Molina PE, Abumrad NN. Differential effects of hemorrhage and LPS on tissue TNF- $\alpha$ , IL-1 and associate neuro-hormonal and opioid alterations. *Life Sci* 2000; 66:399-408
- Cunningham ME, Shaw TA, Bernstein LH, Tinghitella TJ, Claus RE, Brogan DA, McMillen MA. Cholecystokinin-stimulated monocytes produce inflammatory cytokines and eicosanoids. *Am J Gastroenterol* 1995; 90: 621-626
- Lieb K, Fiebich BL, Grawitz MB, Hull M, Berger M. Effect of substance P and selected other neuropeptides on the synthesis of interleukin-1 beta and interleukin-6 in human monocytes: a re-examination. *J Neuroimmunol* 1996; 67: 77-81
- Gu ZY, Ling YL, Meng AH, Cong B, Huang SS. Effect of cholecystokinin octapeptide on the response of rabbit pulmonary artery induced by LPS in vitro. *Zhongguo Bingli Shengli Zazhi* 1999; 15: 484-487
- Meng AH, Ling YL, Wang DH, Gu ZY, Li SJ and Zhu TN. Cholecystokinin-octapeptide alleviates tumor necrosis factor-alpha induced changes in rabbit pulmonary arterial reactivity and injuries of endothelium in vitro. *Shengli Xuebao* 2000; 52:502-506
- Widmann C, Gibson S, Jarpe MB, Johnson GL. Mitogen-activated protein kinase: conservation of a three-kinase module from yeast to human. *Physiol*

- Rev 1999; 79:143-180
- 23 Tapia JA, Ferris HA, Jensen RT, Garcia LJ. Cholecystokinin activates PYK2/CAKbeta by a phospholipase C-dependent mechanism and its association with the mitogen-activated protein kinase signaling pathway in pancreatic acinar cells. *J Biol Chem* 1999; 274: 31261-31271
- 24 Feng DY, Zheng H, Tan Y and Cheng RX. Effect of phosphorylation of MAPK and Stat3 and expression of c-fos and c-jun proteins on hepatocarcinogenesis and their clinical significance. *World J Gastroenterol* 2001; 7: 33-36
- 25 Fleischer F, Dabew R, Ke BG and Wagner ACC. Stress kinase inhibition modulates acute experimental pancreatitis. *World J Gastroenterol* 2001; 7: 259-265
- 26 Browning DD, Windes ND and Ye RD. Activation of p38 mitogen-activated protein kinase by lipopolysaccharide in human neutrophils requires nitric oxide-dependent cGMP accumulation. *J Biol Chem* 1999; 274:537-542
- 27 Monstein HJ, Nylander AG, Salehi A, Chen D, Lundquist L and Hakanson R. Cholecystokinin-A and cholecystokinin-B/gastrin receptor mRNA expression in the gastrointestinal tract and pancreas of the rat and man. *Scand J Gastroenterol* 1996; 31:383-390
- 28 Metzler W, Hofken T, Weber H, Printz H, Goke B, Wagner AC. Hyperthermia, inducing pancreatic heat-shock protein, fails to prevent cerulein-induced stress kinase activation. *Pancreas* 1999; 19:150-157
- 29 Wagner AC, Metzler W, Hofken T, Weber H, Goke B. p38 MAP kinase is expressed in the pancreas and is immediately activated following cerulein hyperstimulation. *Digestion* 1999; 60: 41-47
- 30 Schafer C, Clapp P, Welsh MJ, Benndorf R, Williams JA. HSP27 expression regulates CCK-induced changes of the actin cytoskeleton in CHO-CCK-A cells. *Am J Physiol* 1999; 277:C1029-1031
- 31 Wysk M, Yang D, Lu HT, Flavell RA and Davis RJ. TNF-induced cytokine expression mediated by the p38 MAP kinase activator MKK3. *Proc Natl Acad Sci USA* 1999; 96: 3763-3768
- 32 Hoffmeyer A, Wilde AG, Flory E, Neufeld B, Kunz M, Rapp UR and Ludwig S. Different mitogen-activated protein kinase signaling pathways cooperate to regulate tumor necrosis factor- $\alpha$  gene expression in T lymphocytes. *J Biol Chem* 1999; 274:4319-4327

Edited by Ma JY

• BASIC RESEARCH •

# Effect of cholesterol liposomes on calcium mobilization in muscle cells from the rabbit sphincter of Oddi

Xin-Jiang Wang, Jing-Guo Wei, Chun-Mei Wang, Yao-Cheng Wang, Qiu-Zhen Wu, Jia-Kuan Xu, Xiang-Xin Yang

Xin-Jiang Wang, Jing-Guo Wei, Yao-Cheng Wang, Qiu-Zhen Wu, Jia-Kuan Xu, Xiang-Xin Yang, Department of Radiology, Tangdu Hospital, Chun-Mei Wang, Department of Electron Microscope, Fourth Military Medical University, Xi'an 710038, Shaanxi Province, China

Correspondence to: Dr. Xin-Jiang Wang, Department of Radiology, Tangdu Hospital, the Fourth Military Medical University, Xi'an 710038, Shaanxi Province, China. tdradio@fmmu.edu.cn

Telephone: +86-29-3577163 Fax: +86-29-3577163

Received 2001-04-08 Accepted 2001-06-10

## Abstract

**AIM:** To analyze the influence of cholesterol liposome on the  $\text{Ca}^{2+}$  mobilization of cultured muscle cells in rabbit sphincter of Oddi's.

**METHODS:** New Zealand rabbit was sacrificed and the sphincter of Oddi (SO) segment was obtained aseptically. The SO segment was cut into pieces and cultured in DMEM solution. Then the smooth muscle cells were subcultured, and the 4th-7th passage cells were used for further investigation. The intracellular  $\text{Ca}^{2+}$  increase was measured under confocal microscope after the addition of  $20\text{mmol}\cdot\text{L}^{-1}$  KCl,  $10^{-7}\text{mol}\cdot\text{L}^{-1}$  acetylcholine and  $10^{-7}\text{mol}\cdot\text{L}^{-1}$  cholecystokinin, and different antagonists were added to analyze the  $\text{Ca}^{2+}$  mobilization pathway. After the cells were incubated with  $1\text{g}\cdot\text{L}^{-1}$  cholesterol liposome (CL) (molar ratio was  $\sim 2:1$ ), the intracellular  $\text{Ca}^{2+}$  increase was measured again to determine the effect of CL on cellular  $\text{Ca}^{2+}$  mobilization.

**RESULTS:** The resting cellular calcium concentration of cultured SO cell was  $108\text{nmol}\cdot\text{L}^{-1}\pm 21\text{nmol}\cdot\text{L}^{-1}$ . The intracellular  $\text{Ca}^{2+}$  increases induced by  $20\text{mmol}\cdot\text{L}^{-1}$  KCl,  $10^{-7}\text{mol}\cdot\text{L}^{-1}$  ACh and  $10^{-7}\text{mol}\cdot\text{L}^{-1}$  CCK were  $183\%\pm 56\%$ ,  $161\%\pm 52\%$  and  $130\%\pm 43\%$ , respectively. When the extracellular  $\text{Ca}^{2+}$  was eliminated by  $2\text{mmol}\cdot\text{L}^{-1}$  EGTA and  $5\mu\text{mol}\cdot\text{L}^{-1}$  verapamil, the intracellular  $\text{Ca}^{2+}$  increases induced by KCl, ACh and CCK were  $20\%\pm 14\%$ ,  $82\%\pm 21\%$  and  $104\%\pm 23\%$ , respectively. After the preincubation with heparin, the  $\text{Ca}^{2+}$  increases were  $62\%\pm 23\%$  and  $23\%\pm 19\%$  induced by ACh and CCK, as for preincubation with procaine they were  $72\%\pm 28\%$  and  $85\%\pm 37\%$  induced by ACh and CCK, respectively. Pretreatment with CL for 18h, the resting cellular  $\text{Ca}^{2+}$  concentration elevated to  $152\text{nmol}\cdot\text{L}^{-1}\pm 26\text{nmol}\cdot\text{L}^{-1}$ , however, the cellular  $\text{Ca}^{2+}$  increase percentages in response to these agonists were  $67\%\pm 32\%$ ,  $56\%\pm 33\%$  and  $34\%\pm 15\%$ .

**CONCLUSION:** KCl elicits the SO cellular  $\text{Ca}^{2+}$  increase depends on influx of extracellular  $\text{Ca}^{2+}$ , ACh evoked the SO

**cellular  $\text{Ca}^{2+}$  increase is through the mobilization of intracellular  $\text{Ca}^{2+}$  pool and influx of extracellular  $\text{Ca}^{2+}$  as well, CCK excites the SO cells mainly through mobilization of intracellular IP3-sensitive  $\text{Ca}^{2+}$  store. After the incorporation with cholesterol liposome, KCl, ACh and CCK induced cellular  $\text{Ca}^{2+}$  increase percentages decreased.**

Wang XJ, Wei JG, Wang CM, Wang YC, Wu QZ, Xu JK, Yang XX. Effect of cholesterol liposomes on calcium mobilization in muscle cells from the rabbit sphincter of Oddi. *World J Gastroenterol* 2002;8(1):144-149

## INTRODUCTION

Biliary tract diseases are becoming more common in recent years in China<sup>[1-10]</sup>. Sphincter of Oddi (SO) is an important part located at the distal part of biliary tract. And it is well accepted that SO plays an important role in the regulation of biliary system hydraulic pressure and bile flow<sup>[11-13]</sup>. SO dysfunction (SOD) is one of the causes responsible for biliary tract disorders<sup>[14-16]</sup>, pancreatitis<sup>[17-18]</sup> and other disorders<sup>[19-21]</sup>. The mechanism underlying the occurrence of SOD is controversial, however, several investigators have noticed the relation between hypercholesterolemia and SOD<sup>[22-24]</sup>. Szilvassy *et al*<sup>[23]</sup> reported that patient has an impaired SO relaxation due to high serum lipids, but normalization of serum lipids improved the sphincter of Oddi relaxation. Wei *et al*<sup>[24]</sup> found the abnormalities in ultrastructure of SO in rabbits with hypercholesterolemia. Therefore, hypercholesterolemia might be one of causes of SOD. Meanwhile, the effect of cholesterol on gallbladder contractility has been interpreted by many authors<sup>[25-27]</sup>, who found that the cholesterol incorporated into membrane can impair the cellular signal transduction and contractility as well.

The thin optical sectioning capability of laser scanning confocal microscopy rejects light from out-of-focus planes and permits imaging of  $[\text{Ca}^{2+}]_i$  in single alive cells in optical sections less than  $1\mu\text{m}$  thick, which makes it possible to measure intracellular  $\text{Ca}^{2+}$  alteration instantaneously. So, this experiment was designed to analyze the effect of different agonists on  $\text{Ca}^{2+}$  mobilization of SO cells and cholesterol liposome on this process, in order to explore the mechanism that hypercholesterolemia affected the SO motility.

## MATERIAL AND METHODS

### Materials

The fluo 3/AM was obtained from Molecular Probes (USA), trypsin, HEPES, cholecystokinin-octapeptide (CCK) and bovine serum albumin (BSA) were from Sigma Chemicals (USA), and Dulbecco's modified Eagle's medium (DMEM) was from Gibco Laboratories (USA). The ethylene glycol-bis( $\beta$ -amino ethyl ether)-N,N,N',N'-tetraacetic acid (EGTA), verapamil, procaine, egg phosphatidylcholine and cholesterol were obtained from Shanghai Chemical Co. (China), and the acetylcholine from Suzhou Chemical Co. The dimethyl sulfoxide (DMSO) was purchased from Beijing



Chemical Co. All other chemicals were commercial products of the highest available grade of purity.

### Cells preparation

The New Zealand rabbits (<30d) were euthanized by intravenous injection of ketamine (20mg·kg<sup>-1</sup>), and the segment of Oddi was removed quickly and washed by PBS solution containing penicillin (500×10<sup>3</sup>u·L<sup>-1</sup>). The experiments were conducted in accordance with the institutional ethical guidelines. Mucosa and serosa were dissected carefully, then washed twice with culture medium. The sphincter strip was cut into 1-2 mm<sup>3</sup> squares and placed into culture chamber, the chamber was everted and added into 3mL DMEM medium, and pH was adjusted to 7.4 by addition of 24mmol·L<sup>-1</sup> NaHCO<sub>3</sub> before the use. After 3 h incubation at 37°C, when the tissue squares stuck to the chamber then turn over the chamber, replaced the medium every 4-5 d.

**Subculture:** Cells migrated from the explants 10-15d, as the chamber was confluent with cells, then subcultured by addition with 2.5g·L<sup>-1</sup> trypsin at 37°C for 10 min. The trypsin was inactivated by bovine serum, and the cell suspension was centrifuged at 1000r·min<sup>-1</sup> for 7 min. The supernatant was removed and cell pellet resuspended in fresh medium to a concentration of 5-7×10<sup>5</sup>·mL<sup>-1</sup> and repassaged into several chambers.

**Differentiation:** Three glass cover slips (18mm×18mm) placed into a 6cm diameter chamber, then cell suspension was added and incubated for 48 h. The slips covered with cells and fixed with 950mL·L<sup>-1</sup> ethanol for 30min, washed with PBS for 5min and desiccated naturally. The  $\beta$ -actin staining was performed with immunohistological kits. The positive stain was localized in long, straight, noninterrupted fibrils scattered densely along the longitudinal axis. Under phase-contrast microscope, the cultured cells showed a characteristic “hill- and - valley” growth pattern, and the 4th-7th passage cells were used in this experiments.

### Preparation of cholesterol liposome

Liposomes were prepared as described previously<sup>[28,29]</sup>. Cholesterol (200mg) and phosphatidylcholine (100mg) were added into 5mL chloroform and soluted completely. After the organic solution was evaporated, the container was placed in the desiccator overnight at 4°C. Then PBS (pH 7.2) was added into the container, the final concentration of CL was 10g·L<sup>-1</sup>. After the sonication, the mixture was centrifuged at 21 000×g for 30min to sediment the undispersed lipid, then the supernatant was collected. The cholesterol-to-phospholipid molar ratio (FC/ PL) of the liposome was ~2:1. Control liposome (Cholesterol 100mg and phosphatidylcholine 200mg) was prepared in the same way, FC/PL molar ratio was ~0.5:1. Both liposomes were sterilized by filtration through a 0.45 $\mu$ m filter and mixed with sterile DMEM (Dulbecco's modified Eagle's medium) at a concentration of 1g·L<sup>-1</sup>, which is in accordance with the serum concentration of rabbit model with hypercholesterolemia<sup>[57]</sup>, pH was adjusted to 7.4, control and cholesterol-rich media were determined to be isomolar before experimentation.

### Calcium measurement

A 10mm hole was made in a plastic chamber (Made in Denmark), then a 22mm glass coverslip was used to seal the hole tightly from the bottom. Then it was cleaned thoroughly and sterilized by ultra-violet lamp for 2h. The cell suspension was added into the chambers and incubated for 48h, they were incubated with or without CL overnight.

**Preparation of fluo-3/AM:** The concentration of free cytosolic Ca<sup>2+</sup> in SMCs was determined using the fluorescent Ca<sup>2+</sup> indicator fluo-3/ AM. Fifty  $\mu$ g fluo-3 was dissolved in 50 $\mu$ L dimethyl sulfoxide (DMSO) (about 885 $\mu$ mol·L<sup>-1</sup>), and mixed thoroughly. Then it was

subdivided into ten vials and stored at -20°C. Five  $\mu$ L of vial of stock solution was diluted by D-Hanks with a proportion of 1:200(V/V). The final concentration of fluo-3 was about 4.5 $\mu$ mol·L<sup>-1</sup>. This loading solution should be used in 3 h, to maximize loading efficiency. **Ca<sup>2+</sup> measurement:** The SO cells culture media was removed and washed for 10 min with D-Hanks solution. Remove the final wash solution, add the loading solution, incubate about 50 min at 37°C. Then remove the loading solution, wash the cells with D-Hanks, measure the fluorescence soon after loading. The measurement was performed under Bio-Rad MRC 1024 laser scanning confocal microscope, select cellular Ca<sup>2+</sup> indicator from the method menu, then select the button for fluo-3, numerical aperture being 1.3, and pixel 512. The data was treated at Compaq Pentium 90. The peak excitation was about 506nm and the peak emission was about 526nm.

### Solution

HEPES buffered solution (in mmol·L<sup>-1</sup>): 134 NaCl, 6 KCl, 2 CaCl<sub>2</sub>, 1 MgCl<sub>2</sub>, 10 HEPES, 10 Glucose, 0.49 EDTA; D-Hanks: 138 NaCl, 5.4 KCl, 0.37 Na<sub>2</sub>HPO<sub>4</sub>·H<sub>2</sub>O, 0.44 KH<sub>2</sub>PO<sub>4</sub>, 4.17 NaHCO<sub>3</sub>. PBS: 138 NaCl, 2.7 KCl, 10 Na<sub>2</sub>HPO<sub>4</sub>·H<sub>2</sub>O, 1.6 KH<sub>2</sub>PO<sub>4</sub>; High K<sup>+</sup> solution contained the following (in mmol·L<sup>-1</sup>): 120 NaCl, 20 KCl, 2 CaCl<sub>2</sub>, 1 MgCl<sub>2</sub>, 10 HEPES, 10 Glucose. Heparin was diluted by D-Hanks with 7×10<sup>5</sup>U·L<sup>-1</sup>, procaine concentration was 10mmol·L<sup>-1</sup>.

### Statistical analyses

Results were expressed as  $\bar{x} \pm S\bar{x}$ . Student's test or an analysis of variance (ANOVA) was performed to test the statistical significance as necessary,  $P < 0.05$  was regarded as significant.

## RESULTS

Cultured SO cells showed a typical smooth muscle cell characteristics which presented as “hill-and -valley” and  $\alpha$ -SM actin positive staining, filament was demonstrated along the longitudinal axis of the cells (Figure 1). Loading with fluo-3/AM for 50min, the fluorescence distributed inhomogenously under LSCM, which may represent the Ca<sup>2+</sup> pool, is inhomogenous. All experiments were conducted at room temperature (21°C-23°C). The value of Ca<sup>2+</sup> concentration was calculated and based on the following equation:  $[Ca^{2+}]_i = K_d \times (F - F_{min}) / (F_{max} - F)$ , where  $K_d$  is the dissociation constant for Ca<sup>2+</sup> (316nmol·L<sup>-1</sup>),  $F_{max}$  is fluorescence maxima which was obtained by saturating intracellular signal values;  $F_{min}$  is fluorescence minima which represented zero-Ca<sup>2+</sup> signal. The resting cellular Ca<sup>2+</sup> concentration was 108±21nmol·L<sup>-1</sup>.



**Figure 1** Cultured SO cells characterized with  $\alpha$ -SM actin positive staining, filament were demonstrated along the longitudinal axis of the cells.

### Distinctive agonists induced alteration of intracellular fluorescence

At the presence of extracellular  $\text{Ca}^{2+}$ , intracellular  $\text{Ca}^{2+}$  concentration changed under the LSCM after the addition of agonists, and it showed spatially heterogeneous alteration of fluorescent intensity in SO cells (Figure 2).

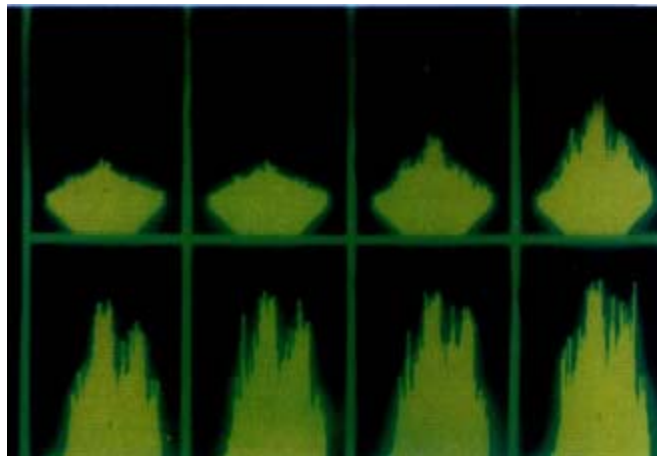


**Figure 2** At the presence of extracellular  $\text{Ca}^{2+}$ , intracellular  $\text{Ca}^{2+}$  concentration changed under the LSCM(1 image·s<sup>-1</sup>) after the addition of agonists, and it shows spatially heterogeneous alteration of fluorescent intensity in SO cells.

After the addition of 20mmol·L<sup>-1</sup> KCl, the increase of intracellular fluorescence was 183±56% ( $n=4$ ), 10<sup>-7</sup> mol·L<sup>-1</sup> ACh caused fluorescence increase was 161±52 % ( $n=4$ ), 10<sup>-7</sup> mol·L<sup>-1</sup> CCK agonized an increase of 130±43 % ( $n=4$ ), the maximum  $\text{Ca}^{2+}$  concentration were 297±66nmol·L<sup>-1</sup>, 275±58nmol·L<sup>-1</sup> and 251±45nmol·L<sup>-1</sup>, respectively.( $n=4$ , Figure 3).

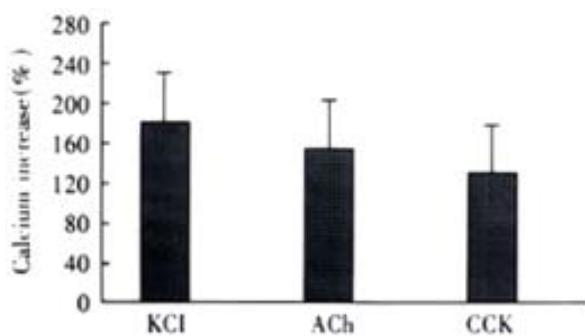


**Figure 3** Intracellular fluorescence increases induced by different agonists.  $\text{Ca}^{2+}$  Concentration increased from resting level of 108±21nmol·L<sup>-1</sup> to 297±66nmol·L<sup>-1</sup>, 275±58nmol·L<sup>-1</sup> and 251±45nmol·L<sup>-1</sup>, respectively. ANOVA was performed for the analysis,  $F=0.9184$ , no significant difference between three groups ( $n=4$ ).

The elimination of extracellular  $\text{Ca}^{2+}$  was performed by incubation of 2mmol·L<sup>-1</sup> EGTA and 10μmol·L<sup>-1</sup> verapamil for 10min. The extracellular  $\text{Ca}^{2+}$  was chelated by EGTA (a highly specific chelator for free  $\text{Ca}^{2+}$  ions) and inward  $\text{Ca}^{2+}$  current was inhibited by verapamil (inhibitor of L-type  $\text{Ca}^{2+}$  channels). Compared with the presence of extracellular  $\text{Ca}^{2+}$ , under this circumstance, the cellular fluorescence decreased from the peak rapidly.

At absence of extracellular  $\text{Ca}^{2+}$  treated by EGTA and verapamil, 20mmol·L<sup>-1</sup> KCl induced an  $\text{Ca}^{2+}$  increase of 20%±14% ( $P<0.01$ , vs control,  $t=4.882$ ), with maximal  $\text{Ca}^{2+}$  concentration of 131±17nmol·L<sup>-1</sup>, which indicated the induction of KCl depends on the presence of extracellular  $\text{Ca}^{2+}$ . Under the same condition, ACh increased the cellular  $\text{Ca}^{2+}$  by 82%±21%, with a

maximal  $\text{Ca}^{2+}$  concentration of 192nmol·L<sup>-1</sup>±22nmol·L<sup>-1</sup>. After pretreatment of heparin (inhibitor of IP3-sensitive  $\text{Ca}^{2+}$  release channel) and procaine(inhibitor of IP3-insensitive  $\text{Ca}^{2+}$  release channel), the cellular fluorescence increase by 62%±23 % and 72%±28%, respectively, the maximal cellular calcium was 175nmol·L<sup>-1</sup>±26nmol·L<sup>-1</sup> and 186nmol·L<sup>-1</sup>±30nmol·L<sup>-1</sup>, and there was no significant difference from that of untreated cells (Figure 4).

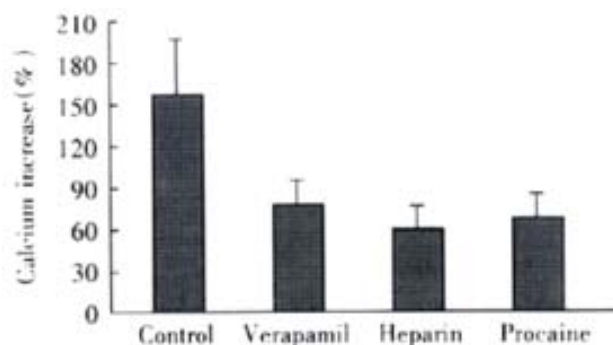


**Figure 4** Effect of different antagonists on ACh induced cellular  $\text{Ca}^{2+}$  increase ( $\bar{x}\pm Sx$ ,  $n=4$ ). Maximal  $\text{Ca}^{2+}$  concentration increased to 192±22nmol·L<sup>-1</sup>, 175nmol·L<sup>-1</sup>±26nmol·L<sup>-1</sup> and 186±30nmol·L<sup>-1</sup>, respectively. ANOVA was performed for the analysis,  $F=1.324$ , with no significant difference between the three experimental groups ( $n=4$ ).

CCK induced an cellular  $\text{Ca}^{2+}$  increase of 104%±23% after the elimination of extracellular  $\text{Ca}^{2+}$ . After incubation of heparin and procaine, CCK induced calcium increase were 23%±19% and 85%±37%, which was different from that of acetylcholine(Figure 5).

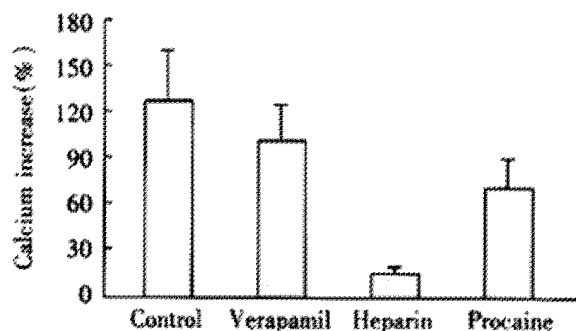


**Figure 5** Effect of different antagonists on CCK induced cellular  $\text{Ca}^{2+}$  increase ( $\bar{x}\pm Sx$ ,  $n=4$ ). Maximal  $\text{Ca}^{2+}$  concentration increased to 220±26nmol·L<sup>-1</sup>, 133±21nmol·L<sup>-1</sup> and 201±40nmol·L<sup>-1</sup>, respectively. SNK-q test was performed, there was a statistical difference between heparin treated group and other two groups,  $P<0.01$ .

### Intracellular calcium increase after the incubation of cholesterol liposome

After the incubation of 1g·L<sup>-1</sup> CL for 18h, many CL incorporated into the membrane, the cells changed slightly as mentioned by others<sup>[45]</sup>. The intracellular calcium concentration of control liposome(FC/PL molar ratio with~0.5:1) treated cells were 117±19nmol·L<sup>-1</sup>, there was no significant difference as compared with untreated cells. However, the resting cellular  $\text{Ca}^{2+}$  concentration was elevated obviously by incubation of CL(FC/PL molar ratio with~2:1), which was 152±26nmol·L<sup>-1</sup>. But, after addition of agonists, the  $\text{Ca}^{2+}$  concentrations increased to 257±54nmol·L<sup>-1</sup>, 238±57nmol·L<sup>-1</sup> and 204nmol·L<sup>-1</sup>±26nmol·L<sup>-1</sup>, respectively, the calcium increase percentages were significantly decreased, the cellular fluorescence increases induced by KCl, ACh and CCK were 67±32%( $t=3.597$ ), 56±33% ( $t=3.410$ ) and 34±15%( $t=4.216$ ), respectively, ( $P<0.05$ , vs control) (Figure 6).

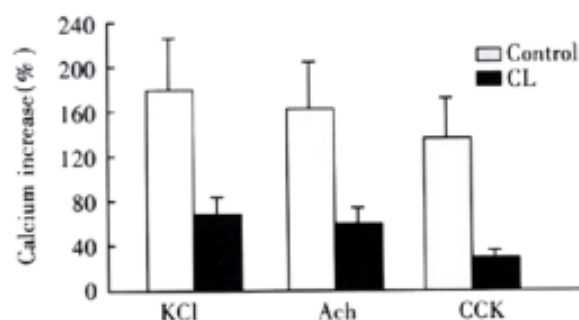


**Figure 6** Effect of cholesterol liposome on cellular  $\text{Ca}^{2+}$  mobilization ( $\bar{x} \pm \text{Sx}$ ,  $n=4$ ). Agonists induced cellular fluorescence increase percentages were markedly less than that of control group.

## DISCUSSION

The present study shows that  $\text{Ca}^{2+}$  mobilization of SO cells evoked by potassium, acetylcholine and cholecystinin were impaired after the cells incubated with cholesterol liposome (CL). And it also indicated that CL affects the different pathways of  $\text{Ca}^{2+}$  mobilization, for our results demonstrated that KCl induced intracellular  $\text{Ca}^{2+}$  increase depends on the extracellular  $\text{Ca}^{2+}$  influx, acetylcholine may agonize the  $\text{Ca}^{2+}$  increase through both intra- and extracellular pathway, while CCK elicited SO cells via mobilizing intracellular  $\text{Ca}^{2+}$  store. These observations agree with other authors' in gallbladder muscle cells<sup>[30-34]</sup>.

Based on literatures and our results, potassium excited the smooth muscle cells depend on  $\text{Ca}^{2+}$  influx through L-type voltage-dependent  $\text{Ca}^{2+}$  channel which could be inhibited by verapamil. As for acetylcholine and cholecystinin,  $2\text{mmol}\cdot\text{L}^{-1}$  EGTA and  $10\text{mm}$  verapamil could not inhibit the cellular  $\text{Ca}^{2+}$  increase completely, demonstrating that both ACh and CCK elicit SO cells do not depend on influx of extracellular calcium. However, heparin could inhibit the cellular  $\text{Ca}^{2+}$  increase induced by CCK, which indicate a CCK evoked  $\text{Ca}^{2+}$  increase of SO cells through IP<sub>3</sub>-sensitive pathway.

The normal function of SO is the precondition of biliary tract homeostasis, and the motility was under the coordination of hormone and innervation<sup>[35-38]</sup>. SOD is responsible for many disorders including gallbladder stasis, stone formation and unexplainable upper abdominal ache post-cholecystectomy<sup>[13]</sup>. Additionally, it was proved that the occurrence of SOD was correlated with intestinal dysmotility<sup>[20,39,40]</sup> and it was also correlated with recurrent and chronic pancreatitis<sup>[41,42]</sup>. On the other hand, most researches on SO were concentrated on the SO manometry, in such a situation, the results and conclusions were always full of discrepancy due to the complex effect of hormone and nerve or differences in species<sup>[12,13]</sup>. Therefore, isolated and cultured SO cells were used to study its characteristics in order to rule out complex influences *in vivo*<sup>[43-46]</sup>.

It was well known that motility regulation of smooth muscle cells depends on several mechanisms, including: influx of extracellular  $\text{Ca}^{2+}$ , intracellular  $\text{Ca}^{2+}$  mobilization and sensitivity modulation of intracellular  $\text{Ca}^{2+}$ . If this process was inhibited, the contractility will be impaired. In our previous experiments, high molar ratio CL (molar ratio~2:1) impaired the SO muscle cell contractility<sup>[43]</sup>, whereas, low molar ratio CL(0.5:1) had no effect on cells contractility. According to previous literatures, cholesterol enrichment of the SMC membrane occurs rapidly, and the aortic smooth muscle cells in hypercholesterolemic rabbit has impaired relaxation<sup>[47-49]</sup>, and reduced contraction as well<sup>[50]</sup>. Cholesterol incorporation into

membrane could also result in an alteration of membrane conduction of ions<sup>[51,63]</sup>. Because the cholesterol liposome was readily incorporated into cells membrane, that the duration, CL and cells incubation needed, was not a routine one. In another previous experiment, we used 2h for incubation<sup>[43]</sup>. Broderick *et al* used 3h in the study of CL effect on arterial smooth muscle<sup>[50]</sup>.

Our aim was mainly to observe the  $\text{Ca}^{2+}$  mobilization alteration affected by CL. There are many evidence *in vivo* and *in vitro* showing an impaired contractility in human and animal gallbladders with cholesterol stones<sup>[28,52]</sup>. Li *et al*<sup>[53]</sup> measured the actin and myosin isoform in gallbladders smooth muscle following feeding in prairie dogs and found that cholesterol feeding induced a shift in actin isoforms, but whether it is really responsible for the decreased contractility is uncertain. It was proved that cholesterol could alter smooth muscle membrane and cell function by changing the physical state of the membrane phospholipid bilayer<sup>[54]</sup>, and therefore affect the function of integral membrane proteins, such as  $\text{Ca}^{2+}$  and potassium channels, as well as transmembrane receptors<sup>[26]</sup>. Membrane fluidity decreased with excessive cholesterol incorporation and subsequently restricted optimal function of membrane proteins, such as receptor binding of ligands, receptor coupling with G proteins and activation of enzymes<sup>[55,56]</sup>. Thus, it could explain the impaired activation of signal transduction pathways responsible for contractile responses to receptor-dependent agonists, such as CCK and ACh. It has been shown that muscle cell contraction, membrane fluidity, membrane cholesterol and phospholipid content are reversible after the membrane cholesterol was leached out by incubation of cholesterol-free liposomes for several hours<sup>[27,28]</sup>. Whether the effects of cholesterol liposome observed in this study were due to cytotoxicity Other authors reported that high concentration of CL might have influence to cultured muscle cells<sup>[46]</sup>. The similar procedures had been done by many researchers<sup>[27,29,64]</sup>, and the cholesterol was within the serum concentration range of hypercholesterolemia rabbit model<sup>[57]</sup>. So, the cytotoxicity of liposomes to cells in this study, if any, might be unconsiderable.

The effect of cholesterol on SO has not been elucidated yet. SO manometry of hypercholesterolemic rabbit shows that abnormal SO motility had been observed before the formation of gallstone<sup>[57]</sup>, basal pressure rose and amplitude of phasic contraction decreased that represented an impaired relaxation and decreased contraction, too. Szilvassy *et al*<sup>[58]</sup> observed that the SO of hypercholesterolemic rabbits restored the nitrergic transmitter mediated relaxation by farnesol treatment. The SO segments of rabbits, prairie dogs and guinea pigs belong to extraduodenal type<sup>[59-61]</sup> and were able to pump fluid from the bile duct to duodenum. Therefore, it could be concluded that cholesterol affected the SO contractility which was responsible for a reduced peristaltic function to pump bile into duodenum. CCK receptors located in SO neurons and muscle cells were G-protein coupled receptors<sup>[62]</sup> which could be affected by excessive cholesterol incorporation resulting in decreased release of neural mediators or an impaired contraction. Therefore, we can conclude that hypercholesterolemia could not only impair relaxation but also contraction of rabbits sphincter of Oddi, which could lead to the occurrence of SO dysfunction.

In summary, the present study shows that potassium induced rabbits SO cells  $\text{Ca}^{2+}$  increase depends on  $\text{Ca}^{2+}$  influx through L-type channel; acetylcholine induces SO cells  $\text{Ca}^{2+}$  increase from both intra- and extra-cellular  $\text{Ca}^{2+}$  release; cholecystinin evokes the SO cells by mobilizing IP<sub>3</sub>-sensitive  $\text{Ca}^{2+}$  stores; and cholesterol liposome could affect the intracellular  $\text{Ca}^{2+}$  increase induced by



different agonists.

## REFERENCES

- Fang CH, Yang JZ, Kang HG. A PCR study on Hp DNA of bile, mucosa and stone in gallstones patients and its relation to stone nuclear formation. *Shijie Huaren Xiaohua Zazhi* 1999;7: 233-235
- Gu SW, Luo KX, Zhang L, Wu AH, He HT, Weng JY. Relationship between ductule proliferation and liver fibrosis of chronic liver disease. *Shijie Huaren Xiaohua Zazhi* 1999;7:845-847
- Zhou LS, Shi JS, Wang ZR, Wang L. Tumor necrosis factor  $\alpha$  in gallbladder and gallstone. *Shijie Huaren Xiaohua Zazhi* 2000;8: 426-428
- Fang CH, Yang J. A study on DNA of aerobic and anaerobic bacteria in bile, mucosa and stone in gallstone patients. *Shijie Huaren Xiaohua Zazhi* 2000; 8:66-68
- Li XP, Mao XZ. Effect of estrogen, cholic acid loading and bile draining on hepatobiliary functions in rats. *Shijie Huaren Xiaohua Zazhi* 2000;8:1009-1012
- He XS, Huang JF, Liang LJ, Lu MD, Cao XH. Surgical resection for hepato portal bile duct cancer. *World J Gastroenterol* 1999;5: 128-131
- Huang ZQ. New development of biliary surgery in China. *World J Gastroenterol* 2000;6:187-192
- Li LB, Cai XI, Li JD, Mu YP, Wang YD, Yuan XM, Wang XF, Bryner B, Finley RK Jr. Will intraoperative cholangiography prevent biliary duct injury in laparoscopic cholecystectomy *World J Gastroenterol* 2000;6:21
- Yang YK, Qiu KX, Zhan YZ, Zhan EY, Yang HM, Zheng P. Determination of cholesterol in human biliary calculus by TLC scanning. *World J Gastroenterol* 2000;6:62
- Chen XM, LaRusso NF. Human intestinal and biliary cryptosporidiosis. *World J Gastroenterol* 1999;5:424-429
- Coelho JC, Moody FG. Certain aspects of normal and abnormal motility of sphincter of Oddi. *Dig Dis Sci* 1987;32:86-94
- Toouli J. What is sphincter of Oddi dysfunction? *Gut* 1989;30:753-761
- Dodds WJ. Biliary tract motility and its relationship to clinical disorders. *AJR* 1990;155:247-258
- Herman F, Delforge M, Basten B, Masy V, Lilet H, Brassine A. Dysfunction of the sphincter of Oddi in cholecystectomy patients. *Rev Med Liege* 1998;53:193-198
- Toouli J. Biliary motility disorders. *Baillieres Clin Gastroenterol* 1997; 11:725-740
- Eversman D, Fogel EL, Rusche M, Sherman S, Lehman GA. Frequency of abnormal pancreatic and biliary sphincter manometry compared with clinical suspicion of sphincter of Oddi dysfunction. *Gastrointest Endosc* 1999;50:637-641
- Guelrud M, Morera C, Rodriguez M, Jaen D, Pierre R. Sphincter of Oddi dysfunction in children with recurrent pancreatitis and anomalous pancreaticobiliary union: an etiologic concept. *Gastrointest Endosc* 1999;50:194-199
- Tomas A, Vida F, Ponce J. Acute recurrent pancreatitis in a patient with Oddi's sphincter dysfunction. *Gastroenterol Hepatol* 1999;22: 279-281
- Chen SZ, Sha JP, Chen XC, Hou CC, Fu WH, Liu W. Dysrelaxation of sphincter of Oddi in patients with bile reflux gastritis: study on effect of nifedipine of gallbladder emptying. *Shijie Huaren Xiaohua Zazhi* 1999;7:1020-1023
- Chen SZ, Bu X, Hou CC, Li S, Chen XC. Mechanism of nifedipine for improving abnormal gallbladder emptying function in patients with irritable bowel syndrome. *Shijie Huaren Xiaohua Zazhi* 1998; 6: 423-426
- Chen SZ, Zhao H, Wu CY, Fu WJ, Chen XC. Gallbladder emptying function in patients with bile reflux gastritis. *Shijie Huaren Xiaohua Zazhi* 1998; 6: 427-429
- Szilvassy Z, Nagy I, Szilvassy J, Jakab I, Csati S, Lonovics J. Impaired nitrenergic relaxation of the sphincter of Oddi of hyperlipidaemic rabbits. *Eur J Pharmacol* 1996;301: R17-18
- Szilvassy Z, Nagy I, Madacsy L, Hajnal F, Velosy B, Takacs T, Lonovics J. Beneficial effect of lovastatin on sphincter of Oddi dyskinesia in hypercholesterolemia and hypertriglyceridemia. *Am J Gastroenterol* 1997; 92: 900-902
- Wei JG, Wang YC, Du F, Yu HJ. Dynamic and ultrastructural study of sphincter of Oddi in early-stage cholelithiasis in rabbits with hypercholesterolemia. *World J Gastroenterol* 2000;6: 102-106
- Chen Q, Amaral J, Oh S, Biancani P, Behar J. Gallbladder relaxation in patients with pigment and cholesterol stones. *Gastroenterology* 1997;113: 930-937
- Chen Q, De Petris G, Yu P, Amaral J, Biancani P, Behar J. Different pathways mediate cholecystokinin action in cholelithiasis. *Am J Physiol* 1997;272: G838-G844
- Chen Q, Amaral J, Biancani P, Behar J. Excess membrane cholesterol alters human gallbladder muscle contractility and membrane fluidity. *Gastroenterology* 1999;116:678-685
- Yu P, Chen Q, Biancani P, Biancani J. Membrane cholesterol alters gallbladder muscle contractility in prairie dogs. *Am J Physiol* 1996; 271:G56-G61
- Bialecki RA, Tulenko TN. Excess membrane cholesterol alters calcium channels in arterial smooth muscle. *Am J Physiol* 1989;257: C306-C314
- Xu QW, Shaffer EA. The potential site of impaired gallbladder contractility in an animal model of cholesterol gallstone disease. *Gastroenterology* 1996; 110:251-257
- Mansour A, Dawoud I, Gad-El-Hak-N. The potential site of disordered gallbladder contractility during the early stage of cholesterol gallstone formation. *Hepatogastroenterology* 1998;45: 1404-1409
- Yu P, Chen Q, Harnett KM, Amaral J, Biancani P, Behar J. Direct G protein activation reverses impaired CCK signaling in human gallbladders with cholesterol stones. *Am J Physiol* 1995; 269: G659-G665
- Behar J, Rhim BY, Thompson W, Biancani P. Inositol trisphosphate restores impaired human gallbladder motility associated with cholesterol stones. *Gastroenterology* 1993; 104:563-568
- Yu P, De Petris G, Biancani P, Amaral J, Behar J. Cholecystokinin-coupled intracellular signaling in human gallbladder muscle. *Gastroenterology* 1994;106:763-770
- Hogan WJ, Geenen JE. Biliary dyskinesia. *Endoscopy* 1988;20:179-183
- Luman W, Williams AJ, Pryde A, Smith GD, Nixon SJ, Heading RC, Palmer KR. Influence of cholecystectomy on sphincter of Oddi motility. *Gut* 1997;41:371-374
- Mawe GM, Kennedy AL. Duodenal neurons provide nicotinic fast synaptic input to sphincter of Oddi neurons in guinea pig. *Am J Physiol* 1999;277: G226-234
- Middelfart HV, Matzen P, Funch-Jensen P. Sphincter of Oddi manometry before and after laparoscopic cholecystectomy. *Endoscopy* 1999;31:146-151
- Soffer EE, Johlin FC. Intestinal dysmotility in patients with sphincter of Oddi dysfunction. A reason for failed response to sphincterotomy. *Dig Dis Sci* 1994; 39:1942-1946
- Evans PR, Dowsett JF, Bak YT, Chan YK, Kellow JE. Abnormal sphincter of Oddi response to cholecystokinin in postcholecystectomy syndrome patients with irritable bowel syndrome. The irritable sphincter. *Dig Dis Sci* 1995; 40: 1149-1156
- Tarnasky PR, Hoffman B, Aabakken L, Knapp WL, Coyle W, Pineau B, Cunningham JT, Cotton PB, Hawes RH. Sphincter of Oddi dysfunction is associated with chronic pancreatitis. *Am J Gastroenterol* 1997; 39: 1125-1129
- Di-Francesco V, Brunori MP, Rigo L, Toouli J, Angelini G, Frulloni L, Bovo P, Filippini M, Vaona B, Talamini G, Cavallini G. Comparison of ultrasound-secretin test and sphincter of Oddi manometry in patients with recurrent acute pancreatitis. *Dig Dis Sci* 1999; 44: 336-340
- Wang XJ, Wei JG, Wang YC, Xu JK, Wu QZ, Wu DC, Yang XX. Effect of cholesterol liposome on contractility of rabbit Oddi's sphincter smooth muscle cells. *Shijie Huaren Xiaohua Zazhi* 2000; 8: 633-637
- Zhang JS, Wei JG, Zhang ML, Wang D, Shi YH, Ji ZL. Effects of cholesterol liposome on cytoskeleton of rabbit sphincter of Oddi cells in culture. *J Fourth Milit Med Univ* 1997;18:528-531
- Zhang JS, Wei JG, Wu JZ, Chen JY. Culture and morphologic observation of rabbit Oddi's sphincter cells. *Shijie Huaren Xiaohua Zazhi* 1999;7:316-319
- Zhang JS, Wei JG, Wu JZ, Zhang YH, Wang H. Experimental study of the effects of cholesterol liposome on rabbit sphincter of Oddi cells proliferation in culture. *J Fourth Milit Med Univ* 1998;19:494-497
- Tulenko TN, Laury-Kleintop L, Walter MF, Mason RP. Cholesterol, calcium and atherosclerosis: is there a role for calcium channel blockers in atheroprotection? *Int J Cardiol* 1997;62: S55-66
- Weisbrod RM, Griswold MC, Du Y, Bolotina VM, Cohen RA. Reduced responsiveness of hypercholesterolemic rabbit aortic smooth muscle cells to nitric oxide. *Arterioscler Thromb Vasc Biol* 1997;17:394-402
- Kitagawa S, Yamaguchi Y, Shinozuka K, Kwon YM, Kunitomo M. Dietary cholesterol enhances impaired endothelium-dependent relaxations in aortas of salt-induced hypertensive Dahl rats. *Eur J Pharmacol* 1996;297:

- 71-76
- 50 Van Diest MJ, Herman AG, Verbeuren TJ. Influence of hypercholesterolemia on the reactivity of isolated rabbit arteries to 15-Lipoxygenase metabolites on arachidonic acid, comparison with platelet-derived agents and vasodilators. *Prostaglandins Leukot Essent Fatty Acids* 1996;54:135-145
- 51 Cox RH, Tulenko TN. Altered contractile and ion channel function in rabbit portal vein with dietary atherosclerosis. *Am J Physiol* 1995;268: H2522-2530
- 52 Behar J, Lee KY, Thompson WR, Biancani P. Gallbladder contraction in patients with pigment and cholesterol stones. *Gastroenterology* 1989; 97:1479-1484
- 53 Li YF, Bowers RL, Russell DH, Moody FG, Weisbrodt NW. Actin and myosin isoforms in gallbladder smooth muscle following cholesterol feeding in prairie dogs. *Gastroenterology* 1990;99: 1460-1466
- 54 Gleason MM, Medow MS, Tulenko TN. Excess membrane cholesterol alters calcium movements, cytosolic calcium levels, and membrane fluidity in arterial smooth muscle cells. *Circ Res* 1991;69:216-227
- 55 Squier TC, Bigelow DJ, Thomas DD. Lipid fluidity directly modulates the overall protein rotational mobility of the Ca-ATPase in sarcoplasmic reticulum. *J Biol Chem* 1988;263:9178-9186
- 56 Fong TM, McNamee MG. Stabilization of acetylcholine receptor secondary structure by cholesterol and negatively charged lipids. *Biochemistry* 1987; 26:3871-3880
- 57 Du F, Wei JG. Function of Oddi's sphincter disorders in formation of cholelithiasis (abstract). *Zhonghua Waikao Zazhi* 1999;37:383
- 58 Szilvassy Z, Sari R, Nemeth J, Nagy I, Csati S, Lonovics J. Improvement of nitergic relaxation by farnesol of the sphincter of Oddi from hypercholesterolaemic rabbits. *Eur J Pharmacol* 1998;353:75-78
- 59 Calabuig R, Ulrich -Baker MG, Moody FG, Weems WA. Propulsion in the opossum sphincter of Oddi. *Am J Physiol* 1990;258:G138-G142
- 60 Calabuig R, Weems WA, Moody FG. Choledochoduodenal flow: effect of the sphincter of Oddi in opossums and cats. *Gastroenterology* 1990;99:1641-1646
- 61 Toouli J. Sphincter of Oddi motility. *Br J Surg* 1984;71:251-256
- 62 Wank SA. G protein-coupled receptors in gastrointestinal physiology I. CCK receptors: an exemplary family. *Am J Physiol* 1998; 274 ( Gastrointest. Liver physiol.37):G607-G613
- 63 Zhou Q, Jimi S, Smith TL, Kummerow FA. The effect of cholesterol on the accumulation of intracellular calcium. *Biochim Biophys Acta* 1991; 1085:1-6
- 64 Broderick R, Bialecki R and Tulenko TN. Cholesterol-induced changes in rabbit arterial smooth muscle sensitivity to adrenergic stimulation. *Am J Physiol* 1989;257: H170-H178

Edited by Ma JY



• BASIC RESEARCH •

# Early diagnosis and treatment of severe acute cholangitis

Wei-Zhong Zhang, Yi-Shao Chen, Jin-Wei Wang, Xue-Rong Chen

Wei-Zhong Zhang, Yi-Shao Chen, Jin-Wei Wang, Xue-Rong Chen, Department of Surgery, Huangyan First Hospital, Huangyan 318020, Zhejiang Province, China

**Correspondence to:** Dr. Wei-Zhong Zhang, Department of Surgery, Huangyan First Hospital, Huangyan 318020, Zhejiang Province, China. pgmh@mail.tzptt.zj.cn

Telephone: +86-576-4016922

Received 2001-07-05 Accepted 2001-11-15

## Abstract

**AIM:** To investigate the diagnostic standard for early identification of severe acute cholangitis in order to lower the incidence of morbidity and mortality rate.

**METHODS:** A diagnostic standard was proposed in this study as follows: documented biliary duct obstruction by ultrasound or computerized tomography or other imaging tools with the manifestation of systemic inflammatory response syndrome (SIRS). The surgical procedures included emergency common bile duct exploration with T tube insertion or cholecystostomy with secondary common bile duct exploration. And incidence of postoperative multiple organ dysfunction syndrome (MODS), duration of systemic inflammatory response and hospital mortality were analyzed.

**RESULTS:** Forty-three patients conforming to the diagnostic standard described above were employed in this study. 1 patient was admitted in acutely ill condition and complicated with acute relapse of chronic bronchitis, cholecystostomy procedure was performed but the patient was complicated with postoperative acute lung injury which was treated by assisted mechanical ventilation for 5 d; 2 wk later, two-stage common bile duct Exploration and T tube insertion were performed. The remaining 42 patients underwent primary common bile duct exploration and T tube insertion, 1 developed acute lung injury and recovered 3 d later, 2 patients developed acute renal dysfunction, 1 of which recovered 2 d later and the other died on d 4. For all patients, the postoperative systemic inflammatory response persisted for 2 to 8 d with median of 3 d.

**CONCLUSION:** Early diagnosis of severe acute cholangitis can be made using this diagnostic standard, further development of systemic inflammatory response could be prevented and incidence of MODS as well as hospital mortality decreased.

Zhang WZ, Chen YS, Wang JW, Chen XR. Early diagnosis and treatment of severe acute cholangitis. *World J Gastroenterol* 2002;8(1):150-152

## INTRODUCTION

Severe acute cholangitis takes a severe clinical course, systemic inflammatory response syndrome (SIRS) appears at early stage and followed by multiple organ dysfunction syndrome (MODS), which signifies poor prognosis<sup>[1-8]</sup>. Recently, the perioperative management and technique of anesthesia have been much improved,

however, the mortality and morbidity of the patients with severe acute cholangitis remain high, especially in local hospitals. This study was performed to investigate the standard for early diagnosis of severe acute cholangitis and its surgical timing in order to decrease the complications.

## MATERIALS AND METHODS

### Diagnostic criteria

In this study, we proposed the diagnostic criterion for severe acute cholangitis as follows: documented obstruction of biliary duct by ultrasound, CT or other radiological imaging<sup>[9-19]</sup> if the patient presents two or more of the following conditions: ① temperature more than 38°C or less than 36°C, ② elevated heart rate more than 90·min<sup>-1</sup>, ③ respiratory rate more than 20·min<sup>-1</sup> or PaCO<sub>2</sub> less than 4.27KPa, and ④ white blood cell count more than 12×10<sup>9</sup>·L<sup>-1</sup>, less than 4×10<sup>9</sup>·L<sup>-1</sup>, or immature granulocyte more than 0.10<sup>[20]</sup>.

### Clinical materials

Between January 1997 and November 2000, 43 consecutive patients conforming to proposed diagnostic criterion for severe acute cholangitis were admitted in surgical department of our hospital, of which 26 were male and 17 were female, the average age was 53±8 years and the average APACHE II score was 9. 2±2.6. 27 patients had stones only in common bile duct; the remaining 16 had both intrahepatic and extrahepatic stones.

After admission, proper preoperative preparation was carried out and all patients underwent emergency biliary duct decompression, including common bile duct exploration with T tube drainage or cholecystostomy with secondary choledochostomy.

After operation, patients were intensively monitored on multiple organ systems. Hospital mortality was taken as death during hospitalization for the severe cholangitic attack, and death attributed to the underlying biliary sepsis in the absence of other obvious contributory cause within 48 h after emergency biliary duct drainage. When postoperative serum creatinine doubled or exceeded 180μmol·L<sup>-1</sup> among patients who had a normal preoperative value or when it increased 100μmol·L<sup>-1</sup> over its deranged preoperative level, the diagnosis was renal dysfunction. Respiratory dysfunction was taken as the necessity for mechanical ventilation at any time after admission because of acute cholangitis. And duration of systemic inflammatory response was measured.

## RESULTS

One patient aged 65 years was admitted in critically ill condition with APACHE II score of 15 and was complicated with acute relapse of chronic bronchitis, therefore, cholecystostomy procedure was performed but he was complicated with postoperative acute lung injury which was treated by assisted mechanical ventilation for 5 d; 2 wk later, common bile duct was explored and T tube inserted. After 20 d, he was discharged. The remaining 42 patients underwent first-stage common bile duct exploration and T tube placement, however, 1 developed acute lung injury and was managed by mechanical ventilation for 3 d; 2 patients developed acute renal dysfunction, one of which recovered 2 d later and the other died on d4. For all

patients, the postoperative systemic inflammatory response persisted for 2 to 8 d with median of 3 d.

## DISCUSSION

Acute cholangitis caused by obstruction of common bile duct can easily induce systemic inflammatory response and later MODS or MOF, the clinical mortality is high. In China, a symposium on hepatic and biliary duct stones was held by Chinese Association of Surgery at Chongqing city in 1983, and the diagnostic standards for severe acute cholangitis was recommended. The diagnosis was met when patient presents shock or two of following six parameters: nervous symptoms; pulse more than  $120 \cdot \text{min}^{-1}$ ; white blood cell counts more than  $20 \times 10^9 \cdot \text{L}^{-1}$ ; temperature more than  $39^\circ\text{C}$  or less than  $35^\circ\text{C}$ ; biliary duct filled with pus and highly pressured; positive blood culture. In western country, diagnosis of severe acute cholangitis was established when septic shock or mental obtundation was confirmed in patients with acute cholangitis<sup>[21]</sup>. However, many patients with severe acute cholangitis were not manifested with nervous dysfunction and hypotension; the incidence of Reynolds' pentad was low; recent study showed that culture is far less sensitive than PCR method in detecting microbes present in blood<sup>[22-23]</sup>; and with progress in technique of modern imaging, obstruction of biliary duct can be identified early and accurately and proper management can be achieved timely; last but not least, patients with the diagnosis of severe acute cholangitis by this standard usually presented severe systemic inflammatory response, suggestive of the presence of multiple organ dysfunction, so if the patients were operated on at this time, second hit would ensue and course leading to MOF was accelerated<sup>[24]</sup>, mortality increased accordingly. At that time, when diagnosis was established, biliary drainage was of immediate concern, the surgical procedures included common bile duct exploration and T tube insertion, or cholecystostomy when patient's condition was unstable, but mortality rate carried between 10 per cent and 40 per cent.<sup>[1-3, 25]</sup>

In the era of minimally-invasive surgery, when the diagnosis of severe acute cholangitis is confirmed, the principle of management has much changed<sup>[26-32]</sup>. Non-operative biliary decompression is attempted before any definitive surgical procedure is undertaken. A nasobiliary catheter by endoscopy can be left in place to provide short-term biliary decompression until the patient's cholangitis resolves. The goal of such treatment is to convert an urgent or emergent problem into one that can be managed in an elective setting. Emergent surgical decompression of the common bile duct is reserved for patients in whom endoscopic procedure is either unsuccessful or unavailable. Should a surgical procedure be necessary, the goal is to establish biliary decompression only by means of a choledochotomy, and placement of a large diameter T-tube. Overall, non-operative drainage can be accomplished with morbidity rates of less than 40 per cent and overall mortality of less than 10 per cent.

Lai *et al* in early 1990s conducted a randomized prospective study on the role of endoscopic biliary drainage for severe acute cholangitis, the diagnosis of severe acute cholangitis was based on the presence of either septicemic shock or evidence of progressive biliary sepsis including mental confusion and persistent or relapsing fever despite appropriate antibiotic treatment, however, the mortality rate remained up to 10 percent. Recently, they conducted a retrospective study to evaluate the combined endoscopic and laparoscopic approach in managing gallstone cholangitis, in their series, 60 patients had severe acute cholangitis defined by the presence of septic shock, mental confusion, or persistent high fever despite antibiotic treatment and the mortality rate among patients with severe acute cholangitis decreased to 5.0 per cent (3/60)<sup>[21]</sup>. They concluded that combined approach is safe and effective for managing gallstone cholangitis. Other authors had reported similar advantages of nonoperative

decompression<sup>[27-30]</sup>.

The advent of endoscopic retrograde cholangiopancreatography, endoscopic sphincterotomy and newer laparoscopic procedures including common bile duct exploration has remarkably decreased the mortality of severe acute cholangitis<sup>[33-37]</sup>. However, the performance of these procedures is dependent on training, technical skills and experience of the surgeon. In the hands of an experienced surgeon, a laparoscopic approach is reasonable for the treatment of acute cholangitis in the tertiary hospitals<sup>[33]</sup>. But in the primary or local hospitals which don't have the experienced endoscopic surgeon or equipment, the management of patients with severe acute cholangitis has to be turned to traditional procedures. Furthermore, a recent multicenter randomized trial comparing surgical treatment with endoscopic management in patients with common bile duct stones showed that surgical treatment was associated with lower major complications like MODS (4% vs 13%) and less retained stones (6% vs 16%) than endoscopic management<sup>[38]</sup>. And other complications of nonoperative management were also noted.<sup>[39-40]</sup>

As we know, in the situation of severe acute cholangitis, the intraductal pressure rises secondary to obstruction, bacteria and endotoxins can leak into the systemic circulation and induce systemic inflammatory response<sup>[4-7]</sup> and a frequent complication of this inflammatory response is the development of organ system dysfunction or failure<sup>[20, 41-42]</sup>. Therefore, the management of severe acute cholangitis should be based on the early awareness of the disease by clinicians, the objective of this study was to establish the early diagnosis of severe acute cholangitis.

An American College of Chest Physicians/Society of Critical Care Medicine Consensus Conference (ACCP/SCCM) was held in August 1991 to produce a series of universal definitions for SIRS (systemic inflammatory response syndrome), sepsis and other clinical conditions related to sepsis, the aim of the consensus conference was to improve our ability to make early detection of the disease possible, and thus allow early therapeutic intervention to decrease morbidity and mortality<sup>[20, 42]</sup>. Based on this background, we recommended a new diagnostic standard since January 1997, that was, SIRS manifestation with documented obstruction of biliary duct by imaging, and surgical procedure for decompression mainly was common bile duct exploration and T tube drainage. 43 consecutive patients conforming to proposed diagnostic criterion for severe acute cholangitis were employed in this study. 1 patient aged 65 years was admitted in acutely ill condition and complicated with acute relapse of chronic bronchitis, cholecystostomy procedure was performed but he was complicated with postoperative acute lung injury which was treated by assisted mechanical ventilation for 5 d; 2 wk later, two-stage common bile duct Exploration and T tube insertion were performed. The remaining 42 patients underwent primary common bile duct exploration and T tube insertion, however, 1 developed acute lung injury and recovered later; 2 patients developed acute renal dysfunction, one of which recovered 2 d later and the other died on d4. Therefore, all patients in this cohort were diagnosed and managed timely, preventing SIRS from further progressing, thus the incidence of MOD was low (9.3%, 4/43) and mortality rate decreased (2.3%, 1/43).

In conclusion, the preliminary results of this prospective study showed that if the systemic inflammatory response is identified early in the disease process of severe acute cholangitis, MODS can be effectively prevented and mortality decreased, the proposed definition for severe acute cholangitis is practical and should be clinically accepted. Furthermore, a randomized controlled prospective study should be done to confirm this conclusion.

## REFERENCES

- 1 Xi XM. Treatment of severe acute cholangitis in 106 elderly patients with integrated traditional and western medicine. *Xin Xiaohuabingxue Zazhi*

- 1993; 1: 182-183
- 2 Liu YG, Xu FH. 57 cases of severe acute cholangitis with multiple organ system failure. *Xin Xiaohuabingxue Zazhi* 1996; 4: 124
- 3 Fulcher AS. Case 1: Recurrent pyogenic cholangitis. *Radiology* 1998; 208: 341-344
- 4 Dong JH, Huang ZQ, Han BL, Duan HC, Li K, Peng ZM, Wang AC. Clinical and pathophysiological characteristics of the new experimental model of biliary sepsis in rabbits. *Xin Xiaohuabingxue Zazhi* 1994; 2: 140-143
- 5 Lei ZM, Li J, Yang WJ, Li DY. Change of nitric oxide and endothelin and its significance in the course of biliary obstruction by stones. *Shijie Huaren Xiaohua Zazhi* 2000; 8(suppl 8): 16
- 6 Kimmings AN, van Deventer SJH, Rauws EAJ, Huibregtse K, Gouma DJ. Systemic inflammatory response in acute cholangitis and after subsequent treatment. *Eur J Surg* 2000; 166: 700-705
- 7 Shi TF, Yang WL. Study on bacterial translocation of intestine and endotoxin concentration of plasma in obstructive jaundice. *World J Gastroenterol* 1998; 4 (Suppl 2): 92
- 8 Shang D, Guan FL, Jin PY, Chen HL, Cui JH. Effect of combined therapy of Yinchenhao Chengqi decoction and endoscopic sphincterotomy for endotoxemia in acute cholangitis. *World J Gastroenterol* 1998; 4: 443-445
- 9 Guo GH, Xu JH, Sun SM, Ma T, Wu LB, Yang YH, Zhuang QW, Jing XB. Experimental study of cholangiogram for refractory jaundice. *World J Gastroenterol* 1999; 5: 75-76
- 10 Li T, Li HP, Huang QR. Imaging features of primary extrahepatic bile duct carcinoma. *Xin Xiaohuabingxue Zazhi* 1996; 4: 266-267
- 11 Gong B, Zhou DY, Zhang FM, Hu B, Cheng HY. Endoscopic treatment of 207 patients with bile duct diseases. *Xin Xiaohuabingxue Zazhi* 1996; 4:270-272
- 12 Li ZS. Current situation in ERCP studies in China. *Shijie Huaren Xiaohua Zazhi* 2000; 8:446-448
- 13 Li ZS. Progress in endoscopic management of pancreas disease. *World J Gastroenterol* 1998; 4: 178-180
- 14 Lu WF. ERCP and CT diagnosis of pancreas divisum and its relation to etiology of chronic pancreatitis. *World J Gastroenterol* 1998; 4: 150-152
- 15 Li LB, Cai XJ, Li JD, Mu YP, Wang YD, Yuan XM, Wang XF, Bryner B, Finley RK Jr. Will intraoperative cholangiography prevent biliary duct injury in laparoscopic cholecystectomy *World J Gastroenterol* 2000; 6(Suppl 3): 21
- 16 Assy N, Jacob G, Spira G, Edoute Y. Diagnostic approach to patients with cholestatic jaundice. *World J Gastroenterol* 1999; 5: 252-262
- 17 Lu B, Sun J, Zhou K, Chai ZB, Zhou J. Percutaneous transhepatic gallbladder cholangiography in the diagnosis of obstructive jaundice. *Shijie Huaren Xiaohua Zazhi* 2000; 8(Suppl 8): 7
- 18 Long ST, Long F, Xu QR, Tang XY, Gao ZW. Percutaneous transhepatic cholangiography with gastrointestinal imaging in the diagnosis of obstructive hepatobiliary disease. *Huaren Xiaohua Zazhi* 1998; 6(Suppl 7): 456
- 19 Ma BY, Yuan CX, Peng YL, Hu YK. Ultrasonographic diagnosis of 584 patients with obstructive jaundice. *Shijie Huaren Xiaohua Zazhi* 2001; 9: 116-117b
- 20 Fry DE. Sepsis syndrome. *Am Surg* 2000; 66: 126-132
- 21 Poon RTP, Liu CL, Lo CM, Lam CM, Yuen WK, Yeung C, Fan ST, Wong J. Management of gallstone cholangitis in the era of laparoscopic cholecystectomy. *Arch Surg* 2001; 136: 11-16
- 22 Kane TD, Alexander JW, Johannigman JA. The detection of microbial DNA in the blood: a sensitive method for diagnosing bacteremia and /or bacterial translocation in surgical patients. *Ann Surg* 1998; 227: 1-9
- 23 Zhang WZ, Han TQ, Tang YQ, Zhang SD. Rapid detection of sepsis complicating acute necrotizing pancreatitis using polymerase chain reaction. *World J Gastroenterol* 2001; 7: 289-292
- 24 Schwartz JD, Shamamian P, Schwartz DS, Grossi EA, Jacobs CE, Steiner F, Minneci PC, Baumann FG, Colvin SB, Galloway AC. Cardiopulmonary bypass primes polymorphonuclear leukocytes. *J Surg Res* 1998; 75: 177-182
- 25 Li ZH, Luo YT, Zhong ZM. Surgical procedures in 21 patients with acute obstructive suppurative cholangitis. *Xin Xiaohuabingxue Zazhi* 1995; 3: 45
- 26 Feng ZT, Song QY, Liu JD, Pan YM, Li SM, Dong CJ, Liu WG. Endoscopic therapy of acute suppurative cholangitis. *Shijie Huaren Xiaohua Zazhi* 2000; 8(Suppl 8): 86
- 27 Gong JP, Zhou YB, Han BL, Li ZH. Endoscopic sphincterotomy in treatment of secondary common bile duct stones. *Shijie Huaren Xiaohua Zazhi* 1999; 7: 320-322
- 28 Liu HY, Tong WH, Hu WM, Li HR, Wen ZS, Wang JK, Huang WX, Liu X. Percutaneous expandable metallic stent biliary endoprotheses used in malignant and benign obstructive jaundice. *World J Gastroenterol* 2000; 6(Suppl 3): 51
- 29 Kozarek RA. Metallic biliary stents for malignant obstructive jaundice: a review. *World J Gastroenterol* 2000; 6: 643-646
- 30 Hong DF, Gao M, Bryner U, Cai XJ, Mou YP. Intraoperative endoscopic sphincterotomy for common bile duct stones during laparoscopic cholecystectomy. *World J Gastroenterol* 2000; 6: 448-450
- 31 Ren X, Kong QY, Xu XH, Zhang GL. Management of acute obstructive suppurative cholangitis by nonoperative biliary decompression procedure. *Xin Xiaohuabingxue Zazhi* 1996; 4: 507-508
- 32 Hu B, Zhou DY, Gong B, Zhang FM, Wang SZ, Cheng HY, Wu MC. Metal stent implantation for palliation of malignant biliary obstruction- a report of 57 cases. *China Natl J New Gastroenterol* 1996; 2: 149-151
- 33 Lillemo KD. Surgical treatment of biliary tract infections. *Am Surg* 2000; 66:138-144
- 34 Schwesinger WH, Sirinek KR, Strodel III WE. Laparoscopic cholecystectomy for biliary tract emergencies: state of the art. *World J Surg* 1999; 23: 334-342
- 35 Crawford DL, Phillips EH. Laparoscopic common bile duct exploration. *World J Surg* 1999; 23: 343-349
- 36 Hammarstrom LE, Andersson R, Stridbeck H, Ihse I. Influence of bile duct stones on patient features and effect of endoscopic sphincterotomy on early outcome of edematous gallstone pancreatitis. *World J Surg* 1999; 23: 12-17
- 37 Geenen DJ, Geenen JE, Jafri FM, Hogan WJ, Catalano MF, Johnson GK, Schmalz MJ. The role of surveillance endoscopic retrograde cholangiopancreatography in preventing episodic cholangitis in patients with recurrent common bile duct stones. *Endoscopy* 1998; 30: 18-20
- 38 Suc B, Escat J, Cherqui D, Fourtanier G, Hay JM, Fingerhut A, Millat B. Surgery vs endoscopy as primary treatment in symptomatic patients with suspected common bile duct stones. *Arch Surg* 1998; 133: 702-708
- 39 Wojtun S, Gil M, Gil J. Recognition of ERC-induced pancreatitis in patients with choledocholithiasis by an analysis of laboratory findings. *Hepatogastroenterology* 2000; 47: 550-553
- 40 Tiscornia OM, Hamamura S, de Lehmann ES, Otero G, Waisman H, Tiscornia WP, Bank S. Biliary acute pancreatitis: a review. *World J Gastroenterol* 2000; 6: 157-168
- 41 Barkun AN, Barkun JS, Baillie J. A Taiwanese woman with acute cholangitis. *Endoscopy* 2000; 32: 890-894
- 42 Dellinger RP, Bone RC. To SIRS with love. *Crit Care Med* 1998; 26: 178-179

Edited by Wang JH and Xu XQ

• BASIC RESEARCH •

# Upregulation of vascular endothelial growth factor by hydrogen peroxide in human colon cancer

Jian-Wei Zhu, Bao-Ming Yu, Yu-Bao Ji, Ming-Hua Zheng, Dong-Hua Li

Jian-Wei Zhu, Bao-Ming Yu, Yu-Bao Ji, Ming-Hua Zheng, Dong-Hua Li, Shanghai Institute of Digestive Surgery, Ruijin Hospital, Shanghai Second Medical University, Shanghai 200025, China

Correspondence to: Dr. Jian-Wei Zhu, Shanghai Institute of Digestive Surgery, Ruijin Hospital, Shanghai Second Medical University, Shanghai 200025, China. tozhujw@263.net

Telephone: +86-21-64370045-662211

Received 2001-07-19 Accepted 2001-09-27

## Abstract

**AIM:** To evaluate the effect of reactive oxygen species such as hydrogen peroxide on the progression of human colon cancer.

**METHODS:** Human colon carcinoma cell lines, LS174T and HCT8, were treated respectively with  $10^{-5}$ ,  $10^{-7}$  or  $10^{-9}$  mol·L<sup>-1</sup> hydrogen peroxide for 24h, and co-cultured with human endothelial cell line ECV-304. The migration of ECV-304 induced by cancer cells was calculated and the expression level of vascular endothelial growth factor in cancer cells was determined by RT-PCR analysis and ELISA. Dactinomycin of 1.5mg·L<sup>-1</sup> which could block transcription of cancer cells was applied to observing the effects of H<sub>2</sub>O<sub>2</sub> on transcriptional activity and the relative half-life of VEGF mRNA. Finally, to evaluate the effect of H<sub>2</sub>O<sub>2</sub> on NF-κB activity in colon cancer cells, NF-κB in cytoplasm and nucleus of the cells were detected with FITC-tagged antibody and its presence in the nucleus(Fn) vs cytoplasm(Fc) was monitored by measuring the green fluorescence integrated over the nucleus by laser scanning cytometry(LSC).

**RESULTS:** Exogenous hydrogen peroxide of low concentration increased the migration of endothelial cell induced by colon cancer cells. When cancer cells were treated with  $10^{-5}$  mol·L<sup>-1</sup> H<sub>2</sub>O<sub>2</sub>, the migration number of endothelial cells induced by LS174T cells was 203±70, and the number induced by HCT8 cells was 145±65. The two values were significantly higher than those treated with other concentrations of H<sub>2</sub>O<sub>2</sub> ( $P<0.01$ ). The expression of vascular endothelial growth factor in cancer cells, which could be blocked by dactinomycin, were increased to a certain degree, while the relative half-life of VEGF mRNA was not prolonged after treatment with hydrogen peroxide. The activity of NF-κB in colon cells rose after the cells were exposed to hydrogen peroxide for 24h. The Fn values in HCT8 cells were 91±13 (0 mol·L<sup>-1</sup> H<sub>2</sub>O<sub>2</sub>) and 149±40 ( $10^{-5}$  mol·L<sup>-1</sup> H<sub>2</sub>O<sub>2</sub>) ( $P<0.05$ ), in LS174T cells were 127±35 (0 mol·L<sup>-1</sup> H<sub>2</sub>O<sub>2</sub>) and 192±11 ( $10^{-5}$  mol·L<sup>-1</sup> H<sub>2</sub>O<sub>2</sub>) ( $P<0.05$ ). It is similar to the case of VEGF expression in cancer cells.

**CONCLUSION:** Hydrogen peroxide increases vascular endothelial growth factor expression in colon cancer cells, and it is likely that reactive oxygen species such as hydrogen peroxide facilitates the development of colon cancer.

Zhu JW, Yu BM, Ji YB, Zheng MH, Li DH. Upregulation of vascular

endothelial growth factor by hydrogen peroxide in human colon cancer. *World J Gastroenterol* 2002;8(1):153-157

## INTRODUCTION

Reactive oxygen species (ROS) can be easily produced in intracolonic cavity, due to large amounts of bacteria and dietary metabolites in it. Several reports on the relationship between ROS and cancer suggested that ROS such as oxygen radicals, hydroxyl radicals and hydrogen peroxide (H<sub>2</sub>O<sub>2</sub>), were involved in the pathogenesis of colon tumors<sup>[1-14]</sup>. H<sub>2</sub>O<sub>2</sub>, a special intermediate in redox reaction, is able to cross cell membranes in a free manner and modify protein and nucleic acid after being changed into radicals, and now it is thought to be a kind of signal molecular which plays an important role in the growth of tumor cells. Evidences have been given in some reports that H<sub>2</sub>O<sub>2</sub> could promote cell growth and related gene expression in human tumors such as prostate cancer and breast cancer. Considering the special environment in colon and rectum we think it is necessary to evaluate the effects of ROS, especially H<sub>2</sub>O<sub>2</sub>, on the progression of colorectal cancer<sup>[15-27]</sup>. As angiogenesis, which induced by several factors such as vascular endothelial growth factor(VEGF), is often demonstrated in solid tumors, and thought to be an essential requirement for the development of malignant tumors<sup>[28-33]</sup>, we investigated the effects of H<sub>2</sub>O<sub>2</sub> on VEGF expression in colon cancers in this study to find evidences that ROS such as H<sub>2</sub>O<sub>2</sub> plays a role in the progression of the tumor.

## MATERIALS AND METHODS

### Cell culture and culture conditions

Human colon cancer cell lines, LS174T and HCT8, and human umbilical vein endothelial cell line ECV-304 were purchased from American Type Culture Collection. These cell lines were cultured and maintained in RPMI1640 supplemented with 100 ml·L<sup>-1</sup> fetal bovine serum at 37°C in 50 ml·L<sup>-1</sup> carbon dioxide and 950 ml·L<sup>-1</sup> air.

### H<sub>2</sub>O<sub>2</sub> treatment of cancer cells and MTT assay

To determine the effects of H<sub>2</sub>O<sub>2</sub> on the growth of cancer cells, LS174T and HCT8 cells were grown (10<sup>3</sup> per well) on 96-well plates and treated with the culture media containing H<sub>2</sub>O<sub>2</sub> (ten concentrations from 10<sup>-10</sup> mol·L<sup>-1</sup> to 10<sup>-1</sup> mol·L<sup>-1</sup>) (300 ml·L<sup>-1</sup> H<sub>2</sub>O<sub>2</sub> solution was purchased from Sigma). After 48h, MTT assay showed that H<sub>2</sub>O<sub>2</sub> inhibited the growth of cancer cells when its concentration was >10<sup>-5</sup> mol·L<sup>-1</sup>, while had no effect on cell growth when its concentration was ≤10<sup>-5</sup> mol·L<sup>-1</sup>. Therefore, those concentrations of H<sub>2</sub>O<sub>2</sub>, 10<sup>-5</sup>, 10<sup>-7</sup> and 10<sup>-9</sup> mol·L<sup>-1</sup>, were used in subsequent studies.

### Endothelial cell migration induced by cancer cells

To clarify the effects of H<sub>2</sub>O<sub>2</sub> on the migration of vascular endothelial cells, which could be promoted by VEGF, colon cancer cells were co-cultured with endothelial cells. LS174T and HCT8 cells were plated on 12-well plates (Falcon) at a density of 4×10<sup>5</sup> per well. Four hours later, the cells were washed with serum-free medium, and

exposed to  $10^{-5}$ ,  $10^{-7}$  or  $10^{-9}$  mol·L<sup>-1</sup> H<sub>2</sub>O<sub>2</sub> with the H<sub>2</sub>O<sub>2</sub>-containing complete media for 24h. Cell culture inserts with polyethylene terephthalate membranes (PET) and 8 μm pore size (Becton Dickinson, USA) were then placed into the 12-well plates, and endothelial cells ECV-304 were seeded into the inserts with a density of  $1 \times 10^4$ . Six hours later, the cells on the upper surface of the PET membranes were wiped off completely, and the inserts were fixed and stained. The migration capacity of endothelial cells was estimated by counting the number of the cells beneath the PET membranes. The controls were the groups without cancer cells in the wells or without treating cancer cells with H<sub>2</sub>O<sub>2</sub>.

### Expression of VEGF in colon cancer cell

To determine the effects of H<sub>2</sub>O<sub>2</sub> on expression of VEGF, LS174T and HCT8 were grown to 90% confluence to avoid the effects of cell density and incubated in complete media in the presence of H<sub>2</sub>O<sub>2</sub> ( $10^{-5}$ ,  $10^{-7}$  and  $10^{-9}$  mol·L<sup>-1</sup>) for 24h. Total RNA was extracted and resuspended in sterile RNase-free water for storage at -70°C. Access RT-PCR system (Promega) with the sensitive feature was used to determine the relative VEGF mRNA expression. All primers were synthesized by Life Technology, Hongkong.

VEGF sense: 5'-AAGCCATCCTGTGTGCCCTG ATG-3'  
antisense: 5'-GCGAATTCCTCTGCCGCGCTGAC-3'  
β-actin sense: 5'-AACACCCAGCCATGTACGTTG-3'  
antisense: 5'-CGGATGTCCACGTCACACTTCAT-3'

The 50 μL mixture for reverse transcription and PCR amplification were added in one-tube including AMV reverse transcriptase 5U, Tfl DNA polymerase 5U, MgSO<sub>4</sub>, 20 μL dNTP mixture, reaction buffer and 20 pmol of each primer and 0.1 μg total RNA sample. The condition for RT-PCR included a 48°C reverse transcription, a 94°C AMV inactivation and denaturation, a 60°C annealing and a 72°C extension. PCR amplification was subjected to 40 cycles. A volume of 10 μL RT-PCR products was added in 20 g·L<sup>-1</sup> agarose gel containing 0.5 mg·L<sup>-1</sup> EB. After electrophoresis, the density and area of each band were measured using Fluro-sTM image software (Bio-Rad, USA). The relative RNA level of VEGF in tumor cells was calculated using the house-keeping gene β-actin as an internal control. The experiments were repeated at least four times.

### Analysis VEGF transcriptional activity and VEGF mRNA half-life

To confirm that the effect of H<sub>2</sub>O<sub>2</sub> on expression of VEGF in colon cancer cells was due to an increase in transcription, transcription activity of cancer cells was blocked by Dactinomycin (ActD, purchased from Sigma). LS174T cells were incubated in the presence of ActD ( $1.5 \text{ mg} \cdot \text{L}^{-1}$ ) for 4h before their exposure to  $10^{-5}$  mol/L H<sub>2</sub>O<sub>2</sub> in serum-free medium. Total RNA was extracted from cells after 24h, and RT-PCR analysis was made. Control cells were treated with ActD without H<sub>2</sub>O<sub>2</sub>.

To determine the effect of H<sub>2</sub>O<sub>2</sub> on VEGF mRNA stability, LS174T cells were incubated in the presence or absence of  $10^{-5}$  mol·L<sup>-1</sup> H<sub>2</sub>O<sub>2</sub> for 24h. Further transcription in cells was then blocked by addition of  $1.5 \text{ mg} \cdot \text{L}^{-1}$  ActD. Total RNA was extracted from cells at 0, 0.25, 0.5, 1, 2 and 4h. RT-PCR analysis was made and the relative level of VEGF mRNA expression at each point was compared with the control value (total RNA extracted from cells before ActD treatment was defined as 100%). The relative half-life of VEGF mRNA was determined by plotting relative VEGF mRNA expression levels on a semilogarithmic axis versus time.

### Determination of VEGF protein levels

The VEGF protein levels in the supernatant were

determined with an enzyme-linked immunosorbent assay (ELISA) kit. Examinations were repeated three times.

### Activity of transcriptional factor NF-κB in colon cancer cells

To evaluate the effects H<sub>2</sub>O<sub>2</sub> on NF-κB activity in colon cancer cells, NF-κB in cytoplasm and nucleus of the cells was detected with FITC-tagged antibody and its presence in the nucleus vs cytoplasm was monitored by measuring the green fluorescence integrated over the nucleus by laser scanning cytometry (LSC) according to the Deptala's report. Briefly, the cells were first attached to the microscope slides, and exposed to  $10^{-5}$  mol·L<sup>-1</sup> H<sub>2</sub>O<sub>2</sub> for 0.5, 1, 3, 6, 12 and 24h. The cells on slides were fixed and incubated with NF-κB P65 antibody (Santa Cruz) and FITC-tagged goat-antirabbit Ig (Santa Cruz) at room temperature. Cellular DNA was then counterstained by addition of a solution containing propidium iodide and RNase (Sigma). The cells were placed on microscope slides mounted under coverslips and analyzed by LSC. At least  $10^3$  cells were analyzed by LSC per slide. Fluorescence intensity in nucleus (Fn) and in cytoplasm (Fc) were detected and the activity of NF-κB was detected by estimating the value of Fn or Fn/Fc.

### Statistics

When appropriate, data were expressed as  $\bar{x} \pm s$ . Analysis of variance and *t* test were applied to assess the significance of differences. Statistical significance was accepted at  $P < 0.05$ .

## RESULTS

### H<sub>2</sub>O<sub>2</sub> promotes the migration of endothelial cells induced by colon cancer cells

The migration of endothelial cells induced by cancer cells was promoted to a certain degree when LS174T and HCT8 cells were exposed to  $10^{-5}$ ,  $10^{-7}$  or  $10^{-9}$  mol·L<sup>-1</sup> H<sub>2</sub>O<sub>2</sub> for 24h. When cancer cells were treated with  $10^{-5}$  mol·L<sup>-1</sup> H<sub>2</sub>O<sub>2</sub>, the migration number of endothelial cells induced by LS174T cells was  $203 \pm 70$ , and the number induced by HCT8 cells was  $145 \pm 65$ . The two values were significantly higher than those treated with other concentrations of H<sub>2</sub>O<sub>2</sub> (Table 1, Figure 1). When there was no cancer cell in the co-culture system, the number of random motility of endothelial cells was about ten cells.

### Upregulation of VEGF expression by H<sub>2</sub>O<sub>2</sub>

Electrophoresis of RT-PCR products showed the three positive bands, 243, 375 and 509 bp, representing VEGF121, VEGF165 and β-actin respectively. The internal control demonstrated a stable expression in colon cells treated with each dose of H<sub>2</sub>O<sub>2</sub>. The analysis of electrophoresis showed that expression levels of VEGF were elevated in LS174T and HCT8 cells with H<sub>2</sub>O<sub>2</sub> exposure, especially with  $10^{-5}$  mol·L<sup>-1</sup> H<sub>2</sub>O<sub>2</sub> (Figure 2). After inhibition of transcriptional activity by ActD before addition of H<sub>2</sub>O<sub>2</sub>, induction of VEGF mRNA expression was completely inhibited in LS174T cells (Figure 3), indicating that H<sub>2</sub>O<sub>2</sub>-induced VEGF expression possibly occurred at the transcriptional level. The relative half-life of VEGF mRNA in LS174T cells treated with H<sub>2</sub>O<sub>2</sub> was similar to that of the cells without H<sub>2</sub>O<sub>2</sub> exposure, demonstrating that the stability of VEGF mRNA was not affected by the treatment with H<sub>2</sub>O<sub>2</sub> (Figure 4). To determine whether secretion of VEGF is increased by H<sub>2</sub>O<sub>2</sub> in colon cancer cells, the supernatant was assayed and the results showed that H<sub>2</sub>O<sub>2</sub> also promoted the VEGF protein expression. The levels of VEGF protein peaked when LS174T and HCT8 cells were incubated in the media containing  $10^{-5}$  mol·L<sup>-1</sup> H<sub>2</sub>O<sub>2</sub>. This situation is similar to the increase of VEGF expression.

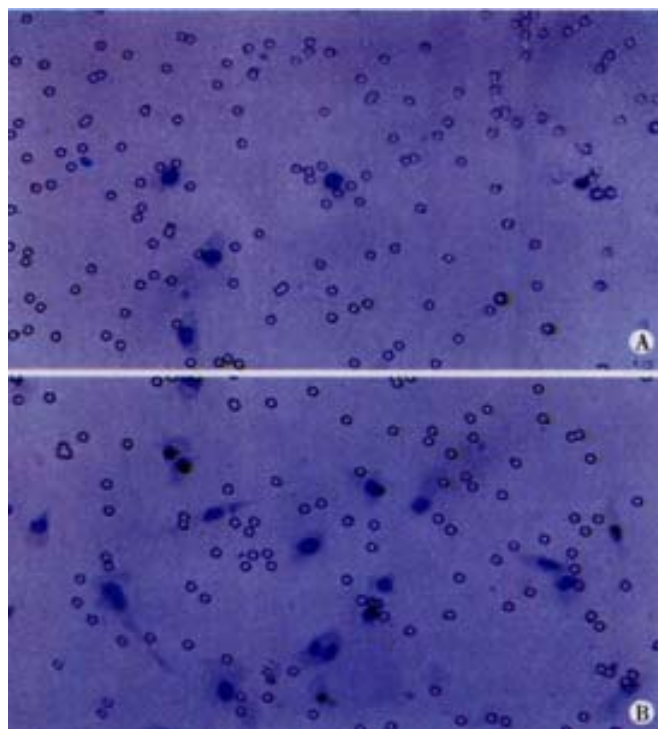
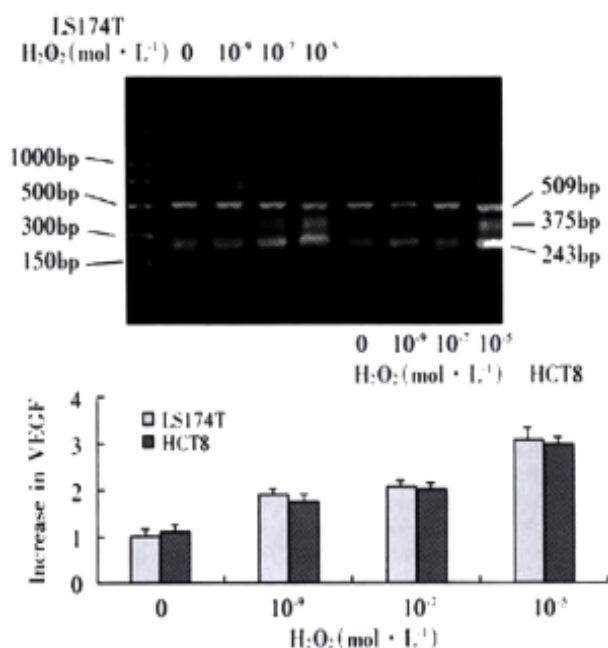
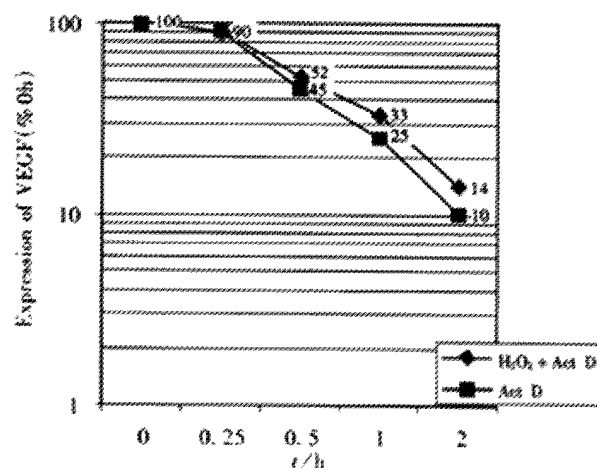


**Table 1** The migration of endothelial cells induced by colon cancer cells ( $\bar{x} \pm s$ )

| Cell line | H <sub>2</sub> O <sub>2</sub> in media(mol·L <sup>-1</sup> ) |                  |                  |                  |
|-----------|--------------------------------------------------------------|------------------|------------------|------------------|
|           | 0                                                            | 10 <sup>-9</sup> | 10 <sup>-7</sup> | 10 <sup>-5</sup> |

|        |        |        |        |                     |
|--------|--------|--------|--------|---------------------|
| LS174T | 155±38 | 162±38 | 174±40 | 202±70 <sup>a</sup> |
| HCT8   | 113±73 | 114±71 | 122±68 | 145±65 <sup>b</sup> |

<sup>a</sup> $P < 0.01$ ,  $t = 3.4751$ , vs LS174T, without H<sub>2</sub>O<sub>2</sub> treatment <sup>b</sup> $P < 0.01$ ,  $t = 3.4183$ , vs HCT8, without H<sub>2</sub>O<sub>2</sub> treatment

**Figure 1** The migration of endothelial cells induced by LS174T cells was increased after the cancer cells were exposed to 10<sup>-5</sup>mol·L<sup>-1</sup> H<sub>2</sub>O<sub>2</sub>. The regular circles is the 8μm pores located in PET membrane. A: induced by cancer cells without H<sub>2</sub>O<sub>2</sub> treatment. B: induced by cancer cells with H<sub>2</sub>O<sub>2</sub> treatment. ×200**Figure 2** Expression levels of VEGF were increased in LS174T and HCT8 after exposure to 10<sup>-9</sup>, 10<sup>-7</sup> and 10<sup>-5</sup>mol·L<sup>-1</sup> H<sub>2</sub>O<sub>2</sub>, demonstrating a dose-dependent feature.**Figure 3** LS174T cells were treated with 1.5mg·L<sup>-1</sup> Act D for 4h, followed by exposure to 10<sup>-5</sup> mol·L<sup>-1</sup> H<sub>2</sub>O<sub>2</sub> for 24h. RT-PCR was done. The control was those without Act D treatment.**Figure 4** Effect of H<sub>2</sub>O<sub>2</sub> on the half-life of VEGF mRNA in LS174T cells with or without H<sub>2</sub>O<sub>2</sub> exposure following Act D treatment. No difference in half-life was showed between the two groups.

### H<sub>2</sub>O<sub>2</sub> increases the activity of NF-κB

LS174T and HCT8 cells were incubated in the presence of H<sub>2</sub>O<sub>2</sub> (10<sup>-5</sup>mol·L<sup>-1</sup>) for 0.5, 1, 3, 6, 12 and 24h in complete medium. NF-κB activity peaked after exposure to H<sub>2</sub>O<sub>2</sub> for 24h. We investigated the changes of NF-κB activity in LS174T and HCT8 cells treated with 10<sup>-5</sup>, 10<sup>-7</sup> and 10<sup>-9</sup> mol·L<sup>-1</sup> H<sub>2</sub>O<sub>2</sub> in media. Compared with the cells without H<sub>2</sub>O<sub>2</sub> treatment, administration of 10<sup>-5</sup> mol·L<sup>-1</sup> H<sub>2</sub>O<sub>2</sub> for 24h led to a more remarkable increase in green fluorescence intensity measured over nuclear area (Fn) (Table 2, Figure 5), indicating the increase of NF-κB activity in LS174T and HCT8 cells.

**Table 2** Change of NF-κB activity in colon cancel cells ( $\bar{x} \pm s$ )

| Cell line | H <sub>2</sub> O <sub>2</sub> (mol·L <sup>-1</sup> ) |                  |
|-----------|------------------------------------------------------|------------------|
|           | 0                                                    | 10 <sup>-5</sup> |

|           |           |                     |
|-----------|-----------|---------------------|
| HCT8 Fn   | 91±13     | 149±40 <sup>a</sup> |
| Fn/Fc     | 0.75±0.14 | 2.18±0.54           |
| LS174T Fn | 127±35    | 192±11 <sup>b</sup> |
| Fn/Fc     | 2.18±1.17 | 3.99±1.38           |

<sup>a</sup> $P < 0.05$ ,  $t = 3.4179$ , vs HCT8, no H<sub>2</sub>O<sub>2</sub> treatment

<sup>b</sup> $P < 0.05$ ,  $t = 3.0981$ , vs LS174T, no H<sub>2</sub>O<sub>2</sub> treatment

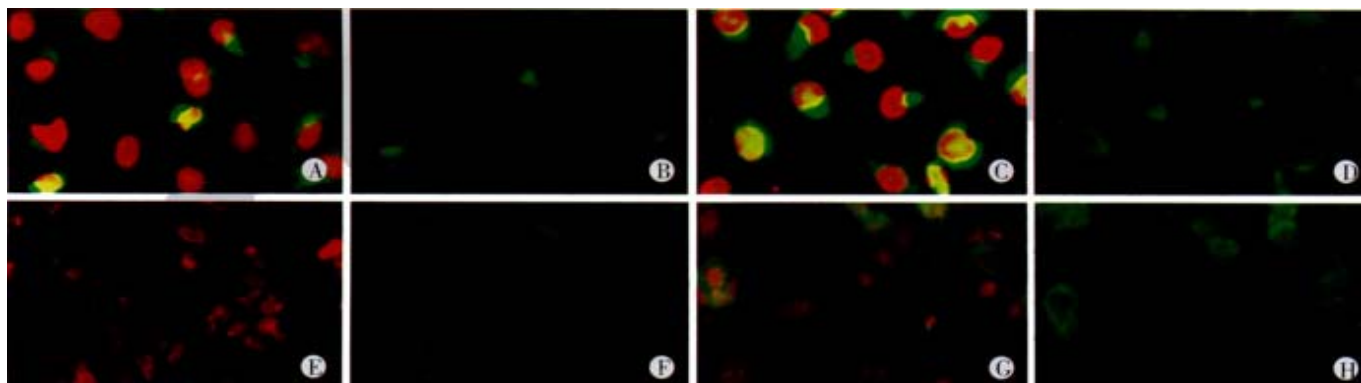


**Figure 5** Measurement of nuclear and cytoplasmic NF- $\kappa$ B associated fluorescence by LSC. The red fluorescence represents the nuclear area, and the intensity of green fluorescence over nucleus(Fn) reflects NF- $\kappa$ B activity. A, B: LS174T cells without H<sub>2</sub>O<sub>2</sub> treatment. C, D: Increase in NF- $\kappa$ B activity of LS174T cells with H<sub>2</sub>O<sub>2</sub> exposure. E, F: HCT8 cells without H<sub>2</sub>O<sub>2</sub> treatment. G, H: Increase in NF- $\kappa$ B activity of LS174T cells with H<sub>2</sub>O<sub>2</sub> exposure.

## DISCUSSION

The reactive oxygen species(ROS), which are ubiquitous and occur naturally in all aerobic species, may be divided into two categories :free oxygen radicals ( $\cdot$ OH, $\cdot$ NO and O<sub>2</sub> $\cdot^-$ ) and nonradical ROS such as H<sub>2</sub>O<sub>2</sub>. For decades, H<sub>2</sub>O<sub>2</sub> has been one of the ROS that has been well investigated in flammatory response and oxidant-induced stress. Recently, numerous evidence has been presented to show that H<sub>2</sub>O<sub>2</sub> can act as a signaling molecule involved in many cellular function such as apoptosis and proliferation<sup>[1-10]</sup>.And the regulation of series of genes involved in carcinogenesis and progression is associated with the function of H<sub>2</sub>O<sub>2</sub><sup>[3,5,6,9,11-14]</sup>.Several reports have suggested that ROS such as H<sub>2</sub>O<sub>2</sub> plays a role in the pathogenesis of tumor in colon, where there are a great deal of bacteria and dietary metabolites<sup>[15-27]</sup>. Diet rich in fat increased the formation of ROS in feces, which then possibly damaged the stem cells in the colon<sup>[20,22,26]</sup>. However, up to date, little information has been available about the role of H<sub>2</sub>O<sub>2</sub> the special reactive oxygen intermediate, in the biological behaviors of colon cancer cells.

VEGF is a potent and unique angiogenic protein that stimulates capillary formation and has specific mitogenic and chemotactic activity for vascular endothelial cells<sup>[28]</sup>.In colon cancer, VEGF levels are elevated and correlated with a poor clinical outcome<sup>[29-33]</sup>. VEGF expression is regulated by some pathological processes such as hypoxia<sup>[34-36]</sup>and by numerous cytokines and growth factors including interleukin1 $\beta$ , interleukin 6, platelet-derived growth factor, transforming growth factor $\beta$ , epidermal growth factor, hepatocyte growth factor, insulin-like growth factor, angiotensin II, hypoxia -inducible factor I and EIF4E etc.<sup>[37-52]</sup> Recently, oncogene p53 is also found to be a regulator of VEGF gene in colon cancer cells<sup>[53,54]</sup>.In the present study, we found, to our knowledge, for the first time, that exogenous H<sub>2</sub>O<sub>2</sub> could up-regulate the expression of VEGF in human colon cancer cells and the migration of endothelial cells induced by the cancer cells after we reviewed those results from RT-PCR assay, ELISA and migration experiment of endothelial cells. Considering the important role of VEGF in neovascularization in solid tumors, we believe that hydrogen peroxide may have the promoting effects on the progression of colon cancer. Related studies also found that hydrogen peroxide could not only increase the expression of VEGF in cultured human vascular smooth muscle cell, human retinal pigment epithelial, melanoma cells and glioblastoma cells, but also promote the growth of prostate and breast cancer cells<sup>[55-58]</sup>.

NF- $\kappa$ B activation, as expressed by its translocation from the cytoplasm to nucleus, can be conveniently assayed by LSC by measuring the intensity of NF- $\kappa$ B-associated immunofluorescence over the area of cell nucleus and comparing it with the intensity over cytoplasm<sup>[59]</sup>. NF- $\kappa$ B, as a transcriptional factor controlling a variety

of target genes such as adhesion molecular and apoptosis, is closely related to the pathogenesis and progression of tumors. NF- $\kappa$ B activity in cells like leukocyte, could be increased by hydrogen peroxide and NF- $\kappa$ B activation was an essential step before VEGF expression level was increased by hydrogen peroxide in murine osteoblastic cells<sup>[60,61]</sup>.It is noteworthy in the present experiment that the increase of NF- $\kappa$ B activity was accompanied by the promotion of expression of VEGF in colon cancer cells exposed to hydrogen peroxide. Thereby, we estimate that the NF- $\kappa$ B activation may be the prerequisite of the effect of hydrogen peroxide on VEGF expression in colon cancer cells.

In view that such reactive oxygen species as hydrogen peroxide are likely to promote the development of colon cancer, it would be helpful in releasing oxidative stress by antioxidants in the colon cancer therapy.

## REFERENCES

- 1 Rhee SG. Redox signaling:hydrogen peroxide as intracellular messenger. *Exper Mol Med* 1999;35:53-59
- 2 Gata L,Paul J,Ba GN, Tew KD, Tapiero H. Oxidative stress induced in pathologies:the role of antioxidants. *Biomed Pharmac Ther* 1999;53:169-180
- 3 Schwieger A, Bauer L, Hanusch J, Sers C, Schafer R, Bauer G.Ras oncogene expression determines sensitivity for intercellular induction of apoptosis. *Carcinogenesis* 2001;22:1385-1392
- 4 Chen Y, Kramer DL, Diegelman P, Vujcic S, Porter CW. Apoptotic signaling in polyamine analogue-treated SK-MEL-28 human melanoma cells. *Cancer Res* 2001;61:6437-6444
- 5 Del Bello B, Valentini MA, Zunino F, Comporti M, Maellaro E. Cleavage of Bcl-2 in oxidant- and cisplatin-induced apoptosis of human melanoma cells. *Oncogene* 2001;20:4591-4595
- 6 Chung YM, Yoo YD, Park JK, Kim YT, Kim HJ.Increased expression of peroxiredoxin II confers resistance to cisplatin. *Anticancer Res* 2001; 21:1129-1133
- 7 Dare E, Li W, Zhivotovsky B, Yuan X, Ceccatelli S.Methylmercury and H(2)O(2) provoke lysosomal damage in human astrocytoma D384 cells followed by apoptosis. *Free Radic Biol Med* 2001;30:1347-1356
- 8 Moriya K, Nakagawa K, Santa T, Shintani Y, Fujie H, Miyoshi H, Tsutsumi T, Miyazawa T, Ishibashi K, Horie T, Imai K, Todoroki T, Kimura S, Koike K. Oxidative stress in the absence of inflammation in a mouse model for hepatitis C virus-associated hepatocarcinogenesis. *Cancer Res* 2001; 61:4365-4370
- 9 Joseph P, Muchnok TK, Klishis ML, Roberts JR, Antonini JM, Whong WZ, Ong T. Cadmium-induced cell transformation and tumorigenesis are associated withtranscriptional activation of c-fos, c-jun, and c-myc proto-oncogenes: role of cellular calcium and reactive oxygen species. *Toxicol Sci* 2001;61:295-303
- 10 Huang RP, Peng A, Golarad A, Hossain MZ, Huang R, Liu YG, Boynton AL. Hydrogen peroxide promotes transformation of rat liver non-neoplastic epithelial cells through activation of epidermal growth factor receptor. *Mol Carcinog* 2001;30:209-217
- 11 Chen YR, Shrivastava A, Tan TH.Down-regulation of the c-Jun N-terminal kinase (JNK) phosphatase M3/6 and activation of JNK by hydrogen peroxide and pyrrolidine dithiocarbamate. *Oncogene* 2001; 20:367-374
- 12 Zmijewski JW, Song L, Harkins L, Cobbs CS, Jope RS. Oxidative stress

- and heat shock stimulate RGS2 expression in 1321N1 astrocytoma cells. *Arch Biochem Biophys* 2001;392:192-196
- 13 Mendoza L, Carrascal T, De Luca M, Fuentes AM, Salado C, Blanco J, Vidal-Vanaclocha F. Hydrogen peroxide mediates vascular cell adhesion molecule-1 expression from interleukin-18-activated hepatic sinusoidal endothelium: implications for circulating cancer cell arrest in the murine liver. *Hepatology* 2001;34:298-310
  - 14 Hardman RA, Afshari CA, Barrett JC. Involvement of mammalian MLH1 in the apoptotic response to peroxide-induced oxidative stress. *Cancer Res* 2001;61:1392-1397
  - 15 Risau W. Development and differentiation of endothelium. *Kidney Int Suppl* 1998; 67:s3-6
  - 16 Landriscina M, Cassano A, Ratto C, Longo R, Ippoliti M, Palazzotti B, Crucitti F, Barone C. Quantitative analysis of basic fibroblast growth factor and vascular endothelial growth factor in human colorectal cancer. *Br J Cancer* 1998;78:765-770
  - 17 Ishigami SI, Arai S, Furutani M, Niwano M, Harada T, Mizumoto M, Mori A, Onodera H, Imamura M. Predictive value of vascular endothelial growth factor in metastasis and prognosis of human colorectal cancer. *Br J Cancer* 1998;78:1379-1384
  - 18 Nanashima A, Ito M, Sekine I, Naito S, Yamaguchi H, Nakagoe T, Ayabe H. Significance of angiogenic factor in liver metastatic tumors originating from colorectal cancers. *Dig Dis Sci* 1998;43:2634-2640
  - 19 Wang MP, Cheung N, Yuen ST, Leung SY, Chung LP. Vascular endothelial growth factor is up-regulated in the early pre-malignant stage of colorectal tumor progression. *Int J Cancer* 1999;81:845-850
  - 20 Zebrowski BK, Liu W, Ramirez K, Akagi Y, Mills GB, Ellis LM. Markedly elevated level of vascular endothelial growth factor in malignant ascites. *Ann Surg Oncol* 1999;6:373-378
  - 21 Dachs GU, Chaplin DJ. Microenvironmental control of gene expressions: implications for tumor angiogenesis, progression and metastasis. *Semi Radiat Oncol* 1998; 8:208-216
  - 22 Ortega N, L'Fagih FE, Plouet J. Control of vascular endothelial growth factor angiogenic activity by the extracellular matrix. *Biol Cell* 1998; 90:381-390
  - 23 Neufeld G, Cohen T, Gengrinovitch S, Poltorak Z. Vascular endothelial growth factor and its receptors. *FASEB J* 1998;90:381-390
  - 24 Lufc FC, Mervaa E, Muller DN, Gross V, Schmidt F, Park JK, Schmitz C, Lippoldt A, Breu V, Dechend R, Dragun D, Schneider W, Ganten D, Haller H. Hypertension-induced end organ damage: A new transgenic approach to an old problem. *Hypertension* 1999;33:212-218
  - 25 Semenza GL, Agani F, Iyer N, Kotch L, Laughner E, Leung S, Yu A. Regulation of cardiovascular development and physiology by hypoxia-inducible factor 1. *Ann N Y Acad Sci* 1999;874:262-268
  - 26 Nanthan CA, Franklin S, Abreo KW, Nassar R, Debenedetti A, Williams J, Stucker FJ. Expression of eIF4E during head and neck tumorigenesis: possible role in angiogenesis. *Laryngoscope* 1999;109:1253-1258
  - 27 Arri S, Mori A, Uchida S, Fujimoto K, Shimada Y, Imamura M. Implication of vascular endothelial growth factor in the development and metastasis of human cancers. *Hum Cell* 1999;12:25-30
  - 28 Holash J, Wiegand SJ, Yancopoulos GD. New model of tumor angiogenesis: dynamic balance between vessel regression and growth mediated by angiopoietins and VEGF. *Oncogene* 1999;18:5356-5362
  - 29 Lamszus K, Lateral J, Westphal m, Rosen EM. Scatter factor/hepatocyte growth factor content and function in human gliomas. *Int J Dev Neurosci* 1999;17:517-530
  - 30 Saari A, Karpanen T, Alitalo K. Mechanism of angiogenesis and their use in the inhibition of tumor growth and metastasis. *Oncogene* 2000;19:6122-6129
  - 31 Akagi Y, Liu W, Zebrowski B, Xie K and Ellis LM. Regulation of vascular endothelial growth factor expression in human colon cancer by insulin-like growth factor 1. *Cancer Res* 1998;58:4008-4014
  - 32 Akagi Y, Liu W, Xie K, Zebrowski B, Shaheen RM and Ellis LM. Regulation of vascular endothelial growth factor expression in human colon cancer by Interleukin-1 $\alpha$ . *Br J Cancer* 1999;80:1506-1511
  - 33 Bouvet M, Ellis LM, Nishizaki M, Fujiwara T, Liu W, Bucana CD, Fang B, Lee JJ and Roth JA. Adenovirus-mediated wild-type p53 gene transfer down-regulates vascular endothelial growth factor expression and inhibits angiogenesis in human colon cancer. *Cancer Res* 1998;58:2288-2292
  - 34 Kondo Y, Arai S, Furutani M, Ishigami S, Mori A, Onodera H, Chiba T, Imamura M. Implication of vascular endothelial growth factor and p53 status for angiogenesis in noninvasive colorectal carcinoma. *Cancer* 2000;88:1820-1827
  - 35 Pool-Zobel BL, Abrahamse SL, Collins AR, Kark W, Gugler R, Oberreuther D, Siegel Treptow-van Lishaut S, Rechkemmer G. Analysis of DNA strand breaks, oxidized bases, and glutathione S-transferases in human colon cells from biopsies. *Cancer Epidemiol Biomarkers Prev* 1999;8:609-614
  - 36 Kondo S, Toyokuni S, Iwasa Y, Tanaka T, Onodera H, Imamura M. Persistent oxidative stress in human colorectal carcinoma, but not in adenoma. *Free Radic Biol Med* 1999;27:401-410
  - 37 Bras A, Sanches R, Cristovao L, Fidalgo P, Mexia J, Leitao N, Rueff J. Oxidative stress in familial adenomatous polyposis. *Eur J Cancer* 1999;8:305-310
  - 38 Wen RW, Giacosa A, Hull WE, Haubner R, Spiegelhalter B, Bartsch H. The antioxidant/anticancer potential of phenolic compounds isolated from olive oil. *Eur J Cancer* 2000;36:1235-1247
  - 39 Van Rossen ME, Sluiter W, Bonthuis F, Jeekel H, Marquet RL, Van Eijck CH. Scavenging of reactive oxygen species leads to diminished peritoneal tumor recurrence. *Cancer Res* 2000;60:5625-5629
  - 40 Owen RW, Spiegelhalter B, Bartsch H. Generation of reactive oxygen species by the faecal matrix. *Gut* 2000;46:225-232
  - 41 Edmiston KH, Shoji Y, Mizoi T, Ford R, Nachman A, Jessup JM. Role of nitric oxide and superoxide anion in elimination of low metastatic colorectal carcinomas by unstimulated hepatic sinusoidal endothelial cell. *Cancer Res* 1998;58:1524-1531
  - 42 Giardina C, Inan MS. Nonsteroidal anti-inflammatory drugs, short-chain fatty acids, and reactive oxygen metabolism in human colorectal cancer cells. *Biochim Biophys Acta* 1998;1401:277-288
  - 43 Polyak K, Li Y, Zhu H, Lengauer C, Willson JK, Markowitz SD, Trush MA, Kinzler KW, Vogelstein B. Somatic mutations of the mitochondrial genome in human colorectal tumor. *Nat Genet* 1998;20:291-293
  - 44 Jessup JM, Battle P, Waller H, Edmiston KH, Stolz DB, Watkins SC, Locker J, Skena. Reactive nitrogen and oxygen radicals formed during hepatic ischemia-reperfusion kill weakly metastatic colorectal cancer cells. *Cancer Res* 1999;59:1825-1829
  - 45 Liegibel UM, Abrahamse SL, Pool-Zobel BL, Rechkemmer G. Application of confocal laser scanning microscopy to detect oxidative stress in human colon cells. *Free Radic Res* 2000;32:535-547
  - 46 Zheng ZH, Zhang H, Pan YX, Gao Y, Yang JZ. Prevention of postoperative abdominal adhesions by an antibody to VEGF in mice. *Shijie Huaren Xiaohua Zazhi* 1999;7:227-229
  - 47 Pan X, Ke CW, Pan WF, He X, Cao GW, Qi ZT. Killing effect of DT/VEGF system on gastric carcinoma cell. *Shijie Huaren Xiaohua Zazhi* 2000;8:393-396
  - 48 Mao H, Yuan AL, Zhao MF, Lai ZS, Zhang YL, Zhou DY. Effect of p38MAPK signal pathway on ultrastructural change of liver cancer cells induced by VEGF. *Shijie Huaren Xiaohua Zazhi* 2000;8:536-538
  - 49 Pan X, Pan W, Ni CR, Ke CW, Cao GW, Qi ZT. Killing effect of tetracycline controlled expression of DT/VEGF system on liver cell cancer. *Shijie Huaren Xiaohua Zazhi* 2000;8:867-873
  - 50 Pan X, Pan W, Ke CW, Zhang B, Cao GW, Qi ZT. Tetracycline controlled DT/VEGF system gene therapy mediated by adenovirus vector. *Shijie Huaren Xiaohua Zazhi* 2000;8:1121-1126
  - 51 Assy N, Paizi M, Gaitini D, Baruch Y, Spira G. Clinical implication of VEGF serum levels in cirrhotic patients with or without portal hypertension. *World J Gastroenterol* 1999;5:296-300
  - 52 Tian XJ, Wu J, Meng L, Dong ZW, Shou CC. Expression of VEGF121 in gastric carcinoma MGC803 cell line. *World J Gastroenterol* 2000;6:281-283
  - 53 Bruce WR, Giacca A, Medline A. Possible mechanisms relating diet and risk of colon cancer. *Cancer Epidemiol Biomarkers Prev* 2000;9:1271-1279
  - 54 Bianchi NO, Bianchi MS, Richard SM. Mitochondrial genome instability in human cancers. *Mutat Res* 2001;488:9-23
  - 55 Ellis EA, Guberski DL, Somogyi-Mann M, Grant MB. Increased H<sub>2</sub>O<sub>2</sub>, vascular endothelial growth factor and receptors in the retina of the BBZ/Wor diabetic rat. *Free Radic Biol Med* 2000;28:91-101
  - 56 Castilla MA, Carmelo C, Gazapo RM, Martin O, Gonzalez-Pacheco FR, Tejedor A, Bragado R, Arroyo MV. Role of vascular endothelial growth factor (VEGF) in endothelial cell protection against cytotoxic agents. *Life Sci* 2000; 67:1003-1013
  - 57 Haklar G, Sayin-Ozveri E, Yuksel M, Aktan AO, Yalcin AS. Different kinds of reactive oxygen and nitrogen species were detected in colon and breast tumors. *Cancer Lett* 2001;165:219-224
  - 58 Wartenberg M, Dierschagen H, Hescheler J, Sauer H. Growth stimulation versus induction of cell quiescence by hydrogen peroxide in prostate tumor spheroids is encoded by the duration of the Ca<sup>2+</sup> response. *J Biol Chem* 1999; 274:27759-27767
  - 59 Deptala A, Bedner E, Gorczyca W, Darzynkiewicz Z. Activation of nuclear factor KappaB (NF- $\kappa$ B) assayed by laser scanning cytometry. *Cytometry* 1998; 33: 376-382
  - 60 Kaul N, Choi J, Forman HJ. Transmembrane redox signaling activates NF-KappaB in macrophages. *Free Radical Biol Med* 1998; 24: 202-207
  - 61 Chua CC, Hamdy RC, Chua BH. Mechanism of transforming growth factor- $\beta$  1 induced expression of vascular endothelial growth factor in murine osteoblastic MC3T3-E1 cells. *Biochim Biophys Acta* 2000; 1497: 69-76

• BASIC RESEARCH •

# An analysis of 10218 ulcerative colitis cases in China

Xue-Liang Jiang, Hui-Fei Cui

Xue-Liang Jiang, Department of Gastroenterology, Chinese PLA General Hospital of Jinan Command, Jinan 250031, China  
Hui-Fei Cui, Department of Biochemical Pharmaceutics, Shandong University, Jinan 250012, Shandong Province, China  
Supported by the Key Research Fund of Jinan Command, No.9801  
Correspondence to: Dr. Xue Liang Jiang, Department of Gastroenterology, Chinese PLA General Hospital of Jinan Command, 25 Shifanlu, Jinan 250031, Shandong Province, China. chfjxl@jn-public.sd.cninfo.net  
Telephone: +86-531-2600132 Fax: +86-531-2600132  
Received 2001-07-19 Accepted 2001-08-01

## Abstract

**AIM:** To analyze the characteristics of ulcerative colitis (UC) in China.

**METHODS:** From 1981 to 2000, a total of 10218 patients of UC reported in Chinese medical literature and including our cases diagnosed were analyzed according to the diagnostic criteria of Lennard-Jones.

**RESULTS:** The number of cases increased by 3.08 times over the past 10 years (2506 patients were diagnosed from 1981 to 1990 while 7512 patients were diagnosed from 1991 to 2000). Lesion range were described in 7966 patients, 5592 (70.20%) were proctosigmoiditis or proctitis, 1792 (22.50%) left-sided colitis, 582 (7.30%) pancolitis. Among the 8122 patients, 2826 (34.8%) had first episode, 4272 (52.6%) had chronic relapse, 869 (10.7%) were of chronic persist type, 154 (1.9%) were of acute fulminant type. The course of the illness were described in 5867 patients, 4427 (75.5%) were less than 5 years, 910 (15.5%) between 5 and 10 years, 530 (9.1%) more than 10 years. Six hundred and sixteen patients (6.1%) had extraintestinal manifestations. The mean age at the diagnosis was 40.7 years (range 6-80 years, and the peak ages 30-49 years). The male to female ratio was 1.09. Among 270 patients diagnosed in our hospital, 36 had histories of smoking, there was no negative association between the severity of UC and smoking ( $P > 0.05$ ), 21 smokers were followed up for one year, 15 of them had given up smoking when the disease were diagnosed, and one year later, 7 patients relapsed, another 6 patients continued smoking, and one year later, 2 patients relapsed. Among 270 UC patients diagnosed in our hospital, 4 patients (1.48%) from 2 families had familial history of UC. Treatment was mentioned in 6859 patients, only 5-ASA and/or corticosteroid only in 1276 patients (18.6%), only Chinese herbs in 1377 patients (20.1%), combined Chinese and western medicine in 4056 patients (59.1%), surgery was performed in 87 patients (1.3%), other treatments in 63 patients (0.9%).

**CONCLUSIONS:** In China, number of UC patients increased significantly in the past 10 years. Lesions are commonly located to left side colon. The course is short with rare extraintestinal manifestations. The age of onset is relatively high. Males and females are nearly equally affected. No negative relation was found between smoking and severity of the disease. Familial relatives are rarely involved

## Traditional Chinese medicine (TCM) is widely used in the treatment of UC.

Jiang XL, Cui HF. An analysis of 10218 ulcerative colitis cases in China. *World J Gastroenterol* 2002;8(1):158-161

## INTRODUCTION

Ulcerative colitis (UC) was first described by Wilks in 1859. In China, the first case of UC was reported in 1956<sup>[1]</sup>. The diagnostic criteria of UC was published firstly in 1978 and was revised in 1993 on the National Conference of Chronic non-infective Diarrhea Disease in Taiyuan city, China<sup>[2-4]</sup>. The criteria are similar to Lennard-Jones, on the three major aspects: mainly by exclusion. A multi-center study was set up in Chinese PLA General Hospital of Jinan Command (Shandong province, China) in 1999, with eight comprehensive hospitals from different areas using unique diagnostic criteria and method treatment<sup>[1]</sup>.

UC was thought to be infrequent in China in the past, however, it was increasing over the last 20 years<sup>[1,2,5]</sup>. Figure 1.

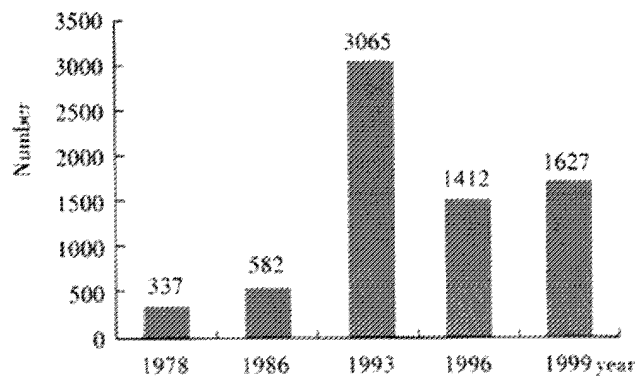


Figure 1 Cases reported on the conferences in China.

No precise statistics are available in China, in our hospital, 57 cases were admitted from 1981 to 1990, whereas 213 cases were hospitalized from 1991 to 2000<sup>[1]</sup>. According to the statistics of World Digestology Network (<http://www.wd.org.cn>) data base, more than 1560 Chinese papers on this subject were published in the past 20 years, of which, 102 articles were published on World Chinese Journal of Digestology (founded in 1993) and World Journal of Gastroenterology (founded in 1995), regarding the animal model<sup>[6-16]</sup>, etiology and pathogenesis<sup>[17-36]</sup>, diagnostic criteria<sup>[1-4]</sup> and results of treatment, etc<sup>[37-102]</sup>. Of these 1560 papers, a total of 10218 patients of UC were reported in Chinese medical literature including those diagnosed in our hospital.

## MATERIALS AND METHODS

The diagnosis of UC was based on endoscopic or radiological findings and mucosal biopsies or surgical pathology using Lennard-Jones criteria. Only those verified were included in the study. A total of 10218 patients of UC reported in Chinese medical literature including ours according to the diagnostic criteria of Lennard-Jones were



analyzed. Redit test was used, a value of  $P < 0.05$  was regarded as statistically significant.

## RESULTS

### Case number

From 1981 to 2000, a total of 10218 cases of UC were reported, of these, 2506 were diagnosed from 1981 to 1990 whereas 7512 were diagnosed from 1991 to 2000, an increasing to 3.08 times in the past 10 years.

### Extent of lesions range

As described in 7966 patients, 5592 (70.20%) were proctosigmoiditis/proctitis, 1792 (22.50%) left-sided colitis, 582 (7.30%) pancolitis.

### Clinical types

Of those described in 8122 cases, 34.8% (2826 patients) were first presentation, 52.6% (4272 patients) were chronic relapsing, 10.7% (869 patients) were chronic persistent, 1.9% (154 patients) were acute fulminant.

### Course

Of those described in 5867 cases, 4427 (75.5%) patients were less than 5 years, 910 patients (15.5%) between 5 and 10 years, 530 patients (9.1%) more than 10 years.

### Extraintestinal manifestations

618 patients (6.1%) had extraintestinal manifestations.

### Age

The mean age at the diagnosis was 40.7 years (range 6-80 years, peak age range 30-49 years).

### Sex

The male to female ratio was 1.09.

### Smoking

In our 270 patients, 36 patients (30 male, 6 female) had histories of smoking (more than 20 cigarette one day), there was no negative association between the severity of UC and smoking ( $P > 0.05$ , Table 1), 21 smokers were followed up for one year, 15 of them had given up smoking when the disease were diagnosed, and one year later, 7 patients relapsed, another 6 patients continued smoking, and one year later, 2 patients relapsed.

**Table 1** The association between the severity of UC and smoking

| Group/severity | mild | moderate | severe |
|----------------|------|----------|--------|
| Smokers        | 20   | 11       | 5      |
| Non-smokers    | 130  | 72       | 32     |

Redit test,  $P > 0.05$

### Family study

In our 270 UC patients, 4 patients (1.48%) from 2 families had familial history of UC. In one family, the patients were mother and son, in the other family, the patient were two sisters, and their mother had a history of bloody stool more than 9 years without seeking medical advise.

### Treatment

Of the 10218 patients, treatment was mentioned in 6859 cases, only 5-ASA and/or corticosteroid only in 1276 patients (18.6%), only

Chinese herbs in 1377 patients (20.1%), combined Chinese and western medicine in 4056 patients (59.1%), surgery was performed in 87 patients (1.3%), other treatments in 63 patients (0.9%). Figure 2.

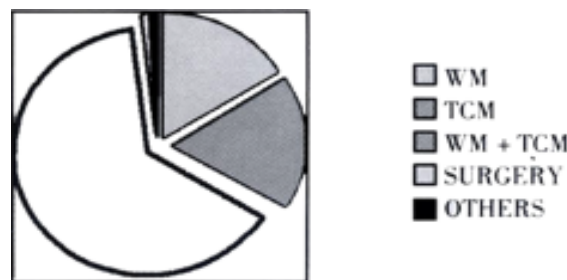


**Figure 2** Treatment of UC in China. WM:western medicine TCM:traditional Chinese medicine.

## DISCUSSION

The characteristic features of UC in China are as follows:

### UC increased significantly in the past 10 years

The incidence of UC varies greatly in different geographical areas of the world<sup>[90-92,95,101-102]</sup>. A high incidence is seen in Northern Europe and North America. In the western world, a sharp rise in the incidence of UC has been observed since early 1950s<sup>[95]</sup>, and now the incidence is stable. UC has been thought uncommon in China, however, an analysis of 1560 papers and 10218 cases indicate that the incidence is rising in recent years. From 1981 to 1990, 2506 patients were diagnosed while 7512 patients were diagnosed from 1991 to 2000. The number of cases increase by 3.08 times in the past 10 years. This is due to increasing awareness, better health care and improved study diagnostics. However, it may also be a real increase, reflecting changes in life style and dietary composition. These may shed some light on the role of environmental factors in the etiology of UC<sup>[1]</sup>.

### Lesions mostly affect left sided colon

In China, UC is usually restricted to the rectum, sigmoid and descending colon, proctocolitis are common. Our data showed 92.7% were restrict to left colon (70.20% proctosigmoiditis/proctitis, 22.50% left-sided colitis), 7.30% pancolitis, the later was commonly seen in the Western countries<sup>[101]</sup>.

### The course of illness is shorter with less extraintestinal manifestations

Occasionally, the disease may present as a single mild episode of diarrhea, but may at anytime relapse. In China, 34.8% were first presentation, 52.6% chronic relapsing, 10.7% chronic persistent, only 1.9% acute fulminant. Usually, the history revealed months or years of general ill health with continuous or intermittent diarrhea. In China, among that, the course of UC is commonly less than 5 years (75.5%), only 9.1% more than 10 years. Symptoms may be mild, systemic complications are rare, only 6.1% has extraintestinal manifestations, much less than that in the Western countries<sup>[99]</sup>.

### The onset of illness is relatively higher

In china, the onset of UC is relatively higher in the middle and old-age group (30-49 years old), mean age at the diagnosis was 40.7 years, but may occur at any age ( range 6-80 years), while in the western countries the peak age is 30 years old<sup>[91]</sup>.

### Male and female are nearly equally affected

The reports on sex difference are variable, but there seem to be a



tendency to a male preponderance especially in high incidence areas. Our data suggest that the male to female ratio was 1.09, with nearly equal frequencies.

### No relation between smoking and severity of illness

Smoking is the only consistent risk factor in case-control studies of UC, and there is no apparent relation seen between ulcerative colitis and cigarette smoking in our cases.

### Familial relatives are rarely involved

Genetic study of UC are rarely performed in China. In our 270 UC patients, 4 patients (1.48%) from 2 families had family history of UC, which is much rarer than expected. The familial tendency may be much lower than that seen in western countries<sup>[91,102]</sup>.

### Traditional Chinese medicine are widely used for the treatment of UC

SASP, is still the major drug used for the treatment of UC in China, which is effective in inducing remission and maintenance in mild-to-moderate cases. 5-ASA is too costly, corticosteroids are more commonly used, whereas 6-MP is only used by some authors. Heparin or oral low molecular weight heparin has been found to paradoxically induce remission in occasional patients with corticosteroid-resistant UC in China<sup>[48,57,60]</sup>. In China, herb medicine as heartleaf houttuynia<sup>[12,13]</sup>, has been widely used in patients with mild-to-moderate disease, as well as an adjunct to patient with moderate-to-severe disease. Combined Chinese and western medicine is the predominance treatment in China.

## REFERENCES

- Jiang XL, Wang ZK, Qin CY. Current research status and strategy on ulcerative colitis in China. *Shijie Huaren Xiaohua Zazhi* 2000;8:610-613
- Jiang XL. Diagnosis and treatment of ulcerative colitis. *Shijie Huaren Xiaohua Zazhi* 2000;8:332
- Jiang XL, Quan QZ, Wang ZK. Diagnosis, clinical types and criteria of effectiveness of ulcerative colitis. *Shijie Huaren Xiaohua Zazhi* 2000;8:332-334
- An ZY. Diagnostic criteria of ulcerative colitis. *Xin Xiaohuabingxue Zazhi* 1994;2:57
- Jiang XL, Pan BR, Ma JY, Ji ZH, Ma LS. Review for the 20th century and prospect for the 21st century of digestology. *Shijie Huaren Xiaohua Zazhi* 2000;8:1161-1176
- Cui SY, Zhang HB, Wu CZ, Sun GC, Zhao WP, Xu T, Li M. The clinical and experimental treatment of ulcerative colitis using Bupisan. *Xin Xiaohuabingxue Zazhi* 1997;5:219-220
- Yi JY, Xia B, Huang MF, Fu N, Deng CS. Observation of experimental model of ulcerative colitis in rats. *Xin Xiaohuabingxue Zazhi* 1997;5:721-722
- Zhu BX, Lu YM, Ye SM. Effects of sulfphasalazine on oxygen free radicals in experimental colitis. *Xin Xiaohuabingxue Zazhi* 1997;5:769-770
- He QW, Chen YM, Jia YL, Li XY, Jiang HY. The pathogenetic effects of immunocomplex on ulcerative colitis. *Huaren Xiaohua Zazhi* 1998;6:87
- Zou YH, Zhang YB, Chen WQ, Zhong TJ, Liu XQ, Zhao H, Lian ZC, Su Q, Su XR, Huang HD. Effects of Chinese medicine compound Weichangkang on rat ulcerative colitis and its NO abnormality. *Huaren Xiaohua Zazhi* 1998;6:288-290
- Jiang XL, Quan QZ, Wang D, Sun ZQ, Wang YJ. A new ulcerative colitis model induced by compound method and the change of immunity and ultrastructures. *Shijie Huaren Xiaohua Zazhi* 1999;7:381
- Jiang XL, Quan QZ, Wang D, Sun ZQ, Wang YJ, Qi F. Effect of heartleaf houttuynia herb on colonic pressure in rats with ulcerative colitis. *Shijie Huaren Xiaohua Zazhi* 1999;7:639
- Jiang XL, Quan QZ, Wang D, Sun ZQ, Wang YJ, Qi F. Experimental and clinical study of heartleaf houttuynia herb on ulcerative colitis. *Shijie Huaren Xiaohua Zazhi* 1999;7:786
- Zheng L, Gao ZQ, Wang SX. A chronic ulcerative colitis model in rats. *World J Gastroenterol* 2000;6:150-152
- Li L, Wang ZL, Ke JT, Zhang M, Shao JF, Zhong CN. Animal model selection for experimental ulcerative colitis. *Shijie Huaren Xiaohua Zazhi* 2001;9:584-585
- Jiang XL, Cui HF. A new chronic ulcerative colitis model produced by combination methods in rats. *World J Gastroenterol* 2000;6:742-746
- Wu XN. New advance on pathogenesis of ulcerative colitis. *Xin Xiaohuabingxue Zazhi* 1995;129-131
- Xu CT, Wang RL, Ma LS. Alterations of serum motilin, peptide YY, IgG and ferritin in patients with ulcerative colitis. *Xin Xiaohuabingxue Zazhi* 1997;5:247-248
- Zhang L, Wang AM, Guo RF, Zhang WN. Serum soluble interleukin-2 receptor level in patients with ulcerative colitis. *Xin Xiaohuabingxue Zazhi* 1997;5:251-252
- Chen X, Zhang ZY, Xu ED, Na JH, Yang NH. Bone mineral density and serum Ca, P and Mg in ulcerative colitis patients. *Xin Xiaohuabingxue Zazhi* 1997;5:385-386
- Jiang XL, Quan QZ, Liu TT, Wang YJ, Sun ZQ, Qi F, Ren HB, Zhang WL, Zhang L. Detection of blood platelet activation in patients with ulcerative colitis. *Xin Xiaohuabingxue Zazhi* 1997;5:736
- Jiang XL, Quan QZ, Sun ZQ, Wang YJ, Qi F. Expression of adhesion molecules in tissues and peripheral lymphocyte of patients with ulcerative colitis. *Huaren Xiaohua Zazhi* 1998;6:54-55
- Li HM. The characteristic of pathogenesis and the rule of treatment in spleen-weak patients with chronic colitis and ulcerative colitis. *Huaren Xiaohua Zazhi* 1998;6:726
- Jin W, Wu SH, Zhang ZJ, Lin PG, Ren XQ, Sui WL. Effect of Chinese herb Changyannin on T lymphocyte subgroup in patients with ulcerative colitis. *Shijie Huaren Xiaohua Zazhi* 1999;7:616-617
- Jiang XL, Quan QZ, Sun ZQ, Wang YJ, Qi F, Wang D, Zhang XL. Expression of lymphocyte apoptosis in patients with ulcerative colitis. *Shijie Huaren Xiaohua Zazhi* 1999;7:903-904
- Jiang XL, Quan QZ, Wang D, Sun ZQ, Wang YJ, Qi F. One case report of ulcerative colitis accompanied with acute myocardial infarction. *Shijie Huaren Xiaohua Zazhi* 1999;7:963
- Jiang XL, Quan QZ, Sun ZQ, Wang YJ, Qi F, Wang D, Zhang XL. Detection of soluble CD44v6 in patients with inflammatory bowel disease. *Shijie Huaren Xiaohua Zazhi* 1999;7:1028
- Tai WP, Luo HS. The role of short chain fatty acid on the etiology and treatment of ulcerative colitis. *Shijie Huaren Xiaohua Zazhi* 2000;8:96-97
- Jiang XL, Quan QZ, Cheng GR, Sun ZQ, Wang YJ, Wang YP. Expression of apoptosis on biopsy tissue in patients with ulcerative colitis. *Shijie Huaren Xiaohua Zazhi* 2000;8:107-108
- Jiang XL, Quan QZ, Liu T, Dong XC. Recent advances in research of ulcerative colitis. *Shijie Huaren Xiaohua Zazhi* 2000;8:216-218
- Wen B, Ma GF. Determination of plasma nitric oxide, motilin and their significances in ulcerative colitis. *World J Gastroenterol* 1998;4:69s
- Xia B, Guo HJ, JBA Crusius 2, Deng CS, SGM Meuwissen, AS Pena. In vitro production of TNF $\alpha$ , IL-6 and sIL-2R in Chinese patients with ulcerative colitis. *World J Gastroenterol* 1998;4:256
- Wang JN, Li ZF, Fu Y, Ke Y, Xu RC, Lin GB. The change of serum TNF $\alpha$  and IL-6 in patients with ulcerative colitis. *Shijie Huaren Xiaohua Zazhi* 1999;7:727-728
- Luo YJ, Yu JP. Molecular marker of IBD activity. *Shijie Huaren Xiaohua Zazhi* 2001;9:698-701
- Feng BS, Niu ZX, Zhang LF. LPO Change in experimental ulcerative colitis in rats. *Xin Xiaohuabingxue Zazhi* 1995;3(Suppl 4):7
- Cui SL, Tang B, Wang WM, Chen K, Liang J, Wang SC. Clinical investigation of serum TNF- $\alpha$  and IL-8 levels in patients with ulcerative colitis. *Xin Xiaohuabingxue Zazhi* 1997;5:719-720
- Li GQ, Feng YK. Clinical presentation and differential diagnosis of ulcerative colitis. *Shijie Huaren Xiaohua Zazhi* 2000;8:334-335
- Chen ZH, Shao XY. Examination of X ray and colonoscopy in ulcerative colitis. *Shijie Huaren Xiaohua Zazhi* 2000;8:335-336
- Wang Q, Xu L. Laboratory test and activity evaluation of ulcerative colitis. *Shijie Huaren Xiaohua Zazhi* 2000;8:336-337
- Han Y, Li SR. Current medical therapy for ulcerative colitis. *Shijie Huaren Xiaohua Zazhi* 2000;8:1273-1275
- Xu CT, Pan BR. Current medical therapy for ulcerative colitis. *World J Gastroenterol* 1999;5:64-72
- Du YC, Wang JM, Du XL. Effectiveness evaluation of different pathway of administration in ulcerative colitis. *Xin Xiaohuabingxue Zazhi* 1993;1:187-188
- Zhou ZY. Treatment of 97 ulcerative colitis patients. *Xin Xiaohuabingxue Zazhi* 1995;3:167
- Wang JD. Drug treatment of ulcerative colitis. *Xin Xiaohuabingxue Zazhi* 1996;4:338
- Li Q, Shen J. Treatment and follow up of 58 patient with ulcerative colitis. *Xin Xiaohuabingxue Zazhi* 1996;4:535
- Zhu XL, Li SX. Curative effect of drug injection via intra arterial catheter in ulcerative colitis. *Huaren Xiaohua Zazhi* 1998;6:705-706
- Chen QP. Surgical treatment of ulcerative colitis. *Shijie Huaren Xiaohua Zazhi* 2000;8:339-340
- Jiang XL, Qin CY, Li GQ. Other treatments for ulcerative colitis. *Shijie Huaren Xiaohua Zazhi* 2000;8:341-342

- 49 Rampton DS, Phil D. New treatments for inflammatory bowel disease. *World J Gastroenterol* 1998;4:369
- 50 Qing GL, Zhang AG, Niu YH, Yu DS, Guo YR. Treatment of ulcerative colitis with SASP suppository. *Xin Xiaohuabingxue Zazhi* 1994;2:120
- 51 Cui GT, Bu XZ, Chen ZX, Chen JS, Zhang PY. Treatment of ulcerative colitis with cimitidine and microwave. *Xin Xiaohuabingxue Zazhi* 1996;4:345
- 52 Sun QJ. Treatment of ulcerative colitis with metronidazole and anisodamine. *Xin Xiaohuabingxue Zazhi* 1996;4:510
- 53 Liu JY, Li YF, Fan MM. Treatment of ulcerative colitis with 4-ASA. *Xin Xiaohuabingxue Zazhi* 1997;5:183
- 54 Li SQ, Zhang JB. Treatment of ulcerative colitis with sucralfate paste. *Xin Xiaohuabingxue Zazhi* 1997;5:330
- 55 Zhou BX, Lv YM. Influence of sulphasalazine on propane dialdehyde of ulcerative colitis intestinal mucosa. *Xin Xiaohuabingxue Zazhi* 1997;5:619
- 56 Cui GT, Lv ZF. Treatment of ulcerative colitis with ranitidine enema. *Xin Xiaohuabingxue Zazhi* 1997;5:86s
- 57 Jiang XL, Liu T. Treatment of refractory ulcerative colitis with heparin. *Shijie Huaren Xiaohua Zazhi* 1999;7:694
- 58 Qin QY, Han GQ. Treatment of ulcerative colitis with aminosaliclate and corticosteroids. *Shijie Huaren Xiaohua Zazhi* 2000;8:338-339
- 59 Li RP, Wang YB. Treatment of inflammatory bowel disease with immunosuppressive agent. *Huaren Xiaohua Zazhi* 1998;6:718
- 60 Cui HF, Jiang XL. Treatment of corticosteroid-resistant ulcerative colitis with oral low molecular weight heparin. *World J Gastroenterol* 1999;5:448-450
- 61 Qiu BX, Qiu SS. Treatment of ulcerative colitis with traditional Chinese medicine. *Xin Xiaohuabingxue Zazhi* 1997;5:58s-59s
- 62 Jiang B, Wu XW, Wang Y, Si YL, Hu WJ. Treatment of ulcerative colitis with traditional Chinese herb Ziqintang. *Xin Xiaohuabingxue Zazhi* 1994;2:174
- 63 Wu ZQ, Wang HL. Treatment of ulcerative colitis with traditional Chinese herb. *Xin Xiaohuabingxue Zazhi* 1996;4:356-357
- 64 Cao GL. Treatment of ulcerative colitis with traditional Chinese herb Changanye. *Xin Xiaohuabingxue Zazhi* 1997;5:100s
- 65 Li L, Wei JQ, Zhang CQ. Treatment of ulcerative colitis with traditional Chinese herb Sanhuangtang and Binpengsan. *Xin Xiaohuabingxue Zazhi* 1997;5:125s
- 66 Li SL, Meng FS, Wang SL, Wang SQ. Treatment of ulcerative colitis with traditional Chinese herb. *Xin Xiaohuabingxue Zazhi* 1997;5:132
- 67 Wu B, Liu CL, Li WH. Treatment of ulcerative colitis with traditional Chinese herb. *Xin Xiaohuabingxue Zazhi* 1997;5:185s
- 68 Zhao XX, Long ZX, Han CB. Treatment of nonspecific ulcerative colitis with Chinese medicine. *Huaren Xiaohua Zazhi* 1998;6:78-79
- 69 Chen ZS, Nie ZW, Shun QL, Yan H. Clinical and pharmacological effect of Jianpiling on chronic ulcerative colitis. *Shijie Huaren Xiaohua Zazhi* 1999;7:960-963
- 70 Wang ZK, Xin ZP, Fan SD. Treatment of ulcerative colitis with traditional Chinese medicine. *Shijie Huaren Xiaohua Zazhi* 2000;8:340-341
- 71 Chen ZS, Zhou CM, Lu Y, Nie ZW, Sun QL, Wang YX, Chi Y. Study on TCM syndrome-typing of chronic ulcerative colitis. *China Natl J New Gastroenterol* 1996;2:141-143
- 72 Zhao LM, Guan DA, Pei HW. Treatment of ulcerative colitis with traditional Chinese medicine and western medicine. *Xin Xiaohua bingxue Zazhi* 1993;1:105
- 73 Zhu YJ, Chen WS, Wang XL. Treatment of ulcerative colitis with traditional Chinese medicine and western medicine. *Xin Xiaohua bingxue Zazhi* 1994;2:103
- 74 Guo SH, Guo JS. Treatment of ulcerative colitis with traditional Chinese medicine and western medicine. *Xin Xiaohua bingxue Zazhi* 1994;2:122
- 75 Liu QM, Bi F, Zhou SJ. Treatment of ulcerative colitis with traditional Chinese and western medicine. *Xin Xiaohua bingxue Zazhi* 1995;3:115-116
- 76 Chen ZS, Yan H, Lu Y. Advance of treatment on ulcerative colitis with traditional Chinese and western medicine. *Xin Xiaohua bingxue Zazhi* 1996;4:301-303
- 77 Sheng YZ, Ru PY, Wang SY. Treatment of ulcerative colitis with combined therapy. *Xin Xiaohua bingxue Zazhi* 1996;4:346
- 78 Ding ZQ, Wang YF, Lv CL. Treatment of ulcerative colitis with traditional Chinese medicine and western medicine. *Xin Xiaohua bingxue Zazhi* 1996;4:355-356
- 79 Sun SR, Liang LJ, Guo JQ, Song DL. Treatment of ulcerative colitis with traditional Chinese medicine and western medicine. *Xin Xiaohua bingxue Zazhi* 1997;5:400
- 80 Chen HW, Miao ZD. Treatment of ulcerative colitis with cimitidine and Yunzhigantai. *Huaren Xiaohua Zazhi* 1999;6:1009
- 81 Wang BH. Advances in treatment of ulcerative colitis. *Shijie Huaren Xiaohua Zazhi* 1999;7:177-179
- 82 Wu HG, Zhou LB, Huang C, Pan YY, Chen HP, Shi Z, Hua XG. Gene expression of cytokines in acupuncture and moxibustion treatment for ulcerative colitis in rats. *Huaren Xiaohua Zazhi* 1998;6:853-855
- 83 Wu HG, Lu HB, Zhao C, Shi Z, Liu HR, Chen HP. The mechanism of iNOS gene modulation on acupuncture and moxibustion treatment for ulcerative colitis in rats. *World J Gastroenterol* 2000;6(Suppl 3):64
- 84 Wu HG, Zhou LB, Shi DR, Liu SM, Liu HR, Zhang BM, Chen HP, Zhang LS. Morphological study on colonic ulcerative colitis treated by moxibustion. *World J Gastroenterol* 2000;6:861-865
- 85 Hu QY, Hu XY, Jiang Y. Clinical investigation of ulcerative colitis patients treated by integrated traditional Chinese and Western medicine. *World J Gastroenterol* 1998;4:93
- 86 Jiao JL, Wang SM, Li YC, Yao LY, Li SJ, Meng YX, Liu QG, Liu GQ. Treatment of ulcerative colitis with Kuijiekang. *Shijie Huaren Xiaohua Zazhi* 2000;8:572
- 87 Hu FF, Ni DQ. Treatment of ulcerative colitis with folic acid and TCM. *Shijie Huaren Xiaohua Zazhi* 2000;8:1144
- 88 Zhou QH, Gu SL, Yu J. Clinical and experimental study on treatment of retention enema for chronic nonspecific ulcerative colitis with quick-acting kuijie powder. *World J Gastroenterol* 2000;6(Suppl 3):76
- 89 Wu HG, Zhou LB, Pan YY, Huang C, Chen HP, Shi Z, Hua XG. Study of the mechanisms of acupuncture and moxibustion treatment for ulcerative colitis rats in view of the gene expression of cytokines. *World J Gastroenterol* 1999;5:515-517
- 90 Xia B, S. ShivanandaI, Zhang GS, Yi JY, JBA CRUSIUS, AS PE A. Inflammatory bowel disease in Hubei Province of China. *China Natl J New Gastroenterol* 1997;3:119-120
- 91 Xia B, JBA Crusius, SGM Meuwissen, AS Pena. Inflammatory bowel disease definition, epidemiology, etiologic aspects, and immunogenetic studies. *World J Gastroenterol* 1998;4:446-458
- 92 Shivananda S. Epidemiology and disease outcome in inflammatory bowel disease: observations from the European Collaborative Study. *World J Gastroenterol* 1998;4:25s
- 93 Geng X, Taniguchi M, Dai HH, Lin JJC, Lin J, Das KM. Autoimmunity in ulcerative colitis: humoral and cellular immune response by tropomyosin in ulcerative colitis. *World J Gastroenterol* 2000;6:9
- 94 Rask-Madsen J. Current concepts of the pathogenesis of IBD. *World J Gastroenterol* 1998;4:20-22
- 95 Russel M. The epidemiology of IBD worldwide. *World J Gastroenterol* 2000;6:6
- 96 Das KM, Farag SA. Current medical therapy of inflammatory bowel disease. *World J Gastroenterol* 2000;6:6
- 97 Rampton DS. Management of difficult inflammatory bowel disease: where are we now. *World J Gastroenterol* 2000;6:8
- 98 Rampton DS. Management of difficult inflammatory bowel disease: where are we now. *World J Gastroenterol* 2000;6:315-323
- 99 Das KM, Farag SA. Current medical therapy of inflammatory bowel disease. *World J Gastroenterol* 2000;6:483-489
- 100 Das KM, Farag SA. Current medical therapy of inflammatory bowel disease. *World J Gastroenterol* 2000;6:6
- 101 Salupere R. Inflammatory bowel disease in Estonia: a prospective epidemiologic study 1993-1998. *World J Gastroenterol* 2001;7:387-388
- 102 Kirsner JB. Historical origins of current IBD concepts. *World J Gastroenterol* 2001;7:175-184

• BASIC RESEARCH •

# Screening and identification of proteins mediating senna induced gastrointestinal motility enhancement in mouse colon

Xin Wang, Yue-Xia Zhong, Mei Lan, Zong-You Zhang, Yong-Quan Shi, Ju Lu, Jie Ding, Kai-Cun Wu, Jian-Ping Jin, Bo-Rong Pan, Dai Min Fan

Xin Wang, Mei Lan, Zong-You Zhang, Yong-Quan Shi, Jie Ding, Kai-Cun Wu, Dai Min Fan, Institute of Digestive Disease, Xijing Hospital, Fourth Military Medical University, Xi'an 710032, Shaanxi Province, China

Yue-Xia Zhong, Department of Emergency, Tangdu Hospital, Fourth Military Medical University, Xi'an 710032, Shaanxi Province, China  
Ju Lu, Class EE 87, Department of Electronic Engineering, Tsinghua University, Beijing 100084, China

Jian-Ping Jin, Department of Physiology and Biophysics, Case Western Reserve University School of Medicine, Cleveland, 44106-4970, Ohio, USA

Bo-Rong Pan, Oncology Center of Xijing Hospital, Fourth Military Medical University, Xi'an 710032, Shaanxi Province, China

Supported by the National Natural Science Foundation of China, No. 39970901

Correspondence to: Prof. Dai-Ming Fan, Institute of Digestive Diseases, Xijing Hospital, Fourth Military Medical University, Xi'an 710033, Shaanxi Province, China. Daimfan@pub.xaonline.com

Telephone: +86-29-3375221 Fax: +86-29-2539041

Received 2001-08-24 Accepted 2001-11-05

## Abstract

**AIM:** To isolate the proteins involved in pharmacologic action of senna extract (SE) from mouse gastrointestinal tract and to explore the molecular mechanism of gastrointestinal motility change induced by SE.

**METHODS:** SE was administrated to mice by different routes. Gastrointestinal motility of mice was observed using cathartic, gastrointestinal propellant movement experiments and X-ray analysis. Mouse model for gastrointestinal motility enhancement was established through continuous gastric administration of SE at progressively increased dose. At 3 h and week 3, 4, 6 and 10, morphological changes of gastrointestinal tissues were found under light microscope. Ultrastructural changes of intestinal and colonic tissues at week 6 were observed under transmission electron microscope. The colonic proteomic changes in model mice were examined by two-dimension polyacrylamide gel electrophoresis with immobilized pH gradient isoelectric focusing to screen the differentially expressed proteins, and their molecular masses and isoelectric points were determined. Two N-terminal sequences of the samples were also determined by mass spectrometry.

**RESULTS:** SE (0.3g) caused diarrhea after gastric administration in 1-6h and enhanced gastrointestinal propellant ( $65.1 \pm 7.5\%$ ;  $45.8 \pm 14.6\%$ ,  $P < 0.01$ ) in mice, but intramuscular and hypodermic injection had no cathartic effect. X-ray analysis of gastrointestinal motility demonstrated that gastric administration of SE enhanced gastric evacuation and gastrointestinal transferring function. At 3 h and week 3 and 4 after gastric administration of SE, light microscopic examination revealed no apparent change in gastrointestinal mucosal tissues, but transmission

**electron microscopic examination revealed inflammatory changes in whole layer of intestinal and colonic wall. Twenty differential proteins were detected in the colonic tissues of the model mice by two-dimensional electrophoresis, and the N-terminal amino acid sequences of two proteins were determined.**

**CONCLUSION:** SE causes diarrhea and enhances gastrointestinal motility through digestive tract administration. Long-term gastric administration of SE induces inflammatory changes and cell damage in the whole gastrointestinal tract. The differential proteins screened from the colonic tissues of the model mice might mediate the enhancing effect of SE on gastrointestinal motility.

Wang X, Zhong YX, Lan M, Zhang ZY, Shi YQ, Lu J, Ding J, Wu KC, Jin JP, Pan BR, Fan DM. Screening and identification of proteins mediating senna induced gastrointestinal motility enhancement in mouse colon. *World J Gastroenterol* 2002;8(1):162-167

## INTRODUCTION

Senna, a traditional Chinese medicine, has potent cathartic effect<sup>[1-4]</sup>. Its extract(SE), composed of a few dozens of chemical substances, possesses multiple pharmacological activities. Especially, it can promote the motility and secretion of gastrointestinal tract. However, its application is greatly restricted due to its toxicity<sup>[5-17]</sup>. Much attention is being paid to the effect of traditional Chinese medicine on the regulation of gastrointestinal motility<sup>[18-37]</sup>. We analyzed the role of senna in gastrointestinal motility and in diarrhea of mice and observed its action pattern, the ultrastructural changes in the active sites, and the changes in protein expression. In doing so we intended to screen from the gastrointestinal tissues the biological molecules mediating diarrhea and the enhancement of gastrointestinal movement, to elucidate the mechanism of catharsis induced by senna at the molecular level, and to lay a foundation for the development of pharmaceutical agents enhancing gastrointestinal motility.

## MATERIALS AND METHODS

### Materials

Imported senna (Shaanxi Medicine Corporation) was used, and its quality was confirmed by the Institute of Pharmaceutics, Fourth Military Medical University. The extract was obtained through solvent recovery and stored at -20°C. Acrylamide, bisacrylamide, SDS, Tris base, PMSF (all from Sino-America Biotechnology Co); ultrapure urea (Shanghai Biotechnology Co); ampholyte pH 3-10L, IPG dry strips pH 3-10L, IPGphorTM Isoelectric Focusing System (Pharmacia Co); ultradispersor GF-1 (Jiangsu Qilin Medical Equipment Factory); two-dimensional electrophoresis bath DYY-III 26, gradient mixer (Beijing 61 Factory); electrophoresis apparatus (Bio-Rad Co) were used.

### **Induction of diarrhea by SE in different Administration routes**

Thirty Balb/c mice (both sexes, 8 week, 18g-23g) were used. Before experimental manipulation, the mice was fasted without water deprivation for 24h, and each was kept in a single cage re-based with filter paper. After being divided into different groups, the mice were administered 0.3g SE in different routes, and the diarrhea status was examined.

### **Effect of SE on gastrointestinal motility in mice**

**Effect of SE on gastrointestinal motility for carbon** Thirty Balb/c mice (both sexes, 6-8weeks, 18-23 g) were divided randomly into 3 groups: Group I, II, and Control Group. SE of 0.3g was delivered to each mouse in Group I through gastric administration; 0.3g SE was im injected into each mouse in Group II; and the same volume of 9g·L<sup>-1</sup> NaCl was delivered through gastric administration to the mice in control group. After 20 min, 0.1 mL of 100 g·L<sup>-1</sup> mixture of Arabic gum and charcoal powder was administrated to all mice. Then, all mice were killed after 20 min. Whole gastrointestinal tract was taken out and pulled straight. The length of gastrointestinal tract from pylorus to anus and that from pylorus to the anterior extremity of carbon powder were measured. Percentage of migration distance of carbon powder out of whole length was calculated.

**Effect of SE on gastrointestinal motility for barium** Eight Balb/c mice (both sexes, 8weeks, 18~20 g), fasting without water deprivation within 24 h prior to the experimental manipulation, were divided randomly into 2 groups. SE of 0.3g was given through gastric administration to each mouse in Group I, and the same volume of 9 g·L<sup>-1</sup> NaCl to each mouse in the control group. After 20 min, 0.8 mL of 1.6kg·L<sup>-1</sup> barium sulfate suspension was given to each mouse. The mice were put into cloth bags that could restrict their movement, and the bags were placed on the flat of the X-ray digital machine. The migration of barium in the gastrointestinal tract was visualized and X-ray photos were taken at 5 and 40 min, 1, 1.5, 2, and 3h after barium administration<sup>[38]</sup>.

### **Effect of SE on morphology of gastrointestinal tissue**

Thirty Balb/c mice (both sexes, 8weeks, 18-23 g) were fed separately according to their sexes. Ten were classified into the control group, and 20 into the experimental group. SE was given through gastric administration to the mice in the experimental group once a day. The frequency of drug delivery increased progressively from 1·d<sup>-1</sup> to 4·d<sup>-1</sup> and the dosage increased progressively from 0.1g·d<sup>-1</sup> to 0.8g·d<sup>-1</sup> in 6 weeks. The same volume of 9 g·L<sup>-1</sup> NaCl was given to the control group. Four mice in the experimental group and 2 in the control group were killed at 3 h, 3, 4 and 6week after reagent administration. Gastric, intestinal and colonic tissues were obtained and fixed in 40 g·L<sup>-1</sup> paraformaldehyde and embedded routinely with paraffin. Sections were made. Morphological changes were examined under light microscope after HE staining. Intestinal and colonic tissues at week 6 were collected and fixed with 30 g·L<sup>-1</sup> glutaraldehyde for 6h at 4°C. Ultrathin sections were routinely made. Cellular ultrastructural changes in the whole layer of the intestinal wall were examined under transmission electron microscope.

### **Two-dimensional polyacrylamide gel electrophoresis of proteins<sup>[39]</sup>**

**Establishment of animal model for chronic gastrointestinal motility enhancement** Forty Balb/c mice (both sexes, 8 weeks, 18-20 g) were selected. Twenty five mice in the experimental group received SE through gastric administration once a day, with the frequency and dosage increasing progressively from 0.1g, 1·d<sup>-1</sup> to 0.8g, 4·d<sup>-1</sup>.

Fifteen mice in the control group received the same volume of 9 g·L<sup>-1</sup> NaCl.

### **Preparation of protein sample from intestinal tissue of mice**

Twenty mice were killed at 6 weeks after receiving gastric administration of SE (10 mice) and 9g·L<sup>-1</sup> NaCl (10 mice). The colons were collected and put immediately into ice-cold 9g·L<sup>-1</sup> NaCl containing 0.1mmol·L<sup>-1</sup>PMSF. The colonic tracts were dissected and colonic contents were washed out. The moisture on the tissues was absorbed with filter paper, and the tissues were put into liquid nitrogen immediately. The whole procedure must be finished in 5 min. Then, the tissues were either stored at -70°C until used again, or taken for immediate use. In the latter case, the tissues were weighed on electric scale, and lysed by adding tissue lytic solution (9.5mol·L<sup>-1</sup> urea, 20g·L<sup>-1</sup> NP, 402g·L<sup>-1</sup> ampholyte pH 3-10, 20g·L<sup>-1</sup> 2-ME, 1.5 mmol·L<sup>-1</sup> EDTA, 40 mmol·L<sup>-1</sup>Tris and ion-free water) by a mass volume ratio of 1 : 5. Tissue homogenate was prepared with high-speed disperser in ice-bath (3500 r·min<sup>-1</sup>×5s×5), and DNase and RNase (both 0.4 g·L<sup>-1</sup>) were added into the homogenate. After the incubation for 20 min in ice-bath and addition of PMSF (0.1 mmol·L<sup>-1</sup>), the homogenate was centrifuged at 10,000×g for 10 min. The supernatant was harvested and stored in designated volume at -70°C until used again. The total protein concentration in the supernatant was measured by Bradford method<sup>[40-42]</sup>.

**Solid-phase pH gradient isoelectric focusing** For each group, 100 µg protein sample was solved in 250µL mixture of deuterioxide solution and IPG buffer, placed at room temperature for 1h, and then applied to sample tank which was placed with IPG dry gel strip (13 cm in length), and covered with mineral oil. The isoelectric focusing program was: deuterioxidation for 12 h; isoelectric focusing 0-300 V, 1 h; 300-500 V, 1 h; 500-1000 V, 1 h; 1000-2000 V, 1 h; 2000-4000 V, 1 h; 4000-8000 V, 4 h. All operations above were performed at 20°C.

**Equilibration and transfer of IPG slab gels** The slab gels were collected and equilibrated with SDS-balanced buffer (50mmol·L<sup>-1</sup> Tris, 6 mol·L<sup>-1</sup> urea, 300 g·L<sup>-1</sup> glycerol, 10 g·L<sup>-1</sup> DTT, ion-free water) for 15 min followed by a second equilibration with balanced buffer (50 mmol·L<sup>-1</sup> Tris, 6 mol·L<sup>-1</sup> urea, 300 g·L<sup>-1</sup> glycerol, 25 g·L<sup>-1</sup> idocetamide, ion-free water) for another 15 min. Two pieces of 125 g·L<sup>-1</sup> separation gel (17cm×17cm×0.15cm) was prepared in absence of sticking gels. IPG slab gels were fixed on the top of the separation gel using 5 g·L<sup>-1</sup> agarose. Protein marker was applied at the other terminus.

**Second dimension SDS-PAGE** Two pieces of 125 g·L<sup>-1</sup> SDS-PAGE (17cm×17cm×0.15cm) were prepared and underwent polymerization for 2 h in absence of sticking gels; IPG slab gels were fixed onto the top of SDS-PAGE gels; electrophoresis was performed for 11 h at room temperature (15°C -20°C) with constant electric current (20 mA/gel, 40mA in total) and terminated when the marker arrived at the bottom.

**Silver staining of gels** The gels were collected and stained with silvery salt based on a modified protocol. The gels were fixed with the fixing solution (300 g·L<sup>-1</sup> ethanol, 0.5 mol·L<sup>-1</sup> sodium acetate, 5 g·L<sup>-1</sup> glutaraldehyde, 2 g·L<sup>-1</sup> sodium thiosulfate), rinsed with ion-free water for 15 min×3, stained with 1 g·L<sup>-1</sup> AgNO<sub>3</sub> and 0.1 g·L<sup>-1</sup> formaldehyde for 20 min, washed with ion-free water for 30sec, and colored with 25 g·L<sup>-1</sup> sodium carbonate, 0.5 g·L<sup>-1</sup> sodium thiosulfate and 0.1 g·L<sup>-1</sup> formaldehyde. The color development was terminated with 10 g·L<sup>-1</sup> acetic acid.

**Analysis of protein map on two-dimensional gels** After silvery salt staining, the gels were scanned with transmission laser scanner at 500 bpi resolution and analyzed with image pattern analyzer under identical conditions. The position, shape and density information for each

detected spot was compared to screen obviously differentially expressed proteins and to determine their molecular masses and isoelectric points.

**Identification of the screened proteins by sequencing<sup>[43]</sup>** One mg colonic proteins from the animal model was sampled and underwent solid-phase pH gradient isoelectric focusing and second dimension SDS-PAGE and transferred from gel slabs to polyvinylidene difluoride (PVDF) membranes (transferring buffer: CAPS, DTT, methanol and ion-free water, pH 11.0; transferring condition: 350 mA, 4.5 h, 10°C). The proteins on the PVDF membranes were stained with 1 g·L<sup>-1</sup> Coomassie brilliant blue. PDVF membrane was air-dried at room temperature. The protein spots stained with Coomassie brilliant blue were excised from the membrane, and their amino acid sequences at the N-termini were determined by mass spectrometry.

### Statistical analysis

Student's *t* test and  $\chi^2$  test were used for data measurement and enumeration, respectively.

## RESULTS

### Cathartic Effect of SE in different Administration routes

One to 1.5 h after gastric administration of SE, mice started to suffer from diarrhea, defecating water-thin feces, which lasted 4-5h. When the mice received im and sc injection of extract of doubled dosage, they did not develop diarrhea within 6 h (Table 1).

**Table 1** Carthartic effect of SE in different administration routes

|     | Groups        | Dose/g | n | Administration routes | Diarrhea (in 6h)  |
|-----|---------------|--------|---|-----------------------|-------------------|
| I   | Normal saline | 0.3    | 6 | ig                    | -                 |
| II  | SE            | 0.3    | 6 | ig                    | +(6) <sup>b</sup> |
| III | Normal saline | 0.3    | 6 | im                    | -                 |
| IV  | SE            | 0.3    | 6 | im                    | -                 |
| VC  | SE            | 0.3    | 6 | sc                    | -                 |

<sup>b</sup>*P*<0.01, vs all other groups.

### Effect of SE on gastrointestinal motility in mice

**Effect of SE on gastrointestinal propellant movement** While ig administration of SE could enhance gastric motility, im delivery did not show such effect (Table 2).

**Table 2** Effect of SE on gastrointestinal propellant rate in mice ( $\bar{x}\pm s$ )

|     | Group         | Dose/g | Administration routes | n  | Propellant rate/%      |
|-----|---------------|--------|-----------------------|----|------------------------|
| I   | Normal saline | 0.3    | ig                    | 10 | 45.8±14.6              |
| II  | SE            | 0.3    | ig                    | 10 | 65.1± 7.5 <sup>b</sup> |
| III | SE            | 0.3    | im                    | 10 | 48.3±12.4              |

<sup>b</sup>*P*<0.01, vs I, III groups.

### X-ray analysis of SE effect on gastrointestinal motility

In mice with gastric administration of SE (0.3 g), barium sulfate was excreted at 40 min, and more at 2 h. The migration speed was significantly higher than that shown in the control group (Figure 1).

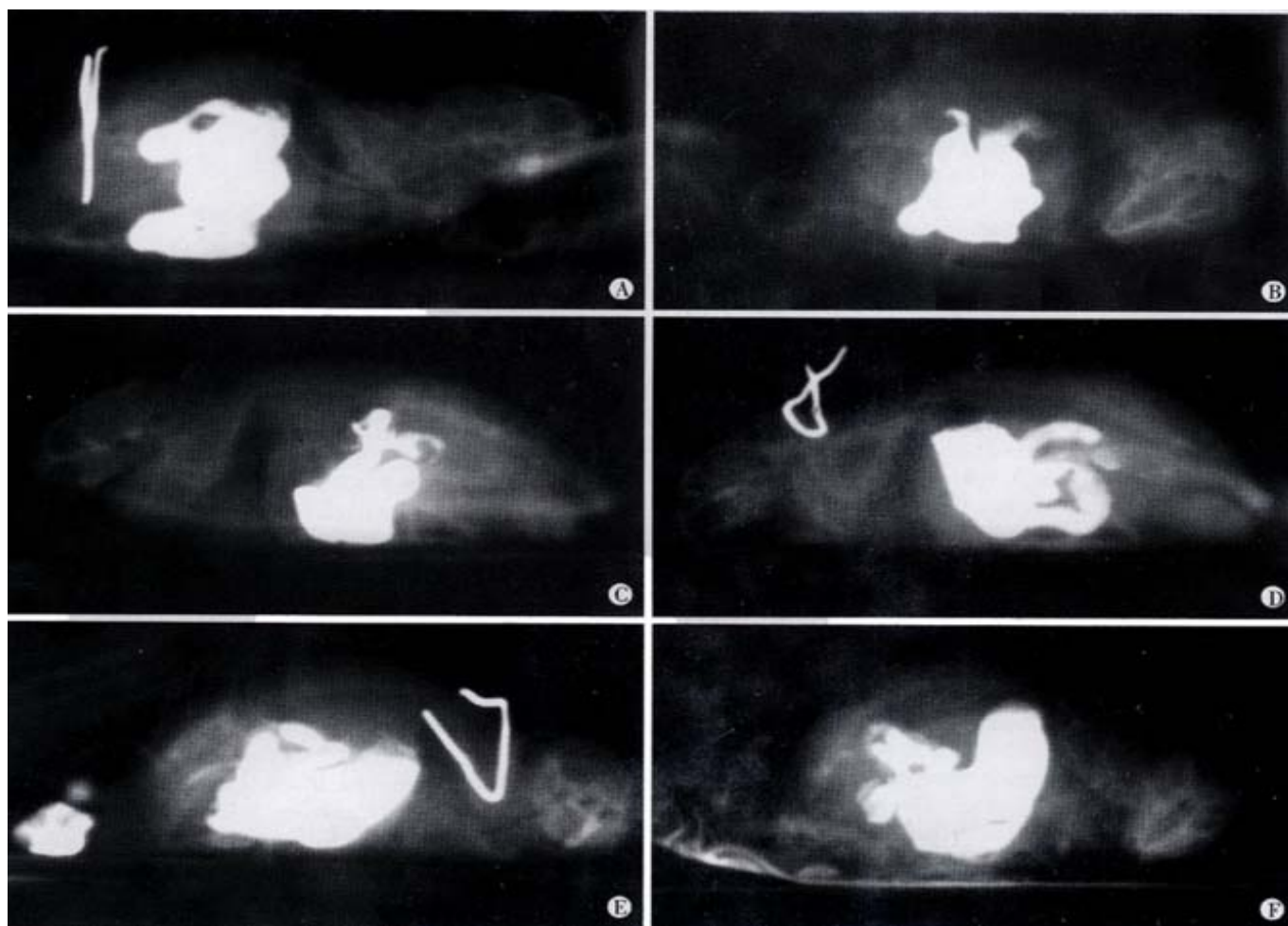


**Figure 1** X- rays of gastrointestinal peristalsis in mice administered with SE  
A, B, C: 5min, 2h, 3h after 9 g·L<sup>-1</sup> NaCl gastric administration, respectively D, E, F: 5 min, 2h, 3h after 0.3 g SE gastric administration, respectively



**Morphological effects of SE on gastrointestinal tissue** No pathological changes were observed in gastrointestinal tissues under light microscopy examination at 3 h, 3, 4 and 6 weeks after gastric administration of SE. However, at week 6, it was observed under transmission electron microscope that some small intestine epithelial cells underwent degeneration and necrosis. Although the microvilli were normal, the mitochondria in the cells were slightly swollen, with

part of the cristae broken. In the mucosa, macrophages containing phagocytic particles were found to increase, and so were plasmacytes. Cell degeneration and necrosis occurred more frequently in the mucosal epithelial cells in colon than those in the small intestine (Figure 2). The mitochondrial abnormalities mentioned above were observed in both small intestine and colon smooth muscle cells, along with the occurrence of vacuolation.

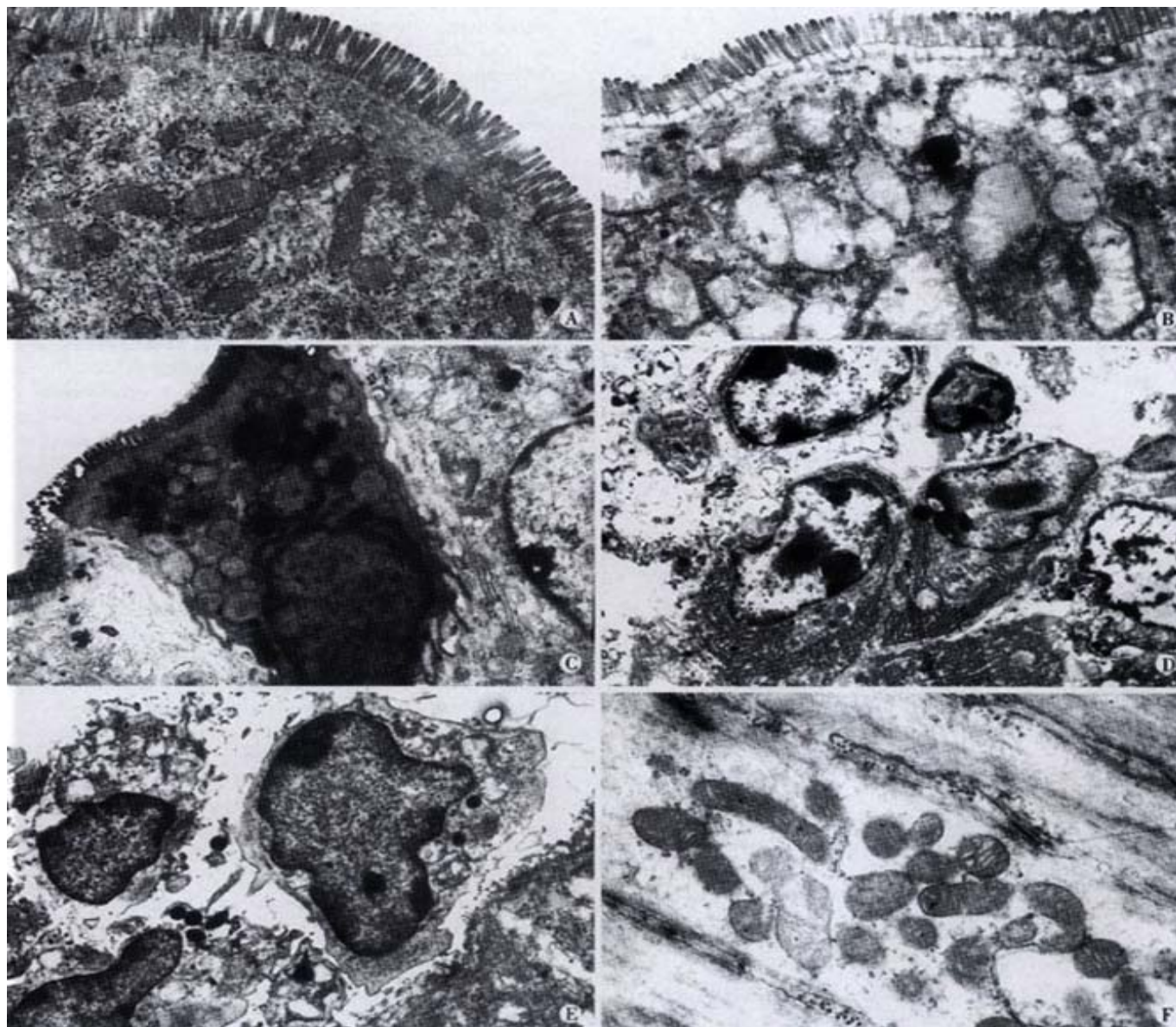


**Figure 2** Ultrastructure of intestine and colon cells in mice receiving SE at week 10.

A: Normal epithelial cell; B: Intestinal cell after treatment with SE; C: Colon cell after treatment with SE; D: Increase in submucosal plasmacytes; E: Increase in submucosal macrophages; F: Minor degeneration of smooth muscle cells in intestine

### **Gastrointestinal proteins in mice**

**Establishment of mice model for chronic gastrointestinal movement enhancement** Gastrointestinal propellant movement experiment and X-ray analysis of gastrointestinal motility demonstrated that gastric administration of SE could significantly enhance the gastrointestinal motility in Balb/c mice. Therefore, continuous gastric administration of SE might keep the gastrointestinal tract in constant enhanced motility. At week 6, the weight of the mice in the model group was significantly lower than that in the control group.

**Differential expression of gastrointestinal tissue proteins in mice** In the first dimension IPG isoelectric focusing, pH gradient was pH 3-10 L, 100 µg protein sample was added. In the second dimension IPG -PAGE 125 g·L<sup>-1</sup> uniform gel was used, the gels were stained with silver salt (Figure 3).

**Identification of differentially expressed proteins** The colonic proteins of one control mouse and one model mouse were screened and compared, and the process repeated for 5 such pairs. Twenty proteins were found different in abundance (Table 3).

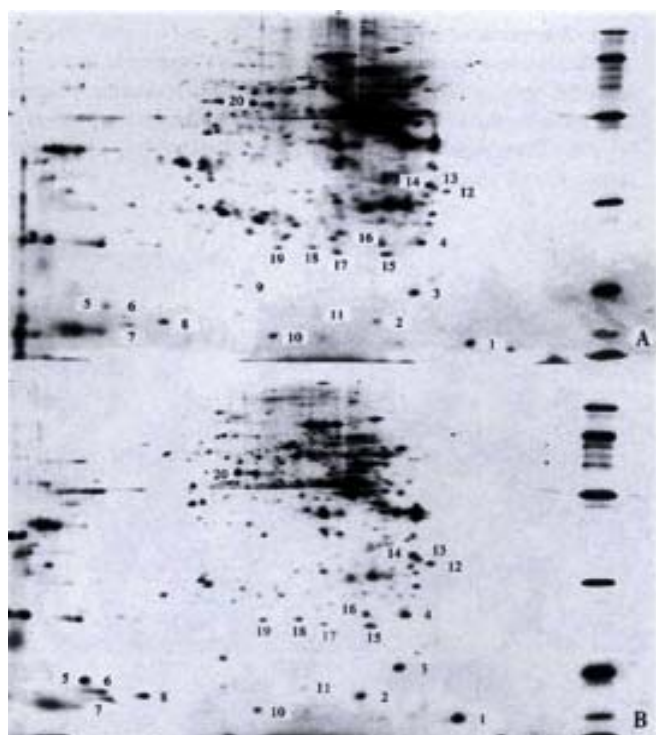


**Figure 3** Proteins on two-dimension electrophoresis maps  
A: Normal mice; B: Model mice

**Table 3** Identification of the differential proteins

| No. | Molecular mass/ku | Isoelectric point/pI | No. | Molecular mass/ku | Isoelectric Point/pI |
|-----|-------------------|----------------------|-----|-------------------|----------------------|
| 1   | 15.0              | 3.9                  | 11  | 18.0              | 5.9                  |
| 2   | 17.5              | 5.2                  | 12  | 33.0              | 4.3                  |
| 3   | 19.0              | 4.7                  | 13  | 34.0              | 4.5                  |
| 4   | 26.0              | 4.6                  | 14  | 35.0              | 4.6                  |
| 5   | 18.0              | 8.8                  | 15  | 24.0              | 5.1                  |
| 6   | 17.5              | 8.6                  | 16  | 26.0              | 5.2                  |
| 7   | 16.5              | 8.5                  | 17  | 24.5              | 5.7                  |
| 8   | 17.0              | 8.0                  | 18  | 25.0              | 6.1                  |
| 9   | 20.0              | 7.0                  | 19  | 25.0              | 6.5                  |
| 10  | 16.0              | 6.6                  | 20  | 52.0              | 7.0                  |

**Identification of differential proteins by sequencing** The N-terminal amino acid sequences of protein No. 4 and No 12 were determined by sequencing (No. 4: N-MIX/IYR-C; No 12: N-GFXDX/L-C). Protein database search showed that these two proteins were unknown proteins.

## DISCUSSION

Senna is a traditional Chinese medicine containing various chemicals, the effective components of which are sennoside A, B, C and D. It has been shown that sennosides are decomposed into Rhein anthrone by bacteria in colon, and then take effects on the colonic smooth muscle, significantly promoting colonic motility in animals and humans. The mechanism is that sennoside and its active forms affect on the intestinal mucosal epithelium and submucosal nerve bundles, stimulating prostaglandin (PG) synthesis and endogenous acetylcholine release, and subsequently enhancing colonic smooth muscle contraction.<sup>[44-46]</sup> Meanwhile, sennosides may affect directly the colonic smooth muscle, evoking its spontaneous spike potential and promoting its contraction<sup>[47]</sup>. In addition, sennosides can stimulate the colonic mucosa to release PG, NO and 5-HT, efficiently inducing the excretion of water and electrolytes by epithelial cells<sup>[48-50]</sup>. Our study showed that 1-1.5 h after gastric administration of SE, mice started

to suffer from diarrhea, defecating water-thin feces, which lasted 4-5h. When the mice received im injection of extract of doubled dosage, they did not develop diarrhea within 6 h, but after 6 h, 3 mice had light diarrhea. It suggested that the possible pathway might be that the drug delivered through im injection entered blood circulation and was excreted into the intestinal tract with bile. With hypodermic injection of larger dosage of extract, no mice developed diarrhea. However, no enhanced gastrointestinal motility was observed after im injection of SE. These results indicate that the cathartic effect of SE can only be exerted through the digestive tract rather than other pathways.

Our study also indicated that SE could promote the propellant movement in mice, a result in agreement with the reports of other researchers. Although most researchers believe that the active components of senna mainly work on colon and promote colonic motility. We think that it may also affect small intestine, as our gastrointestinal propellant movement experiment has revealed that it promoted the motility of mice small intestine in mice. In order to locate the effective site of the drug, we continuously observed the movement of marked liquid (BaSO<sub>4</sub>) in the gastrointestinal tract after administration of SE, and discovered that it inhibited rather than promoted gastric empty; however, it promoted small intestinal motility, and especially colonic motility.

We made histological examinations of mouse gastrointestinal tracts at different stages after gastric administration of SE. No apparent change was found under light microscope, but transmission electron microscopy showed lesions and degenerative changes of small intestinal mucosal epithelial cells, increase in submucosal macrophages and plasmacytes, minor degeneration of smooth muscle cells, and severe extensive degeneration and necrosis of colonic epithelial cells. Mings *et al*<sup>[10]</sup> observed the changes in guinea pig colonic epithelial cells after continuous gastric administration of sennoside for 2 weeks, and discovered epithelial cell degeneration. These results show that SE can injure the intestinal cells.

Using improved two-dimensional electrophoresis of proteomic analysis<sup>[42,51,52]</sup>, we compared the protein expression in the colon tissues of promoted gastrointestinal motility model mice and that of normal controls. The conditions in the whole process were identical for the two groups, and the location, shape, size and density of many protein spots were similar on the two-dimensional electrophoresis maps. Hence, the two groups were comparable. Image analysis showed differential proteins in the colon tissues of the model animals; the differences were primarily the increase or decrease in the amount of protein expression. Most of the differential proteins had moderate or low molecular mass, as shown in Table 3, which are probably regulatory proteins induced or affected by SE. Two of the proteins were sequenced with mass spectrometry and were confirmed to be novel ones through protein database search. However, the pharmacological functions they mediate remain to be discovered.

SE administered through the gastrointestinal tract promotes diarrhea and gastrointestinal motility, especially that of the small intestine and the colon; it also injures the digestive tract mucosa and smooth muscles, and promotes differential protein expression in the colon tissues of model animals. We have isolated and identified some of the molecules that may be involved in mediating the motility promotion and secretion effect of senna, and will continue to investigate the molecular mechanism of the aforementioned effects so as to lay the foundation for further research.

## REFERENCES

- 1 Arezzo A. Prospective randomized trial comparing bowel cleaning preparations for colonoscopy. *Surg Laparosc Endosc Percutan Tech* 2000; 10:215-217
- 2 Chilton AP, O'Sullivan M, Cox MA, Loft DE, Nwokolo CU. A blinded, randomized comparison of a novel, low-dose, triple regimen with fleet phospho-soda: a study of colon cleanliness, speed and success of

- colonoscopy. *Endoscopy* 2000;32:37-41
- 3 Krumbiegel G, Schulz HU. Rhein and aloe-emodin kinetics from senna laxatives in man. *Pharmacology* 1993;47:120-124
  - 4 Valverde A, Hay JM, Fingerhut A, Boudet MJ, Petroni R, Pouliquen X, Msika S, Flamant Y. Senna vs polyethylene glycol for mechanical preparation the evening before elective colonic or rectal resection: a multicenter controlled trial. *Arch Surg* 1999;134:514-519
  - 5 Lan M, Wang X, Wu HP, Fan DM. Biological effects of senna extract on human intestinal epithelial cells. *Shijie Huaren Xiaohua Zazhi* 2001; 9:555-559
  - 6 Stickel F, Seitz HK, Hahn EG, Schuppan D. Liver toxicity of drugs of plant origin. *Z Gastroenterol* 2001;39:225-232, 234-237
  - 7 Adam SE, Al-Yahya MA, Al-Farhan AH. Combined toxicity of Cassia senna and Citrullus colocynthis in rats. *Vet Hum Toxicol* 2001;43:70-72
  - 8 Tasaka AC, Weg R, Calore EE, Sinhorini IL, Dagli ML, Haraguchi M, Gorniak SL. Toxicity testing of Senna occidentalis seed in rabbits. *Vet Res Commun* 2000;24:573-582
  - 9 Calore EE, Weg R, Haraguchi M, Calore NM, Cavaliere MJ, Sesso A. Mitochondrial metabolism impairment in muscle fibres of rats. chronically intoxicated with Senna occidentalis seeds. *Exp Toxicol Pathol* 2000;52:357-363
  - 10 Mascolo N, Mereto E, Borrelli F, Orsi P, Sini D, Izzo AA, Massa B, Boggio M, Capasso F. Does senna extract promote growth of aberrant crypt foci and malignant tumors in rat colon? *Dig Dis Sci* 1999;44: 2226-2230
  - 11 Mengs U, Grimminger W, Krumbiegel G, Schuler D, Silber W, Volkner W. No clastogenic activity of a senna extract in the mouse micronucleus assay. *Mutat Res* 1999;444:421-426
  - 12 Mukhopadhyay MJ, Saha A, Dutta A, De B, Mukherjee A. Genotoxicity of sennosides on the bone marrow cells of mice. *Food Chem Toxicol* 1998;36:937-940
  - 13 Haraguchi M, Calore EE, Dagli ML, Cavaliere MJ, Calore NM, Weg R, Raspantini PC, Gorniak SL. Muscle atrophy induced in broiler chicks by parts of Senna occidentalis seeds. *Vet Res Commun* 1998;22: 265-271
  - 14 Calore EE, Cavaliere MJ, Haraguchi M, Gorniak SL, Dagli ML, Raspantini PC, Calore NM, Weg R. Toxic peripheral neuropathy of chicks fed Senna occidentalis seeds. *Ecotoxicol Environ Saf* 1998;39:27-30
  - 15 Cavaliere MJ, Calore EE, Haraguchi M, Gorniak SL, Dagli ML, Raspantini PC, Calore NM, Weg R. Mitochondrial myopathy in Senna occidentalis-seed-fed chicken. *Ecotoxicol Environ Saf* 1997;37:181-185
  - 16 Calore EE, Cavaliere MJ, Haraguchi M, Gorniak SL, Dagli ML, Raspantini PC, Perez Calore NM. Experimental mitochondrial myopathy induced by chronic intoxication by Senna occidentalis seeds. *J Neurol Sci* 1997;146:1-6
  - 17 Brusick D, Mengs U. Assessment of the genotoxic risk from laxative senna products. *Environ Mol Mutagen* 1997;29:1-9
  - 18 Zhang HX, Ren P, Huang X, Li Yuan. Regulation of the traditional Chinese medicine on gastrointestinal hormone and motility. *Shijie Huaren Xiaohua Zazhi* 2000; 8:
  - 19 Zhu JZ, Yang GH, Leng EF, Chen DF. Effects of the traditional Chinese medicine on gastrointestinal motility. *Shijie Huaren Xiaohua Zazhi* 1999;7:689-690
  - 20 Pang L, Zhou DR. Regulation of the traditional Chinese medicine on gastrointestinal motility. *Huaren Xiaohua Zazhi* 1998; 6: 535
  - 21 Qin XM, Li HF, Wang LD. Effects of metoclopramide on gastrointestinal myoelectric activity in rats. *Chin Natl J New Gastroenterol* 1997;5:169
  - 22 Zheng TZ, Li W, Qu SY, Ma YM, Ding YH, Wei YL. Effects of Dangshen on isolated gastric muscle strips in rats. *World J Gastroenterol* 1998;4:354-356
  - 23 Lin J, Cai G, Xu JY. A comparison between Zhishi Xiaopiwan and cisapride in treatment of functional dyspepsia. *World J Gastroenterol* 1998;4:544-547
  - 24 Zhang ZQ, Zhang HP, Ha CL, Li XZ, Lu GQ, Chen GL, Zhang GH. Clinical analysis of therapeutic effect of traditional Chinese medicine on peptic ulcer. *World J Gastroenterol* 1998; 4: 88-89
  - 25 Li W, Zheng TZ, Qu SY. Effect of cholecystokinin and secretin on contractile activity of isolated gastric muscle strips in guinea pigs. *World J Gastroenterol* 2000; 6: 93-95
  - 26 Lin XZ, Ma DL, Cui ZQ, Kang Y. Effects of rhubarb and the active ingredients of rhubarb on the cytoplasmic free calcium in INT-MNC of rabbits. *World J Gastroenterol* 2000;6:301-303
  - 27 Tian XL, Mourelle M, Li YL, Guarner F, Malagelada JR. The role of Chinese herbal medicines in a rat model of chronic colitis. *World J Gastroenterol* 2000; 6(Suppl 3): 40
  - 28 Ma XS, Fan XP, Chen Z, Li CW, Xing YS. Effects of rhizoma atractylodis macrocephalae on the contraction of isolated ileum of guinea pig. *Xin Xiaohuabingxue Zazhi* 1996;4: 603-604
  - 29 Wang ZH, Lu LS. Effect of Weichanglong on gastrointestinal motility disorders. *Xin Xiaohuabingxue Zazhi* 1997;5:448-449
  - 30 Li Y, Sun SY, Zou Z, Chen SN, Wang XY. Influences of 6 formula compositions combined of 8 kinds of Chinese medicinals on gastro intestinal motility in mice. *Huaren Xiaohua Zazhi* 1998;6:208-209
  - 31 Pang L, Zhou DR. Regulative action of Chinese traditional medicine in gastrointestinal motility. *Huaren Xiaohua Zazhi* 1998;6:535-536
  - 32 Gao F, Zhang SB, Zhang LY, Liu F, Tong WD, Li FZ. An experiment study of the smallintestinal transit injured by contact laxatives. *Shijie Huaren Xiaohua Zazhi* 1999;7:659-660
  - 33 Zhu JZ, Yang GH, Leng ER, Chen DF. Gastrointestinal motility promoting action of traditional Chinese medicine. *Shijie Huaren Xiaohua Zazhi* 1999;7:689-690
  - 34 Wang J, Hou JY. Effect of granulae Li Wei on gastrointestinal activity. *Shijie Huaren Xiaohua Zazhi* 2000;8:377-381
  - 35 Hao Q, Li Y, Yin HT. Comparative effect of different varieties of Bupleurum and Citrus on gastrointestinal motility in mice. *Huaren Xiaohua Zazhi* 1998;6:205-207
  - 36 Li SZ, Tan XH. Effect of Astragalus membranaceus on intestinal blood flow and motility in dogs. *Xin Xiaohuabingxue Zazhi* 1997;5:659-660
  - 37 Wang X, Zhang ZY, Shi YQ, Lan M, Wang QL, Wu HP, Jin JP, Fan DM. Preliminary study on protein differential expression of small bowel in BALB/c mice induced by croton oil. *Chin J Gastroenterol Hepatol* 2000;9:103-106
  - 38 Pfeifer A, Klatt P, Massberg S, Ny L, Sausbier M, Hirneiss C, Wang GX, Korth M, Aszodi A, Andersson KE, Krombach F, Mayerhofer A, Ruth P, Fassler R, Hofmann F. Defective smooth muscle regulation in cGMP kinase I-deficient mice. *EMBO J* 1998;17:3045-3051
  - 39 Wang X, Wang BL, Zhang ZY, Lan M, Wang JC, Yao LB, Chen NC, Jin JP, Fan DM. Improvement and application of two-dimensional gel electrophoresis in proteome analysis. *J Cell Mol Immunol* 2001;17:191-192
  - 40 Radloff M, Delling M, Marti T, Gercken G. Hsp27 phosphorylation is induced in alveolar macrophages exposed to Cdo-coated silica particles. *Biochem Biophys Res Commun* 1998;248:219-222
  - 41 Staudenmann W, Hatt PD, Hoving S, Lehmann A, Kertesz M, James P. Sample handling for proteome analysis. *Electrophoresis* 1998;19:901-908
  - 42 Arnott D, O'Connell KL, King KL, Stults JT. An integrated approach to proteome analysis: Identification of proteins associated with cardiac hypertrophy. *Anal Biochem* 1998;258:1-18
  - 43 Qiu YC, Benet LZ, Burlingame AL. Identification of the hepatic protein targets of reactive metabolites of acetaminophen *in vivo* in mice using two-dimensional gel electrophoresis and mass spectrometry [J]. *J Biol Chem* 1998;273:17940-17953
  - 44 Yagi T, Miyawaki Y, Nishikawa A, Yamauchi K, Kuwano S. Suppression of the purgative action of rhein anthrone, the active metabolite of sennosides A and B, by indomethacin in rats. *J Pharm Pharmacol* 1991; 43:307-310
  - 45 Yagi T, Yamauchi K, Kuwano S. The synergistic Purgative action of aloe-emodin anthrone and rhein anthrone in mice: Synergism in large intestinal propulsion and water secretion. *J Pharm Pharmacol* 1997;49: 21-25
  - 46 Nijs G, de-witte P, Geboesk J. Influence of rhein anthrone and rhein on small intestine transit rate in rats: evidence of prostaglandin mediation. *Eur J Pharmacol* 1992;218:199-203
  - 47 Lan M, Wang X, Liu Na, Fan DM. Effect of senna extract on contraction of colonic smooth muscle cells in guinea pig. *Di-si Junyi Daxue Xuebao* 2001;(in press)
  - 48 van Gorkom BA, Karrenbeld A, van Der Sluis T, Koudstaal J, de Vries EG, Kleibeuker JH. Influence of a highly purified senna extract on colonic epithelium. *Digestion* 2000;61:113-120
  - 49 Izzo AA, Mascolo N, Capasso F. Nitric oxide as a modulator of intestinal water and electrolyte transport. *Dig Dis Sci* 1998;43:1605-1620
  - 50 Izzo AA, Sautebin L, Rombola L, Capasso F. The role of constitutive and inducible nitric oxide synthase in senna- and cascara-induced diarrhoea in the rat. *Eur J Pharmacol* 1997;323:93-97
  - 51 Wang X, Zhang ZY, Shi YQ, Lan M, Ma Z, Jin JP, Fan DM. Differential expression of colonic proteins induced by extract of senna in mice. *Di-si Junyi Daxue Xuebao* 2001;22:16-19
  - 52 Wang X, Shi YQ, Zhao YQ, Wang JC, Yao LB, Zhang ZY, Lan M, Jin JP, Fan DM. Differential display of Vincristine-resistance-related proteins in gastric cancer SGC7901 cell line. *Zhonghua Zhongliu Zazhi* 2001;23: 281-284



• BASIC RESEARCH •

# Preventive effect of glutamine on intestinal barrier dysfunction induced by severe trauma

Jun-You Li, Yi Lu, Sen Hu, Dan Sun, Yong-Ming Yao

Jun-You Li, Yi Lu, Sen Hu, Dan Sun, Yong-Ming Yao, Burn Institute, Chinese PLA 304 Hospital, Beijing 100037, China  
Supported by the Key Project of the "Tenth Five-Year Plan" of the Chinese PLA (01L081)

Correspondence to: Jun-You LI, Burn Institute, Chinese PLA 304 Hospital, 51 Fu Cheng Road, Beijing 100037, China. WuZG@A-1.net.cn  
Telephon: +86-10-66867395 Fax: +86-10-68429998

Received 2001-06-03 Accepted 2001-11-15

## Abstract

**AIM:** To investigate the mechanism underlying intestinal barrier function damage after severe trauma and the therapeutic effect of glutamine.

**METHODS:** Burned patients, and animal models of severe trauma replicated by hemorrhagic shock combined with endotoxin infusion and burn injury, were included in a serial experiment. Effects of oral glutamine on intestinal barrier function were observed in scalded rats. Parameters measured in these experiments were as follows: plasma levels of diamine oxidase (DAO), tumor necrosis factor (TNF $\alpha$ ), endotoxin (LPS), and lactate as well as D-lactate by biochemical methods, lactose/mannitol (L/M) ratio in urine by SP-3400, and pathological examination of intestinal mucosa under light microscopy.

**RESULTS:** Plasma DAO activity was significantly increased after injury. There was a negative correlation between plasma DAO and intestinal mucosal DAO or pH<sub>i</sub> ( $r=-0.93$ , plasma  $0.80\pm0.93$ ,  $2.83\pm1.71$ ,  $1.14\pm0.64$ ,  $2.36\pm2.06$  and  $2.49\pm1.67$  vs intestinal  $0.52\pm0.12$ ,  $0.34\pm0.03$ ,  $0.45\pm0.18$ ,  $0.37\pm0.26$  and  $0.41\pm0.07$ ;  $r=-0.533$ , plasma  $0.87\pm0.75$ ,  $1.89\pm1.13$ ,  $1.21\pm0.23$ ,  $3.03\pm2.61$  and  $4.70\pm1.22$  vs pH<sub>i</sub>  $7.03\pm0.05$ ,  $7.05\pm0.06$ ,  $7.14\pm0.096$ ,  $7.20\pm0.08$  and  $7.05\pm0.07$ ;  $P<0.01-0.05$ ). Positive correlations were found between DAO activity and plasma TNF $\alpha$ , LPS, lactate, L/M and D-lactate ( $r=0.817$ ,  $0.842$ ,  $0.872$ , and  $0.951$ ; plasma DAO  $0.87\pm0.75$ ,  $1.89\pm1.13$ ,  $1.21\pm0.23$ ,  $3.03\pm2.61$  and  $4.70\pm1.22$  vs TNF $\alpha$   $0.08\pm0.02$ ,  $0.03\pm0.25$ ,  $0.17\pm0.09$ ,  $0.34\pm0.15$  and  $0.33\pm0.18$ ; vs LPS  $0.14\pm0.03$ ,  $0.16\pm0.04$ ,  $0.21\pm0.02$ ,  $0.18\pm0.16$  and  $0.37\pm0.10$ ; vs lactate  $9.03\pm2.19$ ,  $18.30\pm2.56$ ,  $9.81\pm2.83$ ,  $12.01\pm6.83$ ,  $12.01\pm6.84$  and  $43.61\pm11.27$ ; vs L/M  $0.03\pm0.01$ ,  $0.41\pm0.27$ ,  $0.62\pm0.20$ ,  $1.70\pm0.60$ ;  $r=0.774$ , plasma DAO  $1.25\pm0.41$ ,  $2.17\pm0.71$ ,  $2.29\pm0.87$ ,  $1.23\pm0.55$  and  $1.11\pm0.47$  vs D-lactate  $8.37\pm2.48$ ,  $18.25\pm6.18$ ,  $13.96\pm4.94$ ,  $8.93\pm3.00$  and  $12.39\pm4.94$ ; all  $P<0.01$ ), respectively. Damage of intestinal mucosa was found by pathological examination. Intestinal barrier function was improved to a certain extent by oral glutamine in scalded rats.

**CONCLUSION:** Intestinal barrier function was damaged in the early stage after trauma. Plasma DAO activity, D-lactate content, intestinal pH<sub>i</sub> and urine L/M may be sensitive markers of intestinal mechanical injury, and glutamine may protect against intestinal barrier dysfunction after severe trauma.

Li JY, Lu Y, Hu S, Sun D, Yao YM. Preventive effect of glutamine on intestinal barrier dysfunction induced by severe trauma. *World J Gastroenterol* 2002;8(1):168-171

## INTRODUCTION

It is generally accepted that the intestine may serve as an important organ in the development of severe complications under critically ill conditions, including trauma, burns, shock, etc.<sup>[1-3]</sup> Hemorrhagic shock and/or gut ischemia-reperfusion injury commonly occur in the early stage after acute insults, leading to gut-derived sepsis as a result of gut barrier dysfunction<sup>[4-10]</sup>. In order to investigate the mechanism underlying intestinal barrier function damage and its potential interventional measures, burned patients and animal models of severe trauma were employed in our current experiments<sup>[6,11-15]</sup>.

## MATERIALS AND METHODS

### Animal models

Animal models of severe trauma were replicated by hemorrhagic shock combined with endotoxin infusion. Male Wistar rats, weighing 190g-230g, were anaesthetized with intraperitoneal injection of 30g·L<sup>-1</sup> barbitone sodium (35mg·kg<sup>-1</sup>), and the femoral artery and jugular vein were cannulated under aseptic conditions. The rats were then bled via the jugular vein catheter until a mean arterial pressure of 30-35 mmHg (4.6 kPa) was reached. At the end of shock, endotoxin (*E.coli*O55 B5, Sigma) was infused through tail vein at a dose of 2mg·kg<sup>-1</sup>. A goat model of hemorrhagic shock combined with endotoxin challenge was established according to the previous report ( $n=20$ )<sup>[5]</sup>. Animals received *E.coli*O26 B6 endotoxin via portal vein 24h after the recovery from shock, and the dosage was 30 ng·kg<sup>-1</sup>·min<sup>-1</sup>, which was given in a continuous infusion lasting for 5d. Wistar rats were divided randomly into three groups: normal controls, early feeding with standard feed phase Gln 0.5g after scalding, and animals (except control group) sustained a 30% TBSA full-thickness scald covering the back and flanks<sup>[6]</sup>. Determination of plasma diamine oxidase in 21 burned patients (17 male and 4 female) at the age of 33±10 years, with burn area (64±21)%, and (35±20)% III/0. Plasma DAO activity was determined on day 1, 3, 7, 14 and 21 postburn. Blood and intestinal DAO levels were tested according to our previous report<sup>[17]</sup>. Plasma lactate and D-lactate concentrations were determined by biochemical methods as described by Brandt *et al*<sup>[18]</sup>. Microassay for quantitation of endotoxin in blood was made with new PCA treatment using chromogenic limulus amebocyte lysate<sup>[19]</sup>.

**Tumor necrosis factor (TNF $\alpha$ ) assay.** Plasma TNF content was measured by radioimmunoassay. Lactulose/mannitol (L/M) ratio tests in urine were made by SP-3400<sup>[20]</sup>.

**Pathological examination.** Tissue samples were examined under light microscopy.

### Statistical Analyses

Data were expressed as the mean±standard error, and were statistically evaluated by Students *t* test and correlation analysis. Differences were considered to be significant with  $P<0.05$ .

## RESULTS

Plasma DAO levels were elevated in double-peak patterns, one at early stage after trauma and another during invading infection in animal models. Similar results were also obtained in burned patients. Meanwhile, intestinal DAO levels were decreased to certain extent after trauma in animal model. There was a significantly negative correlation between plasma and intestinal DAO activity (Table 1; Figures 1 and 2).

**Table 1** Changes in plasma DAO in trauma animal model ( $\bar{x} \pm s \times 10^3 \text{U} \cdot \text{L}^{-1}$ )

| Animal model | Before injury | T (after injury)/h   |                       |                      |                      |                      |
|--------------|---------------|----------------------|-----------------------|----------------------|----------------------|----------------------|
|              |               | 2                    | 6                     | 24                   | 48                   | 72                   |
| Goat         | 0.9±0.8       | 1.9±1.1 <sup>a</sup> |                       | 1.2±0.2              | 3.0±2.6              | 4.7±1.2 <sup>b</sup> |
| Rats         | 1.3±0.4       | 2.2±0.7 <sup>b</sup> | 2.3±0.87 <sup>b</sup> | 1.2±0.6              | 1.1±0.5              |                      |
| Scalded rats | 0.8±0.9       | 0.8±1.8 <sup>b</sup> |                       | 1.1±0.6              | 2.4±2.1 <sup>a</sup> |                      |
| Burned pigs  | 4.1±1.4       | 4.7±1.5              |                       | 4.7±1.4              | 4.8±1.1              | 5.8±1.4 <sup>a</sup> |
| Gun shooting | 1.5±0.6       | 1.2±0.5              | 2.0±0.6 <sup>b</sup>  | 1.9±0.2 <sup>b</sup> |                      |                      |

Dog in hypothermia

<sup>a</sup> $P < 0.05$ ; <sup>b</sup> $P < 0.01$ , vs before injury.

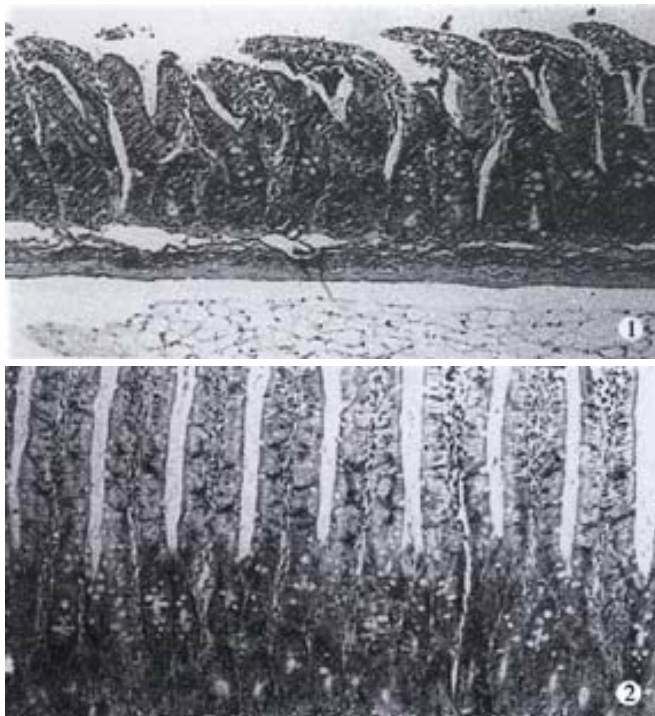


**Figure 1** Pathological changes of intestinal mucosa after 8d in scalded rats. HE×100

**Figure 2** Pathological changes of intestinal mucosa after 8d oral GLN in scalded rats. HE×100

Plasma DAO concentrations and the level of the related index, and plasma  $\text{TNF}\alpha$  significantly increased at various intervals after trauma in goats. Plasma endotoxin levels notably increased at 24h and 72h after injury. Blood lactic acid significantly increased from 2h to 72h after trauma. The plasma DAO activity was obviously correlated with plasma  $\text{TNF}\alpha$ , LPS and lactate ( $P < 0.01$ ; Table 2 and 3). Changes in DAO activity were significantly related with plasma  $\text{TNF}\alpha$  and LPS levels in scalded rats. Plasma DAO activity and plasma D-lactate were significantly correlated in rats secondary to hemorrhage followed by endotoxin challenge ( $r = 0.774$ ;  $P < 0.01$ ).

Glutamine could protect against intestinal barrier function damage. The results indicated that plasma DAO activity was decreased in animals with early glutamine supplementation compared with those without glutamine treatment (10h after trauma  $P < 0.05$ ).

Results of intestinal pathological examination. The pathologic examination of the intestine showed that the damage of epithelial cells of intestinal mucosa, hemorrhage and necrosis, accompanied by the inflammatory cell infiltration in intestinal wall in goats suffering from hemorrhagic shock combined with endotoxin infusion. It was revealed that there was disruption of intestinal mucosa after scald and gut ischemia-reperfusion combined with endotoxin challenge in rats, whereas oral glutamine supplementation could markedly improve intestinal mucosa following acute insults (Figure 2).

**Table 2** Changes in parameters in goats after hemorrhagic shock combined with endotoxin infusion

|                                                        | Before injury | T (after injury)/h      |                        |                        |                          |
|--------------------------------------------------------|---------------|-------------------------|------------------------|------------------------|--------------------------|
|                                                        |               | 2                       | 24                     | 48                     | 72                       |
| $\text{TNF}/\mu\text{g} \cdot \text{L}^{-1}$           | 0.08±0.02     | 0.03±0.25 <sup>a</sup>  | 0.17±0.09 <sup>a</sup> | 0.34±0.15 <sup>a</sup> | 0.33±0.18 <sup>a</sup>   |
| $\text{LPS}/\times 10^3 \text{Eu} \cdot \text{L}^{-1}$ | 0.14±0.03     | 0.16±0.04               | 0.21±0.02 <sup>a</sup> | 0.18±0.16              | 0.37±0.10 <sup>b</sup>   |
| $\text{Lactate}/\text{nmol} \cdot \text{L}^{-1}$       | 9.03±2.19     | 18.30±2.56 <sup>a</sup> | 9.81±2.83              | 12.01±6.84             | 43.61±11.27 <sup>b</sup> |
| L/M rat                                                | 0.03±0.01     | 0.41±0.27               | 0.62±0.20              |                        | 1.70±0.60 <sup>b</sup>   |
| Intestinal pH                                          | 7.03±0.05     | 7.05±0.06 <sup>b</sup>  | 7.14±0.09 <sup>b</sup> | 7.20±0.08 <sup>a</sup> | 7.05±0.07 <sup>b</sup>   |

<sup>a</sup> $P < 0.05$ ; <sup>b</sup> $P < 0.01$ , vs before injury.

**Table 3** Correlation analysis in goats subjected to hemorrhagic shock combined with endotoxin infusion

| X   | Y                  | r      | P     |
|-----|--------------------|--------|-------|
| DAO | $\text{TNF}\alpha$ | 0.817  | <0.01 |
| DAO | LPS                | 0.842  | <0.01 |
| DAO | Lactate            | 0.872  | <0.01 |
| DAO | L/M                | 0.951  | <0.01 |
| DAO | Intestinal pH      | -0.553 | <0.05 |

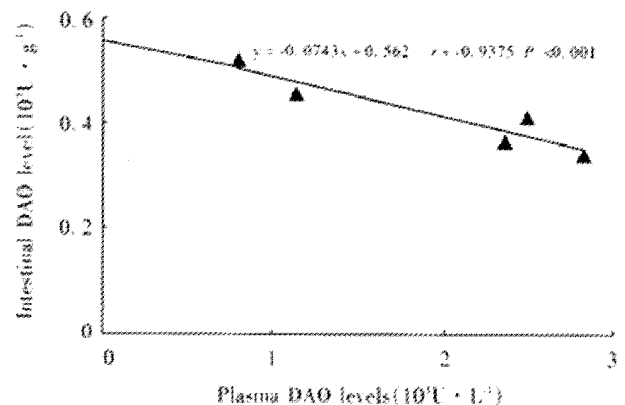


**Figure 3** Relationship between intestinal and plasma DAO level.

## DISCUSSION

DAO is located in the upper part of intestinal mucosa in human as well as in mammals, and is a highly active intracellular enzyme. Under certain circumstances, intestinal mucosa cells became necrosed and dropped into the intestinal cavity, leading to decrease in intestinal mucosal DAO, and increase in DAO activity inside the intestinal cavity. DAO can also enter into the mucosal space between cells, lymphatic vessel<sup>[21-27]</sup> and blood flow, making plasma DAO markedly elevated. Gut as an important organ, may play an important role in the pathogenesis of serious complications. Intestinal mucosal surface layer with tight epithelial cells is an important component for intestinal barrier function, thus it can be seen that intestinal epithelial tissue integrated property is a key part to preserve intestinal barrier function. The changes in DAO activity is an ideal index to investigate intestinal barrier function damage after trauma, specially the changes in plasma DAO activity<sup>[2,6,10,11]</sup>. Therefore, intestinal barrier function injury after severe trauma could result in bacterial/toxin translocation, in turn evoke systemic inflammatory response syndrome



and multiple organ dysfunction syndrome<sup>[3,28-29]</sup>.

The intestinal blood flow might keep relatively low despite of systemic circulation recovery during trauma, which was evident by significant decrease in intestinal mucosal pH<sub>i</sub><sup>[30-33]</sup>. This may be the pathological basis for intestinal origin sepsis and multiple organ dysfunction syndrome. The changes in intestinal permeability were reflected by blood D-lactate and L/M rate in urine. Secretory IgA is an important component part for regulation intestinal immune function, it can prevent the bacteria from adhering to intestinal epithelial cells, and prevent gut-derived bacteria from invading through the intestinal barrier, which might reduce the toxicity of bacterial products to epithelial cells. Therefore, IgA may possess the beneficial effect on the preservation of intestinal mechanical barrier<sup>[34-37]</sup>. From our data that changes in several indexes of intestinal barrier function in various animal models after trauma, it was shown that DAO was released to increase in blood, and decreased in intestinal tissues. Thus, determination of DAO activity might reflect the condition of intestinal injury and repaired process.

The change in plasma D-lactate, lactulose, mannitol and ratio of L/M could reflect the increased intestinal permeability. The intestinal IgA levels appear to be associated with the local immunological dysfunction<sup>[38-41]</sup>. The change in intestinal pH<sub>i</sub> showed that intestinal hemorrhagic injury may result in the release of intestinal mucosal enzyme, subsequently leading to significant elevation of plasma DAO activity. This study showed that there is a close relationship between plasma DAO and TNF $\alpha$ , LPS, D-lactate, lactate, L/M, and the change of intestinal pathology and intestinal barrier function index was similar, indicating that intestinal barrier function was damaged after trauma.

We also observed that the plasma DAO activity was increased 2h and 72h after trauma, especially at 72h, and change of plasma TNF $\alpha$  and LPS was similar to the former. These results suggest that stress injury can cause changes of intestine barrier function index following intestinal ischemia-reperfusion injury, repair or endo/inextra protection, but the trends and degrees of changes were varied. Therefore, it is important to reduce development of SIRS to MODS by protection of intestinal barrier function in early trauma, and prevention of translation of intestinal origin bacteria and toxins<sup>[6,10,14,42-45]</sup>.

Recent studies have shown that GLN may provide protection against intestinal barrier function injury after trauma<sup>[46-52]</sup>. Blood DAO activity was reduced to different extents at 10h, 5d and 8d after early stage of oral GLN in scalded rats. Intestinal pathological examination showed that the damage of epithelial cells of intestinal mucosa could be markedly improved, and the close correlation between plasma DAO and LPS and TNF $\alpha$  could also be changed after scalding<sup>[6]</sup>. The results indicate that GLN can protect against the intestinal barrier function damage after trauma.

## REFERENCES

- Li JY, Hu S, Sun XQ, Yan M, Jin H, Jiang XG, Zhou BT, Sheng ZY. Study on pathophysiological changes during early stage of sepsis after trauma. *Zhong guo wei zhong bing ji jiu yi xue* 2001;13:291-294
- Li JY, Sun SR, Xue LB, Lu Y, Jing H, Gu ZR. Sequential changes in diamine oxidase activity after burns. *Zhong hua zheng xing shao shang za zhi* 1997;13:40-42
- Swank GM, Deitch EA. Role of the gut in multiple organ failure: bacterial translocation and permeability changes. *World J Surg* 1996;20:411-417
- Chen HL, Wu JZ, Pei DK, Guan FL. Damage of gut barrier in the pathogenesis of multiple organ dysfunction syndrome. *Zhong hua pu tong wai ke za zhi* 1998;13:50-53
- Hu S, Sheng ZY, Xue XB, Zhou BT, Lu JY, Jin H, Yu Y, Sun XQ, Li JY, Zheng YQ, Xiong DX. A serilized studies of animal models of posttraumatic multiple organ dysfunction syndrome. *Jie fang jun yi xue za zhi* 1996;21:5-9
- Li JY, Lu Y, Xue LB, Wan SY, Sun SR, Yu Y, Xu HJ, Sheng ZY. The effect of oral glutamine gut mucosa Function and structure in scalded rat. *Jie fang jun yi xue za zhi* 1996;21:91-93
- Yao YM, Sheng ZY, Wu Y, Yu Y, Lu LR. Relationship between plasma D-lactate levels and acute intestinal injury in rats following ischemia-reperfusion. *Zhong hua zheng xing shao shang za zhi* 1998;14:266-269
- Lu Y, Sheng ZY, Li JY, Sun XQ, Jin H, Jiang XG. The relationship between the ICAM-1 expression of hemangioendothelial cell and the dysfunction of murine small bowel in an intestinal ischemia-reperfusion model. *Zhong guo pu tong wai ke za zhi* 2000;15:145-147
- Cui XL, Sheng ZY, Guo ZR, He LX, Zao J, Ren XW, Sun SR, Jiang LX. Mechanisms of early gastro-intestinal ischemia after burn: hemodynamic and hemorrhologic features. *Zhong hua zheng xing shao shang za zhi* 1998;14:262-265
- Li JY, Lu Y, Fu XB, Jin H, Hu S, Sun XQ, Sheng ZY. The significance of changes in diamine oxidase activity in intestinal injury after trauma. *Zhong guo wei zhong bing ji jiu yi xue* 2000;12:482-484
- Li JY, Lu Y, Hu S, Jin H. An experimental study on monitoring of barrier function of small intestine. *Chuang shang wai ke za zhi* 2001;3:109-112
- Li JY, Lu Y, Jin H, Hu S, Sun XQ, Jiang XG, Sheng ZY. Sequential changes of diamine oxidase activity after trauma. *An ji suan he sheng wu zi yuan* 1999;21:17-19
- Fang WH, Yao YM, Shu HG, Yu Y, Wu Y, Zheng YQ. The time course and tissue distribution of endotoxin in rats after thermal injury. *Zhong hua zheng xing shao shang za zhi* 1999;15:298-300
- Fu XB, Yang YH, Sun XQ, Gu XM, Sheng ZY. Protective effects of endogenous basic fibroblast growth factor activated by 2.3 butanedion monoxide on functional changes of ischemic intestine, liver and kidney in rats. *Zhong guo wei zhong bing ji jiu yi xue* 2000;12:69-72
- Fu XB, Sheng ZY, Wang YP, Ye YX, Xu MH, Sun TZ, Zhou BT. Basic fibroblast growth factor reduces the gut and liver morphologic and functional injuries after ischemia and reperfusion. *J Trauma* 1997;42:1080-1087
- Wu CT, Li ZL. Effect of DAO on intestinal damage in acute necrotizing pancreatitis in dogs. *Shi jie hua ren xiao hua za zhi* 1999;7:64-65
- Li JY, Yu Y, Hao J, Jin H, Xu HJ. Determination of diamine oxidase activity in intestinal tissue and blood using spectrophotometry. *An ji suan he sheng wu zi yuan* 1996;18:28-30
- Sun XQ, Fu XB, Zhang R, Lu Y, Deng Q, Zhang C, Jiang XG, Sheng ZY. Plasma D-lactate levels as a useful marker of increased intestinal permeability after severe injuries. *Zhong guo wei zhong bing ji jiu yi xue* 2000;12:476-478
- Yao YM, Tian HM, Wang YP, Yu Y, Shi ZG, Sheng ZY. Microassay for quantitation of endotoxin in blood with new PCA treatment using chromogenic limulus amoebocyte lysate. *Shang hai yi xue jian yan za zhi* 1993;8:31-33
- Zhu XF, Xiong DX, Sheng ZY. Establish measuring Method of alterations in intestinal permeability. *Zhong guo wei sheng tai za zhi* 1994;6:36-38
- Hosoda N, Nishi M, Nakagawa M, Hiramatsu Y, Hioki K, Yamamoto D M. Structural and functional alterations in the gut of parenterally or enterally fed rats. *J Surg Res* 1989;47:129-133
- Yan BG, Yang ZC, Huang YS, Liu ZY, Li A. Effect of delayed rapid fluid resuscitation on plasma diamine oxidase in early postburn dogs. *Shi jie hua ren xiao hua za zhi* 2000;8:178-180
- Lu Y, Li JY, Sun SR, Jin H, Jiang XG, Sun XQ, Sheng ZY. Relationship between change of plasma diamine oxidase activity and gut injury in rats during gut ischemia-reperfusion. *An ji suan he sheng wu zi yuan* 2000;22:50-53
- Liu MH, Gao LX. The effect of oral glutamine supplementation on small intestinal function in burned rats. *Ying yang xue bao* 1995;17:17-21
- Dong HL, Cai JW, Si ZX. Effects of radiation on intestinal and plasma DAO activity in rats. *Shi jie xiao hua za zhi* 1998;6:698
- Bragg LE, Thompson JS, West WW. Intestinal diamine oxidase levels reflect ischemic injury. *J Surg Res* 1991;50:228-233
- Ci XL, Wang BS, Zhang SW, Zhang NN. Experimental treatment with herbal medicines for impaired intestinal mucosal barrier induced by endotoxin plus tumor necrosis factor- $\alpha$ . *Zhong guo wei zhong bing ji jiu yi xue* 1999;11:262-265
- Rush BF, Sori AJ, Murphy TF, Smith S, Flanagan JJ, Machiedo GW. Endotoxemia and bacteremia during hemorrhagic shock: The link between and sepsis? *Ann Surg* 1988;207:549-552
- Yao YM, Sheng ZY, Tian HM, Wang YP, Yu Y, Fu XB, Lu LY, Wang DW, Ma YY. Gut-derived endotoxemia and multiple system organ failure following gunshot wounds combined with hemorrhagic shock an experimental study in the dog. *J Trauma* 1995;38:742-746
- Hu S, Jin H, Lu Y, Li JY, Zhou BT. The changes of PH on gastroduodenal mucosa after hemorrhage shock and resuscitation in goats. *Zhong guo wei zhong bing ji jiu yi xue* 1997;9:708-710
- Murray MJ, Gonze MD, Nowak LR, Cobb CF. Serum D(-)-Lactate levels as an aid to diagnosing acute intestinal ischemia. *The American Journal of Surgery* 1994;167:575-578
- Sun XQ, Lu Y, Jin H, Li JY, Jiang XG, Hu S, Fu XB. Change of intestine mucosal barrier induced by intestine ischemia-reperfusion injury.

- Chuang shang wai ke za zhi* 1999;1:208-210
- 33 Murray MJ, Barbose JJ, Cobb CF. Serum D-lactate levels, as a predictor of acute intestinal ischemia in a rat model. *J Surg Res* 1993;54:507-509
  - 34 Doe WF. The intestinal immune system. *Gut* 1989;30:1679-1685
  - 35 Yu Y, Shi ZG, Chai JK, Guo ZY, Yao YM, Li G, Ho XX, Jiang W, Wang HB, Sheng ZY. The clinical significance of changes in IgA levels in intestinal tract after major burns. *Zhong guo wei zhong bing ji jiu yi xue* 1998;10:725-727
  - 36 Yu Y, Sheng ZY, Tian HM, Wang YP, Yu Y, Lu LR, Chang GY, Ma RS. An experimental study on injury of intestinal immuno-barrier in rat after scald. *Zhong hua zheng xing shao shang wai ke za zhi* 1996;12:86-89
  - 37 Biesbrock AR, Reddy MS, Levine MJ. Interaction of a salivary mucin-secretory immunoglobulin a complex with mucosal pathogens. *Infection and Immunity* 1991;59:3492-3497
  - 38 Harmatz PR, Cater EA, Sullivan D, Hatz RA, Baker R, Breazlale E, Grant K, Bloch KJ. Effect of thermal injury in the rat on transfer of IgA protein into bile. *Ann Surg* 1989;210:203-207
  - 39 Cappeler WA, Bloch KJ, Hatz RA, Carter EA, Fagundes J, Sullivan DA, Harmatz PR. Reduction in biliary IgA after burn injury. *Ann Surg* 1992;215:338-341
  - 40 Alverdy JC, Aoys E. The Effect of dexamethasone and endotoxin administration on biliary IgA and bacterial adherence. *J Surg Res* 1992;53:450-454
  - 41 Yu Y, Chai JK, Li JY, Jin H, Dong N. A preliminary study on the relationship between level of IgA in intestinal content and urine after burns. *An ji suan he sheng wu zi yuan* 2001;23:49-51
  - 42 Diebel LN, Liberati DM, Brown WJ, Dulchavsky SA, painter TM, Diglio CA, Montgomery PC. Secretory immunoglobulin A blocks hypoxia-augmented bacterial passage across madin-darby canine kidney cell monolayers. *J Trauma* 1997;43:759-763
  - 43 Noguchi Y, James JH, Fischer JE, Hasselgren PO. Increased glutamine consumption in small intestine epithelial cell during sepsis in rats. *Am J Surg* 1997;173:199-205
  - 44 Yu B, Wang SL, You ZY, Li A, Zhao Y. Effects of L-Glutamine on ghe tut nutrient metabolism in severe burnedminiswines. *Chang nei yu chang wai ying yang* 1995;2:7-10
  - 45 Li N, Liu FN, Li YS, Kang J, Li FJ, Li JS. The Changes of plasma glutamine and its influence on intestinal permeability after abdominal Surgery. *Chang nei chang wai ying yang* 1998;5:3-6
  - 46 Rhoads JM, Keku EO, Quinn J, Woosely J, Lecce JG. L-Glutamine stimulates jejunal sodium and chloride absorption in pig rotavirus enteritis. *Gastroenterology* 1991;100:683-691
  - 47 Yu B, Wang SL, You ZY, Zhao Y, Li A. Enhancement of gut absorptive function by early enteral feeding enriched with L-Glutamine in severe burned miniswines. *Zhong hua wai ke za zhi* 1995;33:742-744
  - 48 Wu F, Jin XQ, Wu SX, Li J, Xu JL. The experimental study of cholestasis due to parenteral nutrition. *Chang nei chang wai ying yang* 1998;5:96-98
  - 49 Yang JT, Wang ZG, Zhu PF. The Effects of glutamine supplementation on the cellular immunity in traumatized rats. *Ying yang xue bao* 1999;21:8-12
  - 50 Dai DW, Wu SM, Li M, Chen HJ, Cai W. Protective effect of Glutamine in the anoxia/reoxygenation induced injury of human intestinal epithelial cells *in vitro*. *An ji suan he sheng wu zi yuan* 1997;19:1-3
  - 51 Tu WF, Li JS, Zhu WM, Li ZD, Liu FN, Chen YM, XU JG, Shao HF, Xiao GX, LI A. Infiluence of glutamine on gut bacteria/endotoxin translocation in acute severe pancreatites. *Chang wai yu chang nei ying yang* 1999;6:29-32
  - 52 Yu B, Wang SL, You ZY, Zhao Y, Li A. Protection against intestinal injury with oral feeding L-glutamine in severe burned mini-swines. *Zhong hua wai ke za zhi* 1998;14:19-21

Edited by Ma JY

• BASIC RESEARCH •

# Localization of neurokinin B receptor in mouse gastrointestinal tract

Hong Wang, Yuan-Qiang Zhang, Yu-Qiang Ding, Jin-Shan Zhang

Hong Wang, Yuan-Qiang Zhang, Jin-Shan Zhang, Department of Histology and Embryology, Yu-Qiang Ding, Institute of Neurosciences, the Fourth Military Medical University, Xi'an, 710032, China

Supported by the Grants of the National Natural Science Foundation of China, No.39600045, No.39870109

Correspondence to: Professor Yuan Qiang Zhang, Changle Road 17, Xi'an 710032, China. Zhangyuanqiang@fmmu.edu.cn

Telephone: +86-29-3374508 Fax: +86-29-3374508

Received 2001-07-19 Accepted 2001-10-20

## Abstract

**AIM:** To observe the location of neurokinin receptor (NK3r) in the mouse gastrointestinal tract.

**METHODS:** The abdomens of 8 male Kunming mice were opened under anaesthesia with sodium pentobarbital. The exposed gut organs were kept moisture and temperature at the same time. Then the esophagus, jejunum, ileum, colon, etc were respectively cut and the segments from the stomach to the distal colon were opened along the mesenteric border. A circular 4mm~6mm enteric part(pieces of 1 cm<sup>2</sup> were to be prepared) and mucosa and submucosa were removed, then the longitudinal muscle layer was pulled off from the circular muscle layer under microphotograph. They were rinsed in 50n mol·L<sup>-1</sup> potassium phosphate-buffered saline(PBS). Immunohistochemistry and immunoreactive fluorescence were used in the staining procedures.

**RESULTS:** There was not NK3r-Like(-Li) positive material on the smooth muscle cells of the esophagus, stomach, and intestines and other regions. The nerve cell bodies with immunoreactivity for NK3r were mainly distributed in the submucosal nerve plexus or myenteric nerve plexus of the gastrointestinal tract except for the esophagus, stomach and rectum. The reaction product was located on the surface of the nerve cell plasma. It was occasionally observed in the cell plasma endosomes, but was very weakly stained. Among the NK3-like positive neurons in the plexus, the morphological type in many neurons appeared like Dogiel II type cells. Some neuron cell bodies were big, having many profiles, some were long ones or having grading structure. Cell body diameter was about 10μm-46μm and 8μm-42μm in myenteric plexus and submucous plexus.

**CONCLUSION:** This study not only described the distribution of neurokinin B receptor in the mouse gut in detail, but also provided a morphological basis for deducing the functional identity of the NK3r-LI immunoreactivity neurons, suggesting the possibility that these neurons were closely related to gastrointestinal tract contraction and relaxing activity.

Wang H, Zhang YQ, Ding YQ, Zhang JS. Localization of neurokinin B receptor in mouse gastrointestinal tract. *World J Gastroenterol* 2002;8(1):172-175

## INTRODUCTION

The tachykinin family of neuropeptides mainly includes neurokinin A(NKA) neurokinin B(NKB), and the neurotransmitters in the peripheral and central nerve systems<sup>[1]</sup>. Tachykinin and their receptors (NK1/NK2/NK3) play an important role in the nerve system. Various studies have been undertaken in NK3 receptor's distribution in rat CNS<sup>[2,3]</sup>. Our previous experiments suggest that NK3 receptor in the paraventricular and supraoptic nuclei of the rat hypothalamus may be involved in the modulation of the release of vasopressin from the hypothalamus when the internal environment was disturbed<sup>[3]</sup>. Some research results<sup>[4]</sup> implicated that tachykinin located in the intestine intrawall neurons is attributable to the activation of gut and its modification. Pharmacological research work has proved that NK3r was located in neurons rather than in muscle cells<sup>[5,6]</sup>. Having characterized the antisera, researchers localized the neurokinin receptor in the rat/guinea gut<sup>[6,7]</sup>. NK2r was also detected in the muscularis mucosa of the small intestine and the colon. NK2r was localized in the plasma membrane of smooth muscle cells and was present on numerous nerve terminals in both the submucosal and the myenteric plexus of the small intestine<sup>[4,7,8]</sup>, but NK1r-Li reactive product existed only in the neurons that resemble the interstitial cells of Cajal<sup>[9-11]</sup>. Mann *et al*<sup>[12]</sup> and Grady *et al*<sup>[7]</sup> reported that in rat myenteric plexus there were neurons that could express NK1r. These neurons had colocalization with NK3r-Li positive neurons. Although all these results implicated that tachykinin receptors existed in the mouse gastrointestinal tract, and that they might be related to intestinal muscle contractile activity<sup>[13]</sup> in addition to its influence in blood pressure and increase of vascular penetration. Up to now, we have not seen reports about this receptor's distribution in mouse gastrointestinal tract. Our aim was to further investigate this receptor distribution in mouse gut.

## MATERIALS AND METHODS

### *Animals and material preparation*

Ten male Kunming mice weighing 20g-30g were chosen and the abdomens of 8 mice were opened under anaesthesia with sodium pentobarbital. To keep moisture and temperature we cleaned the exposed gut organs with 0.01 mol·L<sup>-1</sup> PBS (phosphate-buffered saline, pH 7.0) continuously. Then the esophagus, jejunum, ileum, colon, etc were respectively cut and the segments from the stomach to the distal colon were opened and cleaned by 0.01 mol·L<sup>-1</sup> PBS containing smooth muscle relaxing medicine. And they were filled with 40g·L<sup>-1</sup> polyformaldehyde and the two ends were closed tightly and fixed for 6-8 h. The stomachs were fixed for 8 h following Peng Xi's suggestion(1999)<sup>[14]</sup> and incubated in 300g·L<sup>-1</sup> sucrose for 24 h (overnight) together with other organs after cut and cleaned with 0.01 mol·L<sup>-1</sup> PBS. Gastrointestinal tract was processed from stomach to the distal colon and was opened along the mesenteric border. A circular 4-6mm enteric part(pieces of 1 cm<sup>2</sup> were to be prepared)

was obtained, the longitudinal muscle layer was pulled off from the circular muscle layer with fine forceps and processed for immunohistochemical examination along the mesenteric border rinsed in phosphate-buffered saline and prepared for layer separation. Gastrointestinal tracts were cut into small pieces of 1 cm<sup>2</sup> and mucosa and submucosa were removed with forceps. Then they were rinsed in 50 nmol·L<sup>-1</sup> potassium phosphate-buffered saline(PBS) and prepared for layer separation. These procedures can be done under anatomy microphotography.

### Staining procedures

Staining procedures: whole-mount free-floating tissues and slide-mounted sections were washed in 50 mmol·L<sup>-1</sup> KPBS, incubated with 0.3% H<sub>2</sub>O<sub>2</sub> (30min), rinsed again in 50 mmol·L<sup>-1</sup> KPBS, and incubated in diluent containing of 50mm KPBS, 4g·L<sup>-1</sup> Triton X-100, 10 g·L<sup>-1</sup> bovine serum albumin, and 10 ml·L<sup>-1</sup> normal goat serum for 30min at 22°C, then transferred to NK3r affinity-purified antibodies diluted to 1:50 in the same diluent for 48-96 h at 4°C. Tissues were washed in 50 mmol·L<sup>-1</sup> KPBS with 0.2g·L<sup>-1</sup> TritonX-100 and incubated with biotinylated goat anti-rabbit IgG(Vector) diluted to 1:200 for 3 h at 22°C(Vector), followed by avidin-biotin complex coupled with horseradish peroxidase 1:200 for 2 h at 22°C(Vector). The horseradish peroxidase reaction product was visualized with 0.4 g·L<sup>-1</sup> diaminobenzidine tetrahydrochloride and 0.1 mL·L<sup>-1</sup> H<sub>2</sub>O<sub>2</sub> dissolved in 0.1 mol·L<sup>-1</sup> sodium acetate. The reaction was terminated by two consecutive 9 g·L<sup>-1</sup> NaCl washes.

The gastrointestinal tracts of the remaining mice were pulled off and cut on a cryostat at -20°C, rinsed by 0.01 mol·L<sup>-1</sup> PBS and incubated in 40 g·L<sup>-1</sup> formaldehyde fixative overnight at 4°C. They were incubated again in 300 g·L<sup>-1</sup> sucrose and embedded by OCT on the next day. Their cryostat sections were 10µm in thickness, and immunohistochemically stained after the slides were cooled according to the earlier procedure.

## RESULTS

Immunohistochemical results showed that NK3-Li neurons and fibers existed in enteric plexus(submucous plexus and myenteric plexus) in the duodenum, jejunum, ileum and colon (Figures 1-8). Staining intensity in myenteric plexus was a little stronger. And the esophagus and the stomach were immunoreactively negative. No positive immunoreactive product was found in esophagus smooth muscle cells.

NK3-Li positive substance existed mostly in the membrane, some or a little in the plasma, but none in the nuclei. The surface of the positive neurons was well stained and was more apparent than those in the cell body(Figures 1,2,4,8). The neurons stained in

myenteric plexus had high intensity, the NK3-Li neurons and fibers were web-like(Figure 3). And the fibers between the positive neurons were often of a beaded or granular appearance(Figure 7). Between fibers just like necklace among longitudinal muscle-myenteric plexus neuronal fibers there were striated fibers, that connect with them. From the cryostat sections, NK3r-Li immunoreactive product was found in intestinal myenteric plexus.

Among the NK3-like positive neurons in the plexus, the morphological type of many neurons were like Dogiel II type cells: round or ellipse shape or presenting several dividing beaded profiles. Some neuron cell bodies were bigger, having many profiles, some of which were long or having grading structures. Results by microscopic counting are shown in Figures 1 and 2.

**Table 1** The number of NK3r immunoreactivity neuron cell bodies in mouse gastrointestinal Tract\*

| Region    | Neuronal density / (cells·cm <sup>-2</sup> ) ( $\bar{x} \pm s$ ) |                  |
|-----------|------------------------------------------------------------------|------------------|
|           | Myenteric plexus                                                 | Submucous plexus |
| Esophagus | Almost no                                                        | Almost no.       |
| Stomach   | Almost no.                                                       | Almost no.       |
| Duodenum  | 82±14                                                            | 95±12            |
| Jejunum   | 249±37                                                           | 237±31           |
| Ileum     | 143±24                                                           | 140±19           |
| Colon     | 118±17                                                           | 107±15           |

\*neurons in areas of 0.05 cm<sup>2</sup> were counted.

**Table 2** Morphological characteristics of NK3r stained neurons in the mouse gastrointestinal tract

| plexus    | Region     | Shape               |            | d (cell soma)/µm |       |
|-----------|------------|---------------------|------------|------------------|-------|
|           |            | Unipolar or bipolar | Multipolar | Major            | Minor |
| Myenteric | Oesophagus | (+/-)               | (+)        |                  |       |
|           | Stomach    | (+/-)               | (+)        |                  |       |
|           | Duodenum   | ++                  | +++        | 17-38            | 10-26 |
|           | Jejunum    | ++                  | +++        | 25-46            | 13-20 |
|           | Ileum      | ++                  | +++        | 21-37            | 12-18 |
|           | Colon      | +                   | ++         | 15-36            | 14-16 |
| Submucous | Rectum     | +/-                 | +          | 13-34            | 8-19  |
|           | Stomach    | (+/-)               | (+)        |                  |       |
|           | Duodenum   | ++                  | +++        | 16-35            | 8-11  |
|           | Jejunum    | ++                  | +++        | 19-42            | 10-13 |
|           | Ileum      | ++                  | +++        | 14-35            | 9-17  |
|           | Colon      | +                   | ++         | 13-27            | 8-15  |

(+/-) almost no; (+) very rare; + infrequent; ++ common; +++ abundant



**Figure 1** NK3r-like(Li) neurons in myenteric nerve plexus of duodenum, mainly located on cell membrane. Arrow: positive neuron; Duo: duodenum, mp: myenteric plexus.

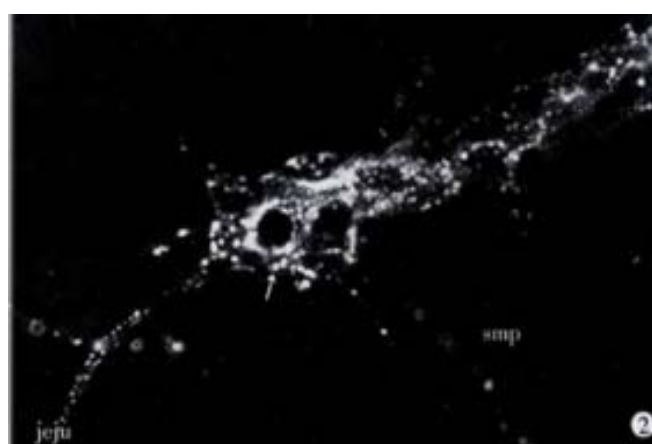


**Figure 2** NK3r-Li neurons in submucosa neural plexus of jejunum. Arrow: positive neuron cell bodies; Smp: submucosa nerve plexus; Jeju: jejunum.

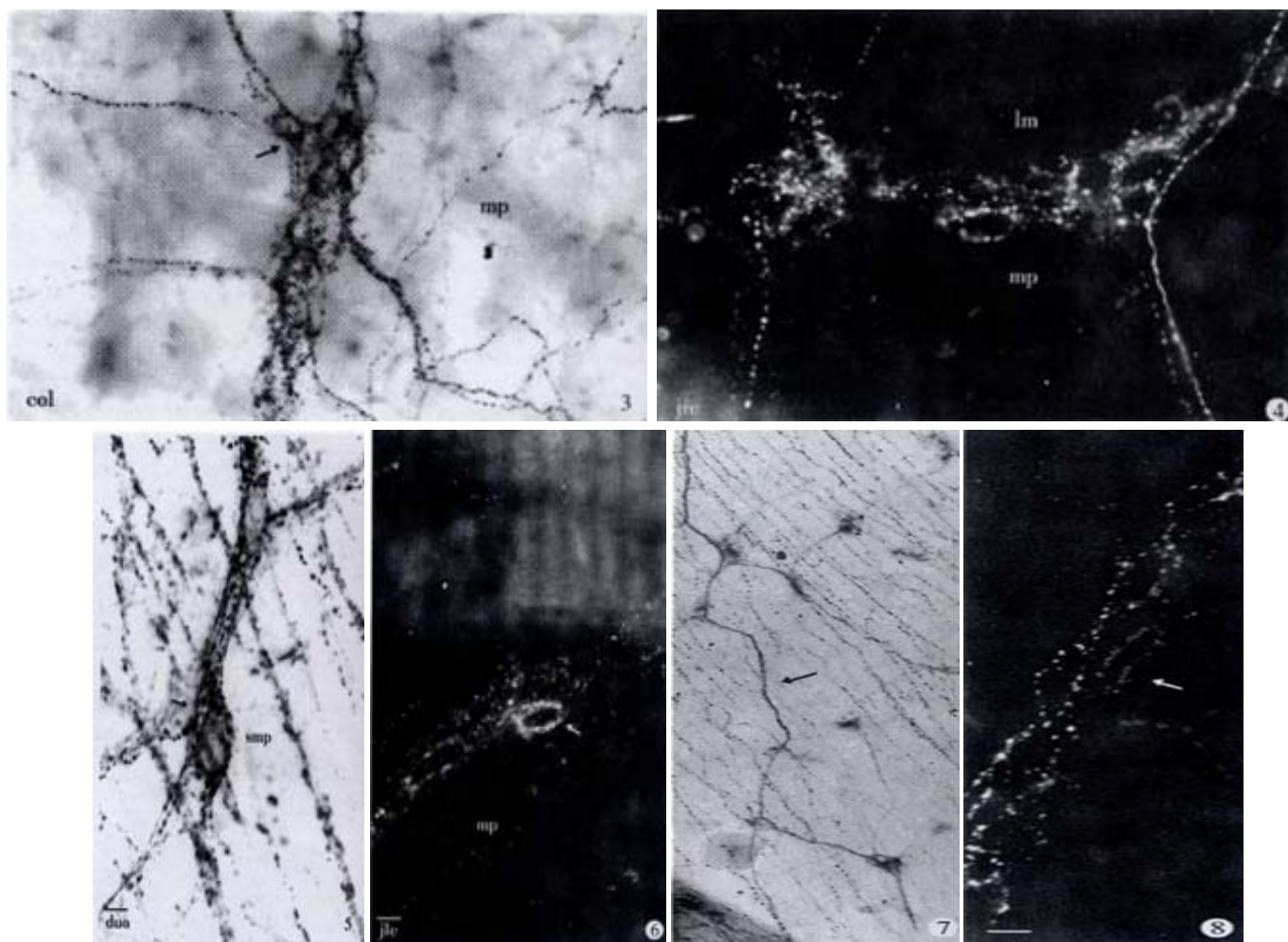


**Figure 3** NK3r-Li product mainly found on the cell membrane in the colon's myenteric plexus. Dark arrow: positive neuron; Col: colon; mp: myenteric plexus.

**Figure 4** The NK3r-Li neurons in the myenteric nerve plexus of the ileum. Mp: myenteric plexus; Ile: ileum; Lm: longitudinal muscles; Cm: circular muscles.

**Figure 5** The NK3r-Li neurons in the submucosa nerve plexus of the duodenum. Dark arrow: positive neuron; Smp: submucosa nerve plexus. Bar=20µm in Figures 1-5

**Figure 6** NK3r-Li neurons in the neuron ganglion of the ileum myenteric nerve plexus; mp: myenteric plexus. Bar=40µm

**Figure 7** The NK3r-Li nerve fibers like a necklace.

**Figure 8** The higher magnification of Dogiel II type NK3r-Li neurons. Arrow: positive products on the cell membrane. Bar=6µm in Figures 7,8

## DISCUSSION

There were some reports about tachykinin B receptor(NK3r) distribution in mammal gastrointestinal tract<sup>[7,12]</sup>. It was proved that NK3r-Li neurons were localized in enteric nervous system of rats and guinea pig<sup>[15]</sup>. We observed the NK3r distribution in mouse gastrointestinal tract. Our results were consistent with the previous results, and support the research work of Mann *et al*<sup>[12]</sup>, and Grady *et al*<sup>[7]</sup>, but we must claim several valuable differences: ① In our experiments we found that immunoreactivity was mainly located in the enteric nervous system neurons, rather than in mouse esophagus or other parts of the gut smooth muscles, which was different from the results of Maggi *et al*<sup>[5]</sup> and Guard *et al*<sup>[16]</sup>. ② We also found that there were different morphological type of NK3r-Li neurons in mouse jejunum and ileum nervous plexus: the first part gut plexus had more neurons than the second part gut plexus. In ileum plexus NK3r-Li neurons were mostly of Dogiel II type neurons<sup>[17]</sup>, which was different from the results by other authors that NK3r-Li neurons were only located in the ileum. ③ Although the immunoreactive products existed mainly in the enteric system neurons membrane, they were also detected in some positive neurons plasma. On the whole, cell

morphology(size and shape) was similar to the cells that were observed and described by Mann *et al.* and Furness<sup>[18]</sup>. We also found that there were some small cell body neurons, which did not have clear characteristic positive shapes, so we might deduce that they had possibly different functions or belonged to dividing disparity. The location of the NK3r-Li immunoreactivity observed through the subnuclei of the NTS (solitary tract nucleus) suggested that NK3r-Li immunoreactive neurons might be involved in the medullar integration of the information conveyed by the afferent vagus nerve from the lower digestive tract<sup>[19]</sup>. The distribution of the NK3r-containing neurons coincided with the afferent fibers arising from the lower digestive tract. Vagal afferent fibers from the stomach and intestine terminated preferentially in the subnuclei medialis and commissuralis and in the substantia gelatinosa of the NTS (solitary tract nucleus)<sup>[20]</sup> as well. In the NTS, the subnucleus centralis represented the preferential termination sites for afferent fibers arising from the esophagus(vagus nerve). No or very few NK3r-Li neurons have been found in this subnucleus. We also found the supporting example for these references of NK3 receptor in the central nervous system and added proof to NK3 receptor in the peripheral nervous system. In the rat



brain, by situ hybridization method for NK3r mRNA, the results agreed well with the immunohistochemical results, however low levels of NK3r mRNA were found in rat stomach and intestines<sup>[21]</sup> which suggests that our detection of a large population of enteric neurons with NK3r immunoreactivity contradicts with Tsuchida *et al.*'s results<sup>[22]</sup>. Binding studies also failed to detect NK3r in the gastrointestinal tract<sup>[22]</sup>. Our experiments showed that morphology of NK3r-Like neurons was in agreement with Dogiel II type neurons in size, shape and localization. The number of neurons was not very large and was less than the proportion of NK1r-Li neurons in the enteric nervous system. Considering NK3r-Li neurons' size in diameter, and the morphologic and pharmacological results, we speculate that NK3r-Li neurons are possibly a part of afferent internal neurons related to the enteric construction, relaxing the activity of mouse enteric nervous system, which was closely related to with some vice sympathetic nerve fiber functions. This is determined according to Furness *et al.*'s<sup>[23]</sup> dividing method in guinea enteric nervous system neurons that is regarded as right, but at the same time it needs further verifications by functional test. Functional experiments supported the neuronal localization of the NK3r: the NK3 agonists NKB senktide stimulated contraction of rat duodenum and guinea pig ileum<sup>[24,25]</sup>. The response of the guinea pig ileum were abolished by tetrodotoxin and reduced by atropine which indicated the presence of NK3r in the cholinergic neurons of the myenteric plexus<sup>[26]</sup>. Indeed, senktide stimulated acetyl choline to release from the myenteric neurons<sup>[16]</sup>. Barthó *et al.* (1999)<sup>[24,25]</sup> proved that NK3r existed in rodent gastrointestinal (interwall) neurons and regulated tachykinin inducing the excitement of the enteric nervous system thus influencing construction<sup>[27]</sup>. Our findings that neurons in the myenteric plexus could express NK3r is of particular interest and NK3r reacting production existed mainly on the plasma membrane of gastrointestinal tract intrawall neurons, implicating that tachykinin B transmitter possibly influence membrane receptor thus influencing the contraction and relaxing smooth muscle and even regulating the exocrine of gastrointestinal tract as well as the contents that some articles have described<sup>[28-33]</sup>.

In summary, our research not only observed the distribution of NK3r-like neurons and fibers in mouse gastrointestinal tract, but also provided new insight into the cellular colocalization of receptor proteins in the mouse gut tract and a base for investigating NK3r-like neuron functions in the gut tract. These results might also give implications about muscle activity of contracting or relaxing action related to the neurokinin receptor.

## REFERENCES

- Blanchet F, Gauchy C, Perez S, Soubrie P, Glowinski J, Kemel ML. Distinct modifications by neurokinin1 (SR140333) and neurokinin2 (SR48968) tachykinin receptor antagonists of the N-methyl-D-aspartate-evoked release of acetylcholine in striosomes and matrix of the rat striatum. *Neuroscience* 1998; 85:1025-1036
- Chen LW, Guan ZL, Ding YQ. Mesencephalic dopaminergic neurons expressing neuromedin K receptor (NK3): a double immunocytochemical study in the rat. *Brain Res* 1998; 780:148-152
- Ding YQ, Shigemoto R, Takada M, Ohishi H, Nakanishi S, Mizuno N. Localization of the neuromedin K receptor (NK3) in the central nervous system of the rat. *J Comp Neurol* 1996; 364:290-310
- Portbury AL, Furness JB, Southwell BR, Wong H, Walsh JH, Bunnett NW. Distribution of neurokinin-2 receptors in the guinea-pig gastrointestinal tract. *Cell Tissue Res* 1996; 286:281-292
- Maggi CA, Patacchini R, Rovero P, Giachetti A. Tachykinin receptors and tachykinin receptor antagonists. *J Auton Pharmacol* 1993; 13:23-93
- Bertrand PP, Galligan JJ. Tachykinin- and synaptically-activated chloride current in myenteric neurons of guinea-pig ileum. *J Physiol (Lond)* 1994; 481:47-60
- Grady EF, Baluk P, Böhm S, Gamp PD, Wong H, Payan DG, Ansel J, Portbury AL, Furness JB, McDonald DM, Bunnett NW. Characterisation of antisera specific to NK1, NK2, NK3 neurokinin receptors and their utilization to localize receptors in the rat gastrointestinal tract. *J Neurosci* 1996; 16:6975-6986
- Alex G, Kunze WA, Furness JB, Clerc N. Comparison of the effects of neurokinin 3 receptor blockade on two forms of slow synaptic events in myenteric AH neurons. *Neuroscience* 2001; 104:263-269
- Portbury AL, Furness JB, Young HM, Southwell BR, Vigna SR. Localization of NK1 receptor immunoreactivity to neurons and interstitial cells of the guinea-pig gastrointestinal tract. *J Comp Neurol* 1996; 367:342-351
- Vigna SR, Bowden JJ, McDonald DM, Fisher J, Okamoto A, McVey DC, Payan DG, Bunnett NW. Characterisation of antibodies to the rat substance P(NK1) receptor and to a chimeric substance P receptor expressed in mammalian cells. *J Neurosci* 1994; 14:834-845
- Sternini C, Su D, Gamp PD, Bunnett NW. Cellular sites of expression of the neurokinin-1 receptor in the rat gastrointestinal tract. *J Comp Neurol* 1995; 358:531-540
- Mann PT, Southwell BR, Ding YQ, Shigemoto R, Mizuno N, Furness JB. Localisation of neurokinin 3(NK3) receptor immunoreactivity in the rat gastrointestinal tract. *Cell Tissue Res* 1997; 289:1-9
- Furness JB, Clerc N. Responses of afferent neurons to the contents of the digestive tract, and their relation to endocrine and immune responses. *Progr. Brain Res* 2000; 122:157-170
- Peng X, Feng JB, Wang SHL. Methods of showing rats stomach myenteric neural plexus. *Jiepouxue Zazhi* 1999; 22:368-369
- Li JC, Busch LC, Kuhnelt W. Immunohistochemical study on the gastroenteric nervous system in trisomy 16 mice-an animal model of Down syndrome. *World J Gastroenterol* 2000;6:793-799
- Guard S, Watson SP. Tachykinin receptor types: classification and membrane signaling mechanisms. *Neurochem Int* 1991; 18:149-165
- Furness JB, Clerc N, Gola M, Kunze WA, Fletcher EL. Identification of component neurons and organisation of enteric nerve circuits. In : *Neurogastroenterology - From the Basics to the Clinics. Kluwer Academic Publishers, Dordrecht, The Netherlands* 2000:134-147
- Furness JB, Clerc N, Lomax AEG, Bornstein JC, Kunze WA. Shapes and projections of tertiary plexus neurons of the guinea-pig small intestine. *Cell and Tissue Res* 2000;300:383-387
- Carpentier C, Baude A. Immunocytochemical localization of NK3 receptors in the dorsal vagal complex of rat. *Brain Research* 1996; 734:327-331
- Furness JB, Clerc N, Kunze WA. Memory in the enteric nervous system. *Gut* 2000; 47:60-62
- Tsuchida K, Shigemoto R, Yokota Y, Nakanishi S. Tissue distribution and quantitation of the mRNAs for three rat tachykinin receptors. *Eur J Biochem* 1990; 193:751-757
- Mantyh PW, Gates T, Mantyh CR, Maggio JE. Autoradiographic localization and characterization of tachykinin receptor binding sites in the rat brain and peripheral tissues. *J Neurosci* 1989; 9:258-279
- Furness JB, Bornstein JC, Pompolo S, Young HM, Kunze WA, Yuan SY, Kelly H. The nerve circuits for motility control in the gastrointestinal tract. *J Smooth Muscle Res* 1993; 29:143-144
- Bartho L, Lenard JRL, Patacchini R, Halmi V, Wilhelm M, Holzer P, Maggi CA. Tachykinin receptors are involved in the "local efferent" motor response to capsaicin in the guinea-pig small intestine and esophagus. *Neuroscience* 1999; 90:221-228
- Kunze WA, Clerc N, Furness JB, Gola M. The soma and neurites of primary afferent neurons in the guinea-pig intestine respond differentially to deformation. *J Physiol* 2000;526:375-385
- Guard S, Watson SP. Evidence for NK3 receptor-mediated tachykinin release in the guinea-pig ileum. *Eur J Pharmacol* 1987; 144:409-412
- Clerc N, Furness JB, Kunze WA, Thomas EA, Bertrand PP. Long term effects of synaptic activation at low frequency on excitability of enteric AH neurons. *Neuroscience* 1999;90: 279-289
- Furness JB, Bornstein JC, Kunze WA, Clerc N. The enteric nervous system and its extrinsic connections. In : Yamada, T., Alpers, D.H., Laine, L., Owyang, C., Powel, D.W. eds. *Textbook of gastroenterology*, Vol. 1, 3rd ed., Lippincott, Williams & Wilkins, Philadelphia. 1999: 11-35
- Furness JB, Kunze WA, Clerc N. Nutrient tasting and signaling mechanisms in the gut. II. The intestine as a sensory organ: neural, endocrine, and immune responses. *Am J Physiol* 1999; 277:G922-G928
- Jiang ZW, Li JS, Li N, Li YS, Liu FL, Sheng XQ, Cheng YM. Recovery of the allografted small intestine functions. *China Natl J New Gastroenterol* 1997;3:67-68
- Liu CY, Liu JZ, Zhou JH, Wang HR, Li ZY, Li AJ, Liu KJ. TRH microinjection into DVC enhances motility of rabbits gallbladder via vagus nerve. *World J Gastroenterol* 1998;4:162-164
- Huang XQ. Helicobacter pylori infection and gastrointestinal hormones: a review. *World J Gastroenterol* 2000;6:783-788
- Pan QS, Fang ZP, Huang FJ. Identification, localization and morphology of APUD cells in gastroenteropancreatic system of stomach containing teleosts. *World J Gastroenterol* 2000;6:842-847

• BASIC RESEARCH •

# Study on of bioadhesive property of carbomer934 by a gamma camera *in vivo*

Jie Fu, Xun Sun, Zhi-Rong Zhang

Jie FuXun Sun, Zhi-Rong Zhang, West China School of Pharmacy, Sichuan University, Chengdu 610041, China

Supported by the Nation Distinguished Youth Scientific Fund (No. 39925039)

Correspondence to: Zhi-Rong Zhang, Ph.D., West China School of Pharmacy, Sichuan University, Chengdu, 610041, China. zrzzl@mail.sc.cninfo.net

Telephone: +86-28-5501566 Fax: +86-28-5456898

Received 2001-07-19 Accepted 2001-10-27

## Abstract

**AIM: To study the bioadhesive property of carbomer934 in dog alimentary tract.**

**METHODS: Carbomer934 and ethylcellulose were radiolabelled with technetium-99m; and Gastrointestinal emptying rate of materials was measured using the technique of gamma scintigraphy.**

**RESULTS: After oral administration, the maximum intestinal radioactivity of non-bioadhesive granules and bioadhesive granules were observed in the second hour and the sixth hour respectively. Constants of stomach emptying rate of nonadhesive granules, bioadhesive granulesI and bioadhesive granulesII were  $0.774h^{-1}$ ,  $0.265h^{-1}$  and  $0.321h^{-1}$  respectively on the base of gastric residual amount. Compared to nonadhesive material (ethylcellulose), the migration rate of adhesive material (carbomer934) was remarkably slower in dog alimentary canal.**

**CONCLUSION: It is concluded that, in the dog, interactions between gastrointestinal mucus layer and adhesive material or nonadhesive material were significantly different. Carbomer934 had stronger *in vivo* bioadhesive property than ethylcellulose.**

Fu J, Sun X, Zhang ZR. Study on of bioadhesive property of carbomer934 by a gamma camera *in vivo*. *World J Gastroenterol* 2002;8(1):176-179

## INTRODUCTION

A problem frequently encountered with controlled release dosage forms is the inability to increase residence time of the dosage form in the stomach and proximal portion of the small intestine. Under fast condition, gastric residence of a dosage form is typically short, which is not more than an hour and it is also common for dosage forms to transit rapidly through the small intestine for not more than 3h<sup>[1]</sup>. Rapid GI transit phenomena may consequently diminish the extent of absorption of many drugs. Since many drug compounds are absorbed exclusively in the small intestine or in a limited segment of the intestine, it would therefore be beneficial to develop sustained release dosage forms, which remain in the stomach for an extended period of time. Several approaches have been tried to prolong gastric residence, one of which is the use of oral bioadhesive formulation<sup>[2,3]</sup>. A number of charged and neutral polymers have been classified as bio/

mucoadhesives, since they are known to bind very strongly to mucus via non-covalent bonds.<sup>[4,5]</sup> Carbomer is a polyacrylic acid polymer, crosslinked with allyl sucrose. As a mucoadhesive polymer, carbomer has been investigated extensively by the pharmaceutical researchers because of its high viscosity at low concentration and low toxicity.<sup>[6-15]</sup> *In vitro* experiment has proved that carbomer934 have good bioadhesion with the gastrointestinal mucus<sup>[16-19]</sup>. Our research strategy is to investigate the *in vivo* bioadhesion of carbomer934 through measuring the migration rate of radioactive carbomer934 granules in dog alimentary tract by a gamma camera. Gamma scintigraphy is an elegant imaging technique which allows the intestinal performance of pharmaceutical formulations to be visualized.<sup>[20]</sup> Over the past 20 years the approach has become the technique of choice for probing the complex interaction of drug preparation/formulations with the heterogeneous environment of the gut.<sup>[21-29]</sup>

## MATERIALS AND METHODS

### Materials and apparatus

Ethylcellulose200cps (EC, imported from Roth Co. Ltd., obtained from Shanghai Chemical Agents Distributing Factory); Stearic acid(AP, supplied by Shanghai Stock and Accommodate Station of Chemical Agents); Carbomer934 (Cb934, purchased from Shanghai Shenxing Pharmacy Co. Ltd); <sup>99m</sup>TcO<sub>4</sub>(China Institute for A-energy and Isotope); γ-ray camera(Orbiter, Semens Co. Ltd, Germany); and Dog (provided by Laboratory Animal Center, Sicuan University).

### Methods

**Radiolabeling of Cb934 and ethylcellulose** Procedures of Cb934 and ethylcellulose radiolabelled were described in brief as follows: In vacuum bottle, 1ml of 0.1mol·L<sup>-1</sup> hydrochloric acid containing 1mg SnCl<sub>2</sub> and 1mg vitamin C was added to 2mL of 15g·L<sup>-1</sup>Cb934(or 30g·L<sup>-1</sup>EC) of ethanol solution, then with incorporation of Tc <sup>99m</sup>O<sub>4</sub>. The mixture was warmed at 90°C for 10 minutes. Radioactivity chemical purity of radiolabelled materials measured by TLC was beyond 95%.

**Preparation of radioactive granules** According to the materials proportion of granules listed in Table 1, the mixed materials were solved in ethanol and dried in a rotated vaporizing apparatus. The product was crushed, then manually sieved. The collecting fraction have a size range of 20-40 mesh. An amount of the final blend was filled into hard gelatin capsules (size No.0). Each capsule has an activity of about 111MBq technetium99m at the time of administration.

**Table 1** Component proportion of radioactive granules

| granules        | Percentage/% |       |              |
|-----------------|--------------|-------|--------------|
|                 | EC           | Cb934 | Stearic acid |
| Non-bioadhesive | 100          | 0     | 0            |
| Bioadhesive I   | 0            | 100   | 0            |
| Bioadhesive II  | 0            | 50    | 50           |

### Measurement of migration rate of granules in dog alimentary tract

The study was an open-labeled, three-period, three treatment crossover study in three dogs (15-20kg). Each subject received the

following treatment in a randomized order: Treatment A: control nonbioadhesive granules,  $2 \times 111\text{MBq}$  radioactivity following 24 h fast. Treatment B: bioadhesive granulesI,  $2 \times 111\text{MBq}$  radioactivity following 24 h fast. Treatment C: bioadhesive granulesII  $2 \times 111\text{MBq}$  radioactivity following 24 h fast. Percentage of granules in different segments of dog alimentary canal could be determined according to radioactivity by a  $\gamma$ -ray camera.

## RESULTS

### Migration rate of three kinds of granules

The dog alimentary tract was divided into three segments of stomach, intestine and colon(including colon,rectum and anus). Radioactivity was measured respectively in different segments (Tables). The gastric emptying rate of granules containing Cb934 (bioadhesive granules I and bioadhesive granulesII) was significantly slower than the control non-bioadhesive granules. After 4h, percentage of non-bioadhesive granules in stomach was only 7.63%, while bioadhesive granulesI 45.92% and bioadhesive granulesII 37.52%. In the sixth hour, percentage of non-bioadhesive granules, bioadhesive granulesI and bioadhesive granulesII in dog stomach was 0, 23.2% and 15% respectively.

**Table 2** Non-bioadhesive granules in alimentary tract of dog ( $n=3$ )

| Sites     | Granules in different segment of alimentary tract(%) |      |      |      |      |     |
|-----------|------------------------------------------------------|------|------|------|------|-----|
|           | 1h                                                   | 2h   | 4h   | 6h   | 8h   | 12h |
| Stomach   | 83.7                                                 | 26.9 | 7.6  | 0    | 0    | 0   |
| Intestine | 16.3                                                 | 73.2 | 59.7 | 0    | 0    | 0   |
| Colon     | 0                                                    | 0    | 32.6 | 43.2 | 10.6 | 0   |

**Table 3** Bioadhesive granulesI in alimentary tract of dog ( $n=3$ )

| Sites     | Granules in different segment of alimentary tract(%) |      |      |      |      |      |
|-----------|------------------------------------------------------|------|------|------|------|------|
|           | 1h                                                   | 2h   | 4h   | 6h   | 8h   | 12h  |
| Stomach   | 100                                                  | 79.6 | 45.4 | 23.3 | 7.5  | 0    |
| Intestine | 20.4                                                 | 54.7 | 59.7 | 55.1 | 30.9 | 0    |
| Colon     | 0                                                    | 0    | 0    | 21.8 | 61.6 | 54.3 |

**Table 4** Bioadhesive granules II in alimentary tract of dog ( $n=3$ )

| Sites     | Granules in different segment of alimentary tract(%) |      |      |      |      |      |
|-----------|------------------------------------------------------|------|------|------|------|------|
|           | 1h                                                   | 2h   | 4h   | 6h   | 8h   | 12h  |
| Stomach   | 100                                                  | 67.1 | 37.5 | 15   | 0    | 0    |
| Intestine | 0                                                    | 32.8 | 51.6 | 57.9 | 29.6 | 0    |
| Colon     | 0                                                    | 0    | 10.9 | 29.7 | 70.4 | 64.8 |

Non-bioadhesive granules were emptied to intestine in the first hour and the maximum intestinal radioactivity was observed in the

second hour, then intestinal radioactivity was completely eliminated in the sixth hour, bioadhesive granulesI and bioadhesive granulesII began to intestine migrated to in the second hour, and the maximum intestinal radioactivity was observed in the sixth hour. Furthermore considerable intestinal radioactivity could be inspected in the eighth hour. Compared with the non-bioadhesive granules, the bioadhesive granules had delayed onset of emptying to intestine and the maximum radioactivity in intestine. This result indicated that bioadhesion of Cb934 granules on the intestinal mucus was stronger than nonbioadhesive granules. In the fourth hour, a considerable non-bioadhesive pellets have entered the colon and were completely discharged out of anus in the eighth hour. Meanwhile, only very small parts of bioadhesive granules migrated into colon, and as long as the twelfth hour a great deal of granules were still in the dog alimentary tract.

### Emptying half life of three kinds of granules in dog stomach

Emptying rate of stomach is fit to the first order kinetics<sup>[30]</sup>.  $\text{Log}V_t = \text{Log}V_0 - \text{Kemt}/2.303$   $V_t$ :Gastric residual amount at the time of  $t$   $V_0$ :Gastric residual amount at the time of 0 in stomach  $\text{Kemt}$ : Constant of stomach emptying rate.

Constants of stomach emptying rate of nonadhesive granules, bioadhesive granulesI and bioadhesive granulesII can be calculated as  $0.774\text{h}^{-1}$ ,  $0.265\text{h}^{-1}$ ,  $0.321\text{h}^{-1}$  respectively on the base of gastric residual amount. According to gastric residual amount of the first three points of time, constant of gastric emptying rate of bioadhesiveI granules can be calculated as  $0.265\text{h}^{-1}$ , while according to the latter three points of time, constant can be calculated as  $0.449\text{h}^{-1}$ .

### Pictures of $\gamma$ -ray camera

A majority of nonadhesive granules have been emptied into intestine in the second hour (Figure 1B), then reached colon in the fourth hour (Figure 1C) and a great deal collected at anus in the seventh hour (Figure 1D). In the fourth hour, most bioadhesiveI granules still mustered in the stomach(Figure 2C) and reached colon in the twelfth hour(Figure 2D). In the fifth hour, most bioadhesiveII granules were still in the intestine (Figure 3C) and reached colon in the seventh hour.

## DISCUSSION

According to radioactivity measured by a gamma camera, migration rate of granules containing Cb934 was significantly slower than nonbioadhesive granules. It can be concluded that Cb934 has good bioadhesive properties *in vivo* and is a possible candidate material for oral bioadhesive preparation.

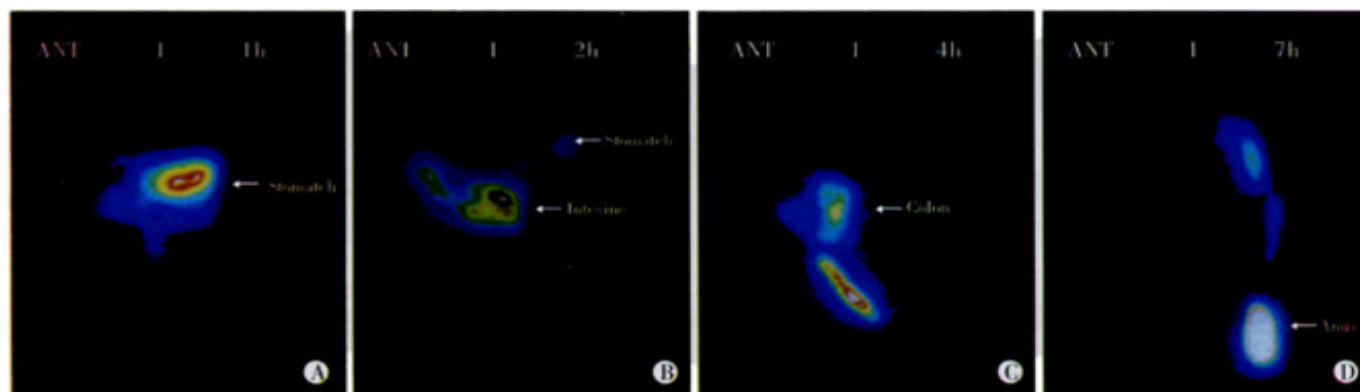


**Figure 1** Radioactivity in alimentary tract of dog swallowing nonadhesive granules.

A, B, C, D: radioactivity at 1, 2, 4 and 7h.

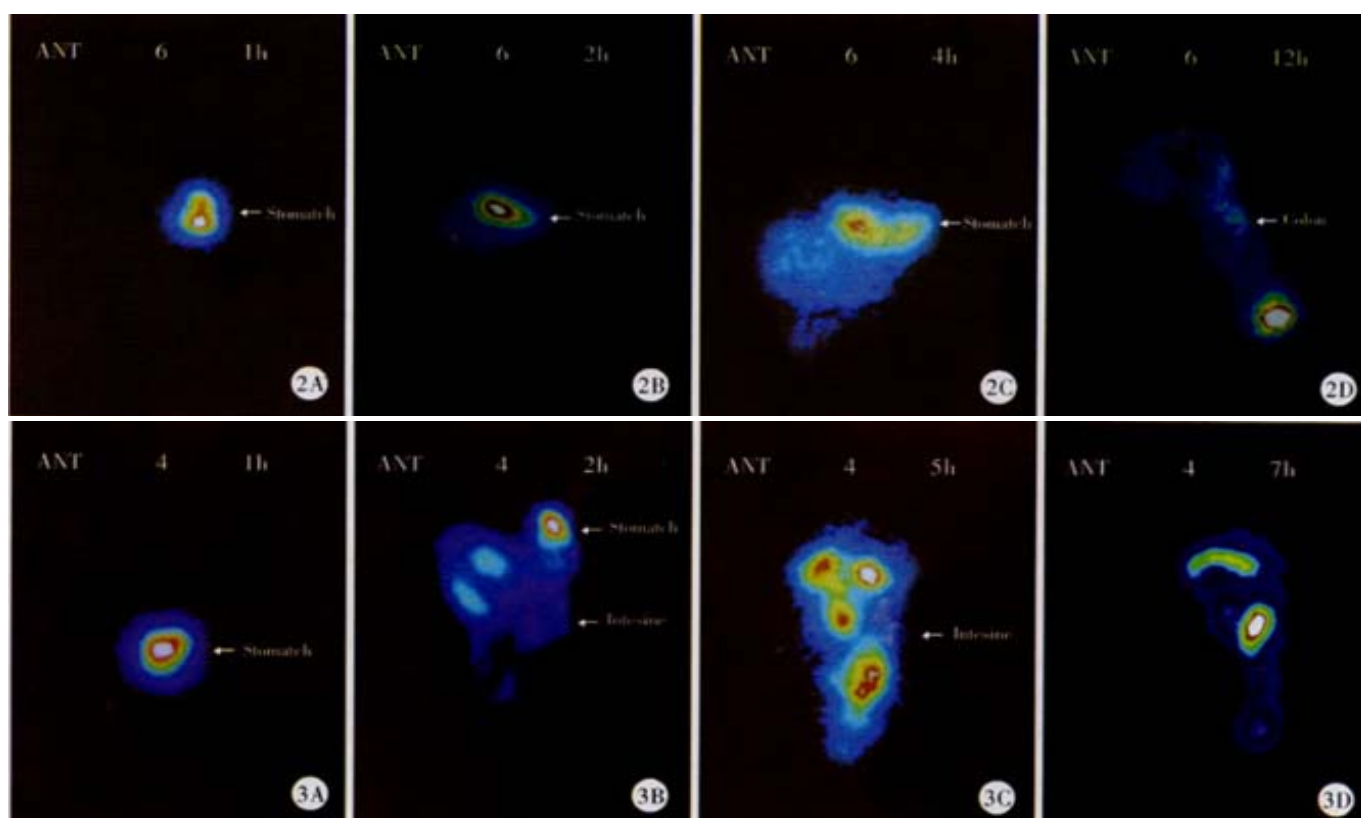


**Figure 2** Radioactivity in alimentary tract of dog swallowing bioadhesive granules.

A, B, C, D: radioactivity at 1, 2, 4 and 12h.

**Figure 3** Radioactivity in alimentary tract of dog swallowing bioadhesive granules.

A, B, C, D: radioactivity at 1, 2, 4 and 7h.

Compared with the rate constant ( $0.265\text{h}^{-1}$ ) at gastric prophase emptying, gastric anaphase emptying rate constant ( $0.449\text{h}^{-1}$ ) of bioadhesive granules became larger. This result showed that gastric emptying rate of Cb934 granules became faster as time went along. It can be inferred that Cb934 was excessively hydrated and caused a lubricative effect, which quickened the gastric emptying of granules. This implied that materials, which not only have good bioadhesive properties and but also can maintain gel status to avoid excessive hydrating, should be preferably considered in oral bioadhesive preparation design.

## REFERENCES

- Barara Naisbett, John Woodley. The potential use of tomato lectin for oral drug delivery: 3. Bioadhesion *in vivo*. *Int J Pharm* 1995; 114: 227-236
- Schnurch A.B, Humenberger C, Vlaenta C. Basic studied on bioadhesive delivery systems for peptide and protein drugs. *Int J Pharm* 1998; 165: 217-225
- Arango M.A, Ponchel G, Orecchioni A.M, Renedo M.J, Duchene D, Irache J.M. Bioadhesive potential of gliadin nanoparticulate systems. *Eur J Pharm Sci* 2000; 11:333-341
- Madsen F, Eberth K, Smart JD. A rheological examination of the mucoadhesive/mucus interaction: the effect of mucoadhesive type and concentration. *J Control Release* 1998; 50:167-178
- Eouani C, Piccerelle Ph, Prinderre P, Bourret E, Joachim J. In-vitro comparative study of buccal mucoadhesive performance of different polymeric films. *Eur J Pharm Biopharm Sci* 2001; 52:45-55
- Nakanishi T, Kaiho F, Hayashi M. Improvement of drug release rate from Carbopol 934P formulation. *Chem Pharm Bull* 1998; 46:171-173
- Tan Y.T.F, Peh KK, Al-Hanbali O. Investigation of interpolymer complexation between carbopol and various grades polyvinylpyrrolidone and effects on adhesion strength and swelling properties. *J Pharm Pharmaceut Sci* 2001; 4:7-14
- Nakanishi T, Kaiho F, Hayashi M. Use of sodium salt of Carbopol 934P in oral peptide delivery. *Int J Pharm* 1998; 171: 177-183
- Callens C, Adriaens E, Dierckens K, Remon JP. Toxicological evaluation of a bioadhesive nasal powder containing a starch and Carbopol 974P on rabbit nasal mucosa and slug mucosa. *J Control Release* 2001; 76:81-91
- Repka MA, McGinity JW. Bioadhesive properties of hydroxypropylcellulose topical films produced by hot-melt extrusion. *J Control Release* 2001; 70:341-351
- Khan GM, Zhu JB. Studies on drug release kinetics from ibuprofen-carbomer hydrophilic matrix tablets: influence of co-excipients on release rate of the drug. *J Control Release* 1999; 57:197-203
- Ozeki T, Yuasa H, Kanaya Y. Controlled release from solid dispersion composed of poly(ethylene oxide)-Carbopol interpolymer complex with various cross-linking degrees of Carbopol. *J Control Release* 2000; 63:287-295
- Khan GM, Zhu JB. Formulation and *in vitro* evaluation of ibuprofen-carbopol 974P-NF controlled release matrix tablets: influence of co-excipients on release rate of the drug. *J Control Release* 1998; 54:185-190
- Muramatsu M, Kanada K, Nishida A, Ouchi K, Saito N. Application of Carbopol to controlled release preparations. Carbopol as a novel coating material. *Int J Pharm* 2000; 199: 77-83
- Senel S, Capan Y, Sargon MF, Giray CB, Hincal AA. Histological and bioadhesion studies on buccal bioadhesive tablets containing a penetration enhancer sodium glycodeoxycholate. *Int J Pharm* 1998; 170: 239-245
- Bogataj M, Mrhar A, Korosec L. Influence of physicochemical and biological parameter on drug release from microspheres adhered on vesical and intestinal mucosa. *Int J Pharm* 1999; 177: 211-220
- Riley RG, Smart JD, Tsibouklis J, Dettmar PW, Hampson F, Davis JA, Kelly G, Wilber WR. An investigation of mucus/polymer rheological synergism using synthesised and characterised poly(acrylic acid)s. *Int J Pharm* 2001; 217: 87-100
- Hagerstrom H, Paulsson M, Edsman K. Evaluation of mucoadhesion for two polyelectrolyte gels in simulated physiological conditions using a rheological method. *Eur J Pharm Sci* 2001; 9:301-309
- Dash AK, Gong Z., Miller DW, Han HY, Laforet JP. Development of a rectal nicotine delivery system for the treatment of ulcerative colitis. *Int J Pharm* 1999; 190: 21-34
- Connor AL, Wray H, Cottrell J, Wilding IR. A scintigraphic study to

- investigate the potential for altered gut distribution of loperamide from a loperamide-simethicone formulation in man. *Eur J Pharm Sci* 2001; 13: 369-374
- 21 Sangalli ME, Maroni A, Zema L, Busetti C, Giordano F, Gazzaniga A. *in vitro* and *in vivo* evaluation of an oral system for time and/or site-specific drug delivery. *J Control Release* 2001; 73:103-110
- 22 Digenis GA, Sandefer EP, Page RC, Doll WJ, Gold TB, Darwazeh NB. Bioequivalence study of stressed and nonstressed hard gelatin capsules using amoxicillin as a drug marker and gamma scintigraphy to confirm time and GI location of *in vivo* capsule rupture. *Pharm Res* 2000; 17: 572-580
- 23 Krishnaiah YSR, Satyanrayana S, Rama Prasad YV, Rao SN. Gamma scintigraphic studies on guar gum matrix tablets for colonic drug delivery in healthy human volunteers. *J Control Release* 1998; 55: 245-252
- 24 Ishibashi T, Pitcairn GR, Yoshino H, Mizobe M, Wilding IR. Scintigraphic Evaluation of a new capsule-type colon specific drug delivery system in healthy volunteers. *J Pharma Sci* 1998; 87: 531-535
- 25 Billa N, Yuen KH, Khader MAA, Omar A. Gamma-scintigraphic study of the gastrointestinal transit and *in vivo* dissolution of a controlled release diclofenac sodium formulation in xanthan gum matrices. *Int J Pharm* 2000; 201: 109-120
- 26 Haruta S, Kawai K, Jinnouchi S, Ogawara KI, Higaki, Tamura S, Arimori K, Kimura T. Evaluation of absorption kinetics of orally administered theophylline in rats based on gastrointestinal transit monitoring by gamma scintigraphy. *J Pharma Sci* 2001; 90: 464-473
- 27 Tang GH, Tang XL. Application of nuclear medicine techniques in drug development. *Acta Pharmaceutica Sinica* 2001; 36: 390-395
- 28 Wilson CG. *In vivo* monitoring of dosage forms. *J Pharm Pharmacol* 1998; 50: 383-386
- 29 Wilding IR, Coupe AJ, Davis SS. The role of scintigraphy in oral drug delivery. *Adv Drug Deliv Rev* 2001; 46: 103-124
- 30 Liang WQ. Biopharmaceutics and pharmacokinetics. Beijing: Renming Health Press. 2000:134-136

Edited by Ma JY



• BASIC RESEARCH •

# Gastric myoelectrical activity and gastric emptying in diabetic patients with dyspeptic symptoms

Hui-Bin Qi, Jin-Yan Luo, You-Ling Zhu, Xue-Qin Wang

Hui-Bin Qi, Jin-Yan Luo, You-Ling Zhu, Xue-Qin Wang, Department of Gastroenterology, The Second Hospital of Xi'an Jiaotong University, Xi'an 710004, Shannxi, China

Correspondence to: Hui-bin Qi, Xiwu Road 36, Xi'an 710004, Shannxi, China. qihuibin123@163.net

Telephone: +86-29-7262029 Fax: +86-29-7231758

Received 2001-04-05 Accepted 2001-07-10

Qi HB, Luo JY, Zhu YL, Wang XQ. Gastric myoelectrical activity and gastric emptying in diabetic patients with dyspeptic symptoms. *World J Gastroenterol* 2002;8(1):180-182

## INTRODUCTION

Recently, electrogastrography (EGG) has received more and more attention. Although gastroenterologists are interested in its clinical application, concerns remain to the reliability and analysis of the EGG and the correlation between the EGG and gastric motility<sup>[1-13]</sup>. This study was to investigate gastric myoelectrical activity and gastric emptying (GE) and their relationship in diabetic patients with dyspeptic symptoms using electrogastrography and isotopic method.

## MATERIALS AND METHODS

### Subjects

The study was performed on 22 healthy asymptomatic subjects (11 women, 11 men, mean age 50 yr) and 32 non-insulin dependent diabetes mellitus (NIDDM) patients with dyspeptic symptoms (15 women, 17 men, mean age 51 yr) based on clinical and laboratory diagnoses. NIDDM was diagnosed by the WHO criteria (1980). All patients had a minimum 3-month history of chronic, persistent, or recurrent epigastric pain and fullness, early satiety, nausea and/or vomiting. The result of esophagogastroduodenoscopic examination were negative for any focal lesions, including esophagitis, gastric, or duodenal ulcers or erosions, or esophageal or gastric malignancy. Exclusion criteria were: ① history of abdominal surgery; ② history of gastroesophageal reflux disease or irritable bowel syndrome; ③ evidence of cardiovascular, pulmonary, hepatic, or renal disease. All subjects fasted an overnight before the study and took no medications known to affect gastrointestinal motility during 3 d before the study.

### Gastric emptying test

Gastric emptying test was taken by using SPECT technique. The standard meal for gastric emptying test consisted of 100g scrambled eggs labeled with <sup>99m</sup>Tc-DTPA (11.1 MBq) and 200mL of water. After eating, the anterior/posterior images of the stomach were taken by the same operator using a technetium scanner for 2 h. Retention and half-emptying time ( $T_{1/2}$ ) were calculated by a specialist at the Department of Nuclear Medicine. Delayed gastric emptying was defined as the half-emptying time  $\geq x+2s$  as controls.

### Recording of gastric myoelectrical activity

Gastric myoelectrical activity was measured with surface EGG. The EGG recording including a 30-min fasting study using an EGG recording unit (Digitrapper, Syneetics Medical, Sweden), after which the patient ate a standard test meal

(1883J). This was immediately followed by another 30-min recording. The EGG data was analyzed by the "multigram" Synectics software package running on a personal computer. The EGG parameters including dominant frequency (DF), dominant power (DP), postprandial / preprandial DF, postprandial / preprandial DP.

### Statistical analysis

Data were expressed as  $\bar{x} \pm s$ . Statistical analyses used are *t* test and  $\chi^2$  test. Statistical significance is taken as  $P < 0.05$ .

## RESULTS

### Gastric emptying test

The mean percentage of gastric retention and half-emptying time in diabetic patients with dyspeptic symptoms were substantially higher than in the healthy subjects (Table 1). Of 32 patients, 15 (47%) had delayed gastric emptying. Of 22 controls, 1 (5%) had delayed gastric emptying. The incidence of gastric emptying delay was higher in patients than in controls ( $P < 0.01$ ).

Table 1 Gastric Emptying In NIDDM ( $\bar{x} \pm s$ )

| Groups   | n  | Percentage of gastric retention % |                         |                          |                          | $T_{1/2}$ min            |
|----------|----|-----------------------------------|-------------------------|--------------------------|--------------------------|--------------------------|
|          |    | 30min                             | 60min                   | 90min                    | 120min                   |                          |
| NIDDM    | 32 | 75 $\pm$ 7 <sup>a</sup>           | 61 $\pm$ 8 <sup>b</sup> | 54 $\pm$ 10 <sup>b</sup> | 43 $\pm$ 10 <sup>b</sup> | 92 $\pm$ 10 <sup>b</sup> |
| Controls | 22 | 61 $\pm$ 7                        | 45 $\pm$ 6              | 33 $\pm$ 4               | 24 $\pm$ 10              | 49 $\pm$ 9               |

<sup>a</sup> $P < 0.05$  vs controls; <sup>b</sup> $P < 0.01$  vs controls

### Electrogastrographic findings

EGG dominant frequency corresponds to gastric slow wave. DF ranging from 2.4 to 3.7 cycle per min (cpm) was considered as normogastria, DF < 2.4 cpm was defined as bradygastria, DF > 3.7 cpm was defined as tachygastria. DF < 2.4 cpm and/or DF > 3.7 cpm was defined as dysrhythmia or abnormal EGG. The patients had a lower incidence of normogastria than did controls both in the fed state (34% vs 86%,  $P < 0.01$ ) and in the fasting state (38% vs 96%,  $P < 0.01$ ). However, the patients had a higher incidence of dysrhythmia (tachygastria and bradygastria) than did controls both in the fed state (66% vs 14%,  $P < 0.01$ ) and in the fasting state (63% vs 5%,  $P < 0.01$ ). The mean postprandial dominant frequency and postprandial/preprandial dominant frequency ratio were lower in patients than in controls (2.61 $\pm$ 0.29 cpm vs 3.76 $\pm$ 0.14 cpm,  $P < 0.05$ ; 1.01 $\pm$ 0.10 vs 1.28 $\pm$ 0.11,  $P < 0.05$ ). The mean postprandial dominant power increase and the mean postprandial/preprandial dominant power ratio was significantly less in the patients than in the controls (121.50 $\pm$ 67.02 V<sup>2</sup>.cpm vs 688.61 $\pm$ 72.73 V<sup>2</sup>.cpm,  $P < 0.01$ ; 0.71 $\pm$ 0.60 vs 2.40 $\pm$ 0.61,  $P < 0.01$ ). No differences were found in the mean preprandial dominant frequency and the mean preprandial dominant power (2.57 $\pm$ 0.24 cpm vs 2.91 $\pm$ 0.22 cpm,  $P > 0.05$ ; 144.10 $\pm$ 27.40 V<sup>2</sup>.cpm vs 288.40 $\pm$ 56.72 V<sup>2</sup>.cpm,  $P > 0.05$ ).

### Comparison of EGG and gastric emptying

Of 32 diabetic patients with dyspeptic symptoms, 15 (47%) had

delayed gastric emptying and 21 (66%) patients with dysrhythmia. 12 patients with dysrhythmia had slow gastric emptying. There was no significant correlation between gastric electrical rhythm and gastric emptying ( $P>0.05$ ).

## DISCUSSION

Gastric emptying and EGG were measured in diabetic patients with dyspeptic symptoms in this study. The results showed that fifteen of 32 (47%) diabetic patients with dyspeptic symptoms had delayed gastric emptying, and 21 of 32 (66%) patients had abnormal gastric myoelectrical activity. 12 patients with dysrhythmia had slow gastric emptying. The major abnormalities in gastric myoelectrical activity observed in diabetic patients with dyspeptic symptoms were the abnormal rhythmicity of the gastric slow wave and the reduced postprandial increase in the dominant power.

Our findings in this study are similar to those in previous studies in patients with various gastric motor disorders<sup>[14-19]</sup>. In studies using cutaneous electrodes, abnormal EGG were found in 50% of patients with functional dyspepsia<sup>[14]</sup>. In an electrogastrographic study using cutaneous electrodes, a high proportion of adult patients (60%) with functional dyspepsia had abnormally slow gastric emptying and abnormalities in gastric myoelectrical activity<sup>[15]</sup>. We found that 66% of the patients had abnormal rhythmicity of the gastric slow wave (bradygastria and tachygastria) and some patients had a reduced postprandial increase in the dominant power. EGG findings similar to those in this study have been also reported in studies in patients with gastroparesis<sup>[20,21]</sup>. However, Pfaffenbach *et al.* reported that the EGG values obtained in diabetics did not differ significantly from those in healthy subjects and did not correlate with radioscinigraphy, the EGG values in diabetics with delayed gastric emptying (about 40%) did not differ from data in diabetics without gastroparesis<sup>[22]</sup>. Jebbink *et al.* also reported that no differences between patients with functional dyspepsia and healthy volunteers were found in the incidence of dysrhythmias<sup>[23]</sup>. These discrepancies probably result from differences in patient selection, differences in definition of dyspepsia and EGG analysis method<sup>[24]</sup>. Prior studies have demonstrated that gastric emptying in dyspeptic patients was found to be delayed in 30~80% of the patients<sup>[15,20, 25-28]</sup>. In agreement with prior studies, this study demonstrated 47% delayed gastric emptying in diabetic patients with dyspeptic symptoms. The present study shows that 12 patients with dysrhythmia had delayed gastric emptying, but there was no correlation between gastric rhythmicity and gastric emptying. An other interesting finding was the reduced increment of amplitude (power), expressed as absolute or relative changes (fed/fasting power ratio). A possible cause for a decrease in the power ratio was the reduced gastric distention or/and contractility of the stomach. An increase in amplitude were reported in numerous studies in normal adults and in normal children<sup>[29-32]</sup>. Some authors believed that it was related to the increased contractility of the stomach after the meal<sup>[30,33-35]</sup>, whereas others reported a major effect of gastric distention. Faure *et al.* suggested that both gastric distention and motor activity contributed to the increase in EGG amplitude, the greater contribution being attributable to gastric distention<sup>[36]</sup>. Gastric emptying and EGG findings were agreement with our finding in previous study<sup>[37]</sup> and other authors' findings<sup>[38]</sup>. A study by Barbar *et al.* showed that EGG did not correlate with nuclear scintigraphic gastric emptying studies in children with suggestive symptoms of gastric motility disorders<sup>[38]</sup>. Zhang *et al.* reported that they can't predict a delayed GET by an abnormal EGG<sup>[39]</sup>. However, controversial findings were reported. Pfaffenbach *et al.* reported that in 25 adult patients with functional dyspepsia, patients with delayed gastric emptying showed significantly more pre- and post prandial tachygastrias than patients with normal gastric emptying<sup>[40]</sup>. Gastric emptying is a complex procedure. EGG reflects gastric myoelectrical

activity and gastric emptying reflects gastric motility, so EGG and gastric emptying should complement each other in studying gastric motor disorders<sup>[14,41]</sup>.

In conclusion, diabetic patients with dyspeptic symptoms have delayed gastric emptying and abnormalities in gastric myoelectrical activity including dysrhythmia and the reduced postprandial increase in the dominant power. However, the abnormal EGG isn't able to predict delayed gastric emptying.

## REFERENCES

- Mathur R, Pimentel M, Sam CL, Chen JD, Bonorris GG, Barnett PS, Lin HC. Postprandial improvement of gastric dysrhythmias in patients with type II diabetes: identification of responders and nonresponders. *Digestive Diseases and Sciences* 2001;46:705-712
- Sanmiquel CP, Mintchev MP, Bowes KL. Electrogastrography: An noninvasive technique to evaluate gastric activity. *Can J Gastroenterol* 1998;12:423-430
- Ma GR, Guo SC, Sun J. Study on the relations between some common gastrointestinal disorders and testing results of electrogastrogram. *Chin Natl J Gastroenterol* 1996;2:81
- Zhang J, Chen D, Gao HY. Function of electrogastrogram in the diagnosis of GI diseases in children. *Chin Natl J Gastroenterol* 1996;2 (Suppl. 1):81-82
- Ouyang S. The new investigation on wave form of electrogastrography. *Chin Natl J Gastroenterol* 1996;2(Suppl. 1):79
- Wang DS, Zhang LD, Chai JY, Zhang Y, Lu YY. Specific EGG wave figure in gastric and duodenal ulcer. *Chin Natl J Gastroenterol* 1996;2 (Suppl. 1):88
- Li JS. Experience in clinical application of electrogastrogram. *Chin Natl J Gastroenterol* 1996;2(Suppl. 1):83
- Ravelli AM. Electrogastrography in childhood. *Chin Natl J Gastroenterol* 1996;2(Suppl. 1):18-21
- Koch KL. Clinical applications of electrogastrography. *Chin Natl J Gastroenterol* 1996;2(Suppl. 1):15-17
- Chen JD. Spectral analysis of electrogastrogram and its clinical significance. *Chin Natl J Gastroenterol* 1996;2(Suppl. 1):11-13
- Chung OY. The clinical significance of gastric dysrhythmias. *Chin Natl J Gastroenterol* 1996;2(Suppl. 1):5-8
- Chen YM, Zhao S, Wan P, Wang J, Fan H, Luo HM, Long YL, Ma BD. Electrogastrography in patients with uremia. *Huaren Xiaohua Zazhi* 1998;6:979-981
- Wang SY. The clinical significance of electrogastrogram application. *Xin Xiaohuabingxue Zazhi* 1994;2(Suppl. 2):157-158
- Parkman HP, Miller MA, Trate D, Knight LC, Urbain JL, Maurer AH, Fisher RS. Electrogastrography and gastric emptying scintigraphy are complementary for assessment of dyspepsia. *J Clin Gastroenterol* 1997;24:214-219
- Lin Z, Eaker EY, Sarosiek I, McCallum RW. Gastric myoelectrical activity and gastric emptying in patients with functional dyspepsia. *Am J Gastroenterol* 1999;94:2384-2389
- Reizzo G, Chiloiro M, Guerra V, Borrelli O, Salvia G, Cucchiara S. Comparison of gastric electrical activity and emptying in healthy and dyspeptic children. *Digestive Diseases and Sciences* 2000;45: 517-524
- Feng YY, Xu RP, Wang Y. The influence of fasting electrogastrograph in patients with functional dyspepsia using cisapride treatment. *Chin Natl J Gastroenterol* 1996;2(Suppl. 1):88
- Li YS, Zhu RM. Mechanisms of functional dyspepsia. *Huaren Xiaohua Zazhi* 1998;6:439-440
- Fu M, Xu GM. Stomach motility in 30 patients with gastric dysrhythmia. *Xin Xiaohuabingxue Zazhi* 1995;3:81-83
- Qi HB, Luo JY, Dai XG, Wang XQ. A study on motility in patients with diabetic gastroparesis. *Xin Xiaohuabingxue Zazhi* 1997; 5:661-662
- Huang YQ, Wang X, Liu L, Li C. Serum NO and the changes of cutaneous electrogastrogram in patients with NIDDM. *Shijie Huaren Xiaohua Zazhi* 2000;8:1177-1178
- Pfaffenbach B, Wegener M, Adamek RJ, Schaffstein J, Lee YH, Ricken D. Antral myoelectric activity, gastric emptying, and dyspeptic symptoms in diabetics. *Scand J Gastroenterol* 1995;30:1166-1171
- Jebbink HJA, Van Berge-Henegouwen GP, Bruijs PPM, *et al.* Gastric myoelectrical activity and gastrointestinal motility in patients with functional dyspepsia. *Eur J Clin Invest* 1995;25:492-437
- Levanon D, Zhang M, Chen JD. Efficiency and efficacy of the electrogastrogram. *Digestive Diseases and Sciences* 1998;43:1023-1030
- Soykan I, Lin Z, Sarosiek I, McCallum RW. Gastric myoelectrical activity, gastric emptying, and correlations with symptoms and fasting blood glucose levels in diabetic patients. *Am J Med Sci* 1999;317:226-231

- 26 Lin X, Chen JZ. Abnormal gastric slow waves in patients with functional dyspepsia assessed by multichannel electrogastrography. *Am J Physiol Gastrointest Liver Physiol* 2001;280:G1370-1375
- 27 Lu CL, Chen CY, Chang FY, Kang LJ, Lee SD, Wu HC, Kuo TS. Impaired postprandial gastric myoelectrical activity in Chinese patients with nonulcer dyspepsia. *Digestive Diseases and Sciences* 2001; 46:242-249
- 28 Chen JD, Ke MY, Lin XM, Wang Z, Zhang M. Cisapride provides symptomatic relief in functional dyspepsia associated with gastric myoelectrical abnormality. *Aliment Pharmacol Ther* 2000;14:1041-1047
- 29 Chen JD, Co E, Liang P, Sutphen J, Torres-Pinedo RB, Orr WC. Patterns of gastric myoelectrical activity in human subjects of different ages. *Am J Physiol* 1997;272:G1022-G1027
- 30 Riezzo G, Chilioro M, Guerra V. Electrogastrography in healthy children: evaluation of normal values, influence of age, gender and obesity. *Digestive Diseases and Sciences* 1998;43:1646-1651
- 31 Cucchiara S, Franzese A, Salvia G, Alfonsi L, Iula VD, Montisci A, Moreira FL. Gastric emptying delay and gastric derangement in IDDM. *Diabetes Care* 1998;21:438-443
- 32 Lin Z, Chen JD, Schirmer BD, McCallum RW. Postprandial response of gastric slow waves: correlation of serosal recordings with the electrogastrograms. *Digestive Diseases and Sciences* 2000;45:645-651
- 33 Zhang KG, Hu YB, Shi XH, Xiao SD. Response of the electrogastrogram in normal subjects to water, milk and solid meal. *Xin Xiaohuabingxue Zazhi* 1996;4:194-195
- 34 Zhou SC, He QN, He P, Feng ZT, Wang YJ. The effect erythromycin on cutaneous electrogastrogram in patients with non-ulcer dyspepsia. *Xin Xiaohuabingxue Zazhi* 1996;4:59-60
- 35 Huang LX, Zhao JX. The effect erythromycin on gastric electrical rhythm in patients with diabetes mellitus. *Xin Xiaohuabingxue Zazhi* 1996;4:612
- 36 Faure C, Wolff P, Navarro J. Effect of meal and intravenous erythromycin on manometric and electrogastrographic measures of gastric motor and electrical activity. *Dig Dis Sci* 2000;45:525-528
- 37 Luo JY, Zhu YL, Wang XQ, Qi HB. Assessment of clinical values of electrogastrography and gastric emptying test. *Weichangbing Xue* 2000; 5:223-225
- 38 Barbar M, Steffen R, Wyllie R, Goske M. Electrogastrography versus gastric emptying scintigraphy in children with suggestive symptoms of gastric motility disorders. *J Pediatr Gastroenterol Nutr* 2000;30:193-197
- 39 Zhang KG, Hu YB, Wang CD, Mo JZ, Wang SX, Xiao SD. Studies in patients with NIDDM by gastric emptying time and electrogastrogram. *Chin Natl J Gastroenterol* 1996;2:81
- 40 Pfaffenbach B, Adamek RJ, Bartholomaeus C, Wegener M. Gastric dysrhythmias and delayed gastric emptying in patients with functional dyspepsia. *Digestive Diseases and Sciences* 1997;42:2094-2099
- 41 Quigley EMM. The evaluation of gastrointestinal function in diabetic patients. *World Journal of Gastroenterology* 1999;5:277-282

Edited by Wang QY

• BASIC RESEARCH •

# Proliferation of intestinal crypt cells by gastrin-induced ornithine decarboxylase

Zi-Li Zhang, Wei-Wen Chen

Zi-Li Zhang, Wei-Wen Chen, Guangzhou University of Traditional Chinese Medicine (TCM), Guangzhou 510405, China  
Supported by National Natural Science Foundation of China, No. 39970906

Correspondence to: Dr. Chen Weiwen, Piwei Institute, Guangzhou University of TCM, Guangzhou 510405, China. pwxh@gzhtcm.edu.cn  
Telephone: +86-20-86591233 ext 2444

Received 2001-07-03 Accepted 2001-10-16

## Abstract

**AIM:** To determine whether the gastrin stimulated intestinal crypt cell (IEC-6) proliferation by induction of ornithine decarboxylase (ODC).

**METHODS:** IEC-6 cells were grown in DMEM containing 50 mL·L<sup>-1</sup> dialyzed fetal bovine serum for 24h and then were treated with gastrin. The proliferative capability of the cells was monitored subsequently on d 1, 2, 3, and 4 after treatment with MTT assay at absorbance 570nm. The cellular ODC mRNA expression, ODC activity, and putrescine content were examined by RT-PCR method, radiometric technique and high-performance liquid chromatography (HPLC) analysis respectively after 12h of treatment.

**RESULTS:** On d1 after exposure of IEC-6 cells to pentagastrin, the proliferation increased initially and reached a peak on d3 at 250 μg·L<sup>-1</sup> concentration. Pentagastrin 500 μg·L<sup>-1</sup> increased cell proliferation on day 1 and day 2, and then decreased. Compared with control group, pentagastrin 250 μg·L<sup>-1</sup> increased ODC mRNA level by 1.09-fold ( $P < 0.05$ ), ODC activity by 1.71-fold ( $P < 0.01$ ), and putrescine content 5.30-fold ( $P < 0.01$ ), respectively. Similarly, pentagastrin of 500 μg·L<sup>-1</sup> also increased ODC mRNA level by 1.16-fold ( $P < 0.05$ ), ODC activity 1.63-fold ( $P < 0.05$ ), and putrescine content 4.41-fold ( $P < 0.01$ ), respectively. But there was not significant difference between them.

**CONCLUSION:** Gastrin is an agent which promotes IEC-6 cell proliferation involved in regulating ODC activity mechanism.

Zhang JL, Chen WW. Proliferation of intestinal crypt cells by gastrin-induced ornithine decarboxylase. *World J Gastroenterol* 2002;8(1):183-187

## INTRODUCTION

Increasing evidence has demonstrated that cell proliferation, differentiation and migration in the intestinal mucosa is dependent on the supply of polyamines to the dividing cells<sup>[1-8]</sup>. Intracellular polyamine levels are highly regulated<sup>[9-15]</sup> and completely depend on the activation or inhibition of ornithine decarboxylase (ODC), which is the first rate-limiting step in polyamine biosynthesis<sup>[16-22]</sup>. In addition to the general effect of metabolic hormones, the amount of ODC in the gastrointestinal mucosa is also regulated by growth-related gut peptides present in the diet or secreted from digestive glands<sup>[23-29]</sup>. Gastrin is an important gut peptide which stimulates cell proliferation in the mucosa under physiological condition<sup>[30]</sup>. Administration of gastrin significantly increases ODC activity and intracellular polyamine levels in intestinal epithelial cells<sup>[30]</sup>. Intestinal epithelial restitution is a complex process. Because of the limitation to

study such issues in natural mucosae, cultured rat small intestinal epithelial cell lines (IEC-6) were commonly employed to characterize the physiological events such as growth, differentiation, metabolism and so on during restitution in detail. In the present study, we investigated the influence of gut peptide gastrin on the proliferation, expression of the ODC gene, ODC activity and polyamine biosynthesis in cultured normal rat intestinal crypt cells (IEC-6 cell line).

## MATERIALS AND METHODS

### *Chemicals and supplies*

IEC-6 cell line (CRL-1592) was purchased from American Type Culture Collection (ATCC, Rockville, MD) at passage 13. Disposable culture was purchased from Corning Glass Works (Corning, NY). Dulbecco's modified Eagle's medium containing 4500 mg·L<sup>-1</sup> D-glucose, L-glutamine, 25 mmol·L<sup>-1</sup> HEPES buffer and pyridoxine hydrochloride (DMEM), dialyzed fetal bovine serum (dFBS), trypsin-EDTA solution, gentamicin sulfate and insulin, Dulbecco's PBS (D-PBS), and biochemicals such as pentagastrin, putrescine, sodium dodecyl sulfate (SDS) and 3-(4,5-dimethylthiazol-2-yl)-2,5-diphenyl-tetrazolium bromide (MTT) were from Sigma (St. Louis, MO). L-[1-<sup>14</sup>C]ornithine (sp act 1.93 TBq·mol<sup>-1</sup>) was purchased from NEN (Boston, MA).

### *General experimental protocol*

To insure the highest level of viability, the culture was started as soon as possible upon receipt of the vial. Thaw the vial by gentle agitation in 37°C water bath and decontaminate by dipping in 700 mL·L<sup>-1</sup> ethanol, transfer the vial contents to 25 cm<sup>2</sup> tissue culture flasks containing 10 mL DMEM supplemented with 50 g·L<sup>-1</sup> dFBS, 10 mg·L<sup>-1</sup> insulin, and 50 mg·L<sup>-1</sup> gentamicin sulfate (cDMEM) then place into the incubator for 15 min prior to addition of the vial contents to allow the medium to reach its normal pH (7.2). Incubate the cells at 37°C in a humidified atmosphere of 900 mL·L<sup>-1</sup> air-100 mL·L<sup>-1</sup> CO<sub>2</sub>. Stock cells were subcultured once a week; and the medium was changed three times weekly. The cells were restarted from frozen stock every five to six passages. Tests for mycoplasma were routinely negative. For cell counting and subculturing, the cells were dispersed with 0.5 g·L<sup>-1</sup> trypsin and 0.2 g·L<sup>-1</sup> EDTA. Remove the solution and add 1 - 2 mL of trypsin-EDTA solution. Allow the flask to sit at room temperature until the cells detach. Add fresh culture medium, aspirate and dispense into new culture flasks.

### *Treatment of pentagastrin on IEC-6 cells*

IEC-6 cell numbers were directly measured with the help of a cell counter, and plated in 96-wells with 200 μL cDMEM, or 6-wells with 2000 μL cDMEM. The cells were incubated in a humidified atmosphere at 37°C in 900 mL·L<sup>-1</sup> air-100 mL·L<sup>-1</sup> CO<sub>2</sub>, which was followed by a period of different experimental treatments. Pentagastrin was dissolved in two or three drops of 300 g·L<sup>-1</sup> ammonium hydroxide (sterile), adjusted to pH 7.5, and then diluted with medium to the desired concentrations before use. Media pentagastrin were prepared immediately before the experiments.

In the first series of studies, we examined the effect of pentagastrin on cell proliferation in IEC-6 cells. Cells were plated in

96-well microplates at a density of  $1 \times 10^4$  cells per well with 200  $\mu$ L cDMEM and grown in incubator under the condition described above. After 24h, 10  $\mu$ L media pentagastrin were added at final concentrations of 500 and 250  $\mu$ g $\cdot$ L $^{-1}$ . Control cells were fed with fresh medium without gastrin as well. To determine the time course of cell proliferation, cell numbers were measured at different time points after exposure of the cells to pentagastrin with MTT assay.

In the second series of studies, we examined the effect of pentagastrin on cellular ODC mRNA levels, ODC enzyme activity and putrescine content in IEC-6 cells. Cells were plated in 6-well microplates at a density of  $2 \times 10^6$  cells per well with 2000  $\mu$ L cDMEM and grown under incubator at the condition described above. After 24h, 100  $\mu$ L media pentagastrin were added at final concentrations of 250 and 500  $\mu$ g $\cdot$ L $^{-1}$ , respectively. Control cells were fed with fresh medium without gastrin as well. Cultures were harvested at 12h after exposure of the cells to pentagastrin. The dishes were placed on ice, the monolayers were washed three times with ice-cold D-PBS, and different solutions were then added according to the assays to be conducted.

### Measurement of ODC mRNA level

Total RNA was isolated from IEC-6 cells using RNA TRIzol reagent from Gibco (Gaithersburg, MD). Isolation and extraction were performed according to the manufacturer's protocol. Briefly, the cells were washed with Dulbecco's PBS and were lysed with 1.0mL Trizol/well.

RNA was extracted with 0.2mL chloroform and precipitated with 0.5 mL isopropanol. The precipitated RNA was washed with 1mL 700mL $\cdot$ L $^{-1}$  ethanol and redissolved in RNase-free water. The concentration of the extracted RNA was calculated by measuring the absorbance at 260nm. The ratio of the absorbance at 260nm to that at 280nm was always  $>1.9$ .

Aliquots of RNA (5  $\mu$ g) were reverse-transcribed using an RT-PCR kit from Gibco (Gaithersburg, MD). Briefly, 5  $\mu$ g RNA in 10  $\mu$ L of diethyl pyrocarbonate-treated water (DEPC-water) was mixed with 1  $\mu$ L of 50  $\mu$ mol $\cdot$ L $^{-1}$  oligo(dT) $_{20}$ , heated at 65 $^{\circ}$ C for 5min, and then placed on ice. The following reagents were added to the tubes: 4  $\mu$ L of 5 $\times$  concentrated cDNA synthesis buffer, 1  $\mu$ L of 0.1mol $\cdot$ L $^{-1}$  DTT, 1  $\mu$ L of RNaseOUT (40MU $\cdot$ L $^{-1}$ ), 1  $\mu$ L of DEPC-water, 2  $\mu$ L of 10mmol $\cdot$ L $^{-1}$  dNTP Mix, and 1  $\mu$ L of ThermoScript RT (15MU $\cdot$ L $^{-1}$ ). The reaction mixture was incubated for 50min at 50 $^{\circ}$ C before the reaction was terminated by incubating the tube at 85 $^{\circ}$ C for 5min. The mixture was added with 1  $\mu$ L RNase H and incubated at 37 $^{\circ}$ C for 20min. The tube was stored at -80 $^{\circ}$ C until PCR was performed using the Platinum Taq DNA polymerase with rat-specific primers prepared on a DNA synthesizer (Seagon, Shanghai, China). The primers were designed according to sequences of rat ornithine decarboxylase gene (EC 4.1.1.17), as follows: upstream primer: 5' $\rightarrow$ TGG CTG GCG CTG GTC TGT AGT $\leftarrow$ 3'; downstream primer: 5' $\rightarrow$ AGC TCC TGC CTG GGT.CTT.ATG A $\leftarrow$ 3'.

The cDNA amplification products were predicted to be 300bp in length for ODC. To initiate the PCR, 2  $\mu$ L RT products were added to the PCR master mix, including 5  $\mu$ L 10 $\times$  PCR reaction buffer, 2  $\mu$ L 50mmol $\cdot$ L $^{-1}$  MgCl $_2$ , 0.2  $\mu$ L Platinum Taq DNA polymerase (5MU $\cdot$ L $^{-1}$ ), 1  $\mu$ L 10  $\mu$ mol $\cdot$ L $^{-1}$  each of the primers, 10mmol $\cdot$ L $^{-1}$  dNTP Mix and 37.8  $\mu$ L DEPC-water. Tubes were placed in a programmed tempcontrol system (PE) as follows: 1) incubation at 94 $^{\circ}$ C for 2min (initial denaturation); 2) 40 cycles of the following sequential steps: 94 $^{\circ}$ C for 30s (denaturation), 60 $^{\circ}$ C for 30s (annealing), and 72 $^{\circ}$ C for 1min (extension); and 3) incubation at 72 $^{\circ}$ C for 7min (final extension). The PCR products were size-fractionated by agarose gel electrophoresis. After electrophoresis and ethidium bromide staining, DNA bands were visualized and the relative levels of mRNA for ODC were corrected for cDNA loading as measured with an ultraviolet transilluminator.

### Assay for ODC activity

ODC activity was determined with radiometric technique in which the amount of  $^{14}$ CO $_2$  liberated from DL-[L- $^{14}$ C]ornithine was estimated. Samples were collected as described above and placed in 0.5mL of 20mmol $\cdot$ L $^{-1}$  Tris buffer (pH7.4) containing 0.05mmol $\cdot$ L $^{-1}$  EDTA, 0.05mmol $\cdot$ L $^{-1}$  pyridoxal phosphate, and 5mmol $\cdot$ L $^{-1}$  dithiothreitol. The cells were frozen and thawed three times, scraped, and transferred to Eppendorf tubes. Cells were centrifuged at 12000g at 4 $^{\circ}$ C for 15min. The ODC activity of an aliquot of the supernatant was determined during incubation in stoppered vials in the presence of 7.6nmol of [ $^{14}$ C] ornithine (sp act 1.93TBq $\cdot$ mol $^{-1}$ ) for 15min at 37 $^{\circ}$ C. The  $^{14}$ CO $_2$  liberated by the decarboxylation of ornithine was trapped on a piece of filter paper impregnated with 20  $\mu$ L of 2mol $\cdot$ L $^{-1}$  NaOH, which was suspended in a center well above the reaction mixture. The reaction was stopped by the addition of trichloroacetic acid to a final concentration of 100g $\cdot$ L $^{-1}$ . The  $^{14}$ CO $_2$  trapped in the filter paper was measured by liquid scintillation spectroscopy at a counting efficiency of 95%. Aliquots of the 12000g supernatant were assayed for total protein, by Lowry method. Enzymatic activity was expressed as picomoles of CO $_2$  per milligram of protein per hour.

### Analysis of cellular putrescine

The cellular putrescine content was analyzed by HPLC as described previously<sup>[5]</sup>. In brief, after monolayers were washed three times with ice-cold D-PBS, 0.5mol $\cdot$ L $^{-1}$  perchloric acid were added and the monolayers were frozen at -80 $^{\circ}$ C until ready for extraction, dansylation, and HPLC cells were harvested, and centrifuged at 1600g for 10min. This supernatant was collected, neutralized to pH 7.0 with 3mol $\cdot$ L $^{-1}$  KOH, and centrifuged to remove the precipitate. A 0.5mL aliquot of solution was delivered to clean Eppendorf tubes. After addition of 0.25mL saturated Na $_2$ CO $_3$  and 0.5mL dansyl chloride solution (10g $\cdot$ L $^{-1}$  acetone), reaction was allowed to proceed by heating at 70 $^{\circ}$ C for 30min and then added to 1.5mL toluene. After mixing and centrifugation, the organic protein portion was collected and dried by vacuum centrifugation. To the residue, 300  $\mu$ L methanol was added and filtered, and an aliquot of 200  $\mu$ L was used for HPLC analysis. Solvent A and B were composed of acetonitrile, water, glacial acetic acid, and triethylamine in the volume proportions of 80:20:0.02:0.001 and 95:5:0.02:0.005, respectively. The mobile phases used in this separation consisted of 60% solvent A and 40% solvent B. Each sample was run for 20min, and the equilibration delay between injections was 2min. Sufficient mobile phases (A and B) were prepared fresh before starting the automatic injector. The polyamine putrescine was measured by comparing ratios of polyamines to 1,10-diaminodecane peak areas with a standard curve. Protein was dissolved in 1mol $\cdot$ L $^{-1}$  NaOH and determined by the Lowry method. The results were expressed as nanomoles of polyamines per milligram of protein.

### Statistics

All data are expressed as  $\bar{x} \pm s$  from three-four dishes. The significance of the difference between means was determined by independent *t* test using SPSS statistical software.

## RESULTS

### Effect of gastrin on the proliferation Of IEC-6 cells

IEC-6 cells were grown in cDMEM in the presence or absence of pentagastrin. Exposure of IEC-6 cells to pentagastrin, the proliferation increased initially on d1 and reached a peak on d3 in 250  $\mu$ g $\cdot$ L $^{-1}$  concentration. Pentagastrin 500  $\mu$ g $\cdot$ L $^{-1}$  increased cell proliferation on d1 and d2 and then decreased as shown in Figure 1.



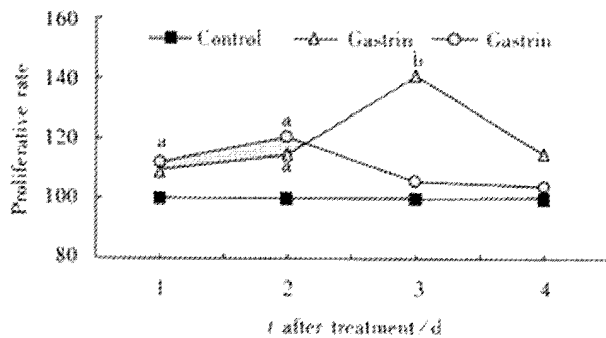


**Figure 1** Gastrin effect on IEC-6 proliferation by the MTT assay. <sup>a</sup> $P < 0.05$ , <sup>b</sup> $P < 0.01$  vs control.

### ODC mRNA amount in IEC-6 cells treated with gastrin

Administration of pentagastrin 250 and 500  $\mu\text{g}\cdot\text{L}^{-1}$  significantly raised the ODC mRNA levels by 1.16-fold and 1.09-fold, respectively as compared with control group (Figure 2). But there was no significant difference between the two doses of gastrin.

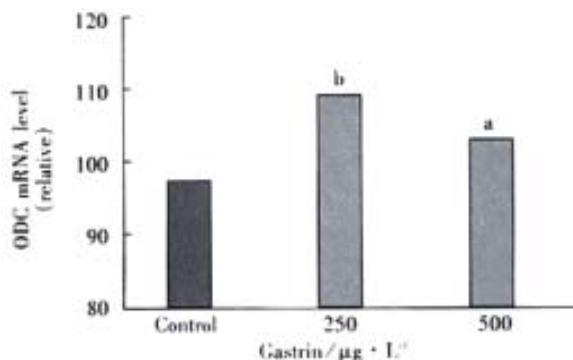


**Figure 2** ODC mRNA levels in IEC-6 cells. <sup>a</sup> $P < 0.05$ , <sup>b</sup> $P < 0.01$  vs control.

### Gastrin induction of ODC activity

In these studies, IEC-6 cells were grown in cDMEM in the presence or absence of pentagastrin. This exposure of IEC-6 cells to pentagastrin 250 and 500  $\mu\text{g}\cdot\text{L}^{-1}$  caused ODC activity to increase significantly by 1.71-fold and 1.63-fold, respectively at 12h after treatment as compared with control group. But there was no significant difference between them (Figure 3).

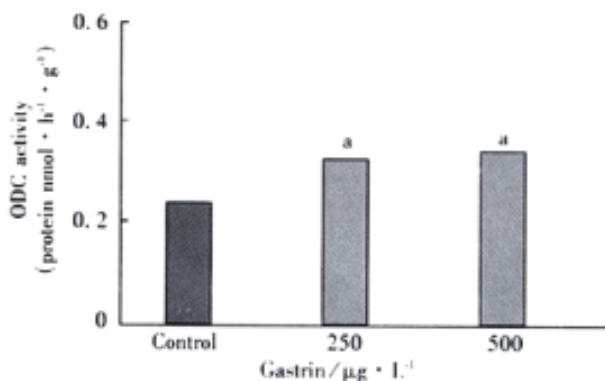


**Figure 3** ODC activity in IEC-6 cells exposed to pentagastrin. <sup>a</sup> $P < 0.05$  vs control.

### Effect of pentagastrin on putrescine content in IEC-6 cells

Increases in ODC activity in cells exposed to pentagastrin were paralleled with increases in cellular putrescine levels. Compared with a value of  $0.46 \pm 0.02 \mu\text{mol}\cdot\text{g}^{-1}$  from 4 cultures in the control group, the cellular putrescine levels treated with pentagastrin 250 and 500  $\mu\text{g}\cdot\text{L}^{-1}$  significantly increased ( $P < 0.01$ ), the values were  $2.44 \pm 0.05 \mu\text{mol}\cdot\text{g}^{-1}$  and  $2.03 \pm 0.03 \mu\text{mol}\cdot\text{g}^{-1}$  from 4 cultures, which were 5.30-fold and 4.41-fold of control group, respectively.

### DISCUSSION

Numerous studies have demonstrated that polyamine biosynthesis plays a critical role in the control of normal mucosal growth and repair<sup>[1-12]</sup> and that ODC in small intestinal mucosa has a high basal activity compared with most tissues and significantly increases in response to a variety of chronic and acute mitogenic stimuli<sup>[16-29]</sup>. The rapid and striking increases in ODC and polyamine levels are absolutely required for the stimulation of intestinal mucosal growth<sup>[16-21]</sup>.

IEC-6 cells which were established by Quaroni *et al* are derived from neonatal normal rat small intestine and have characteristics of crypt-type epithelial cells as judged by morphological and immunologic criteria which do not exhibit differentiated morphology or specific gene expression. They are nontumorigenic and retain the undifferentiated character of epithelial stem cells. These cells exhibit a number of features of normal cells in culture: i.e. a normal rat diploid karyotype, strong density inhibition of growth, lack of growth in soft agar, and a low plating efficiency when seeded at low density. The establishment of IEC-6 cell lines play an important role in functional researches of small intestine epithelial cells such as growth, differentiation, metabolism, the pharmacological effects, and the pathophysiological changes and the mechanism of intestinal mucosa resulted from various pathogenic factors. This cell line also provided an appropriate *in vitro* model for the study on cell proliferation and mucosal healing. This cell line was broadly used in the studies on cellular, molecular and genetic mechanism of small intestinal mucosal repair since the establishment<sup>[31-40]</sup>.

The gastrointestinal mucosa must maintain a barrier against the harsh luminal contents of acid, enzymes, bacteria, and toxins. Disruption of this barrier is the salient feature of a variety of common and important gastrointestinal disorders, including inflammatory bowel disease and peptic ulcers. The mucosal epithelium of the small intestine has the capacity for rapid renewal and adaptation after injury or resection. Crypt cell proliferation leading to intestinal growth and promoting re-establishment of mucosal integrity after injury are essential processes for the differentiation, maintenance, and repair of the intestinal epithelium and are regulated via a complex interplay of nutrients, pancreatic and biliary secretions, and both locally derived and circulating growth factors<sup>[41-51]</sup>.

It is of interest and important to investigate the effect of growth-related gut peptides on the regulation of ODC activity in intestinal epithelial cells. The current study clearly shows that, in small intestinal crypt cells maintained in cDMEM, gastrin stimulates cell proliferation, increases ODC mRNA levels, ODC activity and polyamine content, in which the effects of pentagastrin 250  $\mu\text{g}\cdot\text{L}^{-1}$  seems to be better than those of 500  $\mu\text{g}\cdot\text{L}^{-1}$ . Consistent with the results reported by other authors<sup>[30]</sup> higher dosage of pentagastrin ( $>1000 \mu\text{g}\cdot\text{L}^{-1}$ ) inhibited IEC-6 cell proliferation (data not shown).

In summary, our results indicate that the increased ODC activity in IEC-6 cells treated with gastrin is associated with a rise in ODC mRNA levels and an increase of intracellular putrescine resulting in cell proliferation. It suggests that the induction of ODC activity by gastrin plays an important role in the regulation of cell proliferation in the intestinal mucosa under physiological condition.

**ACKNOWLEDGEMENTS** We would like to thank Prof. Wang

Zhou, Drs Han and Yu, and Mr Pan for their technical advice and excellent assistance.

## REFERENCES

- 1 Loser C, Eisel A, Harms D, and Folsch UR. Dietary polyamines are essential luminal growth factors for small intestinal and colonic mucosal growth and development. *Gut* 1999 Jan; 44: 12-16
- 2 Bardocz S, Grant G, Brown DS, and Pusztai A. Putrescine as a source of instant energy in the small intestine of the rat. *Gut* 1998; 42: 24-28
- 3 Greco S, Huguency I, George P, Perrin P, Louisot P, and Biol MC. Influence of spermine on intestinal maturation of the glycoprotein glycosylation process in neonatal rats. *Biochem J* 2000; 345(Pt 1): 69-75
- 4 Banan A, McCormack SA, and Johnson LR. Polyamines are required for microtubule formation during gastric mucosal healing. *Am J Physiol* 1998;274: G879-885
- 5 Patel AR, Li J, Bass BL, and Wang JY. Expression of the transforming growth factor beta gene during growth inhibition following polyamine depletion. *Am J Physiol* 1998; 275: C590-598
- 6 McCormack SA, Blanner PM, Zimmerman BJ, Ray R, Poppleton HM, and Patel TB. Polyamine deficiency alters EGF receptor distribution and signaling effectiveness in IEC-6 cells. *Am J Physiol* 1998; 274: C192-205
- 7 Wang JY, Wang J, Golovina VA, Li L, Platoshy O, and Yuan JX. Role of K(+) channel expression in polyamine-dependent intestinal epithelial cell migration. *Am J Physiol Cell Physiol* 2000; 278: C303-314
- 8 Wang JY, Viar MJ, Shi HJ, Patel AR, and Johnson LR. Differences in transglutaminase mRNA after polyamine depletion in two cell lines. *Am J Physiol* 274 (Cell Physiol. 43): C522-C530
- 9 Wang W and Higuchi CM. Dietary soy protein is associated with reduced intestinal mucosal polyamine concentration in male Wistar rats. *J Nutr* 2000; 130: 1815-1820
- 10 Noack J, Kleessen B, Proll J, Dongowski G, and Blaut M. Dietary guar gum and pectin stimulate intestinal microbial polyamine synthesis in rats. *J Nutr* 1998; 128: 1385-1391
- 11 Patel AR, and Wang JY. Polyamine depletion is associated with an increase in JunD/AP-1 activity in small intestinal crypt cells. *Am J Physiol* 1999;276:G441-450
- 12 Ray RM, Viar MJ, Yuan Q, and Johnson LR. Polyamine depletion delays apoptosis of rat intestinal epithelial cells. *Am J Physiol Cell Physiol* 2000; 278: C480-489
- 13 Ray RM, Zimmerman BJ, McCormack SA, Patel TB, and Johnson LR. Polyamine depletion arrests cell cycle and induces inhibitors p21(Waf1/Cip1), p27(Kip1), and p53 in IEC-6 cells. *Am J Physiol* 1999; 276: C684-691
- 14 McCormack SA, Ray RM, Blanner PM, and Johnson LR. Polyamine depletion alters the relationship of F-actin, G-actin, and thymosin beta4 in migrating IEC-6 cells. *Am J Physiol* 1999; 276: C459-468
- 15 Li L, Li J, Rao JN, Li M, Bass BL, and Wang JY. Inhibition of polyamine synthesis induces p53 gene expression but not apoptosis. *Am J Physiol* 1999; 276: C946-954
- 16 Guo Y, Harris RB, Rosson D, Boorman D, and O'Brien TG. Functional Analysis of Human Ornithine Decarboxylase Alleles. *Cancer Res* 2000;60: 6314-6317
- 17 Noda J, Iwakiri R, Fujimoto K, Matsuo S, and Aw TY. Programmed cell death induced by ischemia-reperfusion in rat intestinal mucosa. *Am J Physiol* 1998 Aug; 274 (Gastrointest.Liver Physiol. 37):G270-276
- 18 Ray RM, Viar MJ, Patel TB, and Johnson LR. Interaction of asparagine and EGF in the regulation of ornithine decarboxylase in IEC-6 cells. *Am J Physiol* 1999; 276: G773-780
- 19 Wang JY, Li J, Patel AR, Summers S, Li L, and Bass BL. Synergistic induction of ornithine decarboxylase by asparagine and gut peptides in intestinal crypt cells. *Am J Physiol* 1998; 274: C1476-1484
- 20 Jacoby RF, Cole CE, Tutsch K, Newton MA, Kelloff G, Hawk ET, and Lubet RA. Chemopreventive efficacy of combined piroxicam and difluoromethylornithine treatment of Apc mutant Min mouse adenomas, and selective toxicity against Apc mutant embryos. *Cancer Res* 2000; 60: 1864-1870
- 21 Meyskens FL, and Gerner EW. Development of difluoromethylornithine (DFMO) as a chemoprevention agent. *Clin. Cancer Res* 1999;5:945-951
- 22 Hori T, Wanibuchi H, Yano Y, Otani S, Nishikawa A, Osugi H, Kinoshita H, and Fukushima S. Epithelial cell proliferation in the digestive tract induced by space restriction and water-immersion stress. *Cancer Lett* 1998; 125: 141-148
- 23 Gke M, Kanai M, and Daniel KP. Intestinal fibroblasts regulate intestinal epithelial cell proliferation via hepatocyte growth factor. *Am J Physiol* 1998;274 (Gastrointest-Liver Physiol.5): G809-G818
- 24 DeMarco V, Dyess K, Strauss D, West CM, and Neu J. Inhibition of glutamine synthetase decreases proliferation of cultured rat intestinal epithelial cells. *J Nutr* 1999; 129: 57-62
- 25 Jehle PM, Fussgaenger RD, Angelus NK, Jungwirth RJ, Saile B, and Lutz MP. Proinsulin stimulates growth of small intestinal crypt-like cells acting via specific receptors. *Am J Physiol* 1999; 276: E262-268
- 26 Taupin DR, Kinoshita K, and Podolsky DK. Intestinal trefoil factor confers colonic epithelial resistance to apoptosis. *Proc Natl Acad Sci U S A* 2000; 97: 799-804
- 27 Rao JN, Li J, Li L, Bass BL, and Wang JY. Differentiated intestinal epithelial cells exhibit increased migration through polyamines and myosin II. *Am J Physiol* 1999; 277: G1149-1158
- 28 Qing Y, Viar MJ, Ray RM, and Johnson LR. Putrescine does not support the migration and growth of IEC 6 cells. *Am J Physiol* 2000; 278 (Gastrointest-Liver Physiol.1): G49-G56
- 29 Pfeffer LM, Yang CH, Pfeffer SR, Murti A, McCormack SA, and Johnson LR. Inhibition of ornithine decarboxylase induces STAT3 tyrosine phosphorylation and DNA binding in IEC-6 cells. *Am J Physiol Cell Physiol* 2000; 278: C331-335
- 30 Jonson L, Bundgaard JR, Johnsen AH, and Rourke JJ. Identification and expression of gastrin and cholecystokinin mRNAs from the turtle, *Pseudemys scripta*: evidence of tissue-specific tyrosyl sulfation (1). *Biochim Biophys Acta* 1999; 1435: 84-93
- 31 Chen XM, and Larusso NF. Mechanisms of attachment and internalization of *Cryptosporidium parvum* to biliary and intestinal epithelial cells. *Gastroenterology* 2000;118:368-378
- 32 Miyazaki Y, Shinomura Y, Tsutsui S, Kitamura S, Hiraoka S, and Matsuzawa Y. Calphostin C induces expression of amphiregulin mRNA via reactive oxygen species in IEC-6 cells. *Life Sci* 1998; 63: PL361-365
- 33 Sonoyama K, Rutatip S, and Kasai T. Gene expression of activin, activin receptors, and follistatin in intestinal epithelial cells. *Am J Physiol* 2000; 278 (Gastrointest.Liver Physiol.37):G89-97
- 34 Fabbri A, Falzano L, Frank C, Donelli G, Matarrese P, Raimondi F, Fasano A, Fiorentini C. *Vibrio parahaemolyticus* thermostable direct hemolysin modulates cytoskeletal organization and calcium homeostasis in intestinal cultured cells. *Infect Immun* 1999; 67: 1139-1148
- 35 Kumar CK, Nguyen TT, Gonzales FB, and Said HM. Comparison of intestinal folate carrier clone expressed in IEC-6 cells and in *Xenopus* oocytes. *Am J Physiol* 1998; 274: C289-294
- 36 Shinohara H, Killion JJ, Bucana CD, Yano S, and Fidler IJ. Oral administration of the immunomodulator JBT-3002 induces endogenous interleukin 15 in intestinal macrophages for protection against irinotecan-mediated destruction of intestinal epithelium. *Clin Cancer Res* 1999; 5: 2148-2156
- 37 Jobin C, Holt L, Bradham CA, Streetz K, Brenner DA, and Sartor RB. TNF receptor-associated factor-2 is involved in both IL-1 beta and TNF-alpha signaling cascades leading to NF-kappa B activation and IL-8 expression in human intestinal epithelial cells. *J Immunol* 1999; 162: 4447-4454
- 38 Rivard N, Boucher MJ, Asselin C, and L'Allemain G. MAP kinase cascade is required for p27 downregulation and S phase entry in fibroblasts and epithelial cells. *Am J Physiol* 1999; 277: C652-664
- 39 Erwin CR, Helmrath MA, Shin CE, Falcone RA Jr, Stern LE, and Warner BW. Intestinal overexpression of EGF in transgenic mice enhances adaptation after small bowel resection. *Am J Physiol* 1999; 277 (Gastrointest-Liver Physiol. 3): G533-G540
- 40 Sturm A, Sudermann T, Schulte KM, Goebell H, and Dignass AU. Modulation of intestinal epithelial wound healing *in vitro* and *in vivo* by lysophosphatidic acid. *Gastroenterology* 1999; 117: 368-377

- 41 Quaroni A, Tian JQ, Goke M, and Podolsky DK. Glucocorticoids have pleiotropic effects on small intestinal crypt cells. *Am J Physiol* 1999; 277: G1027-1040
- 42 Nishimura S, Takahashi M, Ota S, Hirano M, and Hiraishi H. Hepatocyte growth factor accelerates restitution of intestinal epithelial cells. *J Gastroenterol* 1998; 33: 172-178
- 43 Varedi M, Greeley GH Jr, Herndon DN, and Englander EW. A thermal injury-induced circulating factor(s) compromises intestinal cell morphology, proliferation, and migration. *Am J Physiol* 1999; 277: G175-182
- 44 Ruthig DJ, and Meckling Gill KA. Both (n-3) and (n-6) fatty acids stimulate wound healing in the rat intestinal epithelial cell line, IEC-6. *J Nutr* 1999; 129: 1791-1798
- 45 Bocker U, Damiao A, Holt L, Han DS, Jobin C, Panja A, Mayer L, and Sartor RB. Differential expression of interleukin 1 receptor antagonist isoforms in human intestinal epithelial cells. *Gastroenterology* 1998; 115: 1426-1438
- 46 Vreugdenhil AC, Dentener MA, Snoek AM, Greve JW, and Buurman WA. Lipopolysaccharide binding protein and serum amyloid A secretion by human intestinal epithelial cells during the acute phase response. *J Immunol* 1999; 163: 2792-2798
- 47 Awane M, Andres PG, Li DJ, and Reinecker HC. NF-kappa-B-inducing kinase is a common mediator of IL-17-, TNF-alpha-, and IL-1 beta-induced chemokine promoter activation in intestinal epithelial cells. *J Immunol* 1999; 162: 5337-5344
- 48 Nikawa T, Rokutan K, Nanba K, Tokuoka K, Teshima S, Engle MJ, Alpers DH, and Kishi K. Vitamin A up-regulates expression of bone-type alkaline phosphatase in rat small intestinal crypt cell line and fetal rat small intestine. *J Nutr* 1998; 128: 1869-1877
- 49 Cario E, Rosenberg IM, Brandwein SL, Beck PL, Reinecker HC, and Podolsky DK. Lipopolysaccharide activates distinct signaling pathways in intestinal epithelial cell lines expressing Toll-like receptors. *J Immunol* 2000; 164: 966-972
- 50 Shigematsu T, Miura S, Hirokawa M, Hokari R, Higuchi H, Watanabe N, Tsuzuki Y, Kimura H, Tada S, Nakatsumi RC, Saito H1, and Ishii H. Induction of endothelin-1 synthesis by IL-2 and its modulation of rat intestinal epithelial cell growth. *Am J Physiol* 1998; 275 (Gastrointest.Liver Physiol.3): G556-G563
- 51 Rhoads JM, Argenzio RA, Chen W, Graves LM, Licato LL, Blikslager AT, Smith J, Gatzky J, and Brenner DA. Glutamine metabolism stimulates intestinal cell MAPKs by a cAMP-inhibitable, Raf-independent mechanism. *Gastroenterology* 2000; 118: 90-100

• BASIC RESEARCH •

# Study on the mechanism of regulation on peritoneal lymphatic stomata with Chinese herbal medicine

Shi-Ping Ding, Ji-Cheng Li, Jian Xu, Lian-Gen Mao

Shi-Ping Ding, Ji-Cheng Li, Lian-Gen Mao, Department of Lymphology, Department of Histology and Embryology, Medical College of Zhejiang University, School of Medicine, Hangzhou 310031, China

Jian Xu, Hangzhou First People's Hospital, Hangzhou 310001, China

Supported by the National Natural Science Foundation of China, No. 39970934, Scientific Research Fund by the Science Technology Committee of Hangzhou, State Administration of Traditional Chinese Medicine, No. 927031, Zhejiang Provincial Administration of Traditional Chinese Medicine, fund for outstanding talents by the Chinese Ministry of Health and Analysis and Testing Fund of Zhejiang Province, No. 00159

Correspondence to: Dr. Ji-Cheng Li, Department of Lymphology, Department of Histology and Embryology, Zhejiang University, School of Medicine, Hangzhou 310031, China. lijc@mail.hz.zj.cn

Telephone: +86-571-87217139 Fax: +86-571-87217139

Received 2001-08-23 Accepted 2001-11-05

## Abstract

**AIM:** To study the mechanism of Chinese herbal medicine (CHM, the prescription consists of *Radix Salviae Miltiorrhizae*, *Radix Codonopsis*, *Pilosulae*, *Rhizoma Atractylodis Alba* and *Rhizoma Alismatis*, *Leonurus Heterophyllus* Sweet, etc) on the regulation of the peritoneal lymphatic stomata and the ascites drainage.

**METHODS:** The mouse model of live fibrosis was established with the application of intragastric installations of carbon tetrachloride once every three days; scanning electron microscope and computer image processing were used to detect the area and the distributive density of the peritoneal lymphatic stomata; and the concentrations of urinary ion and NO in the serum were analyzed in the experiment.

**RESULTS:** Two different doses of CHM could significantly increase the area of the peritoneal lymphatic stomata, promote its distributive density and enhance the drainage of urinary ion such as sodium, potassium and chlorine. Meanwhile, the NO concentration of two different doses of CHM groups was  $133.52 \pm 23.57 \mu\text{mol/L}$ , and  $137.2 \pm 26.79 \mu\text{mol/L}$  respectively. In comparison with the control group and model groups ( $48.36 \pm 6.83 \mu\text{mol/L}$ , and  $35.22 \pm 8.94 \mu\text{mol/L}$ ,  $P < 0.01$ ), there existed significantly marked difference, this made it clear that Chinese herbal medicine could induce high endogenous NO concentration. The effect of Chinese herbal medicine on the peritoneal lymphatic stomata and the drainage of urinary ion was altered by adding NO donor (sodium nitroprusside, SNP) or NO synthase (NOS) inhibitor (N(G)-monomethyl-L-arginine, L-NMMA) to the peritoneal cavity.

**CONCLUSION:** There existed correlations between high NO concentration and enlargement of the peritoneal lymphatic stomata, which result in enhanced drainage of ascites. These data supported the hypothesis that Chinese herbal medicine could regulate the peritoneal lymphatic stomata by accelerating the synthesis and release of endogenous NO.

Ding SP, Li JC, Xu J, Mao LG. Study on the mechanism of regulation on

peritoneal lymphatic stomata with Chinese herbal medicine. *World J Gastroenterol* 2002;8(1):188-192

## INTRODUCTION

Numerous investigations have demonstrated that the peritoneal lymphatic stomata are small openings of the subperitoneal lymphatic vessels both in animals and in humans<sup>[1-18]</sup>. It has also been observed that particles, cells and solutions containing vital dyes are absorbed rapidly by the peritoneal lymphatic stomata<sup>[19-22]</sup>. Subsequent researches suggested that the peritoneal cavity is an integral part of the lymphatic system with enormous absorption powers, functioning primarily by means of the subperitoneal lymphatics via the peritoneal lymphatic stomata<sup>[23-29]</sup>. Thus, it has important clinical implications, especially in ascites drainage<sup>[30-32]</sup>. In recent years, therapeutic effect of Chinese herbal medicine (CHM) on the ascites has also drawn world wide attention among he scholars. It is further confirmed that Chinese herbal medicine can regulate the lymphatic stomata and promote the excretion of substance from the peritoneal cavity, which showed a good future in the treatment of the hepatocirrhosis with ascites<sup>[33-44]</sup>. However, it is still unclear how the lymphatic stomata is regulated by the Chinese herbal medicine. This article aimed at the regulation of CHM on the lymphatic stomata in the mouse liver fibrosis model induced by  $\text{CCl}_4$ , which provided theoretical evidence on ascites. Furthermore, by the application of NO donor (SNP) and NOS inhibitor (L-NMMA), the effect of NO was studied on the peritoneal lymphatic stomata in order to clarify the mechanism of CHM on the regulation of the peritoneal lymphatic stomata.

## MATERIAL AND METHODS

### Experimental CHM

By examining a computerized media index, the conventional remedies of CHM was selected for the treatment of hepatocirrhosis with ascites. The Chinese composite prescription was supplied by Zhejiang Academy of Traditional Chinese Medicine. The prescription consisted of *Radix Salviae Miltiorrhizae*, *Radix Codonopsis*, *Pilosulae*, *Rhizoma Atractylodis Alba* and *Rhizoma Alismatis*, *Leonurus Heterophyllus* Sweet. The medicament was immersed in the  $750 \text{ mL} \cdot \text{L}^{-1}$  alcohol for 24 hrs, then purified with rotatory evaporator (ZFQ85A type, produced by Shanghai 11th Factory of Electron Tube). The crude drug content was  $15.2 \text{ g} \cdot \text{mL}^{-1}$ .

### Animal and grouping

Ninety healthy mature NIH male mice, weighing 25g-30g, provided by the Experimental Animal Center of Zhejiang Academy of Medical Sciences, were selected and divided at random into six groups (each of 15 mice): the control group (NS group), model group, low dose of CHM group (CHM I), high dose of CHM group (CHMII), the donor group (DR group) and the inhibitor group (IR group).

### Mouse liver fibrosis model

Except the NS group, the other experimental mice were fed freely with  $50 \text{ mL} \cdot \text{L}^{-1}$  alcohol solution instead of water for 1 week, then the

mice were given 100ml·L<sup>-1</sup> CCl<sub>4</sub> rape-seed oil solution 0.1ml/10g by gastrogavage every 3 days for 6 weeks to induce liver fibrosis. After liver fibrosis was confirmed by pathological examination, low dose of the Chinese herbal medicine (0.1ml/10g/day) was given to CHM I group, high dose of the Chinese herbal medicine (0.2ml/10g/day) was give to CHMII group, normal saline (0.2ml/10g/day) was given to DR group, for 3 weeks respectively. After the 10th week, DR and IR group was additionally injected intraperitoneally with 50μg/10g/day NO donor (SNP) or 80μg/10g/day NOS inhibitor (L-NMMA) for two days respectively. Model group was untreated and NS group was given 0.2ml/10g of normal saline per day.

#### **Preparation of samples for scanning electron microscopic examination and computer image processing**

The diaphragmatic peritoneum on the right side was cut into 5.0×5.0 mm<sup>2</sup> pieces and put into 25ml·L<sup>-1</sup> glutaraldehyde solution for 1 h, then postfixed for 1h in 10ml·L<sup>-1</sup> OsO<sub>4</sub>, dehydrated in a graded series of alcohol, CO<sub>2</sub> critical-point dried, mounted on aluminum tubs and sputter-coated with gold. Specimens were examined with a Stereoscan 260 SEM operated at 25kV. The result was treated with the computer image processing system attached to SEM. The system consists of video, A/D, IBM386. Software was designed for processing and quantitatively analyzing the area and the distributive density of the lymphatic stomata.

#### **Urinary volume and ionic concentration analysis**

Mouse urine was collected in 2 hrs and ionic concentration of Na<sup>+</sup>, K<sup>+</sup> and Cl<sup>-</sup> was measured using auto-biochemical analyzer (Beckman CX ∇7 type).

#### **Measurement of serum NO**

Five hundred microliters of the serum was de-proteinized with 200mL of 75mM zinc sulfate and 250mL of 55mM sodium hydroxid and subsequently were centrifuged at 3000rpm for 10min. One hundred microliters of the deproteinized solution was mixed with 0.3ml ddH<sub>2</sub>O and 0.25g newly-activated Cadmium sufficiently for 1h. The nitrite concentration was determined by mixing 0.1ml of the supernatants from the mixed solution with an equal volume of Griess reagent (1 part of 0.2% N-(1-naphthyl) ethylenediamine dihydrochloride to 1 part of 1% sulfanilamide in 2% phosphoric acid ) for 15min. The absorbance at 545 nm was measured, and the nitrite concentration was determined from a standard curve calibrated with NaNO<sub>2</sub> solution<sup>[45]</sup>.

#### **Statistic analysis**

The experimental results were described by  $\bar{x} \pm s$  and the difference among the groups was analyzed by *t* test.

## **RESULTS**

### **Changes of peritoneal lymphatic stomata**

In SEM, there were cuboidal and flattened cells in the mesothelium. The lymphatic stomata which was round or ellipse were located only among the cuboidal cells and most of them were distributed in cluster. In NS group and model groups, there were few and small lymphatic stomata (Figures 1,2). In contrast, there were many and large lymphatic stomata in CHMI and CHMII groups (Figure3, 4). In DR group, there were fewer and larger lymphatic stomata than in the model group (Figure 5), while in the IR group fewer and smaller than that of the CHMII group (Figure 6).

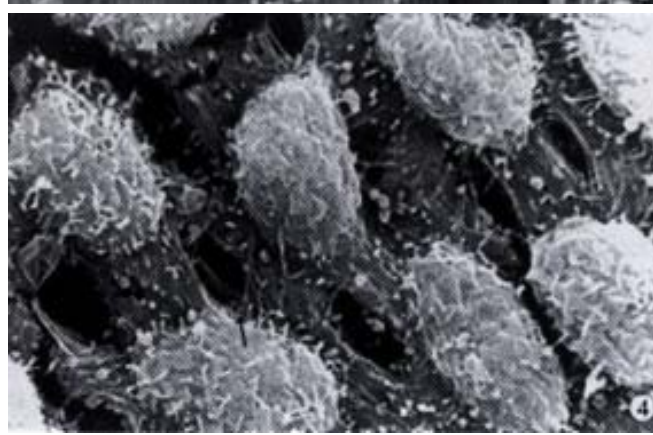
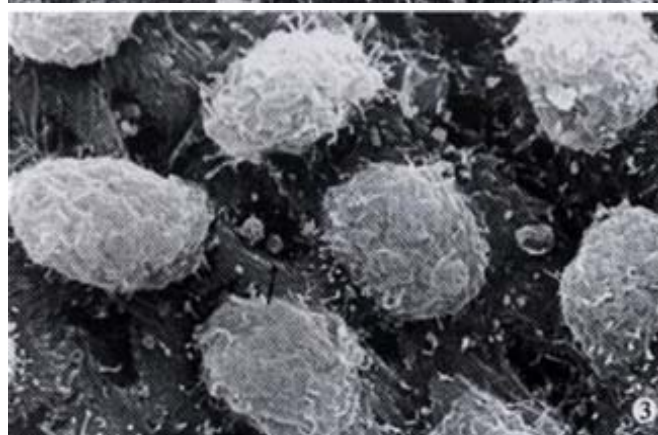
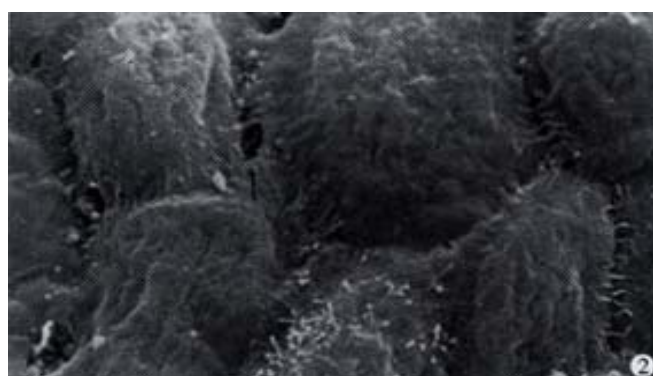
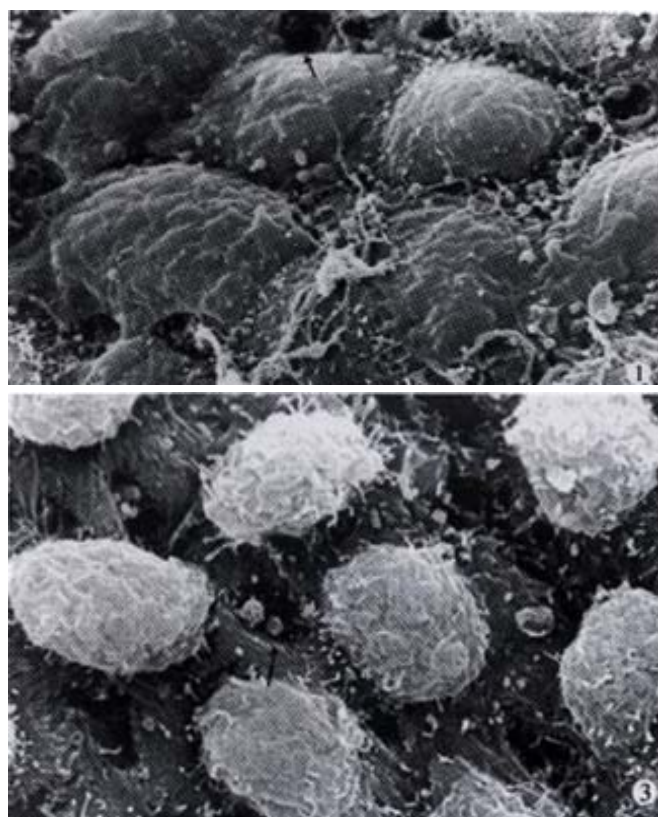


**Figure 1** SEM observation of mouse diaphragmatic peritoneum in the control group. Both the area and distribution density of the peritoneal lymphatic stomata (arrow) are small. ×3500

**Figure 2** SEM observation of mouse diaphragmatic peritoneum in model group showing the peritoneal stomata (arrow).×3500

**Figure 3** SEM observation of mouse diaphragmatic peritoneum in CHMI group. The area and distribution density of the peritoneal lymphatic stomata (arrow) are significantly increased. ×3500

**Figure 4** SEM observation of mouse diaphragmatic peritoneum in CHMII group. The area and distribution density of the peritoneal lymphatic stomata (arrow) are significantly increased. ×3500



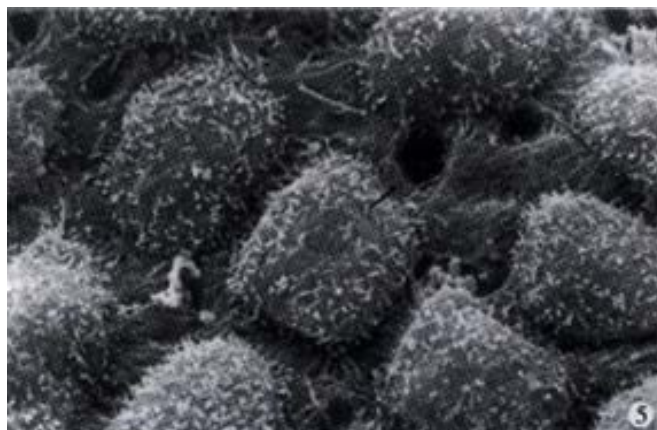


**Figure 5** SEM observation of mouse diaphragmatic peritoneum in DR group. Compared with model group, the area and distribution density of the peritoneal lymphatic stomata (arrow) are relatively increased.  $\times 3500$

**Figure 6** SEM observation of mouse diaphragmatic peritoneum in IR group. Compared with CHMII group, the area and distribution density of the peritoneal lymphatic stomata (arrow) are relatively decreased.  $\times 3500$

With image processing, the average area of the stomata was  $3.59 \pm 1.29 \mu\text{m}^2$  in NS group and  $3.02 \pm 1.11 \mu\text{m}^2$  in model group, whereas in CHMI group and CHMII group, the average area of the stomata was  $5.89 \pm 0.33 \mu\text{m}^2$ , and  $5.93 \pm 1.87 \mu\text{m}^2$  respectively. There were significant differences in the enlargement of the stomata between CHMI and CHMII groups, based on the analysis of variance ( $P < 0.01$ ). By comparing the area at the 99% confidence interval of population means, we found that the stomata area of CHMI and CHMII groups were much larger than those of NS and model groups (Table 1).

When the mouse was injected intraperitoneally by SNP, the average area of the stomata was  $4.37 \pm 0.10 \mu\text{m}^2$ , which was larger than that of the corresponding model group. When the mouse was injected intraperitoneally by L-NMMA, the average area of the stomata was  $2.70 \pm 1.30 \mu\text{m}^2$ , which was smaller than that of the corresponding CHMII group. These showed that the area of the stomata could be altered by SNP or L-NMMA significantly ( $P < 0.05$  or  $P < 0.01$ ).

**Table 1** The influence of CHM, NO donor and NOS inhibitor ( $n=15$ ) on the area of the lymphatic stomata

| Groups              | Mean ( $\mu\text{m}^2$ ) | SD   | Min. ( $\mu\text{m}^2$ ) | Max. ( $\mu\text{m}^2$ ) |
|---------------------|--------------------------|------|--------------------------|--------------------------|
| NS                  | 3.59                     | 1.29 | 0.91                     | 8.93                     |
| model group         | 3.02                     | 1.11 | 1.83                     | 7.53                     |
| CHMI <sup>bd</sup>  | 5.89                     | 0.33 | 2.00                     | 9.82                     |
| CHMII <sup>bd</sup> | 5.93                     | 1.87 | 2.08                     | 10.15                    |
| DR <sup>c</sup>     | 4.37                     | 0.10 | 1.92                     | 8.70                     |
| IR <sup>f</sup>     | 2.70                     | 1.30 | 1.75                     | 9.19                     |

<sup>a</sup> $P < 0.05$ , <sup>b</sup> $P < 0.01$ , vs NS group; <sup>c</sup> $P < 0.05$ , <sup>d</sup> $P < 0.01$ , vs model group; <sup>e</sup> $P < 0.05$ , <sup>f</sup> $P < 0.01$ , vs CHMII group

The average distribution density of the stomata of NS group, and model group were  $66.99 \pm 5.43/0.01\text{mm}^2$ ,  $42.80 \pm 13.35/0.01\text{mm}^2$ , whereas those of CHMI and CHMII group were  $92.08 \pm 4.44/0.01\text{mm}^2$ , and  $96.24 \pm 4.62/0.01\text{mm}^2$  respectively. The results showed that CHM can promote the distribution density of the stomata significantly (Figure 7) ( $P < 0.01$ ).

When the mouse was injected intraperitoneally by SNP, the average distribution density of the stomata was  $79.06 \pm 5.37\text{mm}^2/0.01\text{mm}^2$ , which was much higher than that of the corresponding model group. When the mouse was injected intraperitoneally by L-NMMA, the average distribution density of the stomata was  $60.82 \pm 30.79\text{mm}^2/0.01\text{mm}^2$ , which was much lower than that of the corresponding CHM group. The above statistics show that the distribution density of the stomata could be altered by SNP or L-

NMMA significantly ( $P < 0.01$ ).

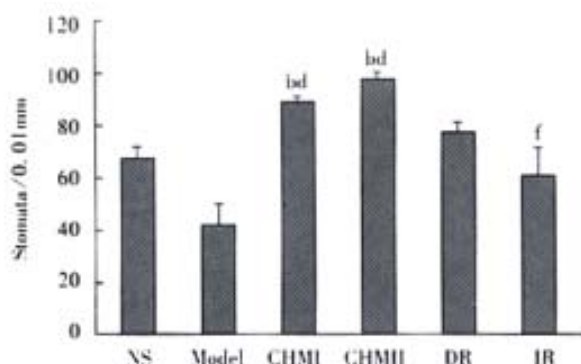


**Figure 7** The influence of CHM, NO donor and NOS inhibitor on the distribution density of the lymphatic stomata.

### Comparison of urinary ionic concentration

Subsequent experiment showed that the excretion of  $\text{Na}^+$ ,  $\text{K}^+$  and  $\text{Cl}^-$  in CHMI and CHMII group was significantly higher than those in NS group and model groups respectively ( $P < 0.01$ ) (Table 2).

When NO donor was injected intraperitoneally, the excretion of  $\text{Na}^+$ ,  $\text{K}^+$  and  $\text{Cl}^-$  in DR group was significantly higher than those in the model group ( $P < 0.05$  or  $P < 0.01$ ). When NO inhibitor was injected intraperitoneally, the excretion of  $\text{Na}^+$ ,  $\text{K}^+$  and  $\text{Cl}^-$  in IR group decreased significantly in comparison with the corresponding CHMII group ( $P < 0.05$  or  $P < 0.01$ ).

**Table 2** The effect of CHM, NO donor, NOS inhibitor on the urinary ion of the mice (mmol/L,  $n=15$ )

| Groups      | $\text{Na}^+$                  | $\text{K}^+$                   | $\text{Cl}^-$                  |
|-------------|--------------------------------|--------------------------------|--------------------------------|
| NS          | $91.55 \pm 23.42$              | $106.15 \pm 34.16$             | $111.18 \pm 30.05$             |
| model group | $97.48 \pm 42.12$              | $129.65 \pm 46.91$             | $121.90 \pm 41.65$             |
| CHMI        | $202.09 \pm 35.30^{\text{bd}}$ | $217.30 \pm 57.78^{\text{bd}}$ | $176.00 \pm 0.00^{\text{bc}}$  |
| CHMII       | $170.78 \pm 17.05^{\text{bd}}$ | $210.11 \pm 51.49^{\text{bd}}$ | $184.72 \pm 13.81^{\text{bd}}$ |
| DR          | $126.74 \pm 51.27^{\text{d}}$  | $142.16 \pm 6.33^{\text{c}}$   | $134.18 \pm 30.36^{\text{c}}$  |
| IR          | $139.28 \pm 26.02^{\text{f}}$  | $88.29 \pm 22.59^{\text{f}}$   | $154.98 \pm 14.88^{\text{e}}$  |

<sup>a</sup> $P < 0.05$ , <sup>b</sup> $P < 0.01$ , vs NS group; <sup>c</sup> $P < 0.05$ , <sup>d</sup> $P < 0.01$ , vs model group; <sup>e</sup> $P < 0.05$ , <sup>f</sup> $P < 0.01$ , vs CHMII group

### Comparison of NO concentration

There were significant difference in the concentration of NO between groups. The NO concentration of NS, model groups was  $48.36 \pm$

6.83  $\mu\text{mol/L}$  and  $35.22 \pm 8.94 \mu\text{mol/L}$  respectively, however that of CHMI and CHMII group was  $133.52 \pm 23.57 \mu\text{mol/L}$  and  $137.2 \pm 26.79 \mu\text{mol/L}$ . The results showed that the concentration of NO in CHMI and CHMII groups was higher than that in NS and model groups ( $P < 0.01$ ) (Figure 8). The results indicated that Chinese herbal medicine could induce higher endogenous NO. When NO donor was injected intraperitoneally, NO concentration in DR group was  $62.56 \pm 18.91 \mu\text{mol/L}$ , which was significantly higher than that in the model group ( $P < 0.05$ ). When NO inhibitor was injected intraperitoneally, NO concentration in IR group was  $99.88 \pm 21.03 \mu\text{mol/L}$ , which decreased significantly as compared with that of CHMII group ( $P < 0.01$ ).

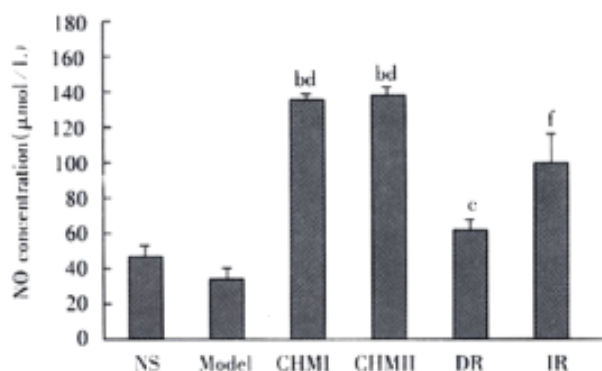


**Figure 8** The change of NO concentration by using CHM, NO donor and NOS inhibitor in the mice.

## DISCUSSION

In the mesothelial cells constituting the lymphatic stomata, there exists bundles of actin microfilaments, the contraction and relaxation of the microfilaments could result in the change of the diameter of the lymphatic stomata. Because the lymphatic stomata is the main pathway of the drainage of the material from the peritoneal cavity<sup>[23-29]</sup>, further investigation on regulating mechanism of the lymphatic stomata could promote the treatment of ascites and other associated illness.

With regard to the regulation of patency of the stomata, some authors have proposed that the peritoneal lymphatic stomata open passively when the diaphragm stretches during expiration, and close passively when it contracts during inspiration. Tsilibary and Wissig observed the regulation of the stomata by means of intravenously injecting carbacholine and succinylcholine, which cause the contraction and relaxation of the mouse diaphragm<sup>[3]</sup>. Their experimental results showed that stomata opened and closed with drug-induced relaxation and contraction of the diaphragm. Changes of the intra-abdominal pressure also play an important role on the regulation of the peritoneal lymphatic stomata. When the intra-abdominal pressure is increased experimentally by injecting normal saline intraperitoneally, the amount of the peritoneal lymphatic stomata is much larger than that of the normal group. On the contrary, when the intra-abdominal pressure is decreased experimentally, the patent number of the peritoneal lymphatic stomata is much less than that of the normal group<sup>[3]</sup>.

Li *et al* and Lv *et al* further confirmed the effect of some Chinese herbal medicine such as Radix Salviae Miltiorrhizae, Radix Codonopsis Pilosulae, Rhizoma Atractylodis Alba and Rhizoma Alismatis in the regulation of the peritoneal lymphatic stomata significantly by increasing the average diameter and the average distribution densities respectively, which can enhance fluid drainage into the vascular system<sup>[37-44]</sup>. This is of important clinical significance in treating ascites caused by liver cirrhosis. In the present study, the prescription is made up according to the traditional Chinese medicinal therapeutic principle in treating “hypocondriac pain”, “lump” and “tympanites”. The drug has the effects of activating blood

circulation to remove stasis, strengthening Spleen, supplementing Qi, and smoothening Qi to eliminate fullness. Our study showed that the CHM in the experiment could regulate the peritoneal lymphatic stomata significantly by increasing the average area and the average distribution densities respectively. Meanwhile, the medicines could enhance the drainage of urinary ion such as sodium, potassium and chlorine. The finding has further confirmed Li *et al*'s results<sup>[37-39]</sup> and Lv *et al*'s results<sup>[40-44]</sup>.

It can also be seen that both dosage of CHM could induce higher concentration of NO, that is, the high endogenous NO production is associated with the enlargement of the peritoneal lymphatic stomata and the increase of the drainage of urinary ion. Further results indicated that great changes could occur in the area and the distribution density of the lymphatic stomata when the NO donor or NOS inhibitor was injected intraperitoneally. When NO donor was injected intraperitoneally, i.e., the concentration of the endogenous NO increased, the area and the distribution density of the lymphatic stomata in the NO donor group were much larger than those of the model group ( $P < 0.05$  or  $P < 0.01$ ). Moreover, when NO inhibitor was given, the concentration of the endogenous NO decreased, these indexes of the lymphatic stomata in NO inhibitor group were much less than those of the corresponding large dose of CHM ( $P < 0.01$ ). Thus, it could be seen that the effect of CHM on the peritoneal lymphatic stomata was altered by adding NO donor or NOS inhibitor to the peritoneal cavity.

It has confirmed that the endothelium-derived relaxing factor (EDRF) is nitric oxide<sup>[46-49]</sup>, which has an effect in relaxing the blood vessel. Li *et al* reported that, with the proceeding of the peritoneal dialysis. Clinically, numerous macrophages were found to enter the peritoneal cavity to form milky spots. Damages of mesothelial cells, increased density of their distribution and enlargement of the peritoneal lymphatic stomata were found to be associated with the increase of macrophage NO quantity. Furthermore, increased NO production was related to the enlargement of the peritoneal lymphatic stomata in the long-term peritoneal dialysis. Therefore, Li *et al* proposed that NO could relax the lymphatic stomata which lead to the enhanced lymph absorption or ultrafiltration failure<sup>[50]</sup>. On these grounds, we suggested that the regulation of CHM on the lymphatic stomata may be related to endogenous NO. Chinese herbal medicine may regulate the lymphatic stomata by accelerating the synthesis and release of endogenous NO. Nitric oxide as an endothelium-derived relaxing factor, mediates its biological effects by activating soluble guanylyl cyclase and increasing cyclic GMP synthesis from GTP and decreasing the concentration of  $\text{Ca}^{2+}$ . These reactions result in the strong relaxation of the lymphatic stomata, with the area and the distribution densities of the lymphatic stomata enlarged, which would lead to the drainage of ascites from the peritoneal cavity.

## REFERENCES

- 1 Leak LV, Rahil K. Permeability of the diaphragmatic mesothelium: the ultrastructural basis for stomata. *Am J Anat* 1978;151:557-593
- 2 Tsilibary EC, Wissig SL. Absorption from the peritoneal cavity: SEM study of the mesothelium covering the peritoneal surface of the muscular portion of the diaphragm. *Am J Anat* 1977;149:127-133
- 3 Tsilibary EC, Wissig SL. Lymphatic absorption from the peritoneal cavity: regulation of patency of mesothelial stomata. *Microvasc Res* 1983;25:22-39
- 4 Tsilibary EC, Wissig SL. Light and electron microscope observation of the lymphatic drainage units of the peritoneal cavity of rodents. *Am J Anat* 1987;180:195-207
- 5 Li JC, Yu SM. Ultrastructural study on the peritoneal stomata in human fetuses. *Jiepo Xuebao* 1990;21:359-361
- 6 Li JC, Yu SM. Study on the ultrastructure of the peritoneal stomata in humans. *Acta Anat* 1991;141:26-30
- 7 Li JC. Electron microscopic study of mesothelial cells in the diaphragm peritoneum of human fetus using the freeze-fracture replica method. *Zhongguo Yixue Kexueyuan Xuebao* 1991;13:189-194
- 8 Li JC. A scanning electron microscopic study on capillary configuration of

- human diaphragmatic peritoneum. *Keji Tongbao* 1992;8:57-61
- 9 Li JC, Chen XB. Study of the human peritoneal stomata and its clinical significance. *Zhonghua Shiyian Waikexue* 1992;9:38-39
  - 10 Li JC, Gao YS, Yong TW. Study on the pelvic stomata and computer image processing. *Zhongguo Yixue Kexueyuan Xuebao* 1994;16:264-269
  - 11 Li JC, Gao YS. The study of quantitative image processing on the ultrastructure of the pelvic stomata in humans. XVIIIth meeting of the European group of lymphology, Belgium, Brussels, 1994: Abstracts
  - 12 Li JC, Zhao ZR, Gao YS, Zhou JL. Study on human pelvic stomata by using the self-made SEM image processing system. *Zhonghua Wuli Yixue Zazhi* 1995;17:104-106
  - 13 Li JC, Zhou JL, Gao YS. The ultrastructure and computer imaging of the lymphatic stomata in the human pelvic peritoneum. *Ann Anat* 1997;179:215-220
  - 14 Li JC, Lv ZL, Shi YH, Shen Y, Yu SM. Experimental study on the peritoneal stomata. *Zhongguo Zhongyi Jichu Yixue Zazhi* 1998;4:20
  - 15 Gao YS, Li JC, Xu LS, Qian BQ. A SEM image processing system and its application in peritoneal stomata study. *Shengwu Yixue Gongchengxue Zazhi* 1993;10:239-243
  - 16 Azzali G. The lymphatic vessels and the so-called "lymphatic stomata" of the diaphragm: A morphologic ultrastructural and three-dimensional study. *Microvasc Res* 1999;57:30-40
  - 17 Fukuo Y, Shinohara H, Matsuda T. The distribution of lymphatic stomata in the diaphragm of the golden hamster. *Anat Rec* 1990;169:13-21
  - 18 Negrini D, Mukenge S, Del Fabbro M, Gonano C, Miserocchi G. Distribution of diaphragmatic stomata. *J Appl Physiol* 1991;70:1544-1549
  - 19 Bettendorf U. Lymph flow mechanism of the subperitoneal diaphragmatic lymphatics. *Lymphology* 1978;11:111-116
  - 20 Mahedero G, Moran JM, Salas J. Absorption of intralipid and interferences from nutrients infused into the peritoneal cavity of the rat. *Am J Surg* 1992;164:45-50
  - 21 Marco AJ, Domingo M, Ruberte J, Carretero A, Briones V, Dominguez L. Lymphatic drainage of listeria monocytogenes and Indian ink inoculated in the peritoneal cavity of the mouse. *Lab Animals* 1992;26:200-205
  - 22 Negrini D, Mukenge S, Del Fabbro M, Gonano C. Distribution of diaphragmatic lymphatic lacunae. *J Appl Physiol* 1992;72:1166-1172
  - 23 Li JC, Shi YH, Chen XB, Yu SM. Study on the peritoneal stomata and absorptive mechanism of ascites. *Zhongguo Yixue Kexueyuan Xuebao* 1992;14:328-333
  - 24 Li JC, Jiang BY. A scanning electron microscopic study on three-dimensional organization of human diaphragmatic lymphatics. *Functional and Developmental Morphology* 1993;3:129-131
  - 25 Li JC, Jiang BY. Studies on three-dimensional configuration of diaphragmatic lymphatics and absorptive mechanism of lymph from the peritoneal cavity. *Zhongguo Yixue Kexueyuan Xuebao* 1994;16:183-187
  - 26 Li JC, Chen XB, Zhang CW, Zhou LJ, Yu SM. Ultrastructural study on human lymphatic drainage units in peritoneal stomata of human. *Jiepo Xuebao* 1995;26:101-104
  - 27 Li JC, Shen Y, Gao YS, Yong TW. Quantitative study of a SEM image processing system on the absorptive mesothelium of the diaphragmatic peritoneum. *Zhongguo Yixue Kexueyuan Xuebao* 1995;17:264-268
  - 28 Li JC, Zhao ZR, Zhou JL, Yu SM. A study of three-dimensional organization of the human diaphragmatic lymphatic lacunae and lymphatic drainage units. *Ann Anat* 1996;178:537-544
  - 29 Li JC, Chen XB, Yu SM. The ultrastructure of vesicle-containing cells and ER-cells of human peritoneum. *Ann Anat* 1996;178:365-367
  - 30 Khoroshaev VA, Vorozheikin VM, Baibekov IM. Routes of resorption of peritoneal fluid in the diaphragm in liver cirrhosis (morphologic study). *Arkh Patol* 1991;53:40-44
  - 31 Hasbargen JA, Hasbargen BJ, Fortenberry EJ. Effect of intraperitoneal neostigmine on peritoneal transport characteristics in CAPD. *Kidney Int* 1992;42:1398-1400
  - 32 Li JC, Yu SM. Study on the relation between the peritoneal stomata and net ultrafiltration in CAPD. *Zhonghua Shenjangbing Zazhi* 1994;10:49-52
  - 33 Zhang B, Wang LT. The cytological mechanism of Chinese herbal medicines in antagonizing liver fibrosis. *Zhongxiyi Jiehe Ganbing Zazhi* 1997;7:249-252
  - 34 Li J, Li YH, Xue LC, Wu CZ. Protective effect of Tanshinone on experimental damage of hepatocytes. *Zhongxiyi Jiehe Ganbing Zazhi* 1996;6:29-30
  - 35 Aiza I, Perez GO, Schiff ER. Management of ascites in patients with chronic liver disease. *Am J Gastroenterol* 1994;89:1994-1996
  - 36 Zhao JP, Yuan SH, Li JC, Liu JD. Advances in the treatment of cirrhosis. *Yixue Zongshu* 1999;5:477-479
  - 37 Li JC, Lv ZL, Wu NP, Zhou JL, Shi YH. A scanning electron microscopy and computer image processing morphometric study of the pharmacological regulation of patency of the peritoneal stomata. *Ann Anat* 1996;178:443-447
  - 38 Li JC, Lv ZL, Shi YH, Shen Y, Chen YF. Study on pharmacological regulation of the peritoneal stomata and its computer image processing. *Zhongguo Yixue Kexueyuan Xuebao* 1996;18:219-223
  - 39 Li JC, Ding WY, Shen Y, Shi YH, Zhong HL, Yu SM, Lv ZL. The influence of Chinese herbal medicines on the peritoneal lymphatic stomata in the mice. *Zhongguo Bingli Shengli Zazhi* 1999;15:414
  - 40 Lv ZL, Li JC. The influence of Chinese herbal medicines for diuresis on the peritoneal stomata in mice. *Zhongxiyi Jiehe Ganbing Zazhi* 1996;6:31-32
  - 41 Lv ZL, Li JC, Shi YH, Chen HM. The mechanism of Jianpi-yiqi Chinese herbal medicine treating the cirrhosis. *Zhongyao Yaoli Yu Linchuang* 1996;11-12
  - 42 Lv ZL, Li JC. The mechanism of Chinese herbal medicine for blood circulation to eliminate turbid in curing ascites: observation on the regulation of red sage root on the peritoneal lymphatic stomata. *Shiyong Zhongxiyi Jiehe Zazhi* 1996;9:1147-1148
  - 43 Lv ZL, Li JC, Shi YH, Chen HM. Experimental observation on the regulation of Chinese herbal medicine on the peritoneal lymphatic stomata. *Zhongyi Zazhi* 1996;37:560-561
  - 44 Lv ZL, Li JC. Experimental study on the regulation of Chinese herbal medicine for diuresis to dispel tympanites on the peritoneal lymphatic stomata of the mouse. *Zhongguo Zhongxiyi Jiehe Zazhi* 1997;17:199-200
  - 45 Mao HM. Determination of nitrate in serum by a copper-coated cadmium reduction method. *Linchuang Jianyan Zazhi* 1995;13:6-8
  - 46 Murad F. Discovery of some of the biological effects of nitric oxide and its role in cell signaling (Nobel Lecture). *Angew Chem Int Ed* 1999;38:1856-1868
  - 47 Yu J, Guo F, Ebert MPA, Malfertheiner P. Expression of inducible nitric oxide synthase in human gastric cancer. *World J Gastroenterol* 1999;5:430-431
  - 48 Huang YQ, Xiao SD, Zhang DZ, Mo JZ. Nitric oxide synthase distribution in esophageal mucosa and hemodynamic changes in rats with cirrhosis. *World J Gastroenterol* 1999;5:213-216
  - 49 Peng X, Feng JB, Wang SL. Distribution of nitric oxide synthase in stomach wall in rats. *World J Gastroenterol* 1999;5:92
  - 50 Li JC, Zhang K, Yang ZR. Effects of peritoneal dialysis on macrophage nitric oxide production and its relation with peritoneal lymphatic stomata. *Shenzangbing Yu Touxishen Yizhi Zazhi* 2000;9:13-17

• REVIEW •

# Early diagnosis for colorectal cancer in China

Ya-Li Zhang, Zhen-Su Zhang, Ba-Ping Wu, Dian-Yuan Zhou

Ya-Li Zhang, Zhen-Su Zhang, Ba-Ping Wu, Dian-Yuan Zhou, PLA Institute for Digestive Diseases, Nanfang Hospital, The First Medical University of PLA, Guangzhou 510515, Guangdong Province, China  
 Supported by Key University Teacher Funds by the Ministry of Education  
**Correspondence to:** Dr. Ya-Li Zhang, PLA Institute for Digestive Diseases, Nanfang Hospital, Guangzhou 510515, China. zhangyl@fimmu.edu.cn

Telephone: +86-20-85141544

Received 2001-03-05 Accepted 2001-06-25

## Abstract

**AIM:** To review the present studies on early diagnosis of colorectal cancer.

**METHODS:** The detective rate for early cancer is 1.7%-26.1% based on various statistical data, with much higher detective rate in endoscopy. Since early cancer means invasion involved in the mucosa or submucosa, the diagnosis can only be made when the invasive depth is identified. Pathological tissue materials from both surgical operation or endoscopic resection are suitable for early cancer evaluation.

**RESULTS:** Incidence of polyp malignancy is 1.4%~20.4%. The various constitutive proportion of polyps may explain the different rates. Malignant incidence is higher in adenomatous polyps, that for villous polyps can reach 21.3%-58.3%. Type II early stage of colorectal carcinoma is rarely reported in China. It is showed that majority of them were not malignant, most of type IIa being adenoma or hyperplasia, and IIb being inflammatory and IIc might be the isolated ulcers. The occurrence of malignancy of type II is far lower than that of polypoid lesion. In China, the qualitative diagnosis and classification of neoplasm generally adopted the WHO standard, including surgical excision or biopsies. There is impersonal evaluation between colorectal pre-malignancy and cancer. The former emphasizes the dysplasia of nuclei and gland, while the latter is marked with cancer invasion. Diagnosis of early stage colorectal cancer in endoscopy is made with too much caution which made the detective rate much lower. Mass screening for asymptomatic subjects and follow-up for high risk population are mainly used to find the early stage colorectal cancer in China. Fecal occult blood test is also widely made as primary screening test, galactose oxygenase test of rectal mucus (T antigen), fecal occult albumin test are also used. The detective rate of colorectal cancer is 24-36.5 per 105 mass population.

**CONCLUSION:** Although carcinoma associated antigen in blood or stool, microsatellite DNA instability for high risk familial history, molecular biology technology for stool oncogene or antioncogene, telomerase activity and exfoliative cytological examination for tumor marker, are utilized, none of them is used in mass screening by now.

Zhang YL, Zhang ZS, Wu BP, Zhou DY. Early diagnosis for colorectal cancer in China. World J Gastroenterol 2002;8(1):21-25

## INTRODUCTION

The colorectal cancer is one of the most common malignant tumors which threatens the people's health<sup>[1-3]</sup>. The occurrence of colorectal cancer has been rising over the past 3 decades. At present, the colorectal cancer is the second cause of death in western countries, and the forth in China<sup>[4,5]</sup>. It is clear that the prognosis of colorectal cancer is related to early diagnosis<sup>[6-8]</sup>. For instance, the five-year survival after operation of colorectal cancer, diagnosed in early stage, is over 80%, but in the advanced stage it is lower than 40%. So, it is very important to improve the colorectal cancer's prognosis by means of early diagnosis<sup>[9-13]</sup>. Recently, much attention has been paid to early detection for colorectal cancer in China. The popularity of the colonoscopy and the mass screening for colorectal cancer in the population who have no symptoms has raised the rate of the early diagnosis of colorectal cancer greatly. However, the study and progress vary among regions in the country, and there are also misdiagnoses. This paper reviews the present study of early diagnosis of colorectal cancer in China.

## THE DETECTIVE RATE OF EARLY STAGE COLORECTAL CANCER IN CHINA

At present, the data of detective rate for early stage colorectal cancer are not perfect, and the detective rate is 1.7%-26.1%, based on various reports (Table 1)<sup>[14-20]</sup>. The major reason for the different rate is the various statistical data. In virtue of the endoscopy popularity, the early stage of cancers are detected increasingly. Most of them can be treated by non-surgically. So, there are great differences between the endoscopic and the surgical data. For example, 997 cases of colorectal cancer were treated surgically during 1990-1999 in Nan Fang Hospital, 21 cases are in early stage (2.1%), while 1087 cases of colorectal cancer were found from 20 353 colonoscoped cases during the corresponding period, in which, 146 early stage of cancers were identified (13.4%). Because most of early cancers are polyps-like and easy to be resected under endoscopy, the percentage of early stage cancer in surgical samples is low.

Table 1 The detective rate for early stage of colorectal cancer in China

| Authors                           | Colorectal cancer |                      |      |
|-----------------------------------|-------------------|----------------------|------|
|                                   | Total<br>n        | Early stage<br>n (%) | Year |
| Lu <i>et al</i> <sup>[14]</sup>   | 569               | 85(15.1)             | 1997 |
| Ni <i>et al</i> <sup>[15]</sup>   | 132               | 15(11.4)             | 1997 |
| Yang <i>et al</i> <sup>[16]</sup> | 721               | 65(22.9)             | 1997 |
| NI <i>et al</i> <sup>[17]</sup>   | 296               | 32(10.8)             | 1997 |
| Cai <i>et al</i> <sup>[18]</sup>  | 1058              | 59(5.6)              | 1999 |
| Zeng <i>et al</i> <sup>[19]</sup> | 300               | 5(1.7)               | 1996 |
| Sun <i>et al</i> <sup>[20]</sup>  | 180               | 47(26.1)             | 1998 |

## MORPHOLOGY OF EARLY STAGE COLORECTAL CANCER UNDER ENDOSCOPY

There are two types of early colorectal cancer based on the morphological classification under endoscopy. Type I also called protruded or polyps type, can be further grouped as pedunculated (Ip), subpedunculated (Isp) and sessile (Is) superficial type. Type II can be classified as elevated (IIa), flat (IIb) and depressed (with or without protruded)<sup>[6,19]</sup>. Since early cancer means invasion involving the mucosa or submucosa, which is not related to the tumor size or special morphology, the diagnosis only can be



made when the invasive depth is identified. Pathological tissues from both surgical operation and endoscopic resection are suitable for early cancer evaluation. It is important that early cancer diagnosis can not be made based on the endoscopic biopsy since invasion is not observed.

Histopathological examination of polyps under endoscopy is a crucial method to detect early cancer in China, and most of them are polyp malignancy<sup>[9,14,21,22]</sup>. Generally, polyp formation is mostly involved in the proliferation of mucosa and submucosal tissues. As long as cancerous tissues do not touch upon pedicle, they can attribute to early-stage carcinoma. If pedicle of polyp invasion in colorectal cancer can not be observed for incomplete resection or embedded in the wrong direction, diagnosis of early-stage carcinoma can not be made rashly. Incidence of polyp malignant transformation is 1.4%-20.4% (Table 2). Different result may be from various constitutive proportion of polyps. Malignant incidence is high in adenomatous polyps. In villous polyps, it can reach 21.3%-58.3% according to the documents in China<sup>[23-31]</sup>. Moreover, as some adenomatous ingredient are observed by biopsy, some advanced colorectal cancers are diagnosed as polyp malignancy by pathologists. This kind of lesions can not be included in the early-stage carcinoma. In our previous study, 87/127 (68.6%) advanced colorectal carcinoma had residual of adenoma.

**Table 2** The malignant transformation rate of polyps in China

| Authors                            | Area      | n    | Incidence (%) |
|------------------------------------|-----------|------|---------------|
| Zhou <i>et al</i> <sup>[22]</sup>  | Guangzhou | 539  | 3.4           |
| Cai <i>et al</i> <sup>[23]</sup>   | Guangzhou | 216  | 9.7           |
| Zhang <i>et al</i> <sup>[24]</sup> | Changchun | 2000 | 5.1           |
| Shen <i>et al</i> <sup>[25]</sup>  | Kunming   | 533  | 6.4           |
| Zhu <i>et al</i> <sup>[26]</sup>   | Beijing   | 219  | 1.4           |
| Zhu <i>et al</i> <sup>[27]</sup>   | Nanjing   | 644  | 5.8           |
| Wang <i>et al</i> <sup>[28]</sup>  | Xi'an     | 548  | 9.7           |
| Zhang <i>et al</i> <sup>[29]</sup> | Zhejiang  | 321  | 14.6          |
| Zhang <i>et al</i> <sup>[30]</sup> | Ha-erbing | 494  | 20.4          |
| Gao <i>et al</i> <sup>[31]</sup>   | Shanghai  | 334  | 6.6           |

Type II early stage of colorectal carcinoma is rarely reported in China. Huang *et al* first summarized 6304 patients detected by colonoscopy from 1974 to 1996 in a hospital of Beijing<sup>[32]</sup>, only 36 Type II lesions were discovered, including 31 (86.1%) type IIa, 4 (11.1%) type IIb and 1 (7%) type IIc. Thirty-two tubular adenomas, 3 villous adenoma and 1 carcinoid were confirmed by histopathological examination. Only one case was identified as malignancy by follow-up.

In 137 cases of early stage colorectal cancer detected in Nanfang Hospital from 1990 to 1999, 95.6% were polypoid type, only 6 cases were considered as type II (4.4%) (Table 3). We also analyzed the histopathological features of 186 cases of type II lesions, only 3.2% were diagnosed as early stage carcinoma (Table 4). It indicated that the majority of so-called type II cancer under endoscopy were not real malignancy. Most of type IIa were adenoma or hyperplasia polyps, and most of type IIb were inflammatory changes of mucosa. A large number of type IIc cases might be the isolated ulcers. The occurrence of malignancy of type II is far lower than that of polypoid lesion.

**Table 3** Morphology of 137 cases of early stage colorectal cancer under endoscopy

| Morphology | Type           | n   | Ratio |
|------------|----------------|-----|-------|
| Polypoid   | I              | 131 | 95.6  |
| Elevated   | IIa            | 2   | 1.4   |
| Flat       | IIb            | 1   | 0.7   |
| Depressed  | IIc or IIc+IIa | 3   | 2.3   |

**Table 4** Histopathology of 186 cases of type II lesion

| Morphology | Type           | n (%)     | Histopathologic diagnosis |          |          |
|------------|----------------|-----------|---------------------------|----------|----------|
|            |                |           | Early cancer              | Adenoma  | Other    |
| Elevated   | IIa            | 155(83.3) | 2(1.3)                    | 86(55.4) | 67(43.3) |
| Flat       | IIb            | 22(11.8)  | 1(4.5)                    | 2(9.00)  | 19(86.4) |
| Depressed  | IIc or IIc+IIa | 9(4.8)    | 3(33.3)                   | 4(44.4)  | 2(22.2)  |

## THE DIAGNOSTIC STANDARD FOR EARLY STAGE OF COLORECTAL CANCER

In China, the qualitative diagnosis and classification of neoplasm generally adopted the WHO standard for both surgical excision and biopsies<sup>[17,33]</sup>. The evaluation is objective between colorectal pre-malignancy and cancer. The former emphasizes the dysplasia of nuclei and gland, while the latter is marked with cancer invasion<sup>[34-37]</sup>. Although pathologists hold different opinions about the classification of dysplasia, it could be classified generally into 3 grades. The simplest classification depends on the ratio of dysplasia karyon in epithelium. Mild dysplasia indicates the crowding nuclei limited within 1/2 depth of epithelium in basement, moderate dysplasia means that atypical nuclei occupied more than 1/2 epithelium, and severe dysplasia refers to the atypical nuclei occupying the whole epithelium with integrated basement. The essential difference between dysplasia and malignancy is invasion. The malignancy is manifested by the destroyed basement, and sporadic dysplasia glands. It is called intra-mucosal cancer if the cancer cell invasion limited within the mucosa. If the cancer destroyed mucosal muscle into submucosa, it is called sub-mucosal cancer. These two types are generally designated as early stage cancer. From the literature reviews, we found that the diagnosis of early stage colorectal cancer in China is made with much cautions under endoscopy. On the one hand, pathologic diagnosis generally adopted the WHO standard, which depends on the invasion, and sometimes it is difficult to observe the invasion on biopsy sections. On the other hand, patients always feel panic to cancer, once the colorectal cancer is diagnosed, they would rather choose surgical operation than endoscopic resection. Besides, they often require consultation of the pathological sections, if diagnostic standard is different, this may cause the psychological pressure to the pathologic doctors in different regions.

In European countries, colorectal cancer is the most common malignant tumor of digestive tract. But the diagnostic rate of early cancer is usually reported less than 9%. In Japan, the diagnostic rate of early stage of cancer detected by endoscopy is 17%-53%. The cases of early stage cancer reported in China is the same as in European countries but far lower than in Japan<sup>[14-20]</sup>. Schlemper RJ *et al* compared the differences in pathological diagnosis of early carcinoma from stripping or surgically resected specimens of colonic mucosa between Japan and Europe-America<sup>[34]</sup>. It was found that 4 cancer cases were diagnosed by Japanese pathologists in 11 adenoma with mild dysplasia based on European-American standard. This is because Japanese pathologists emphasize the nuclei dysplasia and gland structural change evaluating malignancy<sup>[37]</sup>, but pathologists in China usually take above changes as markers of pre-malignancy.

## DETECTION FOR EARLY STAGE OF COLORECTAL CANCER

Mass screening for asymptomatic subjects and follow-up for high risk population are the major ways to find the early stage of colorectal cancer in China<sup>[38-42]</sup>. High risk factors are old age, histories of colorectal polyps, familial history of cancer and some colorectal related positive tests<sup>[43-51]</sup>. Since mass screening for asymptomatic population need a large amount of work, and exact diagnosis must depend on endoscopic and histopathological examination, screening test has been paid much attention. So far, fecal occult blood test is widely used as primary screening test in China<sup>[52-55]</sup>. Other screening tests include galactose oxygenase



test of rectal mucus(T antigen)<sup>[56-60]</sup>, and fecal occult albumin test<sup>[61,62]</sup>. If the screening tests appear positive, colonoscopy is then taken. Although carcinoma associated antigen in blood or stool<sup>[63-81]</sup>, microsatellite DNA instability for high risk familial history<sup>[82-86]</sup>, molecular biology technology for stool oncogene or antioncogene<sup>[87-99]</sup>, telomerase activity<sup>[100-104]</sup> and exfoliative cytological examination<sup>[105,107]</sup> have been used for tumor marker, none of them is used in mass screening.

There are some excellent work reported in China on mass screening for colorectal cancer. Most of them are based on immune fecal occult blood test(Table 5)<sup>[54,55,62]</sup>. In mass screening (age above 35 years), the occurrence of colorectal cancer is 24-36 per 10<sup>5</sup> population.

**Table 5** Mass screening for colorectal cancer in asymptomatic population

| Authors           | Region    | Age(yrs) | Population | Cancer | Dukers(%)<br>A/B | Detection<br>rate    |
|-------------------|-----------|----------|------------|--------|------------------|----------------------|
| Li <i>et al</i>   | North     | >35      | 102 800    | 25     | 52.0             | 24/10 <sup>5</sup>   |
| Zhen <i>et al</i> | East      | >35      | 62 667     | 16     | 57.2             | 25.5/10 <sup>5</sup> |
| Zhou <i>et al</i> | Mid-south | >45      | 24 677     | 9      | 55.6             | 36.5/10 <sup>5</sup> |

Tantigen detection in rectal mucus is also used in some mass screenings<sup>[57-60,108,109]</sup>. In 3820 asymptomatic population, the positive rate of T antigen is 9.1%, among them, 2 cases of early cancer and 28 cases of adenoma were identified. The detective rate of pathologic change is 12.7%. It is shown that T antigen test is not specific for colorectal examination. In 103 cases of T antigen positive subjects, 85 cases were found without any lesion under colonoscopy. The sensitivity is not better than that of feces occult blood examination<sup>[110-114]</sup>.

Since screening tests used so far are not specific for colorectal detection, there are some misdiagnoses either by feces occult blood examination or rectal mucous T antigen test. To improve the detective rate of the early stage cancer, it is suggested that combined complementary screening should be taken. Zhejiang University School of Medicine optimized the screening protocol for colorectal cancer among a high-incidence population<sup>[113]</sup>. Through increasing the cases for colonoscopy follow-up, the detective rate of early cancer was increased. Beijing General Hospital reported that by combined test of sequential fecal occult blood and albumin in the screening of colorectal neoplasma, 3 cases of carcinoma were found from 883 positive asymptomatic subjects<sup>[114]</sup>. The Nanfang Hospital recommended the complementary schemes by combining occult blood and T antigen detection. In 5 cases of colorectal cancer, which were found by colonoscopy in 2832 asymptomatic subjects, 3 were positive in feces occult blood examination and 2 in T antigen test. The missed cases will be reduced if complementary screening was taken<sup>[13]</sup>. Our study showed that the mass screening can reduce the colorectal occurrence(Table 6)<sup>[113]</sup>.

## FUTURE STUDY IN EARLY DIAGNOSIS FOR COLORECTAL CANCER

It is definite that asymptomatic mass screening is the important way to identify the early cancer. Because of the poor specificity of screening test, and the high cost, it is difficult to popularize. Target screening will be highlighted. In 1992, Sidransky *et al* first extracted DNA successfully from feces and reported ras gene variation with Southern-Blot<sup>[116]</sup>. It is considered an effective screening for colorectal cancer in the 21st century. PCR-SSCP technology has a high sensitivity, good specificity and easy manipulation. Gene mutation such as P53, ras, c-erbB-2, APC and MCC was identified in feces

(Table 7)<sup>[94-96,117,118]</sup>. Since no specific gene mutation is found in colorectal cases, the detective rate by molecular technique is low. Though combined genes detection can enhance the screening rate, it is too complex and expensive.

**Table 6** The follow-up results in 3,641 cases of asymptomatic population

|                 | Cancer (n) | Adenoma |                                 |
|-----------------|------------|---------|---------------------------------|
|                 |            | n       | >1.0 cm<br>Dysplasia(>II grade) |
| First screen    | 4          | 48      | 17(35.4%)<br>12(25.0%)          |
| Two years later | 0          | 18      | 4(22.2%)<br>2(11.1%)            |

**Table 7** Gene mutation analysis in colorectal cancer stool (Nanfang Hospital)

| Gene | n  | Tissue DNA |      | Fecal DNA |      |
|------|----|------------|------|-----------|------|
|      |    | Positive   | %    | Positive  | %    |
| APC  | 41 | 20         | 48.8 | 14        | 34.1 |
| MCC  | 45 | 13         | 28.9 | 11        | 24.4 |
| P53  | 32 | 32         | 37.5 | 10        | 31.3 |

Analysis of gene offers possibility and practical significance for detecting high risk population. For example, HNPCC generally represents the microsatellite DNA instability and characteristic DNA mismatch repair gene. Therefore, detecting MIN and DNA mismatch repair gene may identify some high risk population with cancer familial predisposition<sup>[119-122]</sup>. We analyzed 46 cases of colorectal carcinoma for MIN, and found 14 cases of MIN positive patients, 12 of them with familial predisposition (85.7%). It is suggested that MIN might reflect colorectal carcinoma with familial predisposition in some extent.

## REFERENCES

- Zhang YL, Nie J, Zhou J, Guo W, Guan CP, Zhou DY. Incidence and geographical features of colorectal cancer in patients under 30 years of age in china. *Zhonghua Xiaohua Neijing Zazhi* 1997;14:11-14
- Zhang ZS, Zhang YL. Progress in research of colorectal cancer in China. *Shijie Huaren Xiaohua Zazhi* 2001;9:489-494
- Wang SH, Zheng YQ. A clinicopathologic analysis of 354 cases of large intestinal cancer in western Hunan. *Xin Xiaohuabingxue Zazhi* 1996;4:325-326
- Jing F, Zhou SZ, Tao YF, Fang RY, Xiang YB, Shun L, Gao YT. Cancer incidence trend in Shanghai 1972-1994. *Zhongliu* 1999;19:255-258
- Yu JP, Dong WG. Current situation about early diagnosis of cancer of large intestine. *Shijie Huaren Xiaohua Zazhi* 1999;7:553-554
- Li GY, Lu YM, Chen FL, Gong JZ. Current situation about diagnosis and treatment of early colorectal cancer. *Huaren Xiaohua Zazhi* 1998; 6: 377-382
- Zhang Y. Guwai Yixue. Advances of diagnosis and treatment of early colorectal cancer. *Zhongliuxue Fengzhe* 1999; 26: 114-118
- Xiao XW. The value of selective chemoembolization in the treatment of hepatometastases in colorectal carcinoma. *World J Gastroenterol* 1998;4(Suppl 2):38-41
- Jia XD, Han C. Chemoprevention of tea on colorectal cancer induced by dimethylhydrazine in Wistar rats. *World J Gastroenterol* 2000;6: 699-703
- Feng FC, Zhang YL. Canceration and endoscope treatment of large intestine polys. *Zhongguo Shiyong Neike Zazhi* 1996;16: 390-392
- Sheng J, Zhang ZZ, Mo SJ, Liu SY, Wang YL. Endoscopic diagnosis and therapy for early colorectal cancer. *Zhonghua Xiaohua Neijing Zazhi* 1998; 15: 297-298
- Cheng FQ, Du H, Zhu C, Jiang H, Wang HZ, Liu SY. Endoscopic diagnosis and therapy for early colorectal cancer: report of 63 cases. *Zhonghua Xiaohua Neijing Zazhi* 1998; 15: 94-96
- Zhou DY, Feng FC, Zhang YL, Lai ZS. Study on combination mass screening protocol for colorectal cancer. *Zhonghua Neijing Zazhi* 1994; 33:367-369
- Lu YM, Gu F, Lin SR, Zhu ZM. Significance of clinical screening colonoscopy and colonoscopic polypectomy with pathology in diagnosis of early colon cancer. *Zhonghua Xiaohua Neijing Zazhi* 1997; 14: 222-224
- Ni PY, Qu HT. Summary of five years follow up colonoscopy on patients with colorectal polyps and cancer. *Zhongguo Neijing Zazhi* 1997; 3: 1-2
- Yang YX, Li HB, Liu FS, Zhu XD, Zhang YR, Li XL, Xu QX. Preliminary approach of the relationship between colorectal polyps and

- carcinoma:analysis to 2,237 cases. *Zhongguo Neijing Zazhi* 1997; 3: 17-18
- 17 Zhang YL. The diagnosis standard of endoscopic biopsy for colorectal cancer. *Zhonghua Xiaohua Neijing Zazhi* 2001; 18: 135-138
  - 18 Cai BY, Yu DY, Wang Y, Gong BQ, Ma B. The clinical pathological analysis of 1058 cases of colon carcinoma. *Qiqihaer Yixueyuan Xuebao* 1999; 20: 5-6
  - 19 Zeng XJ, Guo RD, Guo PC. A Clinical Analuses of 300 Cases of Carcinoma of the Large Intestine. *Fujian Yiyao Zazhi* 1996;18:13-15
  - 20 Shun CJ, Yao Q, Xu JZ, Yu BM. Detection of early large intestine cancer during clinical symptomatic inspection: clinical and pathological characteristics. *Zhongliu* 1998; 18: 49-51
  - 21 Zhang YL. Canceration and endoscope biopsy diagnosis of large intestine polys. *Zhonghua Xiaohua Neijing Zazhi* 1999;16:188-200
  - 22 Zhou DY, Zhang YC, Zhang YL, Feng HC, Hu Q, Xiao GS. Study on anaplasia potentiality of colorectal adenoma. An analysis of 611 adenomas by endoscope biopsy. *Zhongguo Guangdian Yixue Zazhi* 1992; 1:166-169
  - 23 Cai KY, Huang SZ, Yu XB, Yu JP. An analysis of follow up colonoscopy on 216 aged patients with colorectal polyps. *Fubu Waikes* 2000; 13: 105-106
  - 24 Zhang B, Zhen YG, Zhang DH. The clinical pathological features of colorectal polyps by colonoscope management in 2000 cases. *Zhongguo Shiyong Waikes Zazhi* 1999; 19: 661-662
  - 25 Sheng LJ, Feng SZ, Zhang L, Pu P. Pathological analysis of 533 cases of large bowel polyps. *Yunnan Yiyao* 1995; 16: 267-268
  - 26 Zu C, Zhang JP, Zhang ZQ, Zhao DH. Treatment of large bowel polyps in elderly people with over five years;a follow-up. *Zhonghua Xiaohua Zazhi* 1995; 15: 198-199
  - 27 Zu MQ. Endoscopic Excision of Colonic Polyps. A report of 456 cases. *Zhongguo Zhongliu Linchuang*1995; 22: 334-337
  - 28 Wang ZX, Xu DP, Zhou HZ, Lei PS, Cheng SZ. An analysis of canceration of 53 large intestine polys. *Zhongliu Fangzhi Yanjiu* 1994; 21: 236-238
  - 29 Zhang HZ, Tian HY, Xu JH. Clinical analysis of 321 cases of colorectal polyps. *Shiyong Zhongliu Zazhi* 1994; 9: 30-31
  - 30 Zhang ZY, Pan LN, Wu HX, Li SY. Relation of colorectal polyps and colorectal cancer.A report of 494 cases. *Neijing* 1994; 11: 1-2
  - 31 Gao WD, Yao LQ, Zhou PH, Gu SH. Treatment on canceration colorectal adenomas by colonscope. *Zhonghua Neijing Zazhi* 1996; 2: 42-43
  - 32 Han Y, Li SY. Diagnosis and treatment on early colorectal neoplasmas of type flat and concave by endoscopy. *Zhonghua Neijing Zazhi* 1997; 3: 39-41
  - 33 Zhang YL. The dysplasia of colorectal adenoma. In: Zhang YL eds. Colorectal cancer: Basic and clinical research. *Shanghai Sci Press* 1999: 13-15
  - 34 Schlemper RJ,Itabashi M, Kato Y, Lewin KJ, Riddell RH, Shimoda T, Sipponen P, Stolte M, Watanabe H. Differences in the diagnostic criteria used by Japanese and Western pathologists to diagnose colorectal carcinoma. *Cancer* 1998; 82: 60-69
  - 35 Schlemper RJ, Borchard F, Dixon MF, Koike M, Mueller J, Stolte M, Watanabe H. International comparability of the pathological diagnosis for early cancer of the digestive tract: Munich meeting. *J Gastroenterol* 2000; 35(Suppl 12):102-110
  - 36 Riddell RH. East meets West: what is early cancer? *Can J Gastroenterol* 1999;13:495-497
  - 37 Lauwers GY, Shimizu M, Correa P, Riddell RH, Kato Y, Lewin KJ, Yamabe H, Sheahan DG, Lewin D, Sipponen P, Kubilis PS, Watanabe H. Evaluation of gastric biopsies for neoplasia: differences between Japanese and Western pathologists. *Am J Surg Pathol* 1999; 23: 511-518
  - 38 Chen K, Jiao DA, Zheng S, Zhou L, Yu H, Yuan YC, Yao KY, Ma XY, Zhang Y. Diagnostic value of fecal occult blood testing for screening colorectal cancer. *China Natl J New Gastroenterol* 1997;3:166-168
  - 39 Zhou DY, Feng FC, Zhang YL. Route of early diagnosis on colorectal cancer. *Zhonghua Xiaohua Zazhi* 1992;12:319-321
  - 40 Zhou DY, Zhang YL. Progress on biologic characteristics and early diagnosis of colorectal cancer. *Guowai Yixue: Xiaohua Jibing Fengce* 1992;1:17-18
  - 41 Zhang YL, Zhou DY, Zhang WD, Lai ZS. Speculation on early diagnosis of colorectal cancer. *Yixue Yu Zhexue* 1993;43-44
  - 42 Zhang YL, Zhou DY. Prophylactic and therapeutic strategy of colorectal cancer. *Weichangbingxue He Ganchangbingxue Zazhi* 1994;3:241-243
  - 43 Xu SB, Zhang WX, Wang LL. Expression of antigen a new tumor marker Sc6 byimmunohistochemical method. *Xin Xiaohuabingxue Zazhi* 1994;2(Suppl 2):49-50
  - 44 Feng FC, Huang W, Zhou DY, Zhang YL, Lai ZS. Study on detection of cancer associated antigen in serum and feces by monoclonal antibodies against human colorectal cancer. *Xin Xiaohuabingxue Zazhi* 1995;3:36-38
  - 45 Chen B, Zhou SJ, Fan DM. Establishment of a quick ConA-mAb-LISA for detection of serum MC3-Ag, a novel colorectal cancer-associated antigen. *Xin Xiaohuabingxue Zazhi* 1995;3(Suppl 4):12-13
  - 46 Luo YH, Fang DC, Lu R, Liu FX, Liang ZY, Liu WW, Men RP, Zhou ZC. Heterozygosity loss at the APC/MCC locus in colorectal cancer. *Xin Xiaohuabingxue Zazhi* 1996;4:309-311
  - 47 Zhuang XQ, Yuan SZ, Wang XH, Lai RQ, Luo ZQ. Expression and prognostic significance of EGF receptor and proliferating cell nuclear antigen in colorectal cancer. *Xin Xiaohuabingxue Zazhi* 1996;4:483-484
  - 48 Liu Y, Li QM, Lu MZ. Expressions of nm23-H1, p53 and PCNA in human colorectal carcinoma tissues. *Xin Xiaohuabingxue Zazhi* 1997;5: 431-432
  - 49 Zhao J, Pan X, Yin GP, Shan LC, Wang CL. Peripheral blood CD44 contents in 26 patients with colorectal cancer. *Xin Xiaohuabingxue Zazhi* 1997;5:510-511
  - 50 Feng FC, Huang W, Zhang YL, Wang JD, Zhou DY. Clinical significance of serum sIL-2R and TNF in patients with colorectal carcinoma. *Xin Xiaohuabingxue Zazhi* 1997;5:567-568
  - 51 Qiu SL, Huang JQ. Significance of CD44 gene products for colorectal carcinoma diagnosis and prognosis evaluation. *Xin Xiaohuabingxue Zazhi* 1997;5(Suppl 6):32-33
  - 52 Zhang YL, Zhou DY, Lai ZS. Evaluation of immunological fecal occult blood test for colorectal tumor by specific antibody coated staphylococcal protein A coagglutination. *J Med Coll PLA* 1992; 7:382-358
  - 53 Yu SP, Zheng SJ, Zhou HY. Evaluation of colorectal carcinoma screening with fecal monoclonal antibody. *World J Gastroenterol* 1998;4(Suppl 2):9-11
  - 54 Chen K, Jiao DA, Zheng S, Zhou L, Yu H, Yuan YC, Yao KY, Ma XY, Zhang Y. Diagnostic value of fecal occult blood testing for screening colorectal cancer. *China Natl J New Gastroenterol* 1997;3:166-168
  - 55 Zhu WX. Comparative fecal occult blood test with the kit of RPHA-Z and RPHA-T. *Zhonghua Yixue Zazhi* 1987: 673-674
  - 56 Zhou DY, Zhang YL, Nai ZS. A study on the screening of large intestinal carcinoma by reactum mucus T-antigen method. *Zhonghua Xiaohua Zazhi* 1991;11:261-262
  - 57 Xu SY, Lin GJ, Lu Y. Clinical significance of T-antigen in the premalignant condition of colorectal cancer. *Zhonghua Xiaohua Neijing Zazhi* 1998; 15: 285-288
  - 58 Li DB, Wang HB. Application of T-antigen detective kit in screening colorectal cancer. *Zhongguo Gangchangbing Zazhi* 1998; 18: 27-28
  - 59 Lu Y, Xu SY, Wang QY, Li ZM. Determination of T-antigen in large intestinal mucus by galactose oxidase method. *Zhonghua Yixue Jianyan Zazhi* 1995; 18: 133-135
  - 60 Tan J, Zhang Q, Fang XZ, Kan AP, Cai XL, Zhang SM, Zhang L, Zhang SH. Clinical significance of galactose oxidase-schiff reaction in the detection of carcinoma and precancerous lesions of large intestine. *Zhonghua Zhongliu Zazhi* 1997; 19: 157-159
  - 61 Wang ZH. Mass screening for colorectal cancer by semi-quantum testing fecal occult albumin. *Zhongguo Lingchuang Mianyixue Zazhi* 1993: 39-42
  - 62 Wang ZH, Li SY, Cheng ZM. Preparation of rabbit anti-human immuno-carboxylate and its application in screening of colorectal tumor. *Zhongguo Zhongliu Lingchuang* 1999; 26: 450-452
  - 63 Feng FC, Huang W, Zhong DY, Zhang YL. Study on detection of cancer associated antigen in serum and feces by monoclonal antibodies against human colorectal cancer. *Xingxiaohuabing Zazhi* 1995;3:36-38
  - 64 Hu JY, Su JZ, Pi ZM, Zhu JG, Zhou GH, Sun QB. Radioimmunoimaging of colorectal cancer using 99mTc labeled monoclonal antibody. *World J Gastroenterol* 1998;4:303-306
  - 65 Fang DC, Luo YH, Lu R, Liu WW, Lui FX, Liang ZY. Loss of heterozygosity at APC, MCC and DCC genetic loci in colorectal cancers. *China Natl J New Gastroenterol* 1995;1:21-24
  - 66 Zhao CH, Jiang CY, Zhang YY, Liu XX, Luo DC, Zhang XT, Lin YQ. Analysis of LDH activities and its isoenzyme patterns in colorectal cancer tissues. *China Natl J New Gastroenterol* 1997;3:41-42
  - 67 Wu GJ, Shan XN, Li MF, Shi SL, Zheng QP, Yu L, Zhao SY. A preliminary study on the loss of heterozygosity at 17p13 in gastric and colorectal cancers. *China Natl J New Gastroenterol* 1997;3:160-162
  - 68 Zhang J, Lai MD, Chen J. Methylation status of p16 gene in colorectal carcinoma and normal colonic mucosa. *World J Gastroenterol* 1999;5: 451-454
  - 69 Xu QW, Li YS, Zhu HG. Relationship between expression P53 protein, PCNA and CEA in colorectal cancer and lymph node metastasis. *World J Gastroenterol* 1998;4:218-219
  - 70 Cai Q, Lu HF, Sun MH, Du X, Fan YZ, Shi DR. Expression of two CD44 variant proteins (v3 and v6) in human colorectal carcinoma and its relevance for prognosis. *World J Gastroenterol* 2000;6(Suppl 3):75
  - 71 He SW, Shen KQ, He YJ, Xie B, Zhao YM. Regulatory effect and mechanism of gastrin and its antagonists on colorectal carcinoma. *World J Gastroenterol* 1999;5:408-416

- 72 He Y, Zhou J, Wu JS, Dou KF. Inhibitory effects of EGFR antisense oligodeoxynucleotide in human colorectal cancer cell line. *World J Gastroenterol* 2000;6:747-749
- 73 Jiang CP, Chen YQ, Zhu JW, Shen HX, Yu X. Immunohistochemical study of gastrin in colorectal carcinoma tissues and its adjacent mucosa. *China Natl J New Gastroenterol* 1997;3:84-86
- 74 Chen DW, Wang YH, Chen XY, Wang Q, Gao H. Clinical significance of immunohistochemical study of P53 protein in colorectal carcinoma. *China Natl J New Gastroenterol* 1996;2:25-26
- 75 Hu JY, Wang S, Zhu JG, Zhou GH, Sun QB. Expression of B7 costimulation molecules by colorectal cancer cells reduces tumorigenicity and induces antitumor immunity. *World J Gastroenterol* 1999;5: 147-151
- 76 Feng S, Song JD. Determination of  $\alpha$ -glucuronidase in human colorectal carcinoma cell lines. *China Natl J New Gastroenterol* 1997;3:251-252
- 77 Hu JY, Su JZ, Pi ZM, Zhu JG, Zhou GH, Sun QB. Radioimmunoinaging of colorectal cancer using  $^{99m}\text{Tc}$  labeled monoclonal antibody. *World J Gastroenterol* 1998;4:303-306
- 78 Zhou ZF, Yuan SZ. Prognostic value of silver stained nucleolar organizer regions in colorectal carcinoma. *China Natl J New Gastroenterol* 1995;1:43-47
- 79 Xu YH, Song JD. Expression of tumor associated antigen-LEA in pre-malignant and malignant lesions of colorectal mucosa. *Shijie Huaren Xiaohua Zazhi* 1999;7:992
- 80 Xu SP, Zheng SJ, Zhou HY, Guo XL. Colorectal cancer mass screening by cancer associated monoclonal antibody in feces. *Zhonghua Xiaohua Zazhi* 1998; 18: 216-217
- 81 Wu BP, Zhang YL, Zhang ZS, Zhang LL, Guo W, Zhou DY. Microsatellite instability, MMR gene expression in colorectal cancer with familial predisposition. *Zhonghua Liuxingbingxue Zazhi* 1998;19:331
- 82 Wang YP, Waltraut F, Peter P. Analysis of hMLH1 and hMSH2 gene mutation in hereditary non-polyposis colorectal cancer. *Zhonghuayixue Yichuanxue Zazhi* 1998;15: 333-336
- 83 Wu BP, Zhang YL, Zhou DY, Gao CF, Lai ZS. Microsatellite instability, MMR gene expression and proliferation kinetics in colorectal cancer with familial predisposition. *World J Gastroenterol* 2000;6:902-905
- 84 Zhang LL, Zhang ZS, Zhang YL, Wu BP, Guo W, Liu XX, Zhou DY. Microsatellite instability in multiple primary colorectal cancers. *Shijie Huaren Xiaohua Zazhi* 1999;7:397-399
- 85 Capozzi E, Della Puppa L, Fornasari M, Pedroni M, Boiocchi M, Viel A. Evaluation of the replication error phenotype in relation to molecular and clinicopathological features in hereditary and early onset colorectal cancer. *Eur J Cancer* 1999; 35:289-295
- 86 Lin H, Lin JY, Zhang YL, Zhang ZS, Zhou MY, Zhou DY. The detection of the mutation of APC gene in the stool of the patients with sporadic colorectal carcinoma. *Zhonghua Xiaohua Zazhi* 2000;20:60-61
- 87 Ji DJ, Cao Y, Zhang YL, Jiang P, Yu N, Feng FC, Zhou DY. Synchronous studies on variations of p53 gene transcriptions and expressions in colorectal carcinomas HT-29 and Lovo cell lines. *Shijie Huaren Xiaohua Zazhi* 2000;8:77-79
- 88 Zhen S, Cai YH, Chao J, Zhen L, Mo YQ, Zhang YM, Geng LY, Shi ZZ, Gu JR. Colorectal cancer associated gene analysis by SSH technique. *Zhonghua Yixue Zazhi* 1997; 77: 256-259
- 89 Mo YQ, Zhen L, Cai XH, Chao J, Zhu LJ, Zhen S. Expression of new cancer associated gene - HSU 17714 in colorectal cancer and other malignant tumors. *Zhongguo Zhongliu Linchuang* 1997; 24: 504-508
- 90 Li M, Wang B, Yu BM, Zhen MH. Relationship between p53 gene mutation and prognosis in colorectal cancer. *Shijie Huaren Xiaohua Zazhi* 1999;7:425-426
- 91 Zhuan XQ, Lai RQ, Sun GH, Wang XH, Yuan SZ. The expression of p53 protein and PCNA in colorectal tumors. *Shijie Huaren Xiaohua Zazhi* 1999;7:616
- 92 Shen XB, Zhang XC, Mei LX, Zhao XM, Hu JG. The signification of the expression of nm23/NDPK and p53 in colorectal cancer. *Shijie Huaren Xiaohua Zazhi* 1999;7:809-810
- 93 Lin H, Lin JY, Zhang YL, Zhang ZS, Zhou MY, Zhou DY. The detection of the mutation of APC gene in the stool of the patients with sporadic colorectal carcinoma. *Zhonghua Xiaohua Zazhi* 2000; 20: 60-61
- 94 Gan YB, Cai XH, Zheng S. Detection of Ki-ras gene mutations in tumor tissues and stools of patients with colorectal carcinoma. *Zhejiang Yike Daoxue Xuebao* 1995; 24: 241-247
- 95 Luo CY, Li SY, Zhu XG. The detection of the rearrangements of bcl-2 gene in the cancer tissues and the stool of the patients with colorectal carcinoma by semi-nest PCR. *Zhonghua Shiyang Waikexue Zazhi* 1999;16: 197-198
- 96 Cao GW, Qi ZT, Pan X, Zhang XQ, Miao XH, Feng Y, Lu XH, Kuriyama S, Du P. Gene therapy for human colorectal carcinoma using human CEA promoter controlled bacterial ADP-ribosylating toxin genes human CEA: PEA & DTA gene transfer. *World J Gastroenterol* 1998;4: 388-391
- 97 Xu CT, Pan BR. The study of gene change in colorectal tumors. *Huaren Xiaohua Zazhi* 1998;6:58-60
- 98 Yu BM, Zhao R. The recent study on molecular biology in colorectal cancer. *Shijie Huaren Xiaohua Zazhi* 1999;7:173-175
- 99 Liu BY, Sun ZL, Pan SW, Chui DX, Yuan XJ, Li D, Lei YF, Wang S. Gene expression and early diagnosis in colorectal cancer. *Shijie Huaren Xiaohua Zazhi* 2000;8:43-44
- 100 Sun ZJ, Zhang YL, Zhang ZS, Guo W, Zhou DY. Study on activity of telomerase in colorectal cancer screening. *Zhonghua Liuxingbingxue Zazhi* 1998;19:327
- 101 Jiang CY, Ding K, Liu XX, Zhao CH, Zhu S. Study on histoenzymes markers in colorectal cancer. *Zhongguo Zhongxiyi Jiehe Waikexue Zazhi* 1998; 4: 336-339
- 102 Wang W, Luo HS, Yu BP. Telomerase and colorectal cancer. *Shijie Huaren Xiaohua Zazhi* 2000;8:800-802
- 103 Cuo SL, Huang JQ, Wang YF, Peng ZH. Telomerase analysis in pre-malignant and malignant tumors in colon. *Huaren Xiaohua Zazhi* 1998; 6: 992-993
- 104 Wu XW, Li SY, Wang ZH, Wu X, Cheng ZM, Wu ZT. The evaluation of colonic exfoliative cell for the screening of colorectal cancer. *Aizheng* 1997; 16: 386-387
- 105 Fan RY, Li SR, Wu X, Wu ZT, Cheng ZM, Deng YJ, Chao JB, Zhang HG. The expression of telomerase in exfoliate cells of colorectal cancer. *Shijie Huaren Xiaohua Zazhi* 2000;8:814-815
- 106 Li J, Li SR, Cao JB, Gao G. Laser-induced fluorescence spectrum of colon cancer *in vivo*. *Shijie Huaren Xiaohua Zazhi* 1999;7:164-165
- 107 Luo DC, Dai HJ, Ni YZ, Ci W. A study on the screening of large intestinal carcinoma by t-antigen monoclonal antibody method. *Zhongguo Aizheng Zazhi* 1998; 8: 256-257
- 108 Liu SC, Bai X, Wei YG, Wang ZL. Reresearch of galactose oxidase in screening carcinoma of the large intestine. *Huaren Xiaohua Zazhi* 1998; 6: 990-991
- 109 Zhou DY, Feng FC, Zhang YL, Lai ZS. Comparative analysis of detecting rectum mucus T-antigen and Immuno-fecal occult blood test in screening colorectal cancer. *Chinese Med J* 1993;106:739-742
- 110 Zhou DY, Feng FC, Pan DS, Lai ZS, Zhang WD, Zhang YL, Wan TM, Li LB, Xu GL, Zhou D. Evaluation of optimized screening protocol for colorectal cancer among a high-incidence population. *Zhonghua Xiaohua Zazhi* 1993;13:315-317
- 111 Liu XY, Zheng S, Yang G, Yu H, Zhou L, Zhang X, Shun QY, Shen GF, Shen YZ, Ding XF. Evaluation of combined test of sequential fecal occult blood and albumin in the screening of colorectal neoplasia. *Zhonghua Fangzhi Yanjiu* 1997; 24: 197-200
- 112 Li SY, Zhang CL, Xu ED, Yang TZ, Cheng NP, Liu YH, He YN. Evaluation of combined test of sequential fecal occult blood and albumin in the screening of colorectal neoplasia. *Zhonghua Zhongliu Zazhi* 1995; 17: 381-383
- 113 Zhou DY, Zhang YL, Feng FC, Lai ZS, Pan DS. Combined test of spa fecal occult blood and rectum mucus t-antigen in the screening and follow-up of colorectal cancer. *Weichangbingxue* 1997;2:67-69
- 114 Sidransky D, Tokino T, Hamilton SR, Kinzler KW, Levin B, Frost P, Vogelstein B. Identification of ras oncogene mutations in the stool of patients with curable colorectal tumors. *Science* 1992; 256:102-105
- 115 Eguchi S, Kohara N, Komuta K, Kanematsu T. Mutations of the p53 gene in the stool of patients with resectable colorectal cancer. *Cancer* 1996; 77(Suppl): 1707-1710
- 116 Sidransky D. Molecular screening: how long can we afford to wait? *J Natl Cancer Inst* 1994; 86: 955-956
- 117 Luo CY, Li SY. The detection and their clinical significance of C-erbB-2 amplification and p53 mutation in the stools of patients with colorectal carcinomas. *Zhonghua Putong Waikexue Zazhi* 1999; 14: 371-373
- 118 Lin JY, Lin H, Zhou DY, Jiang P, Zhang YL. Detection of suppress oncogene mutations in tumor tissues and stools of patients with colorectal carcinoma. *Zhonghua Liuxingbingxue Zazhi* 1998; 19: 326
- 119 Yu N, Qiu HM, Ding YQ, Xu L, Zhang SJ. The relation between DNA replication error and clinicopathological features of colorectal carcinoma. *Zhonghua Binglixue Zazhi* 1998; 27: 359-361
- 120 Yu N, Qiu HM, Ding YQ, Xu L. MSI-a useful molecular indicator of hereditary nonpolyposis colorectal cancer: a report of 4 cases. *Diyi Junyi Daoxue Xuebao* 1999;19: 160-162
- 121 Guo QX, Wei N, Guo CH, Lin LM, Chen BJ. Analysis on microsatellite DNA instability in sporadic nonpolyposis colorectal cancer. *Shandong Yike Daxue Xuebao* 1999; 37: 114-116
- 122 Wu BP, Zhang YL, Zhou DY, Gao CF, Lai ZS. Microsatellite instability, MMR gene expression and proliferation kinetics in colorectal cancer with familial predisposition. *World J Gastroenterol* 2000;6:902-905

• ESOPHAGEAL CANCER •

# RRR- $\alpha$ -tocopheryl succinate inhibits human gastric cancer SGC-7901 cell growth by inducing apoptosis and DNA synthesis arrest?

Kun Wu, Yan Zhao, Bai-He Liu, Yao Li, Fang Liu, Jian Guo, Wei-Ping Yu

Kun Wu, Yan Zhao, Bai-He Liu, Yao Li, Fang Liu, Jian Guo, Department of Nutrition and Food Hygiene, Public Health School, Harbin Medical University, Harbin 150001, Heilongjiang Province, China  
Wei-Ping Yu, Genetics Institute, Texas University of USA, Austin, USA  
Supported by National Natural Science Foundation of China, No.39870662  
Correspondence to: Prof. Kun Wu, Department of Nutrition and Food Hygiene, Public Health School, Harbin Medical University, Harbin 150001, Heilongjiang Province, China. wukun@public.hr.hl.cn  
Telephone: +86-451-3648665

Received 2001-04-25 Accepted 2001-10-15

## Abstract

**AIM:** To investigate the effects of growth inhibition of human gastric cancer SGC-7901 cell with RRR- $\alpha$ -tocopheryl succinate (VES), a derivative of natural Vitamin E, via inducing apoptosis and DNA synthesis arrest.

**METHODS:** Human gastric cancer SGC-7901 cells were regularly incubated in the presence of VES at 5, 10 and 20 mg·L<sup>-1</sup> (VES was dissolved in absolute ethanol and diluted in RPMI 1640 complete condition media correspondingly to a final concentration of VES and 1 mL·L<sup>-1</sup> ethanol), succinic acid and ethanol equivalents as vehicle (VEH) control and condition media only as untreated (UT) control. Trypan blue dye exclusion analysis and MTT assay were applied to detect the cell proliferation. 37 kBq of tritiated thymidine was added to cells and [<sup>3</sup>H] TdR uptake was measured to observe DNA synthesis. Apoptotic morphology was observed by electron microscopy and DAPI staining. Flow cytometry and terminal deoxynucleotidyl transferase-mediated dUTP nick end labeling (TUNEL) assay were performed to detect VES-triggered apoptosis.

**RESULTS:** VES inhibited SGC-7901 cell growth in a dose-dependent manner. The growth curve showed suppression by 24.7%, 49.2% and 68.7% following 24h of VES treatment at 5, 10 and 20 mg·L<sup>-1</sup>, respectively, similar to the findings from MTT assay. DNA synthesis was evidently reduced by 35%, 45% and 98% after 24h VES treatment at 20 mg·L<sup>-1</sup> and 48h at 10 and 20 mg·L<sup>-1</sup>, respectively. VES induced SGC-7901 cells to undergo apoptosis with typically apoptotic characteristics, including morphological changes of chromatin condensation, chromatin crescent formation/margination, nucleus fragmentation and apoptotic body formation, typical apoptotic sub-G1 peak by flow cytometry and increase of apoptotic cells by TUNEL assay in which 90% of cells underwent apoptosis after 48h of VES treatment at 20 mg·L<sup>-1</sup>.

**CONCLUSION:** VES can inhibit human gastric cancer SGC-7901 cell growth by inducing apoptosis and DNA synthesis arrest. Inhibition of SGC-7901 cell growth by VES is dose- and time-dependent. Therefore VES can function as a potent chemotherapeutic agent against human gastric

## carcinogenesis.

Wu K, Zhao Y, Liu BH, Li Y, Liu F, Guo J, Yu WP. RRR- $\alpha$ -tocopheryl succinate inhibits human gastric cancer SGC-7901 cell growth by inducing apoptosis and DNA synthesis arrest. *World J Gastroenterol* 2002;8(1):26-30

## INTRODUCTION

Vitamin E is characterized as a fat-soluble membrane antioxidant<sup>[1,2]</sup>. Vitamin E succinate (RRR- $\alpha$ -tocopheryl succinate; VES), a derivative of natural vitamin E, however, does not possess antioxidant properties unless the succinate group is removed by a nonspecific esterase. VES has been demonstrated to be a potent growth inhibitor of various cancer cell types *in vitro* and *in vivo*<sup>[3,4]</sup>. For example, VES has been shown to inhibit the growth of human monoblastic leukemia cells *in vitro*<sup>[5]</sup>, murine B-16 melanoma cells *in vitro*<sup>[6]</sup>, hamster buccal pouch tumor cells *in vivo*<sup>[7]</sup>, avian lymphoid cells *in vitro*<sup>[8,9]</sup>, murine EL4 T lymphoma cells *in vitro*<sup>[4,10]</sup>, human gastric cancer cells *in vitro* and *in vivo*<sup>[11-13]</sup>, and human breast cancer cells *in vitro* and *in vivo*<sup>[14,15]</sup>.

The exact mechanisms are not clearly known, but the inhibitory effect of VES on the proliferation of rapidly dividing cells can be attributed to the induction of cell cycle blockage<sup>[16]</sup>, increased secretion and activation of transforming growth factor- $\beta$ , (TGF- $\beta$ ) and TGF- $\beta$  receptor II<sup>[9,14,17]</sup>, and the induction of apoptosis<sup>[18-20]</sup>. In many instances, growth inhibition following terminal differentiation<sup>[21-23]</sup> or anticancer drug treatment<sup>[24-26]</sup> results in apoptosis. Apoptosis, namely, programmed cell death, is an active and physiological process characterized by a series of morphological and biological alterations including condensation of cytoplasm, loss of plasma membrane microvilli, segmentation of nucleus and extensive degradation of chromosomal DNA into oligomers of 180bp<sup>[27-30]</sup>. The exact mechanisms of apoptosis are still unclear, but our earlier studies indicated that VES can secrete and activate biologically active TGF- $\beta$  and then TGF- $\beta$  increases the kinase activity of c-Jun N-terminal kinase (JNK) followed by phosphorylation of c-Jun, and finally activated c-Jun triggers apoptosis in human gastric cancer SGC-7901 cells<sup>[31]</sup>.

Gastric cancer is common in China<sup>[32-41]</sup>. Since VES is a potential tumor chemopreventive and chemotherapeutic agent, it is worthwhile to investigate the manner in which VES inhibits the cell growth and thereafter gain a better understanding of the molecular events involved. In this study, we demonstrate the ability of VES to inhibit cell proliferation, arrest DNA synthesis and induce human gastric cancer SGC-7901 cells to undergo apoptosis, address the involvement of certain apoptosis-related events in this process and prove that VES-triggered apoptosis is different from VES-induced DNA synthesis arrest.

## MATERIALS AND METHODS

### Materials

VES, DAPI (4',6-diamidino-2'-phenylindole dihydrochloride,

succinic acid, MTT [3-(4,5-dimethylthiazole-2-yl)-2,5-diphenyltetrazolium bromide] and propidium iodide were purchased from Sigma Co. Ltd. RPMI 1640 media was obtained from Gibco, BRL. *In situ* cell death detection kit was purchased from Boehringer Mannheim, Indianapolis, Inc.  $^3\text{H}$ -TdR was supplied by Chinese Academy of Sciences.

## Methods

**Cell culture** Human gastric cancer cell lines SGC-7901 were maintained in RPMI 1640 medium supplemented with 100mL·L<sup>-1</sup> fetal calf serum (FCS), 100kU·L<sup>-1</sup> penicillin, 100mg·L<sup>-1</sup> streptomycin and 2mmol·L<sup>-1</sup> L-glutamine under 50mL·L<sup>-1</sup> CO<sub>2</sub> in a humidified incubator at 37°C. SGC-7901 cells were incubated for different time periods in the presence of VES at 5, 10 and 20mg·L<sup>-1</sup> (VES was dissolved in absolute ethanol and diluted in RPMI 1640 complete condition media correspondingly to a final concentration of VES and 1mL·L<sup>-1</sup> ethanol), succinic acid and ethanol equivalents as vehicle (VEH) control and condition media only as untreated (UT) control.

**Growth curve** Exponentially growing SGC-7901 cells were trypsinized and aliquoted into 24-well flat-bottomed tissue culture plates at  $5 \times 10^4$ ·well<sup>-1</sup>. The cells were allowed to attach overnight and then incubated for seven days in the presence or absence of VES. Cell number and viability were determined by trypan blue dye exclusion analysis.

**MTT assay** The cells were inoculated in a 96-well plate ( $5 \times 10^3$ ·well<sup>-1</sup>) as described previously<sup>[42]</sup>. In brief, cells after 24h of incubation were treated with VES and controls and then cultured for six days. The cells in eight wells at every dose were supplemented with 0.2mL of 5g·L<sup>-1</sup> MTT every day. After 4h, culture media were discarded followed by addition of 0.2ml of DMSO and vibration for 10min. The absorbance (A) was measured at 570nm using a microplate reader. The percentage of viable cells was calculated as follow: (A of experimental group / A of control group) × 100%. [ $^3\text{H}$ ] Thymidine incorporation. The cells were treated with VES for 24 or 48h as described previously<sup>[43]</sup>. 37kBq of tritiated thymidine were added to cells during the last 6h of culture and harvested onto glass fiber filters. [ $^3\text{H}$ ] TdR uptake was measured in a Beckman LS5000 TD liquid scintillation counter.

**Electron microscopy** The cells treated with VES or VEH were trypsinized and harvested after 24h and 48h, respectively. Subsequently the cells were immersed with Epon 821, imbedded in capsules and converged for 72h at 60°C, the cells were prepared into ultrathin section (60nm) and stained with uranyl acetate and lead citrate. Cell morphology was examined by transmission electron microscopy.

**DAPI staining** Treated cells were pelleted and washed three times with distilled water, and then stained with 2mg·L<sup>-1</sup> DAPI in 100% methanol for 15min at 37°C. Cells were viewed using a fluorescence microscope with ultraviolet (UV) excitation at 300~500nm. Cells with nuclei that contained clear condensed chromatin or cells with fragmented nuclei were scored as apoptosis.

**TUNEL assay** Apoptosis of SGC-7901 cells was analyzed by using *in situ* cell death detection kit. The method is essentially based on the terminal deoxynucleotidyl transferase-mediated dUTP nick end labeling (TUNEL) technique, and it can detect apoptosis at very early stages. In brief, cells were treated in the presence or absence of VES and fixed overnight in 100g·L<sup>-1</sup> formaldehyde, treated with proteinase K and then H<sub>2</sub>O<sub>2</sub>, labeled with fluorescein dUTP in a humid box for

1h at 37°C. The cells were then combined with POD-Horseradish peroxidase, colorized with DAB (3,3-diaminobenzidine) and counterstained with methyl green. Cells were visualized with light microscope.

**Flow cytometry** Cells were incubated with various doses of VES, harvested, washed with phosphate-buffered saline (PBS) twice and fixed with 700mL·L<sup>-1</sup> ethanol at 4°C overnight. Fixed cells were washed twice with PBS and stained with 800μL propidium iodide and 200μL deoxyribonulcease-free ribonuclease A in PBS. The fluorescence intensity of propidium iodide-stained nuclei was determined by a FACscan.

**Statistical analysis** Student's *t* test was used to assess statistical significance of differences. If *P* < 0.05, the difference was considered significant.

## RESULTS

### Inhibition of Human Gastric Cancer SGC-7901 Cell Proliferation by VES

**Growth curve** VES has been previously shown to function as a growth inhibitory agent. In this study, VES inhibited SGC-7901 cell growth in a dose-dependent manner. The growth curve showed that cell growth was suppressed by 24.7%, 49.2% and 68.7% following 24h of VES treatment at 5, 10 and 20mg·L<sup>-1</sup>, respectively. The percentage of inhibition was 100% on day 4 with the treatment of VES at 20mg·L<sup>-1</sup> (Figure 1).

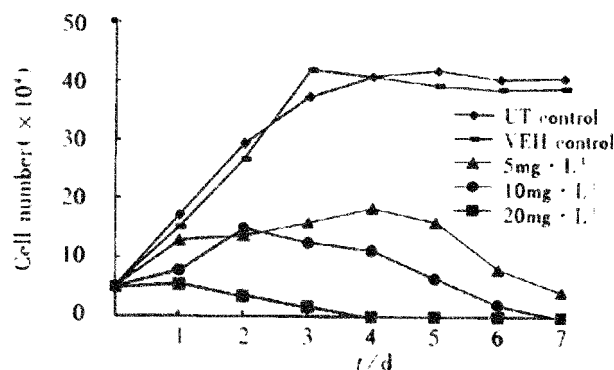


Figure 1 Growth curve of SGC-7901 cell treated with VES.

**MTT assay** SGC-7901 cells were treated in the presence or absence of VES for six days and cell viability was daily measured by MTT proliferation analysis. VES significantly inhibited cell growth and VES at 10 and 20 mg·L<sup>-1</sup> had an obviously inhibitory effect by 100% on the 5th and 4th days, respectively (Table1), similar to the findings from growth curve.

Table 1 Effect of VES on the viability of SGC-7901 cells

| Group                     | Rate of viable cells/% |       |      |       |       |      |
|---------------------------|------------------------|-------|------|-------|-------|------|
|                           | 1                      | 2     | 3    | 4     | 5     | 6    |
| UT control                | 100                    | 100   | 100  | 100   | 100   | 100  |
| VEH control               | 105.5                  | 102.4 | 92.1 | 95.3  | 105.7 | 97.5 |
| 5 mg·L <sup>-1</sup> VES  | 94.8                   | 101.2 | 91.4 | 144.3 | 91.4  | 74.6 |
| 10 mg·L <sup>-1</sup> VES | 91.4                   | 64.6  | 20.8 | 4.2   | 0     | 0    |
| 20 mg·L <sup>-1</sup> VES | 53.4                   | 32.9  | 4.3  | 0     | 0     | 0    |

### DNA synthesis arrest by VES

VES treatment of SGC-7901 cells inhibited [ $^3\text{H}$ ] thymidine



uptake with a dose-response relationship. DNA synthesis was evidently reduced by 35%, 45% and 98% after 24h VES treatment at 20 mg·L<sup>-1</sup> and 48h at 10 and 20 mg·L<sup>-1</sup>, respectively, compared with UT control ( $P<0.01$ ). On the other hand, VEH control did not affect SGC-7901 cell proliferation (Table 2).

**Table 2** Inhibitory effect of VES on DNA synthesis incorporated with <sup>3</sup>H-TdR ( $\bar{x}\pm s$ ,  $n=6$ )

| Group                     | Radioactive intensity/Bq·10 <sup>4</sup> cell <sup>-1</sup> |                            |
|---------------------------|-------------------------------------------------------------|----------------------------|
|                           | 24h(% of inhibition ratio)                                  | 48h(% of inhibition ratio) |
| UT control                | 64.1±10.2(0)                                                | 143.2±13.7(0)              |
| VEH control               | 63.8±10.3(1)                                                | 141.9±14.7(0)              |
| 5 mg·L <sup>-1</sup> VES  | 61.8±10.4(4)                                                | 137.1±16.3(4)              |
| 10 mg·L <sup>-1</sup> VES | 57.2±10.7(11)                                               | 79.3±10.0(45) <sup>b</sup> |
| 20 mg·L <sup>-1</sup> VES | 41.4± 8.0(35) <sup>b</sup>                                  | 2.2±0.3(98) <sup>b</sup>   |

<sup>b</sup> $P<0.01$ , vs UT control.

### VES induction of apoptosis

**Morphological changes** Apoptotic characteristics including chromatin condensation, chromatin crescent formation/margination, DNA fragmentation and apoptotic body formation were seen by electron microscopy (Figure 2) and by fluorescence microscopy of DAPI-labelled cells (Figure 3). The cells undergoing apoptosis evidently increased when the concentration of VES was elevated and reaction time was prolonged.

**Flow cytometry** VES-induced apoptosis was studied further in SGC-7901 cells using flow cytometry. Cell cycle analysis after VES treatment revealed the presence of a sub-G1 apoptotic peak (Figure 4).

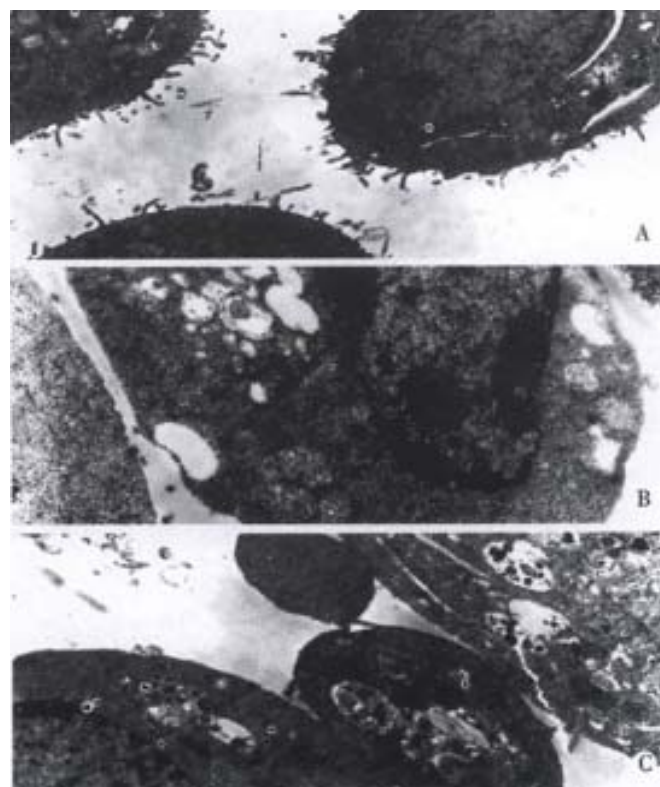


**Figure 2** VES-induced apoptosis in SGC-7901 cells with transmission electron microscope

A: Normal cell; B: Apoptotic cell with chromatin condensation, chromatin crescent formation/margination; C: Cell with apoptotic body.

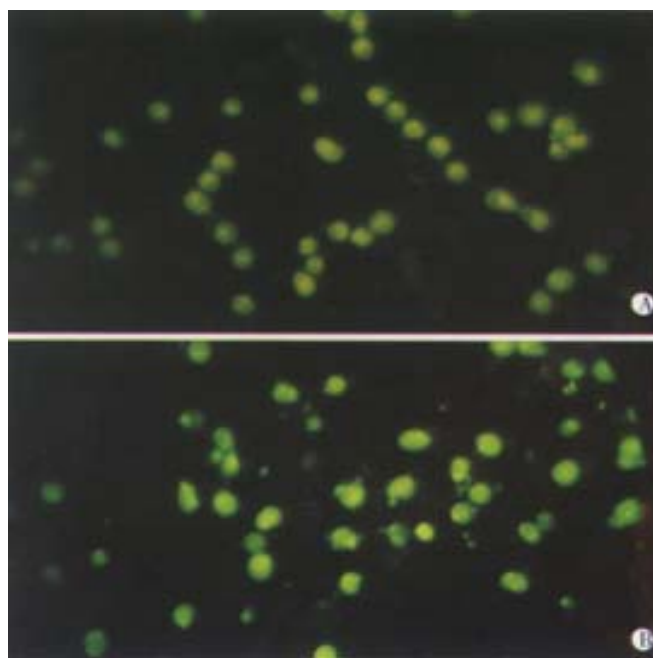


**Figure 3** VES-induced apoptosis in SGC-7901 cells with DAPI staining UT control; VES at 20 mg·L<sup>-1</sup>

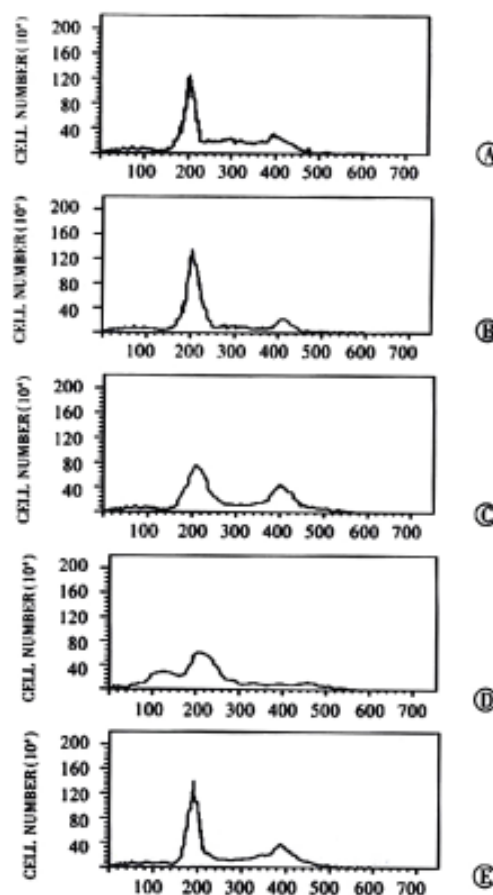


**Figure 4** VES-induced apoptosis in SGC-7901 cells with flow cytometry A: UT control; B: VEH control; C: VES at 5 mg·L<sup>-1</sup>; D: VES at 10 mg·L<sup>-1</sup>; E: VES at 20 mg·L<sup>-1</sup>.

**TUNEL assay** Apoptotic cell death was determined by TUNEL assay according to the manufacturer's instructions. The results showed that apoptotic cells increased with the increase of the concentration of VES in an obviously dose-dependent manner. The percentage of apoptosis was 90% after VES treatment at 20 mg·L<sup>-1</sup> (Figure 5 and Table 3).

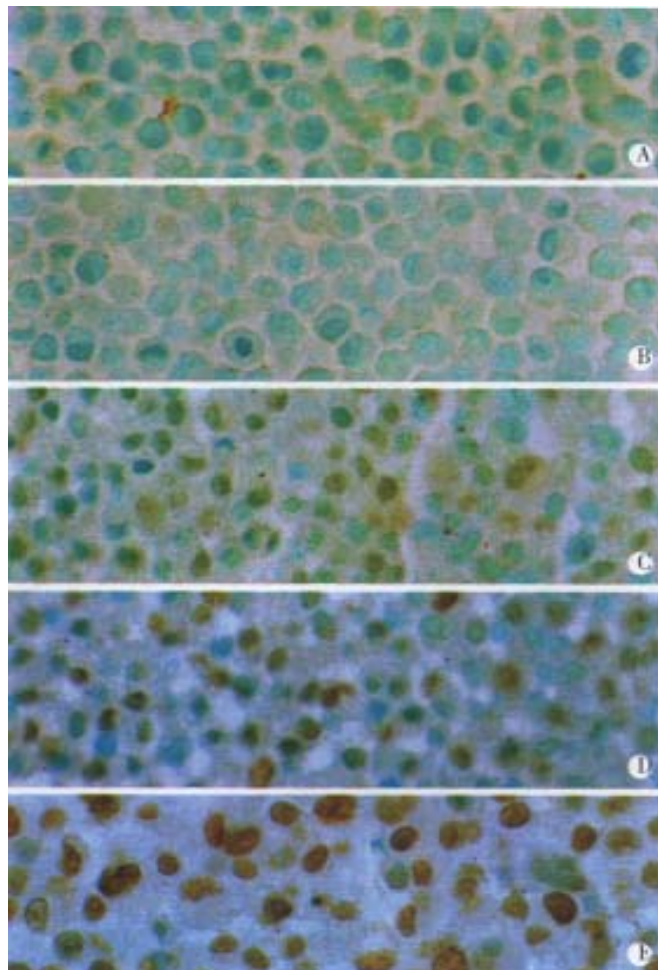


**Figure 5** VES-induced apoptosis by TUNEL assay.

A: UT control; B: VEH control; C: VES at 5 mg·L<sup>-1</sup>; D: VES at 10 mg·L<sup>-1</sup>; E: VES at 20 mg·L<sup>-1</sup>.

**Table 3** Induction of apoptosis after 48h of VES treatment in SGC-7901 cells

| Group                     | Apoptotic cells/10 <sup>4</sup> cells | Rate of apoptosis/% |
|---------------------------|---------------------------------------|---------------------|
| UT control                | 6                                     | 0.06                |
| VEH control               | 28                                    | 0.28                |
| 5 mg·L <sup>-1</sup> VES  | 1248 <sup>b</sup>                     | 12.48               |
| 10 mg·L <sup>-1</sup> VES | 5736 <sup>b</sup>                     | 57.63               |
| 20 mg·L <sup>-1</sup> VES | 8996 <sup>b</sup>                     | 89.96               |

<sup>b</sup>P<0.01, vs UT control.

## DISCUSSION

Cell growth is regulated by the interaction of cell proliferation and cell death. When cell growth is inhibited, the decrease of cell proliferation and increase of cell death will occur. Cell proliferation is performed by continuously proceeding into cell cycle and will be suppressed if cell cycle is disturbed<sup>[44-46]</sup>. The disorder of DNA synthesis, however, is a common reason for the disturbance of cell cycles<sup>[47,48]</sup>. Cell death is another principal reason for cell growth inhibition and is relevant to cell proliferation. Apoptotic cell death is a naturally occurring process of cell suicide which plays a crucial role in the development and homeostasis of metazons by eliminating superfluous or unwanted cells (reviewed by<sup>[49-53]</sup>).

Previous studies showed that VES can block DNA synthesis in tumor cells<sup>[43,54]</sup>. The percent of DNA synthesis arrest is more than 90% when human breast cancer cells are treated with VES at 10 mg·L<sup>-1</sup>, similar to the rate of breast cancer cell growth inhibition which exceeds 80%<sup>[15]</sup>. A recent study shows that VES can function as an apoptosis inducer in tumor cells. In this study, VES was found to inhibit cell proliferation in human gastric cancer SGC-7901 cells by trypan blue exclusion analysis and MTT assay. Cell growth was inhibited by 100% with treatment of VES at 10 mg·L<sup>-1</sup> on day 7 and at 20 mg·L<sup>-1</sup> on day 4 in the former experiment, while on the 6<sup>th</sup> and 4<sup>th</sup> days in the latter one. Meanwhile, VES significantly suppressed cell growth by DNA synthesis arrest via preventing SGC-7901 cells from progressing into S-phase, ultimately blocking the cell proliferation. In order to further elucidate the mechanisms of inhibitory effects of VES on cell growth, we determined the incidence of VES-mediated apoptosis in SGC-7901 cells by electron microscopy, DAPI staining, flow cytometry and TUNEL assay on the basis of morphological and molecular level. The results demonstrated that VES-treated SGC-7901 cells were characteristic by typical apoptotic alterations, including morphological changes by electron microscopy and DAPI staining, typical apoptotic sub-G<sub>1</sub> peak observed by flow cytometry; increase of apoptotic cells with the elevation of the concentration of VES in a clearly dose-dependent manner by TUNEL assay. The data above implicated that VES inhibits human gastric cancer SGC-7901 cell growth by inducing apoptosis and DNA synthesis arrest.

Apoptosis is a complex and programmed process which is regulated by a variety of factors<sup>[55-60]</sup>. The antiproliferative actions of VES may be due, in part, to the ability of VES to induce autocrine acting biologically active TGF-βs<sup>[9,14,17]</sup>. In addition, VES-mediated apoptosis is inhibited when c-Jun mutant is transfected into breast cancer cells<sup>[61]</sup>. JNK, mitogen-activated protein kinase (MAPK) family member, plays an important role in the course of VES-triggered apoptosis<sup>[31,61]</sup>. Although the exact mechanisms involved in VES-induced apoptosis have not been well known up to now, the ability of a compound to induce 90% apoptosis in a tumor cell population within 48h is noticeable. It is also noteworthy that VES can selectively inhibit the growth of tumor cells but not normal cells<sup>[8,62-64]</sup>. The research in our laboratory demonstrated that VES inhibited benzo (a)pyrene (B(a)P)-induced forestomach carcinogenesis in female mice<sup>[11]</sup>, while the inhibition and inhibitory mechanisms of VES *in vivo* are worth further investigating.

## REFERENCES

- Wang YF, Li QF, Wang H, Mao Q, Wu CQ. Effects of vitamin E on experimental hepatic fibrosis in rats. *Huaren Xiaohua Zazhi* 1998; 6: 207-209
- Jiang ZS, Gao Y. Biological feature of matrix metalloproteinase and its action in metastasis of liver cancer. *Shijie Huaren Xiaohua Zazhi* 2000;8:1403-1404
- Kline K, Yu W, Zhao B, Israel K, Charpentier A, Simmons-Menchaca M, Sanders BG. Vitamin E Succinate: Mechanisms of action as tumor cell growth inhibitor. In: Prasad KN, Santamaria L, Williams RM, eds. *Nutrients in Cancer Prevention and Treatment*. Totowa, NY: Humana, 1995:39-56
- Yu W, Sanders BG, Kline K. RRR-α-tocopheryl succinate inhibits EL4 thymic lymphoma cell growth by inducing apoptosis and DNA synthesis arrest. *Nutr Cancer* 1997;27:92-101
- Fariss MW, Fortuna MB, Everett CE, Smith JD, Trent DF, Djuric Z. The selective antiproliferation effects of α-tocopheryl hemisuccinate and cholesteryl hemisuccinate on murine leukemia cells result from the action of the intact compounds. *Cancer Res* 1994;54:3346-3351
- Ottino P, Duncan JR. Effect of α-tocopheryl succinate on free radical and lipid peroxidation levels in BL6 melanoma cells. *Free Radical Biol Med* 1997;22:1145-1151
- Schwartz J and Shklar G. The selective cytotoxic effect of carotenoids and α-tocopherol on human cancer cell lines *in vitro*. *J Oral Maxillofac Surg* 1992;50:367-373
- Kline K, Yu W, Sanders BG, Vitamin E. Mechanisms of action as tumor cell growth inhibitors. In: Prasad KN, Cole WC, eds. *Cancer and Nutrition*. Amsterdam: IOS, 1998:37-53

- 9 Simmons-Menchaca M, Qian M, Yu W, Sanders BG, Kline K. RRR- $\alpha$ -Tocopheryl succinate inhibits DNA synthesis and enhances the production and secretion of biologically active transforming growth factor- $\alpha$  by avian retrovirus-transformed lymphoid cells. *Nutr Cancer* 1995; 24:171-185
- 10 Yu W, Sanders BG, Kline K. Modulation of murine EL-4 thymic lymphoma cell proliferation and cytokine production by Vitamin E succinate. *Nutr Cancer* 1996;25:137-149
- 11 Wu K, Shan YJ, Zhao Y, Yu JW, Liu BH. Inhibitory effects of RRR- $\alpha$ -tocopheryl succinate on benzo(a)pyrene (B(a)P)-induced forestomach carcinogenesis in female mice. *World J Gastroenterol* 2001;17:60-65
- 12 Wu K, Guo J, Shan YJ, Liu BH. The effects of vitamin E succinate on apoptosis in human gastric cancer. *Weisheng Dulixue Zazhi* 1999;13:84-90
- 13 Wu K, Ren Y, Guo J. The effects of vitamin E succinate on the cyclic regulation protein of human gastric cancer cells. *Weisheng Dulixue Zazhi* 1998;12:203-207
- 14 Turley JM, Ruscetti FW, Kim SJ, Fu T, Gao FV, Birchenall-Roberts MC. Vitamin E succinate inhibits proliferation of BT-20 human breast cancer cells: increased binding of cyclin A negatively regulates E2F transactivation activity. *Cancer Res* 1997;57:2668-2675
- 15 Malafa MP, Neitzel LT. Vitamin E succinate promotes breast cancer tumor dormancy. *J Surg Res* 2000;93:163-170
- 16 Kim SJ, Bang OS, Lee YS, Kang SS. Production of inducible nitric oxide is required for monocytic differentiation of U937 cells induced by vitamin E-succinate. *J Cell Sci* 1998;111 (Pt 4):435-441
- 17 Ariazi EA, Satomi Y, Ellis MJ, Haag JD, Shi W, Sattler CA, Gould MN. Activation of the transforming growth factor beta signaling pathway and induction of cytostasis and apoptosis in mammary carcinomas treated with the anticancer agent perillyl alcohol. *Cancer Res* 1999;59:1917-1928
- 18 Neuzil J, Weber T, Schroder A, Lu M, Ostermann G, Gellert N, Mayne GC, Olejnicka B, Negre-Salvayre A, Sticha M, Coffey RJ, Weber C. Induction of cancer cell apoptosis by alpha-tocopheryl succinate: molecular pathways and structural requirements. *FASEB J* 2001;15:403-415
- 19 Turley JM, Fu T, Ruscetti FW, Mikovits JA, Bertolette DC, Birchenall-Roberts MC. Vitamin E succinate induces Fas-mediated apoptosis in estrogen receptor-negative human breast cancer cells. *Cancer Res* 1997;57:881-890
- 20 Yu W, Israel K, Liao QY, Aldaz CM, Sanders BG, Kline K. Vitamin E succinate (VES) induces Fas sensitivity in human breast cancer cells: role for Mr 43,000 Fas in VES-triggered apoptosis. *Cancer Res* 1999;59:953-961
- 21 Foehr ED, Bohuslav J, Chen LF, DeNoronha C, Gelezianus R, Lin X, O'Mahony A, Greene WC. The NF-kappa B-inducing kinase induces PC12 cell differentiation and prevents apoptosis. *J Biol Chem* 2000; 275:34021-34024
- 22 Sementchenko VI, Watson DK. Ets target genes: past, present and future. *Oncogene* 2000;19:6533-6548
- 23 Steff AM, Trop S, Maira M, Drouin J, Hugo P. Opposite Ability of Pre-TCR and alphabetaTCR to induce apoptosis. *J Immunol* 2001;166:5044-5050
- 24 Liu HF, Liu WW, Fang DC, Men RP. Relationship between Fas antigen expression and apoptosis in human gastric carcinoma and adjacent noncancerous tissues. *Huaren Xiaohua Zazhi* 1998;6:321-322
- 25 Xu HY, Yang YL, Guan XL, Song G, Jiang AM, Shi LJ. Expression of regulating apoptosis gene and apoptosis index in primary liver cancer. *World J Gastroenterol* 2000;6:721-724
- 26 Lacour S, Hammann A, Wotawa A, Corcos L, Solary E, Dimanche-Boitrel MT. Anticancer agents sensitize tumor cells to tumor necrosis factor-related apoptosis-inducing ligand-mediated caspase-8 activation and apoptosis. *Cancer Res* 2001;61:1645-1651
- 27 Liang WJ, Huang ZY, Ding YQ. Time effect of TNF $\alpha$  on apoptosis of Lovo cells of human colorectal carcinoma. *Huaren Xiaohua Zazhi* 1998;6:27-29
- 28 Nagata S. Symposium on apoptosis and medical diseases-Fas-induced apoptosis. *Internal Med* 1998;37:179-181
- 29 Leblanc V, Delumeau I, Tocqué B. Ras-GTPase activating protein inhibition specifically induces apoptosis of tumour cells. *Oncogene* 1999;18:4884-4889
- 30 Lu SY, Pan XZ, Peng XW, Shi ZL, Lin L, Chen MH. Effect of Hp infection on gastric epithelial cell kinetics in stomach diseases. *Shijie Huaren Xiaohua Zazhi* 2000;8:386-388
- 31 Wu K, Liu BH, Zhao DY, Zhao Y. The effect of vitamin E succinate on the expression of TGF- $\beta$ 1, c-Jun and JNK1 in human gastric cancer SGC-7901 cells. *World J Gastroenterol* 2001;17:83-87
- 32 Mao ZB, Meng XY, Ge ZJ, Li RZ, Shi GS. Expression of arylamidase isoenzyme in gastric carcinoma and precancerous lesions. *Huaren Xiaohua Zazhi* 1998;6:323-325
- 33 Wang LP, Yu JY, Deng YJ, Tian YW, Wu X, Liu G, Ding HY. Relationship between the expression of somatostatin and epidermal growth factor receptor in gastric carcinoma. *Huaren Xiaohua Zazhi* 1998;6:606-609
- 34 Zhang QX, Dou YL, Shi XY, Ding Yi. Expression of somatostatin mRNA in various differentiated types of gastric carcinoma. *World J Gastroenterol* 1998;4:48-51
- 35 Liu ZM, Shou NH. Expression significance of mdrl gene in gastric carcinoma tissue. *Shijie Huaren Xiaohua Zazhi* 1999;7:145-146
- 36 Yu WL, Huang ZH. Progress in studies on gene therapy for gastric cancer. *Shijie Huaren Xiaohua Zazhi* 1999;7:887-889
- 37 Chen GY, Wang DR. The expression and clinical significance of CD44v in human gastric cancers. *World J Gastroenterol* 2000;6:125-127
- 38 Wang RQ, Fang DC, Liu WW. MUC2 gene expression in gastric cancer and preneoplastic lesion tissues. *Shijie Huaren Xiaohua Zazhi* 2000;8:285-288
- 39 Guo YQ, Zhu ZH, Li JF. Flow cytometric analysis of apoptosis and proliferation in gastric cancer and precancerous lesion. *Shijie Huaren Xiaohua Zazhi* 2000;8:983-987
- 40 Chen SY, Wang JY, Ji Y, Zhang XD, Zhu CW. Effects of *Helicobacter pylori* and protein kinase C on gene mutation in gastric cancer and precancerous lesions. *Shijie Huaren Xiaohua Zazhi* 2001;9:302-307
- 41 Xu AG, Li SG, Liu JH, Gan AH. Function of apoptosis and expression of the proteins Bcl-2, p53 and C-myc in the development of gastric cancer. *World J Gastroenterol* 2001;7:403-406
- 42 Liu BH, Wu K, Zhao DY. Inhibition of human gastric cancer SGC-7901 cell growth by vitamin E succinate. *Weisheng Yanjiu* 2000;29:172-174
- 43 Liu BH, Wu K. Study on the growth inhibition of Vitamin E Succinate in human gastric cancer cell. *Aibian Jibian Tubian* 2000;12:79-81
- 44 Sturla LM, Westwood G, Selby PJ, Lewis IJ, Burchill SA. Induction of cell death by basic fibroblast growth factor in Ewing's sarcoma. *Cancer Res* 2000;60:6160-6170
- 45 Wang H, Chow DA. Natural antibody-induced intracellular signaling and growth control in C3H 10T1/2 fibroblast variants. *Immunology* 2000;101:458-467
- 46 Shen MR, Droogmans G, Eggermont J, Voets T, Ellory JC, Nilius B. Differential expression of volume-regulated anion channels during cell cycle progression of human cervical cancer cells. *J Physiol* 2000;529:385-394
- 47 Keller C, Krude T. Requirement of Cyclin/Cdk2 and protein phosphatase 1 activity for chromatin assembly factor 1-dependent chromatin assembly during DNA synthesis. *J Biol Chem* 2000;275:35512-35521
- 48 Khan SH, Moritsugu J, Wahl GM. Differential requirement for p19ARF in the p53-dependent arrest induced by DNA damage, microtubule disruption, and ribonucleotide depletion. *Proc Natl Acad Sci U S A* 2000;97:3266-3271
- 49 Green DR, Reed JC. Mitochondria and apoptosis. *Science* 1998;281: 1309-1312
- 50 Xue XC, Fang GE, Hua JD. Gastric cancer and apoptosis. *Shijie Huaren Xiaohua Zazhi* 1999;7:359-361
- 51 Ashkenazi A, Dixit VM. Apoptosis control by death and decoy receptors. *Curr Opin Cell Biol* 1999;11:255-260
- 52 Wu K, Zhao Y, Yu W. Study on apoptosis. *Guowai Yixue Yichuanxue Fence* 2001;24:134-138
- 53 Li Y, Wu K. Effectors of apoptosis. *Guowai Yixue Weishengxue Fence* 2001;28:50-54
- 54 Wu K, Guo J, Shan YJ. Inhibitory effects of VES on the growth of human squamous gastric carcinoma cells. In: Johnson IT and Fenwick GR, eds. Dietary anticarcinogens and antimutagens-Chemical and biological aspects. RS-C, UK: Athenaum Press 2000:304-307
- 55 Yang WC, Wang LD. The mechanisms of cell proliferation control by tumor inhibitory genes and oncogenes. *Xin Xiaohuabingxue Zazhi* 1997;5:262-263
- 56 Aravind L, Dixit VM, Koonin EV. The domains of death: evolution of the apoptosis machinery. *TIBS* 1999;24:47-53
- 57 Gu XH, Li QF, Wang YM. Expression of hepatocyte apoptosis and Fas/FasL in liver tissues of patients with hepatitis D. *Shijie Huaren Xiaohua Zazhi* 2000;8:35-38
- 58 Sun BH, Zhao XP, Wang BJ, Yang DL, Hao LJ. FADD and TRADD expression and apoptosis in primary human hepatocellular carcinoma. *World J Gastroenterol* 2000;6:223-227
- 59 Zhao Y, Wu K. Cell death molecule Fas/CD95 and apoptosis. *Aibian Jibian Tubian* 2001;13:55-58
- 60 Yang JQ, Yang LY, Zhu HC. Mitomycin C induced apoptosis of human hepatoma cell. *Shijie Huaren Xiaohua Zazhi* 2001;9:268-272
- 61 Yu W, Simmons-Menchaca M, You H. RRR- $\alpha$ -Tocopheryl Succinate induction of prolonged activation of c-Jun amino-terminal kinase and c-Jun during induction of apoptosis in human MDA-MB-435 breast cancer cells. *Mol Carcinogenesis* 1998;22:247-267
- 62 Simmons-Menchaca M, Qian M, Yu W, Sanders BG, Kline K. RRR- $\alpha$ -tocopheryl succinate inhibits DNA synthesis and enhances the production and secretion of biologically active transforming growth factor- $\beta$  by avian retrovirus-transformed lymphoid cells. *Nutr Cancer* 1995;24:171-185
- 63 Kline K, Sanders BG. RRR- $\alpha$ -tocopheryl succinate inhibition of lectin-induced T cell proliferation. *Nutr Cancer* 1993;19:241-252
- 64 Neuzil J, Weber T, Gellert N, Weber C. Selective cancer cell killing by alpha-tocopheryl succinate. *Br J Cancer* 2000;84:87-89



• ESOPHAGEAL CANCER •

# Morphological and functional changes of mitochondria in apoptotic esophageal carcinoma cells induced by arsenic trioxide

Zhong-Ying Shen, Jian Shen, Qiao-Shan Li, Cai-Yun Chen, Jiong-Yu Chen, Yi Zeng

Zhong-Ying Shen, Jian Shen, Qiao-Shan Li, Department of Pathology, Medical College of Shantou University, Shantou 515031, Guangdong Province, China

Cai-Yun Chen, Central Lab. Medical College of Shantou University  
Jiong-Yu Chen, Central Lab. of Tumor Hospital, Medical College of Shantou University

Yi Zeng, Institute of Virology, Chinese Academy of Preventive Medicine, Beijing 100052, China

Supported by the National Natural Science Foundation of China No. 39830380

Correspondence to: Dr. Zhong-Ying Shen, Department of Pathology, Medical College of Shantou University, 22 Xinglin Road, Shantou 515031, Guangdong Province, China. zhongyingshen@yahoo.com  
Telephone: +86-754-8538621 Fax: +86-754-8537516

Received 2001-06-02 Accepted 2001-11-20

## Abstract

**AIM:** To demonstrate that mitochondrial morphological and functional changes are an important intermediate link in the course of apoptosis in esophageal carcinoma cells induced by  $\text{As}_2\text{O}_3$ .

**METHODS:** The esophageal carcinoma cell line SHEEC1, established in our laboratory, was cultured in 199 growth medium, supplemented with  $100\text{mL}\cdot\text{L}^{-1}$  calf serum and  $3\mu\text{mol}\cdot\text{L}^{-1}\text{As}_2\text{O}_3$  (the same below). After 2, 4, 6, 12, 24 h of drug adding, the SHEEC1 cells were collected for light-and electron-microscopic examination. The mitochondria were labeled by Rhodamine fluorescence probe and the fluorescence intensity of the mitochondria was measured by flow cytometer and cytofluorimetric analysis. Further, the mitochondrial transmembrane potential (MTP,  $\Delta\Psi\text{m}$ ) change was also calculated.

**RESULTS:** The mitochondrial morphological change after adding  $\text{As}_2\text{O}_3$  could be divided into three stages. In the early-stage (2-6 h) after adding  $\text{As}_2\text{O}_3$ , an adaptive proliferation of mitochondria appeared; in the mid-stage (6-12 h) a degenerative change was observed; and in the late-stage (12-24 h) the mitochondria swelled with outer membrane broken down and then cells death with apoptotic changes of nucleus. The functional change of the mitochondria indicated by fluorescent intensity, which reflected the MTP status of mitochondria, was in accordance with morphological change of the mitochondria. The fluorescent intensity increased at early-stage, declined in mid-stage and decreased to the lowest in the late-stage. 24 h after  $\text{As}_2\text{O}_3$  adding, the cell nucleus showed typical apoptotic changes.

**CONCLUSION:** Under the inducement of  $\text{As}_2\text{O}_3$ , the early apoptotic changes of SHEEC1 cells were the apparent morphological and functional changes of mitochondria, afterwards the nucleus changes followed. It is considered that changes of mitochondria are an important intermediate link in the course of apoptosis of esophageal carcinoma

## cells induced by $\text{As}_2\text{O}_3$ .

Shen ZY, Shen J, Li QS, Chen CY, Chen JY, Zeng Y. Morphological and functional changes of mitochondria in apoptotic esophageal carcinoma cells induced by arsenic trioxide. *World J Gastroenterol* 2002;8(1):31-35

## INTRODUCTION

Esophagus cancer is common in China<sup>[1-11]</sup>. The treatment is still a focus of research<sup>[12-17]</sup>. Induction of cell apoptosis is a novel therapeutic strategies for cancer<sup>[18-25]</sup>. In our previous work, we used  $\text{As}_2\text{O}_3$  to induce apoptosis of esophageal carcinoma cells<sup>[26]</sup>. The pathomorphological changes evinced that cells became smaller, the cells shrank, the nuclei rounded up, chromatin agglutinated and marginated, nuclear membrane broke down and then followed by the degenerative changes of the cells. All these changes indicated typical morphological changes of apoptosis<sup>[27]</sup>. The necrotic changes were also found with a large dosage of  $\text{As}_2\text{O}_3$ <sup>[28]</sup>. We discovered that in the early-stage of cell apoptosis, prior to the obvious change of cell nuclei, the mitochondria showed proliferation. The detailed morphological changes of mitochondria of esophageal carcinoma cells induced by  $\text{As}_2\text{O}_3$  were firstly described in our paper<sup>[29]</sup>. We also found that nitric oxide (NO) was released from the cultured esophageal carcinoma cell line after administration of  $\text{As}_2\text{O}_3$  with increasing amounts at the early apoptotic stage<sup>[30]</sup>. Furthermore, down regulated expression of bcl-2 and over expression of bax were always found in apoptotic cells induced by  $\text{As}_2\text{O}_3$ <sup>[31]</sup>.

Some authors hold that apoptosis is a programmed cell death (PCD); the death signal originates from the inside of cells; the change chiefly involves the cell nucleus with no apparent changes seen in the cytoplasm and cell organelle<sup>[32-33]</sup>; making it different from cell necrosis<sup>[34]</sup>. In our studies, the morphological changes of apoptotic cells induced by  $\text{As}_2\text{O}_3$  were different from the programmed cell death in which the latter showed the nuclear changes at first and then cytoplasm, and the former were vice versa<sup>[35]</sup>. In recent years, it has been explained that apoptosis is related to certain factors, such as Bcl-2/Bax,<sup>[36-39]</sup>  $\text{Ca}^{2+}$ <sup>[40]</sup> and cytochrome c<sup>[41-42]</sup>, which are all located on mitochondria<sup>[43]</sup>. When they are released from mitochondria, they can inhibit or promote cell apoptosis. Therefore, mitochondria are thought to be the apoptosis regulation center<sup>[44]</sup>. Mitochondria are also an important organelle. They are concerned with cell breathing, oxygen metabolism, enzyme activity and energy supply. All of those functions relate to the permeability of the mitochondria and mitochondrial transmembrane potential (MTP,  $\Delta\Psi\text{m}$ ). When MTP decreases, the mitochondria generate morphological and functional changes<sup>[45-47]</sup>.

Rhodamine 123 (Rho123), a kind of fluorescent dye, is traditionally used as a mitochondria probe<sup>[48]</sup>. Rho 123 can quickly gather on living cell mitochondria. The fluorescence intensity of Rho123 represents MTP which reflects the cell in a quiescent or active condition, and in a proliferative or differentiative manner<sup>[49]</sup>. Flow cytometer and fluorescent microphotometry are the satisfactory

instruments to measure Rho123 fluorescent intensity. The purpose of this paper is to study the mitochondrial morphological and functional changes during the cell apoptosis of esophageal carcinoma cell line induced by  $\text{As}_2\text{O}_3$ , thus demonstrating that mitochondrial changes play an important role in the course of cell apoptosis.

## MATERIALS AND METHODS

### Cell line and $\text{As}_2\text{O}_3$ adding

The esophageal carcinoma cell line SHEEC1 is the human embryonic esophageal epithelial cells malignantly transformed by HPV18 E6 E7 in synergy with TPA<sup>[50]</sup>. It is cultured in 199 growth medium, supplemented with  $100\text{mL}\cdot\text{L}^{-1}$  calfserum and antibiotics. In experiments, SHEEC1 cells were cultured separately in culture flasks and on 24-well culture plates (Corning Co.) with the cover slide inside the well, in every well  $10^4$  SHEEC1 cells were inoculated.  $\text{As}_2\text{O}_3$  (Sigma, St. Louis, Mo; Lot A 1010) was prepared in concentration of  $3\mu\text{mol}\cdot\text{L}^{-1}$  with 199 growth medium. The experimental group and the control group without  $\text{As}_2\text{O}_3$  administered were examined at definite times. The experiments were repeated once.

### Examination under light-and electron-microscope

At 2,4,6,12,24 h after  $\text{As}_2\text{O}_3$  adding, one culture flask of SHEEC1 cultured cells was taken for examination. The floating cells in the flasks were collected by centrifugation (CytospinIII, Shandon Co.), Giemsa stained and examined by light-microscope. Cells attached to flask were digested with  $2.5\text{g}\cdot\text{L}^{-1}$  trypsin, centrifuged, the cell pallet was fixed with  $25\text{g}\cdot\text{L}^{-1}$  glutaraldehyde, and were routinely prepared for electron-microscopic examination.

### Rhodamine fluorescent probe labeling and cytofluorimetric analysis (CFA)<sup>[51,52]</sup>

SHEEC1 cells were placed on the slide after reacting with  $\text{As}_2\text{O}_3$  at various times, stained by Rhodamine 123 (Rho123, MW381, Molecular Probe Inc. Eugene) at the concentration of  $10\text{mg}\cdot\text{L}^{-1}$ , and the cells were incubated in  $37^\circ\text{C}$ ,  $50\text{mL}\cdot\text{L}^{-1}$   $\text{CO}_2$  incubator for 15 min. It was examined by fluorescent microscopy and cytofluorimetry. Using the Nikon fluorescent microscope (Fluophot, Nikon) with Low-cost cooled digital CCD camera system and software STARI (Photometrics LTD. USA), the fluorescent image of mitochondria of SHEEC1 cells labeled by Rho123 were displayed on the screen of monitor, the fluorescent intensity of cells was measured by scanning method, and the average amount of cellular fluorescence was calculated by software.

### Flow cytometer (FCM) examination<sup>[53]</sup>

Following  $\text{As}_2\text{O}_3$  treatment, SHEEC1 cell cultured in flasks were harvested with trypsinization, washed once with PBS, resuspended in PBS, and incubated with Rho123 ( $10\text{mg}\cdot\text{L}^{-1}$ ) at  $37^\circ\text{C}$  for 15 min, stained cells were wash twice with PBS, dispersed, filtered through a 360 mesh nylon net to make single cell suspension.  $10^9$  cell $\cdot\text{L}^{-1}$  were detected by flow cytometer (FACSort, B-D Co. USA) using exciting light 488nm and emission light 515nm to detect Rho123 fluorescent intensity. The histogram managed by the computer was drawn according to the fluorescent intensity value of one cell. Partial of SHEEC1 cells were fixed with  $700\text{mL}\cdot\text{L}^{-1}$  alcohol, stained with propidium iodide (Sigma) and analyzed with flow cytometer. The cell cycle and apoptotic cell rate were calculated.

### Calculation of mitochondrial transmembrane potential (MTP. $\Delta\Psi\text{m}$ )<sup>[46]</sup>

Examining  $10^4$  cells by FCM, the average fluorescent intensity of the

cells labeled by Rho 123 before and after  $\text{As}_2\text{O}_3$  adding were drawn as histograms for comparing. By cytofluorimetric analysis the average fluorescent intensity value ( $\bar{x}\pm s$ ) was calculated from one cell.

## RESULTS

### Cell apoptosis

Twenty-four hours after  $\text{As}_2\text{O}_3$  acting on SHEEC1 cells, the apoptotic peak (28% of the cells) before  $\text{G}_1\text{G}_0$  in DNA histogram of FCM examination appeared (Figure 1). Collecting the floating cells by cytospin and Giesma staining, the cell nuclei showed typical cell apoptotic changes with chromatin agglutinated and margined (Figure 2).

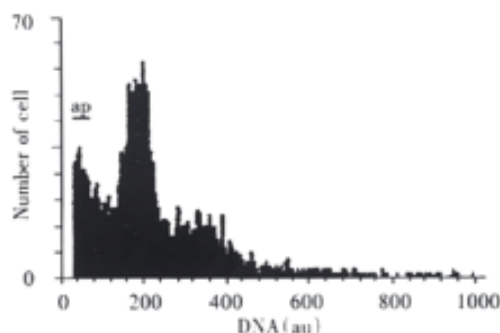


**Figure 1** DNA histogram of SHEEC1 cells 24 h after Figure 2 Apoptotic changes 24 h after  $\text{As}_2\text{O}_3$ .

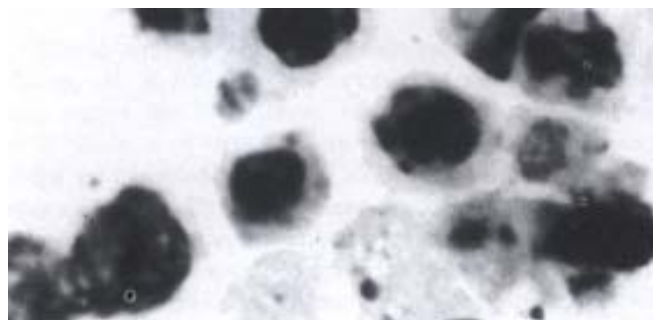


**Figure 2**  $\text{As}_2\text{O}_3$  adding. ap, apoptotic peak. adding, HE $\times 400$ .

### Morphological changes of mitochondria under transmission electron-microscope

Before adding  $\text{As}_2\text{O}_3$  the mitochondria were located around the nucleus in one or two arrays (Figure 3A). There were fixed intervals between mitochondria, in which other organelles were present. When adding  $\text{As}_2\text{O}_3$  2-4 h, the mitochondria increased, which showed either concentration in certain areas or in one pole of the cytoplasm or distributed in inner, middle or outer layer of the cytoplasm (Figure 3B). Mitochondria were oval in shape and different in size. The newly proliferated mitochondria were smaller with dense matrix. Some mitochondria were condensed with indistinct ridges and some mitochondria were crowded closely together. After 6 h, the high electron dense and irregular shaped substances precipitated in the mitochondrial matrix, even filled up the whole mitochondria (Figure 3C). The autophagosomes resulting from wrapping of condensed mitochondria by the lysosomes were frequently seen. After 12 h, the mitochondria swelled, its outer membrane broke down, left a single layer of membrane, which were seen like a balloon or a vacuole. After 24 h, the cell nucleus shrank and chromatin agglutinated locating near the nuclear membrane with mitochondria swelling, or becoming vacuole-like or broken down (Figure 3D).



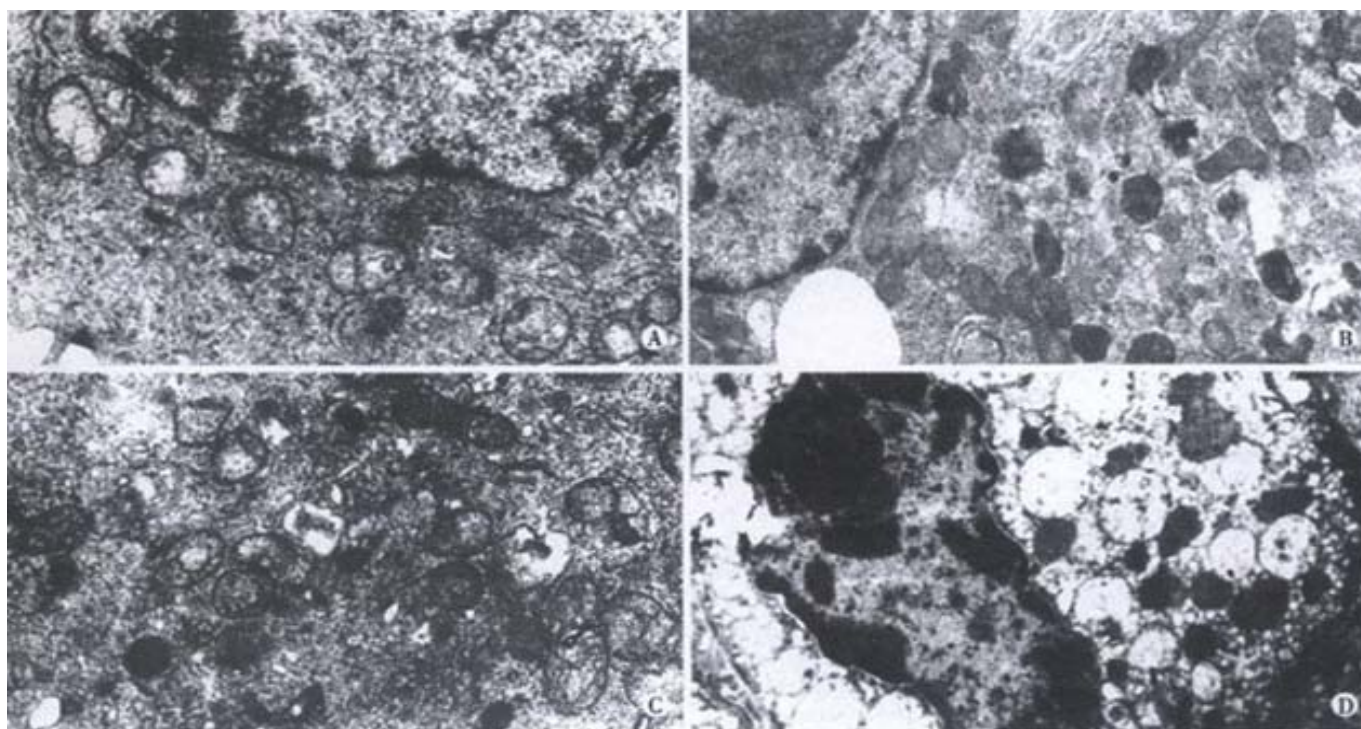


**Figure 3** Apoptotic cells (EM x 15000). Mitochondria in 1-2 arrays located around the cell nucleus, not adding As<sub>2</sub>O<sub>3</sub>; Increment of mitochondria 2-4 h after As<sub>2</sub>O<sub>3</sub> adding; Dense substances deposition in mitochondria 4-6h after As<sub>2</sub>O<sub>3</sub> adding; Apoptotic cell showed cell nucleus shrank, chromatin agglutinated, mitochondria increased and swelled as balloon-like 24h after As<sub>2</sub>O<sub>3</sub> adding.

### Functional changes of mitochondria in cell apoptosis: the dynamic changes of MTP ( $\Delta\Psi_m$ )

**Mitochondrial fluorescence intensity detected by FCM** After As<sub>2</sub>O<sub>3</sub> was added to SHEEC1 cells, the changes of mitochondria fluorescence intensity from different reacting times were seen in histogram (Figure 4 A,B,C,D). A slight increase of mitochondrial fluorescence intensity was observed at 2h after added As<sub>2</sub>O<sub>3</sub>. With treatment of As<sub>2</sub>O<sub>3</sub> for 4-6h, fluorescent intensity of mitochondria was decreased sharply. After 12-24h fluorescent intensity was the lowest.

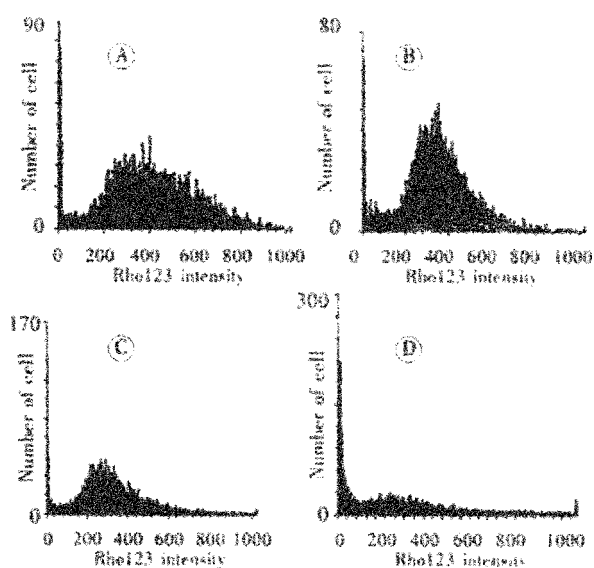


**Figure 4** The histogram of mitochondrial fluorescent intensity by FCM after As<sub>2</sub>O<sub>3</sub> adding.

A: Control; B: 2-4 h; C: 4-6 h; D: 12-24 h.

**Fluorescent intensity by cytofluorimetric analysis** Under fluorescent microscope, the number of mitochondria of cells was increased at first (Figure 5) and then decreased. The fluorescent intensity increased in 2h after As<sub>2</sub>O<sub>3</sub> added, declined in 4-6h and decreased to the lowest in the 12-24h (Table 1). An increment of fluorescence intensity in partial early-stage apoptotic cells after 2 h of As<sub>2</sub>O<sub>3</sub> adding and the intensity decreased hereafter. Following fluorescence associated with the uptake of dye Rho123 allows to evaluate  $\Delta\Psi_m$  modifications, the results showed the dynamic MTP changes in the apoptotic process induced by As<sub>2</sub>O<sub>3</sub>.

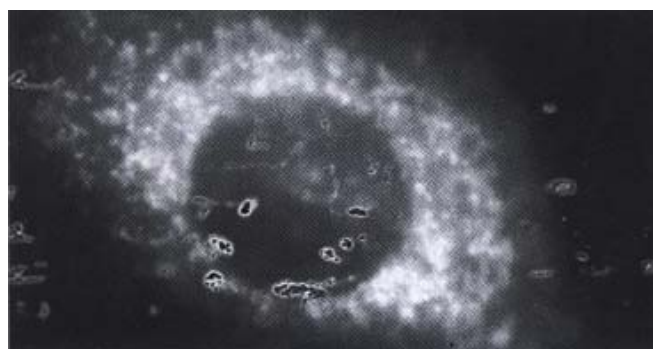


**Figure 5** Increment of mitochondria with Rho123 labeled in cytoplasm of SHEEC1 after 2-4 h As<sub>2</sub>O<sub>3</sub> adding.  $\times 1000$

The Rho123 fluorescence intensity of the labeled mitochondria differed from different reacting times after adding As<sub>2</sub>O<sub>3</sub>. At first fluorescent intensity increased and then the rapidly declining value of fluorescence intensity was in accordance with both results of FCM and CFA. It taking cell morphology into account, the fluorescence intensity changes may reflect the consequence of As<sub>2</sub>O<sub>3</sub> stimulation to mitochondria for different times. 2 h after As<sub>2</sub>O<sub>3</sub> was added, the mitochondria proliferated and the fluorescent intensity increased, soon after the

intensity swiftly declined and went to the lowest at 24 h, which indicated that morphological and functional changes of mitochondria induced by  $As_2O_3$  represented the process cell apoptosis.

**Table 1** Average fluorescence intensity value of SHEEC1 after  $As_2O_3$  adding (arbitrary unit  $\times 10^{-4}/\text{cell}$ )

| T (after $As_2O_3$ )<br>h | Fluorescence<br>intensity ( $\bar{x} \pm s$ ) |
|---------------------------|-----------------------------------------------|
| Control                   | 180.3 $\pm$ 75.7                              |
| 2                         | 206.4 $\pm$ 93.2                              |
| 4                         | 170.2 $\pm$ 80.3                              |
| 6                         | 168.2 $\pm$ 72.2                              |
| 12                        | 114.4 $\pm$ 70.3                              |
| 24                        | 90.7 $\pm$ 85.6                               |

## DISCUSSION

Reports about  $As_2O_3$  inducement of apoptosis of cancer cells have been seen frequently in hemopoietic stem cells and leukemia cells<sup>[54-60]</sup>, but rarely in epithelial tumor cells<sup>[61-64]</sup>. We have tried to explore the possibility of curing esophageal carcinoma by using  $As_2O_3$  treatment *in vitro*. The experimental results have shown that  $As_2O_3$  can induce cancer cell apoptosis, large doses of  $As_2O_3$  can even induce cell necrosis. Our previous works indicated that at the early-stage of cell apoptosis, morphological changes of the mitochondria might be an important phenomenon in the course of esophageal carcinoma cell apoptosis induced by  $As_2O_3$ <sup>[29, 31]</sup>. Our results showed that morphological and functional changes of mitochondria of SHEEC1 cells were induced by  $As_2O_3$ . It could divide into three stages. Two to four h after  $As_2O_3$  administration, the mitochondria proliferated with a lot of new small mitochondria, distributing from the inner layer to the outer layer of cytoplasm. This was the early reaction of mitochondria of SHEEC1 cells to the effect of  $As_2O_3$ . 6 h after  $As_2O_3$  inducement, many ridges on mitochondria were seen. The dense substances began to precipitate in the matrix of mitochondria and the condensed or damaged mitochondria were engulfed by lysosomes to form autophagosomes as seen in lymphocytes<sup>[65]</sup>. Twelve hours after  $As_2O_3$  inducement, the mitochondria were swelling, or vacuolation with mitochondria ridges decreased or disappeared. Twenty-four h after  $As_2O_3$  inducement, apoptotic cells appeared with coagulating chromatin in nucleus and shrinking in the whole cell. The mitochondria swelled like a balloon. During the whole course of cell apoptosis, changes of mitochondria preceded the changes in nuclei.

The fluorescent intensity value detected by CFA and FCM reflects the function of mitochondria<sup>[66]</sup>. The change of Rho123 fluorescent intensity under  $As_2O_3$  treatment may be divided into 3 time phases: 2-4h after  $As_2O_3$  inducement, mitochondria increased fluorescent intensity, but began to decline after 4-6 h and decreased to the lowest after 12-24 h. These functional changes of mitochondria were in accordance with mitochondrial morphological changes.

The functional changes of mitochondria may be accompanied with decreasing the formation of ATP, reducing the activity of dehydrogenase<sup>[67]</sup>, thus influencing cell respiration, cell metabolism, energy supply and even the cell death. If the mitochondrial release cytochrome c or apoptotic inducement factors (AIF), they may activate the caspases enzyme system, which further act upon cell nucleus and cell keratinoprotein to induce irreversible apoptotic changes<sup>[68]</sup>. If the mitochondrial changes resulted in lowering of  $\Delta\Psi_m$ , increase of oxygen free radical and blocking up the formation of ATP, the cells will be finally undergo necrosis, because they lose the ability of electron bond transmission. Therefore, the mitochondrial changes may induce cell apoptosis and also cell necrosis<sup>[69]</sup>. When the inducement factor is strong or highly concentrated it induces cell necrosis. If less in amount and strength, it may give times to activate the caspases enzyme system<sup>[70]</sup>, the cell apoptosis will develop. Mitochondrial fluorescent probe Rho123 is a very useful tool, which may specifically conjugate with mitochondria to indicate cells living

state or metabolic state<sup>[25]</sup>. Detecting Rho123 fluorescence intensity of mitochondria may reveal mitochondrial quantity and function under different kinds of stimuli. The Rho123 fluorescence intensity is stronger in proliferative cells than in quiescent cells, and the intensity decreases in damaged mitochondria caused by harmful stimuli<sup>[48]</sup>. The amount of Rho123 conjugated with mitochondria differs in different types of cells and in different cell functional status<sup>[66]</sup>. The mitochondrial changes of SHEEC1 cells induced by  $As_2O_3$  occurred 2-4 h after drug adding. Under the same cultured conditions, mitochondria were supposed to be the firstly targeting site in the course of cell apoptosis. Therefore, under  $As_2O_3$  inducement, the morphological and functional in mitochondria of SHEEC1 cells, which happened prior to cell nuclear DNA change, may be regarded as the important link in cell apoptosis.

## REFERENCES

- He LJ, Wu M. The distribution of esophageal and cardiac carcinoma and precancerous of 2238. *World J Gastroenterol* 1998; 4(Suppl 2):100
- Yu GQ, Zhou Q, DING Ivan, Gao SS, Zheng ZY, Zou JX, Li YX, Wang LD. Changes of p53 protein blood level in esophageal cancer patients and normal subjects from a high incidence area in Henan, China. *World J Gastroenterol* 1998; 4:365-366
- Gao SS, Zhou Q, Li YX, Bai YM, Zheng ZY, Zou JX, Liu G, Fan ZM, Qi YJ, Zhao X, Wang LD. Comparative studies on epithelial lesions at gastric cardia and pyloric antrum in subjects from a high incidence area for esophageal cancer in Henan, China. *World J Gastroenterol* 1998; 4:332-333
- Wang LD, Zhou Q, Wei JP, Yang WC, Zhao X, Wang LX, Zou JX, Gao SS, Li YX, Yang CS. Apoptosis and its relationship with cell proliferation, p53, Waf1p21, bcl-2 and c-myc in esophageal carcinogenesis studied with a high risk population in northern China. *World J Gastroenterol* 1998; 4:287-293
- Qiao GB, Han CL, Jiang RC, Sun CS, Wang Y, Wang YJ. Overexpression of P53 and its risk factors in esophageal cancer in urban areas of Xi'an. *World J Gastroenterol* 1998; 4:57-60
- Jiao LH, Wang LD, Xing EP, Yang GY, Yang CS. Frequent inactivation of p16 and p15 expression in human esophageal squamous cell carcinoma detected by RT-PCR. *World J Gastroenterol* 1998; 4(Suppl 2):105-
- Bai YM, Wang LD, Seril DN, Liao J, Yang GY, Yang CS. Expression of hMSH2 in human esophageal cancer from patients in a high incidence area in Henan, China. *World J Gastroenterol* 1998; 4(Suppl 2):107
- Qi YJ, Wang LD, Nie Y, Cai C, Yang GY, Xing EP, Yang CS. Alteration of p19 mRNA expression in esophageal cancer tissue from patients at high incidence area in northern China. *World J Gastroenterol* 1998; 4(Suppl 2):108
- Zhang X, Geng M, Wang YJ, Cao YC. Expression of epidermal growth factor receptor and proliferating cell nuclear antigen in esophageal carcinoma and pre-cancerous lesions. *Huaren Xiaohua Zazhi* 1998; 6:229-230
- Wang D, Su CQ, Wang Y, Ye YK. Deletion of p16 gene at a high frequency in esophageal carcinoma. *Huaren Xiaohua Zazhi* 1998; 6:1052-1053
- Zou JX, Wang LD, SHI Stephanie T, Yang GY, Xue ZH, Gao SS, Li YX, YANG Chung S. p53 gene mutations in multifocal esophageal precancerous and cancerous lesions in patients with esophageal cancer in high risk northern China. *Shijie Huaren Xiaohua Zazhi* 1999; 7:280-284
- Deng LY, Zhang YH, Xu P, Yang SM, Yuan XB. Expression of interleukin 1 $\beta$  converting enzyme in 5-FU induced apoptosis in esophageal carcinoma cells. *World J Gastroenterol* 1999; 5:50-52
- Xiao ZF, Zhang Z, Wang Z, Zhang HZ, Wang M, Shi ML, Yin WB. Value of CT Scan on radiotherapy of esophageal carcinoma. *Huaren Xiaohua Zazhi* 1998; 6(Suppl 7): 181-184
- Fu JH, Rong TH, Huang ZF, Yang MT, Wu YL. Comparative assessment of three prostheses types of palliative intubation for late stage esophageal carcinoma. *Huaren Xiaohua Zazhi* 1998; 6:984-986
- Chen KN, Xu GW. Diagnosis and treatment of esophageal cancer. *Shijie Huaren Xiaohua Zazhi* 2000; 8:196-202
- Wu XY, Zhang XF, Yin FS, Lu HS, Guan GX. Clinical study on surgical treatment of esophageal carcinoma in patients after subtotal gastrectomy. *World J Gastroenterol* 1998; 4(Suppl 2):68-69
- Gao ZD, Xu XY, Mao AW, Zhou XF, Jiang H. Combination of arterial infusion chemotherapy and radio therapy in the treatment of 36 cases of middle and late stage esophageal cancer. *World J Gastroenterol* 1998; 4(Suppl 2):72
- Guo WJ, Yu EX, Zheng SG, Shen ZZ, Luo JM, Wu GH, Xia SA. Study on the apoptosis and cell cycle arrest in human liver cancer SMMC7721 cells induced by Jianpili qi herbs. *Shijie Huaren Xiaohua Zazhi* 2000; 8:52-55
- Tu SP, Jiang SH, Qiao MM, Cheng SD, Wang LF, Wu YL, Yuan YZ,

- Wu YX. Effect of trichosanthin on cytotoxicity and induction of apoptosis of multiple drugs resistance cells in gastric cancer. *Shijie Huaren Xiaohua Zazhi* 2000; 8:150-152
- 20 Liang WJ, Huang ZY, Ding YQ, Zhang WD. Lovo cell line apoptosis induced by cyclo heximide combined with TNF  $\alpha$ . *Shijie huaren Xiaohua Zazhi* 1999; 7:326-328
  - 21 Lu XP, Li BJ, Chen SL, Lu B, Jiang NY. Effect of chemotherapy or targeting chemotherapy on apoptosis of colorectal carcinoma. *Shijie Huaren Xiaohua Zazhi* 1999; 7:332-334
  - 22 Shen YF, Zhuang H, Shen JW, Chen SB. Cell apoptosis and neoplasms. *Shijie Huaren Xiaohua Zazhi* 1999; 7:267-268
  - 23 Sun ZX, Ma QW, Zhao TD, Wei YL, Wang GS, Li JS. Apoptosis induced by norcantharidin in human tumor cells. *World J Gastroenterol* 2000; 6:263-265
  - 24 Zhu HZ, Ruan YB, Wu ZB, Zhang CM. Kupffer cell and apoptosis in experimental HCC. *World J Gastroenterol* 2000; 6:405-407
  - 25 Evan G and Littlewood T. A matter of life and cell Death. *Science* 1998; 281: 1317-1320
  - 26 Shen ZY, Tan LJ, Cai WJ, Shen J, Chen C, Tang XM, Zheng MH. Arsenic trioxide induces apoptosis of oesophageal carcinoma *in vitro*. *Intern J Mol Med* 1999;4:33-37
  - 27 Shen ZY, Tan LJ, Cai WJ, Shen J, Chen CY, Tang XM. Morphologic study on apoptosis of esophageal carcinoma cell line induced by arsenic trioxide. *Shijie Huaren Xiaohua Zazhi* 1998; 6:(Suppl 7)226-229
  - 28 Shen J, Wu MH, Cai WJ, Shen ZY. The effects of arsenite trioxide in various concentration on the esophageal carcinoma cell line. *Zhongguo Zhongliu Shengwu Zhiliao Zazhi* 2001; 8:106-109
  - 29 Shen ZY, Shen J, Cai WJ, Hong C, Zheng MH. The alteration of mitochondria is an early event of arsenic trioxide induced apoptosis in esophageal carcinoma cells. *Intern J Mol Med* 2000;5: 155-158
  - 30 Shen ZY, Shen WY, Chen MH, Hong CG, Shen J. Alterations of nitric oxide in apoptosis of esophageal carcinoma cells induced by arsenite. *Shijie Huaren Xiaohua Zazhi* 2000; 8: 1101-1104
  - 31 Shen ZY, Shen J, Chen MH, Li QS, Hong CQ. Morphological changes of mitochondria in apoptosis of esophageal carcinoma cells induced by As<sub>2</sub>O<sub>3</sub>. *Zhonghua Binglixue Zazhi* 2000; 29: 200-203
  - 32 Deng LY, Zhang YH, Zhang HX, Ma CL, Chen ZG. Observation of morphological changes and cytoplasmic movement in apoptosis process. *World J Gastroenterol* 1998; 4: 66-67
  - 33 Floryk D, Ucker DS. Molecular mapping of the physiological cell death process. Mitochondrial events may be disordered. *Ann N Y Acad Sci* 2000; 926: 142-148
  - 34 Shen ZY, Chen CY, Shen J, Cai WJ. Ultrastructural study of apoptosis and necrosis in the esophageal carcinoma cell line induced by arsenic trioxide. *Zhongguo Yixue Wulixue Zazhi* 1999; 16: 91-94
  - 35 Shen ZY, Chen MH, Li QS, Shen J. An ultrastructural study on the programmed cell death of human amniotic epithelium. *Dianzi Xianwei Xuebao* 2000; 19: 259-260
  - 36 Zhang CS, Wang WL, Peng WD, Hu PZ, Chai YB, Ma FC. Promotion of apoptosis of SMMC7721 cells by bcl-2 ribozyme. *Shijie Huaren Xiaohua Zazhi* 2000; 8: 417-441
  - 37 Yuan RW, Ding Q, Jiang HY, Qin XF, Zou SQ, Xia SS. Bcl-2, p53 protein expression and apoptosis in pancreatic cancer. *Shijie Huaren Xiaohua Zazhi* 1999; 7: 851-854
  - 38 Wang LD, Zhou Q, Wei JP, Wang WC, Zhao X, Wang LX, Zou X, Gao SS, Li YX, Yang CS. Apoptosis and its relationship with cell proliferation, p53, waf/p21, bcl-2 and c-myc in esophageal carcinogenesis studied with a high risk population in northern China. *World J Gastroenterol* 1998; 4: 287-293
  - 39 Pastorino JG, Chen ST, Tafani M, Snyder JW and Farber JL. The overexpression of Bax produces cell death upon induction of the mitochondrial permeability transition. *J Biol Chem* 1998; 273: 7770-7775
  - 40 Fang M, Zhang HQ, Xue SB, Li N, Wang L. Intracellular calcium distribution in apoptosis of HL-60 cells induced by harringtonine: intranuclear accumulation and regionalization. *Cancer Letters* 1998; 127: 113-121
  - 41 Mootha VK, Wei MC, Buttle KF, Scorrano L, Panoutsakopoulou V, Mannella CA, Korsmeyer SJ. A reversible component of mitochondrial respiratory dysfunction in apoptosis can be rescued by exogenous cytochrome c. *EMBO J* 2001; 20: 661-671
  - 42 Zimmermann KC, Waterhouse NJ, Goldstein JC, Schuler M, Green DR. Aspirin induces apoptosis through release of cytochrome c from mitochondria. *Neoplasia* 2000;2:505-513
  - 43 Li H, Kolluri SK, Gu J, Dawson MI, Cao XH, Hobbs PD, Lin BZ, Chen GQ, Lu JS, Lin F, Xie ZH, Fontana JA, Reed JC, Zhang XK. Cytochrome c release and apoptosis induced by mitochondrial targeting of nuclear orphan receptor TR3. *Science* 2000; 289: 1159-1164
  - 44 Brenner C and Kroemer G. Apoptosis Mitochondria—the death signal intergrators. *Science* 2000; 289: 1150-1151
  - 45 Heerdt BG, Houston MA, Anthony GM, Augenlicht LH. Mitochondrial membrane potential ( $\Delta \psi_{mt}$ ) in the coordination of p53-independent proliferation and apoptosis pathways in human colonic carcinoma cells. *Cancer Res* 1998; 58: 2869-2875
  - 46 Wakabayashi T, Karbowski M. Structural changes of mitochondria related to apoptosis. *Biol Signals Recept* 2001; 10: 26-56
  - 47 Hail NJ, Lotan R. Mitochondrial permeability transition is a central coordinating event in N-(4-hydroxyphenyl) retinamide-induced apoptosis. *Cancer Epidemiol Biomarkers Prev* 2000; 9: 1293-1301
  - 48 Shapiro HM. Membrane potential estimation by flow cytometer. *Methods* 2000; 21: 271-279
  - 49 Buckman JF, Reynolds IJ. Spontaneous changes in mitochondrial membrane potential in cultured neurons. *J Neurosci* 2001; 21: 5054-5065
  - 50 Shen ZY, Cen S, Shen J, Cai WJ, Xu JJ, Ten ZP, Hu Z, Zeng Y. Study of immortalization and malignant transformation of human embryonic esophageal epithelial cells induced by HPV18E6E7. *J Cancer Res Clin Oncol* 2000; 126: 589-594
  - 51 Canete M, Juaranz A, Lopez-Nieva P, Alonso-Torcal C, Villanueva A, Stockert JC. Fixation and permanent mounting of fluorescent probes after vital labeling of cultured cells. *Acta Histochem* 2001; 103: 117-126
  - 52 Follstad BD, Wang DI, Stephanopoulos G. Mitochondrial membrane potential differentiates cells resistant to apoptosis in hybridoma cultures. *Eur J Biochem* 2000; 267: 6534-6540
  - 53 Bedner E, Li X, Gorczyca W, Melamed MR, Darzynkiewicz Z. Analysis of apoptosis by laser scanning cytometry. *Cytometry* 1999; 35: 181-195
  - 54 Li YM, Broome JD. Arsenic targets tubulins to induce apoptosis in myeloid leukemia cells. *Cancer Res* 1999; 59: 776-780
  - 55 Bazarbachi A, El-Sabban ME, Nasr R, Quignon F, Awaraji C, Kersual J, Dianoux L, Zermati Y, Haidar JH, Hermine O, de-The H. Arsenic trioxide and interferon-alpha synergize to induce cell cycle arrest and apoptosis in human T-cell lymphotropic virus type I-transformed cells. *Blood* 1999; 93: 278-283
  - 56 Jing Y, Dai J, Chalmers-Redman RM, Tatton WG, Waxman S. Arsenic trioxide selectively induces acute promyelocytic leukemia cell apoptosis via a hydrogen peroxide-dependent pathway. *Blood* 1999; 94: 2102-2111
  - 57 Lallemand-Breitenbach V, Guillemin MC, Janin A, Daniel MT, Degos L, Kogan SC, Bishop JM, de-The H. Retinoic acid and arsenic synergize to eradicate leukemic cells in a mouse model of acute promyelocytic leukemia. *J Exp Med* 1999; 189: 1043-1052
  - 58 Rousselot P, Labaume S, Marolleau JP, Larghero J, Noguera MH, Brouet JC, Fermand JP. Arsenic trioxide and melarsoprol induce apoptosis in plasma cell lines and in plasma cells from myeloma patients. *Cancer Res* 1999; 59:1041-1048
  - 59 Huang XJ, Wiernik PH, Klein RS, Gallagher RE. Arsenic trioxide induces apoptosis of myeloid leukemia cells by activation of caspases. *Med Oncol* 1999; 16: 58-64
  - 60 Zhu XH, Shen YL, Jing YK, Cai X, Jia PM, Huang Y, Tang W, Shi GY, Sun YP, Dai J Wang ZY, Chen SJ, Zhang TD, Waxman S, Chen Z, Chen GQ. Apoptosis and growth inhibition in malignant lymphocytes after treatment with arsenic trioxide at clinically achievable concentrations. *J Nat Cancer Inst* 1999; 91: 772-778
  - 61 Chen HY, Liu WH, Qin SK. Induction of arsenic trioxide on apoptosis of hepatocarcinoma cell lines. *Shijie Huaren Xiaohua Zazhi* 2000; 8: 532-535
  - 62 Gu QL, Li NL, Zhu ZG, Yin HR, Lin YZ. A study on arsenic trioxide inducing *in vitro* apoptosis of gastric cancer cell lines. *World J Gastroenterol* 2000; 6: 435-437
  - 63 Tu SP, Jiang SH, Tan JH, Jiang XH, Qiao MM, Zhang YP, Wu YL, Wu YX. Proliferation inhibition and apoptosis induction by arsenic trioxide on gastric cancer cell SGC 7901. *Shijie Huaren Xiaohua Zazhi* 1999; 7: 18-21
  - 64 Tan L, Chen X, Shen ZY. Study on the proliferative inhibition of human esophageal cancer cells with treatment DMSO and As<sub>2</sub>O<sub>3</sub>. *Shanghai Di-er Yike Daxue Xuebao* 1999; 19: 5-8
  - 65 Huo X, Piao YJ, Huang XX, Quao DF. Ultrastructural observation of mitochondria in apoptotic lymphocytes induced with cycloheximide. *Dianzi Xianwei Xuebao* 1998; 17: 702-705
  - 66 Hu Y, Moraes CT, Savaraj N, Priebe W, Lampidis TJ. Rho (0) tumor cells: a model for studying whether mitochondria are targets for rhodamine 123, doxorubicin, and other drugs. *Biochem Pharmacol* 2000; 60: 1897-1905
  - 67 Green DR, Reed JC. Mitochondria and apoptosis. *Science* 1998;281: 1309-1312
  - 68 Sugrue MM, Tatton WG. Mitochondrial membrane potential in aging cells. *Biol Signals Recept* 2001; 10: 176-188
  - 69 Lee HC, Yin PH, Lu CY, Chi CW, Wei YH. Increase of mitochondria and mitochondrial DNA in response to oxidative stress in human cells. *Biochem J* 2000; 348: 425-432
  - 70 Seol JG, Park WH, Kim ES, Jung CW, Hyun JM, Lee YY, Kim BK. Potential role of caspase-3 and -9 in arsenic trioxide-mediated apoptosis in PCI-1 head and neck cancer cells. *Int J Oncol* 2001; 18: 249-255

• ESOPHAGEAL CANCER •

# The sensitivity of digestive tract tumor cells to As<sub>2</sub>O<sub>3</sub> is associated with the inherent cellular level of reactive oxygen species

Fei Gao, Jing Yi, Gui-Ying Shi, Hui Li, Xue-Geng Shi, Xue-Ming Tang

Fei Gao, Jing Yi, Gui-Ying Shi, Hui Li, Xue-Geng Shi, Xue-Ming Tang, Department of Cell Biology, Shanghai Second Medical University, Shanghai 200025, China

Supported by the grants from National Natural Science Foundation of China, No. 39730270 and Shanghai Science and Technology Development fund of Education Committee, No.2000B101

Correspondence to: Prof. YI Jing, Department of Cell Biology, Shanghai Second Medical University, Shanghai 200025, China. yijing@shsmu.edu.cn Telephone: +86-21-63846590 Ext.421 Fax: +86-21-53065329

Received 2001-04-25 Accepted 2001-10-18

## Abstract

**AIM:** To explore the correlation of the inherent cellular ROS level with the susceptibility of the digestive tract tumor cells to apoptosis induced by As<sub>2</sub>O<sub>3</sub>.

**METHODS:** Two gastric carcinoma cell lines, SGC7901 and MKN45, and two esophageal carcinoma cell lines, EC/CUHK1 (alternatively named EC1.71) and EC1867 with low concentration (2 μmol·L<sup>-1</sup>) of As<sub>2</sub>O<sub>3</sub> were cultured respectively, which confirmed the difference in apoptosis susceptibility between SGC7901 and MKN45, and between EC/CUHK1 and EC1867. The cells were incubated with dihydrogenrhodamine123 (DHR123), used as a ROS capture in absence of As<sub>2</sub>O<sub>3</sub>. The fluorescent intensity of rhodamine123, which was the product of cellular oxidation of DHR123, was detected by flow cytometry, and ROS was measured.

**RESULTS:** Apoptosis induced by a low concentration of As<sub>2</sub>O<sub>3</sub> was more readily to occur in SGC7901 (22.4%±2.4%) and EC/CUHK1 (27.0%±2.9%) than in MKN45 (2.1%±0.5%) and EC1867 (0.8%±0.5%). In other words, SGC7901 was more sensitive than MKN45 to As<sub>2</sub>O<sub>3</sub>, meanwhile EC/CUHK1 was more sensitive than EC1867 to As<sub>2</sub>O<sub>3</sub>. The level of inherent cellular ROS in SGC7901 (650±37) was higher than that in MKN45 (507±22) (*P*<0.01), and the level of inherent cellular ROS in EC/CUHK1 (462±17) was higher than that in EC1867 (187±12) (*P*<0.01).

**CONCLUSIONS:** The cellular sensitivity to apoptosis induced by As<sub>2</sub>O<sub>3</sub> is associated with the difference in cellular ROS level. The inherent ROS level might determinate the apoptotic sensitivity of tumor cells to As<sub>2</sub>O<sub>3</sub>.

Gao F, Yi J, Shi GY, Li H, Shi XG, Tang XM. The sensitivity of digestive tract tumor cells to As<sub>2</sub>O<sub>3</sub> is associated with the inherent cellular level of reactive oxygen species. *World J Gastroenterol* 2002;8(1):36-39

## INTRODUCTION

Arsenic trioxide (As<sub>2</sub>O<sub>3</sub>) has proved to be effective in the treatment of acute promyelocytic leukemia (APL)<sup>[1-7]</sup>. While many researchers aimed at the effectiveness of As<sub>2</sub>O<sub>3</sub>-induced apoptosis on the other leukemic cells and some solid tumor cells, a lot of evidence showed that some types of tumor cells were sensitive while others

were insensitive to apoptosis-inducing effect of As<sub>2</sub>O<sub>3</sub><sup>[2,8-20]</sup>. Unraveling the causes of such sensitivity difference in the tumor cells will benefit not only the clinical selection of patients, to which As<sub>2</sub>O<sub>3</sub> can be given, but also understanding the mechanisms underlying the apoptosis induced by As<sub>2</sub>O<sub>3</sub>.

Previously we investigated the sensitivity of a series of digestive tumor cell lines to As<sub>2</sub>O<sub>3</sub>. We identified that there were difference of sensitivity to apoptosis induced by low concentration (2 μmol/L) of As<sub>2</sub>O<sub>3</sub> between the gastric carcinoma cell line SGC7901 and MKN45, and between the esophageal carcinoma cell line EC/CUHK1 (alternatively named EC1.71) and EC1867; SGC7901 was more sensitive than MKN45, and EC/CUHK1 was more sensitive than EC1867 to As<sub>2</sub>O<sub>3</sub><sup>[15-16]</sup>. We found that As<sub>2</sub>O<sub>3</sub> induced cell apoptosis via directly influencing mitochondrion, consequently causing decrease of transmembrane potential and increase of reactive oxygen species (ROS) level<sup>[17]</sup>. Recently it was evidenced that ROS participate the apoptosis induction of acute promyelocytic leukemia<sup>[18,19,21,22]</sup>. But whether the difference of sensitivity of digestive tumor cells to apoptosis-inducing effect of As<sub>2</sub>O<sub>3</sub> is associated with the inherent cellular ROS level is not clearly understood. In this study, we demonstrated the difference between SGC7901 versus MKN45, and EC/CUHK1 versus EC1867, thereby explored the relation between the sensitivity of cell to apoptosis induction of As<sub>2</sub>O<sub>3</sub> and the inherent cellular ROS level.

## MATERIALS AND METHODS

### Cell Lines and Culture Conditions

Gastric carcinoma cell line SGC7901 vs MKN45, and esophageal carcinoma cell line EC/CUHK1 vs EC1867 (kindly provided by professor Shen, Shantou University) were cultured in DMEM medium supplemented with 100kU·L<sup>-1</sup> penicillin, 100mg·L<sup>-1</sup> streptomycin, and 100mL·L<sup>-1</sup> fetal bovine serum (Gibco) in a fully humidified atmosphere with 50mL·L<sup>-1</sup> CO<sub>2</sub> at 37°C. Cells were split when reached to 80% confluency.

### Inducing Cell Apoptosis by As<sub>2</sub>O<sub>3</sub>

About 5×10<sup>5</sup> tumor cells in logarithmic stage were treated with 2 μmol·L<sup>-1</sup> concentration of As<sub>2</sub>O<sub>3</sub> (Sigma) for 72h and analyzed by flow cytometry and electron microscopy for apoptosis<sup>[15-17]</sup>. As<sub>2</sub>O<sub>3</sub> powder was dissolved in small amounts of 1.0 mol·L<sup>-1</sup> NaOH, then diluted to 10.0 mmol·L<sup>-1</sup> with phosphate-buffered saline (PBS) as stock solutions.

### Detection Inherent ROS Level

The cells were incubated with 1 μmol·L<sup>-1</sup> dihydrorhodamine123 (DHR123, Sigma), as a ROS capture<sup>[23-25]</sup>, for 1 or 24h. Blank and positive controls were set, in which DHR123 was either omitted or plus 50 μmol·L<sup>-1</sup> of hydrogen peroxide (H<sub>2</sub>O<sub>2</sub>). DHR123 could be oxidized intracellularly to form the fluorescent compound rhodamine123 (Rh123) by ROS, and be pumped into mitochondria and remained there. After incubated with DHR123, cells were trypsinized and harvested before an immediate detection of



fluorescence intensity of Rh123 by flow cytometry FACscan (Becton Dickinson), and the cellular ROS level was thus measured.

## RUSULTS

### Cell Apoptosis Induced by As<sub>2</sub>O<sub>3</sub>

A significant apoptosis was observed in EC/CUHK1 and SGC7901 cells with 2μmol/L of As<sub>2</sub>O<sub>3</sub> for 3 days while no remarkable apoptosis could be seen in EC1867 and MKN45 cells with the equivalent As<sub>2</sub>O<sub>3</sub>. The characteristic morphological changes were displayed in the apoptotic cells, including the shrinkage of the nuclear membrane, condensation and margination of the chromatin, and nuclear breakage (Figure1). DNA flow cytometry showed that the some cells with fractional DNA, as typical display of apoptosis, appeared, (27.0±2.9)% and (22.4±2.4)% ( $\bar{x} \pm s, n=5$ ) respectively in EC/CUHK1 and SGC7901 cells, but hardly visible in EC1867 (0.8±0.5)% and MKN45 (2.1±0.5)%. (Figure 2).

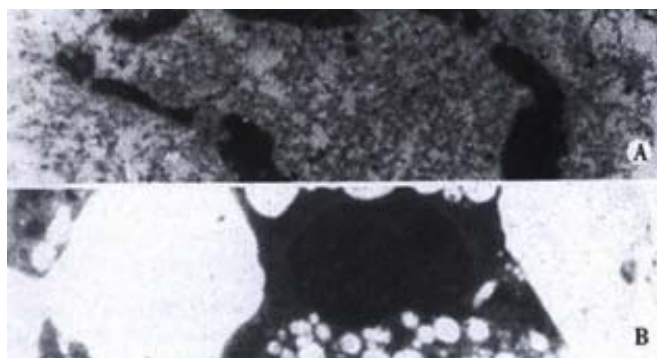


**Figure 1** Apoptotic cells in EC/CUHK1 and SGC7901 with the condensation and margination of chromatin, and nuclear breakage EM×6000

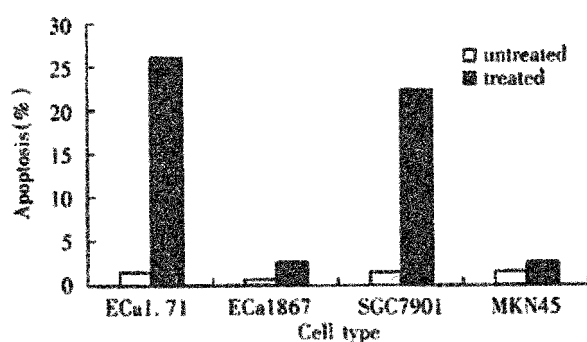


**Figure 2** Flow cytometry with PI staining: apoptosis proportions in EC/CUHK1, EC1867, SGC7901 and MKN45

### Inherent Cellular ROS Level

After incubation with DHR123 for 1 or 24h in absence of As<sub>2</sub>O<sub>3</sub>, the values ( $\bar{x} \pm s, n=3$ ) of fluorescent intensity for Rh123 were 29±4.1 and 650±37 in SGC7901 cells; 21±1.4 and 507±22 in MKN45 cells; 50±3.9 and 462±17 in EC/CUHK1; 46±6.4 and 187±12 in EC1867 cells. The fluorescent intensity in blank control was less than 3. The values for the positive controls (DHR123 plus hydrogen peroxide incubation for 1h) were 80±4.9 in SGC7901; 27±3.0 in MKN45; 72±5.8 in EC/CUHK1; and 19±2.1 in EC1867. Figure 3 displayed the fluorescence histograms for four types of cells after incubation with DHR123 for 24h. The data showed that, in absence of As<sub>2</sub>O<sub>3</sub>, the cellular ROS level was higher in SGC7901 than in MKN45, and higher in EC/CUHK1 than in EC1867. Such differences were augmented in 24h incubation as shown above, where the value in SGC7901 was as 1.3 times as in MKN45, and in EC/CUHK1 was 2.5 times as in EC1867.

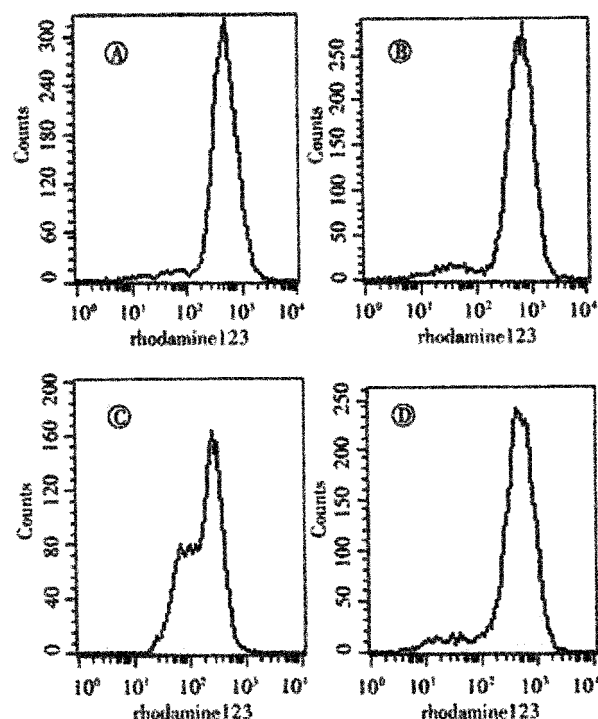


**Figure 3** Flow cytometry displaying the inherent ROS level of cells A: MKN45; B: SGC7901; C: EC1867; D: EC/CUHK1

## DISCUSSION

ROS, including superoxide anion (O<sub>2</sub><sup>-</sup>), hydrogen peroxide (H<sub>2</sub>O<sub>2</sub>), hydroxyl free radical (OH) and singlet oxygen (<sup>1</sup>O<sub>2</sub>), continuously generated from mitochondrial respiratory chain, have powerfully oxidative potential. ROS is capable of attacking lipids, nuclear acids and proteins, resulting in certain degree of oxidative damages<sup>[26-35]</sup>. It has been thought recently to involve in apoptosis triggering and signaling<sup>[36-43]</sup>. Cell possesses an efficient antioxidant defense system, mainly composed of the enzymes such as superoxide dismutase, glutathione peroxidase, and catalase, which can scavenge the ROS excessive to cellular metabolism, and make ROS level relatively stable under physiological conditions<sup>[26-35]</sup>. Though it has been noticed that ROS were involved in As<sub>2</sub>O<sub>3</sub>-induced apoptosis<sup>[18,19,21,22]</sup>, evaluation of ROS level differences directly by a flow cytometric detection of ROS, to our knowledge, has not been frequently reported. Instead, H<sub>2</sub>O<sub>2</sub>, a kind of ROS, was adopted to represent the total ROS level, usually judged from a decrease in activity of glutathione peroxidase or catalase, or a decrease in ratio of reductive/oxidative glutathione<sup>[18,19]</sup>. The total ROS level in the resting cells, however, was directly measured in the present study, by flow cytometric detection of Rh123. The comparative investigation on the inherent ROS levels in the cells showed that there were different apoptosis susceptibility to As<sub>2</sub>O<sub>3</sub>. In this study, inherent ROS level signified the basal cellular level of ROS in absence of any drug or exogenous ROS.

Detecting ROS level by flow cytometry has been a novel approach with characteristic of rapidness, convenience and reproducibility. DHR123, one of common ROS captures, is membrane permeable. It is oxidized by ROS intracellularly to become fluorescent Rh123, and is pumped into mitochondria and remain there, then is detectable by flow cytometry after a period of accumulation<sup>[23-25]</sup>. 6-carboxy-2',7'-dichlorodihydrofluorescein diacetate (DCFH-DA) is another agent used to capture ROS. It is



cleaved by nonspecific esterases to form DCFH, which was further oxidized to form the fluorescent compound DCF and kept inside cells<sup>[19,44,45]</sup>. It proved important, as we realized in this study, to prolong the incubation time with the ROS capture in order to visualize the nuance in ROS, since the absolute quantity of ROS is scarce. We selected two time intervals to visualize the accumulation of Rh123 fluorescence, finding that difference began to display at 1 h and became much pronounced by 24 h. These parameters definitely represented the difference of ROS level inherently existed in the respective types of cells. A similar result was obtained by using DCFH-DA in our study. Recently it was evidenced that NB4 leukemia cell line, which is sensitive to low concentration of  $As_2O_3$  (1-2  $\mu$ mol/L), had higher  $H_2O_2$  level than the U937 leukemia cell line which is insensitive to  $As_2O_3$ , and exposure of cells to low concentration of  $As_2O_3$  elevated the level of  $H_2O_2$  in NB4 but not in U937<sup>[19]</sup>. Though these studies indicated that a higher  $H_2O_2$  level in NB4 might link to its higher sensitivity to  $As_2O_3$ -induced apoptosis<sup>[19]</sup>, whether there existed a difference in total ROS level between cell lines which possessed different susceptibility to  $As_2O_3$ -induced apoptosis, prior to  $As_2O_3$  treatment, has not been documented.

Based on our previous work, we selected two pairs of digestive tract cell lines EC/CUHK1 versus EC1867, SGC7901 versus MKN45 in which one type of cell was susceptible and the other type was unsusceptible to  $As_2O_3$ -induced apoptosis in this study, and measured the inherent levels of total ROS in these cells. The data on both pairs showed that the inherent ROS level was higher in sensitive cells. These results indicated that difference in apoptosis susceptibility of tumor cells to low concentration of  $As_2O_3$ , was associated with the difference in the inherent cellular level of ROS, and what's more, the inherent ROS level might be pivotal in determination of the cellular susceptibility to  $As_2O_3$ -induced apoptosis. The difference of inherent ROS level between cells probably resulted from the differential expression of enzymes involved in ROS generation and elimination<sup>[46-51]</sup>. An interference to the expression of relevant enzymes or simply ROS is likely an approach by which an improved effect and expanded usage of arsenic trioxide can be achieved clinically.

## REFERENCES

- Cai X, Shen YL, Zhu Q, Jia PM, Yu Y, Zhou L, Huang Y, Zhang JW, Xiong S.M., Chen SJ, Wang ZY, Chen Z and Chen GQ. Arsenic trioxide-induced apoptosis and differentiation are associated respectively with mitochondrial transmembrane potential collapse and retinoid acid signaling pathways in acute promyelocytic leukemia. *Leukemia* 2000;14:262-270
- Murgo AJ. Clinical trials of arsenic trioxide in hematologic and solid tumors: overview of the National Cancer Institute Cooperative Research and Development Studies. *Oncologist* 2001; 6(Suppl 2):22-28
- Kinjo K, Kizaki M, Muto A, Fukuchi Y, Umezawa A, Yamato K, Nishihara T, Hata J, Ito M, Ueyama Y, Ikeda Y. Arsenic trioxide ( $As_2O_3$ )-induced apoptosis and differentiation in retinoic acid-resistant acute promyelocytic leukemia model in hGM-CSF-producing transgenic SCID mice. *Leukemia* 2000; 14:431-438
- Ma DC, Sun YH, Chang KZ, Ma XF, Huang SL, Bai YH, Kang J, Liu YG, Chu JJ. Selective induction of apoptosis of NB4 cells from G2+M phase by sodium arsenite at lower doses. *Eur J Haematology* 1998; 61:27-35
- Munshi NC. Arsenic trioxide: an emerging therapy for multiple myeloma. *Oncologist* 2001; 6(Suppl 2):17-21
- Soignet SL, Maslak P, Wang ZG, Jhanwar S, Calleja E, Dardashti LJ, Corso D, DeBlasio A, Gabrilove J, Scheinberg DA, Pandolfi PP, Warrell RP Jr. Complete remission after treatment of acute promyelocytic leukemia with arsenic trioxide. *N Engl J Med* 1998;339:1341-1348
- Zhu XH, Shen YL, Jing YK, Cai X, Jia PM, Huang Y, Tang W, Shi GY, Sun YP, Dai J, Wang ZY, Chen SJ, Zhang TD, Waxman S, Chen Z, Chen GQ. Apoptosis and growth inhibition in malignant lymphocytes after treatment with arsenic trioxide at clinically achievable concentrations. *J Natl Cancer Inst* 1999;91:743-745
- Tu SP, Zhong J, Tan JH, Jiang XH, Qiao MM, Wu YX, Jiang SH. Induction of apoptosis by arsenic trioxide and hydroxy camptothecin in gastric cancer cells *in vitro*. *World J Gastroenterol* 2000;6:532-539
- Shen ZY, Tan LJ, Cai WJ, Shen J, Chen CY, Tang XM. Morphologic study on apoptosis of esophageal carcinoma cell line induced by arsenic trioxide. *Huaren Xiaohua Zazhi* 1998;6(Suppl 7):226-229
- Tu SP, Jiang SH, Tan JH, Jiang XH, Qiao MM, Zhang YP, Wu YL, Wu YX. Proliferation inhibition and apoptosis induction by arsenic trioxide on gastric cancer cell SGC-7901. *Shijie Huaren Xiaohua Zazhi* 1999; 7:18-21
- Chen HY, Liu WH, Qin SK. Induction of arsenic trioxide on apoptosis of hepatocarcinoma cell lines. *Shijie Huaren Xiaohua Zazhi* 2000;8:532-535
- Maeda H, Hori S, Nishitoh H, Ichijo H, Ogawa O, Kakehi Y, Kakizuka A. Tumor growth inhibition by arsenic trioxide ( $As_2O_3$ ) in the orthotopic metastasis model of androgen-independent prostate cancer. *Cancer Res* 2001;61:5432-5440
- Xu HY, Yang YL, Gao YY, Wu QL, Gao GQ. Effect of arsenic trioxide on human hepatoma cell line BEL-7402 cultured *in vitro*. *World J Gastroenterol* 2000;6:681-687
- Gu QL, Li NL, Zhu ZG, Yin HR, Lin YZ. A study on arsenic trioxide inducing *in vitro* apoptosis of gastric cancer cell lines. *World J Gastroenterol* 2000;6:435-437
- Shi YH, Tan LJ, Li H, Shi GY, Shi XG, Tang XM. Study on arsenic trioxide induced apoptosis in tumor cell lines of digestive tract. *Shanghai Di-er Yike Daxue Xuebao* 1999;19:242-245
- Tan LJ, Shi GY, Shi XG, Tang XM. Induction of apoptosis of human esophageal cancer cell lines treated with arsenic trioxide. *Zhongguo Aizheng Zazhi* 1999;9:85-87
- Tan LJ, Shi YH, Shi GY, Li H., Shi XG, Tang XM. Study on the mechanism of  $As_2O_3$ -induced apoptosis of human esophageal carcinoma cell lines. *Shanghai Di-er Yike Daxue Xuebao* 2000;20:12-17
- Dai J, Weinberg RS, Waxman S, Jing Y. Malignant cells can be sensitized to undergo growth inhibition and apoptosis by arsenic trioxide through modulation of the glutathione redox system. *Blood* 1999;93:268-277
- Jing Y, Dai J, Chalmers-Redman RME, Tatton WG, Waxman S. Arsenic trioxide selectively induces acute promyelocytic leukemia cell apoptosis via a hydrogen peroxide-dependent pathway. *Blood* 1999; 94:2102-2111
- Shen ZY, Tan LJ, Cai WJ, Shen J, Chen C, Tang XM, Zheng MH. Arsenic trioxide induces apoptosis of oesophageal carcinoma *in vitro*. *Int J Mol Med* 1999;4:33-37
- Gao F, Yi J, Shi GY, Li H, Jin HF, Shi XG, Tang XM. The susceptibility of leukemia cells to arsenic trioxide-induced apoptosis is determined by cellular reactive oxygen species level. *Shengwu Huaxue Yu Shengwu Wuli Xuebao* 2001;33:109-113
- Gao F, Yi J, Shi GY, Jin HF, Shi XG, Tang XM. Cell cycle-related induction of apoptosis of NB4 cells by arsenic trioxide is associated with difference in reactive oxygen species level in cell cycle. *Shanghai Di-er Yike Daxue Xuebao* 2001;21:296-299
- Shi GY, Gao F, Shi XG, Tang XM. Detection of cellular reactive oxygen species by flow cytometry. *Shanghai Di-er Yike Daxue Xuebao* 2001; 21:122-124
- Navarro-Antolin J, Hernandez-Perera O, Lopez-Ongil S, Rodriguez-Puyol M, Rodriguez-Puyol D, Lamas S. CsA and FK506 up-regulate eNOS expression: role of reactive oxygen species and AP-1. *Kidney Int* 1998;68(Suppl):S20-S24
- Lopez-Ongil S, Hernandez-Perera O, Navarro-Antolin J, Perez de Lema G, Rodriguez-Puyol M, Lamas S, Rodriguez-Puyol D. Role of reactive oxygen species in the signalling cascade of cyclosporine A-mediated up-regulation of eNOS in vascular endothelial cells. *Br J Pharmacol* 1998;124:447-454
- Allen RG and Tresini M. Oxidative Stress and Gene Regulation. *Free Radic Biol* 2000;28:463-499
- Yeldandi AV, Rao MS, Reddy JK. Hydrogen peroxide generation in peroxisome proliferator-induced oncogenesis. *Mutation Res* 2000;448: 159-177
- Sun GY, Liu WW. Free radicals and digestive system neoplasms. *Huaren Xiaohua Zazhi* 1998;6:272-273
- Greene EL, Velarde V, Jaffa AA. Role of reactive oxygen species in bradykinin-induced mitogen-activated protein kinase and c-fos induction in vascular cells. *Hypertension* 2000;35:942-947
- Sun GY, Liu WW, Zhou ZQ, Fang DC, Men RP, Luo YH. Free radicals in development of experimental gastric carcinoma and precancerous lesions induced by N-methyl-N'-nitro N-nitrosoguanidine in rats. *Huaren Xiaohua Zazhi* 1998;6:219-221
- Sun GY, Liu WW, Zhou ZQ, Fang DC, Men RP, Luo YH. Free radicals in development of experimental gastric carcinoma and precancerous lesions induced by N-methyl-N'-nitro N-nitrosoguanidine in rats. *World J Gastroenterol* 1998;4:124
- Mates JM, Sanchez-Jimenez FM. Role of reactive oxygen species in apoptosis: implications for cancer therapy. *Int J Biochem Cell Biol* 2000; 32:157-170

- 33 Chen DZ, Wei MX, Gu YC, Guan XZ. Oxygen free radical harm in Piyinxu and Shenyinxu patients. *Huaren Xiaohua Zazhi* 1998;6:660-662
- 34 Nath KA, Norby SM. Reactive oxygen species and acute renal failure. *Am J Med* 2000;109:665-678
- 35 Thannickal VJ, Fanburg BL. Reactive oxygen species in cell signaling. *Am J Physiol Lung Cell Mol Physiol* 2000;279:L1005-1028
- 36 Perkins C, Kim CN, Fang G, Bhalla KN. Arsenic induces apoptosis of multidrug-resistant human myeloid leukemia cells that express Bcr-Abl or overexpress MDR, MRP, Bcl-2, or Bcl-xL. *Blood* 2000;95:101-022
- 37 Carmody RJ, Cotter TG. Signalling apoptosis: a radical approach. *Redox Rep* 2001;6:77-90
- 38 Fadeel B, Cihlin A, Henter J-I, Orrenius S, Hampton MB. Involvement of caspases in neutrophil apoptosis: regulation by reactive oxygen species. *Blood* 1998; 92:4808-4818
- 39 Zhang C, Gong Y, Ma H, An C, Chen D. Reactive oxygen species involved in trichosanthin-induced apoptosis of human choriocarcinoma cells. *Biochem J* 2001;355:653-661
- 40 Arai T, Endo N, Yamashita K, Sasada M, Mori H, Ishii H, Hirota K, Makino K, Fukuda K. 6-formylpterin, a xanthine oxidase inhibitor, intracellularly generates reactive oxygen species involved in apoptosis and cell proliferation. *Free Radic Biol Med* 2001;30:248-259
- 41 Jones DC, Gunasekar PG, Borowitz JL, Isom GE. Dopamine-induced apoptosis is mediated by oxidative stress and is enhanced by cyanide in differentiated PC12 cells. *J Neurochem* 2000;74:2296-2304
- 42 Moreno-Manzano V, Ishikawa Y, Lucio- Cazana J, Kitamura M. Selective involvement of superoxide anion, but not downstream compounds hydrogen peroxide and peroxynitrite, in tumor necrosis factor- $\alpha$ -induced apoptosis of rat mesangial cells. *J Biol Chem* 2000; 275:12684-12691
- 43 Hildeman DA, Mitchell T, Teague TK, Henson P, Day BJ, Kappler J, Marrack PC. Reactive oxygen species regulate activation-induced T cell apoptosis. *Immunity* 1999;10:735-744
- 44 Sawada M, Nakashima S, Kiyono T, Nakagawa M, Yamada J, Yamakawa H, Banno Y, Shinoda J, Nishimura Y, Nozawa Y, Sakai N. p53 regulates ceramide formation by neutral sphingomyelinase through reactive oxygen species in human glioma cells. *Oncogene* 2001;20:1368-1378
- 45 Sureda FX, Gabriel C, Comas J, Pallas M, Escubedo E, Camarasa J, Camins A. Evaluation of free radical production, mitochondrial membrane potential and cytoplasmic calcium in mammalian neurons by flow cytometry. *Brain Res Brain Res Protoc* 1999;4:280-287
- 46 Atlante A, Calissano P, Bobba A, Giannattasio S, Marra E, Passarella S. Glutamate neurotoxicity, oxidative stress and mitochondria. *FEBS Lett* 2001;497:1-5
- 47 Faist V, Konig J, Hoger H, Elmadfa I. Decreased mitochondrial oxygen consumption and antioxidant enzyme activities in skeletal muscle of dystrophic mice after low-intensity exercise. *Ann Nutr Metab* 2001; 45:58-66
- 48 Caillaud C, Py G, Eydoux N, Legros P, Prefaut C, Mercier J. Antioxidants and mitochondrial respiration in lung, diaphragm, and locomotor muscles: effect of exercise. *Free Radic Biol Med* 1999;26:1292-1299
- 49 Zini R, Morin C, Bertelli A, Bertelli AA, Tillement JP. Effects of resveratrol on the rat brain respiratory chain. *Drugs Exp Clin Res* 1999;25:87-97
- 50 Esposito LA, Melov S, Panov A, Cottrell BA, Wallace DC. Mitochondrial disease in mouse results in increased oxidative stress. *Proc Natl Acad Sci USA* 1999;96:4820-4825
- 51 Paradies G, Petrosillo G, Pistolesi M, Ruggiero FM. The effect of reactive oxygen species generated from the mitochondrial electron transport chain on the cytochrome oxidase activity and on cardiolipin content in bovine heart submitochondrial particles. *FEBS letter* 2000; 466:323-326

Edited by Wang JH and Xu XQ

• ESOPHAGEAL CANCER •

# Nitric oxide and calcium ions in apoptotic esophageal carcinoma cells induced by arsenite

Zhong-Ying Shen, Wen-Ying Shen, Ming-Hua Chen, Jian Shen, Wei-Jie Cai, Zeng Yi

Zhong-Ying Shen, Ming-Hua Chen, Jian Shen, Wei-Jie Cai,  
Department of Pathology

Wen-Ying Shen, Department of Chemistry Medical College of Shantou  
University, Shantou, 515031, Guangdong, China

Zeng Yi, Institute of Virology, Chinese Academy of Preventive Medicine,  
Beijing, 100052, China

Supported by the National Natural Science Foundation of China.  
No. 39830380

Correspondence to: Dr. Zhong-Ying Shen, Department of Pathology,  
Medical College of Shantou University, 22 Xinling Road. Shantou 515031,  
Guandong Province, China. Zhongyingshen@yahoo.com

Telephone: +86-754-8538621 Fax: +86-754-8537516

Received 2001-08-09 Accepted 2001-11-12

## Abstract

**AIM:** To Quantitatively analyze the nitric oxide (NO) and  $\text{Ca}^{2+}$  in apoptosis of esophageal carcinoma cells induced by arsenic trioxide ( $\text{As}_2\text{O}_3$ ).

**METHODS:** The cell line SHEEC1, a malignant esophageal epithelial cell induced by HPV in synergy with TPA in our laboratory, was cultured in a serum-free medium and treated with  $\text{As}_2\text{O}_3$ . Before and after administration of  $\text{As}_2\text{O}_3$ , NO production in cultured medium was detected quantitatively using the Griess Colorimetric method. Intracellular  $\text{Ca}^{2+}$  was labeled by using the fluorescent dye Fluo3-AM and detected under confocal laser scanning microscope (CLSM), which was able to acquire data in real-time enabling  $\text{Ca}^{2+}$  dynamics of individual cells *in vitro*. The apoptotic cells were examined under electron microscopy.

**RESULTS:** Intracellular concentration of  $\text{Ca}^{2+}$  increased from 1.00 units to 1.09-1.38 units of fluorescent intensity at  $\text{As}_2\text{O}_3$  treatment and NO products subsequently released from  $\text{As}_2\text{O}_3$ -treated cells increased from  $0.98-1.00 \times 10^{-2} \mu\text{mol} \cdot \text{L}^{-1}$  up to  $1.48-1.52 \times 10^{-2} \mu\text{mol} \cdot \text{L}^{-1}$  and maintained in a high level continuously. Finally apoptosis of cells occurred, chromatin being agglutinated, cells shrunk, nuclei became round and mitochondria swelled.

**CONCLUSION:**  $\text{Ca}^{2+}$  and NO increased with cell damage and apoptosis in cells treated by  $\text{As}_2\text{O}_3$ . The  $\text{Ca}^{2+}$  is an initial messenger to the apoptotic pathway. To investigate  $\text{Ca}^{2+}$  and NO will be a new direction for studying the apoptotic signaling messenger of the esophageal carcinoma cells induced by  $\text{As}_2\text{O}_3$ .

Shen ZY, Shen WY, Chen MH, Shen J, Cai WJ, Yi Z. Nitric oxide and calcium ions in apoptotic esophageal carcinoma cells induced by arsenite. World J Gastroenterol 2002;8(1): 40-43

## INTRODUCTION

Arsenic trioxide ( $\text{As}_2\text{O}_3$ ) has been proved to be a genotoxic and a carcinogenic agent<sup>[1-6]</sup>. Previous studies also showed that  $\text{As}_2\text{O}_3$  induced cellular apoptosis in leukemia<sup>[7-15]</sup>, in cancer cells of head and neck<sup>[16]</sup> and other cancer cells<sup>[17-22]</sup>. So  $\text{As}_2\text{O}_3$  has antitumoral

effect. We found that  $\text{As}_2\text{O}_3$  induced apoptosis in esophageal squamous carcinoma cells<sup>[23]</sup>. The pathomorphological changes induced by  $\text{As}_2\text{O}_3$  revealed that cells became smaller and shrank, nucleus rounded up, chromatin agglutinated and marginated, the nuclear membrane broke down followed by degenerative changes and cell mortality. All these changes indicated typical morphological changes of apoptosis<sup>[24, 25]</sup>. Mitochondria, an important cellular apparatus, is related to cell breathing, oxygen metabolism, enzyme activity and energy supply. Our data demonstrated that the primary target of  $\text{As}_2\text{O}_3$  inducing apoptosis of esophageal carcinoma cells might be the mitochondria<sup>[26]</sup>. It is likely that  $\text{As}_2\text{O}_3$  is a mitochondriotoxic agent<sup>[27, 28]</sup>. At the early stage of cellular apoptosis induced by  $\text{As}_2\text{O}_3$ , the mitochondria generated morphological and functional changes<sup>[29, 30]</sup>.

NO exerts a wide range of its biological properties via its interaction with mitochondria and NO mediated mitochondria damage<sup>[31]</sup>. In our previous data, an increase level of nitrite, a stable product of NO, was detected in the culture medium of esophageal carcinoma cells in arsenite-treated apoptosis<sup>[32]</sup>. Calcium ions ( $\text{Ca}^{2+}$ ) act as a universal second messenger in a variety of cells. Numerous functions of all types of cells are regulated by  $\text{Ca}^{2+}$  to a greater or lesser degree. Because of the importance of  $\text{Ca}^{2+}$  in biology, numerous methods of analyzing cellular  $\text{Ca}^{2+}$  activity have been established. Confocal laser scanning microscopy (CLSM) allows the precise spatial and temporal analysis of intracellular  $\text{Ca}^{2+}$  activity at the subcellular level. This optical technique has enabled scientists to document the dynamic changes of intracellular  $\text{Ca}^{2+}$  *in vitro*<sup>[33]</sup>.

Arsenic may generate reactive oxygen species to exert its toxicity, which is implicated in DNA damage, signal transduction and apoptosis. What we are interested in is to see if NO and  $\text{Ca}^{2+}$  are involved in arsenic-induced apoptosis and to observe the changes of its target organelle—mitochondria. This study is to investigate which are the original messengers that initiate apoptosis and to detect quantitatively  $\text{Ca}^{2+}$  and NO in the apoptotic process of esophageal carcinoma cell line induced by  $\text{As}_2\text{O}_3$ .

## MATERIALS AND METHODS

### Cell line generation and cell culture

The esophageal carcinoma cell line (SHEEC1) was a malignant transformed cell line of human embryonic esophageal epithelium induced by HPV18 E<sub>6</sub>E<sub>7</sub> in synergy with TPA (12-O-tetradecanoyl-phorbol-13-acetate)<sup>[34]</sup>. Cells were cultured in 50ml flasks and 24-well plate (Corning) with serum-free medium. The culture medium contained of the basal medium (MCDB151) with trace elements (M-6645 Sigma) and added transferrin, hydrocortisone, epidermal growth factor (EGF), insulin (Sigma Chemical Co.) and extracts of bovine hypophysis (Gibco, BRL), but without calf serum, nitrite and nitrate, while containing streptomycin and penicilline ( $50\text{mg} \cdot \text{L}^{-1}$  for each).

### The administration of arsenic

Arsenic trioxide ( $\text{As}_2\text{O}_3$ ) obtained from Sigma Chemical Co. (St. Louis MO, Lot A 1010) at concentrations of 0, 1, 3 and  $5 \mu\text{mol} \cdot \text{L}^{-1}$  was added into the culture flasks and 24-well plates, respectively, for

0, 2, 4, 8, 12 and 24 h. The experiment was repeated once.

### Transmission electron-microscopy (EM) examination

At the endpoints of  $\text{As}_2\text{O}_3$  (24h), cells of each group were digested with 0.25% trypsin, centrifuged, fixed with 2.5% glutaraldehyde, and routinely prepared for electron microscopic examination. The samples were observed under transmission electron microscope (Hitachi 300).

### Cell cycle and apoptotic rate analyzed by flow cytometry (FCM)

Cells of repeated experiment were harvested to measure the ratio of apoptotic cells to survived cells. The cells were washed twice with PBS, dispersed, and filtered through 360 mesh nylon net to make a single cell suspension. It was fixed with 700mL·L<sup>-1</sup> precooled alcohol in ice. Before analysis cells were suspended in PBS and stained with propidium iodide.  $1 \times 10^9$  cells·L<sup>-1</sup> were detected by flow cytometry (FACSort, B-D Co, USA). The DNA histogram was drawn according to the fluorescent intensity value of  $10^4$  cells.

### Procedure of NO detection<sup>[35]</sup>

The nitrite/nitrate colorimetric method, using the kit purchased from Boehringer Mannheim Co, was used to detect NO in culture medium. The culture medium of 0.2 mL from flask was regularly deactivated at 80°C for 5 min and deproteinated by centrifugation in 12000 r·min<sup>-1</sup> for 30min, and the supernatant was determined. The procedure for NO determination was as follows: sample solution of 100μL, 50μL of nicotinamide adenine dinucleotide phosphate (NADPH) and 4μL of the enzyme nitrate reductase (NR) were placed in a 3mL test tube, mixed, incubated for 30 min at room temperature, and added 50μL color reagent I & II, respectively, mixed, and allowed to stand in the dark at room temperature for 10 to 15min. The NO content of the samples and the blank was estimated with Shimadzu UV/120 spectrophotometry by 450nm and was calculated by calibration curve of standard addition method. The standards were prepared from known amounts of stock  $\text{NO}_3$  and  $\text{NO}_2$  and run in parallel with test samples in each assay.

### Determination of intracellular calcium level using CLSM<sup>[33, 36]</sup>

The cells were cultured on the coverslips within the glass bottom of a small cultured dish (No. 0, uncoated, and irradiated. MatTek Co., USA). At the exponential growth period, the cells were stained with  $10 \mu\text{mol} \cdot \text{L}^{-1}$  fluo-3/AM (Molecular Probe) for 30min at 37°C, and washed with  $135 \text{ mol} \cdot \text{L}^{-1}$  NaCl,  $10 \text{ mol} \cdot \text{L}^{-1}$  HEPES,  $0.4 \text{ mol} \cdot \text{L}^{-1}$   $\text{MgCl}_2$ ,  $1 \text{ mol} \cdot \text{L}^{-1}$   $\text{CaCl}_2$ ,  $1 \text{ g} \cdot \text{L}^{-1}$  D-glucose,  $1 \text{ g} \cdot \text{L}^{-1}$  bovine serum albumin, pH 7.3 at least 3 times. Then the cells were placed in the culture medium 199 to maintain them in living state. Before and after administration of  $\text{As}_2\text{O}_3$  the fluorescence intensity was determined by CLSM in dynamic changes for up to 900 s. Using scan-time series menu, time series was used to scan some definite cells repeatedly to monitor the dynamic changes in fluorescent intensity of intracellular  $\text{Ca}^{2+}$  content over time. The parameters of the CLSM (Ultima 312, Meridian Instruments Inc., USA) were as follows: the excited light 488nm, the emission light 530 nm and pinhole 10-40nm. The fluorescent intensity of pixel was collected and managed with the software of the instrument.

## RESULTS

### Cell apoptosis

Ultrastructural morphological changes of mitochondria in  $\text{As}_2\text{O}_3$  treated cells were described in the previous reports<sup>[25,26]</sup>. Cells treated with

$\text{As}_2\text{O}_3$  at different concentrations for 24 h displayed an apoptotic appearance. Under electron microscope, condensed and margined chromatin in most of the nuclei appeared accompanying swelling mitochondria (Figure 1). By flow cytometry, time course study on  $\text{As}_2\text{O}_3$  induced apoptosis revealed that apoptotic peak can be observed as early as 12 h after the incubation of arsenic trioxide in  $3 \mu\text{mol} \cdot \text{L}^{-1}$ . The apoptotic cells accounted for 5.0% of total cell population at 12 h and 28.3% at 24 h (Figure 2).

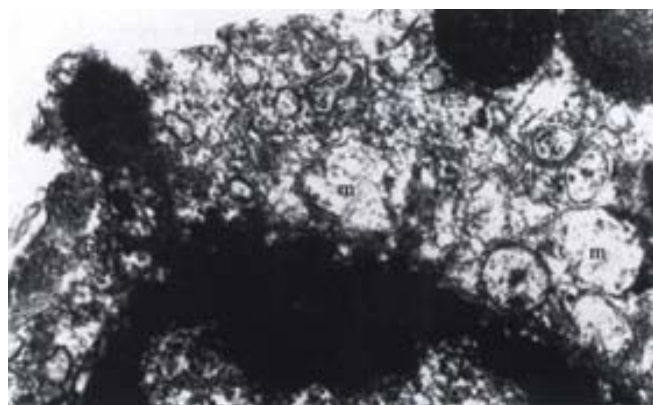


**Figure 1** Ultrastructure of SHEEC1 cell treated with  $3 \mu\text{mol} \cdot \text{L}^{-1}$   $\text{As}_2\text{O}_3$ . Apoptotic appearance displayed with swelling of mitochondria and nuclear chromatin coagulating and merging. m, mitochondria. n, nucleus. EM,  $\times 7000$

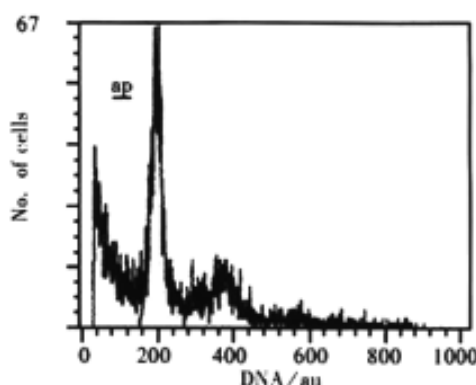


**Figure 2** DNA histogram of SHEEC1 cell in 24 h after  $3 \mu\text{mol} \cdot \text{L}^{-1}$  of  $\text{As}_2\text{O}_3$  adding. ap, apoptotic peak.

### NO determination

When  $\text{As}_2\text{O}_3$  acted on the SHEEC1 for 2-24h, in 0, 1, 3 and  $5 \mu\text{mol} \cdot \text{L}^{-1}$   $\text{As}_2\text{O}_3$ , NO in cultured medium was increased at the time points. The amount of NO released from SHEEC1 was increased from the basal condition ( $0.98\text{-}1.00 \times 10^{-2} \mu\text{mol} \cdot \text{L}^{-1}$ ) up to the high level ( $1.48\text{-}1.52 \times 10^{-2} \mu\text{mol} \cdot \text{L}^{-1}$ ) (8h) and maintained for 24h (Figure 3). The concentration of NO in different groups varied, high concentration of NO in  $5 \mu\text{mol} \cdot \text{L}^{-1}$  of  $\text{As}_2\text{O}_3$  and low concentration of NO in  $1 \mu\text{mol} \cdot \text{L}^{-1}$  of  $\text{As}_2\text{O}_3$ .

### Dynamic change calcium of intracellular calcium

To show the time course of changes in  $\text{Ca}^{2+}$  in individual cells, the changes in fluorescence intensity (arbitrary unit, au) at different representative cells were measured. Upon the initiation of stimulation by  $\text{As}_2\text{O}_3$ , all the cells responded with a rapid rise in  $[\text{Ca}^{2+}]$  from 1.00 au. to 1.09-1.38 au of fluorescent intensity. The peak levels of  $\text{Ca}^{2+}$  in all cells were consistently reached at about 900s after stimulation (Figure 4A). In the control group, without being treated with  $\text{As}_2\text{O}_3$ , the fluorescent intensity of cell, were remained on the basal line (Figure 4B).

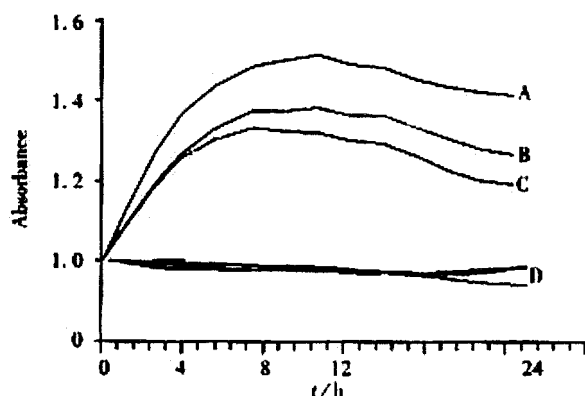


**Figure 3** NO determination of SHEEC1 treated with different concentration of  $\text{As}_2\text{O}_3$ . NO increased markedly in  $5\mu\text{mol}\cdot\text{L}^{-1}$  of  $\text{As}_2\text{O}_3$  group (A), intermediately in  $3\mu\text{mol}\cdot\text{L}^{-1}$  of  $\text{As}_2\text{O}_3$  group (B) and lowly in  $1\mu\text{mol}\cdot\text{L}^{-1}$  of  $\text{As}_2\text{O}_3$  group (C). The control group,  $0\mu\text{mol}\cdot\text{L}^{-1}$  of  $\text{As}_2\text{O}_3$ , were remained on the basal lines (D).

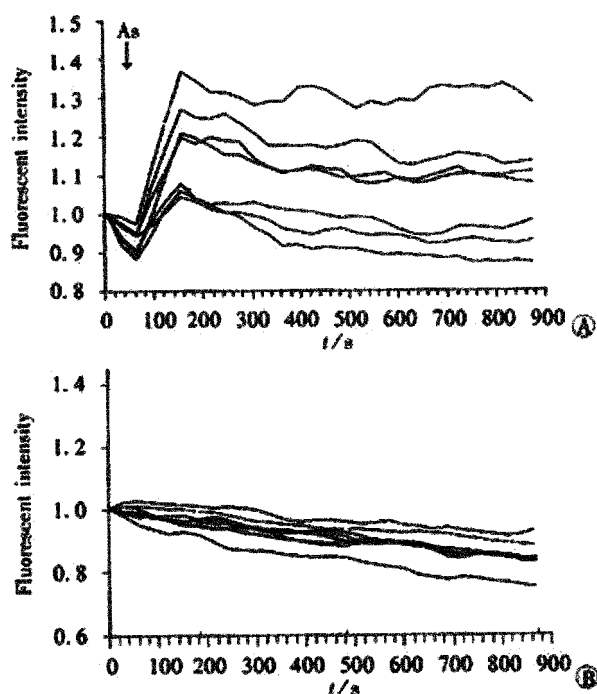


**Figure 4** Dynamic changes of intracellular calcium in 7 cells of SHEEC1 treated with  $\text{As}_2\text{O}_3$ . A, SHEEC1 cells treated with  $\text{As}_2\text{O}_3$  in  $3\mu\text{mol}\cdot\text{L}^{-1}$ . B, Control group without adding  $\text{As}_2\text{O}_3$ .

## DISCUSSION

In general, the process of cell apoptosis involved three phases: the initiation phase, the effector phase and the degradation phase<sup>[37]</sup>. The initiation (or signal transduction) phase is the stage in which specific or non-specific pro-apoptotic signal transduction pathways are activated. The effector (or central control) phase mainly occurs in the mitochondria<sup>[38]</sup> where mitochondria membranes are unstable as a result of the action of the permeability alternation. Some genes such as p53 and bcl-2, activate in this phase<sup>[39-41]</sup>. The degradation (or morphological and biochemical changes) phase manifest the postmitochondrial features of apoptosis, in which soluble intermembrane proteins released from mitochondria played an active role in the activation of proteolytic destruction. In our previous reports, we investigated the early changes of the apoptotic cells

induced by  $\text{As}_2\text{O}_3$  and defined the phase in which  $\text{As}_2\text{O}_3$  was involved<sup>[26, 27]</sup>. Our results demonstrated that  $\text{As}_2\text{O}_3$  acted directly on mitochondria for the early stage of apoptosis. The alteration of mitochondria in arsenic trioxide treated tumor cells could be observed as early as 2 h after the treatment<sup>[27, 30]</sup>. In this study we investigated signal messengers of apoptosis, by first selecting both messengers of NO and  $\text{Ca}^{2+}$  in the apoptotic pathway.

Experiments on the effects of various modulators (dose and time lag) of arsenic in the level of  $\text{Ca}^{2+}$  and NO were carried out. Nitric oxide (NO) is a free radical generated in cells by nitric oxide synthases (NOS)<sup>[42]</sup>. It is a gaseous inter- and intra-cellular messenger that plays as a signaling molecular in many physiological and pathological processes and it is also a cytotoxic agent involved in many diseases, which has been elaborated extensively during the last decade. Various intra- or extra-cellular factors act on mitochondria to produce NO. NO binds to cytochrome oxidase<sup>[43]</sup>, blocks respiratory chain and induces apoptosis<sup>[44, 45]</sup>.

Cells themselves control intracellular  $\text{Ca}^{2+}$  concentration ( $[\text{Ca}^{2+}]_i$ ) strictly with several  $\text{Ca}^{2+}$  regulatory mechanisms, such as  $\text{Ca}^{2+}$  channels,  $\text{Ca}^{2+}$  pumps, and  $\text{Ca}^{2+}$  exchangers. The role of calcium is as the important intracellular signal element in regulating cell death<sup>[46]</sup>. As revealed by previous reports, it seems that calcium changes in apoptosis vary with stimuli and cell lines<sup>[47]</sup>. This data suggested that an early, gradual and sustained increase in intracellular  $\text{Ca}^{2+}$  is necessary for the appearance of apoptotic characteristics. In the examination of CLSM with Fuo-3 AM as a calcium indicator, we found that a rise in intracellular calcium was elicited at once after application of  $\text{As}_2\text{O}_3$ . The mechanism of how arsenic increases intracellular calcium levels was not clear at this moment. Arsenic has been shown to disrupt mitochondria and may elevate intracellular calcium via a signal transduction pathway. Arsenite has also been reported to activate protein kinase C and mitogen-activated protein kinase<sup>[48]</sup>. These kinases are known to be involved in the calcium signal transduction pathway.

According to the previous reports, the relationship between NO,  $\text{Ca}^{2+}$  and mitochondria in apoptosis is as follows: various extracellular factors can induce the increase of intracellular  $\text{Ca}^{2+}$  levels ( $[\text{Ca}^{2+}]_i$ ), modulating cellular signaling and gene expression, and the increased ( $[\text{Ca}^{2+}]_i$ ) effect on NO production through the iNOS pathway<sup>[49, 50]</sup>; mitochondria are a source of NO<sup>[51]</sup>, the production of which may affect energy metabolism,  $\text{O}_2$  consumption and  $\text{O}_2$  free radical formation<sup>[52]</sup>; mitochondrial  $\text{Ca}^{2+}$  uptake in combination with NO production triggers the collapse of mitochondrial membrane potential, affecting mitochondrial respiration and culminating in delayed cell death<sup>[53]</sup>.

In conclusion, our data proved that increased calcium ions and nitric oxide triggered by  $\text{As}_2\text{O}_3$  may play an important role in arsenite-induced apoptosis in esophageal carcinoma cells. The demonstration of the involvement of  $\text{Ca}^{2+}$  and NO in arsenite-induced apoptosis suggests a new direction for studying the apoptotic pathway.

## REFERENCES

- Matsui M, Nishigori C, Toyokuni S, Takada J, Akaboshi M, Ishikawa M, Imamura S, Miyachi Y. The role of oxidative DNA damage in human arsenic carcinogenesis: detection of 8-hydroxy-2'-deoxyguanosine in arsenic-related Bowen's disease. *J Invest Dermatol* 1999; 113:26-31
- Goering PL, Aposhian HV, Mass MJ, Cebrian M, Beck BD, Waalkes MP. The enigma of arsenic carcinogenesis: role of metabolism. *Toxicol Sci* 1999; 49:5-14
- Schaumloffel N, Gebel T. Heterogeneity of the DNA damage provoked by antimony and arsenic. *Mutagenesis* 1998; 13: 281-286
- Ho IC, Yih LH, Kao CY, Lee TC. Tin-protoporphyrin potentiates arsenite-induced DNA strand breaks, chromatid breaks and kinetochores-negative micronuclei in human fibroblasts. *Mutat Res* 2000; 452:41-50
- Gebel T. Suppression of arsenic-induced chromosome mutagenicity by antimony. *Mutat Res* 1998; 412:213-218



- 6 Gebel T, Birkenkamp P, Luthin S, Dunkelberg H. Arsenic (III), but not antimony (III), induced DNA-protein crosslinks. *Anticancer Res* 1998; 18: 4253-4257
- 7 Zhu XH, Shen YL, Jing YK, Cai X, Jia PM, Huang Y, Tang W, Shi GY, Sun YP, Dai J, Wang ZY, Chen SJ, Zhang TD, Waxman S, Chen Z, Chen GQ. Apoptosis and growth inhibition in malignant lymphocytes after treatment with arsenic trioxide at clinically achievable concentrations. *J Natl Cancer Inst* 1999; 91:772-778
- 8 Look AT. Arsenic and apoptosis in the treatment of acute promyelocytic leukemia. *J Natl Cancer Inst* 1998; 90: 86-88
- 9 Shao W, Fanelli M, Ferrara FF, Riccioni R, Rosenauer A, Davison K, Lamph WW, Waxman S, Pelicci PG, Lo-Coco F, Avvisati G, Testa U, Peschle C, Gambacorti-Passerini C, Nervi C, Miller WH. Arsenic trioxide as an inducer of apoptosis and loss of PML/RAR alpha protein in acute promyelocytic leukemia cells. *J Natl Cancer Inst* 1998; 90: 124-133
- 10 Soignet SL, Maslak P, Wang ZG, Jhanwar S, Calleja E, Dardashti LJ, Corso D, DeBlasio A, Gabrilove J, Scheinberg DA, Pandolfi PP, Warrell RP. Complete remission after treatment of acute promyelocytic leukemia with arsenic trioxide. *N Engl J Med* 1998; 339: 1341-1348
- 11 Tamm I, Paternostro G and Zapata JM. Treatment of acute promyelocytic leukemia with arsenic trioxide. *N Engl J Med* 1999; 340: 1043-1045
- 12 Jing Y, Dai J, Chalmers-Redman RM, Tatton WG, Waxman S. Arsenic trioxide selectively induces acute promyelocytic leukemia cell apoptosis via a hydrogen peroxide-dependent pathway. *Blood* 1999; 94:2102-2111
- 13 Huang XJ, Wiernik PH, Klein RS, Gallagher RE. Arsenic trioxide induces apoptosis of myeloid leukemia cells by activation of caspases. *Med Oncol* 1999; 16:58-64
- 14 Lallemand-Breitenbach V, Guillemin MC, Janin A, Daniel MT, Degos L, Kogan SC, Bishop JM, de The H. Retinoic acid and arsenic synergize to eradicate leukemic cells in a mouse model of acute promyelocytic leukemia. *J Exp Med* 1999; 189:1043-1052
- 15 Li YM, Broome JD. Arsenic targets tubulins to induce apoptosis in myeloid leukemia cells. *Cancer Res* 1999; 59:776-780
- 16 Seol JG, Park WH, Kim ES, Jang CW, Hyun JM, Lee YY, Kim BK. Potential role of caspase-3 and -9 in arsenic trioxide-mediated apoptosis in PCI-1 head and neck cancer cells. *Int J Oncol* 2001; 18: 249-255
- 17 Chen HY, Liu WH, Qin SK. Induction of arsenic trioxide on apoptosis of hepatocarcinoma cell lines. *Shijie Huaren Xiaohua Zazhi* 2000; 8: 532-535
- 18 Gu QL, Li NL, Zhu ZG, Yin HR, Lin YZ. A study on arsenic trioxide inducing *in vitro* apoptosis of gastric cancer cell lines. *World J Gastroenterol* 2000; 6: 435-437
- 19 Tu SP, Jiang SH, Tan JH, Jiang XH, Qiao MM, Zhang YP, Wu YL, Wu YX. Proliferation inhibition and apoptosis induction by arsenic trioxide on gastric cancer cell SGC 7901. *Shijie Huaren Xiaohua Zazhi* 1999; 7: 18-21
- 20 Xu HY, Yang YL, Gao YY, Wu QL, Gao GQ. Effect of arsenic trioxide on human hepatoma cell line BEL-7402 cultured *in vitro*. *World J Gastroenterol* 2000; 6:681-687
- 21 Wang W, Qin SK, Chen BA, Chen HY. Experimental study on antitumor effect of arsenic trioxide in combination with cisplatin or doxorubicin on hepatocellular carcinoma. *World J Gastroenterol* 2001; 7:702-705
- 22 Xu HY, Gao YY, Wu QL, Gao GQ, Yang YL, Chen SX, Liu TF. Proliferation inhibition and apoptosis induction by arsenic trioxide on human hepatoma cell line *in vitro*. *Shijie Huaren Xiaohua Zazhi* 2000; 8:1233-1237
- 23 Shen ZY, Tan LJ, Cai WJ, Shen J, Chen C, Tang XM, Zheng MH. Arsenic trioxide induces apoptosis of oesophageal carcinoma *in vitro*. *Int J Mol Med* 1999;4:33-37
- 24 Shen ZY, Tan LJ, Cai WJ, Shen J, Chen CY, Tang XM. Morphologic study on apoptosis of esophageal carcinoma cell line induced by arsenic trioxide. *Shijie Huaren Xiaohua Zhazhi* 1998;6:226-229
- 25 Shen ZY, Chen CY, Shen J, Cai WJ. Ultrastructural study of apoptosis and necrosis in the esophageal carcinoma cell line induced by arsenic trioxide. *Zhongguo Yixue Wulixue Zazhi* 1999; 16: 91-94
- 26 Shen ZY, Shen J, Chen MH, Li QS, Hong CQ. Morphological changes of mitochondria in apoptosis of esophageal carcinoma cells induced by As<sub>2</sub>O<sub>3</sub>. *Zhonghua Binluxe Zazhi* 2000; 29: 200-203
- 27 Shen ZY, Shen J, Cai WJ, Hong CQ, Zheng MH. The alteration of mitochondria is an early event of arsenic trioxide induced apoptosis in esophageal carcinoma cells. *Int J Mol Med* 2000; 5: 155-158
- 28 Kroemer G and de The H. Arsenic trioxide, a novel mitochondriotoxic anticancer agent? *J Natl Cancer Inst* 1999; 91:743-74
- 29 Shen ZY, Chen MH, Li QS, Shen J. An ultrastructural study on the programmed cell death of human amniotic epithelium. *Dianzi Xianwei Xuebao* 2000; 19: 259-260
- 30 Shen ZY, Shen J, Li QS, Chen CY, Chen JY, Zeng Y. The morphological and functional changes of mitochondria in apoptotic esophageal carcinoma cells induced by arsenic trioxide. *World J Gastroenterol* 2001 (in press)
- 31 Rachmilewitz D. Role of nitric oxide in gastrointestinal tract. *World J Gastroenterol* 1998; 4:28-29
- 32 Shen ZY, Shen WY, Chen MH, Hong CQ, Shen J. Alterations of nitric oxide in apoptosis of esophageal carcinoma cells induced by arsenite. *Shijie Huaren Xiaohua Zhazhi* 2000; 8: 1101-1104
- 33 Takahashi A, Camacho P, Lechleiter JD, Herman B. Measurement of intracellular calcium. *Physiol Rev* 1999; 79: 1089-1125
- 34 Shen ZY, Cen S, Shen J, Cai WJ, Xu JJ, Teng ZP, Hu Z, Zeng Y. Study of immortalization and malignant transformation of human embryonic esophageal epithelial cells induced by HPV18E6E7. *J Cancer Res Clin Oncol* 2000; 126:589-594
- 35 Shen WY, Chen MH, Shen ZY, Zhang LM. Microspectrophotometric determination of nitric oxide. *J Shantou Univ Med College* 2000; 13:10-11
- 36 Satoh Y, Nishimura T, Kimura K, Mori S, Saino T. Application of real-time confocal microscopy for observation of living cells in tissue specimens. *Hum Cell* 1998; 11: 191-198
- 37 Kroemer G, Dallaporta B and Resch-Rigon M. The mitochondrial death/life regulator in apoptosis and necrosis. *Annu Rev Physiol* 1998; 60: 619-642
- 38 Brenner C and Kroemer G. Apoptosis Mitochondria—the death signal integrators. *Science* 2000; 289: 1150-1151
- 39 Zhang CS, Wang WL, Peng WD, Hu PZ, Chai YB, Ma FC. Promotion of apoptosis of SMMC7721 cells by bcl-2 ribozyme. *Shijie Huaren Xiaohua Zazhi* 2000; 8: 417-419
- 40 Yuan RW, Ding Q, Jiang HY, Qin XF, Zou SQ, Xia SS. Bcl-2, p53 protein expression and apoptosis in pancreatic cancer. *Shijie Huaren Xiaohua Zazhi* 1999; 7: 851-854
- 41 Wang LD, Zhou Q, Wei JP, Wang WC, Zhao X, Wang LX, Zou X, Gao SS, Li YX, Yang CS. Apoptosis and its relationship with cell proliferation, p53, wafp21, bcl-2 and c-myc in esophageal carcinogenesis studied with a high risk population in northern China. *World J Gastroenterol* 1998; 4: 287-293
- 42 Kuai XL, Ge ZJ, Meng XY, Ni RZ. Expression of nitric oxide synthase in human gastric carcinoma. *Shijie Huaren Xiaohua Zazhi* 2000; 8:22-24
- 43 Li H, Kolluri SK, Gu J, Dawson MI, Cao X, Hobbs PD, Lin B, Chen G, Lu J, Lin F, Xie Z, Fontana JA, Reed JC, Zhang X. Cytochrome c release and apoptosis induced by mitochondrial targeting of nuclear orphan receptor TR3. *Science* 2000; 289: 1159-1164
- 44 Brown GC. Nitric oxide and mitochondrial respiration. *Biochim Biophys acta* 1999; 1411: 351-369
- 45 Brown GC. Regulation of mitochondrial respiration by nitric oxide inhibition of cytochrome c oxidase. *Biochim Biophys Acta* 2001; 1504: 46-57
- 46 Duchon MR. Mitochondria and calcium: from cell signaling to cell death. *J Physiol* 2000; 529: 57-68
- 47 Fang M, Zhang H, Xue S. Role of calcium in apoptosis of HL-60 cells induced by harringtonine. *Sci China* 1998; 41: 600-607
- 48 Jun CD, Oh CD, Kwak HJ, Pae HO, Yoo JC, Choi BM, Chun JS, Park RK, Chung HT. Overexpression of protein kinase C isoforms protects RAW 264.7 macrophages from nitric oxide-induced apoptosis: involvement of c-Jun N-terminal kinase stress-activated protein kinase, p38 kinase, and CPP-32 protease pathways. *J Immunol* 1999; 162: 3395-3401
- 49 Korhonen R, Kankaanranta H, Lahti A, Lahde M, Knowles RG, Moilanen E. Bi-directional effects of the elevation of intracellular calcium on the expression of inducible nitric oxide synthase in J774 macrophages exposed to low and to high concentration of endotoxin. *Biochem J* 2001; 354: 351-358
- 50 Gurr JR, Liu F, Lynn S, Jan KY. Calcium-dependent nitric oxide production is involved in arsenite-induced micronuclei. *Mutat Res* 1998; 416: 137-148
- 51 Giulivi C, Poderoso JJ, Boveris A. Production of nitric oxide by mitochondria. *J Biol Chem* 1998; 273: 11038-11043
- 52 Nishikawa M, Takeda K, Sato EF, Kuroki T, Inoue M. Nitric oxide regulates energy metabolism and Bcl-2 expression in intestinal epithelial cells. *Am J Physiol* 1998; 274: G797-801
- 53 Umansky V, Ushmorov A, Ratter F, Chlichlia K, Bucur M, Lichtenauer A, Rocha M. Nitric oxide-mediated apoptosis in human breast cancer cells requires changes in mitochondrial functions and is independent of CD95 (APO-1/Fas). *Int J Oncol* 2000; 16:109-117

• ESOPHAGEAL CANCER •

# VEGF<sub>165</sub> antisense RNA suppresses oncogenic properties of human esophageal squamous cell carcinoma

Zhong-Ping Gu, Yun-Jie Wang, Jin-Ge Li, Yong-An Zhou

Zhong-Ping Gu, Yun-Jie Wang, Yong-An Zhou, Department of Thoracic Surgery, Jin-Ge Li, Department of Infectious Disease, Fourth Military Medical University, Xi'an 710038, Shaanxi Province, China  
Correspondence to: Zhong Ping Gu, Department of Thoracic Surgery, Fourth Military Medical University, Xi'an 710038, Shaanxi Province, China. Zhongpg@pub.xaonline.com  
Telephone: +86-29-3577737

Received 2001-08-09 Accepted 2001-10-23

## Abstract

**AIM:** To investigate the effect of antisense RNA to vascular endothelial growth factor<sub>165</sub> (VEGF<sub>165</sub>) on human esophageal squamous cell carcinoma cell line EC109 and the feasibility of gene therapy for esophageal carcinoma.

**METHODS:** By using subclone technique, the full length of VEGF<sub>165</sub> amino acid cDNA, which was cut from pGEM-3Zf (+), was cloned inversely into the eukaryotic expression vector pCEP4. The recombinant plasmid pCEP-AVEGF<sub>165</sub> was transfected into EC109 cell with lipofectamine. After a stable transfection, dot blot, enzyme-linked immunosorbent assay (ELISA), laser confocal imaging system analysis, transmission electron microscopy and flow cytometry were performed to determine the biological characteristics of EC109 cell line before and after transfection *in vitro* and whether there was a reversion in the tumorigenic properties of the EC109 cell *in vivo*.

**RESULTS:** The eukaryotic expression vector pCEP-AVEGF<sub>165</sub> was successfully constructed and transfected into EC109 cells. The expression of VEGF<sub>165</sub> was significantly decreased in the transfected cells while the biological characteristics of the cells were not influenced by the expression of antisense gene. The tumorigenic and angiogenic capabilities were greatly reduced in nude mice, as demonstrated by reduced tumor end volume ( $820 \pm 112.5$ ) mm<sup>3</sup> vs ( $7930 \pm 1035$ ) mm<sup>3</sup> and ( $7850 \pm 950$ ) mm<sup>3</sup>,  $P < 0.01$  and microvessel density ( $8.5 \pm 1.2$ ) mm<sup>-2</sup> vs ( $44.3 \pm 9.4$ ) mm<sup>-2</sup> and ( $46.4 \pm 12.6$ ) mm<sup>-2</sup>,  $P < 0.01$  in comparison between experimental groups empty vector transfected group and control group.

**CONCLUSION:** The angiogenesis and tumorigenicity of human esophageal squamous cell carcinoma were effectively inhibited by VEGF<sub>165</sub> antisense RNA. Antisense RNA to VEGF<sub>165</sub> can potentially be used as an adjuvant therapy for solid tumors.

Gu ZP, Wang YJ, Li JG, Zhou YA. VEGF<sub>165</sub> antisense RNA suppresses oncogenic properties of human esophageal squamous cell carcinoma. *World J Gastroenterol* 2002;8(1):44-48

## INTRODUCTION

Angiogenesis, which is defined as the formation of new blood vessel from the pre-existing vascular bed, is essential for solid tumor

growth, for the entrance of tumor cell into the circulation, and for the subsequent establishment and growth of metastasis. Many studies demonstrated that tumor angiogenesis is associated with patient outcome and is an independent prognostic marker in almost all solid tumors, including esophageal carcinoma<sup>[1-10]</sup>. Tumor angiogenesis is a complex process, involving growth factors and extracellular matrix enzymes. Among the many known triggers of tumor angiogenesis, vascular endothelial growth factor (VEGF), also known as vascular permeability factor, is an endothelial cell-specific mitogen and an angiogenesis inducer released by a variety of tumor cells and expressed in human tumors *in situ*. VEGF<sub>165</sub> is the most effective angiogenic factor in the VEGF family. Tumor cells engineered to express VEGF constitutively exhibit enhanced tumor growth and angiogenic phenotypes<sup>[11-13]</sup>. Conversely, inhibition of the expression of VEGF<sub>165</sub> was considered as a therapeutic strategy for the treatment of solid tumors<sup>[14-24]</sup>.

In this report, we constructed antisense RNA to VEGF<sub>165</sub> eukaryotic expression vector and applied gene transfer technology to modulate the expression in stably transfected human esophageal squamous cell carcinoma cells. We assessed the effects of down-regulation of VEGF expression on the biological characteristics *in vitro*, microvessel density and tumorigenic capability in nude mice.

## MATERIALS AND METHODS

### Cell line and vector

The EC109 human esophageal squamous cell carcinoma cell line was generously provided by Dr. Sun (Department of Thoracic Surgery, Tangdu Hospital, Fourth Military Medical University). Cells were maintained in Dulbecco's modified Eagle's medium (DMEM), high glucose media (Life Technologies) and supplemented with 100 mL·L<sup>-1</sup> fetal calf serum (HyClone Laboratories), penicillin, streptomycin, and nonessential amino acids (Life Technologies). The vector pGEM-3Zf (+) (carrying the full length aminoacids cDNA of VEGF<sub>165</sub>) was kindly provided by Dr. Abraham (Columbia University, USA) and vector pCEP4 was a gift from Dr. Li (Department of Infectious Disease, Tangdu Hospital, Fourth Military Medical University, China).

### Plasmid construction

The expression vector for VEGF<sub>165</sub> antisense RNA was constructed by subcloning cDNA fragment that code for VEGF<sub>165</sub> into the eukaryotic expression vector pCEP4. pGEM-3Zf (+) was digested by *Kpn*I and *Hind* III. The fragment was purified by gel. The VEGF<sub>165</sub> amino acids cDNA was cloned inversely in the *Hind* III/*Kpn*I site of pCEP4 to generate plasmid pCEP-AVEGF<sub>165</sub> (Figure 1).

### Transfection and selection

The transfection and selection of the EC109 cells were carried out in a 6-well plate. When the cells reached 70% confluence, the transfection process began. Briefly, solution A was prepared by diluting 10 µg of pCEP-AVEGF<sub>165</sub> into 200 µL serum-free medium, and solution B was prepared by diluting 20 µL Lipofectamine 2000 (Life

Technologies) into 200 $\mu$ L serum-free medium. The two solutions were combined for 20 min at room temperature, and then 0.6mL serum-free medium was added to the tube containing the complex, and subsequently added to the rinsed cells. The medium was replaced with fresh and complete medium 18 h after the start of transfection. Seventy-two hours after transfection, it was replaced again with the selective medium containing 200g $\cdot$ L<sup>-1</sup> hygromycin B (Boehringer Mannheim). Once stable transfections were obtained, the cells were maintained in 100g $\cdot$ L<sup>-1</sup> of hygromycin B. The EC109 cells were transfected with either the empty pCEP4 vector or pCEP-AVEGF<sub>165</sub>.

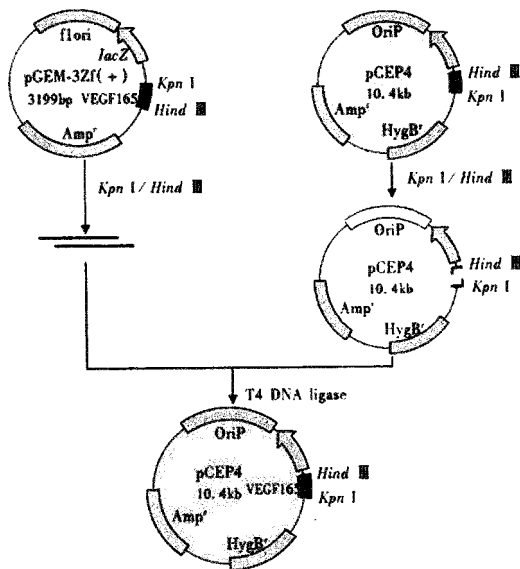


Figure 1 Diagram of the construction of the vector pCEP-AVEGF<sub>165</sub>.

### Dot blot analysis

Total cellular RNA was extracted from the cultured cells using the Trizol isolation kit (Life Technologies) according to the manufacturer's instruction. The recovered total RNA was redissolved in diethyl pyrocarbonate-treated water and 20 $\mu$ g was immobilized onto a gene screen plus membrane (DuPont) by gentle suction with a blotting manifold (Bethesda Research Laboratories). The membrane was then probed with a 5'-end-radiolabeled synthetic oligodeoxyribonucleotide complementary.

### Flow cytometry analysis

Approximately  $5 \times 10^6$  centrifugal sedimentation cells were immediately fixed in 700mL $\cdot$ L<sup>-1</sup> ethanol and stored at 4 $^{\circ}$ C in PBS in preparation for fluorescent-activated cell sorting. Flow cytometry analysis was performed on a FACStar flow cytometer (Becton Dickinson). Histograms of cell number logarithmic fluorescence intensity were recorded for 10 000 cells per sample.

### Transmission electron microscope examination

The centrifugalized cells were placed in 40g $\cdot$ L<sup>-1</sup> glutaraldehyde and then post-fixed in osmium tetroxide and embedded in Epon. Routine thin sections were stained with uranyl acetate and lead citrate. Thin sections were mounted on grids and examined under a transmission electron microscope (JEM-2000EX) at 60kV.

### Laser confocal microscope analysis

Indirect immunofluorescence techniques were applied in the transfected EC109 cells and the parental cells. VEGF<sub>165</sub> protein was detected with mouse anti-human VEGF<sub>165</sub> antibody and sheep anti-mouse IgG-FITC (Dako A/S Denmark). FITC was activated by light with a wavelength of 488nm. The data of laser scanning were 3%. The

expression of VEGF<sub>165</sub> was analyzed by confocal microscope system controlled by software obtained by Bio-Rad.

### Tumorigenicity assay

Athymic Balb/c nude mice were obtained from the Animal Center of Fourth Military Medical University. The mice were maintained in a laminar airflow cabinet under specific pathogen-free conditions and used at 8-12 weeks of age. Cells used for injection were grown to subconfluence, trypsinized, washed once, and resuspended in serum-free DMEM. The cell suspensions were examined microscopically to ensure that they were composed of single-cell suspensions. Mice were injected s.c. on the hind leg with  $5 \times 10^6$  single cells in 0.1mL. The mice were then separated into three groups, depending on whether they were injected with pCEP-AVEGF<sub>165</sub> transfected cells, pCEP4 empty vector transfected cells, or control cells. Each group contained five mice. Calipers was used for the calculation of tumor size. Microvessel density was determined under light microscopy after immunostaining of sections with anti-CD34 monoclonal antibody according to the strepto ABC kit (Dako A/S Denmark) instruction.

### Statistical analysis

The data were analyzed for significance by ANOVA.

## RESULTS

### VEGF<sub>165</sub> antisense vector construction

After ligation, transformation and selection, three clones were found likely to contain the desired recombinant. These clones were digested by restriction enzymes *KpnI/HindIII* or *KpnI/SfiI*. The 640bp or the 660bp fragment was found by using polyacrylamide gel electrophoresis. These recombinant plasmids were the eukaryotic expression vectors of antisense RNA to VEGF<sub>165</sub> (Figure 2).

### Expression of VEGF<sub>165</sub> antisense RNA

Two weeks after being transfected and selected by hygromycin B, the EC109 cells transfected by pCEP-AVEGF<sub>165</sub> expressed antisense RNA to VEGF<sub>165</sub> which was confirmed by dot blot analysis, whereas the cells transfected by pCEP4 empty vector and control group cells were negative (Figure 3).

### Expression of VEGF<sub>165</sub> in vitro

ELISA showed that a great number of VEGF<sub>165</sub> accumulated in the pCEP4 empty vector transfected group and control group cells, whereas in the pCEP-AVEGF<sub>165</sub> transfected group cells, the level of VEGF<sub>165</sub> was very low. The level of VEGF<sub>165</sub> expression was significantly lower in EC109 cells transfected by pCEP-AVEGF<sub>165</sub> than that in the pCEP4 empty vector transfected group and control group cells ( $P < 0.01$ ) determined under confocal microscope, as indicated in Figure 4.

### The change of ultrastructure and cell cycle

There was no substantial change neither in the ultrastructure examined under transmission electron microscope nor in the cell cycle determined by flow cytometer.

### The change of tumorigenic capacity in vivo

The nude mice were sacrificed at week 5. Tumor volume was measured and morphological characteristics were assessed in HE stained sections. pCEP-AVEGF<sub>165</sub> transfected xenografts grew very slowly, pCEP4 empty vector transfected group and nontransfected control xenografts were significantly larger than pCEP-AVEGF<sub>165</sub> transfected xenografts ( $P < 0.01$ ), and the mean tumor volumes were  $(820 \pm 112.5)\text{mm}^3$ ,  $(7930 \pm 1035)\text{mm}^3$  and  $(7850 \pm 950)\text{mm}^3$ ,

respectively. pCEP-AVEGF<sub>165</sub> transfected xenografts had a relatively large area of central necrosis. Immunohistochemical staining for CD34 was performed to evaluate tumor microvessel density. The microvessel density was expressed as the average number of the five highest areas



**Figure 2** Identification of recombinant clone by restriction enzyme.

- 1: Fragment of 640bp digested with *KpnI/Hind III*
- 2: DL2000 markers (2000,1000,750,500,250,100bp)
- 3: Fragment of 660bp digested with *KpnI/SfiI*

identified within a single×200 field, for the pCEP-AVEGF<sub>165</sub> transfected mice, pCEP4 empty vector group and nontransfected controls were  $(8.5\pm1.2)\text{mm}^{-2}$ ,  $(44.3\pm9.4)\text{mm}^{-2}$  and  $(46.4\pm12.6)\text{mm}^{-2}$ , respectively ( $P<0.01$ ).

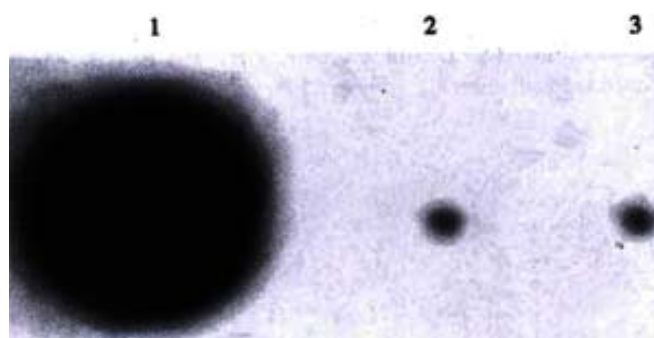


**Figure 3** Expression of antisense RNA to VEGF<sub>165</sub> in EC109 cell

- 1: Transfected by pCEP-AVEGF<sub>165</sub>
- 2: Transfected by empty vector
- 3: Control group

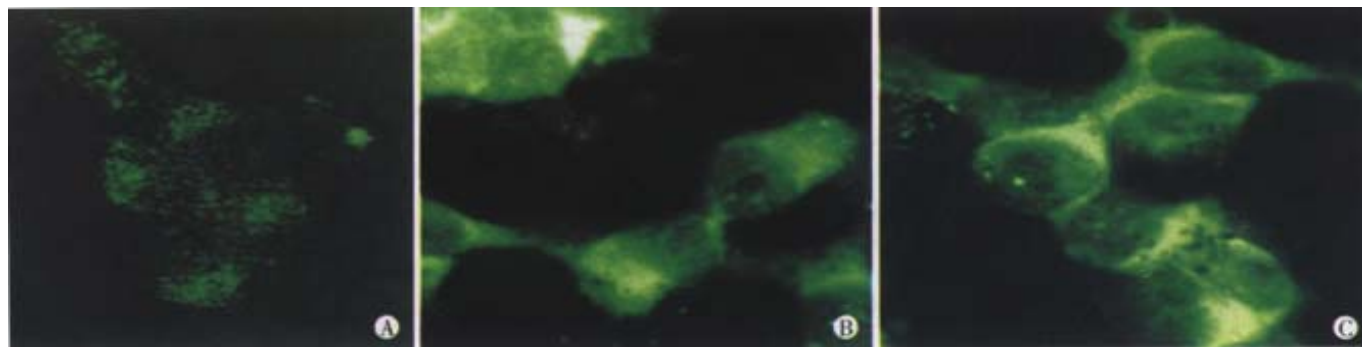


**Figure 4** Expression of VEGF<sub>165</sub> in EC109 cell (×40): transfected by pCEP-AVEGF<sub>165</sub> (A), transfected by empty vector (B), and control group (C).

## DISCUSSION

Mammalian cells require oxygen and nutrients for their survival and are therefore located within 100μm-200μm blood vessels-the diffusion limit for oxygen. For multicellular organisms which grow beyond this size, they must recruit new blood vessels by angiogenesis and vasculogenesis. This process is regulated by a balance between pro- and anti-angiogenic molecules, and is derailed in various diseases, especially cancer. Without blood vessels, tumor can not grow beyond a critical size or metastasize to another organ<sup>[25-29]</sup>. In 1971, Folkman<sup>[30]</sup> proposed that solid tumor growth and metastasis are critically dependent on angiogenesis, the formation of new blood vessels from pre-existing vasculature, and hence, blocking angiogenesis could be a strategy to arrest tumor growth. The induction of angiogenesis is mediated by several factors released by both tumor and host cells. One of the key mediators of angiogenesis is VEGF, a multifunctional growth factor that is overexpressed and secreted by a majority of human and animal tumors. VEGF was purified by Ferrara *et al*<sup>[31]</sup> from the conditioned medium of bovine pituitary folliculo stellate cells. VEGF is a homodimeric 46ku heparin-binding glycoprotein with potent angiogenic, mitogenic, and vascular permeability-enhancing activities specific for endothelial cells. By alternative splicing of messenger RNA, VEGF may exist in at least four different homodimeric molecular species each monomer having 121, 165, 189 or 206 amino acids, respectively (VEGF<sub>121</sub>, VEGF<sub>165</sub>, VEGF<sub>189</sub>, VEGF<sub>206</sub>). Among this family, VEGF<sub>165</sub> is the most important effector. Antiangiogenic therapy targeting VEGF has been

proposed as a means of inhibiting VEGF-dependent tumor growth and metastasis<sup>[32-40]</sup>.

It has been suggested that antisense RNA could block the translation progress of aim protein effectively and inhibit expression<sup>[41-45]</sup>. DeFatta *et al*<sup>[46]</sup> found that reducing eIF4E express on *via* antisense RNA suppressed both the tumorigenic and angiogenic properties of the head and neck squamous cell cancers, cell line FaDu, as demonstrated by lowered capacity to grow in soft agar, reduced expression of angiogenic factors, and loss of tumorigenicity in nude mice. Oku and associates<sup>[47]</sup> transfected human SK-MEL-2 melanoma cells with antisense VEGF which resulted in substantial inhibition of intracerebral tumor growth in nude mice, and a decrease in tumor vascularity, blood flow, and permeability.

The prognosis of human esophageal squamous cell carcinoma after curative resection is dismal. Radiotherapy and several conventional chemotherapeutic agents have been tried to improve the prognosis, but the results are generally disappointing. In this regard, antiangiogenic therapy could be a promising and hopeful strategy for esophageal cancer<sup>[48-51]</sup>. In this study, an antisense RNA to VEGF<sub>165</sub> eukaryotic expression vector pCEP-AVEGF<sub>165</sub> was constructed successfully. We transfected it into human esophageal squamous cell carcinoma cell line EC109. Under immunohistochemistry and confocal microscopy, it was found that the expression of VEGF<sub>165</sub> decreased significantly in the cells transfected with VEGF<sub>165</sub> antisense RNA compared with the empty vector transfected and control group. Under transmission electron microscopy and flow cytometry, we observed that the ultrastructure

and cell cycle had no change among transfected and control groups. In the nude mice tumor model, the tumorigenicity, the rate of tumor growth, and microvessel density were significantly decreased for the tumors derived from antisense RNA transfected cells as compared with the empty vector transfected and parental cells. pCEP-AVEGF<sub>165</sub> transfected tumors had a very low initial growth rate with central necrosis. These results suggested that inhibition of tumor growth might be achieved by VEGF<sub>165</sub> antisense RNA's down-regulation of endogenous VEGF expression in tumor tissues. In the meantime, we found that the VEGF<sub>165</sub> antisense RNA therapy could slow the rate of tumor growth and not inhibit completely the tumorigenicity. This demonstrated that the process of angiogenesis and tumorigenicity is complex and involves multifactors. To the best of our knowledge, this is the first experimental report which shows that VEGF<sub>165</sub> antisense RNA suppresses the growth of human esophageal squamous cell carcinoma *in vivo* in association with decreased vessel number in the treated tumors.

Esophageal carcinoma is still common in China<sup>[52-58]</sup>, and the treatment remains a big problem up to date<sup>[59-65]</sup>. Our present study suggests that antisense RNA to VEGF<sub>165</sub> can potentially be used as an adjuvant therapy for human esophageal squamous cell carcinoma. Further studies are needed to understand the details of the mechanisms for appropriate clinical application.

**ACKNOWLEDGMENTS** We especially thank Dr. Xiao Yan Sun for providing us the EC109 cell line, Dr. Abraham for providing the pGEM-3Zf (+) vector, we also thank Dr. Zhi Pei Zhang for his assistance with the animal experiments, and Prof. Bo Rong Pan for improving the paper.

## REFERENCES

- Carmeliet P, Jain RK. Angiogenesis in cancer and other diseases. *Nature* 2000; 407:249-257
- Park JS, Qiao L, Su ZZ, Hinman D, Willoughby K, McKinstry R, Yacoub A, Duigou GJ, Young CS, Grant S, Hagan MP, Ellis E, Fisher PB, Dent P. Ionizing radiation modulates vascular endothelial growth factor (VEGF) expression through multiple mitogen activated protein kinase dependent pathways. *Oncogene* 2001;20:3266-3280
- Millikan KW, Mall JW, Myers JA, Hollinger EF, Doolas A, Saclarides TJ. Do angiogenesis and growth factor expression predict prognosis of esophageal cancer? *Am Surg* 2000;66:401-5; discussion 405-406
- Kollermann J, Hulpap B. Expression of vascular endothelial growth factor (VEGF) and VEGF receptor Flk-1 in benign, premalignant, and malignant prostate tissue. *Am J Clin Pathol* 2001;116:115-121
- Volm M, Koomagi R, Mattern J. PD-ECGF, bFGF, and VEGF expression in non-small cell lung carcinomas and their association with lymph node metastasis. *Anticancer Res* 1999; 19:651-655
- Assy N, Paizi M, Gaitini D, Baruch Y, Spira G. Clinical implication of VEGF serum levels in cirrhotic patients with or without portal hypertension. *World J Gastroenterol* 1999;5:296-300
- Tian XJ, Wu J, Meng L, Dong ZW, Shou CC. Expression of VEGF 121 in gastric carcinoma MGC803 cell line. *World J Gastroenterol* 2000;6: 281-283
- Volm M, Mattern J, Koomagi R. Inverse correlation between apoptotic (Fas ligand, caspase-3) and angiogenic factors (VEGF, microvessel density) in squamous cell lung carcinomas. *Anticancer Res* 1999;19: 1669-1671
- Borre M, Nerstrom B, Overgaard J. Association between immunohistochemical expression of vascular endothelial growth factor (VEGF), VEGF-expressing neuroendocrine-differentiated tumor cells, and outcome in prostate cancer patients subjected to watchful waiting. *Clin Cancer Res* 2000;6:1882-1890
- Korshunov A, Golanov A. The prognostic significance of vascular endothelial growth factor (VEGF C-1) immunorexpression in oligodendroglioma. An analysis of 91 cases. *J Neurooncol* 2000;48:13-19
- Carmeliet P. Mechanisms of angiogenesis and arteriogenesis. *Nature Med* 2000; 6:389-395
- Ferrara N, Alitalo K. Clinical applications of angiogenic growth factors and their inhibitors. *Nat Med* 1999;5:1359-1364
- Ferrara N. Vascular endothelial growth factor: molecular and biological aspects. *Curr Top Microbiol Immunol* 1999;237:1-30
- Nishizaki M, Fujiwara T, Tanida T, Hizuta A, Nishimori H, Tokino T, Nakamura Y, Bouvet M, Roth JA, Tanaka N. Recombinant adenovirus expressing wild-type p53 is antiangiogenic: a proposed mechanism for bystander effect. *Clin Cancer Res* 1999;5:1015-1023
- Kido Y. Vascular endothelial growth factor (VEGF) serum concentration changes during chemotherapy in patients with lung cancer. *Kurume Med J* 2001;48:43-47
- Takayama K, Ueno H, Nakanishi Y, Sakamoto T, Inoue K, Shimizu K, Ohashi H, Hara N. Suppression of tumor angiogenesis and growth by gene transfer of a soluble form of vascular endothelial growth factor receptor into a remote organ. *Cancer Res* 2000; 60:2169-2177
- Morino F, Tokunaga T, Tsuchida T, Handa A, Nagata J, Tomii Y, Kijima H, Yamazaki H, Watanabe N, Matsuzaki S, Ueyama Y, Nakamura M. Hammerhead ribozyme specifically inhibits vascular endothelial growth factor gene expression in a human hepatocellular carcinoma cell line. *Int J Oncol* 2000;17:495-499
- Sandberg JA, Sproul CD, Blanchard KS, Bellon L, Sweedler D, Powell JA, Caputo FA, Kornbrust DJ, Parker VP, Parry TJ, Blatt LM. Acute toxicology and pharmacokinetic assessment of a ribozyme (angiozyme) targeting vascular endothelial growth factor receptor mRNA in the cynomolgus monkey. *Antisense Nucleic Acid Drug Dev* 2000;10:153-162
- Oshika Y, Nakamura M, Tokunaga T, Ohnishi Y, Abe Y, Tsuchida T, Tomii Y, Kijima H, Yamazaki H, Ozeki Y, Tamaoki N, Ueyama Y. Ribozyme approach to downregulate vascular endothelial growth factor (VEGF) 189 expression in non-small cell lung cancer (NSCLC). *Eur J Cancer* 2000;36:2390-2396
- Nguyen JT, Wu P, Clouse ME, Hlatky L, Terwilliger EF. Adeno-associated virus-mediated delivery of antiangiogenic factors as an antitumor strategy. *Cancer Res* 1998;58:5673-5677
- Brekken RA, Overholser JP, Stastny VA, Waltenberger J, Minna JD, Thorpe PE. Selective inhibition of vascular endothelial growth factor (VEGF) receptor 2 (KDR/Flk-1) activity by a monoclonal anti-VEGF antibody blocks tumor growth in mice. *Cancer Res* 2000; 60:5117-5124
- Kotoh T, Dhar DK, Masunaga R, Tabara H, Tachibana M, Kubota H, Kohno H, Nagasue N. Antiangiogenic therapy of human esophageal cancers with thalidomide in nude mice. *Surgery* 1999;125:536-544
- Gaddipati JP, Mani H, Shefali, Raj K, Mathad VT, Bhaduri AP, Maheshwari RK. Inhibition of growth and regulation of IGFs and VEGF in human prostate cancer cell lines by shikonin analogue 93/637 (SA). *Anticancer Res* 2000;20:2547-2552
- Zimmermann RC, Hartman T, Bohlen P, Sauer MV, Kitajewski J. Preovulatory treatment of mice with anti-vegf receptor 2 antibody inhibits angiogenesis in corpora lutea. *Microvasc Res* 2001;62:15-25
- Risau W. Mechanisms of angiogenesis. *Nature* 1997;386:671-674
- Shibuya M. Structure and function of VEGF/VEGF-receptor system involved in angiogenesis. *Cell Struct Funct* 2001;26:25-35
- Rohan RM, Fernandez A, Udagawa T, Yuan J, D'Amato RJ. Genetic heterogeneity of angiogenesis in mice. *FASEB J* 2000;14:871-876
- Ramanujan S, Koenig GC, Padera TP, Stoll BR, Jain RK. Local imbalance of proangiogenic and antiangiogenic factors: a potential mechanism of focal necrosis and dormancy in tumors. *Cancer Res* 2000;60:1442-1448
- Isner JM, Asahara T. Angiogenesis and vasculogenesis as therapeutic strategies for postnatal neovascularization. *J Clin Invest* 1999;103: 1231-1236
- Folkman J. Tumor angiogenesis: therapeutic implications. *N Engl J Med* 1971;285:1182-1186
- Ferrara N, Henzel WJ. Pituitary follicular cells secrete a novel heparin-binding growth factor specific for vascular endothelial cells. *Biochem Biophys Res Commun* 1989; 161: 851-858
- Hyder SM, Murthy L, Stancel GM. Progesterin regulation of vascular endothelial growth factor in human breast cancer cells. *Cancer Res* 1998; 58: 392-395
- Ferrara N. Role of vascular endothelial growth factor in regulation of physiological angiogenesis. *Am J Physiol Cell Physiol* 2001;280: C1358-366
- Neufeld G, Cohen T, Gengrinovitch S, Poltorak Z. Vascular endothelial growth factor (VEGF) and its receptors. *FASEB J* 1999; 13: 9-22
- Salven P, Lymboussaki A, Heikkila P, Jaaskela-Saari H, Enholm B, Aase K, von Euler G, Eriksson U, Alitalo K, Joensuu H. Vascular endothelial growth factors VEGF-B and VEGF-C are expressed in human tumors. *Am J Pathol* 1998; 153:103-108
- Gerber HP, McMurtrey A, Kowalski J, Yan M, Keyt BA, Dixit V, Ferrara N. Vascular endothelial growth factor regulates endothelial cell survival through the phosphatidylinositol 3'-kinase/Akt signal transduction pathway. Requirement for Flk-1/KDR activation. *J Biol Chem* 1998; 273: 30336-30343
- Bates DO, Heald RI, Curry FE, Williams B. Vascular endothelial growth factor increases Rana vascular permeability and compliance by different signalling pathways. *J Physiol* 2001;533:263-272
- Rousseau S, Houle F, Huot J. Integrating the VEGF signals leading to



- actin-based motility in vascular endothelial cells. *Trends Cardiovasc Med* 2000;10:321-327
- 39 Pepper MS, Wasi S, Ferrara N, Orci L, Montesano R. In vitro angiogenic and proteolytic properties of bovine lymphatic endothelial cells. *Exp Cell Res* 1994; 210: 298-305
- 40 Laughner E, Taghavi P, Chiles K, Mahon PC, Semenza GL. Her2 (neu) signaling increases the rate of hypoxia-inducible factor 1 alpha (hif-1alpha) synthesis: novel mechanism for hif-1-mediated vascular endothelial growth factor expression. *Mol Cell Biol* 2001;21:3995-4004
- 41 Fu L, Mei Y, Li H. Effect of PAI-1 antisense RNA on vascular endothelial growth factor expression in aorta smooth muscle cells cultured in vitro. *Zhonghua Yixue Yi Chuanxue Zazhi* 2001;18:110-113
- 42 Nguyen JT. Vascular endothelial growth factor as a target for cancer gene therapy. *Adv Exp Med Biol* 2000;465:447-456
- 43 Belletti B, Ferraro P, Arra C, Baldassarre G, Bruni P, Staibano S, De Rosa G, Salvatore G, Fusco A, Persico MG, Viglietto G. Modulation of in vivo growth of thyroid tumor-derived cell lines by sense and antisense vascular endothelial growth factor gene. *Oncogene* 1999;18: 4860-4869
- 44 Cheng SY, Huang HJ, Nagane M, Ji XD, Wang D, Shih CC, Arap W, Huang CM, Cavenee WK. Suppression of glioblastoma angiogenicity and tumorigenicity by inhibition of endogenous expression of vascular endothelial growth factor. *Proc Natl Acad Sci U S A* 1996;93:8502-8507
- 45 Inoue K, Slaton JW, Kim SJ, Perrotte P, Eve BY, Bar-Eli M, Radinsky R, Dinney CP. Interleukin 8 expression regulates tumorigenicity and metastasis in human bladder cancer. *Cancer Res* 2000;60:2290-2299
- 46 DeFatta RJ, Nathan CA, De Benedetti A. Antisense RNA to eIF4E suppresses oncogenic properties of a head and neck squamous cell carcinoma cell line. *Laryngoscope* 2000;110:928-933
- 47 Oku T, Tjuvajev JG, Miyagawa T, Sasajima T, Joshi A, Joshi R, Finn R, Claffey K P, Blasberg RG. Tumor growth modulation by sense and antisense vascular endothelial growth factor gene expression: effects on angiogenesis, vascular permeability, blood volume, blood flow, fluorodeoxyglucose uptake, and proliferation of human melanoma intracerebral xenografts. *Cancer Res* 1998; 58:4185-4192
- 48 Wu XY, Zhang XF, Yin FS, Lu HS, Guan GX. Clinical study on surgical treatment of esophageal carcinoma in patients after subtotal gastrectomy. *World J Gastroenterol* 1998;4:68-69
- 49 Chen DF, Yang ZY, Yin WB. Radiotherapy of 180 cases of operable esophageal carcinoma. *China Natl J New Gastroenterol* 1997;3:123-126
- 50 Xiao ZF, Yang ZY, Zhou ZM, Yin WB, Gu XZ. Radiotherapy of double primary esophageal carcinoma. *World J Gastroenterol* 2000;6:145-146
- 51 Zhang YH, Xu P, Yang SM, Yuan XB. Expression of interleukin 1 and LY converting enzyme in 5-FU induced apoptosis in esophageal carcinoma cells. *World J Gastroenterol* 1999;5:50-52
- 52 Zhang HX, Li XL, Zhao WX, Gao XP, Fu HM, Shang YQ. The study of trace elements in the hair of patients with esophageal carcinoma in high risk area. *World J Gastroenterol* 2000;6:20
- 53 Shen ZY, Shen WY, Chen MH, Hong CQ, Shen J. Quantitative detection of nitric oxide (NO) in apoptosis of esophageal carcinoma cell induced by arsenite. *World J Gastroenterol* 2000;6:65
- 54 Wu QM, Li SB, Wang Q, Wang DH, Li XB, Liu CZ. The expression of COX-2 in esophageal carcinoma and its relation to clinicopathologic characteristic. *Shijie Huaren Xiaohua Zazhi* 2001;9:11-14
- 55 Zhang J, Yan XJ, Yan QJ, Duan J, Hou Y, Su CZ. Cloning and expression of HPV16 L-2 DNA from esophageal carcinoma in *E. coli*. *Shijie Huaren Xiaohua Zazhi* 2001;9:273-278
- 56 Zhang X, Geng M, Wang YJ, Cao YC. Expression of epidermal growth factor receptor and proliferating cell nuclear antigen in esophageal carcinoma and pre cancerous lesions. *Huaren Xiaohua Zazhi* 1998;6:229-230
- 57 Wang D, Su CQ, Wang Y, Ye YK. Deletion of p16 gene at a high frequency in esophageal carcinoma. *Huaren Xiaohua Zazhi* 1998;6: 1052-1053
- 58 Gu HP, Shang PZ, Su H, Li ZG. Association of CD15 antigen expression with cathepsin D in esophageal carcinoma tissues. *Shijie Huaren Xiaohua Zazhi* 2000;8:259-261
- 59 Liu J, Chen SL, Zhang W, Su Q. P21WAF1 gene expression with P53 mutation in esophageal carcinoma. *Shijie Huaren Xiaohua Zazhi* 2000; 8:1350-1353
- 60 Wang D, Su CQ, Wang Y, Ye YK. Deletion of p16 gene at a high frequency in esophageal carcinoma. *Huaren Xiaohua Zazhi* 1998;6: 1052-1053
- 61 Shen ZY, Shen WY, Chen MH, Hong CQ, Shen J. Alterations of nitric oxide in apoptosis of esophageal carcinoma cells induced by arsenite. *Shijie Huaren Xiaohua Zazhi* 2000;8:1101-1104
- 62 Shen ZY, Tan LJ, Cai WJ, Shen J, Chen CY, Tang XM. Morphologic study on apoptosis of esophageal carcinoma cell line induced by arsenic trioxide. *Huaren Xiaohua Zazhi* 1998;6:226-229
- 63 Chen J, Zhang ZY, Zhu JQ, Wang CW, Xie Y, Huang DQ. Expression of CD44v6 in esophageal carcinoma and its clinical significance. *Huaren Xiaohua Zazhi* 1998;6:534
- 64 He FX, Fan SH, Ge LZ, Shen YF, Lu XK. Radioprotection of radiated auto blood transfusion on patients with esophageal carcinoma. *Huaren Xiaohua Zazhi* 1998;6:867-868
- 65 Fu JH, Rong TH, Huang ZF, Yang MT, Wu YL. Comparative assessment of three prosthesis types of palliative intubation for late stage esophageal carcinoma. *Huaren Xiaohua Zazhi* 1998;6:984-986

• ESOPHAGEAL CANCER •

# Relationship of tobacco smoking, CYP1A1, GSTM1 gene polymorphism and esophageal? cancer in Xi'an

An-Hui Wang, Chang-Sheng Sun, Liang-Shou Li, Jiu-Yi Huang, Qing-Shu Chen

An-Hui Wang, Chang-Sheng Sun, Liang-Shou Li, Jiu-Yi Huang, Department of Epidemiology, Faculty of Preventive Medicine, Fourth Military Medical University Xi'an 710033, Shaanxi Province, China  
Qing-Shu Chen, Department of Thoracic Surgery, Tangdu Hospital, Fourth Military Medical University, Xi'an 710038, Shaanxi Province, China  
Supported by National Natural Science Foundation of China, No.39670651  
Correspondence to: An-Hui Wang, Department of Epidemiology, Faculty of Preventive Medicine, Fourth Military Medical University Xi'an 710032, Shaanxi Province, China. wanganhui@hotmail.com  
Telephone: +86-29-3374871

Received 2001-06-13 Accepted 2001-11-15

## Abstract

**AIM:** To analyze the association of tobacco smoking, polymorphism of CYP1A1 (7<sup>th</sup> exon) and GSTM1 genotype and esophageal cancer(EC) in Xi'an.

**METHODS:** A hospital based case-control study, with molecular epidemiological method, was carried out. Polymorphism of CYP1A1 and GSTM1 of samples from 127 EC cases and 101 controls were detected by PCR method.

**RESULTS:** There were no significant difference of age and gender between cases and controls. Tobacco smoking was the main risk factor(OR=1.97, 95% CI=1.12-3.48) for EC in Xi'an. The proportions of CYP1A1 *Ile/Ile*, *Ile/Val* and *Val/Val* gene types in cases and controls was 19.7%, 45.7%, 34.6% and 30.7%, 47.5%, 21.8% respectively ( $P=0.049$ ). Individuals with CYP1A1 *Val/Val* genotype compared to those with CYP1A1 *Ile/Ile* genotype had higher risk for EC increased (OR=2.48, 95%CI=1.12-5.54). The proportions of GSTM1 deletion genotype in cases and controls were 58.3% and 43.6% (OR=1.81, 95%CI=1.03-3.18,  $P=0.028$ ). Analysis of gene-environment interaction showed that tobacco smoking and CYP1A1 *Val/Val* genotype; tobacco smoking and GSTM1 deletion genotype had synergism interaction respectively. Analysis of gene-gene interaction did not find synergistic interaction between these two genes. But in GSTM1 deletion group, there was significant difference of distribution of CYP1A1 genotype between cases and controls ( $P=0.011$ ).

**CONCLUSION:** CYP1A1 *Val/Val* and GSTM1 deletion genotypes are genetic susceptibility biomarkers for EC. The risk increases, when person with CYP1A1 *Val/Val* and/or GSTM1 deletion genotype. And these two-metabolic enzymes seem to have interactions with tobacco smoking, in which the mechanism still needs further study.

Wang AH, Sun CS, Li LS, Huang JY, Chen QS. Relationship of tobacco smoking, CYP1A1, GSTM1 gene polymorphism and esophageal cancer in Xi'an. *World J Gastroenterol* 2002;8(1):49-53

## INTRODUCTION

Esophageal cancer (EC) is one of the most common malignant tumors of human being. The incidence of EC varies in different countries. China is the country with highest incidence and

mortality rate of EC. Research showed that risks for EC in different countries or different places were different<sup>[1-6]</sup>. In western countries alcohol intake and tobacco smoking were studied deeply<sup>[7-12]</sup>. It was thought that besides tobacco smoking and alcohol drinking, nutrition factors, life style, viruses infection, heredity or exposure to nitrosamines, fungi or AFB1 maybe involved in the process of EC<sup>[1,3,13-19]</sup>. In China, researches showed risks for EC were different in areas with different incidence<sup>[1-5,16,18,20,21]</sup>. The mortality rate of EC of Xi'an city in Shaanxi province is about 24 per 100,000, which ranks first in all cancer mortalities. Previous studies showed that both of tobacco smoking and family history of EC were main risk factors for EC in Xi'an city<sup>[2,22,23]</sup>.

EC is a multi-etiology disease; environmental risks exposures and genetic susceptibility may take the role part<sup>[2,22-24]</sup>. Almost all of the environmental carcinogens (procarcinogens) are activated to be ultimate carcinogens before initiate the process of carcinogenesis. Some metabolic enzymes are closely related to the activation and detoxification of procarcinogens. Alterations of the key oncogene or tumor suppress gene can disturb the cycle of cell proliferation, which can also initiate the process of carcinogenesis<sup>[23,25,26]</sup>. Susceptibility of cancer is associated with the genetics polymorphism of related metabolic enzymes. Both certain susceptibility related biomarkers and certain environmental carcinogens perhaps are indispensable factors for EC<sup>[20,23,27,28]</sup>. To explore the bio-basis of genetic susceptibility of EC in Xi'an, we carried out a hospital based case-control study to analyze the associations of tobacco smoking, CYP1A1, GSTM1 gene polymorphism and EC.

## MATERIALS AND METHODS

### Selection of patients and controls

All cases with esophageal cancer (confirmed by pathological diagnosis) came from inpatients of Tangdu Hospital during half a year period (December, 1999 to April, 2000). All controls were stratified randomly selected from non-cancer inpatients from different department of the same hospital during the same period. Both cases and controls were confined to residents with long-term living in Xi'an (with similar proportion of gender and age).

### Collected data

Trained interviewers using a structured questionnaire interviewed cases and controls in the hospital. The questionnaire obtained detailed information on residence, occupation, tobacco smoking habit and so on. Here tobacco smoking was defined as smoking at least one cigarette per day and persisting for more than one year. 127 cases (male 97, female 30) and 101 (male 78, female 23) controls were included. Blood samples were also collected for extraction of DNA genome. All blood samples had been stored at -70°C before started DNA extraction.

### PCR methods to detect polymorphism of CYP1A1 and GSTM1

Digested by Proteinase K, DNA genomes were extracted from blood

clot of cases and controls with hydroxybenzene, chloroform method in a uninterrupted period. CYP1A1 and GSTM1 polymorphisms were identified by polymerase chain reaction (PCR) before which DNA samples were stored at 4°C. Primers for GSTM1(P1:5'-GTA CCC TAC TTG ATT GAT GGG-3'; P2:5'-CTG GAT TGT AGC AGA TCA TGC-3') and for CYP1A1 (P3: 5'-CGG AAG TGT ATC GGT GAG ACC A -3' P4: 5'-CGG AAG TGT ATC GGT GAG ACC G -3'; P5:5'-GTA GAC AGA GTC TAG GCC TCA-3') were synthesized by Shenggong bio-technical company of Shanghai. PCR condition for GSTM1 as follows, 50μL solution including 10×buffer 5μL, Mg<sup>2+</sup> 2μL, P1,P2 1μL respectively, template DNA1.5μL, dNTPs 1μL and Taq DNA polymerase 3<sup>U</sup>. After denaturation at 94°C for 10 min, Taq DNA polymerase was added,followed by 30 cycles with 94°C 1min, 60°C 1min, and 72°C 1min.20g·L<sup>-1</sup> agar was used to electrophoresis PCR production, then observed under the violate light. GSTM1 exist genotype was characterized as had a 273bp fragment; while GSTM1 deletion genotype had no fragment (Figure 1).

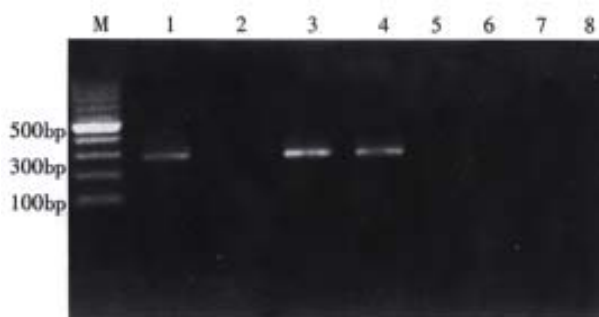


**Figure 1** Identify the GSTM1 genotype  
M:100bp DNA ladder, 3,4 were GSTM1 exist 2,5 were GSTM1 deletion; 1 positive control,6 negative control,7 was blank control (without DNA template)

We used two pairs of primers to detect the polymorphism of CYP1A1 (7<sup>th</sup> exon). For each DNA sample two sets of PCR were carried out using P3, P5 (marked as tube A) and P4, P5 (marked as tube B) respectively. PCR conditions were the same:50μL solution including 10×buffer 5μL,Mg<sup>2+</sup> 2μL, P3,P5 (or P4,P5) 1μL, template DNA 1.5μL, dNTPs 1μL and Taq DNA polymerase 3<sup>U</sup>, then 94°C 10min followed by 94°C 1min,55°C 1min, 72°C 1min, 35 cycles,72°C extending 10 min. PCR products were observed. The PCR was conducted to detect the mutation of A-G in CYP1A1 7<sup>th</sup> exon, the mutation can leads to change of one amino acid (Ile to Val). If there was only tube A had the specifically fragment (200bp), the DNA was regarded as CYP1A1 *Ile/Ile* genotype (pure wild genotype); if only tube B had the positive fragment, CYP1A1 *Val/Val* genotype (pure mutation) was considered; and CYP1A1 *Ile/Val* genotype was identified with both tube A and tube B had the fragment (Figure 2).

### Quality control

DNA extraction and PCR were conducted in different period and places. The genotypes of DNA samples were identified blindly. Every PCR had were set controls as blanket control (without DNA template), positive control and negative control, and when any one of these controls was failure, PCR wasre-conducted.

### Statistical analysis

Data were input into computer, then the values of  $\chi^2$ , odds ratio (OR) and OR95% CI (confidence intermediate) were

calculated. And ORs of gene-environment and gene-gene interaction were also estimated.



**Figure 2** Identified the genotypes of CYP1A1  
M: 100bp DNA ladder; 1(A),2(B) represent *Ile/Ile* genotype; 3(A),4(B) represent *Ile/Val* genotype; 5(A),6(B) represent *Val/Val* genotype; 7(A),8 (B) as blank control( without DNA template).

## RESULTS

### Comparability between cases and controls

The age and gender in cases and controls were comparable(Table 1).

**Table 1** Comparability of age and gender in cases and controls

| Factor    | Case | Control | $\chi^2$ | P     |
|-----------|------|---------|----------|-------|
| Age(year) |      |         |          |       |
| <50       | 28   | 16      |          |       |
| 50-       | 38   | 44      |          |       |
| ≥60       | 61   | 41      | 4.73     | 0.094 |
| Gender    |      |         |          |       |
| Male      | 97   | 78      |          |       |
| Female    | 30   | 23      | 0.02     | 0.80  |

### Risk factors for EC

The proportions of tobacco smoking, *GSTM1* deletion genotype and *CYP1A1* genotype (*Val/Val*) in cases and controls were significantly different ( $P<0.05$ ) (Table 2).

**Table 2** Distributions of smoking, *GSTM1* deletion and *CYP1A1* genotypes

| Factors        | Case | Control | OR   | OR95%CI   | $\chi^2$ | P     |
|----------------|------|---------|------|-----------|----------|-------|
| Smoking        |      |         |      |           |          |       |
| Yes            | 69   | 38      | 1.97 | 1.12-3.48 | 6.28     | 0.012 |
| No             | 58   | 63      |      |           |          |       |
| <i>GSTM1</i>   |      |         |      |           |          |       |
| Deletion       | 74   | 44      | 1.81 | 1.03-3.18 | 4.85     | 0.028 |
| Exist          | 53   | 57      |      |           |          |       |
| <i>CYP1A1</i>  |      |         |      |           |          |       |
| <i>Ile/Ile</i> | 25   | 31      | 1.00 |           | 1.00     |       |
| <i>Ile/Val</i> | 58   | 48      | 1.50 | 0.74-3.03 | 1.48     | 0.22  |
| <i>Val/Val</i> | 44   | 22      | 2.48 | 1.12-5.54 | 5.93     | 0.015 |

### Interaction of tobacco smoking and *GSTM1* deletion genotype or *CYP1A1 Val/Val* genotypes

Analysis showed that there was synergistic interaction between tobacco smoking and *GSTM1* deletion genotype (Table 3).

**Table 3** Interaction of smoking and *GSTM1* deletion genotype.

| Smoking | <i>GSTM1</i> deletion | Case | Control | OR   | OR95%CI   | $\chi^2$ | P      |
|---------|-----------------------|------|---------|------|-----------|----------|--------|
| No      | No                    | 25   | 37      | 1.00 |           |          |        |
| Yes     | No                    | 28   | 20      | 2.07 | 0.90-4.80 | 3.48     | 0.062  |
| No      | Yes                   | 33   | 26      | 1.88 | 0.86-4.13 | 2.93     | 0.087  |
| Yes     | Yes                   | 41   | 18      | 3.37 | 1.49-7.69 | 10.29    | 0.0013 |

$$SIA=3.37/(1.88+2.07-1.00)=1.14$$

Tobacco smoking and CYP1A1 *Val/Val* genotype also appeared synergistic interaction (Table 4).

**Table 4** Interaction of tobacco smoking and CYP1A1 *Val/Val* genotype

| Smoking | CYP1A1( <i>Val/Val</i> ) | Case | Control | OR   | OR95%CI    | $\chi^2$ | P      |
|---------|--------------------------|------|---------|------|------------|----------|--------|
| No      | No                       | 36   | 47      | 1.00 |            |          |        |
| Yes     | No                       | 47   | 32      | 1.92 | 0.98-3.76  | 4.18     | 0.04   |
| No      | Yes                      | 22   | 16      | 1.80 | 0.77-4.20  | 2.18     | 0.14   |
| Yes     | Yes                      | 22   | 6       | 4.79 | 1.62-14.83 | 10.30    | 0.0013 |

$$SIM=4.79/(1.92 \times 1.80)=1.39$$

But CYP1A1 mutation genotypes (*Val/Val*, *Ile/Val*) and GSTM1 deletion genotype did not show significant interaction (Table 5).

**Table 5** Interaction of CYP1A1 mutation genotypes (*Val/Val*, *Ile/Val*) and GSTM1 deletion genotype

| GSTM1 deletion | CYP1A1 mutation | Case | Control | OR   | OR95%CI   | $\chi^2$ | P      |
|----------------|-----------------|------|---------|------|-----------|----------|--------|
| No             | No              | 10   | 20      | 1.00 |           |          |        |
| No             | Yes             | 43   | 37      | 2.32 | 0.89-6.14 | 3.61     | 0.057  |
| Yes            | No              | 15   | 11      | 2.73 | 0.81-9.42 | 3.28     | 0.070  |
| Yes            | Yes             | 59   | 33      | 3.58 | 1.39-9.38 | 8.66     | 0.0033 |

OR of individuals with CYP1A1 mutation genotype and GSTM1 deletion genotype was greater than those with of any other forms of the two genotypes. But there did not show any synergistic interaction between CYP1A1 mutation genotypes and GSTM1 deletion genotype.

Stratified with GSTM1 deletion genotype to analyze the distributions of CYP1A1 genotypes in cases and controls. Results showed that there were significant different in cases and controls ( $P=0.011$ ) in GSTM1 exist genotype CYP1A1 genotypes, whereas there were no significant difference ( $P=0.83$ ) between cases and controls in GSTM1 deletion genotype (Table 6).

**Table 6** Analysis of CYP1A1 genotypes in cases and controls with Stratified GSTM1 deletion

| CYP1A1 genotype | GSTM1 deletion |         | existing GSTM1 |         |
|-----------------|----------------|---------|----------------|---------|
|                 | Case           | Control | Case           | Control |
| <i>Ile/Ile</i>  | 15             | 11      | 10             | 20      |
| <i>Ile/Val</i>  | 35             | 19      | 23             | 29      |
| <i>Val/Val</i>  | 24             | 14      | 20             | 8       |
| $\chi^2$        | 0.39           |         | 9.04           |         |
| P               | 0.83           |         | 0.011          |         |

## DISCUSSION

Under similar environmental carcinogens exposure only a few of individuals get neoplasm, for there were individual difference to environmental exposure. The different liability to cancer was called genetic susceptibility of cancer. Genetic susceptibility can affect on every step of carcinogenesis, including modify the effect of environmental carcinogens<sup>[24,29-35]</sup>. Oncogenes and tumor suppressor genes can also affect individual's susceptibility to cancer. Cancer susceptibility genes includes type I, type II metabolism enzyme gene, DNA repair gene and those affect cell proliferation rate gene. In recent years evidence has accumulated to support the hypothesis that cancer susceptibility gene may be of importance in determining individual susceptibility to cancer<sup>[34,36-46]</sup>.

EC is a multi-factor determined disease; including environmental risk factors and genetic factors. In recent years, more and more researches considered environmental and genetic susceptibility factors and their interactions in evaluating the risks of cancer<sup>[2,17,43,47-50]</sup>. Investigations showed the mortality rate of EC in Shaanxi province did not

decreased during the late 20 years, and risks factors for EC in Xi'an city were discussed in several researches<sup>[2,22,23]</sup>. In this hospital based case-control study, the results showed that tobacco smoking was a risk factor; and tobacco smoking had interactions with GSTM1 deletion genotype and CYP1A1 *Val/Val* genotype.

Most chemical carcinogens in environment are pro-carcinogens. And aromatic hydrocarbons (AHs) in tobacco smoking are pro-carcinogens, they need to be activated to reactive electrophilic forms by type I metabolic enzymes (CYP450s), then initiate the carcinogenesis. On the other hand the reactive electrophilic forms of carcinogen can be detoxified and excreted by type I metabolic enzymes such as GSTM1. Although theoretically the increase of activity of type II metabolic enzymes and/or decrease of activity of type I metabolic enzymes can increase the risk for cancer, there were different results in different researches, some supported this hypothesis and others did not<sup>[27,34,35,37,40-42,51-56]</sup>. Our results showed that individuals with the GSTM1 deletion genotype or/and CYP1A1 *Val/Val* genotype had increased risks for EC.

P450 CYP1A1 gene located in chromosome 15q22 mainly metabolizes pro-carcinogens. There are three kinds of polymorphism of CYP1A1: *MspI* site, 7<sup>th</sup> exon (*Ile/Val*) and AA polymorphism. *MspI* polymorphism include three genotypes: without *MspI* enzyme cleavage site allele gene *m1(m1/m1)* as A genotype; having *MspI* cleavage site allele (*m2/m2*) as C genotype and *m1/m2* as B genotype. In different populations the distribution of these three genotypes were different. CYP1A1 *Ile/Val* polymorphism caused by 7<sup>th</sup> exon 4889<sup>th</sup> base difference (A or G), transition of A to G results in 462<sup>th</sup> amino turned from isoleucine to valine<sup>[13]</sup>, then form three kinds of genotypes: homozygote wild genotype (*Ile/Ile*), mutation genotype (*Val/Val*) and heterozygote *Ile/Val* genotype. Polymorphism of 7<sup>th</sup> exon correlated with polymorphism of *MspI* in Asia and Caucasian populations, and in Americans from Africa these two kind of CYP1A1 polymorphism were independent, CYP1A1 7<sup>th</sup> exon polymorphism and *MspI* site were incomplete linkage. Research showed CYP1A1 *Val/Val* genotype have higher ability to activate pro-carcinogen than CYP1A1 *Ile/Ile* genotype. PAH-DNA adducts in leukocyte were higher in heavy smoking population with CYP1A1 *Val/Val* genotype than those with CYP1A1 *Ile/Val* or *Ile/Ile* genotype. AA polymorphism was new special *MspI* polymorphism, which still under discussion.

Although evidence showed that CYP1A1 mutation genotype (*Val/Val*) had the strongest ability to activate pro-carcinogens, the associations between CYP1A1 genotype and susceptibility to cancers were varied<sup>[30-33,37,57,58]</sup>. Data from Guangdong province in China showed that *MspI* C correlated with no-smoking population's lung cancer susceptibility<sup>[52]</sup>. Study in Shanghai and Haerbin no significant relation was discovered between CYP1A1 (*Ile/Val*) polymorphism and lung cancer susceptibility in non-smoking female patients<sup>[51]</sup>. CYP1A1 *Val/Val* genotype only appear about 3.2%~5% in white population, while in Japanese it was about 19.8%, in Chinese it was 22.3%. Our study showed that distributions of CYP1A1 genotypes in cases and controls were different ( $P=0.049$ ), CYP1A1 *Val/Val* genotype was associated with EC (OR= 2.48, 95%CI=1.12-5.54) and there was interaction of tobacco smoking and CYP1A1 *Val/Val* genotype.

GSTM1 can detoxify a number of reactive electrophilic compound substances, including the carcinogens PAHs. If

individuals with GSTM1 deletion genotype, the ability of detoxify the carcinogens decreased. Individuals with GSTM1 deletion can have the increased risk of cancers<sup>[24,43,46]</sup>. In China there were similar research on GSTM1 deletion genotype and the risks of lung cancer(OR=2.56)<sup>[53]</sup>, and stomach cancer(OR=1.90, 95%CI=1.01-3.56)<sup>[54]</sup>. Researches showed that in Henan province, high incidence of EC in China, GSTM1 deletion gene polymorphisms had not significant relation with EC susceptibility<sup>[20]</sup>. Results of our study indicated GSTM1 deletion genotype was significant different in cases and controls ( $P=0.028$ ) and the OR was 1.81(OR95%CI=1.03-3.18). GSTM1 deletion genotype had synergistic interaction with tobacco smoking.

In summary, we found tobacco smoking, CYP1A1 Val/Val genotype; GSTM1 deletion genotype had associations with EC in Xi'an area. Gene-environment interaction analysis showed that tobacco smoking had synergistic interactions with CYP1A1 Val/Val genotype, and with GSTM1 deletion genotype. Gene-gene interaction analysis did not find synergistic interaction between CYP1A1 mutation genotypes and GSTM1 deletion genotype, though individuals with these two genotypes had increased risk for EC. The synergistic interactions and their mechanisms of tobacco smoking with these two metabolic enzymes gene polymorphisms still need further study with large (population-based) samples and modified designs.

**Acknowledgment** We would like to thank Bing-Quan Gu for their help in collecting blood sample.

## REFERENCES

- Zhang W, Bailey-Wilson JE, Li W, Wang X, Zhang C, Mao X, Liu Z, Zhou C, Wu M. Segregation analysis of esophageal cancer in a moderately high-incidence area of northern China. *Am J Hum Genet* 2000; 67: 110-119
- Li LS, Sun CS, Zhang XL, Qiao GB, Xu DZ, Han CL, Yang WX, Chang GS, Yan MX, Wang Y, Zhang HY. A comparative molecular epidemiological study on esophageal cancer between Xi'an and Lichou. *Jiefangjun Yufangyixue Zazhi* 1999; 17: 255-259
- Zhou XG, Watanabe S. Factor analysis of digestive cancer mortality and food consumption in 65 Chinese countries. *J Epidemiol* 1999; 9: 275-284
- Wang LD, Zou JX, Hong JY, Zhou Q, Deng CJ, Xie DW, Holly C. Identification of a novel genetic polymorphism of human O-6-alkylguanine-DNA alkyltransferase in patients with esophagus cancer. *Huren Xiaohua Zazhi* 1998; 6: 560-463
- Lu JB, Lian SY, Sun XB, Zhang ZX, Dai DX, Li BW, Cheng LP, Wei JR, Duan WJ. A case-control study on the risk factors of esophageal cancer in Linzhou. *Zhonghua Liuxingbingxue Zazhi* 2000; 21: 434-436
- Li WD, Wang XQ, Zhang CL, Han XY, Chen DQ, Zhang T, Pan XF, Jia YT, Mao XZ, Zhang R. Esophageal carcinoma in part of population of yangquan city. *Zhonghua Yixue Zazhi* 1998; 78: 203-206
- Castellsague X, Munoz N, De Stefani E, Vitoria CG, Quintana MJ, Castelletto R, Rolon PA. Smoking and drinking cessation and risk of esophageal cancer (Spain). *Cancer Causes Control* 2000; 11: 813-818
- Lagregren J, Bergstrom R, Lindgren A, Nyren O. The role of tobacco, snuff and alcohol use in the aetiology of cancer of the oesophagus and gastric cardia. *Int J cancer* 2000; 85: 340-346
- Launoy G, Milan C, Faivre J, Pienkowski P, Gignoux M. Tobacco type and risk of squamous cell cancer of the oesophagus in males: a French multicentre case-control study. *Int J Epidemiol* 2000; 29: 36-42
- Talamini G, Capelli P, Zamboni G, Mastromauro M, Pasetto M, Castagnini A, Angelini G, Bassi C, Scarpa A. Alcohol, smoking and papillomavirus infection as risk for esophageal squamous-cell papilloma and esophageal squamous-cell carcinoma in Italy. *Int J cancer* 2000; 86: 874-878
- Castellsague X, Munoz N, De Stefani E, Vitoria CG, Castelletto R, Rolon PA. Independent and joint effects of tobacco smoking and alcohol drinking on the risk of esophageal cancer in men and women. *Int J Cancer* 1999; 82: 657-664
- Castellsague X, Munoz N, De Stefani E, Vitoria CG, Castelletto R, Rolon PA. Influence of mate drinking, hot beverages and diet on esophageal cancer risk in South America. *Int J Cancer* 2000; 88: 658-664
- Dhillon PK, Farrow DC, Vaughan TL, Chow WH, Risch HA, Gammon MD, Mayne ST, Stanford JL, Schoenberg JB, Ahsan H, Dubrow R, West AB, Rotterdam H, Blot WJ, Fraumeni JF Jr. Family history of cancer and risk of esophageal and gastric cancers in the United States. *Int J Cancer* 2001; 93: 148-152
- Nayar D, Kapil U, Joshi YK, Sundara KR, Sriastava SP, Shukla NK, Tandon RK. Nutritional risk factors in esophageal cancer. *J Assoc Physicians India* 2000; 48: 781-787
- Chang F, Syrjanen S, Shen Q, Cintorino M, Santopietro R, Tosi P, Syrjanen K. Evaluation of HPV, CMV, HSV and EBV in esophageal squamous cell carcinomas from a high-incidence area of China. *Anticancer Res* 2000; 20: 3935-3940
- Li T, Lu ZM, Chen KN, Guo M, Xing HP, Mei Q, Yang HH, Lechner JF, Ke Y. Human papillomavirus type 16 is an important infectious factor in the high incidence of esophageal cancer in Anyang area of China. *Carcinogenesis* 2001; 22: 929-934
- Shi QL, Xu DZ, Sun CS, Li LS. Study on family aggregation of esophageal cancer in Linzhou city. *Zhonghua Yufang Yixue Zazhi* 2000; 34: 269-270
- Shen YP, Gao YT, Dai Q, Hu X, Xu TL, Xiang YB, Tang ZL, Li WL. A case-control study on esophageal cancer in Huaian city, Jiangsu province (I): role of the cigarette smoking and alcohol drinking. *Zhongliu* 1999; 19: 363-367
- Lagergren J, Ye W, Lindgren A, Nyren O. Heredity and risk of cancer of the esophagus and GASTRIC cardia. *Cancer Epidemiol Biomarkers Prev* 2000; 9: 757-760
- Lin DX, Tang YM, Lu SX, Kadlubar FF. Glutathione S-transferase M1, T1 genotypes and risks of esophageal cancer: a case-control study. *Zhonghua Liuxingbing Zazhi* 1998; 19: 195-199
- Gao YT, Den J, Xiang YB, Ruan ZX, Wang ZX, Hu BY, Guo MR, Ten WK, Han JJ, Zhang YS. Smoking, related cancers, and other diseases in Shanghai: A 10-year prospective study. *Zhonghua Yufang Yixue Zazhi* 1999; 33: 5-8
- Zhang HY, Sun CS, Li LS, Yan MX. Cytochrome P4501A1 and the genetic susceptibility to esophageal carcinoma. *Zhonghua Yufang Yixue Zazhi* 2000; 34: 69-71
- Wang AH, Zhang HY, Wang Y, Yan MX, Sun CS, Li LS, Huang JY, Cheng QS, Zhu YF. Molecular epidemiological study on esophageal cancer in Xi'an. *Disi Junyi Daxue Xuebao* 2001; 22: 61-63
- Tan W, Song N, Wang GQ, Liu Q, Tang HJ, Kadlubar FF, Lin DX. Impact of genetic polymorphisms in cytochrome P450 2E1 and glutathione S-transferases M1, T1, and P1 on susceptibility to esophageal cancer among high-risk individuals in China. *Cancer Epidemiol Biomarkers Prev* 2000; 9: 551-556
- Hu N, Huang J, Emmert-buck MR, Tang ZZ, Roth MJ, Wang C, Dawsey SM, Li WJ, Wang QH, Han XY, Ding T, Giffen C, Goldstein AM, Taylor PR. Frequent inactivation of the TP53 gene in esophageal squamous cell carcinoma from a high-risk population in China. *Clin Cancer Res* 2001; 7: 883-891
- Taniere P, Martel-Planche G, Puttawibul P, Casson A, Montesano R, Chanvitan A, Hainaut P. TP53 mutations and MDM2 gene amplification in squamous-cell carcinomas of the esophagus in south Thailand. *Int J Cancer* 2000; 88: 223-227
- Shao GZ, Hu Z, Li EM, Li J, Wen BG. Relationship between the GSTM1 genetic polymorphism and susceptibility to squamous cell carcinoma of esophagus. *Shantou Daxue Yixueyuan Xuebao* 1999; 12: 1-3
- Mizobuchi S, Furihata M, Sonobe H, Ohtsuki Y, Ishikawa T, Murakami H, Kurabayashi A, Ogoshi S, Sasaguri S. Association between p53 immunostaining and cigarette smoking in squamous cell carcinoma of the esophagus. *Jpn J Clin Oncol* 2000; 30: 423-428
- van Lieshout EM, Roelofs HM, Dekker S, Mulder CJ, Wobbes T, Jansen JB, Peters WH. Polymorphic expression of the glutathione S-transferase P1 gene and its susceptibility to Barrett's esophagus and esophageal carcinoma. *Cancer Res* 1999; 59: 586-589
- Roth MJ, Dawsey SM, Wang G, Tangrea JA, Zhou B, Ratnasinghe D, Woodson KG, Olivero OA, Poirier MC, Frye



- BL, Taylor PR, Weston A. Association between GSTM1\*0 and squamous dysplasia of the esophagus in the high risk region of Linxian, China. *Cancer Lett* 2000; 156: 73-81
- 31 Morita S, Yano M, Tsujinaka T, Akiyama Y, Taniguchi M, Kaneko K, Miki H, Fujii T, Yoshino K, Kusuoka H, Monden M. Genetic polymorphisms of drug-metabolizing enzymes and susceptibility to head-and-neck squamous-cell carcinoma. *Int J Cancer* 1999; 80: 685-688
  - 32 Butler WJ, Ryan P, Roberts-Thomson IC. Metabolic genotypes and risk for colorectal cancer. *J Gastroenterol Hepatol* 2001;16:631-635
  - 33 Rojas M, Cascorbi I, Alexandrov K, Kriek E, Auburtin G, Mayer L, Kopp-Schneider A, Roots I, Bartsch H. Modulation of benzo<sup>[a]</sup>pyrene diolepoxide-DNA adduct levels in human white blood cells by CYP1A1, GSTM1 and GSTT1 polymorphism. *Carcinogenesis* 2000; 21: 35-41
  - 34 Tanimoto K, Hayashi S, Yoshiga K, Ichikawa T. Polymorphisms of the CYP1A1 and GSTM1 gene involved in oral squamous cell carcinoma in association with a cigarette dose. *Oral Oncol* 1999; 35: 191-196
  - 35 Sato M, Sato T, Izumo T, Amagasa T. Genetic polymorphism of drug-metabolizing enzymes and susceptibility to oral cancer. *Carcinogenesis* 1999; 20: 1927-1931
  - 36 Xing DY, Tan W, Song N, Lin DX. Genetic polymorphism in hOGG1 and susceptibility to esophageal cancer in Chinese. *ZhonghuaYiue Yichuanxue Zazhi* 2000; 17: 377-380
  - 37 Chen S, Xue K, Xu L, Ma G, Wu J. Polymorphisms of the CYP1A1 and GSTM1 genes in relation to individual susceptibility to lung carcinoma in Chinese population. *Mutat Res* 2001;458:41-47
  - 38 Song C, Xing D, Tan W, Wei Q, Lin D. Methylenetetrahydrofolate reductase polymorphisms increase risk of esophageal squamous cell carcinoma in a Chinese population. *Cancer Res* 2001;61:3272-3275
  - 39 Lee JM, Lee YC, Yang SY, Yang PW, Luh SP, Lee CJ, Chen CJ, Wu MT. Genetic polymorphisms of XRCC1 and risk of the esophageal cancer. *Int J Cancer* 2001;95:240-246
  - 40 Chao YC, Wang LS, Hsieh TY, Chu CW, Chang FY, Chu HC. Chinese alcoholic patients with esophageal cancer are genetically different from alcoholics with acute pancreatitis and liver cirrhosis. *Am J Gastroenterol* 2000;95:2958-2964
  - 41 Sato M, Sato T, Izumo T, Amagasa T. Genetically high susceptibility to oral squamous cell carcinoma in terms of combined genotyping of CYP1A1 and GSTM1 genes. *Oral Oncol* 2000;36: 267-671
  - 42 Gsur A, Haidinger G, Hollaus P, Herbacek I, Madersbacher S, Trieb K, Pridun N, Mohn-Staudner A, Vetter N, Vutuc C, Micksche M. Genetic polymorphisms of CYP1A1 and GSTM1 and lung cancer risk. *Anticancer Res* 2001;21:2237-2242
  - 43 Dong CH, Yu SZ, Chen GC, Zhao DM, Hu Y. Association of polymorphisms of glutathione S transferase M1 and T1 genotypes with elevated aflatoxin and increased risk of primary liver cancer. *Huaren Xiaohua Zazhi* 1998; 6: 463-466
  - 44 Bian JC, Shen FM, Shen L, Wang TR, Wang XH, Chen GC, Wang JB. Susceptibility to hepatocellular carcinoma associated with genotypes of GSTM1 AND gstm1. *World J Gastroenterol* 2000; 6:228-230
  - 45 Cai L, Yu SZ, Zhang ZF. Glutathione S-transferase M1, T1 genotypes and the risk of gastric cancer: a case-control study. *World J Gastroenterol* 2001;7:506-509
  - 46 Cai L, Yu SZ. A molecular epidemiologic study on gastric cancer in Changde, Fujian province. *Shijie Huaren Xiaohua Zazhi* 1999; 7: 652-655
  - 47 Lee JM, Lee YC, Yang SY, Shi WL, Lee CJ, Luh SP, Chen CJ, Hsieh CY, Wu MT. Genetic polymorphisms of p53 and GSTP1, but not NAT2, are associated with susceptibility to squamous-cell carcinoma of the esophagus. *Int J Cancer* 2000; 89: 458-464
  - 48 Bartsch H, Nair U, Risch A, Rojas M, Wikman H, Alexandrov K. Genetic polymorphism of CYP genes, alone or in combination, as a risk modifier of tobacco-related cancers. *Cancer Epidemiol Biomarkers Prev* 2000;9:3-28
  - 49 Butkiewicz D, Cole KJ, Phillips DH, Harris CC, Chorazy M. GSTM1, GSTP1, CYP1A1 and CYP2D6 polymorphisms in lung cancer patients from an environmentally polluted region of Poland: correlation with lung DNA adduct levels. *Eur J Cancer Prev* 1999;8: 315-323
  - 50 Liu G, Zhou Q, Wang LD, Hong JY, Deng CJ, Wang YY, Zou JX. Blood clot as a DNA source for studying genetic polymorphism of human carcinogen-metabolizing enzymes. *World J Gastroenterol* 1998; 4(Suppl 2): 108-109
  - 51 Qu YH, Shi YB, Peter S, Zhong LJ, Sun L, Sun XW, Cheng JR, Lin YJ, Xian YB, Dai XD, Gao YT. The genotypes of cytochrome P4501A1 and GST M1 in non-smoking female lung cancer. *Zhongliu* 1998; 18: 80-82
  - 52 Hu YL, Zhang Q. Genetic Polymorphisms of CYP1A1 and susceptibility of lung cancer. *Zhonghua Yixue Yichuanxue ZaZhi* 1999; 16: 26-28
  - 53 Gao JR, Ren CL, Zhang Q. CYP2D6 and GSTM1 genetic polymorphism and lung cancer susceptibility. *Zhonghua Zhongliu Zazhi* 1998; 20: 185-186
  - 54 Cai L, Yu SZ. Preliminary studies on cytochrome P4502E1 and glutathione transferase M1 polymorphisms and susceptibility to gastric cancer. *Zhongguo Gonggong Weisheng* 1999; 15: 895-897
  - 55 Olshan AF, Mark CW, Watson MA, Bell DA. GSTM1, GSTT1, GSTP1, CYP1A1 and NAT1 Polymorphisms, Tobacco use, and the risk of head and neck cancer. *Cancer Epidemiol Biomarkers Prev* 2000; 9:185-191
  - 56 London SJ, Yuan JM, Coetzee GA, Gao YT, Ross RK, Yu MC. CYP1A1 I462V genetic polymorphism and lung cancer risk in a cohort of men in Shanghai, China. *Cancer Epidemiol Biomarkers Prev* 2000;9:987-991
  - 57 Murata M, Watanabe M, Yamanaka M, Kubota Y, Ito H, Nagao M, Katoh T, Kamataki T, Kawamura J, Yatani R, Shiraishi T. Genetic polymorphisms in cytochrome P450 (CYP) 1A1, CYP1A2, CYP2E1, glutathione S-transferase (GST) M1 and GSTT1 and susceptibility to prostate cancer in the Japanese population. *Cancer Lett* 2001; 165: 171-177
  - 58 Shen J, Wang RT, Xing HX, Wang LW, Wang ZX, Wang BY, Li MS, Wang JM, Hua ZL, Guo CH, Wang XR, Xu XP. Research on the interaction models of cytochrome P450 1A1 polymorphism(s) in the agents of stomach cancer. *Zhonghua Yufang Yixue Zazhi* 2001;35:167-170

• REVIEW •

# Changing patterns of traumatic bile duct injuries: a review of forty years experience

Zhi-Qiang Huang, Xiao-Qiang Huang

Zhi-Qiang Huang, Xiao-Qiang Huang, Research Institute of General Surgery, The General Hospital of Chinese PLA, Beijing 100853, China  
Correspondence to: Zhi-Qiang Huang, 28 Fuxin Road, Beijing 100853, China. zhiqianghuang2000@yahoo.com

Telephone: +86-10-66939871 Fax: +86-10-68181689

Received 2001-08-23 Accepted 2001-12-20

## Abstract

**AIM:** To summarize the experiences of treating bile duct injuries in 40 years of clinical practice.

**METHODS:** Based on the experience of more than 40 years of clinical work, 122 cases including a series of 61 bile duct injuries of the Southwest Hospital, Chongqing, and 42 cases (1989-1997) and 19 cases (1998-2001) of the General Hospital of PLA, Beijing, were reviewed with special reference to the pattern of injury. A series of cases of the liver and the biliary tract injuries following interventional therapy for hepatic tumors, most often hemangioma of the liver, were collected. Chinese medical literature from 1995 to 1999 dealing with 2742 traumatic bile duct strictures were reviewed.

**RESULTS:** There was a changing pattern of the bile duct injury. Although most of the cases of bile duct injuries resulted from open cholecystectomy. Other types of trauma such as laparoscopic cholecystectomy (LC) and hepatic surgery were increased in recent years. Moreover, serious hepato-biliary injuries following HAE using sclerotic agents such as sodium morrhuate and absolute ethanol for the treatment of hepatic hemangiomas were encountered in recent years. Experiences in how to avoid bile duct injury and to treat traumatic biliary strictures were presented.

**CONCLUSION:** Traumatic bile duct stricture is one of the serious complications of hepato-biliary surgery, its prevalence seemed to be increased in recent years. The pattern of bile duct injury was also changed and has become more complicated. Interventional therapy with sclerosing agents may cause serious hepatobiliary complications and should be avoided.

Huang ZQ, Huang XQ. Changing patterns of traumatic bile duct injuries: a review of forty years experience. *World J Gastroenterol* 2002;8(1):5-12

## INTRODUCTION

Since the first total cholecystectomy performed by Carl Langenbuch in 1882, there has been the likelihood of bile duct injury. But it was not mentioned until 1905 that Mayo reported the first two cases of bile duct stricture following cholecystectomy treated by choledochoduodenostomy<sup>[1]</sup>. This might be due to the small number of operations performed by that time. However, the number of cases of bile duct injuries has been rapidly increased since then<sup>[2]</sup>. In China, the prevalence of cholelithiasis is increasing, and cholecystectomy has become one of the most frequent operations in daily surgical

practice<sup>[3-5]</sup>. The victims of bile duct injuries often suffered from great misery and the fatality rate can be as high as 30%<sup>[6]</sup>. Efforts have been made in the training and standardization of conventional biliary operations such as cholecystectomy, the result being encouraging. Roslyn<sup>[7]</sup> (1993) revealed 42,474 cases of open cholecystectomy from 1988 to 1989 (8% of cholecystectomies performed in America at the same period of time), and the bile duct injury rate has been lowered to 0.2%. In China, however, the bile duct injury during conventional open cholecystectomy has been claimed to be low, in spite of the lack of statistical data. In recent years, the number of reports on bile duct injuries due to cholecystectomies has been rapidly increased in the Chinese medical literature. The seriousness of the problem caused great concern from the medical professionals<sup>[8]</sup>. Furthermore, the pattern of bile duct injuries at present also differed in some way from the traditional ones which imposed different methods of treatment. These may be complicated and unfamiliar to the practicing physicians and surgeons. In this report, we present our clinical experiences in the treatment of bile duct injuries over the past 40 years and specially the importance in laparoscopic, and bile duct injuries during liver resection and interventional therapy of hepatic lesions.

## CLINICAL MATERIALS

Case records of traumatic bile duct injuries were reviewed. All patients in Group A and Group B series were the cases attended by the senior author either as the director or as senior surgeon of the department. Group A consisted of 61 cases of bile duct injury admitted to the South-west Hospital, Chongqing from 1963 to 1986;<sup>[9]</sup> and Group B were 61 cases admitted to the General Hospital of PLA in Beijing from 1989 to 1997<sup>[10]</sup> and from 1998 to 2001 (Tables 1,2).

Before 1990, the cases of traumatic bile duct stricture were mostly due to open celiotomy by conventional technique. Cases of bile duct stricture following laparoscopic cholecystectomy have been encountered since the turn of 1990 and cases of bile duct injuries resulting from the so-called 'mini-cholecystectomy' have been found in recent years. Up till now, bile duct injuries chiefly result from conventional surgery but not laparoscopic operations. Traumatic injuries and operations of the upper abdominal organs may cause bile duct injury, but biliary tract operations was the most common cause.

**Table 1** Types of primary operations in 61 cases of traumatic biliary strictures (Group A, 1963/1986, South-West Hospital Series)

| Types of operation                                                                | Cases |
|-----------------------------------------------------------------------------------|-------|
| Cholecystectomy                                                                   | 39    |
| Cholecystectomy + choledochostomy                                                 | 10    |
| Gastrectomy (B-II)                                                                | 7     |
| Hepatic injury - Rt lobectomy                                                     | 1     |
| Suture + gauze packing                                                            | 2     |
| Suture + choledochostomy                                                          | 1     |
| Suture + repair of duodenum                                                       | 1     |
| Total cases                                                                       | 61    |
| **29 of the 61 cases were recognized by the operator during the primary operation |       |

**Table 2** Changing trend of primary operations in cases of traumatic biliary strictures (Group B: The General Hospital of PLA Series)

| Types of operations               | Cases       |             |
|-----------------------------------|-------------|-------------|
|                                   | (1989-1997) | (1998-2001) |
| Cholecystectomy                   | 27          | 8           |
| Mini-cholecystectomy              | 2           |             |
| Laparoscopic cholecystectomy(LC)  | 4           | 5           |
| Cholecystectomy + choledochostomy | 9           |             |
| Hepatic resection                 | 3           |             |
| Hepatic resection + HAE           | 1           |             |
| HAE                               |             | 1           |
| Gastrectomy(B-I)                  | 1           |             |
| Total cases                       | 42          | 19          |

In these 122 cases of traumatic bile duct injuries, cholecystectomy, especially simple cholecystectomies, was responsible for the majority of cases. As to the patterns of injuries, laparoscopic surgery, hepatic resection and interventional therapy for hepato-biliary diseases made a significant contribution in the Group B series.

**Gastric resection** The next common cause of extra-hepatic bile duct injury is gastric resection, which has been frequently employed for the treatment of chronic duodenal ulcer disease before the advent of the present anti-ulcer drugs. In series A, there were 2 cases of bile duct injury due to gastric resection probably through a not well-known mechanism which was differed from the ordinary direct operative injury. The first one was a male patient aged 42 years with a history of repeated hemorrhage from chronic duodenal ulcer for 7 years. On operation, a mass involving the posterior duodenal wall and the head of the pancreas was found and a Bancroft's type of gastric resection was performed. Four years following the operation, the patient still suffered from episodes of massive G-I bleeding accompanied with low blood pressure. Therefore, another operation was undertaken. The operation consisted of vagotomy and resection of the remanding portion of the gastric antrum together with the duodenal "ulcer" so as to control bleeding. However, the patient experienced a very stormy postoperative course. Jaundice appeared on the 4<sup>th</sup> postoperative day associated with daily chills and fever, while the gastric aspiration showed no bile. The patient's general condition was thus rapidly deteriorated. Re-operation was performed on the 6<sup>th</sup> postoperative day. A large amount of blood and bile tinged fluid was found inside the peritoneal cavity, and fatty necrosis was found around the head of the pancreas. A cholecystostomy was performed to relieve jaundice and drainage of the abdominal cavity. After the operation, a large amount of bile mixed with pancreatic juice (amylase activity was 1280 Winslow's unit) was drained outdaily through the cholecystostomy tube. Subsequently, further additional operations were performed for intra-abdominal residual abscesses. Eventually, the patient died of sepsis and wide spread intra-cranial hemorrhage. At autopsy, left-sided residual suphrenic abscess and empyema of left thorax was found, the ruptured duodenal stump was healed, and obstruction of the common bile duct at the ampulla below the confluence of the bile and pancreatic ducts was found so that pancreatic fluid was drained through the cholecystostomy tube by retrograde flow. There was no evidence of direct surgical injury or suturing of the lower end of the bile duct as the cause of biliary obstruction, however.

Another case was a middle-aged patient who also suffered from chronic duodenal ulcer complicated with repeated G-I hemorrhage. He was also treated at first by Bancroft's gastric resection and followed by resection of the gastric remnant and the ulcer because episodes of G-I hemorrhage recurred. The patient developed disruption of the duodenal stump and obstructive jaundice. PTC showed bile duct obstruction at the ampulla of Vater. This patient was firstly treated by abdominal drainage and cholecystostomy followed by Roux-en-Y

choledocho-jejunostomy and pancreatico-jejunostomy with an uneventful convalescence. This patient showed no excessive pancreatic drainage through the cholecystostomy tube because of the common bile and the pancreatic ducts were both obstructed at the ampullary level. In these two cases, the obstruction of the ampulla may be the result of operative interruption of blood supply to this particular region. However, the mechanism of such kind of bilio-pancreatic duct injury has not been well understood.

**Interventional therapy and bile duct injury** In recent years, a particular type of bile duct injury was noted<sup>[11]</sup>, i.e., bile duct injuries following interventional treatment for hepatic tumors, most frequently for hepatic hemangiomas<sup>[12]</sup> (Table 3). But such kind of bile duct injuries was usually not categorized under the heading of traumatic bile duct injury in hospital files.

**Table 3** Hepato-biliary complications following HAE for cavernous hemangioma of liver

| Case | Embolizing No. agents   | Complications                                               | Operations                                   | Results                            |
|------|-------------------------|-------------------------------------------------------------|----------------------------------------------|------------------------------------|
| 1    | Sod.mo.+Lip.            | Rt.Lt.CHD,GB Necrosis<br>Biliary cirrhosis<br>Liver abscess | S-R shunt<br>B-jejunostomy                   | Jaundice ↓                         |
| 2    | Ethanol                 | Biliary fistula                                             | Rt. Lobectomy<br>B-jejunostomy               | Jaundice ↓                         |
| 3    | Sod.mo.+Lip.            | Rt-Lt-HD necrosis<br>Liver abscess                          | PTBD<br>Necrosectomy, U-tube                 | Jaundice ↓<br>Jaundice ↑           |
| 4    | Lip.wire<br>Phnyanmycin | GB necrosis<br>HD stricture<br>Liver abscess                | No                                           | Jaundice ↓                         |
| 5    | Sod. Mo+Lip.            | GB,CBD necrosis<br>Liver abscess                            | Cholecystectomy<br>T-tube stent              | Jaundice ↓                         |
| 6*   | Sod. Mo+Lip.            | Bile fistula<br>Rt lobe atrophy<br>Biliary cirrhosis        | B-jejunostomy<br>T-tube stent                | Jaundice ↓                         |
| 7*   | Ethanol                 | Rt liver, GB,duodenum necrosis                              | Cholecystectomy<br>Gastro-jejunostomy        | Died                               |
| 8    | Sod.mo+Lip.             | Rt liver abscess<br>GB necrosis                             | Cholecystectomy<br>Rt lobectomy<br>Repair HD | Jaundice ↓                         |
| 9*   | Sod. Mo+Lip             | Rt liver necrosis<br>HD stricture<br>Portal hypertension    | No                                           | Jaundice ↑<br>Repeated hematemesis |

(Such type of bile duct injury was not included under the category of traumatic biliary injuries in the hospital records)

\* Treated by consultation; Sod mo.=sodium morrhuate; Lip.=iodized oil; B=biliary; GB=gallbladder; CBD=common bile duct; HD=hepatic duct; S-R=spleno-renal; PTBD=percutaneous transhepatic biliary drainage

Since interventional therapy was advocated for hepatocellular carcinoma in recent years with encouraging results, the method of percutaneous transarterial embolism (HAE) has also been advocated and used for the treatment of hepatic hemangioma<sup>[13,14]</sup>. The embolizing agent used was usually sodium morrhuate which is a strong sclerosing agent commonly employed for injection of varicose vein of the lower extremities. But in hepatic hemangioma, after HAE with sodium morrhuate, the patient usually experienced a chronic course of progressive sclerosis of the intrahepatic and extrahepatic hepatic bile duct, persistent jaundice, progression of hepatic fibrosis and portal hypertension<sup>[15]</sup>.

A male patient aged 43 years, he was diagnosed having a hemangioma of the right liver after a routine physical examination with ultrasound scanning. He was advised to have a "catheter treatment" (HAE) for the tumor. According to the doctor's advice, he received a HAE treatment with injection of 10mL iodized oil and 4mL sodium morrhuate. He developed severe right upper abdominal pain, nausea and vomiting immediately after the injection. He was then admitted and treated in the hospital for one week, but he had constant upper abdominal discomfort after discharged from the hospital. Two years later, jaundice appeared which had been diagnosed as "viral hepatitis" and treated accordingly for 3 months. Exploratory celiotomy was

followed. A cholecystectomy was performed, exploring the common bile duct, in which a red-colored mucoid plug was found and removed. Three years later, a percutaneous transhepatic drainage of left intrahepatic bile duct was made because of persistent jaundice. A second operation of choledcho-jejunostomy was then performed. Despite of the operations, jaundice still persisted. He was at last admitted to the General Hospital of PLA in 1999, 6 years after interventional therapy for the liver hemangioma. Preoperative evaluation revealed fibrosis and atrophy of the right liver with the hemangioma still in situ, extensive fibrosis and stricture of the right hepatic duct involving the hepatic duct confluence and the left hepatic duct, and, hypertrophy of the left lateral segment of the liver with dilated intrahepatic bile ducts (Figures 1,2). A third operation was then performed. The left lateral intrahepatic bile duct was chosen for biliary-intestinal anastomosis. Because of the sclerotic changes of the hepatic duct confluence, a trans-round ligament approach for left hepatic duct-jejunostomy of Roux-en-Y type with stent was adopted. Jaundice decreased following the last operation. The other cases of HAE biliary injuries showed more or less similar clinical courses (Table 3). The clinical course and type of subsequent surgical treatment depended on the extensiveness of hepatic and biliary damages and the progression of hepatic fibrosis. Portal hypertension secondary to hepatic fibrosis may be developed and complicated with G-I hemorrhage. In all the cases under this category, the caudate lobe of the liver was found to be much enlarged and in a state of functional compensation.

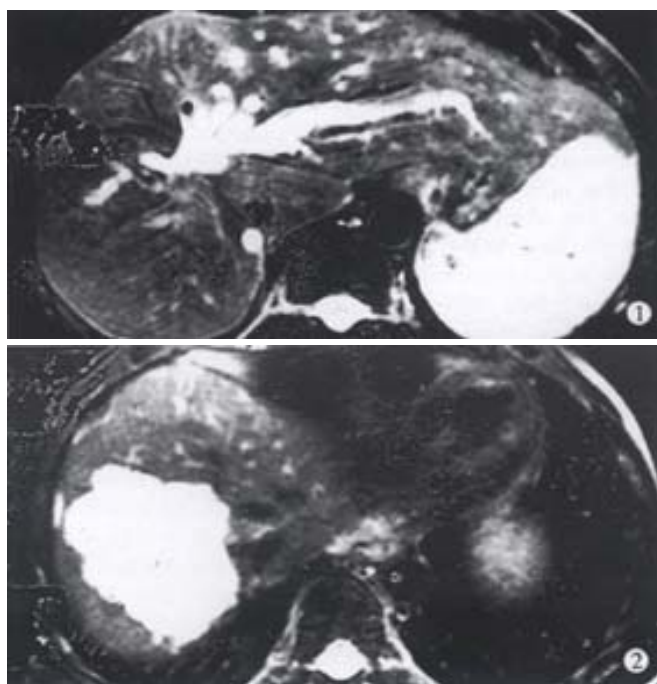


**Figure 1** Hepatobiliary damages 6 years after HAE with splenic hemorrhage: MRI showed atrophy of right liver, hypertrophy of the left lateral segment and obstruction of hepatic duct at the hilum.

**Figure 2** Hemangioma of right liver years after HAE. The same patient. MRI showed hemangioma still in place.

**Hepatic trauma and bile duct injury** Traumatic injury of the liver may be the cause of bile duct injury. Hepatic resections in daily surgical practice as one of the causes of bile duct injury is of increasing importance due to the rapid development of hepatic surgery in recent 20 years. In Group A series, we met a middle-aged male patient who sustained from severe laceration of the right lobe of the liver in a road accident. Resuscitation including emergency right hepatic lobectomy was undertaken in another hospital. However, injury to the left hepatic duct was inflicted and was recognized at

completion of the operation. Hence, repeated operations to treat the bile duct stricture and its complications were necessary subsequently, such as spleno-renal shunt for the treatment of portal hypertension and G-I bleeding, and attempts to recreate a patent biliary-intestinal passage. But operative attempts failed repeatedly because of marked enlargement of the left hepatic lobe and the extreme right posterior rotating displacement of the hilum which became inaccessible to the operation through the conventional surgical approach. The thirteenth operation was performed for the patient to complete a mucosa-to-mucosa anastomosis between the left hepatic duct and a Roux-en-Y jejunal loop through a low thoraco-abdominal incision. The patient recovered from the operation uneventfully and reported to have a satisfactory outcome. There was a young male patient in Group A. He had a severe crushing injury of the liver in a road accident. An external biliary fistula developed following incision and drainage treatment of a subphrenic abscess in right side after the primary operation, and 200-300ml bile was drained from the wound every day. Reoperation revealed traumatic rupture and occlusion of the right hepatic duct. He was treated, during the operation, using the gallbladder to form a conduit bridging between the right hepatic duct and the common bile duct. The biliary fistula healed after the operation.

**Bile duct injury and hepatic resection** In the past 10 years, more and more cases of bile duct injury due to elective liver tumor resections were admitted to the General Hospital of PLA for further treatment. In the Group B series, 1 case of bile duct injuries as a result of hepatic resection was recorded from 1989-1997. From 1998-2001, 3 additional cases were admitted to the General Hospital of PLA. According to our knowledge, besides the above mentioned cases, more than 6 cases were actually caused by hepatic tumor excision in our hospital. Five of these 6 cases had injuries to the left hepatic duct during the resection of tumors involving the left medial segment of the liver (Figure 3). The history of a case of left hepatic duct injury as a result of extended right hepatic resection for neuroblastoma and gauze packing to check bleeding was very illustrative to show the complexity of bile duct injury following hepatic surgery.

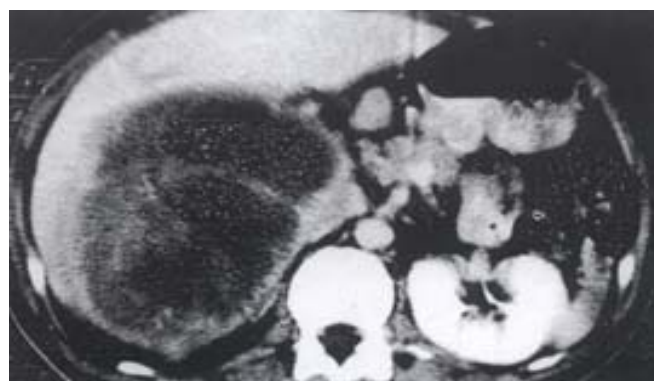


**Figure 3** Neuroblastoma of the right liver: Resection of the tumor with right-sided tri-segmentectomy resulted in injury of the left hepatic duct.

A male patient aged 32 years was admitted to the General Hospital of PLA on 4 January, 2000. He had operative bile duct injury during resection of a neuroblastoma on 27 August, 1998. The tumor, weighting 5.0kg, situated in the right liver, was resected with difficulty and complicated with profuse bleeding. The estimated blood loss was about 27 000 mL. Gauze packing was used to stop the hemorrhage from the liver hilum upon completion of the operation. There was clinical jaundice on the second post-operative day. The gauze packing was removed on the 5<sup>th</sup> postoperative day through the celiotomy wound. On October 21, 1998, PTCD of the left intrahepatic bile duct was performed because of persistent jaundice.

As the indwelling catheter was withdrawn accidentally later on, another PTCD of the left intrahepatic duct was performed on December 23, 1999 when the serum bilirubin level was  $543\mu\text{mol/L}$ . The catheter was kept on draining of bile in the amount of  $500\text{--}700\text{mL}\cdot\text{d}^{-1}$ . Retrograde cholangiography showed complete obstruction of the left segmental bile duct (Figure 4). After admission to the General Hospital of PLA, the patient was reexamined and prepared for reoperation. During the operation, there was so dense fibrous adhesions and rich vascular communications in the hilar region that dissection of the extrahepatic bile duct was very difficult. Therefore, the left segmental bile duct was approached along the surface plane of the left external hepatic segment under the guidance of intraoperative ultrasound scanner. The site of the obstructed left intrahepatic duct was found posterior to the left portal vein. The operation was completed with a cholangio-jejunostomy over a U-typed silicone rubber tube. This case illustrated the changing scope of traumatic bile duct strictures at the present that restorative treatment in many cases may be very complicated, and this might be the reason why this patient carried on his PTCD tube for as long as 2 years before referral to our hospital without further surgical intervention. The use of intraoperative BU-scan was important for the success of the operation in this case. Since bile duct injuries inflicted from hepatic surgery may have a very complicated clinical feature, therefore, for one or another reason, such patients may be withheld from appropriate and timely surgical intervention. This was reflected from what happened to a male patient at 40 years of age in Group B. He was diagnosed as having a cavernous hemangioma of quadrate lobe of the liver by ultrasound. The tumor was resected in another hospital. Following the operation, the patient developed obstructive jaundice, biliary peritonitis, and a big "biloma" in the upper abdomen. Re-exploration of the abdomen was carried out, bile-like fluid of about 2500mL was evacuated, however, the extrahepatic bile duct could not be found. The patient suffered from obstructive jaundice and subphrenic abscess without further treatment for 7 months. At last, when the patient was admitted to the General Hospital of PLA, his general condition was very poor and cachectic, the serum bilirubin level was  $600\mu\text{mol/L}$ . MRI examination showed a large subphrenic collection of fluid and markedly dilated intrahepatic bile ducts (Figure 5). Aspiration of the subphrenic abscesses showed infected bile collection. He was further treated by PTCD of the intrahepatic duct instead of reconstructive operation. In spite of the minimally invasive procedure, the patient developed hepatic coma and recovered only after a period of intensive medical treatment. He was waiting for further surgery when his condition was indicated for the operation. This was a typical case of negligence of medical profession. The difficult situations facing to the surgeon are the lack of knowledge and experience in handling bile duct injury following hepatic operations.



**Figure 4** The same case as Fig 3. Retrograde cholangiography of the intraphepatic duct through a PTBD catheter showing obstruction of left intrahepatic ducts and hypertrophy of the left hepatic segment.

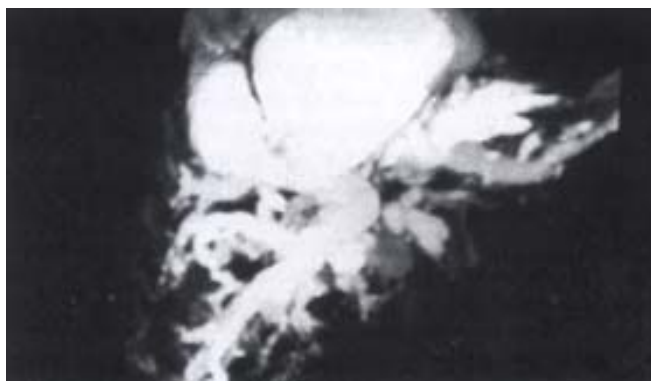


**Figure 5** Bile duct injury in resection of quadrate lobe hemangioma: MRCP showing marked dilatation of the intrahepatic duct system with suphrenic collection of fluid. Extrahepatic bile duct not visualized.

## DISCUSSION

**Safety of cholecystectomy** The current cholecystectomy should be a safe and effective operation. For example, in a review reported on the safety of laparoscopic cholecystectomy for cholelithiasis<sup>[16]</sup>, 4655 consecutive cases of cholecystectomies for gallstones one year before laparoscopic cholecystectomy (LC) was initiated were collected from 34 well equipped hospitals in China. Among these cases, postoperative complications which needed reoperative intervention occurred in 17 cases (0.36%), complications with lasting sequelae in 2 cases (0.05%), and death in 8 cases with a mortality rate of 0.18%. Most of the deaths were related to emergency operation in high risk patients<sup>[16]</sup>. More or less similar result was obtained by Roslyn<sup>[7]</sup> who revealed 42,474 open cholecystectomies performed in the year 1989 in America with a mortality rate of 0.17%. Injury to the bile duct is still a serious complication during cholecystectomy. Presently, incidence of bile duct injuries in open cholecystectomy has been decreased to a rather low level. Clavien *et al*<sup>[17]</sup> reviewed the result of open cholecystectomy in the hospitals in North America and in Europe, injuries to the extrahepatic bile duct was found in 0.2% of the 1, 252 operations. But, bile duct injuries occurred more frequently in laparoscopic cholecystectomy than in conventional open cholecystectomy<sup>[18-21]</sup>. The latest data about laparoscopic cholecystectomy collected by Huang *et al* showed that bile duct injuries occurred in 0.30% and biliary complications (including postoperative bile fistula which might be the result of minor bile duct injuries) occurred in 0.60% of the cases in China<sup>[22]</sup>. The reported incidence of operative injury of the bile duct may be much lower than actually existed, however. This is true in China and as well as in the other parts of the world. Therefore, the reported incidence of traumatic bile duct injury in laparoscopic cholecystectomy was around 0.15% (9/5680)<sup>[23]</sup> from a single hospital to 0.19% in a review series, but the result of about 0.5% in some western countries<sup>[24,25]</sup>. A review of recent Chinese medical literature (1995.1-1999.12) on trauma to the extra-hepatic bile duct<sup>[26]</sup> revealed that the spectrum of bile duct injuries occurring most frequently was the operations related to cholecystectomy, which accounted for 94% in 2,566 cases (Table 4).

**Table 4** Bile duct injury and the type of operations in 2742 cases (Chinese literature review 1995-1999)

| Type of operation                 | No. of cases | %   |
|-----------------------------------|--------------|-----|
| Cholecystectomy                   | 1 933        | 70  |
| Laparoscopic cholecystectomy      | 310          | 11  |
| Cholecystectomy + choledochostomy | 165          | 6   |
| Gastrectomy                       | 66           | 2   |
| HAE*                              | 16           | 0.6 |
| Hepatic resection                 | 10           | 0.4 |
| Other operations                  | 66           | 2   |
| Unspecified                       | 176          | 6   |

\*HAE = Hepatic arterial embolization



There were cases of bile duct injuries from HAE and hepatic resections (0.6% and 0.4% respectively), and bile duct injuries due to laparoscopic cholecystectomy accounting for 11% of the total series. This variations in the disease pattern of benign biliary stricture were in accordance with the current changing practice of hepato-biliary surgery.

**Surgical treatment of traumatic biliary stricture** Since bile duct injury cannot be eradicated by biliary surgery as human beings are not exempt from errors. Therefore, prevention as well as treatment of bile duct injuries is still most important in biliary surgery [27-29]. In our experience, the long-term good results of reparative operation of traumatic bile duct stricture may be as high as 90% and 95% [9,10]. In average, especially when reconstructive surgery was performed in those hospitals lack of expertise in biliary surgery, the result may be far from satisfactory, the postoperative morbidity rate and reoperation rate was high, and the mortality rate may be as high as 30%. Many of the patients carried on a miserable life (so-called biliary cripple) and eventually died of hepatic failure. Option of methods of surgical treatment for traumatic biliary strictures is varied according to different authors. In our experience, the best result was obtained after bilio-enterostomy of Roux-en-Y type with application of plastic reconstructions of hilar bile duct remnant. Therefore, in the two series of cases in this report, satisfactory result was obtained in more than 90% of the treated cases. In our series, all of the patients were referred from elsewhere in our country, and most of them have had multiple unsuccessful operations and came to our hospital as the last resort. One patient with traumatic bile duct injury had been operated upon as many as 12 times. Secondary surgical repair of biliary stricture is more difficult than the primary reparation because of the much distorted local anatomy and, in many of the cases, the level of bile duct stricture may be extended above the hepatic confluence to involving both hepatic ducts (Bismuth classification type IV), which is the most difficult situation to be treated.

In the treatment of traumatic bile duct stricture, the type of surgery seems to have important influence on the outcome of the disease. We preferred cholangio-jejunostomy of the Roux-en-Y type for reconstruction, especially for those late cases and those high strictures in which one or both hepatic ducts may be involved. Therefore, we used such type of operative repair in 47 of the 61 cases (77%) of Group A. Besides, in 4 cases with a functioning distal common bile duct, we adopted the principle of preservation of the sphincter of Oddi's function by using a pedicled gastric or jejunal patch for the repair. With an interposed jejunal loop with artificial nipple formation, hepatico-duodenostomy was employed in 2 cases. By such methods of management, we obtained good long-term result of 95.6% (including 2 reoperations 2 and 30 years after the first repair respectively). Two patients (4.4%) in Group A died of suppurative cholangitis 4 and 12 years respectively after the repair. Based on our experience in bile duct surgery, we have set up some guidelines for the surgery of biliary stricture which were proved to be important in clinical practice. They are: ① Strategy of traumatic biliary stricture repair: primary repair is critical, but early repair is more frequent, thus being, more important; though reoperations are difficult, they should be performed with confidence; operation should be staged in the presence of marked portal hypertension; operations should be a wait till marked biliary cirrhosis with liver dysfunction; ②. Technical essentials in reparative operation: side-to-side bilio-enterostomy is the first choice to minimize late stricture formation; single-layered anastomosis is essential; absorbable or single strand suturing materials should be provided; stent placement of 9 months or 1 year, if possible; good quality stenting tube should be selected to prevent accidental breakage; It should be kept in mind that there were '3 hepatic ducts' at the hilum of liver instead of only 2 as generally believed; ③ Alternatives: T-tube, Y-tube, and U-tube all

have merits for stenting; straight-tube, and shape-memory tube may be used at special occasions; Trans-hepatic tube may also be used for prolonged stenting and instrumentation; Finally, bile duct surgery is more or less alike to cannal engineering.

**LC bile duct stricture** Treatment of traumatic injury of extrahepatic bile duct due to laparoscopic cholecystectomy is a special problem of current biliary surgery. Though the number of laparoscopic injuries was relatively low in comparison with the open technique, for example, 310 of 2742 cases of bile duct injuries (12%) in a literature survey [26] and 4 of 42 cases (9.5%) of bile duct injuries in the General Hospital of PLA from 1989-1997 [10]. In a review of 182 cases of bile duct injuries from 4 medical centers (1999), 30 cases (17%) were due to LC [30]. Reports of LC bile duct injury have appeared since 1991 when the technique of laparoscopic cholecystectomy was first introduced to China mainland, but the number of patients rapidly increased as time went on. Therefore, LC bile duct injuries were found in 5 of the 19 cases treated in the General Hospital of PLA between the years 1998 and 2000, accounting for 26.3%. With accumulated experience of treatment of LC bile duct injuries, certain characteristic features were apparent. Most of the severe bile duct injuries of LC belonged to the so-called "classical injury" classified by Davidoff [31]. Usually there was loss of a segment of the upper bile duct and involvement of one or both hepatic ducts. Sometimes, one of the injured hepatic ducts in the hepatic hilum may be hidden from the operator's sight (the right posterior duct being the most often and also occasionally the left hepatic duct) (Figures 6,7). Retained foreign materials (usually a broken piece of plastic tube which was used for internal stenting) were found more often. Spontaneous biliary duodenal fistula may be found in cases with no clinical jaundice. On the other hand, in many cases, when secondary repair was undertaken, the degree of intra-abdominal inflammatory changes and extent of adhesions was less than in the operation after conventional open surgery, therefore, a repair operation for the injury or anastomosis with the gut can be considered. These characteristic features of LC bile duct injuries demanded a change of surgical policy in the management of bile duct injuries for a better result [32-34].

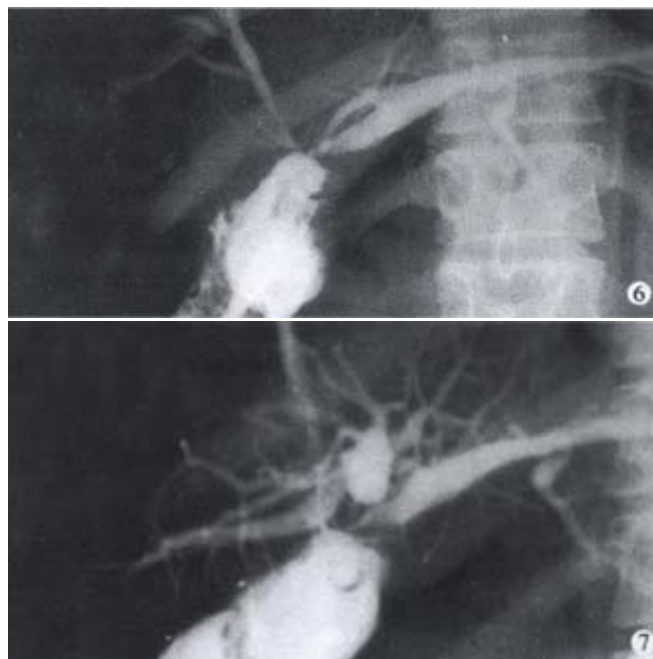


**Figure 6** LC bile duct injury: Bile duct repair by hepatico-jejunostomy of Roux-en-Y type. Postoperative retrograde cholangiography only the right anterior segmental duct and the left hepatic duct visualized.

**Figure 7** The same case. PTC showing the dilated blind end of the right posterior segmental duct which was "missed" during the operation.

**Gastric resection and bile duct injury** Gastric resection is the next most common cause of operative bile duct injury. In a review of 2742 cases of bile duct injuries reported in Chinese literature by Huang *et al*<sup>[35]</sup>, 66 cases occurred during gastric resection operation, accounting for 2.4% of the total. The most severe type of such kind injury was trans-section of the common bile duct together with the hepatic artery and the portal vein. Such type of injury gave a high fatality rate (11/11). Among the patients in series A, two incidences showed a similar clinical manifestations following gastric operation for bleeding chronic penetrating duodenal ulcer. The mechanism of such type of damages may be related to the disruption of blood supply to the duodeno-ampullary region. Disturbance of local blood supply resulted in the coexistence of disruption of the duodenal stump and fibrotic obstruction at the ampulla. Blood supply of the extrahepatic bile duct is segmental. The supra-duodenal portion of the common bile duct received arterial blood supply chiefly from branches sent by the hepatic artery proper, while the lower portion of the common bile duct including the ampullary region received blood supply chiefly from the posterior pancreatico-duodenal artery that was derived from the gastroduodenal artery<sup>[36,37]</sup>. Operation of excising the bleeding duodenal ulcer would inevitably result in the disruption of local blood supply and lead to the dishesion of the duodenal stump and fibrotic occlusion change of the ampulla.

**Interventional therapy and bile duct injury** Since bile duct injuries and its consequences are the ever existing problem of hepato-biliary surgery including interventional therapies of many hepato-biliary affections<sup>[38,39]</sup>. A kind of severe extensive damage of the intraand extra-hepatic bile duct as a result of inadvertent use of sclerosing agents in the treatment of liver tumors (most often hemangioma of the liver) was noted<sup>[11,13,14,40]</sup>. Six cases were admitted to our hospital on account of complications such as liver necrosis and abscesses, biliary intestinal fistula, extensive hepatic fibrosis complicated with portal hypertension, G-I bleeding, extensive destruction of the intra- and hilar bile duct with obstructive jaundice, etc. The sclerosing agents that most commonly employed were sodium morrhuate and absolute ethanol<sup>[13,14,41]</sup>. Furthermore, we have also attended 3 cases through consultation. One case of asymptomatic haemangioma of the right liver was treated in another hospital by injecting 19ml absolute alcohol through the hepatic arterial catheter. The patient suffered from severe abdominal pain soon after the injection and was operated upon because of signs of acute peritonitis on the third day after the procedure. During operation, necrosis of the right liver, the biliary tract and the duodenum was found. The patient developed biliary fistula, and eventually died of multiple organs failure on the 10<sup>th</sup> day after the therapy. The other 2 patients suffered from repeated G-I bleeding because of portal hypertension due to hepatic fibrosis. Trans-hepatic arterial embolization (HAE) is a kind of interventional therapy which was widely employed as the current non-surgical treatment for advanced hepatocellular carcinoma(HCC)<sup>[42-47]</sup>. In general, the embolizing agents consisted of lipoidal oil and small particles of gelform sponge. Particles of 1-2 mm in size would block the small intrahepatic arteriols about 50  $\mu$ m in diameter, and caused necrosis of the tumor mass. The gelform sponge particles will be dissolved in a course of about 2 weeks. While, on the other hand, if liquid materials are used as embolizing agent, such as absolute ethanol and sodium morrhuate, the drug may reach the end of the hepatic arterioles, causing damages to the liver parenchyma wherever the drug reached. Therefore, liquid embolizing agents will cause more extensive liver necrosis and damages to the intrahepatic bile duct by way of the peribiliary plexus. The resulting complications will be necrosis of the gallbladder, destruction of the intrahepatic bile duct system, liver abscesses formation, sclerosis of intra- and extra-hepatic duct, necrosis of the gall bladder with biliary duodenal fistula formation, and hepatic fibrosis (Figures 8, 9). If a more caustic agent (such as absolute ethanol) is used, immediate coagulation necrosis of the bile duct and liver parenchyma will occur. If the drug

was used in excessive amount or being injected too rapidly (as often the case when mechanical automatic injector is used), there will be retrograde flow of the drug causing extensive damage of extrahepatic intra-abdominal organs.

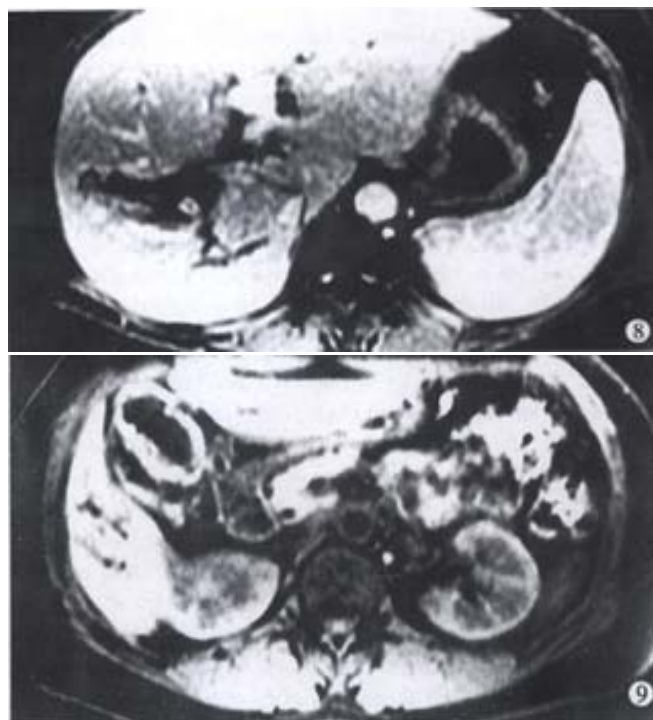


**Figure 8** Fibrosis and obstruction of hepatic duct following HAE with injection of sodium morrhuate: 2 years after the procedure.

**Figure 9** The same case. Necrosis of the gallbladder and the hepatic duct.

Liver receives double-sourced blood supply, arterial blood composed of 25%-30% of the hepatic blood inflow and supply 50% of the total oxygen expenditure of the liver. The hepatic artery, after entering into the liver parenchyma, sends branches to the hepatic duct, forming a complicated peribiliary plexus which by way of the portal vessels reaches hepatic sinusoids<sup>[48]</sup>. The intrahepatic bile duct system, differing from the hepatic cells, received blood supply exclusively from hepatic artery. Blood supply of the common hepatic duct and the right and left hepatic duct is derived directly from the right and left hepatic artery, forming a peribiliary vascular plexus in direct connection with the intrahepatic peribiliary vascular plexus<sup>[49]</sup>. Therefore, inadvertent intra-arterial injection of sclerosing agents into the hepatic artery will result in destruction of the intrahepatic bile duct, as well as sclerosis and obstruction of the right and left hepatic duct at the hilum hepatis. However, the common bile duct under such conditions was often found to be exempt except when retrograde flow of a large amount of the drug occurred. This is explained on the ground of vascular pattern of the common bile duct that the vascular plexus of the common bile duct is derived chiefly from the branches of gastroduodenal artery that connect with the vascular plexus of the intrahepatic bile duct indirectly. Furthermore, as we found in the reported cases of intrahepatic bile duct damage resulting from HAE that in spite of atrophy of the right and left hepatic lobes, the caudate lobe was usually markedly hypertrophied so as to take over the functional role of the liver. This phenomenon is also explained on the basis of blood supply of the caudate lobe. The caudate lobe of liver received bilateral hepatic arterial and portal venous blood supply, therefore, may be exempt from the injurious effect of HAE.

In recent years, HAE has been widely used as a therapeutic modality in the treatment of advanced HCC and was claimed to be safe and effective. However, serious biliary damage was found when

HAE was applied to treat cases of hepatic haemangiomas with sclerosing agents as shown in this report. There may be fundamentally different hemodynamic patterns between malignant and benign lesions of the liver. It was well known that arterial blood supply to HCC is much increased with dilatation and increased number of arterial branches to the tumor. Under such conditions, intra-arterial injection of sclerosing agents may be diverted from the accompanying intrahepatic bile ducts. While, in case of liver hemangioma, configuration of vascularity of the liver remained almost the same as found in the normal liver, therefore, more injected toxic agents will be directed to the intrahepatic biliary plexus and caused damages. A large volume of injected material (such as absolute ethanol) by high speed under pressure injection, and displacement of the intra-arterial catheter may render the situation worst as wide spread retrograde flow may occur as result of arterial spasm. Many cases of bile duct damage resulting from HAE employing sclerosing agents (generally not categorized under traumatic bile duct injury) may not be amendable to surgical treatment because of the extensiveness of the lesion. The authors have treated 11 such cases during the last 10 years (including 3 cases by consultation). Among these cases, 2 were not treated surgically because of extensive sclerotic cholangitis of the intrahepatic bile duct. One case of intrahepatic sclerosing cholangitis resulting from injection of absolute ethanol into a hydatid cyst of the right liver which happened to have a fistula communicating with the hepatic duct. One case of hemangioma of the liver died of multiple organs failure after the injection of absolute ethanol. The other 6 patients were treated by drainage of liver abscess, resection of damaged liver lobe, reconstruction of cholangio-enterostomy with an indwelling U-tube for stenting, and, in one case, a preliminary spleno-renal shunt was required before definite bile duct operation was attempted because of portal hypertension and G-I bleeding. One patient died of liver carcinoma 5 years after surgery. Because of the serious complications in HAE for benign hepatic lesions, re-evaluation of the rationale of such kind of treatment should be undertaken.

**Hepatic resection and bile duct injury** Injury to the extrahepatic bile duct during hepatic surgery occurred most frequently in operations for those lesions located in the perihilar region. Operations involving resection of tumors of quadrate lobe of the liver are most vulnerable because of the close proximity of these structures. Bile duct injury and stricture formation following hepatic resection should deserve more scrutiny because of its detrimental effect on the outcome of the surgery and the difficulty of repairing operation under such situation<sup>[50-52]</sup>. In our experience, bile duct stricture resulting from hepatic surgery has become more common over the past 10 years, the increase of number of patients kept pace with the development and propagation of hepatic surgery in our country. In this report, bile duct injury in hepatic surgery accounted for 0.82%-15.7% of the total bile duct strictures. Furthermore, bile duct injuries occurred only in cases of hepatic trauma in Group A. In Group B, the incidence of bile duct injuries rose to 15.7 % as a result of resection of hepatic tumors. In fact, to our knowledge, numbers of bile duct injury in hepatic surgery were much larger than what was reported. The apparent reason is that many cases were recorded and filed as 'operative complications' or 'bile fistulae' instead of the diagnosis of traumatic bile duct injuries<sup>[53-55]</sup>. Injury to the hilar bile duct is most vulnerable during resection of tumors, either benign or malignant, of the quadrate lobe of the liver. The transverse portion of the left hepatic duct courses along the underneath border of the quadrate lobe and with its peribiliary connective tissue fibers interwoven with that from the hilar plate. Identification and isolation of the left hepatic duct may be difficult especially when the normal anatomical relationship was distorted by local tumor growth. Furthermore, branches of bile duct to the left middle segment of the liver were difficult to be identified and individually divided, laceration injury of the left hepatic duct may occur when the hepatic tumor mass was mobilized. Therefore, we emphasized that technique of mobilizing the left hepatic duct with the hilar

plate for the prevention of bile duct injury should be a safeguard measure in liver resection and should be followed in case of perihilar tumor resection.

In recent years, a kind of small incision (3cm-5cm) cholecystectomy (minilaparotomy) has been introduced<sup>[56-58]</sup>. The result of such type of operation is not different from that of conventional surgery so far as the probability of bile duct injury is concerned.

## REFERENCES

- 1 Braasch JW. Historical perspectives of biliary tract injuries. *Surg Clin North Am* 1994; 74:731-740
- 2 Chapman WC, Halevy A, Blumgart LH, Benjamin IS. Postcholecystectomy bile duct strictures: Management and outcome in 130 patients. *Arch Surg* 1995; 130:597-604
- 3 Guo ZY, Huang ZQ. Characteristics of gallstones in China. *Zhonghua Waike Zazhi* 1987;25:321-329
- 4 Huang ZQ. Development of Hepatobiliary and pancreatic surgery in the last fifty years in China. *Zhonghua Waike Zazhi* 2001; 39:9-16
- 5 Huang ZQ. New development of biliary surgery in China. *World J Gastroenterol* 2000; 6:187-192
- 6 Huang ZQ. Laparoscopic surgery and the evolution of surgical treatment of cholelithiasis. *Zhonghua Waike Zazhi* 1993; 31:387-389
- 7 Roslyn JJ, Binns GS, Hughes EFX, Saunders-Kirkwood K, Zinner MJ, Cates JA. Open cholecystectomy. A contemporary analysis of 42 474 patients. *Ann Surg* 1993;218:129-137
- 8 Huang ZQ. The safety of laparoscopic cholecystectomy should be guarded. *Zhonghua Waike Zazhi* 1995; 33:645-646
- 9 Liu YX, Huang ZQ, Zhou YB, Cai ZJ, Qian GX, Chi YB, Han BL, He ZP, Zhang CZ, Tao JM. Surgical treatment of traumatic bile duct stricture. *Puwai Linchuang* 1986; 1:234-245
- 10 Wang J, Liu YX, Feng YQ, Zhou NX, Gu WQ, Huang XQ, Zhang WZ, Huang ZQ. Surgical treatment of traumatic stricture of bile duct. *Zhonghua Gandan Waike Zazhi* 1998; 4: 73-75
- 11 Huang XQ, Huang ZQ, Duan WD, Zhou NX, Feng YQ. Damage to intra- and extrahepatic bile duct after hepatic artery embolization. *Zhonghua Waike Zazhi* 2000;38:169-172
- 12 Huang XQ, Huang ZQ, Duan WD, Zhou NX, Feng YQ. Hepato-biliary complications following hepatic artery embolism for hepatic hemangioma ( Report of 9 cases). *Zhongguo Shiyong Waike Zazhi* 2001;21:319-320
- 13 Li YH, Li SX. An experimental study of sod morrhuate as an agent for arterial embolization. *Zhonghua Fangshexue Zazhi* 1987;21:357-359
- 14 Yan XF, He JG, Song HZ, Zhao CZ. Interventional therapy of hepatic cavernous hemangioma. *Zhonghua Waike Zazhi* 1994; 32:563-565
- 15 Huang XQ, Huang ZQ, Duan WD, Zhou NX, Feng YQ. Destructive damage of bile duct of hepatic artery embolization in treatment of hepatic cavernous haemangioma. *Acad J PLA Postgrad Med Sch* 2000; 21:88-91
- 16 Huang ZQ, Wang YS, Jia SY. On safety of laparoscopic cholecystectomy (Analysis of 4655 cases from 34 hospitals). *Gandan Yipi Zazhi* 1995; 1:73-76
- 17 Clavien PA, Sanabria JR, Mentha G, Borst F, Buhler L, Roche B, Cywes R, Tibshirani R, Rohner A, Strasberg SM. Recent results of elective open cholecystectomy in a North American and a European Center. *Ann Surg* 1992; 216:613-626
- 18 Dunn D, Fowler S, Nair R, McCloy R. Laparoscopic cholecystectomy in England and Wales: results of an audit by The Royal College of Surgeons of England. *Ann R Coll Surg Engl* 1994; 76:269-275
- 19 Kerin MJ, Gorey TF. Biliary injuries in the laparoscopic era. Clinical review. *Eur J Surg* 1994;160:195-201
- 20 Wherry DC, Marohn MR, Malanoski MP, Hetz SP, Rich NM. An external audit of laparoscopic cholecystectomy in the steady state performed in medical treatment facilities of the department of defense. *Ann Surg* 1996; 224:145-154
- 21 Gouma DJ, Go MNYH. Bile duct injury during laparoscopic and conventional cholecystectomy. *J Am Coll Surg* 1994;178:229-233
- 22 Huang XQ, Feng XQ, Huang ZQ. Complications of laparoscopic cholecystectomy in China.:An analysis of 39 238 cases. *Chin Med J* 1997; 110: 704-706
- 23 Zhou ZD, Chen XR, Mao JS, Yu SM. Prevention and treatment of extrahepatic bile duct injuries in laparoscopic cholecystectomy. *Gandan Waike Zazhi* 1999; 7:261-262
- 24 Huang ZQ. Iatrogenic bile duct injuries: Old problem with new meaning. *Zhongguo Shiyong Waile Zazhi* 1999;19: 451-452
- 25 Martin RF, Rossi RL. Bile duct injuries: Spectrum, mechanism of injury, and their prevention. *Surg Clin North Am* 1994; 74:781-803
- 26 Huang XQ, Huang ZQ. Treatment of iatrogenic bile duct injury. *Zhongguo Shiyong Waike Zazhi* 2001; 21:413-414
- 27 Huang ZQ. Bile duct injury in the era of laparoscopic surgery. *Gandan Waike*

- Zazhi 1998; 6:65-66
- 28 Rutledge R, Fakhry SM, Baker CC, Meyer AA. The impact of laparoscopic cholecystectomy on the management and outcome of biliary tract disease in North Carolina: A statewide, population-based, time-series analysis. *J Am Coll Surg* 1996; 183:31-45
- 29 Strasberg SM, Hertl M, Soper NJ. An analysis of the problem of biliary injury during laparoscopic cholecystectomy. *J Am Coll Surg* 1995; 180:101-124
- 30 Dai XW, Chen YJ, Gao ZQ, Shi JS, Yang FQ, Ma K, et al. Iatrogenic extrahepatic bile duct injury and treatment (a report of 182 cases). *Zhongguo Shiyong Waike Zazhi* 1999; 19:485-487
- 31 Davidoff AM, Pappas TN, Murray EA, Hilleren DJ, Johson RD, Baker ME, Newman GE, Cotton PB, Meyers WC. Mechanism of major biliary injury during laparoscopic cholecystectomy. *Ann Surg* 1992; 215:196-199
- 32 Madariaga JR, Dodson SF, Selby R, Todo S, Iwatsuki S. Corrective treatment and anatomic considerations for laparoscopic cholecystectomy injuries. *J Am Coll Surg* 1994; 179:321-325
- 33 Woods MS, Traverso LW, Kozarek RA, Tsao J, Rossi RL, Gough D, Donohue JH. Characteristics of biliary tract complications during laparoscopic cholecystectomy: A multi-institutional study. *Am J Surg* 1994; 167:27-34
- 34 Kwon AH, Inui H, Kamiyama Y. Laparoscopic management of bile duct and bowel injury laparoscopic cholecystectomy. *World J Surg* 2001; 25:856-861
- 35 Huang XQ, Huang ZQ. Present status of bile duct injuries in China. Proceedings of The 9th National Conference on Biliary and The 2nd Chinese General Surgeon Association, 2000, Nov. Wuhan 49-52
- 36 Xu ND. Anatomy and anatomical variations of extrahepatic biliary passage. In Huang ZQ: Modern Biliary Surgery (Dangdai Dandao Waikexue), Shanghai: Archives of Science and Technology Publisher 1998:26-27
- 37 Chen WJ, Ying DJ, Liu ZJ, He ZP. Analysis of the arterial supply of the extrahepatic bile ducts and its clinical significance. *Clinical Anatomy* 1999; 12: 245-249
- 38 Huang ZQ. Bile duct injury-The ever-lasting theme in hepato-biliary surgery. *Zhonghua Putongwaikao Zazhi* 2001;16:371-373
- 39 Huang FG, Li Y, Xie XD. Side effects and complications of hepatic arterial infusion and embolization of liver carcinoma in aged patients and its management. *World J Gastroenterol* 1998;4:67-68
- 40 Huang XQ, Yang KZ, Huang ZQ, Yi GQ, Wang BZ. Changes of hepatic micro-circulation after obstruction of bile duct: An experimental study. *Zhonghua Shiyong Waikao Zazhi* 1987; 4:151-154
- 41 Cao XC, He NS, Sun JZ, Wang S, Ji XM, Wang JS, Zhang CL, Yang JG, Lu TW, Li JH, Zhang GH. Interventional treatment of huge hepatic cavernous hemangioma. *Chin Med J* 2000; 113:927-929
- 42 Wang JH, Lin G, Yan ZP, Wang XL, Cheng JM, Li MQ. Stage II surgical resection of hepatocellular carcinoma after TAE of 38 cases. *World J Gastroenterol* 1998; 4:133-136
- 43 Li L, Wu PH, Li JQ, Zhang WZ, Lin HG, Zhang YQ. Segmental transcatheter arterial embolization for primary hepatocellular carcinoma. *World J Gastroenterol* 1998; 4:511-512
- 44 Huang FG, Yuan J, Xie XD. Long-term follow-up of patients with carcinoma after hepatic arterial infusion and embolization. *World J Gastroenterol* 1998; 4:66
- 45 Lu MD, Chen JW, Xie XY, Liang LJ, Huang JF. Portal vein embolization by fine needle ethanol injection: experimental and clinical studies. *World J Gastroenterol* 1999; 5:506-510
- 46 Tang ZY. Hepatocellular carcinoma-cause, treatment and metastasis. *World J Gastroenterol* 2001; 7:445-454
- 47 Fan J, Ten GJ, He SC, Guo JH, Yang DP, Weng GY. Arterial chemembolization for hepatocellular carcinoma. *World J Gastroenterol* 1998; 4:33-37
- 48 Stapleton GN, Hickman R, Terblanche J. Blood supply of the right and left hepatic ducts. *Brit J Surg* 1998; 85:202-207
- 49 Lillemoe KD, Melton GB, Cameron JL, Pitt HA, Campbell KA, Talamini MA, Sauter PA, Coleman J, Yeo CJ. Postoperative bile duct strictures: management and outcome in the 1990s. *Ann Surg* 2000; 232:430-441
- 50 Matthews JB, Gertsch P, Baer HU, Schweizer WP, Blumgart LH. Biliary stricture following hepatic resection. *HPB Surgery* 1991;3:181-189
- 51 Yamashita YI, Hamatsu T, Rikimaru T, Tanaka S, Shirabe K, Shimada M, Sugimachi K. Bile leakage after hepatic resection. *Ann Surg* 2001; 233:45-50
- 52 Torzilli G, Makuuchi M, Midorikawa Y, Sano K, Inoue K, Takayama T, Kubota K. Liver resection without total vascular exclusion: hazardous or beneficial. *Ann Surg* 2001; 233:167-175
- 53 Schweizer WP, Matthews JB, Baer HU, Nudelman LI, Triller J, Halter F, Gertsch P, Blumgart LH. Combined surgical and interventional radiological approach for complex benign biliary tract obstruction. *Br J Surg* 1991; 78:559-563
- 54 Tocchi A, Costa G, Lepre L, Liotta G, Mazzoni G, Sita A. The long-term outcome of hepaticojejunostomy in the treatment of benign bile duct stricture. *Ann Surg* 1996; 224:162-167
- 55 Keulemans YC, Bergman JJ, de Wit LT, Rauws EA, Huibregtse K, Tytgat GN, Gouma DJ. Improvement in the management of bile duct injuries. *J Am Coll Surg* 1998; 187:246-254
- 56 Luo KY, Lin SJ, Yang Y, Wang MZ, Liu WZ, Wo HZ, Chen QS. The comparison of conventional open cholecystectomy, laparoscopic cholecystectomy and minor incision cholecystectomy. *Zhonghua Waikao Zazhi* 1997; 35:660-662
- 57 O'Dwyer PJ, Murphy JJ, O'Higgins NJ. Cholecystectomy through a 5 cm sub-costal incision. *Br J Surg* 1990; 77:1189-1190
- 58 Nagakawa T. Biliary surgery via minilaparotomy-A limited procedure for biliary lithiasis. *HPB Surgery* 1993; 6:245-254

Edited by Zhu LH



• GASTRIC CANCER •

# Differential display of vincristine-resistance-related genes in gastric cancer? SGC7901 cell

Xin Wang, Mei Lan, Yong-Quan Shi, Ju Lu, Yue -Xia Zhong, Han-Ping Wu, Hui-Hong Zai, Jie Ding, Kai-Cun Wu, Bo-Rong Pan, Jian-Ping Jin, Dai-Ming Fan

Dai-Ming Fan-Xin Wang, Mei Lan, Yong-Quan Shi, Han-Ping Wu, Hui-Hong Zai, Jie Ding, Kai-Cun Wu, Dai-Ming Fan, Institute of Digestive disease, Xijing Hospital, Fourth Military Medical University, Xi'an 710032, Shaanxi Province, China

Ju Lu, Department of Electronic Engineering, Tsinghua University, Beijing 100084, China

Yue-Xia Zhong, Emergency Department, Tangdu Hospital, Fourth Military Medical University, Xi'an 710038, Shaanxi Province, China

Bo-Rong Pan, Oncology Center of Xijing Hospital, Fourth Military Medical University, Xi'an 710032, Shaanxi Province, China

Jian-Ping Jin, Department of Physiology and Biophysics, Case Western Reserve University School of Medicine, Cleveland, 44106-4970, Ohio, USA

Supported by the National Natural Science Foundation of China, No. 30030140, 39970901

Correspondence to: Prof. Dai-Ming Fan, Institute of Digestive disease, Xijing Hospital, Fourth Military Medical University, Xi'an 710033, Shaanxi Province, China. Daimfan@pub.xao

Telephone: +86-29-3375221 Fax: +86-29-2539041

Received 2001-04-21 Accepted 2001-08-15

## Abstract

**AIM:** To isolate and clone the vincristine-resistance-related genes in gastric cancer SGC7901 cell line and to clarify the multidrug-resistant molecular mechanism of gastric cancer cells.

**METHODS:** The modified differential-display polymerase chain reaction (DD-PCR) was used to examine the differences in the mRNA composition of Vincristine-resistant gastric cancer SGC 7901 cells (SGC7901/VCR), induced by vincristine sulfate versus SGC7901 cells. The differentially expressed cDNA fragments were confirmed by reverse Northern analysis, sequencing, BLAST analysis and Northern blot analysis.

**RESULTS:** DD-PCR identified that 54 cDNA fragments were preferentially expressed in SGC 7901/VCR cells. When these cDNA fragments were analyzed by reverse Northern blot, 20 were reproducibly expressed at a high level in SGC7901/VCR. Sequencing and BLAST analysis revealed that seven of the genes were known genes: ADP-ribosylation factor 4, Cytochrome oxidase subunit II, Ss-A/Ro ribonucleoprotein autoantigen 60kd subunit, ribosomal protein S13, galectin-8 gene, oligophrenin 1 mRNA, ribosomal protein L23 mRNA; thirteen of the genes were unknown genes. The length and abundance of the four unknown genes mRNA were further confirmed by Northern blot analysis.

**CONCLUSION:** The twenty differential known and unknown genes may be related to the vincristine-resistant mechanism in human gastric cancer SGC7901 cell line.

Wang X, Lan M, Shi YQ, Lu J, Zhong YX, Wu HP, Zai HH, Ding J, Wu KC, Pan BR, Jin JP, Fan DM. Differential display of vincristine-resistance-related genes in gastric cancer SGC7901 cell. *World J Gastroenterol* 2002;8(1):54-59

## INTRODUCTION

The primary factor affecting the chemotherapy for gastric cancer is the resistance of cancer cells to anti-tumor drugs. This phenomenon is called multidrug-resistance (MDR). Previous studies have shown that the mechanisms of MDR involved P-glycoprotein (P-gp), multidrug-resistance related protein (MRP 1-5), lung drug-resistance related protein (LRP), and recently discovered breast cancer drug-resistance related protein (BCRP), GSH/GST, PKC, Topo DNA plerosis<sup>[1-3]</sup>, genes related to apoptosis and changes of cellular environment (such as pH, hypoxia and temperature). However, over-expression of the genes encoding these proteins cannot completely account for MDR, nor can the treatment aiming at these mechanisms significantly revert MDR. Thus, it is most likely that MDR involves multi-genes. Little has been known about MDR of gastric carcinoma cells. Preliminary studies have shown specific features in MDR of gastric carcinoma cells<sup>[4-19]</sup>, which cannot be completely explained by any known mechanisms of gastric carcinoma MDR<sup>[20-32]</sup>. We therefore used mRNA differential display to investigate the differential expression of the genes in MDR gastric cells in order to elucidate the molecular mechanism of gastric cancer MDR and to discover the related genes so as to lay the foundation for the eventual solution of the problem.

## MATERIALS AND METHODS

### Induction of vincristine-resistant gastric cancer SGC 7901 cells

Gastric cancer SGC7901 cell (preserved by the Institute), grown in RPMI1640 medium containing 100g·L<sup>-1</sup> fetal bovine serum and cultured in incubator filled with 950mL·L<sup>-1</sup> O<sub>2</sub>, 50 mL·L<sup>-1</sup> CO<sub>2</sub> at 37°C. The procedure of SGC7901/VCR cell induction was as follows<sup>[33]</sup>: SGC7901 cells were harvested at the mid log-growth phase, and then cultured in the medium containing 0.2 mg·L<sup>-1</sup> vincristine; the medium exchanged every two or three days, and then the vincristine concentration was increased by 0.1 mg·L<sup>-1</sup> every other week, until it reached 0.8-1.0mg·L<sup>-1</sup>. SGC7901/VCR cells with stable phenotype were obtained after three months of continuous culture.

### DD-PCR<sup>[34-38]</sup>

Total RNA of gastric cancer SGC7901 and SGC7901/VCR cells was extracted and underwent RNA formaldehyde denatured agarose gel electrophoresis. The purity and RNA content of the samples were measured by OD260/280. Five µg of total RNA were taken from SGC7901 and SGC7901/VCR respectively, and combined with anchoring primers 5'-AAGCTTTTTTTTTTTTA-3', 5'-AAGCTTTTTTTTTTTTG-3', and 5'-AAGCTTTTTTTTTTTC to undergo RT-PCR. The procedure is as follows: to each 20µL reaction system, 5µg total RNA and 1.6µL anchoring primer were added, and the system was put at 70°C for 5 min and then into ice bathing. Buffer of 5×RT 4µL, 10mmol·L<sup>-1</sup> dNTP (each)2µL, RNase inhibitor 20U, M-MuLV retrotranscriptase (MBI) 2µL (40U) were added into the reaction system sequentially, and put in H<sub>2</sub>O to get a total volume of 20µL. The reaction went at 37°C for 1h, and for



10min at 70°C to terminate.

Eight random primers AP1-8 were employed in PCR. Three kinds of cDNA products of retrotranscription were each combined with the eight random primers to form 24 PCR reaction systems. There were 48 PCR reactions for two kinds of cells. In each 20μL PCR reaction system, there were 2μL RT product cDNA, 1μL anchoring primer (4μmol·L<sup>-1</sup>), 1μL random primer (4μL), 10×PCR buffer 2μL, MgCl<sub>2</sub> (25μmol·L<sup>-1</sup>) 1.6μL, dNTP (5μmol·L<sup>-1</sup>) 1.6μL, Taq plus I DNA polymerase (MBI) 0.15μL (0.4U), α-<sup>32</sup>P-dNTP 0.5μL (185kBq), and ion-free water. The conditions of PCR: 95°C 3min; 94°C 30s→40°C 2min→72°C 40s for 40 cycles; and then 70°C 10min for termination. PCR product was 95°C heat denatured for 3min, and underwent ice-bathing, and 60 g·L<sup>-1</sup> urea denatured polyacrylamide gel (sequencing gel) electrophoresis. The gel was preserved with membrane after electrophoresis and underwent X-ray film autoradiography at -70°C in black box for 48h.

### Cloning and restriction enzymatic cleavage identification of differential DNA bands

Differential bands were cut from the gel and the DNA was recovered and amplified with secondary PCR. The primers and conditions were identical to that of DD-PCR. The amplified product was separated with agarose gel electrophoresis, purified and retrieved, cloned into PUCm-T vector (Shanghai Shenggong Co.), and underwent restriction enzymatic cleavage identification.

### Reverse Northern analysis

The plasmids were extracted from the bacteria with positive clones of the 46 differential DNA bands; the quantities were determined through 10 g·L<sup>-1</sup> agarose gel electrophoresis. One μg plasmid was used to solve in 6(SSC buffer, boiled at 100°C for 10min to denature, put into ice-water, and pointed onto two NC membranes, each NC membrane having 46 points, and 1μg plasmid. The location of the points on the two membranes were identical. The NC membranes were dried at room temperature. The samples were alkaline-denatured on the membranes; and the membranes were heated at 80°C for 2h to fix the plasmid DNA and preserved at room temperature.

Preparation of radioactive cDNA probe: Total RNA was extracted from SGC7901 and SGC7901/VCR cells by the same method as in DD-PCR. Ten μg total RNA was taken; 2μL Olig dT<sub>18</sub> (0.5mg·L<sup>-1</sup>) were added, and put at 70°C for 5min, and ice-water bathed for 5min. Buffer of 5×RT 10μL, dNTP (10mmol·L<sup>-1</sup>/each) 2.5μL, RNase inhibitor 2.5μL (50U), α-<sup>32</sup>P-dATP 5μL (1850kBq), α-<sup>32</sup>P-dCTP 5μL (1850kBq), M-MuLV 4μL (80U), and water 50μL were added. The reaction was processed at 37°C for 1h, and 70°C for 5min to terminate. EDTA of 0.5 mol·L<sup>-1</sup> (pH 8.0) 2μL, 100 g·L<sup>-1</sup> SDS 2μL and 10 mol·L<sup>-1</sup> NaOH 1.8μL were put into the retrotranscription product, and incubated at 68°C for 30min. Ten μL 1mol·L<sup>-1</sup> Tris.Cl (pH 7.4) and 3μL 2 mol·L<sup>-1</sup> HCl were added to neutralize at room temperature. Pre-hybridization was made at 42°C for 6h, and different cDNA probes were added onto the two membranes to hybridize at 42°C for 20h. The membranes were washed, dried and underwent X-ray film autoradiography at -70°C for 72h.

### Sequencing and homologous analysis of cDNA clones

The cDNA fragments were sequenced and confirmed through reverse Northern blot to be highly expressed in SGC7901/VCR. BLAST program was used for homologous comparison in genetic library and FASTA was used to analyze the results.

### Northern Blot analysis

The total RNA of the two kinds of cells was extracted by the method

identical to that mentioned above. Sixteen μg total RNA of each sample was denatured; 10 g·L<sup>-1</sup> formaldehyde denature agarose gel electrophoresis (16μg RNA/lane) was performed; the mRNA was transferred onto the NC membranes by capillary blot, and heated at 80°C for 2h to fix the mRNA. Plasmids were extracted from positive clone bacteria; restriction endonuclease cleavage and electrophoresis were performed; the target cDNA fragments were recovered and purified; the cDNA probes were labeled by random primer method, and pre-hybridized on the NC membrane for 3h at 42°C. The probes were added and hybridized at 42°C for 20h. The membranes were washed, dried and undergone for X-ray film autoradiography at -70°C in black box for 48h.

## RESULTS

### DD-PCR separation of differential cDNA of SGC7901/VCR cell

The mRNA of SGC7901 and SGC7901/VCR cells was amplified by RT-PCR, each was divided into 24 groups, and each group was further separated into 150-200 cDNA fragments of diverted length (100-1500bp) after 60 g·L<sup>-1</sup> polyacrylamide gel electrophoresis. The comparison showed that the abundance of certain DNA bands in SGC7901/VCR cells was up-regulated, down-regulated, newly generated or lost. A total of 196 differential cDNA fragments were obtained (Figure 1).

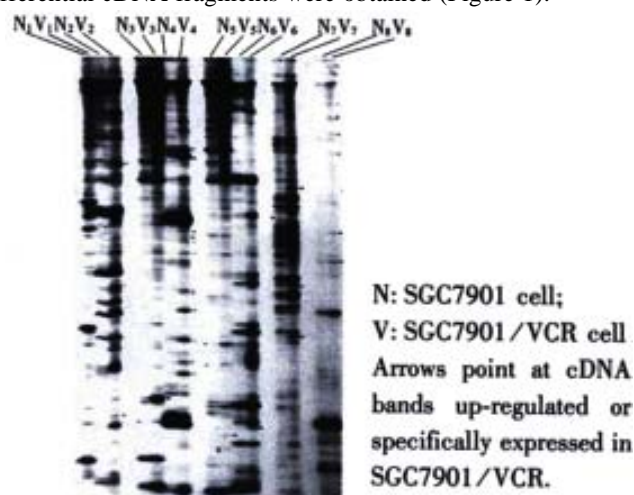


Figure 1 Differential display of mRNA of SGC7901/VCR.

### Cloning and restriction enzymatic cleavage identification of differential cDNA fragments in SGC7901/VCR

Fifty-four of the 196 differential cDNA fragments were specifically or significantly highly expressed in SGC7901/VCR cells. Restriction enzymatic cleavage identification showed that 46 cDNA fragments were successfully cloned (Figure 2).

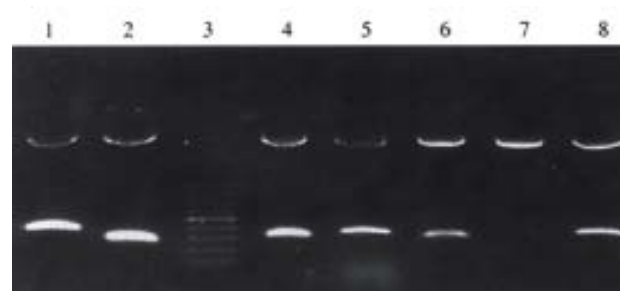
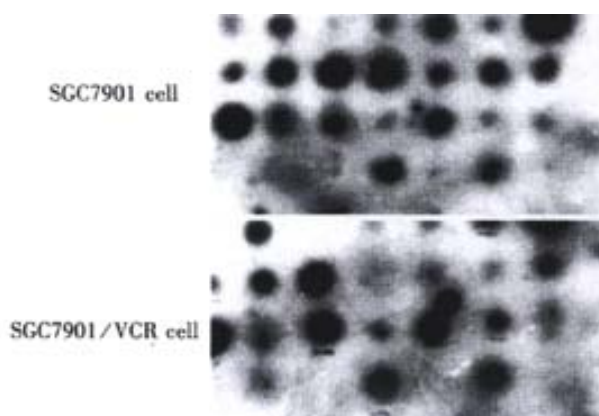


Figure 2 Restriction endonuclease cleavage identification of differential cDNA clones in SGC7901/VCR.

### Reverse northern analysis of differential cDNA fragments

In order to confirm the abundance changes of the differential genes and exclude false positive, reverse Northern blot was performed and the high expression of the 20 cDNA fragments in SGC7901/VCR was further validated (Figure 3).



**Figure 3** Reverse Northern analysis of genes significantly highly expressed in SGC7901/VCR.

### cDNA sequencing and homologous analysis

Sequencing and homologous analysis of the 20 highly expressed genes in SGC7901/VCR cells, confirmed by reverse Northern blot, showed that 7 of the 20 positive clones were highly homologous with known gene sequences (Table 1), and 13 were unknown sequences: GRP-2, GRP-8, GRP-12, GRP-15, GRP-18, GRP-19, GRP-24, GRP-28, GRP-31, GRP-36, GRP-37, GRP-38, GRP-41.

**Table 1** Up-regulated cDNA sequence in SGC7901/VCR homologous with known genes

| Serial number | Homologous genes                                        |
|---------------|---------------------------------------------------------|
| GRP-44(168bp) | ADP-ribosylation factor4 (ARF4) mRNA (1610bp)           |
| GRP-39(181bp) | Cytochrome oxidase subunit II mRNA                      |
| GRP-33(199bp) | Ss-A/Ro ribonucleoprotein autoantigen 60kd subunit mRNA |
| GRP-42(498bp) | Ribosomal protein S13 (RPS13) mRNA (530bp)              |
| GRP-6 (390bp) | Galaectin-8 (LGALS 8) gene, exons4, mRNA                |
| GRP-16(197bp) | Oligophrenin 1 (OPHN1) mRNA (7350bp)                    |
| GRP-1 (442bp) | Ribosomal protein L23 (RPL23) mRNA (490bp)              |

GRP:Gastric cancer drug-resistance related protein; serial numbers are numbering of positive cDNA clones.

#### GRP-2

CAGTGACTTTATTTAATGGGTTTTCAGACATACAGAAAGGGATTCTTTAGATGGGGCTGTGTCAGTCACTAGTCAACCATCTTCACTGTGGAGTCTAGTCACTATGATTTTGTGTTGTAGATCATGAGGATTCATTCAAATGTCTCCTCTTCCACTCCTTCGTAATAGGTTACATGATCTGAAAGTACATCCCTCTTATGACATTGTATTCAAACAGGTTGCTGCTACTTCTCTACTGTCATTAATCTTTTCATCATCTTCTTATTCCTCTTAGC—

#### GRP-8

GTTTGAGAGGATACTCATCTTTTGAATCCTGACCTTAGGTTCCGGCATGTAGACCAAGTGATGAGAAGTGAATACATGGAAGAGTTTAAAGTGTGACTTGA AAAATATGC—

#### GRP-12

GGAACCTGGATTCTTTAATAGTTGTTGAAGCCTCCAGGGGGCCAGGCGGATCACTTGAGGCCAGCCTGGCCAACATAGCGAAACCCTGCCTCTACTAAAA CCACAAAAATCAGCCGGGCATGGTGGCACACGCTTATAATCCAGCTACTTGGGACGCTGAGGTGGGATATAGCTTGAACCCGGGAAGGAGACTGCAGTCAG GGAAGCCTAGGGAAGCCTCAGACCAAGGATGATTGAATAACAAAGAAAAGGTGTAAGTAAAGATCTCCAACCTCTAGGGAGTACTAATTAGGAAAGTTAAGG GTAGAAAAAGATAAATTAAGGAAAATAC—

#### GRP-15

GAAAGACAGAAAAACAAGGGCAAAACAGGAGATGAGGAAATGTTAAAGGATAAAGGAAAGCCAGAGAGTGAGGGAGAGGCAAAAGAAGGAAAGTCAGAGA GGGAGGGAGAGTCAGAGATGGAGGGAGGATCAGAGAGAGAGGAAAACCAGAGATAGAGGGAAGCCAGAGAGTGAAGGAGAGCCAGGGAGTGAACAA GGGCTGCAGGAAAGCGCCAGCTGAGGATGATGTACCCAGGAAAGC—

#### GRP-18

GGAACCTGGATTCTTTAATAGTTGTTGAAGCCTCCAGGGGGCCAGGCGGATCACTTGAGGCCAGCCTGGCCAACATAGCGAAACCCTGCCTCTACTAAAA CCACAAAAATCAGCCGGGCATGGTGGCACACGCTTATAATCCAGCTACTTGGGACGCTGAGGTGGGATATAGCTTGAACCCGGGAAGGAGACTGCAGTCA GGAAGCCTAGGGAAGCCTCAGACCAAGGATGATTGAATAACAAAGAAAAGGTGTAAGTAAAGATCTCCAACCTCTAGGGAGTACTAATTAGGAAAGTTAA GGGTAGAAAAAGATAAATTAAGGAAAATACCGTTGAGAAGCTTAAAGACTGGAGATCTGGATCCCTCGAGTCTAGAGTCGACCTGCA—

#### GRP-19

AAAAGAAGAAAAATAAACACCAAAAAACAAGGAGAATAAAATGGCAGCAGACTTGATGCAAAAAATTAATAAAGGAAATTAAGAGAAATTACAGATGCACCTTTTATT GATTGCAAAAAAGCTTTAGAGCAACAGGTGCTGATTAGATAAAGCAGTTGCTTGATTACAAGAAAAACGGAAAACTAAAGCACTTAAAAAGCTGATAGA ATTGCTGCTGAAGGTTTAGTTTTTGCTACTAAAAATGAAACACATGGTGTATAGTAGAATTAAACTCAGAAACAGACTTTTGTG—

#### GRP-24

GGAACCTGGATTCTTTAATAGTTGTTGAAGCCTCCAGGGGGCCAGGCGGATCACTTGAGGCCAGCCTGGCCAACATAGCGAAACCCTGCCTCTACTAAAA CCACAAAAATCAGCCGGGCATGGTGGCACACGCTTATAATCCAGCTACTTGGGACGCTGAGGTGGGATATAGCTTGAACCCGGGAAGGAGACTGCAGTCAG GGAAGCCTAGGGAAGCCTCAGACCAAGGATGATTGAATAACAAAGAAAAGGTGTAAGTAAAGATCTCCAACCTCTAGGGAGTACTAATTAGGAAAG TTAAGGGTAGAAAAAGATAAATTAAGGAAAATAC—

#### GRP-28

CTGTGGCAATATTGTGTTCCAAATAAAGACTTGGTTTCCTCAGATCTACGCCATTTTCAATCTTCCCTAACAAATACGTGCATTTTAAACAAAGCTGGTATT TGAATACTTACCTGAGGTAACATGCCTTGGTATAGTTTCTTCTAAAGTTCACTGCAGGCTGGGTGCTGTGGCTCGTGCCTGTAATCCTAGCACTTTGGGAGGC CGAGTCGGGAGAATTGCTTGAGCCCGGGAGTTCAAGACCAGCCTGCGGGACAAAATGAGACCCCATCCATA—

#### GRP-31

CTGTGATTTTTTTAAGGTTTAATAATTGAAGGAAGTCAACAGTCATTTATCCGAATTAAACTTGAGGTTAATAAGTTTCAATTCGTAATTTTCCAAACC AACCAATGTAAAAACCCAGATTTTCTGAATTGAGTCATGTAAGGATTTTGTAAAGTG—

#### GRP-36

ACGGCAACTGATAGCTTTAAGGAGGAAGAGAGAATAGAGAGAGTGTGTGTTGGGGGGTGTGTGTGCGTTTAGTCCTATAAAATGTTTACTATTGATTTTT  
TCTGTTTACTACCTCTTTCTCAAATAGGTTGGTTGTGAAGATGGATCTGTGAAACTATTTCAAATTACCCAGACAAAATTCAGTTTGAAAGAAATTTTGATC  
GGCAGAAAAGTAAGCGTCATTTTTCATGGG-

GRP-37

TCATTTTACAAAAGGAACATTAATATTAATATAAGAAAAGAATTTCTTATACGTACCAATATGGTATCACATTTTCAGCTCAACATCAGACATGCAATAAATG  
TATACAAGTACTTCAATTTGCATTAGAACATTTTAAAGAAATACACAATTATTTCTAAATTATTTTATATATACTAAGGCGGTAAAAGCTTAAGACTGG  
AGATCTGGATCCCTCGAGTCTAGAGTCGACCTGCAGGCATGCAAGCTTGGCGTAATCATGGTCATAGCTGTTTCTGTGTGAAATTGTTATCCGCTCACAAT  
TCCACACAACATACGAGCCGGAAGCATA—

GRP-38

TAGAACCCTGAGTGGGAACAGAAATCTCAAAATAAATAAATGGAAATGAGATCATGGCTGTAAATGGTAATTATATTATGTCAAAAACACCTTTAGAGTTACT  
TTAGAGCTCCCTAAAAATAACAATTAAGTAGCTGTAGAGGATATTTCTCTCTCTCTTACATTTATGTGGTGTTCAGGTGGACAAAGTACTTTTG  
---

GRP-41

TCAGAAATGAGAATGCACTGGAGGCTGGTGATTACTTCTGGACCCCTCTTCCCATCCATCGTTTCGGCTAAAAGTCATCATAAATTGGGAGTCCTTCCCTT  
TACTGGTCTAGAAGTTCCCTCAGGAAGCAGCGTCACCTTCTCCCTGCTCTTCACTGAGGAGGGAGGAAGAGGAGCAAGAGAAGACTTTCCGGTTTCCAA  
ATGGCAGATTTGGTTTCGGGCATGTGAGGAGCCACATA—

### Northern blot analysis of unknown differential genes in SGC7901/VCR cell

The cDNA fragments of four genes randomly selected from the 13 unknown genes mentioned above were used to produce probes for Northern blot, and the result was in agreement with that of DD-PCR and reverse Northern analysis. All the four genes were specifically (GRP-2) or highly expressed in SGC7901/VCR.

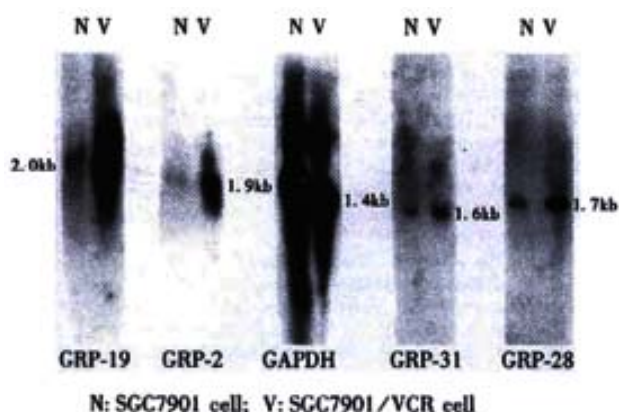


**Figure 4** Northern analysis of unknown genes up-regulated in SGC7901/VCR cells.

### DISCUSSION

MDR is a major obstacle to tumor chemotherapy. In recent years, progress has been made concerning the mechanism of MDR at the molecular level, which includes the separation and identification of some proteins encoded by MDR-related genes, including P-gp, MRP, LRP and BCRP. All of them are membrane proteins, which engender MDR by reducing the accumulation of chemotherapeutic drugs in the target cells or redistributing the drugs, which consequently reduce the drug concentration in the target organelles. Their expressions differ in different tumors. Certain anti-MDR drugs with some specific MDR mechanisms have been applied clinically. The first generation anti-MDR drugs require that the drug concentration to be high enough to revert MDR, so their side-effects often exceed the tolerance of patients. The second and third generation drugs (PSC833, GF 120918, VX-710, LY335979 etc) cannot revert MDR effectively, either. This phenomenon suggests that tumor cells may tolerate anti-tumor drugs through various mechanisms. The changes at the genetic level are usually more sensitive and prompt than those at the protein level, so screening MDR-related genes at the genetic level has great advantages. One method for screening differential expression genes is

mRNA differential display, which contributes substantially in many researches. We employed this technique to screen 20 gene fragments that were highly expressed in gastric cancer MDR cells. This result indicates that MDR involves multi-genes, each playing its own role in the process. Among these genes, seven were separated and identified as known genes.

### Human mitochondrial cytochrome C oxidase subunit II

Human mitochondrial cytochrome C oxidase consists of three subunits. It has essential functions in mitochondrial respiration. Higuchi<sup>[39]</sup> obtained two highly expressed genes in human head and neck squamous epithelium cancer cells that were cisplatin-resistant, using differential display, and one of the two encodes human mitochondrial cytochrome C oxidase subunit II. It is regarded as a sign of cisplatin-resistance. Denis-Gay *et al.*<sup>[40]</sup> discovered that the concentration and activity of mitochondrial cytochrome C oxidase did not change in K562 leukemia cells that were adriamycin-resistant, while the concentrations of most other cytochrome oxidases declined significantly. A noteworthy phenomenon recently reported is that methamphetamine or 3,4-methylenedioxymethamphetamine (MDMA) could suppress the activity of mitochondrial cytochrome C oxidase, which implied that they could probably revert MDR<sup>[41]</sup>.

### Galectin-8 cDNA is closely related to PCTA-1<sup>[42]</sup>

If transferred into tumor 11299 cells, galectin-8 could suppress the formation of the clones by 75%. Galectin-8 is a binding protein of integrin, and has effects against tumor cell adhesion after binding. It can also induce apoptosis, too<sup>[43-45]</sup>.

### Human ribosomal protein L23(RPL23)

It is homologous with *E. coli* ribosomal protein L11. As the drug-resistant mutant strain of *E. coli* lacks L11, it is postulated that L23 may be related to drug-resistance<sup>[46]</sup>.

### Ss-A/Ro ribonucleoprotein autoantigen subunit

Its mRNA (1890 bp) has an open reading frame (ORF), encoding a polypeptide of 417 amino acid residues whose apparent molecular mass is 60ku. It is the antigen of several autoimmune diseases. In ultraviolet radiation resistant bacteria, an RNA-binding protein was recently discovered to mediate the resistance and to be highly homologous with Ss-A/Ro 60ku protein. Therefore, Ss-A/Ro ribonucleoprotein autoantigen 60ku subunit presumably has the similar function in the recovery of cells after UV radiation in higher eukaryotes<sup>[47]</sup>.

### Oligophrenin-1 (OPHN1)

Its gene covers 500 kb genomic DNA and is composed of 25 exons. It is highly expressed primarily in fetal brain, encoding a protein whose

molecular mass is 91ku. It has a typical Rho GTPase activation protein (rhoGAP) domain, the activation of which induces GAP to inactivate Rho and Ras. Therefore, the inactivation of rhoGAP can activate its target molecules and subsequently influence cell differentiation and migration. Its mutation can result in non-specific X-chromosome linked mental retardation, as its loss of function probably interferes with or affects cell signal transduction pathways, impeding cell migration and axonal growth in the development of cells in the neural system<sup>[48,49]</sup>.

### ADP-ribosylation factor 4 (ARF4)

It is a member of the G-protein family, with a molecular mass of about 20ku. It was first identified to activate cholera toxin ribosyltransferase, and was recently discovered to effect essentially in vesicular transport in cell, and to be an activator of phospholipase D<sup>[50]</sup>. Human ribosomal protein S13 (RPS13) is a translation initiation factor and is related to cell growth and differentiation<sup>[51]</sup>. Some of these seven genes are apparently related to MDR, and the relationship of others to MDR remains to be further studied.

Two cDNAs (GRP-24, GRP-41) which are highly expressed in SGC7901/VCR cells, are 100% homologous with human genomic clone fragments. The two genomic clones contain the genes of dynamin, neuroendocrine secretory protein 55 (NESP55), and GANS1. Dynamin is a membrane protein with GTPase activity; its alternative splicing produces six subtypes engaging in endocytosis, exocytosis, pinocytotic vesicle cycle, intracellular and Golgi complex vesicular transport, and cell membrane transport. NESP55 and GANS1 are both G-proteins, involved in cell signal transduction. Further confirmation of homologous genes of the two cDNA fragments is necessary.

We randomly selected 4 cDNA fragments (GRP-2, GRP-19, GRP-28, GRP-31) from the rest 11 unknown genes to do Northern analysis. The result was in agreement with that of reverse Northern analysis; and gave the lengths of the four genes and also confirmed the reliability of reverse Northern blot. The result is conducive to the cloning of the entire length of the genes.

To sum up, we managed to separate and clone 20 significantly highly or specifically expressed genes from drug-resistant gastric cancer SGC7901/VCR cells using DD-PCR. Some known genes are related to drug-resistance and others may enhance drug-resistance. It is necessary to conduct further research on the unknown genes.

### REFERENCES

- Fan K, Fan D, Cheng LF, Li C. Expression of multidrug resistance-related markers in gastric cancer. *Anticancer Res* 2000;20:4809-4814
- Jonker JW, Smit JW, Brinkhuis RF, Maliepaard M, Beijnen JH, Schellens JH, Schinkel AH. Role of breast cancer resistance protein in the bioavailability and fetal penetration of topotecan. *J Natl Cancer Inst* 2000; 92: 1651-1656
- Tan B, Pinwnica WD, Ratner L. Multidrug resistance transporters and modulation. *Curr Opin Oncol* 2000;12: 450-458
- Liu ZM, Shou NH, Jiang XH. Expression of lung resistance protein in patients with gastric carcinoma and its clinical significance. *World J Gastroenterol* 2000; 6:433-434
- Zhang LJ, Chen KN, Xu GW, Xing HP, Shi XT. Congenital expression of Mdr-1 gene in tissues of carcinoma and its relation with pathomorphology and prognosis. *World J Gastroenterol* 1999;5:53-56
- Fan DM, Xiao B, Shi YQ, Ming-Feng, Qiao TD, Chen BJ, Chen Z. A novel cDNA fragment associated with gastric cancer drug resistance was screened out from a library by monoclonal antibody MGr1. *World J Gastroenterol* 1998; 4:110-111
- Liu Y, Lu MZ, Li QM, Wang YL. Expression of p53 C-myc and P-gp in gastric cancer. *Xin Xiaohuabingxue Zazhi* 1997; 5:585-586
- You HN, Chen Q, Jiang HP, Li DG, Zhang WZ. The influence of P-glycoprotein expression on the prognosis of gastric carcinoma. *Xin Xiaohuabingxue Zazhi* 1997; 5(Suppl 6):23-24
- Zhou WJ, Pan FQ. Significance of P-gp and P53 in patients with gastric cancer. *Huaren Xiaohua Zazhi* 1998; 6:318-319
- Xiao B, Shi YQ, Zhao YQ, You H, Liu XL, Fan DM. Expression of Fas gene in gastric cancer cells transduced with Fas gene. *Huaren Xiaohua Zazhi* 1998;6:400-403
- Cheng SD, Wu YL, Zhang YP, Qiao MM, Guo QS. Abnormal drug accumulation in multidrug resistant gastric carcinoma cells. *Shijie Huaren Xiaohua Zazhi* 2001; 9:131-134
- Lage H, Jordan A, Scholz R, Dietel M. Thermosensitivity of multidrug-resistant human gastric and pancreatic carcinoma cells. *Int J Hyperthermia* 2000;16:291-303
- Yin L, Chen K, Li D. Inherent mdr-1 gene expression in fresh tumor tissue specimens from several high-incidence malignancies. *Zhonghua Zhongliu Zazhi* 1997;19:420-422
- Gurel S, Yerci O, Filiz G, Dolar E, Yilmazlar T, Nak SG, Gulten M, Zorluoglu A, Memik F. High expression of multidrug resistance-1 (MDR-1) and its relationship with multiple prognostic factors in gastric carcinomas in patients in Turkey. *J Int Med Res* 1999;27:79-84
- Anzai H, Kitadai Y, Bucana CD, Sanchez R, Omoto R, Fidler IJ. Expression of metastasis-related genes in surgical specimens of human gastric cancer can predict disease recurrence. *Eur J Cancer* 1998; 34:558-565
- Motoo Y, Su SB, Nakatani MT, Sawabu N. Expression of multidrug resistance gene (mdr-1) mRNA in gastric and colorectal cancers. *Anticancer Res* 1998;18:1903-1906
- Yeh KH, Chen CL, Shun CT, Lin JT, Lee WJ, Lee PH, Chen YC, Cheng AL. Relatively low expression of multidrug resistance-1 (MDR-1) and its possible clinical implication in gastric cancers. *J Clin Gastroenterol* 1998;26:274-278
- Son YS, Suh JM, Ahn SH, Kim JC, Yi JY, Hur KC, Hong WS, Muller MT, Chung IK. Reduced activity of topoisomerase II in an Adriamycin-resistant human stomach adenocarcinoma cell line. *Cancer Chemother Pharmacol* 1998;41:353-360
- Endo K, Maehara Y, Kusumoto T, Ichiyoshi Y, Kuwano M, Sugimachi K. Expression of multidrug-resistance-associated protein (MRP) and chemosensitivity in human gastric cancer. *Int J Cancer* 1996;68:372-377
- Liu XL, Xiao B, Yu ZC, Guo JC, Zhao QC, Xu L, Shi YQ, Fan DM. Downregulation of Hsp90 could change cell cycle distribution and increase drug sensitivity of tumor cells. *World J Gastroenterol* 1999; 5:199-208
- Darimont BD. The Hsp90 chaperone complex-A potential target for cancer therapy? *World J Gastroenterol* 1999; 5:195-198
- Xiao B, Shi YQ, Zhao YQ, You H, Wang ZY, Liu XL, Yin F, Qiao TD, Fan DM. Transduction of Fas gene or Bcl-2 antisense RNA sensitizes cultured drug resistant gastric cancer cells to chemotherapeutic drugs. *World J Gastroenterol* 1998; 4:421-425
- Yin F, Shi YQ, Zhao WP, Xiao B, Miao JY, Fan DM. Suppression of P-gp induced multidrug resistance in a drug resistant gastric cancer cell line by overexpression of Fas. *World J Gastroenterol* 2000;6:664-670
- Shi YQ, Xiao B, Miao JY, Li MF, Qiao TD, Chen BJ, Chen Z, Han JL, Zhou SJ, Fan DM. A novel cDNA fragment associated with gastric cancer drug resistance screened from a library by mAb MGr1. *Huaren Xiaohua Zazhi* 1998; 6:656-659
- Xiao B, Shi YQ, Zhao YQ, You H, Wang ZY, Liu XL, Yin F, Qiao TD, Fan DM. Transduction of fas gene or bcl-2 antisense RNA sensitizes cultured drug resistant gastric cancer cells to chemotherapeutic drugs. *Huaren Xiaohua Zazhi* 1998;6:675-679
- Liu B, Staren E, Iwamura T, Appert H, Howard J. Effects of Taxotere on invasive potential and multidrug resistance phenotype in pancreatic carcinoma cell line SUIT-2. *World J Gastroenterol* 2001; 7:143-141
- Wang X, Shi YQ, Zhao YQ, Wang JC, Yao LB, Zhang ZY, Lan M, Jin JP, Fan DM. Differential display of Vincristine-resistance-related proteins in gastric cancer SGC7901 cell line. *Zhonghua Zhongliu Zazhi* 2001;23:281-284
- Lin HL, Liu TY, Wu CW, Chi CW. Berberine modulates expression of mdr1 gene product and the responses of digestive track cancer cells to Paclitaxel. *Br J Cancer* 1999;81:416-226
- Zheng GQ, Han FS, Liu XY, Xu GW. Drug resistance mechanism of doxorubicin-resistant human gastric cancer cells BGC-823/DOX. *Zhonghua Waikexue Zazhi* 1997;35:325-328
- Varga A, Sokolowska-Kohler W, Presber W, Von Baehr V, Von Baehr R, Lucius R, Volk D, Nacsas J, Hever A. Toxoplasma infection and cell free extract of the parasites are able to reverse multidrug resistance of mouse lymphoma and human gastric cancer cells *in vitro*. *Anticancer Res* 1999;19:1317-1324
- Nakamura T, Oka M, Aizawa K, Soda H, Fukuda M, Terashi K, Ikeda K, Mizuta Y, Noguchi Y, Kimura Y, Tsuruo T, Kohno S. Direct interaction between a quinoline derivative, MS-209, and multidrug resistance protein (MRP) in human gastric cancer cells. *Biochem Biophys Res Commun* 1999; 255:618-624
- Kellner U, Hutchinson L, Seidel A, Lage H, Danks MK, Dietel M, Kaufmann SH. Decreased drug accumulation in a mitoxantrone-resistant gastric carcinoma cell line in the absence of P-glycoprotein. *Int J Cancer* 1997;71:817-824

- 33 Nitta A, Chung YS, Nakata B, Yashiro M, Onoda N, Maeda K, Sawada T, Sowa M Establishment of a cisplatin-resistant gastric carcinoma cell line OCUM-2M/DDP. *Cancer Chemother Pharmacol* 1997;40:94-97
- 34 Wang X, Huang YX, Wen QS, Wang QL. Silver-staining mRNA differential display method and cloning of tumor related genes in HepG2 cell line. *Di-si Junyi Daxue Xuebao* 2001;22:843-845
- 35 Wang L, Lu W, Chen YG, Zhou XM, Gu JR. Comparison of gene expression between normal colon mucosa and colon carcinoma by means of messenger RNA differential display. *World J Gastroenterol* 1999; 5:533-534
- 36 Ji F, Peng QB, Zhan JB, Li YM. Study of differential polymerase chain reaction of C-erbB 2 oncogene amplification in gastric cancer. *World J Gastroenterol* 1999; 5:152-155
- 37 You H, Xiao B, Cui DX, Shi YQ, Fan DM. Two novel gastric cancer associated genes identified by differential display. *World J Gastroenterol* 1998;4:334-336
- 38 Cui DX, Yan XJ, Su CZ. Differentially expressed genes were isolated in gastric carcinoma by optimised differential display PCR. *Shijie Huaren Xiaohua Zazhi* 1999; 7:139-144
- 39 Higuchi E. Up-regulation of human chorionic gonadotropin alpha subunit gene and human mitochondrial cytochrome oxidase subunit II gene in cis-Diamminedichloroplatinum(II) -resistant human head and neck squamous carcinoma cells. *Hokkaido Igaku Zasshi* 1999;74:231-238
- 40 Denis-Gay M, Petit JM, Mazat JP, Ratinaud MH. Modifications of oxido-reductase activities in adriamycin-resistant leukaemia K562 cells. *Biochem Pharmacol* 1998;56: 451-457
- 41 Burrows KB, Gudelsky G, Yamamoto BK. Rapid and transient inhibition of mitochondrial function following methamphetamine or 3,4-methylenedioxymethamphetamine administration. *Eur J Pharmacol* 2000;398:11-18
- 42 Gopalkrishnan RV, Roberts T, Tuli S, Kang D, Christiansen KA, Fisher PB. Molecular characterization of prostate carcinoma tumor antigen-1, PCTA-1, a human galectin-8 related gene. *Oncogene* 2000;19:4405-4416
- 43 Hadari YR, Arbel-Goren R, Levy Y, Amsterdam A, Alon R, Zaick Y. Galectin-8 binding to integrins inhibits cell adhesion and induces apoptosis. *J Cell Sci* 2000;113:2385-2397
- 44 Bassen R, Brichory F, Caulet-Maugendre S, Bidon N, Delaval P, Desrues B, Dazord L. Expression of Po66-CBP, a type-8 galectin, in different healthy, tumoral and peritumoral tissues. *Anticancer Res* 1999 ;19:5429-5433
- 45 Camby I, Belot N, Rorive S, Lefranc F, Maurage CA, Lahm H, Kaltner H, Hadari Y, Ruchoux MM, Brotchi J, Zick Y, Salmon I, Gabius HJ, Kiss R. Galectins are differentially expressed in supratentorial pilocytic astrocytomas, astrocytomas, anaplastic astrocytomas and glioblastomas, and significantly modulate tumor astrocyte migration. *Brain Pathol* 2001 ;11:12-26
- 46 Mcelwain KB, Boynton JE, Gillham NW. A nuclear mutation conferring thiostrepton resistance in chlamydomonas reinhardtii affects a chloroplast ribosomal protein related to Escherichia coli ribosomal protein L11. *Mol Gen Genet* 1993; 241: 564-572
- 47 Chen X, Quinn AM, Wolin SL. Ro ribonucleoproteins contribute to the resistance of Deinococcus radiodurans to ultraviolet irradiation. *Genes Dev* 2000;14:777-782
- 48 Billuart P, Bienvenu T, Ronce N, des Portes V, Vinet MC, Zemni R, Roest Crollius H, Carrie A, Fauchereau F, Cherry M, Briault S, Hamel B, Fryns JP, Beldjord C, Kahn A, Moraine C, Chelly J. Oligophernin-1 encodes a rho GAP protein involved in X-linked mental retardation. *Nature* 1998;392: 923-926
- 49 Ljubimova JY, Khazenzon NM, Chen Z, Neyman YI, Turner L, Riedinger MS, Black KL. Gene expression abnormalities in human glial tumors identified by gene array. *Int J Oncol* 2001;18:287-295
- 50 Lebeda RA, Haun RS. Cloning and characterization of the human ADP-ribosylation factor 4 gene. *Gene* 1999;237: 209-214
- 51 Ito T, Kim GT, Shinozaki K. Disruption of an Arabidopsis cytoplasmic ribosomal protein S13-homologous gene by transposon-mediated mutagenesis causes aberrant growth and development. *Plant J* 2000;22:257-264



• GASTRIC CANCER •

# Overexpression of cyclin E in Mongolian gerbil with *Helicobacter pylori*-induced gastric precancerosis

Yong-Li Yao, Bo Xu, Yu-Gang Song, Wan-Dai Zhang

Yong-Li Yao, Yu-Gang Song, Wan-Dai Zhang, Institute of Gastrointestinal Diseases, Nanfang Hospital, First Military Medical University, Guangzhou 510515, Guangdong Province, China

Bo Xu, Department of Orthopedics, Nanfang Hospital, First Military Medical University, Guangzhou 510515, Guangdong Province, China

Correspondence to: Yong-Li Yao, Institute of Gastrointestinal Diseases, Nanfang Hospital, First Military Medical University, Guangzhou 510515, Guangdong Province, China. xbyyl@fimmu.edu.cn

Telephone: +86-20-85141544

Received 2001-03-12 Accepted 2001-08-15

## Abstract

**AIM:** To explore dysregulation of cyclin E in malignancies, and to further investigate the role of cyclin E in *Helicobacter pylori* (*H. pylori*)-induced gastric precancerosis.

**METHODS:** Four-week-old specific pathogen-free male Mongolian gerbils were employed in the study. 0.5 mL  $1 \times 10^8$  cfu  $\cdot$  L<sup>-1</sup> suspension of *H. pylori* NTCC11637 in Brucella broth was inoculated orally into each of 20 Mongolian gerbils, and a further 20 gerbils were inoculated with Brucella broth as controls. 10 of the infected gerbils and 10 of the non-infected control gerbils were sacrificed at 25, 45 wk after infection. The expression of cyclin E was analyzed by RT-PCR and immunohistochemical studies with monoclonal antibody to cyclin E in Mongolian gerbil of *H. pylori*-induced gastric precancerosis.

**RESULTS:** *H. pylori* was constantly detected in all infected animals throughout the study. At 25 wk after infection of *H. pylori*, ulcers were observed in the antral and body of stomach ( $n=6$ ). Histological examination showed that all animals developed severe inflammation and multifocal lymphoid follicles appeared in the lamina propria and submucosa of gastric antrum. At 45 wk after infection of *H. pylori*, severe atrophic gastritis ( $n=10$ ), intestinal metaplasia ( $n=8$ ) and dysplasia ( $n=6$ ) could be observed. Cyclin E mRNA levels were significantly more at 25 wk after infection of *H. pylori* ( $1.27 \pm 0.26$ ), and at 45 wk after infection of *H. pylori* ( $1.82 \pm 0.39$ ) than control-animals ( $0.59 \pm 0.20$ ,  $P < 0.01$ ); cyclin E mRNA levels were evaluated by 2.2-fold at 25 wk ( $P < 0.01$ ) and 3.1-fold at 45 wk ( $P < 0.01$ ) precancerosis induced by *H. pylori*, when compared with control gastric epithelium of Mongolian gerbil. Immunohistochemical staining revealed exclusive nuclear staining of cyclin E. Furthermore, there was a sequential increase in cyclin E positive cells from normal epithelium to precancerosis.

**CONCLUSION:** Overexpression of cyclin E occurs relatively early in gastric tumorigenesis in this model.

Yao YL, Xu B, Song YG, Zhang WD. Overexpression of cyclin E in Mongolian gerbil with *Helicobacter pylori*-induced gastric precancerosis. World J Gastroenterol 2002;8(1):60-63

## INTRODUCTION

Gastric cancer is a major health problem<sup>[1-3]</sup> and remains the second

most common cancer in the world<sup>[4-6]</sup>. Although epidemiological studies have indicated that *H. pylori* infection plays a crucial role in gastric carcinogenesis in humans<sup>[7-22]</sup>, there is no direct proof that *H. pylori* is actually associated with gastric carcinogenesis<sup>[23-26]</sup>. The purpose of this study was to elucidate the relationship between *H. pylori* infection and gastric carcinogenesis by using an animal model of long-term *H. pylori* infection, and explore the role played by cyclin E in gastric tumorigenesis<sup>[27-29]</sup>.

Cyclins are positive regulators of cell cycle progression. They function by forming a complex with and activating a class of protein kinases which are essential for cell cycle transitions. As the major regulatory events leading to cell proliferation occur in the G1 phase of the cell cycle, altered expression of cyclins involved in the G1 phase may be an important step in oncogenesis<sup>[30-33]</sup>. Among G<sub>1</sub> cyclins, an accumulating body of evidence suggests that over expression and rearrangement of cyclin E is associated with malignancy. Over expression of cyclin E has also been found in mouse mammary tumors and is associated with tumor development; altered expression of cyclin E can accelerate occurrence and early progression of colorectal cancer, and plays an important role in occurrence of breast cancer<sup>[34-37]</sup>. But cyclin D<sub>1</sub>, over expression in esophageal cancer and breast cancer, has no over expression in gastric cancer, which suggests expression of cyclins has specificity of organs. To gain a further understanding of the role played by cyclin E in gastric tumorigenesis, the study investigates the role of cyclin E in *H. pylori*-induced gastric precancerosis<sup>[38-39]</sup>.

## MATERIALS AND METHODS

### Animals and preparation

Four-week-old specific pathogen-free male Mongolian gerbils, weighing (20 $\pm$ 5)g, were employed in the study. They were housed in individual metabolic cages in a temperature conditioned room (23 $\pm$ 2) $^{\circ}$ C with a 12 h light-dark cycle, allowed access to standard rat chow (provided by Experimental Animal Center, First Military Medical University) and water ad libitum, and acclimatized to the surrounding for 7 d prior to the experiments. *H. pylori* (NTCC11637) was obtained from American Type Culture Collection and cultured on Brucella agar plates containing 70 mL  $\cdot$  L<sup>-1</sup> goat blood in a microaerobic condition (volume fraction; N<sub>2</sub>:85%, O<sub>2</sub>:5%, CO<sub>2</sub>:10%, in aerobic globe box) at 37 $^{\circ}$ C for 3 d. The strain was identified by morphology, Gram's stain, urease production and so on.

### Experimental protocol

Suspension 0.5 mL  $1 \times 10^8$  cfu  $\cdot$  L<sup>-1</sup> of *H. pylori* NTCC11637 in Brucella broth was inoculated orally into each of 20 Mongolian gerbils which had been fasted overnight, for 14 d continuously. A further 20 gerbils were inoculated with Brucella broth as controls. 10 of the infected gerbils and 10 of the non-infected control gerbils were sacrificed at 25, 45 wk after infection. The stomach of each animal was removed and opened for macroscopic observation. For half of each gastric antrum mucosa was dissected for RNA isolation. The remainders of the stomach samples were used for histological examination, which were fixed with neutral-buffered 100 mL  $\cdot$  L<sup>-1</sup>

formalin and processed by standard methods that embedded in paraffin, sectioned and stained with haematoxylin for analyzing histological changes, Giemsa stain for detecting for *H. pylori* and Alcian blue (AB)/PAS stain for examining intestinal metaplasia.

### RNA isolation and RT-PCR analysis

Using Tripure isolation reagent (Boehringer Mannheim, Germany), total cellular RNA was isolated from previously frozen tissues according to the manufacturer's instruction. All RNA samples were analyzed for integrity of 18s and 28s rRNA by ethidium bromide staining of 0.5µg RNA resolved by electrophoresis on 12g·L<sup>-1</sup> agarose-formaldehyde gels. RT-PCR analysis was performed as follows. RNA was incubated at 60°C for 10 min and chilled to 4°C immediately before being reverse transcribed. Reverse transcription of 1µg total RNA using antisense primers was performed in a volume of 20µL for 40 min at 50°C, containing 200 U MMLV reverse transcriptase, 1×buffer RT, 1 MU·L<sup>-1</sup> Rnasin, 0.5mmol·L<sup>-1</sup> dATP, dGTP, dCTP and dTTP respectively and 0.2µmol·L<sup>-1</sup> antisense primers including cyclin E and β-actin respectively. The samples were heated to 99°C for 5 min to terminate the reverse transcription reaction. By using a Perkin-Elmer DNA Thermocycler 4800 (Perkin-Elmer, Norwalk, CT), 5µL cDNA mixture obtained from the reverse transcription reaction was then amplified for cyclin E and β-actin. β-actin was used as the housekeeping gene and amplified with cyclin E as contrast. The amplification reaction mixture consisted of 10×buffer 5µL, 0.2 mmol·L<sup>-1</sup> dATP, dGTP, dCTP and dTTP respectively, 2.5 U Taq DNA polymerase, and 0.2µmol·L<sup>-1</sup> each of sense and antisense primers in a final volume of 50µL. The reaction mixture was first heated at 94°C for 2 min and amplification was carried out for 29 cycles at 94°C for 0.5 min, 53°C for 1 min, 70°C for 1.5 min, followed by an incubation for 7 min at 70°C. The number of amplification cycles was previously determined to keep amplification in the linear range to avoid the "plateau effect" associated with increased numbers of PCR cycles. The PCR primers used were: cyclin E, sense 5'-TAT GGC GAC ACA AGA AAA TG-3' and antisense 5'-GCA AGA GAA GAC AGA CAA CG-3'; β-actin, sense 5'-CCA AGG CCA ACC GCG AGA AGA TGA C-3' and antisense 5'-AGG GTA CAT GGT GGT GCC GCC AGA C-3'. The length of PCR products for cyclin E and β-actin was 770 bp and 587 bp. PCR products were run on a 15g·L<sup>-1</sup> agarose gel in 0.5×TBE buffer and then analyzed by gel image analysis system. The level of cyclin E was reflected with the ratio of cyclin E/β-actin.

### Immunohistochemical staining

Four micrometers paraffin-embedded tissue sections were deparaffinized and rehydrated. Endogenous peroxidase activity was ablated with 10 mL·L<sup>-1</sup> hydrogenperoxide in methanol. The immunostaining for cyclin E was conducted using the StreptAvidin-Biotin-enzyme Complex kit (Boster, Wuhan). Immunostaining by replacing primary antibody with PBS was also conducted as a negative control. The staining was evaluated semiquantitatively on the basis of the percentage of positive cells, and classified as follows<sup>[40]</sup>: diffusely positive (+++) when positive cells accounted for more than 70% of the total cells, partially positive (++) when positive cells were 35%-70%, partially positive (+) when positive cells accounted for 5%-35%, and negative (-) when positive cells accounted for less than 5%.

### Statistical Analysis

Experimental results were analyzed with Chi-square Tests and K Related Samples Test by SPSS software. Statistical significance was determined at  $P < 0.05$ .

## RESULTS

### Histopathological findings

*H. pylori* was detected in gastric antrum and gastric body of all infected animals throughout the study, and more in gastric antrum than gastric body. By the 25th wk after infection of *H. pylori*, ulcers were observed in the antral and body of stomach ( $n=6$ ). Histological examination showed that all animals developed severe inflammation in the area close to ulcers; multifocal lymphoid follicles appeared in the lamina propria and submucosa; and there were mild atrophic gastritis in all infected animals. By the 45th wk after infection of *H. pylori*, severe atrophic gastritis ( $n=10$ ), intestinal metaplasia ( $n=8$ ) and dysplasia ( $n=6$ ) could be observed. Those metaplastic glands appeared more atypical than the surrounding nonmetaplastic and hyperplastic glands. Severe atrophic gastritis, intestinal metaplasia and dysplasia were gastric precancerosis. In the uninfected animals, there were no significant changes throughout the study.

### RT-PCR analysis of cyclin E mRNA expression

There were cyclin E mRNA expression in gastric antrum mucosa of control-animals. cyclin E mRNA levels were significantly more at 25 wk after infection of *H. pylori* ( $1.27 \pm 0.26$ ), and at 45 wk after infection of *H. pylori* ( $1.82 \pm 0.39$ ) than control-animals ( $0.59 \pm 0.20$ ,  $P < 0.01$ ); Cyclin E mRNA levels were evaluated by 2.2-fold at 25 wk ( $P < 0.01$ ) and 3.1-fold at 45 wk ( $P < 0.01$ ) precancerosis induced by *H. pylori*, when compared with control gastric epithelium of Mongolian gerbil (Figure 1-3).

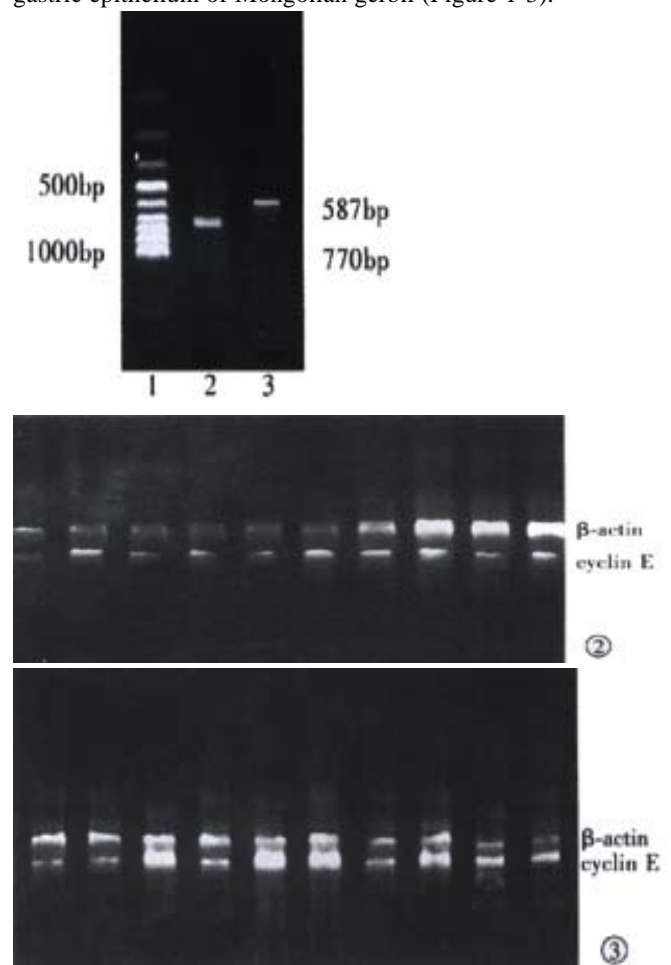


**Figure 1** 1:cyclin E; 2:PCR marker; 3:β-actin

**Figure 2** RT-PCR analysis of cyclin E mRNA levels using β-actin as internal control. Total RNA was first reverse transcribed into cDNA and then amplified by PCR in control.

**Figure 3** In 25 wk after infection of *H. pylori*.

### Immunohistochemical analysis of cyclin E protein expression

To examine whether increased cyclin E mRNA expression were accompanied by increased expression of cyclin E protein, immunohistochemical analysis was performed. cyclin E protein expression lied in nuclei and cytoplasm. Cyclin E protein expressions were evaluated significantly at 25 wk ( $P<0.01$ ) and at 45 wk ( $P<0.01$ ) precancerosis induced by *H. pylori*, when compared with control gastric epithelium of Mongolian gerbil (Figure 4 and Table 1).

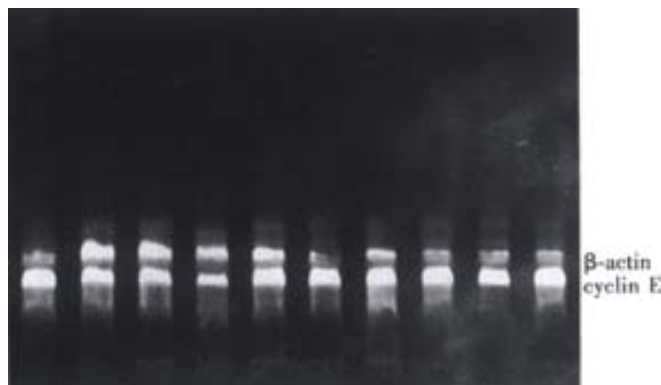


Figure 4 In 45 wk after infection of *H. pylori*.

Table 1 Expression of cyclin E by immunohistochemical staining (n=10)

| Groups                           | Cyclin E |   |    |     | Positive %      |
|----------------------------------|----------|---|----|-----|-----------------|
|                                  | -        | + | ++ | +++ |                 |
| Control                          | 8        | 2 |    |     | 20 <sup>a</sup> |
| 25 wk after <i>H. pylori</i> inf | 2        | 7 | 1  |     | 80 <sup>b</sup> |
| 45 wk after <i>H. pylori</i> inf | 1        | 6 | 2  | 1   | 90 <sup>c</sup> |

K related samples test:  $P=0.002$  Chi-square test:  $\chi^2=12.344$ ,  $P=0.002^b$  vs  $aP=0.007$ , c vs  $aP=0.002$

### DISCUSSION

*H. pylori* infection is now know as a major cause of acute and chronic active gastritis, peptic ulcer disease and atrophic gastritis and is also suspected to be involved in the genesis of gastric adenocarcinoma and mucosa-associated lymphoid tissue lymphoma<sup>[41-49]</sup>. In 1994, the International Agency for Research on Cancer (IRAC), a branch of the World Health Organization (WHO), convened experts from 11 countries to examine the evidence linking a number of infectious agents with human cancer. Although there is no direct proof that *H. pylori* is actually associated with gastric carcinogenesis, epidemiological studies have indicated that *H. pylori* infection plays an important role in gastric carcinogenesis in humans; *H. pylori* was designated as a definite carcinogen (group I) to the human stomach based on prospective case-control studies reported in 1991. Several experiments were conducted in Japan that demonstrated that chronic *H. pylori*-infection models of Mongolian gerbils developed gastric carcinoma. These results will be extremely significant to elucidate the mechanism of gastric carcinogenesis due to *H. pylori* infection<sup>[5,50]</sup>. Apoptosis, a programmed cell death, was ignored, just like *H. pylori*, only to reappear recently. However, the number of current publications dealing with apoptosis of *H. pylori* has increased exponentially. Although gastric epithelial apoptosis is a programmed physiological event in the superficial aspect of the mucosa and is important for healthy cell turnover, *H. pylori* infection reportedly promotes such a cell death sequence<sup>[51-52]</sup>. Because apoptosis regulates the cycle of cell turnover in balance with proliferation, dysregulation of apoptosis or proliferation evoked by *H. pylori* colonization would be linked to the gastric

carcinogenesis<sup>[53-56]</sup>.

Cyclins are positive regulators of cell cycle progression, initially identified in early cleavage embryos of marine invertebrates as proteins that accumulated during interphase and were degraded at mitosis. Cyclins are now known to be positive regulatory subunits of a class of protein kinase termed cyclin-dependent kinases. These protein kinases have been shown in a number of diverse eukaryotic systems to be the master regulators of major cell cycle transitions<sup>[57-59]</sup>. Cyclin E is essential for the G1/S phase transition in the cell cycle. Cyclin E gene amplification and altered expression has been reported in a variety of human cancers<sup>[60-61]</sup>. Now Cyclin E gene has been detected as oncogene<sup>[38]</sup>. Cyclin E was synthesized in the mid-term of the cell cycle, expressed the highest level when entering S phase, and degraded through S phase. The level of cyclin-dependent kinase2 kept constant during the cell cycle. Cyclin E, cyclin-dependent kinase2 and cyclin-dependent kinase inhibitor regulated G1/S phase transition by two-way at late stage of G1 phase, Cyclin E accelerated G1/S phase transition by composing and activating cyclin-dependent kinase2.

In the present study, to explore dysregulation of cyclin E in malignancies, and to further investigate the role of cyclin E in *H. pylori*-induced gastric precancerosis, cyclin E mRNA level was measured by quantitative RT-PCR analysis in Mongolian gerbil gastric antrum mucosa. In addition, the expression and localization of protein product was analyzed by immunohistochemistry. Sample size requirement for obtaining sufficient amounts of RNA for RT-PCR analysis did not allow detection of either cyclin E mRNA level in any specific type of preneoplastic lesions. However, using immunohistochemical technique, cyclin E protein expression in preneoplastic lesions was observed from paraffin-embedded tissue sections. Cyclin E mRNA levels were increased 2.2-fold at 25 wk and 3.1-fold at 45 wk precancerosis induced by *H. pylori*, when compared with normal gastric epithelium of Mongolian gerbil. Immunohistochemical staining revealed exclusive nuclear staining of cyclin E. Furthermore, there was a sequential increase in cyclin E positive cells from normal epithelium to precancerosis. The present study indicated that expression of cyclin E increased from normal epithelium to precancerosis, dysregulation of cyclin E expression occurred relatively early in gastric tumorigenesis in this model and might participate in tumor progression. These findings suggested that *H. pylori*-induced gastric precancerosis was associated with dysregulation of gastric epithelial cell cycle. Further studies were needed to delineate the mechanism of these alterations.

### REFERENCES

- Deng DJ. Progress of gastric cancer etiology: N-nitrosamides in the 1990s. *World J Gastroenterol* 2000;6:613-618
- Chen GY, Wang DR. The expression and clinical significance of CD44v in human gastric cancers. *World J gastroenterol* 2000;6:125-127
- Ma JL, Liu WD, Zhang ZZ, Zhang L, You WC, Chang YS. Relationship between gastric cancer and precancerous lesions. *Shijie Huaren Xiaohua Zazhi* 1998;6:223-224
- Pan ZR. Study on chronic gastritis and gastric cancer. *Xin Xiaohua Bingxue Zazhi* 1996;4:95-96
- Watanabe T, Tada M, Nagai H, Sasaki S, Nakao M. *Helicobacter pylori* infection induces gastric cancer in Mongolian gerbils. *Gastroenterology* 1998;115:642-648
- Zhuang XQ, Lin SR. Study on the relationship between *Helicobacter pylori* and gastric cancer. *Shijie Huaren Xiaohua Zazhi* 2000;8:206-207
- Vandenplas Y. *Helicobacter pylori* infection. *World J Gastroenterol* 2000; 6:20-31
- Takahashi S, Keto Y, Fujita H, Muramatsu H, Nishino T, Okabe S. Pathological changes in the formation of *Helicobacter pylori*-induced gastric lesions in Mongolian gerbils. *Dig Dis Sci* 1998;43:754-765
- Pan KF, Liu WD, Ma JL, Zhou T, Zhang L, Chang YS, You WC. Infection of *Helicobacter pylori* in children and mode of transmission in a high-risk area of gastric cancer. *Shijie Huaren Xiaohua Zazhi* 1998;6:42-44
- Zhang L, Jiang J, Pan KF, Liu WD, Ma JL, Zhou T, Perez-Perez GT,

- Blaser MJ, Chang YS, You WC. Infection of *H. pylori* with cagA+ strain in a high risk area of gastric cancer. *Shijie Huaren Xiaohua Zazhi* 1998;6:40-41
- 11 Zhuang XQ, Lin SR. Study on *Helicobacter pylori* infection in gastric cancer and precancerosis. *Shijie Huaren Xiaohua Zazhi* 2000;8:710-711
- 12 Hu PJ. *Helicobacter pylori* and gastric cancer. *Shijie Huaren Xiaohua Zazhi* 1999;7:1-2
- 13 Huang XQ. *Helicobacter pylori* infection and gastrointestinal hormones: a review. *World J Gastroenterol* 2000;6:783-788
- 14 Shang SH, Zheng JW. Treatment on *Helicobacter pylori* induced diseases. *Shijie Huaren Xiaohua Zazhi* 2000;8:556-557
- 15 Wang XH, Zahgn WD, Zahgn YL, Zeng JZ, Sun Y. Relationship between *Hp* infection and oncogene and tumor suppressor gene expressions in gastric cancer and precancerosis. *Shijie Huaren Xiaohua Zazhi* 1998;6:516-518
- 16 Ye GA, Zhang WD, Liu LM, Shi L, Xu ZM, Chen Y, Zhou DY. *Hp vac A* gene and chronic gastritis. *Shijie Huaren Xiaohua Zazhi* 2001;9:593-594
- 17 Quan J, Fan XG. Experimental studies on *Helicobacter pylori* and gastric cancer. *Shijie Huaren Xiaohua Zazhi* 1999;7:1068-1069
- 18 Lu SY, Pan XZ, Peng XW, Shi ZL, Lin L, Chen MH. Effect of *Hp* infection on gastric epithelial cell kinetics in stomach diseases. *Shijie Huaren Xiaohua Zazhi* 2000;8:386-388
- 19 Xiao SD. *Helicobacter pylori* and gastric cancer. *Shijie Huaren Xiaohua Zazhi* 1998;6:4
- 20 Xia HH. Association between *Helicobacter pylori* and gastric cancer: current knowledge and future research. *World J Gastroenterol* 1998;4:93-96
- 21 Gao XH, Pan BR. *Helicobacter pylori* infection and gastric cancer. *Xin Xiaohua Bingxue Zazhi* 1995;3:223-224
- 22 Zu Y, Shu J, Yang CM, Zhong ZF, Dai HY, Wang X, Qin GM. Study on *Helicobacter pylori* infection and risk of gastric cancer. *Shijie Huaren Xiaohua Zazhi* 1998;6:367-368
- 23 Wu MS, Shun CT, Lee WC, Chen CJ, Wang HP, Lee WJ, Lin JT. Gastric cancer risk in relation to *Helicobacter pylori* infection and subtypes of intestinal metaplasia. *Br J Cancer* 1998;78:125-128
- 24 Forman D. Review article: Is there significant variation in the risk of gastric cancer associated with *Helicobacter pylori* infection? *Aliment Pharmacol Ther* 1998;12:3-7
- 25 Alexander CGA, Amg MC. Association of *Helicobacter pylori* infection with gastric cancer. *Military Med* 2000;165:21-27
- 26 Cai L, Yu SZ, Zhang ZF. *Helicobacter pylori* infection and risk of gastric cancer in Changle County, Fujian Province, China. *World J Gastroenterol* 2000;6:374-376
- 27 Chi J, Fu BY, Nakajima, Hattori and Kushima. Establishment of Mongolian gerbil animal model infected with *Hp* infection and change of inflammation and proliferation before and after *Hp* eradication. *Shijie Huaren Xiaohua Zazhi* 1999;7:557-560
- 28 Zhang WD. Animal model on diseases induced by *H. pylori*: it was difficult for study of *H. pylori*. *Shijie Huaren Xiaohua Zazhi* 1999;7:555-556
- 29 Yasui W, Naka K, Suzuki T, Fujimoto J, Hayashi K, Matsutani N, Yokozaki H, Tahara E. Expression of p27Kip1, cyclin E and E2F-1 in primary and metastatic tumors of gastric carcinoma. *Oncol Rep* 1999;6:983-987
- 30 Matsumoto M, Furihata M, Ishikawa T, Ohtsuki Y, Ogoshi S. Comparison of deregulated expression of cyclin D1 and cyclin E with that of cyclin dependent kinase 4 (CDK4) and CDK2 in human oesophageal squamous cell carcinoma. *Br J Cancer* 1999;80:256-261
- 31 Loden M, Nielsen NH, Roos G, Emdin So, Landberg G. Cyclin E dependent kinase activity in human breast cancer in relation to cyclin E, p27 and p21 expression and retinoblastoma protein phosphorylation. *Oncogene* 1999;18:2557-2566
- 32 Le Cam L, Polanowska J, Fabbriozio E, Olivier M, Philips A Ng Eaton E, Classon M, Geng Y, Sardet C. Timing of cyclin E gene expression depends on the regulated association of a bipartite repressor element with a novel E2F complex. *EMBO J* 1999;18:1878-1890
- 33 Jang SJ, Park YW, Park MH, Lee JD, Lee YY, Jung TJ, Kim IS, Choi IY, Ki M, Choi BY, Ahn MJ. Expression of cell cycle regulators, cyclin E and p21 WAF1/CIP1, potential prognostic markers for gastric cancer. *Eur J Surg Oncol* 1999;25:157-163
- 34 Nielsen NH, Arnerlov C, Cajander S, Landberg G. Cyclin E expression and proliferation in breast cancer. *Anal Cell Pathol* 1998; 17:177-188
- 35 Mishina T, Dosaka Akita H, Hommura F, Nishi M, Kojima T, Ogura S, Shimizu M, Katoh H, Kawakami Y. Cyclin E expression, a potential prognostic marker for non small cell lung cancers. *Clin Cancer Res* 2000;6:11-16
- 36 Quade BJ, Park JJ, Crum CP, Sun D, Dutta A. *In vivo* cyclin E expression as a marker for early cervical neoplasia. *Mod Pathol* 1998;11:1238-1246
- 37 Ohashi R, Gao C, Miyazaki M, Hamazaki K, Tsuji T, Inoue Y, Uemura T, Hirai R, Shimizu N, Namba M. Enhanced expression of cyclin E and cyclin A in human hepatocellular carcinomas. *Anticancer Res* 2001;21:657-662
- 38 Sakaguchi T, Watanabe A, Sawada H, Yamada Y, Yamashita J, Matsuda M, Nakajima M, Miwa T, Hirao T, Nakano H. Prognostic value of cyclin E and p53 expression in gastric carcinoma. *Cancer* 1998;82:1238-1243
- 39 Ling WJ, Ma YJ, Zhang WD, Chen YP. Relationship between classification of spleen syndrome of patients with chronic gastric diseases and gastric carcinoma and cyclin E expression. *Shijie Huaren Xiaohua Zazhi* 2000;8:513-515
- 40 Shimizu M, Nikaido T, Toki T, Shiozawa T, Fujii S. Clear cell carcinoma has an expression pattern of cell cycle regulatory molecules that is unique among ovarian adenocarcinomas. *Cancer* 1999;85:669-677
- 41 Li ZM, Gao CM, Ding JH, Wang JD, Wang YP, Hu X, Liu TK, Takezaki T, Tajima K. Study on seroprevalence of *Helicobacter pylori* infection among upper digestive tract cancer patients and their kindreds. *Chin J Epidemiol* 1999;20:88-90
- 42 Tabata H, Fuchigami T, Kobayashi H, Sakai Y, Nakanishi M, Tomioka K, Nakamura S, Fujishima M. *Helicobacter pylori* and mucosal atrophy in patients with gastric cancer: a special study regarding the methods for detecting *Helicobacter pylori*. *Dig Dis Sci* 1999;44:2027-2034
- 43 Meining AG, Bayerdorffer E, Stolte M. *Helicobacter pylori* gastritis of the gastric cancer phenotype in relatives of gastric carcinoma patients. *Eur J Gastroenterol Hepatol* 1999;11:717-720
- 44 Yamaoka Y, Kodama T, Kashima K, Graham DY. Antibody against *Helicobacter pylori* CagA and VacA and the risk for gastric cancer. *J Clin Pathol* 1999;52:215-218
- 45 Danesh J. *Helicobacter pylori* infection and gastric cancer: systematic review of the epidemiological studies. *Aliment Pharmacol Ther* 1999; 13:851-856
- 46 Harris RA, Owens Dk. Witherell H, Parsonnet J. *Helicobacter pylori* and gastric cancer: what are the benefits of screening only for the CagA phenotype of *H. pylori*? *Helicobacter* 1999;4:69-76
- 47 Hansen S, Melby KK, Aase S, Jellum E, Vollset Se. *Helicobacter pylori* infection and risk of cardia cancer and non cardia gastric cancer. A nested case-control study. *Scand J Gastroenterol* 1999;34:353-360
- 48 Scheiman JM, Cutler AF. *Helicobacter pylori* and gastric cancer. *Am J Med* 1999;106:222-226
- 49 Kuipers EJ. Review article: exploring the link between *Helicobacter pylori* and gastric cancer. *Aliment Pharmacol Ther* 1999;13:3-11
- 50 Honda S, Fujioka T, Tokieda M, Satoh R, Nishizono A, Nasu M. Development of *Helicobacter pylori* induced gastric carcinoma in Mongolian gerbils. *Cancer Res* 1998;58:4255-4259
- 51 Shirin H, Sordillo EM, Oh SH, Yamamoto H, Delohery T, Weinstein B, Moss SF. *Helicobacter pylori* inhibits the G1 to S transition in AGS gastric epithelial cell. *Cancer Res* 1999;59:2277-2281
- 52 Gao H, Wang JY, Shen XZ, Liu JJ. Effect of *Helicobacter pylori* infection on gastric epithelial cell proliferation. *World J Gastroenterol* 2000;6:442-444
- 53 Suzuki H, Ishii H. Role of apoptosis in *Helicobacter pylori* associated gastric mucosal injury. *J Gastroenterol Hepatol* 2000;15:D46-D54
- 54 Rudi J, Kuck D, Strand S, Herbay AV, Mariani SM, Krammer PH, Galle PR, Stremmel W. Involvement of the CD95 (APO1/Fas) receptor and ligand system in *Helicobacter pylori* induced gastric epithelial apoptosis. *J Clin Invest* 1998;102:1506-1514
- 55 Zhuang XQ, Lin SR. Research of *Helicobacter pylori* infection in precancerous gastric lesions. *World J Gastroenterol* 2000;6:428-429
- 56 Gu JZ, Hou TW, Wang XX. Study on precancerous gastric lesions induced by *Helicobacter pylori*. *Shijie Huaren Xiaohua Zazhi* 2001;9:111
- 57 Shin JY, Kim HS, Park J, Park JB, Lee JY. Mechanism for inactivation of the KIP family cyclin dependent kinase inhibitor genes in gastric cancer cells. *Cancer Res* 2000;60:262-265
- 58 Carroll JS, Prall OW, Musgrove EA, Sutherland RL. A pure estrogen antagonist inhibits cyclin E-Cdk2 activity in MCF-7 breast cancer cells and induces accumulation of p130-E2F4 complexes characteristic of quiescence. *J Biol Chem* 2000;275:38221-38229
- 59 Fischer PM, Lane DP. Inhibitors of cyclin-dependent kinases as anti cancer therapeutics. *Curr Med Chem* 2000;7:1213-1245
- 60 Tu JF, Jiang FZ, Chen BC. The relationship between cyclin E expression in primary gallbladder carcinoma and the activity of cell proliferation. *Chin J Exp Surg* 2000;17:20-21
- 61 Huang M, Yang SM, Liao SL, Zhang B, You JF. The effects of cyclin E on the growth and other cell cycle related genes of breast carcinoma cells MCF-7. *Chin J Pathol* 2000;29:192-195

• LIVER CANCER •

# Expression of gap junction genes connexin 32 and connexin 43 mRNAs and proteins, and their role in hepatocarcinogenesis

Xiang-Dong Ma, Xing Ma, Yan-Fang Sui, Wen-Liang Wang

Xiang-Dong Ma, Department of Obstetrics & Gynecology, Xijing Hospital, Fourth Military Medical University, 17 Changle Xilu, Xi'an 710033, Shaanxi Province, China

Xing Ma, Department of Orthopedics, Xinan Hospital, Third Military Medical University, Chongqing, 400038, China

Yan-Fang Sui, Wen-Liang Wang, Department of Pathology, Fourth Military Medical University, Xi'an 710033, Shaanxi Province, China

Correspondence to: Dr. Xiang-Dong Ma, Department of Obstetrics & Gynecology, Xijing Hospital, the Fourth Military Medical University, Xi'an 710033, Shaanxi Province, China. mapping@fmmu.edu.cn

Telephone: +86-27-3373569

Received 2001-02-08 Accepted 2001-03-12

## Abstract

**AIM:** To investigate the relationship between hepatocarcinogenesis and the expression of connexin32 (cx32), connexin43 (cx43) mRNAs and proteins *in vitro*.

**METHODS:** Gap junction genes cx32 and cx43 mRNA in hepatocellular carcinoma cell lines HHCC, SMMC-7721 and normal liver cell line QZG were detected by *in situ* hybridization (ISH) with digoxin-labeled cx32, and cx43 cDNA probes. Expression of Cx32 and Cx43 proteins in the cell lines was revealed by indirect immunofluorescence and flow cytometry (FCM).

**RESULTS:** Blue positive hybridization signals of cx32 and cx43 mRNAs detected by ISH with cx32 and cx43 cDNA probes respectively were located in cytoplasm of cells of HHCC, SMMC-7721 and QZG. No significant difference of either cx32 mRNA or cx43 mRNA was tested among HHCC, SMMC-7721 and QZG ( $P=2.673$ , HHCC vs QZG;  $P=1.375$ , SMMC-7721 vs QZG). FCM assay showed that the positive rates of Cx32 protein in HHCC, SMMC-7721 and QZG were 0.7%, 1.7% and 99.0%, and the positive rates of Cx43 protein in HHCC, SMMC-7721 and QZG were 7.3%, 26.5% and 99.1% respectively. Significant differences of both Cx32 and Cx43 protein expression existed between hepatocellular carcinoma cell lines and normal liver cell line ( $P=0.0069$ , HHCC vs QZG;  $P=0.0087$ , SMMC-7721 vs QZG). Moreover, the fluorescent intensities of Cx32 and Cx43 proteins in HHCC, SMMC-7721 were lower than that in QZG.

**CONCLUSION:** Hepatocellular carcinoma cell lines HHCC and SMMC-7721 exhibited lower positive rates and fluorescent intensities of Cx32, Cx43 proteins compared with that of normal liver cell line QZG. It is suggested that lower expression of both Cx32 and Cx43 proteins in hepatocellular carcinoma cells could play pivotal roles in the hepatocarcinogenesis. Besides, genetic defects of cx32 and cx43 in post-translational processing should be considered.

Ma XD, Ma X, Sui YF, Wang WL. Expression of gap junction genes connexin 32 and connexin 43 mRNAs and proteins, and their role in hepatocarcinogenesis. *World J Gastroenterol* 2002;8(1):64-68

## INTRODUCTION

Carcinoma of the liver is one of the most common malignant tumors which seriously threatens to human life<sup>[1-14]</sup>. About 90% of carcinoma of the liver are hepatocellular carcinoma (HCC)<sup>[15-19]</sup>. In each year, more than 250 thousands of new cases of HCC were reported around the world, among which 110 000 cases (44.7%) occurred in China<sup>[20-24]</sup>. Due to the difficulty in early diagnosis and treatment, the tumor molecular mechanisms, early diagnosis and effective methods of clinical treatment for HCC have been a major research project all over the world.

Gap junctions are intercellular channels formed by the interaction of two hemichannels—connexons, one of which is composed of six protein subunits<sup>[25,26]</sup>. Connexins (Cx) are subunits of gap junctional channels<sup>[27,28]</sup>, by which neighboring cells can exchange low molecular weight ions and molecules, i.e., gap junctional intercellular communication (GJIC)<sup>[29,30]</sup>. GJIC mediated via gap junctions plays important roles in embryogenesis, cell proliferation, tissue homeostasis and in carcinogenesis<sup>[31,32]</sup>. Connexins are encoded by a gene family of at least 16 members, which have been divided into two groups based on primary amino acid sequence homology. Connexin32 (Cx32) and connexin43 (Cx43) are the major gap junction forming proteins in liver tissues. Decreased expression of Cx genes and disordered signal transduction pathway of Cx genes contribute to abnormal gap junctional intercellular communication between contacting cells<sup>[33]</sup>. Uncontrolled tumor cell growth because of the loss of gap junctional intercellular communication due to the down-regulated expression of Cx genes appears to be an important event in cell transformation<sup>[34-37]</sup>. In this study, the hepatocellular carcinoma cell lines HHCC, SMMC-7721 and normal liver cell line QZG were employed to investigate the relationship between hepatocarcinogenesis and cx32, cx43 mRNA and their protein expression.

## MATERIALS AND METHODS

### Cell culture

Hepatocellular carcinoma cell lines HHCC, SMMC-7721 and normal liver cell line QZG, were kindly provided by Professor Chen in the 863 Research Group. The cells were cultured on slides in RPMI 1640 medium (Gibco BRL, USA), supplemented with 100 mL·L<sup>-1</sup> fetal bovine serum (Gibco BRL, USA), incubated in a humidified atmosphere of 950 mL·L<sup>-1</sup> air and 50 mL·L<sup>-1</sup> CO<sub>2</sub> at 37°C. The cells were passaged by trypsinization twice a week.

### Probe labeling

pGEM-cx32 plasmid containing cx32 cDNA 1.5kb, pSG5-cx43 plasmid containing cx43 cDNA 1.1kb were gifts from Professor Li in Hunan Medical University. After amplification, isolation and purification, pGEM3-cx32 plasmid was digested by EcoR I (Gibco BRL, USA) and pSG5-cx43 by BamH I (Gibco BRL, USA). The digested plasmids were electrophorated on 7 g·L<sup>-1</sup> agarose gel with DNA/Hind III + EcoR I Marker (Gibco BRL, USA). cx32, cx43 cDNAs from gel were extracted and purified as the protocol of PCR-pure kit (Clontech, USA), and labeled using Dig



DNA labeling and detection kit (Boehringer Mannheim, Germany).

### *In situ hybridization*

Slides of varied cells were incubated in  $0.2\text{mL}\cdot\text{L}^{-1}$  DEPC at RT for 10 min, then in  $0.2\text{mL}\cdot\text{L}^{-1}$  HCl for 10 min,  $5\text{mg}\cdot\text{L}^{-1}$  PK at  $37^{\circ}\text{C}$  for 10 min. The digestion reaction was stopped in  $0.1\text{mol}\cdot\text{L}^{-1}$  glycine and the slides were fixed in  $40\text{g}\cdot\text{L}^{-1}$  PFA for 10 min, dehydrated in ethanol and air dried in sequence. Prehybridization was performed at  $42^{\circ}\text{C}$  for 30 min. The labeled cDNA probes were denatured in hybridization buffer at  $100^{\circ}\text{C}$  for 10 min, then at  $-20^{\circ}\text{C}$  for 3 min, then added on tissues and coverslipped at  $42^{\circ}\text{C}$  overnight. Washing of sections was done with  $2\times\text{SSC}$ ,  $1\times\text{SSC}$ ,  $0.5\times\text{SSC}$  and Buffer I. The slides were incubated in NSS at  $37^{\circ}\text{C}$  for 30 min, and then Dig-Ap (Boehringer Mannheim, Germany, 1:500) for 2h, finally detected with NBT / BCIP of Dig DNA labeling and detection kit (Boehringer Mannheim, Germany). Positive signals were visualized as intensive blue granules in the cytoplasm. Control sections were used. All results were verified by  $\chi^2$  test.

### *Flow cytometry (FCM) analysis*

Total  $10^6\cdot\text{L}^{-1}$  cells of HHCC, SMMC-7721 and QZG were

collected, and blocked with normal serum (Vector, USA) for 30 min at  $4^{\circ}\text{C}$ , then added mouse-anti Cx32 McAb (Zymed, USA, 1:1000) and mouse-anti Cx43 McAb (Zymed, USA, 1:1000) respectively for 30 min at  $4^{\circ}\text{C}$ , whereas IgG was added for control. FITC-IgG (Jackson, 1:100) was added in the cells for 30 min at  $4^{\circ}\text{C}$ , precipitated and washed by  $0.01\text{mol}\cdot\text{L}^{-1}$  pH7.5 PBS. Detective rates and the fluorescent intensity of Cx32, Cx43 proteins in the cells were measured by ELITE ESP flow cytometer (Coulter, USA) and phoenix software (Coulter, USA).

## RESULTS

### *Detect of cx32, cx43 mRNA in cell lines by ISH*

The cx32, cx43 mRNA in hepatocellular carcinoma cell lines HHCC, SMMC-7721 and normal liver cell line QZG were detected by Dig-labeled cx32, cx43 cDNA probes. After in situ hybridization, blue positive hybridization signals of mRNA were located in cytoplasm of the cells. The results showed that bright blue specific hybridization signals of cx32 mRNA and cx43 mRNA were detected in hepatocellular carcinoma cell lines HHCC, SMMC-7721 and normal liver line QZG.  $\chi^2$  tests did not show any significant difference ( $P > 0.05$ ) between them. The results were showed in Figure 1-3.

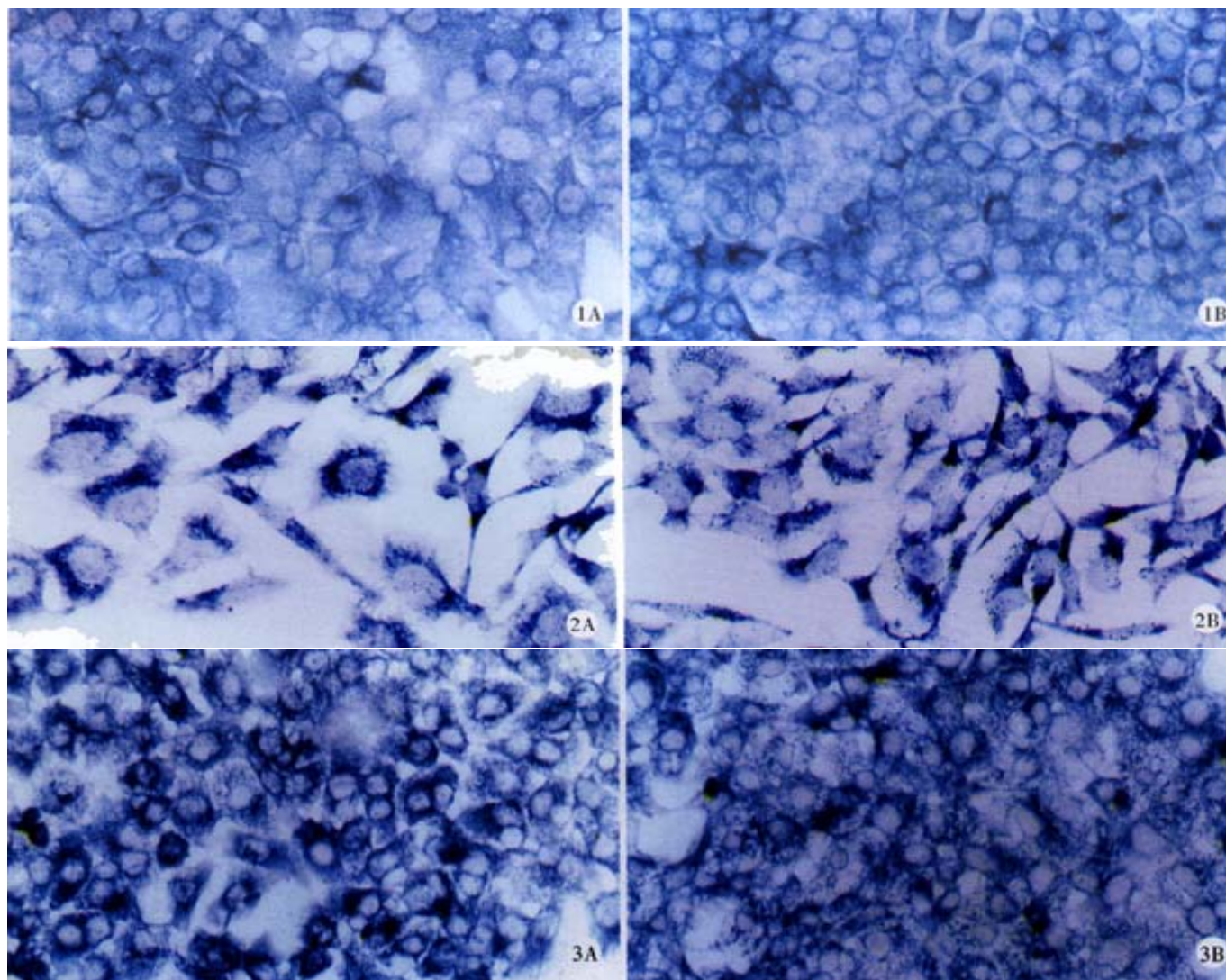


**Figure 1A** Positive signal of cx32 mRNA in HHCC, ISH $\times 400$   
**Figure 2A** Positive signal of cx32 mRNA in SMMC-7721, ISH $\times 400$   
**Figure 3A** Positive signal of cx32 mRNA in QZG, ISH $\times 400$

**Figure 1B** Positive signal of cx43 mRNA in HHCC, ISH $\times 400$   
**Figure 2B** Positive signal of cx43 mRNA in SMMC-7721, ISH $\times 400$   
**Figure 3B** Positive signal of cx43 mRNA in QZG, ISH $\times 400$

### Expressions of Cx32, Cx43 proteins in hepatocellular carcinoma cell lines by FCM

Expression of Cx32, Cx43 proteins in cultured hepatocellular carcinoma cell lines HHCC, SMMC-7721 and normal liver cell line QZG were detected by FCM after immunoreaction with mouse-anti Cx32 McAb, mouse-anti Cx43 McAb. FCM examined both positive rates of Cx proteins expression and their quantities in each cell line.

FCM assay showed that positive rates of Cx32 protein expression in HHCC, SMMC-7721 and QZG were 0.7%, 1.7% and 99.0%, and those of Cx43 protein were 7.3%, 26.5% and 99.1% respectively. The fluorescent intensity of Cx32 protein and Cx43 protein in HHCC, SMMC-7721 were lower than those in QZG. QZG

cells showed both higher positive rates for Cx32, Cx43 proteins and strong fluorescent intensity. The detection rates of Cx32, Cx43 proteins were showed in Figure 4-6 and Table 1.

**Table 1** Positive expression rates of Cx32 and Cx43 proteins in various cell lines

| Cell line | Positive rates % |                   |
|-----------|------------------|-------------------|
|           | Cx32             | Cx43              |
| HHCC      | 0.7 <sup>b</sup> | 7.3 <sup>b</sup>  |
| SMMC-7721 | 1.7 <sup>b</sup> | 26.5 <sup>b</sup> |
| QZG       | 99.0             | 99.1              |

<sup>b</sup>P<0.01, vs QZG.

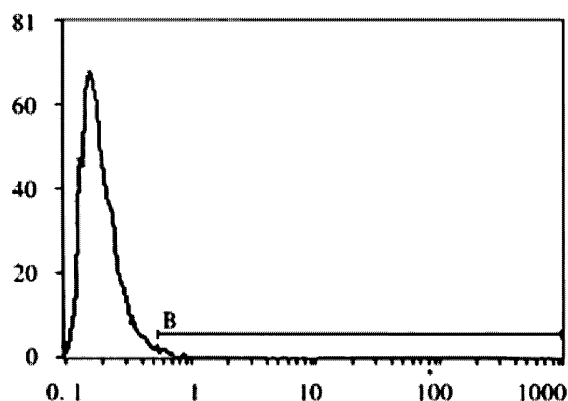


**Figure 4A** Positive expression rate of Cx32 protein in HHCC, FCM  
(X: FL1; Y: cell count)

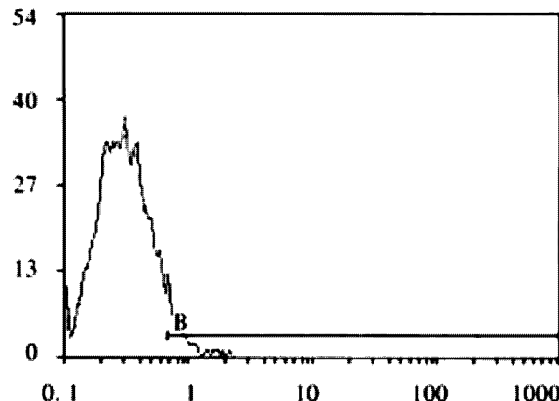


**Figure 4B** Positive expression rate of Cx43 protein in SMMC-7721, FCM  
(X: FL1; Y: cell count)

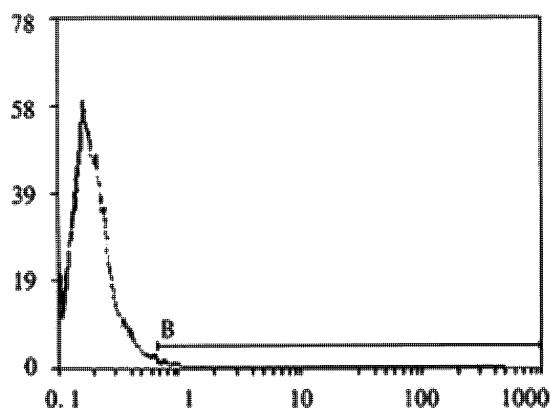


**Figure 5A** Positive expression rate of Cx43 protein in HHCC, FCM  
(X: FL1; Y: cell count)

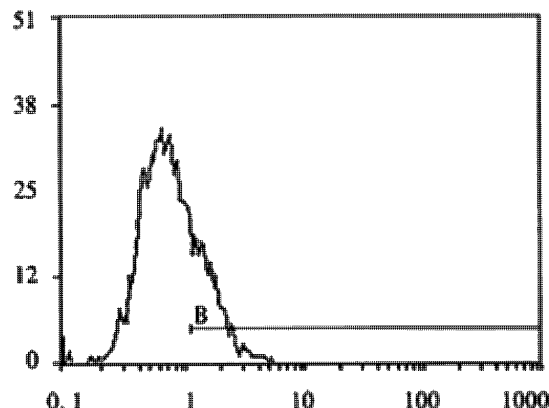


**Figure 5B** Positive expression rate of Cx32 protein in QZG, FCM  
(X: FL1; Y: cell count)

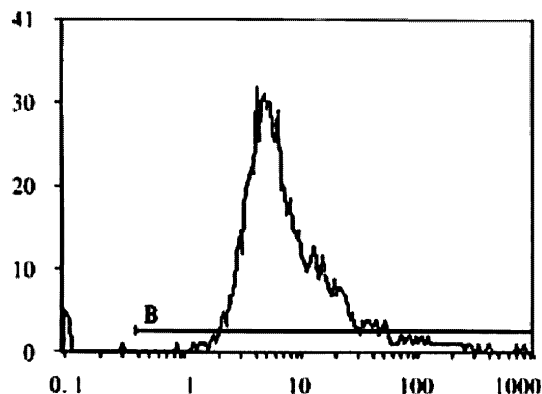


**Figure 6A** Positive expression rate of Cx32 protein in SMMC-7721, FCM  
(X: FL1; Y: cell count)

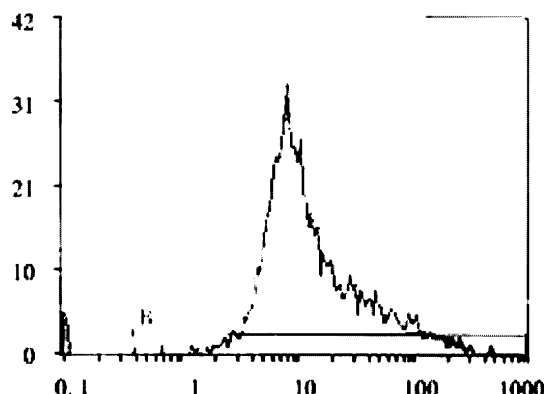


**Figure 6B** Positive expression rate of Cx43 protein in QZG, FCM  
(X: FL1; Y: cell count)

## DISCUSSION

Gap junction intercellular communication (GJIC) mediated by gap junction channels<sup>[38,39]</sup> has been postulated to be an important tool for the maintenance of tissues homeostasis, metabolism, control growth and differentiation<sup>[40,41]</sup>. Carcinogenesis is one of the pathological processes in which disorders of GJIC may play an important role. The inhibited GJIC in many kinds of tumor cells has been found, which could make important contributions to neoplastic progression by allowing tumor cells to escape by either systemic or local control mechanisms<sup>[42-44]</sup>.

Cx32, Cx43 are widely expressed in many tissues, especially in normal liver. This study revealed that Cx32 and Cx43 proteins expressed at a high level in normal liver cell line but at low level in hepatocellular carcinoma cell lines<sup>[45-47]</sup>.

Hepatocarcinogenesis is dramatically enhanced in liver neoplasm tissues lacking of Cx32 and Cx43 proteins, as we shown previously<sup>[48]</sup>. The results showed that cx32 and cx43 mRNAs and their proteins were highly expressed in normal liver tissues and cell lines, and had significantly decreased in hepatocellular carcinoma tissues and cell lines except expression of Cx43 protein in hepatoma cell line SMMC-7721. cx32 is the specific expression gene in human normal liver tissues and cell line whereas cx43 is a kind of variable expressing gene in either normal liver or hepatoma cell lines. Decrease of Cx proteins related with abnormal function of GJIC between hepatocellular carcinoma cells and surrounding normal cells finally results in hepatocarcinogenesis. Aberrant localization of Cx32 and Cx43 may be not only essential for the reduced GJIC in HCC<sup>[49]</sup>, but also disturb the mechanism of a bystander effect<sup>[50]</sup>. Expression of the gap junctional proteins is often decreased in tumor tissues, but recruited expression could suppress malignant phenotypes of the tumor cells. The mechanism is that enhanced GJIC on basis of normal gap junctional protein expression regulates homologous and heterologous communication between tumor cells, surrounding normal hepatocytes and other cells<sup>[51]</sup>.

Many observations demonstrate that the lower expression of Cx32 and Cx43 may be involved in the development of hepatocellular carcinoma<sup>[52]</sup>. It is interesting, moreover, that our results have showed even lower expression of Cx32, Cx43 proteins in hepatocellular carcinoma cell lines HHCC, SMMC-7721 than that in normal liver cell line QZG, but ISH results have shown no decreases of cx32 and cx43 mRNA in hepatocellular carcinoma compared with normal liver cell line. Therefore, it appears that cx32 and cx43 genes transcription is not responsible for aberrant expression of Cx32 and Cx43 proteins during human liver tumorigenesis. Besides, the results have indicated that cx32 and cx43 genes, the specific genes expressing in normal liver tissues, are expected to be the potential unmutated tumor suppressor genes.

Some abnormal regulatory events promote carcinogenesis<sup>[55,56]</sup>, through multiple mechanisms, including post translation process and other potential mechanisms<sup>[53-56]</sup>. The carcinogenesis and development of hepatocellular carcinoma are related with the abnormal expression of cx genes, signal transduction disorders<sup>[57, 58]</sup>, such as reduce of  $[Ca^{2+}]$ <sup>[59,60]</sup> and post-translational phosphorylation on tyrosine of Cx proteins, which are associated with dramatic changes in gap junctional intercellular communication and carcinogenesis<sup>[61]</sup>. The possibility is that defects in post-translational processing of Cx32 and Cx43 proteins may be obstacle for their transportation to cell membranes<sup>[62]</sup>. Furthermore, phosphorylation on tyrosine of Cx protein can affect the structure of Cx proteins, which is related to channel properties<sup>[63]</sup>. Post-translational phosphorylation on tyrosine of Cx32 and Cx43 may be important factors controlling the GJIC in hepatocellular carcinoma and substantially responsible for the assembly and function of these proteins as well. Further investigation is expected to understand the mechanism in detail.

## REFERENCES

- 1 Ma XD, Sui YF, Wang WL. Expression of gap junction genes connexin32 and connexin43 and their proteins in hepatocellular carcinoma and normal liver tissues. *World J Gastroenterol* 2000;6:66-69
- 2 Wang Y, Liu H, Zhao Q, Li X. Analysis of point mutation in site 1896 of HBV procore and its detection in the tissues and serum of HCC patients. *World J Gastroenterol* 2000;6:395-397
- 3 Mei MH, Xu J, Shi QF, Yang JH, Chen Q, Qin LL. Clinical significance of serum intercellular adhesion molecule detection on patients with hepatocellular carcinoma. *World J Gastroenterol* 2000;6:408-410
- 4 Qin Y, Li B, Tan YS, Sun ZL, Zuo FQ, Sun ZF. Polymorphism of p16INK4a gene and rare mutation of p15INK4b gene exon2 in primary hepatocellular carcinoma. *World J Gastroenterol* 2000;6:411-414
- 5 Wang XZ, Chen XC, Yang YH, Chen ZX, Huang YH, Tao QM. Relationship between HBxAg and Fas/FasL in patients with hepatocellular carcinoma. *World J Gastroenterol* 2000;6(Suppl 3):17-20
- 6 Zhao CY, Li YL, Liu SX, Feng ZJ. Changes of IL6 and relevant cytokines in patients with hepatocellular carcinoma and their clinical significance. *World J Gastroenterol* 2000;6(Suppl 3):33-36
- 7 Su ZJ, Zhang YF, Shi MY, Zeng QX, Chen ML. A prospective study of nosocomial infection in 848 cases of liver diseases. *World J Gastroenterol* 2000;6(Suppl 3):38-40
- 8 Li JY, Huang Y, Lin MF. Clinical evaluation of several tumor markers in the diagnosis of primary hepatic cancer. *World J Gastroenterol* 2000;6(Suppl 3):39-41
- 9 Yin ZZ, Jin HL, Yin XZ, Li TZ, Quan JS, Jin ZN. Effect of boschniakia rossica on expression of GSTP, p53 and p21ras proteins in early stage chemical hepatocarcinogenesis and its anti inflammatory activities in rats. *World J Gastroenterol* 2000;6(Suppl 3):49-51
- 10 Lin GY, Chen ZL, Lu CM, Li Y, Wang J, Ping XJ, Huang R. Immunohistochemical study on p53, Hrasp21, cerbB2 protein and PCNA expression in tumor tissues of Han and minority ethnic patients with primary hepatic carcinoma in Xinjiang. *World J Gastroenterol* 2000;6(Suppl 3):53-56
- 11 Jiang Z, Liu L, Fang W, Shou WZ, Zhang DS, Dai MM. Local radioactive treatment of hepatocellular cancer with phosphorus32 glass microspheres to enhance the efficacy of hepatic artery chemoembolism and possibly related with MDR expressed glycoprotein. *World J Gastroenterol* 2000;6(Suppl 3):59-62
- 12 Liu LX, Jiang HC, Zhu AL, Zhou J, Wang XQ, Wu M. Gene expression profiles in liver cancer and normal liver tissues. *World J Gastroenterol* 2000;6(Suppl 3):85-88
- 13 Wang CF, Shao YF, Zhang HZ. Surgical treatment for patients with stage IVa hepatic carcinoma and related studies. *World J Gastroenterol* 2000;6(Suppl 3):86-89
- 14 Lin NF, Tang J, Mohamed-Ishmael HS. Study on environmental etiology of high incidence areas of liver cancer in China. *World J Gastroenterol* 2000;6:572-576
- 15 Tian DY, Yang DF, Xia NS, Zhang ZG, Lei HB, Huang YC. The serological prevalence and risk factor analysis of hepatitis G virus infection in Hubei Province of China. *World J Gastroenterol* 2000;6:585-587
- 16 Zhong DR, Ji XL. Hepatic angiomyolipoma misdiagnosis as hepatocellular carcinoma: A report of 14 cases. *World J Gastroenterol* 2000;6:608-612
- 17 Riordan SM, Williams R. Transplantation of primary and reversibly immortalized human liver cells and other gene therapies in acute liver failure and decompensated chronic liver disease. *World J Gastroenterol* 2000;6:636-642
- 18 Li Y, Su JJ, Qin LL, Yang C, Luo D, Ban KC, Kensler TW, Roebuck BD. Chemopreventive effect of oltipraz on AFB1 induced hepatocarcinogenesis in tree shrew model. *World J Gastroenterol* 2000;6:647-650
- 19 Xu HY, Yang YL, Gao YY, Wu QL, Gao GQ. Effect of ars enic trioxide on human hepatoma cell line BEL7402 cultured in vitro. *World J Gastroenterol* 2000;6:681-687
- 20 Zang GQ, Zhou XQ, Yu H, Xie Q, Zhao GM, Wang B, Guo Q, Xiang YQ, Liao D. Effect of hepatocytic apoptosis induced by TNF $\alpha$  on acute severe hepatitis in mouse models. *World J Gastroenterol* 2000;6:688-692
- 21 Huang XF, Wang CM, Dai XW, Li ZJ, Pan BR, Yu LB, Qian B, Fang L. Expression of chromogranin A and cathepsin D in human primary hepatocellular carcinoma. *World J Gastroenterol* 2000;6:693-698
- 22 Xu HY, Yang YL, Guan XL, Song G, Jiang AM, Shi LJ. Expression of regulating apoptosis gene and apoptosis index in primary liver cancer. *World J Gastroenterol* 2000;6:721-724
- 23 Chen YP, Liang WF, Zhang L, He HT, Luo KX. Transfusion transmitted virus infection in general populations and patients with various liver diseases in south China. *World J Gastroenterol* 2000;6:738-741
- 24 Ma XD, Sui YF, Wang WL. The expression of gap junction protein connexin32 in human hepatocellular carcinoma, cirrhotic and viral hepatitis liver tissues. *Aizheng* 1999; 18:133-135

- 25 Kumar NM, Gilula NB. The gap junction communication channel. *Cell* 1996; 84: 381-388
- 26 Windoffer R, Beile B, Leibold A, Thomas S, Wilhelm U, Leube RE. Visualization of gap junction mobility in living cells. *Cell Tissue Res* 2000; 299:347-362
- 27 Durnick PE, Benjamin DC, Verselis VK, Bargiello TA, Dowd TL. Structure of the amino terminus of a gap junction protein. *Arch Biochem Biophys* 2000; 381:181-190
- 28 Hopperstad MG, Srinivas M, Spray DC. Properties of gap junction channels formed by Cx46 alone and in combination with Cx50. *Biophys J* 2000; 79:1954-1966
- 29 Falk MM. Biosynthesis and structural composition of gap junction intercellular membrane channels. *Eur J Cell Biol* 2000; 79:564-574
- 30 Ruch RJ, Trosko JE. The role of oval cells and gap junctional intercellular communication in hepatocarcinogenesis. *Anticancer Res* 1999; 19: 4831-4838
- 31 Yamasaki H, Naus CC. Role of connexin genes in growth control. *Carcinogenesis* 1996;17:1199-1213
- 32 Krutovskikh V, Yamasaki H. The role of gap junctional intercellular communication (GJIC) disorders in experimental and human carcinogenesis. *Histol Histopathol* 1997;12:761-768
- 33 Hahn AF, Ainsworth PJ, Naus CC, Mao J, Bolton CF. Clinical and pathological observations in men lacking the gap junction protein connexin32. *Muscle Nerve* 2000; 999:S39-49
- 34 Moennikes O, Buchmann A, Rommaldi A, Ott T, Werringloer J, Willecke K, Schwarz M. Lack of phenobarbital-mediated promotion of hepatocarcinogenesis in connexin 32-null mice. *Cancer Res* 2000; 60:5087-5091
- 35 Moennikes O, Buchmann A, Willecke K, Tranb O, Schwarz M. Hepatocarcinogenesis in female mice with mosaic expression of connexin 32. *Hepatology* 2000; 32: 501-506
- 36 Piechocki MP, Toti RM, Fernstrom MJ, Burk RD, Ruch RJ. Liver cell-specific transcriptional regulation of connexin32. *Biochim Biophys Acta* 2000; 1491: 107-122
- 37 Ma XD, Sui YF, Wang WL. Expression of gap junction genes connexin32, connexin43 and their proteins in human hepatocellular carcinoma cell lines and normal liver cell line. *Shiyong Aizheng Zazhi* 1999;14:161-163
- 38 Ma XD, Sui YF, Wang WL, Xu QL. A flow cytometric study of gap junction cx32,cx43 in human hepatocellular carcinoma cell lines. *Xibao Yu Fenzi Mianyixue Zazhi* 1999;15:51-54
- 39 Ma XD, Sui YF, Wang WL, Wang CM. Expression of gap junction proteins Cx32, Cx43 in human hepatocellular carcinoma cell lines and normal liver cell line: Study with laser scanning confocal microscope. *Zhongguo Zhongliu Zazhi* 2000;10:1-2
- 40 Juul MH, Rivedal E, Stokke T, Sanner T. Quantitative determination of gap junction intercellular communication using flow cytometric measurement of fluorescent dye transfer. *Cell Adhes Commun* 2000; 7: 501-512
- 41 Nielsen M, Ruch RJ, Vang O. Resveratrol reverses tumor-promoter-induced inhibition of gap junctional intercellular communication. *Biochem Biophys Res Commun* 2000;275:804-809
- 42 Krutovskikh VA, Troyanovsky S M, Piccoli C, Tsuda H, Asamoto M, Yanaski H. Differential effect of subcellular localization of communication impairing gap junction protein connexin43 on tumor cell growth. *Oncogene* 2000; 19: 505-513
- 43 Christ GJ. Gap junctions and ion channels: relevance to erectile dysfunction. *Int J Impot Res* 2000;12(Suppl 4):S15-25
- 44 Piechocki MP, Burk RD, Ruch RJ. Regulation of connexin 32 and connexin43 by DNA methylation in rat liver cells. *Carcinogenesis* 1999; 20: 401-406
- 45 Ma XD, Sui YF, Wang WL. Expression of gap junction protein connexin32 in human hepatocellular carcinoma, pericancerous liver and normal liver tissues. *Disi Junyi Da xue Xuebao* 1999;20:48-50
- 46 Temme A, Buchmann A, Gabriel HD, Nelles E, Schwarz M, Willecke K. High incidence of spontaneous and chemically induced liver tumors in mice deficient for connexin32. *Curr Biol* 1997; 7: 713-716
- 47 Wang Y, Rose B. An inhibition of gap-junctional communication by cadherins. *J Cell Sci* 1997; 110(pt3): 301-309
- 48 Krutovskikh V, Yamasaki H. Connexin gene mutations in human genetic diseases. *Mutat Res* 2000;462:197-207
- 49 Krutovskikh V, Mazzoleni G, Mironov N, Omori Y, Aguelon AM, Mesnil M, Berger F, Partensky C, Yamasaki H. Altered homologous and heterologous gap-junction intercellular communication in primary human liver tumors associated with aberrant protein localization but not gene mutation of connexin 32. *Int J Cancer* 1994; 54: 87-93
- 50 Kawamura K, Bahar R, Namba H, Seimiya M, Takenaga K, Hamada H, Sakiyama S, Tagawa M. Bystander effect in uracil phosphoribosyltransferase/5-fluoracil-mediated suicide gene therapy is correlated with the level of intercellular communication. *Int J Oncol* 2001; 18:117-120
- 51 Ren P, Ruch RJ. Inhibition of gap junctional intercellular communication by barbiturates in long-term primary cultured rat hepatocytes is correlated with liver tumor promoting activity. *Carcinogenesis* 1996; 17:2119-2124
- 52 Omori Y, Krutovskikh V, Mironov N, Tsuda H, Yamasaki H. Cx32 gene mutation in a chemically induced rat liver tumor. *Carcinogenesis* 1996; 17: 2077-2880
- 53 Neveu MJ, Hully JR, Babcock KL, Hertzberg EL, Nicholson BJ, Paul DL, Pitot HC. Multiple mechanisms are responsible for altered expression of gap junction genes during oncogenesis in rat liver. *J Cell Sci* 1994; 107(pt1): 83-95
- 54 DeoCampo ND, Wilson MR, Trosko JE. Cooperation of bcl-2 and myc in the neoplastic transformation of normal rat liver epithelial cells is related to the down-regulation of gap junction-mediated intercellular communication. *Carcinogenesis* 2000;21:1501-1506
- 55 Kolaja KL, Engelken DT, Klaassen CD. Inhibition of gap-junctional-intercellular communication in intact rat liver by nongenotoxic hepatocarcinogens. *Toxicology* 2000;146:15-22
- 56 Yamasaki H, Krutovskikh V, Mesnil M, Tanaka T, Zaidan-Dagli ML, Omori Y. Role of connexin (gap junction) genes in cell growth control and carcinogenesis. *C R Acad Sci* 1999;322:151-159
- 57 Niessen H, Harz H, Bedner P, Kramer K, Willecke K. Selective permeability of different connexin channels to the second messenger inositol 1,4,5-trisphosphate. *J Cell Sci* 2000;113(pt8):1365-1372
- 58 Niessen H, Willecke K. Strongly decreased gap junctional permeability to inositol 1,4,5,-trisphosphate in connexin32 deficient hepatocytes. *FEBS Lett* 2000;466:112-114
- 59 Suadicani SO, Vink MJ, Spray DC. Slow intercellular Ca(2+) signaling in wild-type and cx43-null neonatal mouse cardiac myocytes. *Am J Physiol Heart Circ Physiol* 2000; 279:H3076-3088
- 60 Rottingen J, Iversen JG. Ruled by waves Intracellular and intercellular calcium signaling. *Acta Physiol Scand* 2000;169:203-219
- 61 Chen BL, Ma XD, Xin XY, Wang DT, Wang CM. The regulation on signal transduction pathway of gap junction gene connexin43 in HeLa cell line by all-trans-retinoic acid. *Shiyong Aizheng Zazhi* 2000; 15:337-340
- 62 Ma XD, Chen BL, Wang DT, Xin XY. Expression of antioncogene connexin43 mRNA and its protein in human cervical carcinoma cell line HeLa. *Xiandai Fuchanke Jinzhan* 1999;8:317-319
- 63 Guan XJ, Ruch RJ. Gap junction endocytosis and lysosomal degradation of connexin43-P2 in WB-F344 rat liver epithelial cells treated with DDT and lindane. *Carcinogenesis* 1996;17:1791-1798



• LIVER CANCER •

# Pharmacokinetics of radioimmunotherapeutic agent of direct labeling mAb $^{188}\text{Re}$ -HAb18

Chao Lou, Zhi-Nan Chen, Hui-Jie Bian, Jie Li, Shou-Bo Zhou

Chao Lou, Zhi-Nan Chen, Hui-Jie Bian, Department of Cell Engineering Research Centre, Jie Li, Department of Oral Cell Biology, Qingdu Hospital, Fourth Military Medical University, Xi'an 710033, Shaanxi Province, China

Shou-Bo Zhou, School of Biological Science, University of Manchester, Oxford Road, United Kingdom

Supported by National Natural Science Foundation of China, No. 39700175 (Dr. Hui-Jie Bian)

Correspondence to: Chao Lou, Cell Engineering Research Centre, Fourth Military Medical University, Xi'an 710033, Shaanxi Province, China. wall1970@sina.com

Telephone: +86-29-3374057

Received 2001-07-19 Accepted 2001-10-24

## Abstract

**AIM:** To label anti-hepatoma monoclonal antibody (mAb) fragment HAb18 F(ab')<sub>2</sub> was labeled with  $^{188}\text{Re}$  for the pharmacokinetic model of  $^{188}\text{Re}$ -HAb18 F(ab')<sub>2</sub> and to evaluate its pharmacokinetic parameters in hepatoma-bearing nude mice.

**METHODS:** HAb18 F(ab')<sub>2</sub> was directly labeled with  $^{188}\text{Re}$  using 2-mercaptoethanol (2-ME) as reducing agents. Labeling efficiency and immunoreactivity of  $^{188}\text{Re}$ -HAb18 F(ab')<sub>2</sub> were evaluated by Whatman 3MM paper chromatography and live cell assay, respectively. Biodistribution analysis was also conducted in nude mice bearing human hepatoma in which animals were sacrificed at different time points (1, 4, 18, 24 and 48h) after  $^{188}\text{Re}$ -HAb18 F(ab')<sub>2</sub> was injected through tail-vein into hepatoma-bearing nude mice. The blood and radioactivity of organs and mass were measured. The concentrations of  $^{188}\text{Re}$ -HAb18 F(ab')<sub>2</sub> were evaluated with a pharmacokinetic 3P97 software.

**RESULTS:** The optimum labeling efficiency and immunoreactive fraction were 91.7% and 0.78% respectively. The parameters of  $^{188}\text{Re}$ -HAb18 F(ab')<sub>2</sub> were:  $T_{1/2}$ , 2.29h;  $V_d$ ,  $1.49 \times 10^{-9} \text{ L} \cdot \text{Bq}^{-1}$ ; AUC,  $20.49 \times 10^9 \text{ Bq} \cdot \text{h} \cdot \text{L}^{-1}$ ; CL,  $0.45 \times 10^{-3} \text{ L} \cdot \text{h}^{-1}$ .  $^{188}\text{Re}$ -HAb18 F(ab')<sub>2</sub> could locate specially in hepatoma with high selective reactivity of HAb18 F(ab')<sub>2</sub>.  $^{188}\text{Re}$ -HAb18 F(ab')<sub>2</sub> was mainly eliminated by kidney. The maximal tumor to blood ratio was at 48h, and maximal tumor to liver ratio was at 18h.

**CONCLUSION:** The pharmacokinetics of  $^{188}\text{Re}$ -HAb18 F(ab')<sub>2</sub> fit a 1-compartment model.  $^{188}\text{Re}$ -HAb18 F(ab')<sub>2</sub> can be uptaken selectively at the hepatoma site.

Lou C, Chen ZN, Bian HJ, Li J, Zhou SB. Pharmacokinetics of radioimmunotherapeutic agent of direct labeling mAb  $^{188}\text{Re}$ -HAb18. *World J Gastroenterol* 2002;8(1):69-73

## INTRODUCTION

$^{188}\text{Re}$  is a new radioisotope<sup>[1-16]</sup>. In the past,<sup>131</sup>I was used as the main radioisotope for radioimmunotherapy (RAIT).<sup>131</sup>I has its favour such

as simple labeling, appropriate partial energy and path length, but the high energy of  $\gamma$ -ray produced harmness to the whole body, and  $\beta$ -energy ( $E_{\max}$ , 0.6 MeV) was low<sup>[17-22]</sup>. So scientists have searched for more effective radioisotope. Rhenium-188 is of particular interest to this study as the  $^{188}\text{Re}$  may be obtained from the  $^{188}\text{W}/^{188}\text{Re}$  generator, and  $^{188}\text{Re}$  decays by  $\beta$ -emission with energies ( $E_{\max}$ =2.12 MeV) similar to  $^{90}\text{Y}$  and  $\gamma$  photons ( $E_{\gamma}$ =155 keV; abundance=15%) that are useful for dosimetry calculations and radioimmunotherapy, with a half-time of 17h. Furthermore,  $^{188}\text{Re}$  has chemical properties similar to  $^{99}\text{Tc}$  m, thus it can be conjugated to antibodies modeling on  $^{99}\text{Tc}$  m labeling methods using direct or indirect method<sup>[23-29]</sup>. Direct methods require attaching the reduced form of Re to the endogenous thiols of antibodies, whereas indirect methods require the reduced Re to be complexed by a bifunctional chelator that is conjugated to the antibody<sup>[30-32]</sup>. There has been considerable interest in the direct labeling of mAb, which would result in the formation of an instant kit formulation for imaging or therapy.

$^{188}\text{Re}$  can be provided at reasonable costs for routine preparation of radiopharmaceuticals for cancer treatment.  $^{188}\text{Re}$  is an important therapeutic radioisotope which is obtained on demand as carrier-free sodium perrhenate by saline elution of the tungsten-188/rhenium-188 generator system. Because of its prominent physical characters,  $^{188}\text{Re}$  will become a new therapeutic isotope.  $^{188}\text{Re}$  is a radioisotope currently under evaluation for a variety of therapeutic application, including that for metastatic bone pain and therapy in oncology.

The HAb18 antibody is a murine IgG<sub>1</sub> anti-hepatoma monoclonal antibody under investigation in our laboratory. It does not cross react with normal liver cells, and only rarely with other malignant tissues. Due to the smaller size, easier penetration into tumor tissues, rapid clearance from circulation, and less human anti-mouse antibody (HAMA) reaction, F(ab')<sub>2</sub> fragments showed that tumor localization is faster and better than the intact antibody. Previous studies of  $^{99}\text{Tc}$  m labeled with HAb18 F(ab')<sub>2</sub> indicated that the conjugate is effective to detect hepatoma in the nude mice model<sup>[33]</sup>. The results encourage us to continue the radioimmunotherapy for hepatoma using  $^{188}\text{Re}$  labeled with HAb18 F(ab')<sub>2</sub>. We have studied the pharmacokinetics of  $^{188}\text{Re}$ -HAb18 F(ab')<sub>2</sub> in hepatoma-bearing nude mice in order to prove if  $^{188}\text{Re}$ -HAb18 F(ab')<sub>2</sub> was located specially in hepatoma, to establish the pharmacokinetic model and get the parameters of pharmacokinetics.

## MATERIALS AND METHODS

### Animals

Five-week Balb/c nude mice (derived from Experimental Animals Center of our university) were implanted with  $1 \times 10^7$  (0.2 mL) human hepatocellular carcinoma (HCC) cells in the right thigh. When the diameter of the tumors reached 1 cm, the tumor bearing mice would be investigated further.

### Monoclonal antibody fragment

HAb18 F(ab')<sub>2</sub> fragment was generated by pepsin digestion and phenyl-sepharose HP column purification with a relative molecular mass of 110,000. The solution containing the antibody fragment was concentrated by lyophilization and reconstituted with distilled water.



### Isotope

A 7.4GBq  $^{188}\text{W}/^{188}\text{Re}$  generator was eluted with normal saline.

### Radiolabeling

The antibody concentrated at  $5\text{g}\cdot\text{L}^{-1}$  was reduced by reaction with a molar excess of 2-ME at  $4^\circ\text{C}$  for 20-30 min. The reduced antibody was isolated from reductant through a PD-10 column (Pharmacia) equilibrated with  $0.05\text{mol}\cdot\text{L}^{-1}$  acetate-buffered saline.

For labeling, the reduced HAb18 F(ab')<sub>2</sub> was mixed with glucoheptonate (GH) solution,  $\text{SnCl}_2$  solution, and 50-100 $\mu\text{L}$  perhenium solution for 2-3 h at  $37^\circ\text{C}$  before it was analyzed by Whatman 3MM paper chromatography which was then developed in  $100\text{g}\cdot\text{L}^{-1}$  trichloroacetic acid (TCA). R<sup>a</sup>-f (distance of some composition moved/distance of extended reagent moved) values for  $100\text{g}\cdot\text{L}^{-1}$  TCA are: mAb 0.0,  $^{188}\text{Re}$ -GH 0.7, and  $^{188}\text{ReO}_4$  0.7. Labeled mAb was differentiated from  $^{188}\text{Re}$  colloid by the method of Thrall *et al* [33]. The same strips impregnated with 10-20  $\text{g}\cdot\text{L}^{-1}$  human serum albumin before development with 5V:2V:1V; water: ethanol:  $5\text{mol}\cdot\text{L}^{-1}$   $\text{NH}_4\text{OH}$  (volum ratio). Colloid remained on the bottom of the strip while mAb-bound isotope migrated with the solvent front.

### Immunoreactivity assessment

The *in vitro* immunoreactivity of the radiolabeled HAb18 F(ab')<sub>2</sub> was evaluated by a live cell assay [9]. Briefly,  $5\times 10^9\cdot\text{L}^{-1}$  HCC cells were centrifuged at  $1000\text{r}\cdot\text{min}^{-1}$  for 5 min and washed twice with  $1\text{g}\cdot\text{L}^{-1}$  bovine serum albumin (BSA) in PBS, then 5 serial 1:2 dilutions were made up in  $10\text{g}\cdot\text{L}^{-1}$  BSA in Eppendorf tubes precoated with BSA. Radiolabeled HAb18 F(ab')<sub>2</sub> at a mass concentration of  $40\mu\text{g}\cdot\text{L}^{-1}$  in  $10\text{g}\cdot\text{L}^{-1}$  BSA was added using a volume equal to half the volume of cell suspension. The total volume of cell-binding assay solution was 0.3 mL. After incubation for 2 h at  $37^\circ\text{C}$ , the total as well as the cell-bound radioactivity were counted in a gamma counter.

### Study of biodistribution in nude mice

Fifteen hepatoma-bearing nude mice were divided into 5 groups randomly, the mice were tail-vein injected via tail vein with  $1.85\text{MBq }^{188}\text{Re}$ -HAb18 F(ab')<sub>2</sub> in a volume of 0.1 mL and then they were sacrificed at 1, 4, 18, 24 and 48h (3 mice at each time). Samples of tumor, heart, liver, spleen, lung, kidney, large intestine, small intestine, muscle, bone were taken and weighed carefully. In addition, the blood sample was drawn from the heart. The radioactive concentrations in tissues were calculated and expressed as percent injected dose per gram (%ID·g<sup>-1</sup>). The radioactivity of tumor/no tumor (T/NT) was also calculated.

### Pharmacokinetics

The concentrations of blood and other organs were mounted by 3P97 software to get the parameters of pharmacokinetics and established the mode of pharmacokinetics was established.

## RESULTS

Table 1 shows the biodistribution of  $^{188}\text{Re}$ -HAb18 F(ab')<sub>2</sub>. The blood concentration was measured by 3P97 software, which fits the 1-compartment model (Table 3). Figure 1 shows the curve of concentration-time in nude mice, and Table 2 shows the parameters of pharmacokinetics. The half-time(h) of each tissue was: tumor (32.99), blood (2.99), lung (5.67), bone (11.76), muscle (9.22), small intestine (7.47), large intestine (15.08), heart (2.29), liver (5.67), spleen (19.76), and kidney (11.53). Table 4 illustrates the influence of various concentrations of  $\text{SnCl}_2$  and GH on the free  $^{188}\text{ReO}_4$  amounts, colloid amounts and labeling efficiency.

Optimal complexation with labeling efficiency of 91.7% was achieved in  $0.8\text{mol}\cdot\text{L}^{-1}$  GH and  $2\text{g}\cdot\text{L}^{-1}$   $\text{SnCl}_2$  solution. As shown in Figure 2, the immunoreactive fraction, 0.78 was determined by plotting the inverse of the bound fraction as compared with the inverse of the cell concentration, which is based on the assumption that the total antigen concentration (i.e., cell density) is a good approximation for the free antigen concentration.

**Table 1** Biodistribution of  $^{188}\text{Re}$ -HAb18 F(ab')<sub>2</sub> in hepatoma-bearing nude mice

| Tissue          | T(post-inj)/h | $^{188}\text{Re}$ -HAb18 F(ab') <sub>2</sub> |            |
|-----------------|---------------|----------------------------------------------|------------|
|                 |               | %ID·g <sup>-1</sup> ( $\bar{x}\pm s$ )       | T/NT ratio |
| Tumor           | 1             | $3.01\pm 0.89$                               | ND         |
|                 | 4             | $3.94\pm 0.82$                               | ND         |
|                 | 18            | $3.43\pm 0.28$                               | ND         |
|                 | 24            | $1.96\pm 0.43$                               | ND         |
|                 | 48            | $0.99\pm 0.32$                               | ND         |
| Blood           | 1             | $4.58\pm 0.63$                               | 0.66       |
|                 | 4             | $1.83\pm 0.10$                               | 2.15       |
|                 | 18            | $0.21\pm 0.04$                               | 16.30      |
|                 | 24            | $0.18\pm 0.03$                               | 10.90      |
|                 | 48            | $0.05\pm 0.01$                               | 19.80      |
| Heart           | 1             | $1.60\pm 0.38$                               | 1.88       |
|                 | 4             | $0.80\pm 0.10$                               | 4.92       |
|                 | 18            | $0.36\pm 0.03$                               | 9.53       |
|                 | 24            | $0.30\pm 0.02$                               | 6.53       |
|                 | 48            | $0.21\pm 0.03$                               | 4.71       |
| Liver           | 1             | $2.07\pm 0.40$                               | 1.45       |
|                 | 4             | $1.57\pm 0.31$                               | 2.51       |
|                 | 18            | $0.77\pm 0.12$                               | 4.45       |
|                 | 24            | $0.66\pm 0.10$                               | 2.97       |
|                 | 48            | $0.47\pm 0.13$                               | 2.11       |
| Spleen          | 1             | $1.22\pm 0.25$                               | 2.47       |
|                 | 4             | $0.91\pm 0.22$                               | 4.33       |
|                 | 18            | $0.47\pm 0.07$                               | 7.30       |
|                 | 24            | $0.45\pm 0.08$                               | 4.36       |
|                 | 48            | $0.41\pm 0.10$                               | 2.40       |
| Lung            | 1             | $1.45\pm 0.23$                               | 2.08       |
|                 | 4             | $0.86\pm 0.29$                               | 4.58       |
|                 | 18            | $0.19\pm 0.04$                               | 18.10      |
|                 | 24            | $0.18\pm 0.04$                               | 10.90      |
|                 | 48            | $0.14\pm 0.05$                               | 7.07       |
| Kidney          | 1             | $59.81\pm 14.52$                             | 0.05       |
|                 | 4             | $47.83\pm 12.87$                             | 0.08       |
|                 | 18            | $18.72\pm 4.94$                              | 0.18       |
|                 | 24            | $15.80\pm 0.99$                              | 0.12       |
|                 | 48            | $7.31\pm 2.10$                               | 0.13       |
| Large intestine | 1             | $1.36\pm 0.38$                               | 2.21       |
|                 | 4             | $0.93\pm 0.24$                               | 4.24       |
|                 | 18            | $0.57\pm 0.06$                               | 6.02       |
|                 | 24            | $0.45\pm 0.00$                               | 4.36       |
|                 | 48            | $0.18\pm 0.03$                               | 5.50       |
| Small intestine | 1             | $1.61\pm 0.43$                               | 1.87       |
|                 | 4             | $0.88\pm 0.29$                               | 4.24       |
|                 | 18            | $0.33\pm 0.05$                               | 10.40      |
|                 | 24            | $0.29\pm 0.05$                               | 6.76       |
|                 | 48            | $0.13\pm 0.05$                               | 7.62       |
| Muscle          | 1             | $0.74\pm 0.29$                               | 4.07       |
|                 | 4             | $0.44\pm 0.12$                               | 8.95       |
|                 | 18            | $0.19\pm 0.08$                               | 18.10      |
|                 | 24            | $0.16\pm 0.06$                               | 12.25      |
|                 | 48            | $0.05\pm 0.02$                               | 19.80      |
| Bone            | 1             | $1.03\pm 0.31$                               | 2.92       |
|                 | 4             | $0.68\pm 0.12$                               | 5.79       |
|                 | 18            | $0.31\pm 0.09$                               | 11.06      |
|                 | 24            | $0.27\pm 0.02$                               | 7.26       |
|                 | 48            | $0.16\pm 0.02$                               | 6.19       |

ND: not done

**Table 2** Pharmacokinetic parameters of <sup>188</sup>Re-HAb18 F(ab')<sub>2</sub> in hepatoma-bearing nude mice

| Parameter             | Unit                                   | Value | Standard error |
|-----------------------|----------------------------------------|-------|----------------|
| C0                    | 1×10 <sup>9</sup> Bq·L <sup>-1</sup>   | 6.18  | 3.14E-01       |
| Ke                    | h <sup>-1</sup>                        | 0.30  | 2.88E-02       |
| Vd                    | 1×10 <sup>-9</sup> L·Bq <sup>-1</sup>  | 1.49  |                |
| T <sub>1/2</sub> (Ke) | h                                      | 2.29  |                |
| AUC                   | 1×10 <sup>9</sup> Bq·h·L <sup>-1</sup> | 20.49 |                |
| CL                    | 1×10 <sup>-3</sup> L·h <sup>-1</sup>   | 0.45  |                |

CO: Concentration at zero time Ke: Elimination rate constant

Vd: Apparent volume of distribution T<sub>1/2</sub>: Half-life time

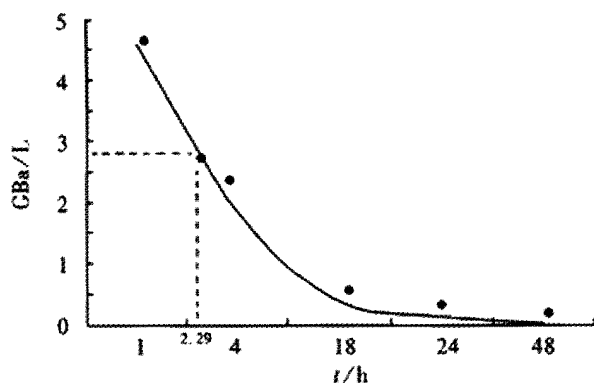
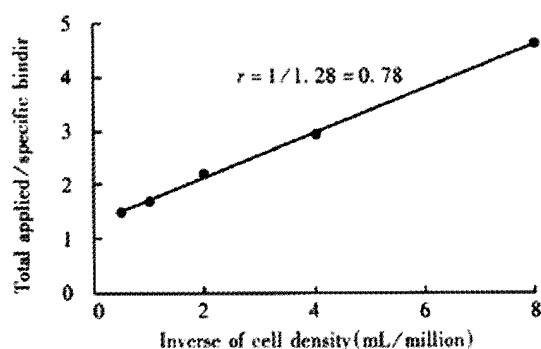
AUC: Area under the curve CL: Clearance

**Table 3** Criteria for goodness of fitting for mean

| REC No. | Mean No | WT   | No. of camp | Weighted sum of squarers | R      | R Squares | Goodness of fit | Max error C-CI | Max error % | AIC    |
|---------|---------|------|-------------|--------------------------|--------|-----------|-----------------|----------------|-------------|--------|
| 1       | 1       | 1    | 1           | 0.672E-01                | 0.9993 | 0.9955    | 0.150           | 0.18           | 100.00      | -9.499 |
| 2       | 1       | 1/c  | 1           | 0.329E+00                | 0.9856 | 0.9781    | 0.331           | 0.52           | 99.1        | -1.560 |
| 3       | 1       | 1/cc | 1           | 0.119E+01                | 0.9200 | 0.9207    | 0.630           | 3.58           | 78.2        | 4.877  |

**Table 4** Effect of various concentration of SnCl<sub>2</sub> and GH on free <sup>188</sup>ReO<sub>4</sub> amounts, colloid amounts and labeling efficiency

| Concentration                           |     | <sup>188</sup> ReO <sub>4</sub> | Colloid | Labeling efficiency(%) |
|-----------------------------------------|-----|---------------------------------|---------|------------------------|
| aSnCl <sub>2</sub> (g·L <sup>-1</sup> ) | 8   | 0.3                             | 3.6     | 90.9                   |
|                                         | 4   | 0.4                             | 2.8     | 90.1                   |
|                                         | 2   | 9.7                             | 2.1     | 82.7                   |
|                                         | 1   | 21.8                            | 1.2     | 71.2                   |
| bGH (mol·L <sup>-1</sup> )              | 0.8 | 1.1                             | 1.1     | 91.7                   |
|                                         | 0.4 | 12.5                            | 2.5     | 78.8                   |
|                                         | 0.2 | 16.6                            | 2.8     | 72.7                   |
|                                         | 0.1 | 20.6                            | 4.1     | 71.3                   |

<sup>a</sup>Molar ratio of 2-ME: F(ab')<sub>2</sub> = 400:1, Concentration of GH=0.5 mol·L<sup>-1</sup><sup>b</sup>Molar ratio of 2-ME: F(ab')<sub>2</sub> = 400:1, Concentration of SnCl<sub>2</sub>=2 g·L<sup>-1</sup>**Figure 1** Concentration-time curve of <sup>188</sup>Re-HAb18 F(ab')<sub>2</sub> in nude mice**Figure 2** Binding assay for determination of immunoreactive fraction of <sup>188</sup>Re-labeled HAb18 F(ab')<sub>2</sub>

## DISCUSSION

The occurrence of hepatoma is high in Southeast Asia, East Africa and Middle Africa. In China, hepatoma is one of the most three common cancers related death, but there is no effective treatment<sup>[34-45]</sup>. The therapy of hepatoma includes surgical operation, chemotherapy and radiotherapy. Targeting diagnosis and therapy of hepatoma with anti-hepatoma Mab have been developed quickly, giving a hopeful prospect to hepatoma treatment. Our research focuses on the targeting therapy of hepatoma.<sup>[46-48]</sup> <sup>188</sup>Re is a generator-produced radioisotope which can be obtained. There were some studies on the biodistribution and pharmacokinetics of <sup>188</sup>Re-mAb. Safavy *et al*<sup>[49]</sup> have reported biodistribution of <sup>188</sup>Re-labeled trisuccin-HuCC49 and trisuccin-C49deltaCh2 conjugates in athymic nude mice bearing intraperitoneal colon cancer xenografts. <sup>188</sup>Re-labeled mAb was injected, and the mice were sacrificed 24h postinjection. Biodistribution of the radiolabeled mAb at 24h after injection showed median tumor uptake values of 23.5% ID·g<sup>-1</sup> and 17.6% ID·g<sup>-1</sup> for the <sup>188</sup>Re-C49deltaCh2 and <sup>188</sup>Re-HuCC49, respectively. Yang *et al*<sup>[50]</sup> have prepared the conjugate of staphylococcal enterotoxin A (SEA) protein which is a bacterial Sag and the F(ab')<sub>2</sub> fragment of HAb18. The F(ab')<sub>2</sub> fragment of mAb HAb18 was prepared by papain digestion method. The conjugate of mAb HAb18 F(ab')<sub>2</sub> fragment and SEA was prepared with chemical conjugating reagent N-succinimidyl-1-(3-(2-pyridyldithio) propionate (SPDP) and purified through chromatography column Superose 12 with FPLC system. The molecular mass was identified with SDS-PAGE assay, the antibody activity of in the conjugate was determined by indirect immunocytochemical ABC method. SEA is a protein, the method of labeling is indirect, SEA and antibody are conjugated by SPDP. <sup>188</sup>Re's labeling method is direct, it is more convenient and quicker than indirect method. In the animal experiment, <sup>188</sup>Re-HAb18F(ab')<sub>2</sub> can inhibit the growth of tumor, but the pharmacokinetics of <sup>188</sup>Re-HAb18F(ab')<sub>2</sub> in animal is seldom reported.

<sup>188</sup>Re-HAb18F(ab')<sub>2</sub> can last a long time at a high level (Table 1). The maximal ratio of tumor: blood was at 48h, and maximal ratio of tumor: liver was at 18h. From Table 1, we can also find that after 1, 4, and 24 h (iv) injection, the radio percent of tumor is 3.83%, 6.48%, and 9.74%, the liver is 1.64%, 2.59% and 3.19%, the kidney is 76.24%, 78.8% and 76.3% respectively, showing that the antibody and its fragments were eliminated from kidney<sup>[51-52]</sup>. The half-time of <sup>188</sup>Re-HAb18 F(ab')<sub>2</sub> in the tumor was 32.99h, it was longer in tumor than that in other organs, this indicated that <sup>188</sup>Re-HAb18 F(ab')<sub>2</sub> was located in tumor, the rate of decay was low. It also showed that the mAb was specifically combined with tumor tissues and its harmness to normal tissues was low. Pharmacokinetic parameters (AUC, blood clearance, half-life, etc) were generated using the 3P97 software.

From 3P97 software, we can see the pharmacokinetics of conform to a 1-compartment model. Table 3 shows the criteria for goodness of fitting. we can judge the compartments from R squares, goodness of fit and AIC. 1, 1/C, 1/C/C represented three weights. To the same weight, when the F test has marked significance ( $P < 0.05$  or  $P < 0.01$ ), we should choose the compartment of small AIC, and when the F test has not prominent significance ( $P > 0.05$ ), we should choose the small compartment.<sup>[53]</sup> From Table 3, it can be seen that the 1-compartment model is the best. <sup>188</sup>Re-HAb18 F(ab')<sub>2</sub> can distribute to the whole body instantly. The elimination rate was corresponded to the concentration of the drug. The higher the concentration was, the higher the speed of elimination was.

The half-time was 32.99h in tumor, being much longer than that in any other organs. It showed that <sup>188</sup>Re-HAb18 F(ab')<sub>2</sub> was located specifically in hepatoma and the elimination was low. It also showed the higher selective reactivity of HAb18 F(ab')<sub>2</sub> with hepatoma, the

harmness to other organs was small. The half-time was 2.29h in blood, and was 32.99h in tumor, the radioation of blood can decrease more rapidly than that of the tumor. The half-time of  $^{188}\text{Re}$  was 17h, which was also lower than that in blood, so the  $^{188}\text{Re}$  can be eliminated through the blood. It has excellent value in the clinical therapy.<sup>[54-62]</sup>

Carrier-free  $^{188}\text{Re}$  is one of  $\beta$  emitting radionuclides recommended for RAIT because of suitable decay characteristics and availability from  $^{188}\text{W}/^{188}\text{Re}$  generator. Some methods are reported in the literature for labeling mAb with  $^{188}\text{Re}$  which imitate the labeling method of  $^{99}\text{Tcm}$ .  $^{188}\text{Re}$  eluted from generator will not bind to organic ligands without reduction to a lower oxidation state. We selected  $\text{SnCl}_2$  as reductant and GH as transfer ligand and stablizer to avoid Sn- or Re-collide formation. Table 1 shows that the concentration of  $\text{SnCl}_2$  and GH solutions is an important parameter to obtain good labeling results. The low percentage of free  $^{188}\text{ReO}_4^-$  and radiocolloid shows that  $0.8 \text{ mol} \cdot \text{L}^{-1}$  GH and  $2 \text{ g} \cdot \text{L}^{-1}$   $\text{SnCl}_2$  are the optimal values. Under these conditions, the labeled HAb18 F(ab')<sub>2</sub> keeps its immunoreactivity (Figure 2).

We believe that a variety of factors make  $^{188}\text{Re}$  a potential alternative to other  $\beta$ -emitting radionuclides for RAIT. They include an efficient generator system and the direct labeling of IgG at high specific activity. The enhanced clearance of  $^{188}\text{Re}$ -IgG from the circulation and the retention of immunoreactivity and tumortargeting of the Re-mAb conjugate are also important factors. In addition, the low-energy (155keV, 15%)  $\gamma$  emission for imaging and the lack of accretion of metabolic products in nontarget tissues are important characteristics for further evaluation of  $^{188}\text{Re}$ -labeled antibodies for tumor therapy.

## REFERENCES

- Guhlke S, Beets AL, Oetjen K, Mirzadeh S, Biersack HJ, Knapp FF Jr. Simple new method for effective concentration of  $^{188}\text{Re}$  solutions from alumina-based  $^{188}\text{W}/^{188}\text{Re}$  generator. *J Nucl Med* 2000; 41: 1271-1278
- Jeong JM, Lee YJ, Kim YJ, Chang YS, Lee DS, Chung JK, Song YW, Lee MC. Preparation of rhenium-188-tin colloid as a radiation synovectomy agent and comparison with rhenium-188-sulfur colloid. *Appl Radiat Isot* 2000; 52: 851-855
- Kotzerke J, Glatting G, Seitz U, Rentschler M, Neumaier B, Bunjes D, Duncker C, Dohr D, Bergmann L, Reske-SN. Radioimmunotherapy for the intensification of conditioning before stem cell transplantation: differences in dosimetry and biokinetics of  $^{188}\text{Re}$ - and  $^{99\text{m}}\text{Tc}$ -labeled anti-NCA-95 mAbs. *J Nucl Med* 2000; 41: 531-537
- Sykes TR, Somayaji VV, Bier S, Woo TK, Kwok CS, Snieckus V, Noujaim AA. Radiolabeling of monoclonal antibody B43.13 with rhenium-188 for immunoradiotherapy. *Appl Radiat Isot* 1997; 48: 899-906
- Sharkey RM, Blumenthal RD, Behr TM, Wong GY, Haywood L, Forman D, Griffiths GL, Goldenberg DM. Selection of radioimmunoconjugates for the therapy of well-established or micrometastatic colon carcinoma. *Int J Cancer* 1997; 72: 477-485
- Roka R, Sera T, Pajor L, Thurzo L, Lang J, Csernay L, Pavics L. Clinical experience with rhenium-188 HEDP therapy for metastatic bone pain. *Orv Hetil* 2000; 141: 1019-1023
- Wunderlich G, Pinkert J, Andreeff M, Stintz M, Knapp FF Jr, Kropp J, Franke WG. Preparation and biodistribution of rhenium-188 labeled albumin microspheres B 20: a promising new agent for radiotherapy. *Appl Radiat Isot* 2000; 52: 63-68
- Zimmerman BE, Cessna JT, Unterweger MP, Li AN, Whiting JS, Knapp FF Jr. A new experimental determination of the dose calibrator setting for  $^{188}\text{Re}$ . *J Nucl Med* 1999; 40: 1508-1516
- Knapp FF Jr. Rhenium-188-a generator-derived radioisotope for cancer therapy. *Cancer Biother Radiopharm* 1998; 13: 337-349
- Hafeli UO, Roberts WK, Meier DS, Ciezki JP, Pauer GJ, Lee EJ, Weinhaus MS. Dosimetry of a W-188/Re-188 beta line source for endovascular brachytherapy. *Med Phys* 2000; 27: 668-675
- Juweid M, Sharkey RM, Swayne LC, Griffiths GL, Dunn R, Goldenberg DM. Pharmacokinetics, dosimetry and toxicity of rhenium -188-labeled anti-carcinoembryonic antigen monoclonal antibody, MN-14, in gastrointestinal cancer [see comments]. *J Nucl Med* 1998; 39: 34-42
- Junfeng Y, Duanzhi Y, Xiaofeng M, Zili G, Jiong Z, Yongxian W, Knapp FF Jr.  $^{188}\text{Re}$  Rhenium sulfide suspension: a potential radiopharmaceutical for tumor treatment following intra-tumor injection. *Nucl Med Biol* 1999; 26: 573-579
- Chen J, Giblin MF, Wang N, Jurisson SS, Quinn TP. In vivo evaluation of  $^{99\text{m}}\text{Tc}/^{188}\text{Re}$ -labeled linear alpha-melanocyte stimulating hormone analogs for specific melanoma targeting. *Nucl Med Biol* 1999; 26: 687-693
- Iznaga-Escobar N.  $^{188}\text{Re}$ -direct labeling of monoclonal antibodies for radioimmunotherapy of solid tumors: biodistribution, normal organ dosimetry, and toxicology. *Nucl Med Biol* 1998; 25: 441-447
- Palmedo H, Guhlke S, Bender H, Sartor J, Schoeneich G, Risse J, Grunwald F, Knapp FF Jr, Biersack HJ. Dose escalation study with rhenium-188 hydroxyethylidene diphosphonate in prostate cancer patients with osseous metastases. *Eur J Nucl Med* 2000; 27: 123-130
- Melendez Alafort L, Ferro Flores G, Arteaga Murphy C, Pedraza Lopez M, Gonzalez Zavala MA, Tendilla JJ, Garcia Salinas L. Labeling peptides with rhenium-188. *Int J Pharm* 1999; 182: 165-172
- van Zanten Przybysz I, Molthoff CF, Ross JC, Plaizier MA, Visser GW, Pijpers R, Kenemans P, Verheijen RH. Radioimmunotherapy with intravenously administered  $^{131}\text{I}$ -labeled chimerical monoclonal antibody Mov18 in patients with ovarian cancer. *J Nucl Med* 2000; 41: 1168-1176
- Behr TM, Behe M, Lohr M, Sgouros G, Angerstein C, Wehrmann E, Nebendahl K, Becker W. Therapeutic advantages of Auger electron-over beta-emitting radiometals radioiodine when conjugated to internalizing antibodies. *Eur J Nucl Med* 2000; 27: 753-756
- Clarke K, Lee FT, Brechbiel MW, Smyth FE, Old LJ, Scott AM. Therapy efficacy of anti-Lewis(y) humanized 3S193 radioimmunotherapy a breast cancer model: enhanced activity when combined with taxol chemotherapy. *Clin Cancer Res* 2000; 6: 3621-3628
- Barendsward EC, O'Donoghue JA, Larson SM, Tschmelitsch J, Welt S, Finn RD, Humm JL.  $^{131}\text{I}$  radioimmunotherapy and fractionated external beam radiotherapy: comparative effectiveness in a human tumor xenograft. *J Nucl Med* 1999; 40: 1764-1768
- Smith Jones PM, Vallabhaajousula S, Goldsmith SJ, Navarro V, Hunter CJ, Bastidas D, Bander NH. In vitro characterization of radiolabeled monoclonal antibodies specific for the extracellular domain of prostate-specific membrane antigen. *Cancer Res* 2000; 60: 5237-5243
- Juweid ME, Zhang CH, Blumenthal RD, Hajjar G, Sharkey RM, Goldenberg DM. Prediction of hematologic toxicity after radioimmunotherapy with  $^{131}\text{I}$ -labeled anticarcinoembryonic antigen monoclonal antibodies. *J Nucl Med* 1999; 40: 1609-1616
- Natowich DJ, Mardirossian G, Ruscowski M, Fogarasi M, Virzi F, Winnard Jr P. Directly and indirectly technetium-99m-labeled antibodies-a comparison of *in vitro* and animal *in vivo* properties. *J Nucl Med* 1993; 34: 109-119
- Colnot DR, Quak JJ, Roos JC, van Lingen A, Wilhelm AJ. Phase I therapy study of  $^{186}\text{Re}$ -labeled chimeric monoclonal antibody U36 in patients with squamous cell carcinoma of the head and neck. *J Nucl Med* 2000; 41: 1999-2010
- Lechner P, Lind P, Snyder M, Haushofer H. Probe-guided surgery for colorectal cancer. *Recent Results Cancer Res* 2000; 157: 273-280
- Willkomm P, Bender H, Bangard M, Decker P, Grunwald F, Biersack HJ. FDG PET and immunoscintigraphy with  $^{99\text{m}}\text{Tc}$ -labeled antibody fragments for detection of the recurrence of colorectal carcinoma. *J Nucl Med* 2000; 41: 1657-1663
- Line BR, Weber PB, Lukasiewicz R, Dansereau RN. Reduction of background activity through radiolabeling of antifibrin Fab' with  $^{99\text{m}}\text{Tc}$ -dextran. *J Nucl Med* 2000; 41: 1264-1270
- Amato R, Kim EE, Prow D, Andreopoulos D, Kasi LP. Radioimmunodetection of residual, recurrent or metastatic germ cell tumors using technetium-99 anti-(alpha-fetoprotein) Fab' fragment. *J Cancer Res Clin Oncol* 2000; 126: 161-167
- Bian HJ, Chen ZN and Deng JL. Direct technetium-99m labeling of anti-hepatoma monoclonal antibody fragment: a radioimmunoconjugate for hepatocellular carcinoma imaging. *World J Gastroenterol* 2000; 6: 348-352
- Dadachova E, Chapman J.  $^{188}\text{Re}(\text{V})$ -DMSA revisited: preparation and biodistribution of a potential radiotherapeutic agent with low kidney uptake. *Nucl Med Commun* 1998; 19: 173-181
- Schmidt PF, Smith SV and Bundesen PG.  $^{188}\text{Re}$  DD-3B6/22 Fab' for use in therapy of ovarian cancer: labeling and animal studies. *Nucl Med Biol* 1998; 25: 639-649
- Ferro-Flores G, Pimentel-Gonzalez G, Gonzalez-Zavala MA, Arteaga de Murphy C, Melendez Alafort L, Tendilla JJ, Croft BY. Preparation, biodistribution, and dosimetry of  $^{188}\text{Re}$ -labeled McAb ior ceal and its F(ab')<sub>2</sub> fragments by avidin-biotin strategy. *Nucl Med Biol* 1999; 26: 57-62
- Thrall JH, Freitas JE, Swanson D, Rogers WL, Clare JM, Brown M, Pitt B. Clinical comparison of cardiac blood pool visualization with technetium-99m red blood cells labeled *in vivo* and with technetium-99m human serum albumin. *J Nucl Med* 1978; 19: 796-803
- Qian S B, Li Y, Qian GX, Chen SS. Efficient tumor regression induced by genetically engineered tumor cells secreting interleukin-2 and membrane-

- expressing allogeneic MHC class I antigen. *J Cancer Res Clin Oncol* 2001; 127: 27-33
- 35 Dai WJ, Jiang HC. Advances in gene therapy of liver cirrhosis: a review. *World J Gastroenterol* 2001;7:1-8
  - 36 Cheng ML, Wu YY, Huang KF, Luo TY, Ding YS, Lu YY, Liu RC, Wu J. Clinical study on the treatment of liver fibrosis due to hepatitis B by IFN- $\alpha$ 1 and traditional medicine preparation. *World J Gastroenterol* 1999;5:267-269
  - 37 Kessel D, Caruso JA, Reiners JJ Jr. Potentiation of photodynamic therapy by ursodeoxycholic acid. *Cancer Res* 2000; 60: 6985-6988
  - 38 Yang SS, Wu CH, Chen TH, Huang YY, Huang CS. TT viral infection through blood transfusion: retrospective investigation on patients in a prospective study of post transfusion hepatitis. *World J Gastroenterol* 2000;6:70-73
  - 39 Kang MA, Kim KY, Seol JY, Kim KC, Nam MJ. The growth inhibition of hepatoma by gene transfer of antisense vascular endothelial growth factor. *J Gene Med* 2000; 2: 289-296
  - 40 Ma XD, Sui YF, Wang WL. Expression of gap junction genes connexin 32, connexin 43 and their proteins in hepatocellular carcinoma and normal liver tissues. *World J Gastroenterol* 2000;6:66-69
  - 41 Huang ZH, Zhuang H, Lu S, Guo RH, Xu GM, Cai J, Zhu WF. Humoral and cellular immunogenicity of DNA vaccine based on hepatitis B core gene in rhesus monkeys. *World J Gastroenterol* 2001;7:102-106
  - 42 Fang JN, Jin CJ, Cui LH, Quan ZY, Choi BY, Ki MR, Park HB. A comparative study on serologic profiles of virus hepatitis B. *World J Gastroenterol* 2001;7:107-110
  - 43 Tietze MK, Wuestefeld T, Paul Y, Zender L, Trautwein C, Manns MP, Kubicka S. IkappaBalpha gene therapy in tumor necrosis factor-alpha- and chemotherapy-mediated apoptosis of hepatocellular carcinomas. *Cancer Gene Ther* 2000; 7: 1315-1323
  - 44 Xu J, Mei MH, Zeng SE, Shi QF, Liu YM, Qin LL. Expressions of ICAM21 and its mRNA in sera and tissues of patients with hepatocellular carcinoma. *World J Gastroenterol* 2001;7:120-125
  - 45 Hu YP, Hu WJ, Zheng WC, Li JX, Dai DS, Wang XM, Zhang SZ, Yu HY, Sun W, Hao GR. Establishment of transgenic mouse harboring hepatitis B virus (adr subtype) genomes. *World J Gastroenterol* 2001;7: 111-114
  - 46 Qiu K, Wang BF, Chen ZN, Fang P, Liu CG, Wan WX, Liu YF. <sup>99m</sup>Tc-labeled HAB18 McAb Fab fragment for radioimmunodiagnosis in nude mice bearing human hepatocellular carcinoma. *World J Gastroenterol* 1998;4:117-120
  - 47 Chen ZN, Bian HJ, Jiang JL. Recent progress in anti-hepatoma monoclonal antibody and its application. *Huaren Xiaohua Zazhi* 1998;6:461-462
  - 48 Ickman S. Antibodies stage a comeback in cancer treatment. *Science* 1998;280:1196-1197
  - 49 Safavy A, Khazaeli MB, Safavy K, Mayo MS, Buchsbaum DJ. Biodistribution study of <sup>188</sup>Re-labeled trisuccin-HuCC49 and trisuccin-HuCC49deltaCh2 conjugates in athymic nude mice bearing intraperitoneal colon cancer xenografts. *Clin Cancer Res* 1999; 5: 2994-3000
  - 50 Yang LJ, Sui YF, Chen ZN. Preparation and activity of conjugate of monoclonal antibody HAB18 against hepatoma F(ab')<sub>2</sub> fragment and staphylococcal enterotoxin A. *World J Gastroenterol* 2001;7:216-221
  - 51 Duan XD, Chen ZN, Bian HJ, Wen AD, Feng Q. Pharmacokinetics of technetium-99m labeled anti-hepatoma monoclonal antibody HAB18 and its F(ab')<sub>2</sub> fragment in mice. *Zhongguo Yaoxue Zazhi* 2000;35:465-467
  - 52 Chen H, Gu SF, Xiao Zh, Zeng FD, Wu WZ, Zhang QH. Pharmacokinetics and bioavailability of sustained release capsules of nicardipine hydrochloride in healthy volunteers. *Zhongguo Yaolixue Tongbao* 2000; 16:107-110
  - 53 Lan Q, Huang Q, Zhuang DL, Wu YF, Sun ZF. Study on the pharmacokinetics of immunoradiotherapeutic agent S-MAb SZ39 in glioma-bearing nude mice. *Zhongguo Yaoxue Zazhi* 1999;34:683-686
  - 54 Hosono MN, Hosono M, Zamora PO. Localization of colorectal carcinoma by rhenium-188-labeled B72.3 antibody in xenograft mice. *Ann Nucl Med* 1998; 12:83-88
  - 55 Gustin JF, Loussouarn A, Bardies M, Gautherot E, Gruaz Guyon A, Sai Maurel C, Barbet J, Curtet C, Chatal JF, Faivre Chauvet A. Two-step targeting of xenografted colon carcinoma using a bispecific antibody and <sup>188</sup>Re-labeled bivalent hapten: biodistribution and dosimetry studies. *J Nucl Med* 2001; 42: 146-153
  - 56 Hosono MN, Hosono M, Mishra AK, Faivre Chauvet A, Gautherot E, Barbet J, Knapp F F, Chatal JF. Rhenium-188-labeled anti-neural cell adhesion molecule antibodies with 2-iminothiolane modification for targeting small-cell lung cancer. *Ann Nucl Med* 2000; 14: 173-179
  - 57 Bian HJ, Chen ZN, Lou C, Mi L, Wang J, Yue XL. <sup>188</sup>Re-labeled HAB18 F(ab')<sub>2</sub> of hepatoma radioimmunodiagnosis. *Zhongliu* 2000; 20:181-183
  - 58 Qingnuan L, Xiaodong Z, Rong S, Wenxin L. Preparation of (<sup>188</sup>Re) Re-AEDP and its biodistribution studies. *Appl Radiat Isot* 2000; 53: 993-997
  - 59 Kostarelos K, Emfietzoglou D. Tissue dosimetry of liposome-radionuclide complexes for internal radiotherapy: toward liposome-targeted therapeutic radiopharmaceuticals. *Anticancer Res* 2000; 20: 3339-3345
  - 60 Iznaga Escobar N, Torres LA, Morales A, Ramos M, Alvarez I, Perez N, Fraxedas R, Rodriguez O, Rodriguez N, Perez R, Lage A, Stabin MG. Technetium-99m-labeled anti-EGF-receptor antibody in patients with tumor of epithelial origin: I. Biodistribution and dosimetry for radioimmunotherapy. *J Nucl Med* 1998; 39: 15-23
  - 61 Blower PJ, Kettle AG, O'Doherty MJ, Coakley AJ, Knapp FF. <sup>99m</sup>Tc (V)DMSA quantitatively predicts <sup>188</sup>Re(V)DMSA distribution in patients with prostate cancer metastatic to bone. *Eur J Nucl Med* 2000; 27: 1405-1409
  - 62 Heppeler A, Froidevaux S, Eberle AN, Maecke HR. Receptor targeting for tumor localisation and therapy with radiopeptides. *Curr Med Chem* 2000; 7: 971-994

Edited by Ma JY

• GASTRIC CANCER •

# High-dose Iodized Oil Transcatheter Arterial Chemoembolization For Patients with Large Hepatocellular Carcinoma

Min-Shan Chen, Jin-Qing Li, Ya-Qi Zhang, Li-Xia Lu, Wei-Zhang Zhang, Yun-Fei Yuan, Yong-Ping Guo, Xiao-Jun Lin, Guo-Hui Li

Min-Shan Chen, Jin-Qing Li, Ya-Qi Zhang, Yun-Fei Yuan, Yong-Ping Guo, Xiao-Jun Lin, Guo-Hui Li, Department of Hepatobiliary Cancer Center of Sun Yet-sen University of Medical Sciences, Guangzhou 510060, China

Li-Xia Lu, Wei-Zhang Zhang, Department of Radiology Cancer Center of Sun Yet-sen University of Medical Sciences, Guangzhou 510060, China

Supported by the "9-5" National Major Project of National Committee of Sciences and Technology, No.96-907-03-02

Correspondence to: Dr. Min-Shan Chen, Department of Hepatobiliary Cancer Center of Sun Yet-sen University of Medical Sciences, 651 Dongfeng Road East, Guangzhou 510060, China. Minshan@8848.net  
Telephone: +86-13902241061 Fax: +86-20-87754506

Received 2001-08-23 Accepted 2001-09-08

## Abstract

**AIM:** To conduct a randomized trial to evaluate the role of using high-dose iodized oil transcatheter arterial chemoembolization (TACE) in the treatment of large hepatocellular carcinoma (HCC).

**METHODS:** From January 1993 to June 1998, 473 patients with unresectable hepatocellular carcinoma were divided into two groups: 216 patients in group A received more than 20mL iodized oil during the first TACE treatment; 257 patients in group B received 5-15mL iodized oil in the same way. The Child's classification and ICG-R15 for evaluating the liver function of the patients were done before the treatment. During the TACE procedure the catheters was inserted into the target artery selectively and the tumor vessels were demonstrated with contrast medium in the hepatic angiography. The anticancer drug mixed with iodized oil (Lipiodol) were Epirubicin and Mitomycin. In group A, 112 cases received 20-29mL Lipiodol in the first procedure, 85 cases 30-39mL, 19 cases more than 40mL. The largest dose was 53 mL and the average dose was 28.3mL. In group B, 119 cases received 5-10mL Lipiodol, 138 cases received 11-15mL, and the average dose was 11.8mL.

**RESULTS:** High-dose Lipiodol chemoembolization caused tolerable side effects and a little hurt to the liver function in the patients with Child grade A or ICG-R15 <20. But the patients with child grade B or ICG-R15 >20 had higher risk of liver failure after high-dose TACE. More type I and type II lipiodol accumulations in CT scan after 4 weeks of TACE were seen in the group A patients than those in the group B patients ( $P < 0.01$ ). The resection rate and complete tumor necrosis rate in group A were higher than those of group B ( $P < 0.05$ ). The 1-, 2-, 3-year survival rates of group A patients with Child grade A were 79.2%, 51.8% and 34.9%, respectively, better than those of group B ( $P < 0.001$ ).

**CONCLUSION:** High-dose Lipiodol can result in more complete tumor necrosis by blocking both arteries and small

portal vein of the tumor. High-dose TACE for treatment of large and hypervascular hepatocellular carcinoma is practically acceptable with the better effect than the routine dose. For the patients with large and hypervascular tumor of Child grade A liver function or ICG-R15 less than 20%, oily chemoembolization with 20-40mL Lipiodol is recommended.

Chen MS, Li JQ, Zhang YQ, Lu LX, Zhang WZ, Yu YF, Guo YP, Lin XJ, Li GH. High-dose Iodized Oil Transcatheter Arterial Chemoembolization For Patients with Large Hepatocellular Carcinoma. *World J Gastroenterol* 2002;8(1):74-78

## INTRODUCTION

Hepatocellular carcinoma (HCC) is one of the most common malignant tumors in human beings. It was estimated that in 1985, about 315, 000 new cases of primary liver cancer occurred worldwide, accounting for 4.1% of all human cancer cases<sup>[1]</sup>. In the same year, 312,000 patients died as a consequence of the disease. In China, HCC is responsible for 130,000 deaths every year and is the second cause of the cancer deaths<sup>[2]</sup>. The crude mortality of HCC was 20.4 per 100,000 population, accounting for 18.8% of the total cancer deaths in 1990-1992<sup>[3]</sup>.

About 80% of HCC are associated with cirrhosis that makes treatment more difficult<sup>[4]</sup>. Surgical resection is the best options for the treatment of HCC and the 5-year survival rate after hepatectomy was about 20%-40%<sup>[5]</sup>. But in only 20% of HCC patients the surgical resection is feasible. About 60%-70% HCC were in late stages at the time of diagnosis and had lost the chance of operation<sup>[6-8]</sup>. Transcatheter arterial chemoembolization (TACE) is one of the most common method for the treatment of the unresectable HCC<sup>[9,10]</sup>. The results achieved by using TACE were much better than those of systemic or regional chemotherapy<sup>[11, 12]</sup>. TACE with anticancer agent suspended in an oily substance has become one of the standard forms of treatment for advanced HCC. In the treatment, iodized oil is used as an embolic agent and carrier of anticancer drugs<sup>[13,14]</sup>. After entering into the small arteries and peritumoral sinusoid of HCC through a catheter, the iodized oil can be retain there to block the terminal blood flow. The more iodized oil entering into the small arteries and peritumoral sinusoid of HCC, the more complete blocking of the terminal blood supply to the cancer will occur<sup>[15,16]</sup>. But in such ease more iodized oil may flow into the portal vein causing infarction or necrosis in the noncancerous hepatic tissue, and thus lead to the more liver dysfunction. Generally the amount of iodized oil recommended is about 5-15 mL at each procedure for fear that more iodized oil could lead to liver dysfunction<sup>[17,18]</sup>. In clinical practice, most patients who received TACE were those with large HCC. For the large and hypervascular liver tumor, using 5-15 mL iodized oil is not enough to attain complete filling of tumor vessel bed. To get a full blocking of the tumor vessels, a larger volume of iodized oil is necessary. Basing on the experience of our clinical practice and the good evaluation of liver function, we conducted a high-dose (more



than 20mL) iodized oil TACE for the large HCC.

## MATERIALS AND METHODS

### Eligibility of patients

From January 1993 to June 1998, 473 patients with large HCC who were eligible for this study were treated at the Tumor Hospital of Sun Yat-sen University of Medical Sciences. The eligibility criteria for entering this study were as follows: ① a diagnosis of HCC was established on the basis of the patient's high serum alpha-fetoprotein (AFP) value, findings obtained at computed tomography(CT) scan and clinical manifestations; ② the largest diameter of the tumor exceeded 5 cm; ③ there was no evidence of portal trunk occlusion by thrombosis, extrahepatic metastasis, jaundice or ascites; ④ during the TACE procedure the catheter was successfully inserted into the target artery selectively as proved by angiography. We excluded patients who had Child's C grade liver function or ICG-R15 (indocyanine green retention rate in 15 min)>30%. All patients were randomly divided into two treatment groups. In Group A, 216 patients received more than 20mL of iodized oil in the first TACE, and in Group B, 257 patients received 5-15mL.

### Clinical Characteristics of the patients

The clinical characteristics of the patients including age, sex, size of tumor, thrombosis in portal branch, AFP, serum alanine aminotransferase(ALT), Child's grading, ICG-R15 were collected before the treatment. The patients in the two groups did not differ significantly with respect to these clinical characteristics (Table 1).

**Table 1** Pretreatment clinical characteristics of 473 patients

| Characteristics   | Group A<br>(N=216) | Group B<br>(N=257) | Probability<br>value |
|-------------------|--------------------|--------------------|----------------------|
| Age               |                    |                    |                      |
| Mean              | 44.6               | 45.1               | 0.348                |
| Range             | 22-67              | 24-71              |                      |
| Sex               |                    |                    |                      |
| Male              | 213                | 246                | 0.065                |
| Female            | 3                  | 11                 |                      |
| Diameter of tumor |                    |                    |                      |
| 6-9.9cm           | 32                 | 9                  | 0.133                |
| 10-14.9cm         | 105                | 135                |                      |
| ≥15cm             | 79                 | 73                 |                      |
| Thrombosis        |                    |                    |                      |
| Yes               | 54                 | 81                 | 0.118                |
| No                | 162                | 176                |                      |
| AFP (μg/L)        |                    |                    |                      |
| ≥400              | 91                 | 114                | 0.626                |
| <400              | 125                | 143                |                      |
| ALT               |                    |                    |                      |
| <40               | 117                | 109                | 0.023                |
| 40-79             | 78                 | 103                |                      |
| 80-119            | 17                 | 39                 |                      |
| ≥120              | 4                  | 7                  |                      |
| Child's class     |                    |                    |                      |
| A                 | 203                | 238                | 0.553                |
| B                 | 13                 | 19                 |                      |
| ICG-R15*          |                    |                    |                      |
| <10               | 71                 | 89                 | 0.314                |
| 10-19             | 127                | 137                |                      |
| 20-29             | 18                 | 31                 |                      |

\*ICG-R15 refers to the indocyanine green retention rate at 15 minutes

### Methods of chemoembolization

During the hepatic angiography that demonstrated the tumor vessels and tumor contour, the catheter was inserted selectively into the target artery. The catheter tip was placed as close as possible to the tumor for attaining the high-selective embolization<sup>[19]</sup>. The first 5-10 mL iodized oil (Lipiodol, Laboratoire Guerbet, Aulnay-sous-Bois, France) were mixed with anticancer drugs, Epirubicin(50 mg·m<sup>-2</sup>) and Mitomycin(8mg·m<sup>-2</sup>), to form an emulsion. The emulsion was slowly injected under fluoroscopic control. The remainder Lipiodol was added according to the state of accumulation of the emulsion within the tumor at the first injection, speed of blood flowing to the tumor, and appearance of portal vein around the tumor (Figure 1). Gelatin sponge impregnated with contrast medium was injected into the tumor, if the blood flow to the tumor wasn't slowed down enough after the Lipiodol injection<sup>[20]</sup>. Any embolization was terminated when the blood flow to the tumor had slowed down.

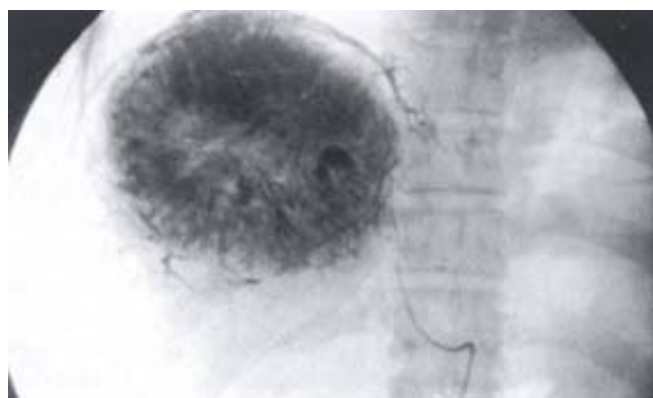


**Figure 1** Portal vein branches around the tumor as visualized by high-dose iodized oil

In group A, 112 cases received 20-29mL Lipiodol in the first procedure, 85 cases 30-39mL, 19 cases more than 40mL; the largest dose was 53 mL and the average dose was 28.3mL. In group B, 119 cases received 5-10mL Lipiodol and 138 cases received 11-15mL; the average dose was 11.8mL.

### Follow-up

Four weeks after TACE, the therapeutic effect was assessed by double phase CT scan and AFP test. The CT was performed after a bolus administration of 50-100mL of contrast material<sup>[21]</sup>. The pattern of Lipiodol accumulation on CT were classified into following four kinds according to Nishimine<sup>[22]</sup>: type I, homogeneous; type II, defective; type III, inhomogeneous; and type IV, only slight accumulation, if any (Table 2). Type I was further subgrouped into type I a (with accumulation around the tumor) and type I b (without accumulation around the tumor). AFP was tested at 4 wk intervals after first TACE.

| Type | I           | II        | III    | IV                     |
|------|-------------|-----------|--------|------------------------|
| L-CT |             |           |        |                        |
| L-CT |             |           |        |                        |
|      | Homogeneous | Defective | Uneven | No/slight Accumulation |

A repeat TACE and other therapies were performed depending on the conditions of the patient after the first TACE. 11 patients underwent totally 5 times TACE; 32 underwent 4; 139 underwent 3; 207 underwent 2; 84 underwent 1. 59 patients underwent percutaneous ethanol injection(PEI) after TACE and 46 patients received surgical

resection. Survival was measured from date of the first treatment until death. The causes of death were determined for 347 patients during the follow-up period. When a patient died from advanced carcinoma, hepatic failure or a deterioration of his or her general condition shortly after the procedure, the patients death was considered to be due to treatment failure.

### Statistical analysis

The changes of liver dysfunction and CT type was analyzed by chi-square test. Cumulative survival rates were estimated by the Kaplan-Meier method. The relationship between each of the variable and survival was assessed by log rank test. "Significant" indicated a calculated two-tailed value of  $<0.05$ .

## RESULTS

### Side Effects

The most frequent side effects of TACE were fever and abdominal pain. In Group A abdominal pain occurred in 53.7% of the patients, fever in 71.3%, vomiting in 20.8%, appetite loss in 41.7% and upper digestive tract bleeding in 0.93%. In group B, abdominal pain occurred in 49.8% patients, fever in 47.5%, vomiting in 14.8%, appetite loss in 42.8% and upper digestive bleeding in 1.17%. The toxic effect of the drugs on the hemopoietic system reflected in slight decreases in the white blood cell counts, platelet counts, and hemoglobin levels of peripheral blood in both groups. Elevations in the serum alanine aminotransferase, alkaline phosphatase, or total bilirubin levels were seen in the patients of both groups, but the changes were not severe and no significant differences were found between the two groups. Liver dysfunction occurred in 24 patients of group A and in 28 patients of group B. The patients with child's grade B or ICG-R15  $>20$  had higher risk of liver failure after high-dose TACE (Table 2).

**Table 2** The comparison of liver dysfunction\*\* in two group

| Group   | Child-Pugh Classification |              | ICG-R15    |              |              |
|---------|---------------------------|--------------|------------|--------------|--------------|
|         | A                         | B            | $<10\%$    | 10-19%       | $\geq 20\%$  |
| Group A | 5.9%(12/203)              | 92.3%(12/13) | 1.4%(1/71) | 7.9%(10/127) | 72.2%(13/18) |
| Group B | 5.5%(13/238)              | 84.2%(15/19) | 2.2%(2/89) | 5.8%(8/137)  | 58.1%(18/31) |

\*\*Liver dysfunction is referred to ascites, jaundice(Tbil  $>34.2\mu\text{mol/L}$ ), or hepatic encephalopathy

### CT and AFP

CT scan was done four weeks after TACE: In group A there were 77 cases of type I, 130 cases of type II, 9 cases of type III; whereas in group B there were 27 cases of type I, 108 cases of type II, 90 cases of type III and 32 cases of type IV (group A vs group B  $P<0.001$ , Figure 2). In group A, the AFP level in 78 of 91 AFP-positive patients ( $\geq 400\mu\text{g}\cdot\text{L}^{-2}$ ) had decreased and in 12 of them down to normal; in group B, 81 of 114 AFP-positive patients had their AFP decrease and in 9 down to normal ( $P<0.01$ ).

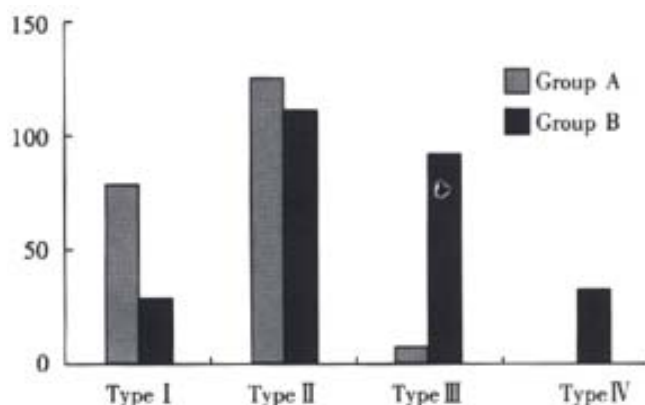


**Figure 2** Comparison of CT type between the two groups.

### Resection

After TACE, 47 cases achieved surgical resection in group A, and 19 of them were found to have complete tumor necrosis pathologically. In group B, 25 patients received surgical resection and only 4 cases were found to have complete tumor necrosis. The resection rate and complete tumor necrosis rate of group A were higher than those of group B ( $P<0.05$ ).

### Survival Rates

The 1-, 2-, 3-year cumulative survival rates of the patients with Child's grade A in group A were 79.2%, 51.8%, 34.9% and in group B was 59.1%, 26.7%, 14.9%, respectively (Figure 3). The cumulative survival rates were significantly better in group A than in group B ( $P<0.001$ ). The 1-, 2-, 3-year cumulative survival rates of the patients with Child's grade B in group A were 42.1%, 21.1%, 7.7% and in group B was 46.8%, 23.7%, 0%, respectively (no significantly difference in between the two groups).

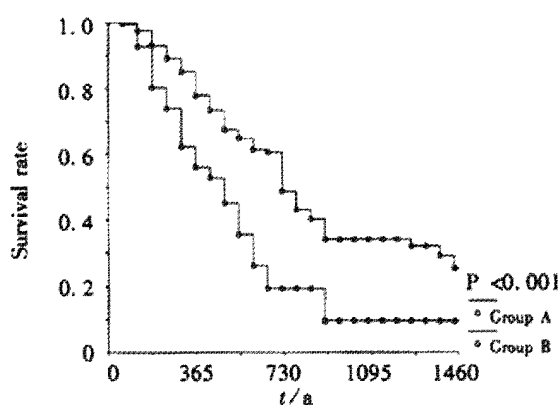


**Figure 3** Cumulative survival rates of patients with Child's A in two groups.

## DISCUSSION

For use in TACE, Iodized oil (mostly lipiodol) mixed with anticancer drugs has been reported to be one of the most effective agents<sup>[23,24]</sup>. Iodized oil plays an important role as an embolic agent. It not only occludes the small arteries supplying the tumor but also acts as the carrier bringing the drug to the tumor. The lipiodol can enter into the microcirculation of the tumor and stay there to stop the blood flow<sup>[25]</sup>. The experimental investigations in animal and human resected specimens revealed that the lipiodol could stay in the small artery, sinusoid, and small portal vein within the tumor. In general, the recommended amount of lipiodol is 5-15mL. The use of large volume of iodized oil is more prone to invade the normal liver parenchyma, causing more liver injury<sup>[26]</sup>. Matsuo<sup>[27]</sup> reported the relationship between the lipiodol dose and the tumor necrosis rates in 198 HCC cases. He found that the prognosis was better in the group of patients with big tumors in which the doses of lipiodol were correspondingly larger tumor diameter, but the total dose must not be more than 10mL in small HCC. Other authors<sup>[28,29]</sup> confirmed that the dose of iodized oil played an important role in TACE. A sufficiently high dose of Lp-TACE would be a factor of good tumor response, if the tumor was large. Therefore the volume of lipiodol is an important factor influencing the antitumor effect of TACE. The large and hypervascular liver tumors have vast vessel bed. So it is necessary to inject high-dose lipiodol to attain complete filling of tumor vessel bed. While the tumor 5cm in diameter needs 5mL lipiodol to fill the vessel bed, the 10cm tumor would need at least 8 times of lipiodol to do the same work. In this situation a high-dose of iodized oil must be used for complete filling of the large tumor<sup>[30,31]</sup>. Some portal branches around the tumors are displayed after the high-

dose lipiodol pooled into the tumor; this is considered to be the sign of complete arterial block. After a certain amount of lipiodol is pooled into the hepatic microcirculation and sinusoid, any additional volume of lipiodol enter into the branches of portal vein via the sinus between hepatic artery and portal vein. And then some lipiodol is seen in the small branches of portal vein around the tumor. As the amount of lipiodol delivered into artery increase, the portal vein branches become more prominent<sup>[32]</sup>. Prominent portal vein appearances were seen in 29% patients given 10 mL or less of lipiodol, in 67% with 10-20 mL, and in 86% with more than 20 mL. It was known that infiltrating portion and nonencapsulated daughter nodules of the tumor are nourished by both the portal vein and the hepatic artery. So even if the tumor arteries are successfully embolized, some tumor cells can survive because the portal vein blood supply still exists. This may be the reason for incomplete tumor necrosis with subsequent tumor recurrence<sup>[28,15]</sup>. High-dose lipiodol fully fills the sinus and stops the portal vein supply to tumor cells after the arteries are embolized. Embolization of both hepatic artery and small portal veins may cause complete necrosis of the tumor infiltrating portion and nonencapsulated daughter nodules<sup>[13,14]</sup>. The visualization of some portal vein tributaries around the tumor may be a sign of complete embolization.

After Lp-TACE it is important to estimate the amount and state of iodized oil accumulating within the tumor, because this has much bearing on the prognosis of the patients<sup>[33]</sup>. Matsuo<sup>[27]</sup> found that the volume of lipiodol infusion correlated with the CT type. If the lipiodol volume is greater than the tumor mass in the small HCC, more type I lipiodol accumulation will be seen in the CT scan after Lp-TACE. He suggested that the lipiodol volume should be greater than the tumor mass, but the maximum dose should be less than 10 mL for fear of liver dysfunction even in the large HCC. Nishimine<sup>[22]</sup> reported that tumors of CT type I have the highest cumulative survival rates and those of the type I have higher cumulative survival rates than type III and type IV. The iodized oil retention was again evaluated by using CT scan one month after TACE. It was found that the patients with iodized oil retention in the tumor greater than 50 per cent of tumor size survived longer than patients with retention of less than 50 per cent<sup>[34-36]</sup>. Our study showed that high-dose lipiodol could bring about more type I and type II lipiodol accumulation than a routine dose. Pathological study of resected specimen after TACE showed that the area of lipiodol retention in CT was the necrotic area of the tumor. The high-dose lipiodol would lead to more lipiodol retention in the necrotic tumor<sup>[37,38]</sup>.

For preventing severe side effects, attention must be paid. The liver reserve function must be evaluated by Child's grading and ICG-R15<sup>[39,40,41,42]</sup>. Our data showed that the liver dysfunction most frequently occurred in the patients with child's B or ICG-R15>20. The patients with Child's A or ICG-R15<20 were usually tolerant of 20-40mL lipiodol. Nonetheless, a high-dose lipiodol is contraindicated for the patients with child's B or ICG-R15>20. Second, to avoid normal liver parenchyma damage a high-selective placement of the catheter is crucial for injecting high-dose lipiodol. We mainly used the 5F Yasilo catheter or 5F RH catheter to perform the high selective catheterization. Subsegmental or segmental embolization is necessary for the high-dose lipiodol infusion<sup>[43,44]</sup>. If the tip of catheter can't pass over all the arteries that flow to normal tissue and organ, high-dose lipiodol injection should be done with caution. Finally, slow injection under fluorescent guidance is also important to let all the lipiodol flow clearly into the tumor vessels. Whenever the lipiodol flows to the outside of tumor, injection should be stopped immediately. In the condition that all the lipiodol selectively enters into the tumor and doesn't flow to the normal liver tissue, the hepatic function will not be deteriorated<sup>[45,46]</sup>. We safely injected 53mL into a large HCC with a diameter >20cm. If the blood flow is still fast toward the tumor after lipiodol infusion, Gelatin

sponge should be prescribed<sup>[47]</sup>. High-dose lipiodol TACE can bring about more tumor necrosis. So high-dose lipiodol TACE results in higher survival rate.

It is concluded that high-dose lipiodol can bring about more completely tumor necrosis by blocking both the arteries and small portal veins of the tumor. High-dose TACE for treatment of large and hypervascular hepatocellular carcinoma is practically acceptable and gives a better effect than those using a routine dose. For the patients with large and hypervascular tumors and with Child A or ICG-R15 less than 20%, chemoembolization with 20-40mL lipiodol is recommended.

## REFERENCES

- 1 Wu MC, Shen F. Progress in research of liver surgery in China. *World J Gastroenterol* 2000;6:773-776
- 2 Tang ZY, Yu YQ, Zhou XD, Ma ZC, Wu ZQ Progress and prospects in hepatocellular carcinoma surgery. *Ann Chir* 1998;52:558-563
- 3 Zhang SW, Li LD, Lu FZ, Mo R, Sun XT, Huanfu XM, Sun J, Zhou YC, Dai XD. Mortality of primary liver cancer from 1990 through 1992. *Zhonghua Zhongliu Zazhi* 1999;21:245-249
- 4 Rabe C, Pilz T, Klostermann C, Berna M, Schild HH, Sauerbruch T, Caselmann WH. Clinical characteristics and outcome of a cohort of 101 patients with hepatocellular carcinoma. *World J Gastroenterol* 2001; 7:208-215
- 5 Wu MC. Progresses in surgical treatment of primary hepatocellular carcinoma. *Huaren Xiaohua Zazhi* 1998;6:921-923
- 6 Sithinamsuwan P, Piratvisuth T, Tanomkiat W, Apakupakul N, Tongyoo S. Review of 336 patients with hepatocellular carcinoma at Songklanagarind Hospital. *World J Gastroenterol* 2000;6:339-343
- 7 Tang ZY. Hepatocellular carcinoma cause, treatment and metastasis. *World J Gastroenterol* 2001;7:445-454
- 8 Yip D, Findlay M, Boyer M, Tattersall MH. Hepatocellular carcinoma in central Sydney: a 10 year review of patients seen in a medical oncology department. *World J Gastroenterol* 1999;5:483-487
- 9 Tu SP, Wu DM, Yuan YZ, Wu YL, Jiang SH, Wu YX. Treatment of hepatocellular carcinoma by transcatheter arterial chemoembolization with hydroxycamptothecin. *Shijie Huaren Xiaohua Zazhi* 1999;7:158-160
- 10 Zhang XQ, Yang XM, Sun HL, Li ZR. Effects of hepatic artery chemoembolization on hepatic carcinoma. *Xin Xiaohuabingxue Zazhi* 1997;5:112-113
- 11 Fan J, Ten GJ, He SC, Guo JH, Yang DP, Weng GY. Arterial chemoembolization for hepatocellular carcinoma. *World J Gastroenterol* 1998;4:33-37
- 12 Okusaka T, Okada S, Ueno H, Ikeda M, Yoshimori M, Shimada K, Yamamoto J, Kosuge T, Yamasaki S, Iwata R, Furukawa H, Moriama N, Sakamoto M, Hirohashi S. Evaluation of the therapeutic effect of transcatheter arterial embolization for hepatocellular carcinoma. *Oncology* 2000; 58: 2093-2099
- 13 Ono Y, Yoshimasu T, Ashikaga R, Inoue M, Shindou H, Fuji K, Araki Y, Nishimura Y. Long-term results of lipiodol-transcatheter arterial embolization with cisplatin or doxorubicin for unresectable hepatocellular carcinoma. *Am J Clin Oncol* 2000; 23: 564-568
- 14 Ueno K, Miyazono N, Inoue H, Nishida H, Kanetsuki I, Nakajo M. Transcatheter arterial chemoembolization therapy using iodized oil for patients with unresectable hepatocellular carcinoma: evaluation of three kinds of regimens and analysis of prognostic factors. *Cancer* 2000; 88: 1574-1581
- 15 Takayasu K, Muramatsu Y, Maeda T, Iwata R, Furukawa H, Muramatsu Y, Moriama N, Okusaka T, Okada S, Ueno H. Targeted transarterial oily chemoembolization for small foci of hepatocellular carcinoma using a unified helical CT and angiography system: analysis of factors affecting local recurrence and survival rates. *Am J Roentgenol* 2001; 176: 681-688
- 16 Mizoe A, Yamaguchi J, Azuma T, Fujioka H, Furui J, Kanematsu T. Transcatheter arterial embolization for advanced hepatocellular carcinoma resulting in a curative resection: report of two cases. *Hepatogastroenterology* 2000; 47: 1706-1710
- 17 Vogl TJ, Trapp M, Schroeder H, Mack M, Schuster A, Schmitt J, Neuhaus P, Felix R. Transarterial chemoembolization for hepatocellular carcinoma: volumetric and morphologic CT criteria for assessment of prognosis and therapeutic success-results from a liver transplantation center. *Radiology* 2000; 214: 349-357
- 18 Ernst O, Sergeant G, Mizrahi D, Delemazure O, Paris JC, L'Hermine C. Treatment of hepatocellular carcinoma by transcatheter arterial chemoembolization: comparison of planned periodic chemoembolization and chemoembolization based on tumor response. *Am J Roentgenol* 1999; 172: 59-64

- 19 Inoue H, Ito T, Siraki K, Sugimoto K, Sakai T, Oomori S, Takase K, Nakano T. Effect of segmental transcatheter arterial chemoembolization on branched chain amino acids and tyrosine ratio in patients with hepatocellular carcinoma. *Int J Oncol* 2000; 17: 977-980
- 20 Kwok PC, Lam TW, Chan SC, Chung CP, Wong WK, Chan MK, Lo HY, Lam WM. A randomized clinical trial comparing autologous blood clot and gelfoam in transarterial chemoembolization for inoperable hepatocellular carcinoma. *J Hepatol* 2000; 32: 955-964
- 21 Katyal S, Oliver JH, Peterson MS, Chang PJ, Baron RL, Carr BI. Prognostic significance of arterial phase CT for prediction of response to transcatheter arterial chemoembolization in unresectable hepatocellular carcinoma: a retrospective analysis. *Am J Roentgenol* 2000; 175: 1665-1672
- 22 Nishimine K, Uchida H, Matsuo N. Segmental transarterial chemoembolization with Lipiodol mixed with anticancer drugs for nonresectable hepatocellular carcinoma: Follow-up CT and therapeutic results. *Cancer Chemother Pharmacol* 1994; (Suppl 33):S60-S68
- 23 Llado L, Virgili J, Figueras J, Valls C, Dominguez J, Rafecas A, Torras J, Fabregat J, Guardiola J, Jaurrieta E. A prognostic index of the survival of patients with unresectable hepatocellular carcinoma after transcatheter arterial chemoembolization. *Cancer* 2000; 88: 50-57
- 24 Pelletier G, Ducreux M, Gay F, Lubinski M, Hagege H, Dao T, Van Steenberghe W, Buffet C, Rougier P, Adler M, Pignon JP, Roche A. Treatment of unresectable hepatocellular carcinoma with lipiodol chemoembolization: a multicenter randomized trial. Groupe CHC. *J Hepatol* 1998; 29: 129-134
- 25 Savastano S, Miotto D, Casarrubea G, Teso S, Chiesura Corona M, Feltrin GP. Transcatheter arterial chemoembolization for hepatocellular carcinoma in patients with Child's grade A or B cirrhosis: a multivariate analysis of prognostic factors. *J Clin Gastroenterol* 1999; 28: 334-340
- 26 Kamada K, Nakanishi T, Kitamoto M, Aikata H, Kawakami Y, Ito K, Asahara T, Kajiyama G. Long-term prognosis of patients undergoing transcatheter arterial chemoembolization for unresectable hepatocellular carcinoma: comparison of cisplatin lipiodol suspension and doxorubicin hydrochloride emulsion. *J Vasc Interv Radiol* 2001; 12: 847-854
- 27 Matsuo N, Uchida H, Sakaguchi H, Nishimine K, Nishimura Y, Hirohashi S, Ohishi H. Optimal lipiodol volume in transcatheter arterial chemoembolotherapy for hepatocellular carcinoma: Study based on lipiodol accumulation patterns and histopathologic findings. *Seminars in Oncology* 1997;24:61-70
- 28 Takayasu K, Arii S, Matsuo N, Yoshikawa M, Ryu M, Takasaki K, Sato M, Yamanaka N, Shimamura Y, Ohto M. Comparison of CT findings with resected specimens after chemoembolization with iodized oil for hepatocellular carcinoma. *Am J Roentgenol* 2000;175: 699-704
- 29 Bizollon T, Rode A, Bancel B, Gueripel V, Ducerf C, Baulieux J, Trepo C. Diagnostic value and tolerance of Lipiodol-computed tomography for the detection of small hepatocellular carcinoma: correlation with pathologic examination of explanted livers. *J Hepatol* 1998;28: 491-496
- 30 Oi H, Kim T, Kishimoto H, Matsushita M, Tateishi H, Okamura J. Effective cases of transcatheter arterioportal chemoembolization with high-dose iodized oil for hepatocellular carcinoma. *Cancer Chemother Pharmacol* 1994;33 Suppl: S69-73
- 31 Oi H, Kishimoto H, Matsushita M, Katsushima S, Tateishi H, Okamura J. Antitumor effect of transcatheter oily chemoembolization for hepatocellular carcinoma assessed by computed tomography: role of iodized oil. *Semin Oncol* 1997;24(Suppl 6): 56-60
- 32 Nakayama A, Imamura H, Matsuyama Y, Kitamura H, Miwa S, Kobayashi A, Miyagawa S, Kawasaki S. Value of lipiodol computed tomography and digital subtraction angiography in the era of helical biphasic computed tomography as preoperative assessment of hepatocellular carcinoma. *Ann Surg* 2001;234: 56-62
- 33 Caturelli E, Siena DA, Fusilli S, Villani MR, Schiavone G, Nardella M, Balzano S, Florio F. Transcatheter arterial chemoembolization for hepatocellular carcinoma in patients with cirrhosis: evaluation of damage to nontumorous liver tissue-long-term prospective study. *Radiology* 2000; 215: 123-128
- 34 Colagrande S, Fagnoli R, Dal Pozzo F, Bindi A, Rega L, Villari N. Value of hepatic arterial phase CT versus lipiodol ultrafluid CT in the detection of hepatocellular carcinoma. *J Comput Assist Tomogr* 2000; 24: 878-883
- 35 Higashi S, Tabata N, Kondo KH, Maeda Y, Shimizu M, Nakashima T, Setoguchi T. Size of lipid microdroplets effects results of hepatic arterial chemotherapy with an anticancer agent in water-in-oil-in-water emulsion to hepatocellular carcinoma. *J Pharmacol Exp Ther* 1999; 289: 816-819
- 36 Vogl TJ, Schroeder H, Trapp M, Straub R, Schuster A, Schuster M, Mack M, Souchon F, Neuhaus P. Multi-sequential arterial chemoembolization of advanced hepatocellular carcinomas: computerized tomography follow-up parameters for evaluating effectiveness of therapy. *Rofo Fortschr Geb Rontgenstr Neuen Bildgeb Verfahr* 2000;172:43-50
- 37 Kamada K, Nakanishi T, Kitamoto M, Aikata H, Kawakami Y, Ito K, Asahara T, Kajiyama G. Long-term prognosis of patients undergoing transcatheter arterial chemoembolization for unresectable hepatocellular carcinoma: comparison of cisplatin lipiodol suspension and doxorubicin hydrochloride emulsion. *J Vasc Interv Radiol* 2001;12: 847-854
- 38 Okusaka T, Okada S, Ueno H, Ikeda M, Yoshimori M, Shimada K, Yamamoto J, Kosuge T, Yamasaki S, Iwata R, Furukawa H, Moriyama N, Sakamoto M, Hirohashi S. Evaluation of the therapeutic effect of transcatheter arterial embolization for hepatocellular carcinoma. *Oncology* 2000;58: 293-299
- 39 Jiao LR, El Desoky AA, Seifalian AM, Habib N, Davidson BR. Effect of liver blood flow and function on hepatic indocyanine green clearance measured directly in a cirrhotic animal model. *Br J Surg* 2000; 87: 568-574
- 40 Hashimoto M, Watanabe G. Hepatic parenchymal cell volume and the indocyanine green tolerance test. *J Surg Res* 2000; 92: 222-227
- 41 Tang ZY. Advances in clinical research of hepatocellular carcinoma in China. *Huaren Xiaohua Zazhi* 1998;6:1013-1016
- 42 Zhou HG, Gu GW. New trend in clinicopathology of primary liver cancer. *Huaren Xiaohua Zazhi* 1998;6:714-715
- 43 Wu ZQ, Fan J, Qiu SJ, Zhou J, Tang ZY. The value of postoperative hepatic regional chemotherapy in prevention of recurrence after radical resection of primary liver cancer. *World J Gastroenterol* 2000; 6:131-133
- 44 Li L, Wu PH, Li JQ, Zhang WZ, Lin HG, Zhang YQ. Segmental transcatheter arterial embolization for primary hepatocellular carcinoma. *World J Gastroenterol* 1998;4:511-512
- 45 Tarazov PG, Polysalov VN, Prozorovskij KV, Grishchenkova IV, Rozengauz EV. Ischemic complications of transcatheter arterial chemoembolization in liver malignancies. *Acta Radiol* 2000; 41: 156-160
- 46 Caturelli E, Siena DA, Fusilli S, Villani MR, Schiavone G, Nardella M, Balzano S, Florio F. Transcatheter arterial chemoembolization for hepatocellular carcinoma in patients with cirrhosis: evaluation of damage to nontumorous liver tissue-long-term prospective study. *Radiology* 2000;215:123-128
- 47 Ono Y, Yoshimasu T, Ashikaga R, Inoue M, Shindou H, Fuji K, Araki Y, Nishimura Y. Long-term results of lipiodol-transcatheter arterial embolization with cisplatin or doxorubicin for unresectable hepatocellular carcinoma. *Am J Clin Oncol* 2000;23:564-568

• LIVER CANCER •

# Anti-hepatoma activity of resveratrol in vitro

Zhong-Jie Sun, Cheng-En Pan, Hong-Shan Liu, Guo-Jun Wang

Zhong-Jie Sun, Cheng-En Pan, Hong-Shan Liu, Guo-Jun Wang,  
Department of Hepatobiliary Surgery, First Hospital of Xi'an Jiaotong  
University, Xi'an 710061, Shaanxi Province, China

Correspondence to: Dr. Zhong-Jie SUN, Department of Hepatobiliary  
Surgery, First Hospital of Xi'an Jiaotong University Xi'an 710061,  
Shaanxi Province, China. szhjje@21cn.com

Telephone: +86-029-5260273 Fax: +86-029-5260273

Received 2001-08-09 Accepted 2001-08-23

## Abstract

**AIM: To study the anti-tumor effect of resveratrol alone and the synergistic effects of resveratrol with 5-FU on the growth of H22 cells line *in vitro*.**

**METHODS: The number of cells was measured by MTT method, the morphological changes of H<sub>22</sub> cells were investigated under microscopy and electron microscopy.**

**RESULTS: Resveratrol inhibited the growth of hepatoma cells line H<sub>22</sub> in a dose- and time-dependent manner. IC<sub>50</sub> of the resveratrol on H<sub>22</sub> cells was 6.57 mg·L<sup>-1</sup>. The synergistic anti-tumor effects of resveratrol with 5-FU increased to a greater extent than for H22 cells treated with 5-FU alone (70.2% vs 28.4%) ( $P < 0.05$ ). Under microscope and electron microscope, characteristics of apoptosis such as typical apoptotic bodies were commonly found in tumor cells in the drug-treated groups.**

**CONCLUSION: Resveratrol can suppresses the growth of H<sub>22</sub> cells *in vitro*, its anti-tumor activity may occur through the induction of apoptosis.**

Sun ZJ, Pan CE, Liu HS, Wang GJ. Anti-hepatoma activity of resveratrol *in vitro*. *World J Gastroenterol* 2002;8(1):79-81

## INTRODUCTION

Hepatoma is common in China<sup>[1-20]</sup>, but only a few chemotherapeutic drugs hold a high place in the treatment of human primary hepatocellular carcinoma (PHC). Resveratrol, a phytoalexin found in grapes, fruits, and root extracts of the weed *Polygonum cuspidatum*, has been an important constituent of Japanese and Chinese folk medicine. Indirect evidence suggests that the presence of resveratrol in white and rose wine may explain for the reduced risk of coronary heart disease associated with moderate wine consumption. This effect has been attributed to the inhibition of platelet aggregation and coagulation, in addition to the antioxidant and anti-inflammatory activity of resveratrol<sup>[21-28]</sup>. Moreover, a recent report shows that resveratrol is a potent cancer chemopreventive agent in assays representing three major stages of carcinogenesis<sup>[29-35]</sup>. The ability to inhibit cellular events associated with tumor initiation, promotion, and progression has been attributed to the anticyclooxygenase activity (COX-1) of resveratrol<sup>[36]</sup>. We report here the results of our findings showing that resveratrol inhibited the growth of hepatoma cells line H<sub>22</sub>.

## MATERIALS AND METHODS

### Reagents

Resveratrol was kindly provided by Prof Li (Environment and

Chemical Engineering School, Xi'an Jiaotong University) and dissolved in dimethylsulfoxide (DMSO); MTT was obtained from Sigma. RPMI 1640 containing 100 mL·L<sup>-1</sup> fetal bovine serum (FBS) was bought from Gibco. All other chemicals were standard commercial products of analytical grade.

### Cell culture

H<sub>22</sub> cells were obtained from Center of Molecular Biology of First Hospital, Xi'an Jiaotong University and routinely cultured in RPMI 1640 containing 100 mL·L<sup>-1</sup> FBS at 37°C in an atmosphere with 50 mL·L<sup>-1</sup> CO<sub>2</sub>.

### Assay of cell proliferation

H<sub>22</sub> cells were plated in 96-well plates (2×10<sup>4</sup>/well) for 24 h before the addition of resveratrol. Medium was then aspirated and replaced with fresh RPMI 1640 + 100 mL·L<sup>-1</sup> FBS containing resveratrol for 48 h. Different compositions to be tested were added according to designed groups: group A (cell control group) with nothing added, group B (DMSO control group) with DMSO 5 mL·L<sup>-1</sup>, group C1-5 with Resveratrol (1.25, 2.50, 5.0, 10.0 and 20.0 mg·L<sup>-1</sup>), group D 1-25-FU (2400 and 1200 mg·L<sup>-1</sup>), group E with Resveratrol 5.0 mg·L<sup>-1</sup>+5-FU 1200 mg·L<sup>-1</sup>. Each group had 4 wells and was cultured for 48 h. The number of cells was determined by MTT (3-[4,5-dimethylthiazol-2-yl]-2,5-diphenyl tetrazolium bromide) method as described in Sigma Technical Bulletin (Sigma, MO). Absorbance at 570 nm (A) was assayed at different time points. The A value was adjusted with the living cell number. Each sample was assayed three times. Inhibition rate (%) = (1 - experimental A/control A) × 100%.

### Morphologic observation

After the cellular culture for 48 h, cells in groups A, C and E were observed and photographed with an Olympus BH-I microscope and a Hitachi-600 electron microscope.

## RESULTS

### Growth inhibition of H<sub>22</sub> cells

H<sub>22</sub> cells at 2×10<sup>4</sup>/well were incubated with different concentrations of resveratrol for 8 - 48 h and the effect of resveratrol on the cells growth was examined by MTT assay. The growth of H<sub>22</sub> cells was markedly inhibited by resveratrol with the IC<sub>50</sub> value of 6.57 mg·L<sup>-1</sup>. Moreover, the cytotoxicity of resveratrol was in concentration-dependent and time-dependent manners (Table 1). The inhibition ability of 5-FU was 49.2% (2400 mg·L<sup>-1</sup>), 28.4% (1200 mg·L<sup>-1</sup>) respectively; The inhibiting ability of resveratrol (5.0 mg·L<sup>-1</sup>) combined with 5-FU (1200 mg·L<sup>-1</sup>) was higher than that of 5-FU alone (70.2% vs 28.4%,  $P < 0.05$ ).

### Morphology observation

Apoptotic cells were found in cells incubated with resveratrol. Light microscopic observation showed that apoptotic cells were characterized with cytoplasmic condensation, vacuolated bubbles, and condensed nuclei (Figure 1). Under electron microscope, H<sub>22</sub> cells exhibited the characteristics of apoptosis including cytoplasmic condensate, pyknotic nuclei, condensed chromatin and apoptotic bodies (Figures 2,



3). Compared with control groups, group C and E had much more cells with the apoptotic characteristics.

**Table 1** Effect of various concentrations of resveratrol on the growth of hepatoma cells H<sub>22</sub>

| c(resveratrol)/mg · L <sup>-1</sup> | 8h                | 12h               | 24h               | 48h               |
|-------------------------------------|-------------------|-------------------|-------------------|-------------------|
| 0.00                                | -                 | -                 | -                 | -                 |
| 1.25                                | 11.4              | 12.6              | 13.4              | 16.8              |
| 2.50                                | 23.4              | 29.3              | 30.2 <sup>a</sup> | 32.6 <sup>a</sup> |
| 5.00                                | 30.5 <sup>a</sup> | 31.2 <sup>a</sup> | 36.4 <sup>a</sup> | 43.5 <sup>a</sup> |
| 10.0                                | 32.2 <sup>a</sup> | 38.3 <sup>a</sup> | 45.1 <sup>a</sup> | 62.2              |
| 20.0                                | 38.2 <sup>a</sup> | 45.9 <sup>a</sup> | 65.2 <sup>b</sup> | 74.9 <sup>b</sup> |

<sup>a</sup>P<0.05; <sup>b</sup>P<0.01 vs control

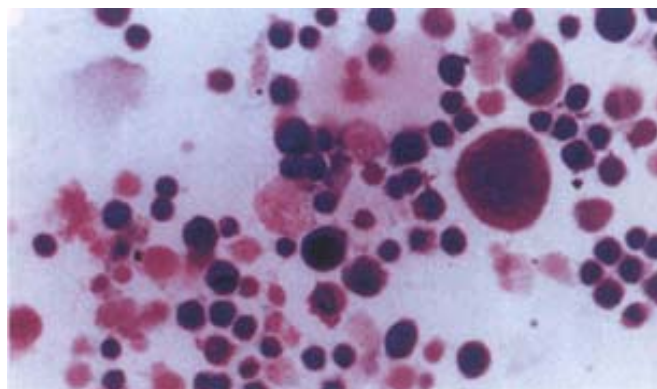


**Figure 1** Treatment with resveratrol for 48 hours: apoptotic cell with condensed nuclei and cytoplasmic condensation (×200).

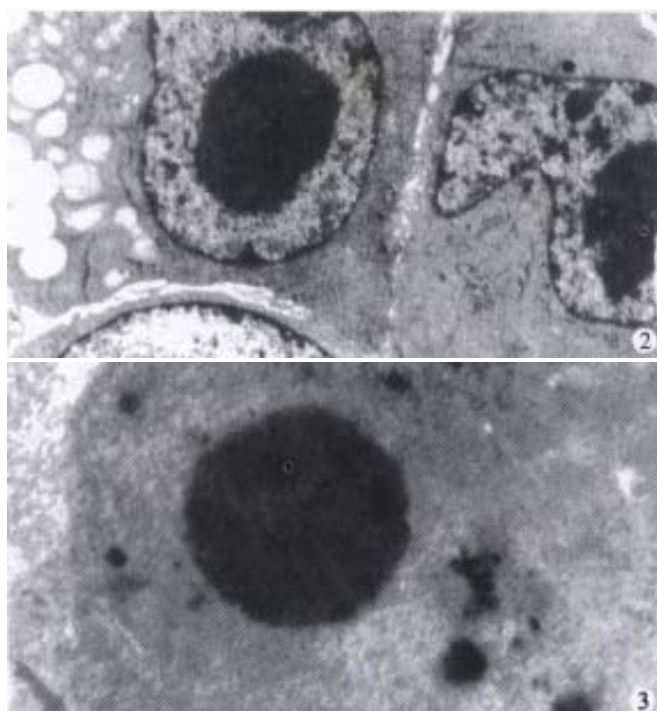


**Figure 2** Cytoplasmic condensation with vacuoles, pyknotic nuclei, some with condensed chromatin inside (×5000).

**Figure 3** Apoptotic body (×10 000).

## DISCUSSION

To date, only a few chemotherapeutic drugs hold a high place in the treatment of human primary hepatocellular carcinoma (PHC) and there is clearly a need for evaluation of new anti-hepatoma drugs. Resveratrol (3,5,4'-trihydroxystibene), a natural compound present in grapes and other food, has been shown to provide cancer

chemopreventive effects in different systems based on its striking inhibition of diverse cellular events associated with tumor initiation, promotion, and progression<sup>[29-35,37]</sup>. At the molecular level, these effects were related to the inhibition of free radical formation and cyclooxygenase activity<sup>[36]</sup>, as well as induction of differentiation. In addition, resveratrol was shown to be a remarkable inhibitor of ribonucleotide reductase and DNA synthesis with cellular arrest in the S phase or the S-G2 phase transition<sup>[38-40]</sup>. In the present study, MTT assay was used to observe the effect of resveratrol on the growth of H<sub>22</sub> mouse hepatoma cells *in vitro*, indicating that the drug could inhibit the growth of hepatoma cells. Its concentration- and time-effect relationships were also significant. Compared with control groups, group C had much more cells with apoptotic characteristics. The plausible mechanisms that could account for the anti-tumor activity of resveratrol might be related to induce apoptosis of tumor cells<sup>[41-48]</sup>.

Resveratrol combined with 5-FU inhibited the cell growth much more strongly than each agent used alone. At a certain concentration, resveratrol inhibits H<sub>22</sub> cell growth with the same effect as using 5-FU alone. Combination of resveratrol and 5-FU could have a cooperative effect. Both drugs inhibit cell growth at different phases of the cell cycle, i.e., resveratrol mainly causes G2/M arrest<sup>[39-40]</sup> and 5-FU mainly inhibits DNA synthesis(S phase) which naturally decreases the cellular growth more significantly. Our study indicates that combined use of resveratrol and 5-FU at low concentration that is used to treat hepatoma may be more efficient than using a single drug at higher concentration. The side-effects produced by 5-FU at the high doses can be avoided by its combination at low doses. These results suggest that resveratrol, may be potentially useful as a biochemical modulator to enhance the therapeutic effects of 5-FU in cancer chemotherapy.

## REFERENCES

- 1 Tang ZY. Hepatocellular Carcinoma Cause, Treatment and Metastasis. *World J Gastroenterol* 2001;7:445-454
- 2 Lin NF, Tang J, Mohamed Ismael HS. Study on environmental etiology of high incidence areas of liver cancer in China. *World J Gastroenterol* 2000;6:572-576
- 3 Yang CS. Chinese diet in the causation and prevention of cancer. *World J Gastroenterol* 1998;4:36-37
- 4 Liu E, Zhang QN, Li WG. Effect of various drinking water on human micronucleus frequency in high-risk population of PHC. *World J Gastroenterol* 1998;4:183-184
- 5 Wu MC. Clinical research advances in primary liver cancer. *World J Gastroenterol* 1998;4:471-474
- 6 Tang ZY. Advances in clinical research of hepatocellular carcinoma in China. *World J Gastroenterol* 1998;4:4-7
- 7 Wu MC, Shen F. Progress in research of liver surgery in China. *World J Gastroenterol* 2000;6:773-776
- 8 Jiang YF, Yang ZH, Hu JQ. Recurrence or metastasis of HCC: predictors, early detection and experimental antiangiogenic therapy. *World J Gastroenterol* 2000;6:61-65
- 9 Li JY, Huang Y, Lin MF. Clinical evaluation of several tumor markers in the diagnosis of primary hepatic cancer. *World J Gastroenterol* 2000;6:39
- 10 Wang CF, Shao YF, Zhang HZ. Surgical treatment for patients with stage IVa hepatic carcinoma and related studies. *World J Gastroenterol* 2000;6:86
- 11 Gu GW, Zhou HG. Traditional Chinese Medicine in prevention of liver cancer. *Shijie Huaren Xiaohua Zazhi* 1999;7:80-81
- 12 Liu WW. Etiological studies of hepatocellular carcinoma. *Shijie Huaren Xiaohua Zazhi* 1999;7:93-95
- 13 Zhou XD. Prevention and treatment of recurrences and metastases of hepatocellular carcinoma. *Shijie Huaren Xiaohua Zazhi* 1999;7:260-261
- 14 Lu B, Dai YM. Abnormal cycle regulation of cells in the HCC. *Shijie Huaren Xiaohua Zazhi* 2001;9:205-208
- 15 Li L, Wu PH, Li JQ, Zhang WZ, Lin HG, Zhang YQ. Segmental transcatheter arterial embolization for primary hepatocellular carcinoma. *World J Gastroenterol* 1998;4:511-512
- 16 Huang FG, Li Y, Xie XD. Side effects and complications of hepatic arterial infusion and embolization of liver carcinoma in aged patients and its management. *World J Gastroenterol* 1998;4:67-68
- 17 Wang JH, Lin G, Yan ZP, Wang XL, Cheng JM, Li MQ. Stage II surgical resection of hepatocellular carcinoma after TAE: a report of 38

- cases. *World J Gastroenterol* 1998;4:133-136
- 18 Cai WX, Zheng H, Sheng J, Ye QL. Combined measurement of serum tumor markers in patients with hepatocellular carcinoma. *World J Gastroenterol* 1998;4:181-182
  - 19 Deng ZL, Ma Y, Yuan L, Teng PK. The importance of hepatitis C as a risk factor for hepatocellular carcinoma in Guangxi. *World J Gastroenterol* 2000;6:75
  - 20 Fan J, Wu ZQ, Tang ZY, Zhou J, Qiu SJ, Ma ZC, Zhou XD, Ye SL. Multimodality treatment in hepatocellular carcinoma patients with tumor thrombi in portal vein. *World J Gastroenterol* 2001;7:28-32
  - 21 Huang K, Lin M, Cheng G. Anti-inflammatory tetramers of resveratrol from the roots of *Vitis amurensis* and the conformations of the seven-membered ring in some oligostilbenes. *Phytochemistry* 2001;58:357-362
  - 22 Surh Y, Chun K, Cha H, Han SS, Keum Y, Park K, Lee SS. Molecular mechanisms underlying chemopreventive activities of anti-inflammatory phytochemicals: down-regulation of COX-2 and iNOS through suppression of NF-kappaB activation. *Mutat Res* 2001;480-481:243-268
  - 23 Olas B, Wachowicz B, Saluk-Juszczak J, Zielinski T, Kaca W, Buczynski A. Antioxidant activity of resveratrol in endotoxin-stimulated blood platelets. *Cell Biol Toxicol* 2001;17:117-125
  - 24 Stojanovic S, Sprinz H, Brede O. Efficiency and mechanism of the antioxidant action of trans-resveratrol and its analogues in the radical liposome oxidation. *Arch Biochem Biophys* 2001;391:79-89
  - 25 Wu JM, Wang ZR, Hsieh TC, Bruder JL, Zou JG, Huang YZ. Mechanism of cardioprotection by resveratrol, a phenolic antioxidant present in red wine (Review). *Int J Mol Med* 2001;8:3-17
  - 26 Russo P, Tedesco I, Russo M, Russo GL, Venezia A, Cicala C. Effects of de-alcoholated red wine and its phenolic fractions on platelet aggregation. *Nutr Metab Cardiovasc Dis* 2001;11:25-29
  - 27 Murcia MA, Martinez-Tome M. Antioxidant activity of resveratrol compared with common food additives. *J Food Prot* 2001;64:379-384
  - 28 Olas B, Zbikowska HM, Wachowicz B, Krajewski T, Buczynski A, Magnuszewska A. Inhibitory effect of resveratrol on free radical generation in blood platelets. *Acta Biochim Pol* 1999;46:961-966
  - 29 Igura K, Ohta T, Kuroda Y, Kaji K. Resveratrol and quercetin inhibit angiogenesis *in vitro*. *Cancer Lett* 2001;171:11-16
  - 30 Gusman J, Malonne H, Atassi G. A reappraisal of the potential chemopreventive and chemotherapeutic properties of resveratrol. *Carcinogenesis* 2001;22:1111-1117
  - 31 Kimura Y, Okuda H. Resveratrol isolated from *Polygonum cuspidatum* root prevents tumor growth and metastasis to lung and tumor-induced neovascularization in Lewis lung carcinoma-bearing mice. *J Nutr* 2001;131:1844-1849
  - 32 Yang CS, Landau JM, Huang MT, Newmark HL. Inhibition of carcinogenesis by dietary polyphenolic compounds. *Annu Rev Nutr* 2001;21:381-406
  - 33 Kozuki Y, Miura Y, Yagasaki K. Resveratrol suppresses hepatoma cell invasion independently of its anti-proliferative action. *Cancer Lett* 2001;167:151-156
  - 34 Nakagawa H, Kiyozuka Y, Uemura Y, Senzaki H, Shikata N, Hioki K, Tsubura A. Resveratrol inhibits human breast cancer cell growth and may mitigate the effect of linoleic acid, a potent breast cancer cell stimulator. *J Cancer Res Clin Oncol* 2001;127:258-264
  - 35 Mollerup S, Ovrebø S, Haugen A. Lung carcinogenesis: resveratrol modulates the expression of genes involved in the metabolism of PAH in human bronchial epithelial cells. *Int J Cancer* 2001;92:18-25
  - 36 MacCarrone M, Lorenzon T, Guerrieri P, Agro AF. Resveratrol prevents apoptosis in K562 cells by inhibiting lipoxygenase and cyclooxygenase activity. *Eur J Biochem* 1999;265:27-34
  - 37 Jang M, Cai L, Udeani G, O, Slowing KV, Thomas CF, Beecher CW, Fong HH, Farnsworth NR, Kinghorn AD, Mehta RC, Moon RC, Pezzuto JM. Cancer chemopreventive activity of resveratrol, a natural product derived from grapes. *Science (Washington DC)* 1997;275: 218-220
  - 38 Fontecave M, Lepoivre M, Elleingand E, Gerez C., Guittet O. Resveratrol, a remarkable inhibitor of ribonucleotide reductase. *FEBS Lett* 1998;421: 277-279
  - 39 Park JW, Choi YJ, Jang MA, Lee YS, Jun DY, Suh SI, Baek WK, Suh MH, Jin IN, Kwon TK. Chemopreventive agent resveratrol, a natural product derived from grapes, reversibly inhibits progression through S and G2 phases of the cell cycle in U937 cells. *Cancer Lett* 2001;163:43-49
  - 40 Ragione FD, Cucciolla V, Borriello A, Pietra V. D., Racioppi L., Soldati G., Manna C., Galletti P., Zappia V. Resveratrol arrests the cell division cycle at S/G2 phase transition. *Biochem Biophys Res Commun* 1998;250: 53-58
  - 41 Pervaiz S. Resveratrol-from the bottle to the bedside? *Leuk Lymphoma* 2001;40:491-498
  - 42 Huang C, Ma WY, Goranson A, Dong ZG. Resveratrol suppresses cell transformation and induces apoptosis through a p53-dependent pathway. *Carcinogenesis (Lond)* 1999;20: 237-242
  - 43 Dorrie J, Gerauer H, Wachter Y, Zunino SJ. Resveratrol induces extensive apoptosis by depolarizing mitochondrial membranes and activating caspase-9 in acute lymphoblastic leukemia cells. *Cancer Res* 2001;61:4731-4739
  - 44 She QB, Bode AM, Ma WY, Chen NY, Dong Z. Resveratrol-induced activation of p53 and apoptosis is mediated by extracellular-signal-regulated protein kinases and p38 kinase. *Cancer Res* 2001;61:1604-1610
  - 45 Tsan MF, White JE, Maheshwari JG, Bremner TA, Sacco J. Resveratrol induces Fas signalling-independent apoptosis in THP-1 human monocytic leukaemia cells. *Br J Haematol* 2000;109:405-412
  - 46 Szende B, Tyihak E, Kiraly-Veghely Z. Dose-dependent effect of resveratrol on proliferation and apoptosis in endothelial and tumor cell cultures. *Exp Mol Med* 2000;32:88-92
  - 47 Bernhard D, Tinhofer I, Tonko M, Hubl H, Ausserlechner MJ, Greil R, Kofler R, Csordas A. Resveratrol causes arrest in the S-phase prior to Fas-independent apoptosis in CEM-C7H2 acute leukemia cells. *Cell Death Differ* 2000;7:834-842
  - 48 Tian XM, Zhang ZX. The anticancer activity of resveratrol on implanted tumor of HepG2 in nude mice. *Shijie Huaren Xiaohua Zazhi* 2001;9:161-164

• LIVER CANCER •

# Characterization of focal hepatic lesions with SPIO-enhanced MRI

Wei-Wei Zheng, Kang-Rong Zhou, Zu-Wang Chen, Ji-Zhang Shen, Cai-Zhong Chen, Shu-Jie Zhang

Wei-Wei Zheng, Kang-Rong Zhou, Zu-Wang Chen, Ji-Zhang Shen, Cai-Zhong Chen, Shu-Jie Zhang, Department of Radiology, Affiliated Zhongshan Hospital, Medical College of Fudan University, Shanghai 200032, P.R.China

Supported by the Health Ministry Programme No.97030220

Correspondence to: Dr. Wei Wei Zheng, Department of Radiology, Zhongshan Hospital, Medical Center of Fudan University, 180 Fenglin Road, Shanghai 200032, China. Viviannc@online.sh.cn

Telephone: +86-21-64041990 Ext.2416

Received 2001-08-08 Accepted 2001-08-23

## Abstract

**AIM:** To evaluate the value of superparamagnetic iron oxide (SPIO) enhanced MRI in characterizing focal hepatic lesions.

**METHODS:** Forty-three patients (32 men, 11 women, mean age 51 years, age range 25-74 years) with previously identified focal hepatic lesions were enrolled into this study. All the patients underwent plain, Gd-DTPA enhanced MRI and the SPIO enhanced MRI 1-7 d later. The surgicopathologic diagnosis was established in 31 cases and the diagnosis in other 12 cases was made on the basis of clinical findings and biochemical tests. The signal changes of lesions were analyzed and the CNRs of lesion-to-liver were measured before and after SPIO enhancement. The data were analyzed by paired *t* test.

**RESULTS:** Focal hepatic lesions included primary hepatocellular carcinoma (HCC, *n*=22), hemangioma (*n*=5), cyst (*n*=4), metastases (*n*=5), cirrhotic nodule (*n*=4), focal nodular hyperplasia (FNH, *n*=5) and other miscellaneous lesions (*n*=6). After SPIO enhancement HCC demonstrated iso- or slight hyperintensity on T1WI and moderate hyperintensity on T2WI, hemangioma showed moderate hyperintensity on T1WI and obvious hyperintensity on T2WI, the SI of cyst had no change either on T1WI or on T2WI, cirrhotic nodules revealed iso-intensity on T2WI, and the SI of FNH decreased significantly on T2WI. No specific manifestations were found in the other 6 miscellaneous lesions after SPIO enhancement.

**CONCLUSION:** SPIO enhanced-MRI can improve the characterization confidence for diagnosis of focal hepatic lesions.

Zheng WW, Zhou KR, Chen ZW, Shen JZ, Chen CZ, Zhang SJ. Characterization of focal hepatic lesions with SPIO-enhanced MRI. *World J Gastroenterol* 2002;8(1):82-86

## INTRODUCTION

Superparamagnetic iron oxide (SPIO) is a newly developed tissue-specific contrast material. Intravenously administered SPIO particles can be specifically taken up by reticulo-endothelial system, and the signal intensities of normal hepatic and splenic parenchyma are significantly decreased on MR images. Therefore, it has been widely applied for lesion detection in the liver<sup>[1-6]</sup>. After SPIO-enhancement the detectability of focal hepatic lesions smaller than

1cm could be increased from 65.9% to 97.5%. However, to our knowledge, the previously reported studies were mainly concerned about the detection of hepatic metastatic lesions and only a few studies focused on the characterization of focal hepatic lesions<sup>[4-13]</sup>. Thus, the purpose of this study is to evaluate the diagnostic value of superparamagnetic iron oxide in demonstrating benign and malignant focal hepatic lesions.

## MATERIAL AND METHODS

### Patients

Forty-three patients (32 men, 11 women, mean age 51 years, age range 25-74 years) with previously identified focal hepatic lesions were enrolled into this study. The pathologically proven diagnosis was achieved in 31 cases and the other 12 cases were diagnosed on the basis of clinical findings and biochemical tests. Most lesions were smaller than 3cm. Three cases previously suspected of having focal hepatic lesion were finally confirmed as cirrhotic nodules after SPIO-enhancement. In the remaining 40 patients showed multiple hepatic lesions were found in 22 and solitary in 18, including malignant lesions in 29 cases and benign lesions in 11 cases. The malignant lesions included: primary hepatocellular carcinoma (HCC, *n*=22) associated with hemangioma or cyst in 4, cholangiocarcinoma with cysts (*n*=1), and cholangiohepatocarcinoma (*n*=1), metastases (*n*=5). The benign lesions included: multiple hemangiomas (*n*=2), focal nodular hyperplasia (FNH, *n*=5), angiolipoleiomyoma (*n*=1), inflammatory pseudotumor with hemangioma and cysts (*n*=1), multiple abscess (*n*=1) and focal inflammation with hemangioma (*n*=1).

### Contrast agent

Gadopentetate dimeglumine (Magnevist; Schering, Berlin, Germany) was manually administered through antecubital intravenous bolus of 0.1mmol/kg. Feridex (Advanced Magnetix, USA) is an iron oxide preparation coated with low-molecular-weight dextran available in 5mL vial containing 11.2mg iron and 61.3mg mannitol/mL. Feridex at a dose of 0.05mL·kg<sup>-1</sup> (0.56mg Fe·kg<sup>-1</sup>) was diluted with 100mL of 5g·L<sup>-1</sup> glucose and infused intravenously at a rate of 3mL·min<sup>-1</sup>.

### Imaging procedure

The GE Signa 1.5T MR imaging system was used. The whole procedure including: ① non-enhanced images: SE T1-weighted (TR/TE=540ms/15ms), FSE T2-weighted with fat suppression (TR/TE=3000-4000ms/98ms); ② Gd-DTPA enhanced images: FMPSGR with dynamic enhancement; and ③ SPIO-enhanced images: 1-7 d later, SE T1-weighted, FSE T2-weighted, FSE T2-weighted with fat suppressed sequences, were performed after SPIO administration. Transverse images were obtained with a slice thickness of 8mm, a section gap of 1-2mm, a field of view of 360mm and matrix size of 256×160.

### Imaging analysis

The images were reviewed by 3 experienced radiologists. The signal intensities (SI) of normal hepatic parenchyma, hepatic lesions and

signal change of lesion-to-liver were measured before and after administration of SPIO. Regions of interest (ROI) with at least 50 pixels on homogeneous background free of artifacts. ROI were chosen to be representative of the tissue being evaluated. Measurements were made at the same anatomic level for unenhanced and enhanced images in each patient. If patient had multiple lesions with the homogeneous character, the typical one was selected, otherwise the lesions were analyzed individually.

## RESULTS

Totally 12 kinds of benign and malignant diseases were observed in 43 patients. The CNR of lesion-to-liver was evaluated on each sequence (Tables 1 and 2). After SPIO-enhancement the ratios of lesion-to-liver were significantly raised on T<sub>1</sub>-weighed images except that of cyst, while on T<sub>2</sub>-weighed images the hepatic cirrhotic nodules and FNH's ratios of lesion-to-liver showed no significant difference before and after SPIO-enhancement.

**Table 1** The CNR of lesion-to-liver on T<sub>1</sub>WI

| Lesion (cases)                | T <sub>1</sub> WI | SPIO-enhanced T <sub>1</sub> WI | P      |
|-------------------------------|-------------------|---------------------------------|--------|
| HCC (22)                      | -10.2±8.3         | 19.9±23.8                       | <0.001 |
| Hemangioma (5)                | -16.4±8.6         | 71±33                           | <0.05  |
| Cyst (4)                      | -457±12.1         | -33.7±17.9                      | >0.05  |
| Metastases (5)                | -15.4±9.3         | 6.8±28.1                        | <0.05  |
| Cirrhosis nodules (4)         | 2.3±9.3           | 21.3±17                         | <0.05  |
| FNH (5)                       | -4.3±14.1         | 18.8±18.6                       | <0.05  |
| Cholangiocarcinoma (1)        | -32               | 0                               | -      |
| inflammatory pseudotumor (1)  | -15               | 47                              | -      |
| Hepatic abscess (1)           | -19               | 1                               | -      |
| Focal inflammatory lesion (1) | -17               | 12                              | -      |
| Angiolipoleiomyoma (1)        | 16                | 85                              | -      |
| Cholangiohepatocarcinoma (1)  | -5                | 34                              | -      |

**Table 2** The CNR of lesion-to-liver on T<sub>2</sub>WI

| Lesion (cases)                | T <sub>2</sub> WI | SPIO-enhanced T <sub>2</sub> WI | P      |
|-------------------------------|-------------------|---------------------------------|--------|
| HCC (22)                      | 98.39±58.59       | 465.77±272.73                   | <0.001 |
| Hemangioma (5)                | 354.57±119.78     | 1452.63±205.68                  | <0.001 |
| Cyst (4)                      | 509.48±145.02     | 1256.33±333.39                  | <0.001 |
| Metastases (5)                | 104.36±52.02      | 416.11±324.94                   | <0.05  |
| Cirrhosis nodules (4)         | 16.34±15.76       | 13.77±12.54                     | >0.05  |
| FNH (5)                       | 65.78±68.4        | 77.5±104.7                      | >0.05  |
| Cholangiocarcinoma (1)        | 63.33             | 766.95                          | -      |
| inflammatory pseudotumor (1)  | 45.58             | 618.01                          | -      |
| Hepatic abscess (1)           | 114.97            | 587.55                          | -      |
| Focal inflammatory lesion (1) | 89.33             | 575.53                          | -      |
| Angiolipoleiomyoma (1)        | 145.26            | 523.91                          | -      |
| Cholangiohepatocarcinoma (1)  | 106.09            | 1390.6                          | -      |

HCC was found in 22 patients. The lesions were iso- or hypointense on T<sub>1</sub>-weighed images and slightly hyperintense on T<sub>2</sub>-weighed images before enhancement. After SPIO administration, 11 cases of the lesions became slightly hyperintense, 10 were isointense and 1 was hypointense on T<sub>1</sub>WI, while on T<sub>2</sub>WI all lesions appeared hyperintense. The mean CNRs of lesion-to-liver on T<sub>1</sub>WI and T<sub>2</sub>WI were greatly improved from -10.2±8.3, 98.4±58.6 to 19.9±23.8, 465.8±272.7 respectively after SPIO administration. The difference had statistical significance ( $P<0.001$ ). After Gd-DTPA administration, 17 cases showed obvious enhancement while the other 5 cases enhanced mildly in early phase. Characteristically, the signal

intensity or enhancement of the lesions decreased significantly in portal and delayed phases (Figure 1A-C).

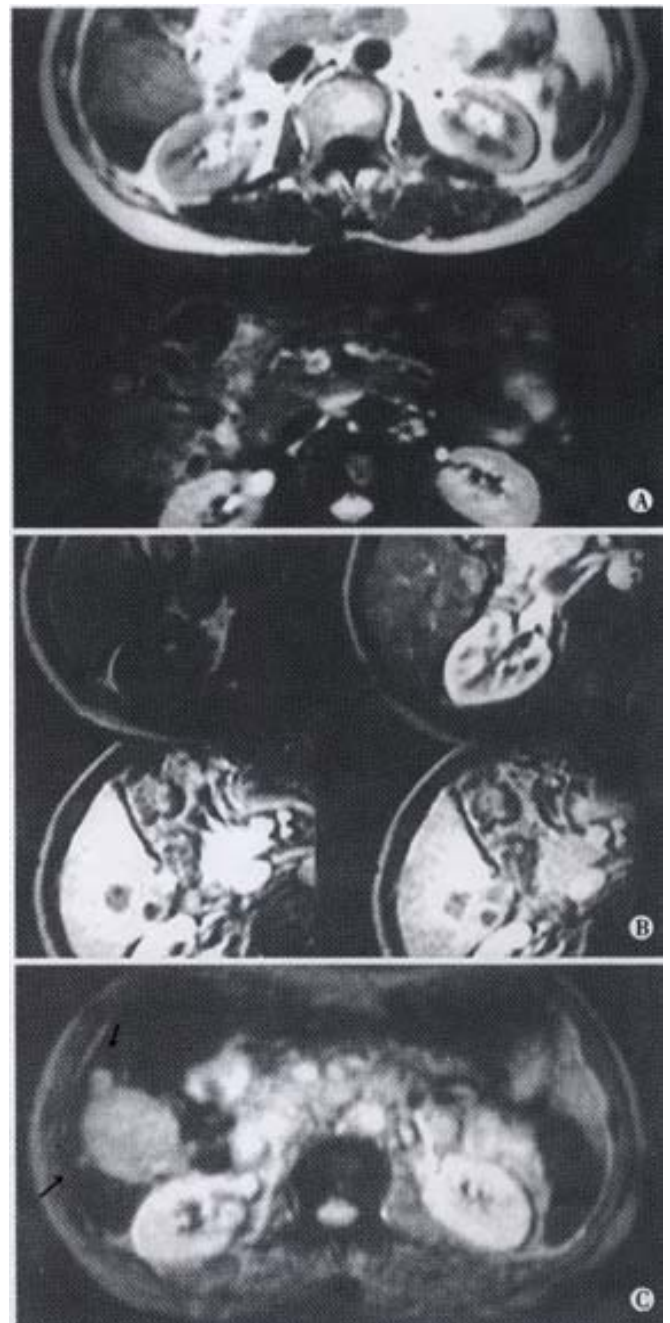


**Figure 1** Primary hepatocellular carcinoma in posterior right lobe. The lesions appear hypointensity on T<sub>1</sub>WI and mildly hyperintensity on T<sub>2</sub>WI (A). On Gd-DTPA enhanced images, early enhancement can be seen in arterial phase and appear relatively hypointensity in portal phase. (B) On SPIO-enhanced image, the conspicuity is clearer than pre-contrasted and Gd-DTPA enhanced images. Two micro-lesions (arrow) are obviously showed (C).

**Hepatic hemangioma** was revealed in 5 cases. The lesions were iso- or hypointense on T<sub>1</sub>WI and markedly hyperintense on T<sub>2</sub>WI in pre-contrast images. After SPIO-enhancement distinct SI increase was noted and the CNR of lesion-to-liver increased from -16.4±8.6 to 71±33 ( $P<0.05$ ) on T<sub>1</sub>WI. The signal intensity showed no perceivable change on T<sub>2</sub>WI, but the CNR of lesion-to-liver was greatly increased because of the signal loss of the background after SPIO administration (Figure 2A, B). After Gd-DTPA enhancement, the lesions were gradually filled by the contrast from peripheral to central area and were kept hyperintense in portal and delayed phases.



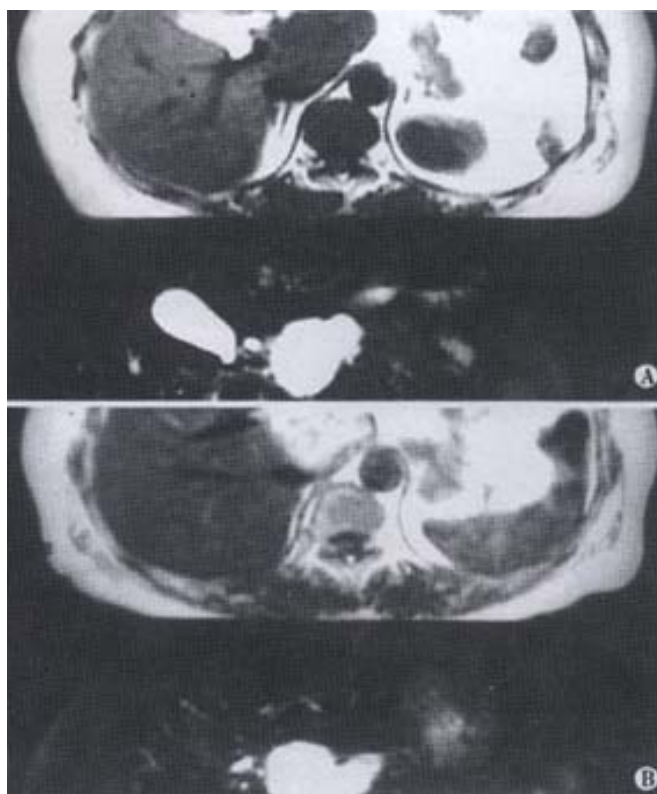


**Figure 2** Hepatic hemangioma. (A) The lesion shows hypointensity on T<sub>1</sub>WI and hyperintensity on T<sub>2</sub>WI on pre-contrast images. (B) After SPIO administration, the lesion become hyperintense on both T<sub>1</sub>WI and T<sub>2</sub>WI (arrow).

**Hepatic cyst** was found in 4 patients. The SI of the cyst had no change after SPIO-enhancement. The hypointensity of cystic lesions on T<sub>1</sub>WI after SPIO-enhancement was characteristic, thus it could be distinguished from other focal hepatic lesions. The hepatic cyst showed no enhancement after Gd-DTPA administration.

**Metastasis** was observed in 5 cases. The lesions were hypointense on T<sub>1</sub>WI pre-enhancement and iso- or hypointense during post-enhancement. On T<sub>2</sub>WI they were mildly hyperintense before enhancement and relatively hyperintense after enhancement because of obvious signal decrease of adjacent normal liver parenchyma. Such change of SI had no diagnostic value because many other focal hepatic lesions could have the similar appearance after SPIO enhancement. The appearance of lesions varied after Gd-DTPA administration, most of them showed peripheral enhancement, or with “bull eyes” sign, or only slightly enhanced.

**Cirrhotic nodule** was found in 4 patients, which was associated with HCC in one patient. On pre-contrast T<sub>1</sub>WI cirrhotic nodules appeared slightly hyperintense differing from other focal hepatic lesions. That the cirrhotic nodule contained Kupffer cells which could take up SPIO particles made it have the same SI as that of the surrounding liver parenchyma after SPIO administration. The cirrhotic nodules showed no early enhancement after Gd-DTPA administration and pertained iso- or hypo-intense in portal and delayed phases.

**Focal nodular hyperplasia (FNH)** was observed in 5 cases. The lesions were slightly hypointense on unenhanced T<sub>1</sub>WI. The appearances of FNH on T<sub>2</sub>WI were variable and could be hyperintense ( $n=2$ ), heterogeneously intense ( $n=2$ ) and iso-intense ( $n=1$ ) which was unable to be detected. After SPIO-enhancement, SI of the lesion decreased markedly and appeared iso- or slightly hyper-intense on T<sub>2</sub>WI, which was characteristic for FNH. On Gd-DTPA enhanced image, the manifestation was also characteristic: it was obviously enhanced in early phase and continuously kept hyperintense in portal and delayed phases (Figure 3A-C).

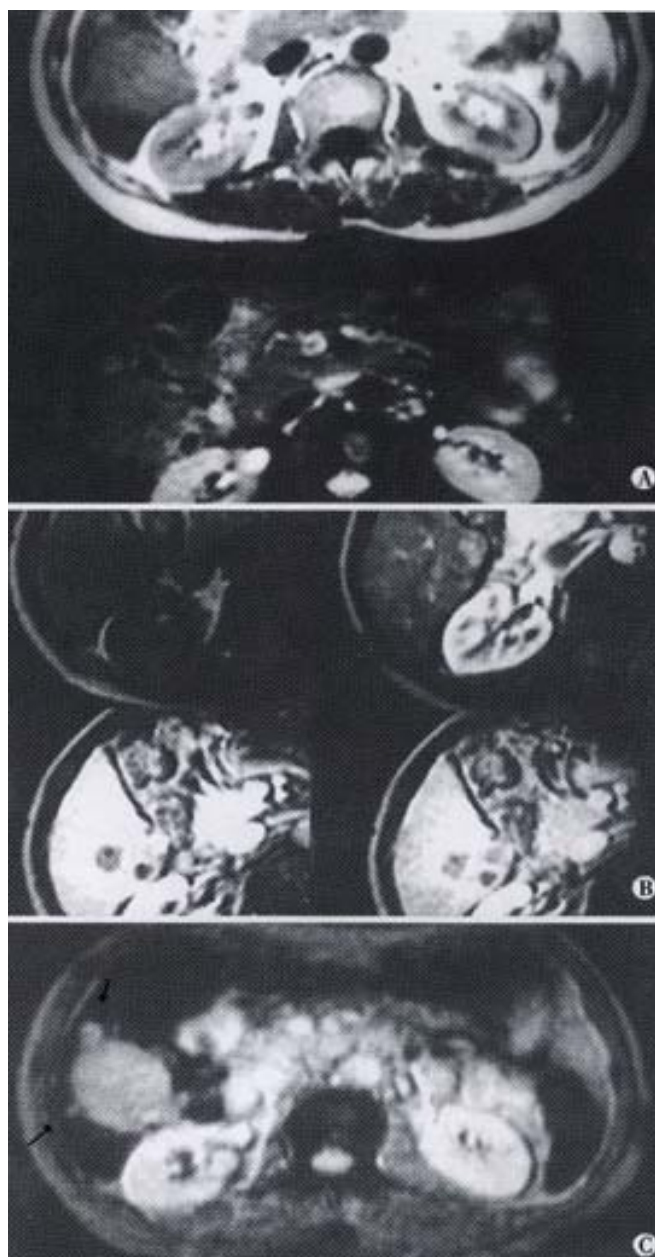


**Figure 3** Focal nodular hyperplasia (FNH). Before enhancement, the lesion (arrow) presents hypointensity on T<sub>1</sub>WI and heterogeneous hyperintensity on T<sub>2</sub>WI (A). After Gd-DTPA administration, the lesion is obviously enhanced in arterial phase and remains hyperintense in portal and delayed phase (B). On T<sub>2</sub>WI after SPIO enhancement, the lesion (arrow) has focal signal loss compared with the un-enhanced image (C).

**Other focal hepatic lesions** were found in 6 cases including cholangiocarcinoma ( $n=1$ ), inflammatory pseudotumor ( $n=1$ ), hepatic abscess ( $n=1$ ), focal inflammatory lesion ( $n=1$ ), angiolipoleiomyoma ( $n=1$ ), and cholangiohepatocarcinoma ( $n=1$ ). These lesions were hypointense on T<sub>1</sub>WI and slightly or moderately hyperintense on T<sub>2</sub>WI before enhancement. The appearances were non-specific after SPIO-enhancement although the contour of lesions was clear and the CNR of lesion-to-liver increased, which was helpful in improving the detectability or conspicuity. The appearances of these lesions on Gd-DTPA enhanced images were also diversified.

## DISCUSSION

As a non-specific extracellular contrast material, Gd-DTPA has been widely used in MR imaging of the liver. Dynamic Gd-DTPA-



enhanced MR images can provide much useful information of the blood supply of lesions and thus highly improving the accuracy of diagnose of focal hepatic lesions. However, Gd-DTPA has several disadvantages such as non-specific distribution, quickly reaching equilibrium throughout extracellular compartment and having slightly nephrotic toxicity. As a negative contrast material, namely reticulo-endothelial system specific contrast agent, the particles of SPIO can be taken up primarily by the hepato-splenic Kupffer cells. The collection of SPIO particles can produce a focal heterogeneous magnetic field which shortens T2 relaxation time predominantly, leading to a significant decrease of SI of normal hepatic parenchyma and remarkable improvement for the focal lesion detection. The prolonged half-life time and widened scanning time-window are also helpful in making examination more convenient<sup>[1,4,5,13-15,17]</sup>.

The signal intensity of normal hepatic parenchyma decreased both on T<sub>1</sub>WI and T<sub>2</sub>WI after SPIO-enhancement, especially on T<sub>2</sub>WI. The SI of HCC changed a little due to lack of Kupffer cells, but the signal loss of background inversely makes the HCC appear hyperintense. As a result, the CNR of lesion-to-liver increased and the detection of HCC after SPIO-enhancement being improved. There are a few of reports dealing with the appearance of HCC on SPIO-enhanced MR images<sup>[9,14,17-22]</sup>. Grangier described HCC's feature in 10 cases after SPIO enhancement and concluded that the HCC presenting iso-intensity on T1WI was the key point for differentiating HCC from hemangioma and cyst<sup>[11]</sup>. However, we believe that it might be inappropriate because the appearances of HCC in our 22 cases on enhanced-T<sub>1</sub>WI were slightly hyperintense, isointense and hypointense which were 50% (11/22), 45.5% (10/22) and 4.5% (1/22) respectively. This might be attributed to more examples in our study or the difference of HCC's differentiation between the two studies. The non-characteristic appearances of HCC on pre- and post-SPIO-enhanced T<sub>2</sub>WI made it difficult to distinguish from other malignant lesions. Moreover, the signal changes on pre- and post-enhanced T<sub>1</sub>WI can exclude the possibility of hemangioma and cyst. Accordingly, the accurate diagnosis of HCC must not merely rely on the appearance of lesion on SPIO-enhanced MRI but on the combination with the clinical findings and biochemical tests. After Gd-DTPA administration, the precise diagnosis in most cases can be made according to the enhancement pattern of the lesion. Typically, HCC is enhanced rapidly in arterial phase and the contrast agent is soon washed out in portal phase. So we believe that, only for those the diagnoses are indefinite or the appearances of lesion are untypical on Gd-DTPA-enhanced images, SPIO-enhanced MRI could be a method of choice to make further diagnosis<sup>[17-21]</sup>.

The hemangioma had high SI on unenhanced T<sub>2</sub>WI and showed no change on SPIO-enhanced T<sub>2</sub>WI. The hemangioma presenting moderate hyper-intensity on T<sub>1</sub>WI after SPIO-enhancement is a key point to distinguish it from cyst and other focal hepatic lesions. However, such typical appearance did not present, owing to the partial volume effect in tiny hemangioma in our study, manifesting iso- or slight hyper-intensity on post-enhanced T<sub>1</sub>WI which might make the diagnosis confused. Grangier and Hahn *et al* reported that on SPIO-enhanced T<sub>2</sub>WI, the SI of hemangioma could decrease significantly and its enhancement pattern was as the same as that on Gd-DTPA enhanced T1WI (the lesion was filled with contrast agent gradually)<sup>[10,11]</sup>. Although the signal of lesion decreased a little, 11 lesions of 5 patients in our study had no such appearance and remained hyper-intensitive namely "Bright Bulb" on SPIO-enhanced T<sub>2</sub>WI. Whether such difference is attributed to the different dosage of contrast agent used in studies (10(mol Fe·kg<sup>-1</sup> in our group vs 15(mol Fe·kg<sup>-1</sup> in others) needs further investigations.

SPIO has unique advantages in diagnosing liver cirrhotic nodules and FNH. Both contain Kupffer cells which can take up the SPIO particles. Accordingly, on post-contrast T<sub>2</sub>WI, the former showed identical intensity to that of adjacent normal hepatic parenchyma and the latter had signal loss of different degree. Hepatic cirrhotic nodule

and FNH were the only two diseases that had signal loss in our study. As hepatic cirrhotic nodules usually have a cirrhosis background, the lesion presented the SI similar to that of surrounding liver parenchyma after SPIO-administration and no early enhancement after Gd-DTPA administration is the key factor to make the accurate diagnosis. In our study there were 3 liver cirrhotic nodules, which had difficulty in characterization on pre- and Gd-DTPA enhanced MR images, accurate diagnoses were made after SPIO-administration. Thus, SPIO-enhanced MRI is supposed to be the first choice when the cirrhotic nodule is suspected to be associated with early stage of canceration and has no obvious early enhancement after Gd-DTPA administration<sup>[15]</sup>. FNH has no cirrhotic background with abnormally arrayed lobuli hepatis. The various appearances on pre-contrast T<sub>2</sub>WI might be corresponding to its different cellular components. Most lesions were iso- or slightly hyperintense on T<sub>2</sub>WI and had signal loss on SPIO-enhanced image. The CNR of lesion-to-liver had no statistical significance between pre- and post-contrast images in our study. This can exactly demonstrate that Kupffer cell in FNH uptake the contrast media and decrease the SI while the background has signal loss at the same time (the mean SI of lesion and liver decreased from 138.6 to 43 and 85.3 to 23.6 respectively on pre- and post-contrast images). The change of SI was different from other diseases and had statistical significance ( $P < 0.05$ ). The central scar was reported to present as mildly hyperintense and 2 cases in our study had this appearance. The characterized appearance of FNH on Gd-DTPA enhanced MR image demonstrated markedly early enhancement as homogeneous hyperintense and iso- to slightly hyperintense in portal or delayed phase. Central scar in 3 lesions enhanced in delayed phase. The results in our study were consistent with other report<sup>[24-29]</sup>.

Cyst had no signal change on both pre- and post-contrast T<sub>1</sub>W, and T<sub>2</sub>W images. There were 4 inflammatory cases and 1 case of abscess in our study which had no visible difference on pre- and post- SPIO enhanced images. Diagnoses were made only by Gd-DTPA enhanced images and confirmed after clinical antibiotics treatment and follow-up. One case of inflammatory pseudotumor was pathologically proven<sup>[30]</sup>. One case of cholangiocarcinoma was diagnosed mainly on Gd-DTPA enhanced images which provided more information of the blood supply of lesions. Another case of angiolipoleiomyoma was misdiagnosed as HCC before surgery on both Gd-DTPA and SPIO-enhanced images because it had early enhancement and no SPIO uptake. When retrospectively reviewed, the patchy hyperintensity on T<sub>1</sub>W and T<sub>2</sub>W images corresponding to fatty component might suggest the diagnosis. Since there was no obvious difference of SI, SPIO-contrasted image had little specificity in diagnosing such hepatic inflammation, cholangiocarcinoma and angiolipoleiomyoma<sup>[30-33]</sup>. To characterize these lesions, SPIO-enhanced image was inferior to Gd-DTPA image although the lesions showed better circumscription.

As a specific MR contrast media, there is no doubt that SPIO has superiority in detection of hepatic micro-lesions. It is also useful in characterization of some lesions and is superior to unenhanced MR with Gd-DTPA enhanced image when differential diagnosis of HCC, FNH and cirrhotic nodule is needed. As most hepatic lesions could be precisely diagnosed by conventional MR combined with Gd-DTPA dynamic contrast enhancement, SPIO-enhanced image would be a supplementary modality to those which are difficult to be defined.

## REFERENCES

- 1 Peter F, Sanjay S. Liver-specific MR imaging contrast agents. *Radiol Clin North Am* 1998;36:287-296
- 2 Anthony B, Janice W, Daniel W, *et al.* Hepatic lesion detection at MR imaging: A comparative study with four sequences. *Radiology* 1997; 203:759-765
- 3 Fretz CJ, Elizondo G, Weissleder R, Hahn PF, Stark DD, Ferrucci JT. Superparamagnetic iron oxide-enhanced MR imaging: Pulse sequence optimization for detection of liver cancer. *Radiology* 1989;172:393-397
- 4 Masayuke M, Kanematsu M, Itoh K, Maetani Y, Kondo H, Matsunaga N, Hoshi H, Shiraishi J. Detection of malignant hepatic tumors:

- comparison of Gadolinium- and Ferumoxide-enhanced MR imaging. *AJR* 2001;177:637-643
- 5 Taylor PM, Hawnaur JM, Hutchinson CE. Superparamagnetic iron oxide imaging of focal liver Disease. *Clinical Radiology* 1995;50:215-219
- 6 Lwakatare F, Yamashita Y, Nakayama M, Takahashi M. SPIO-enhanced MR imaging of focal fatty liver lesions. *Abdom Imaging* 2001;26:157-160
- 7 Ros PR, Freeny PC, Harms SE, Seltzer SE, Davis PL, Chan TW, Stillman AE, Muroff LR, Runge VM, Nissenbaum MA. Hepatic MR imaging with ferumoxides: a multicenter clinical trial of the safety and efficacy in the detection of focal hepatic lesions. *Radiology* 1995;196:481-488
- 8 Winter TC, Freeny PC, Nghiem HV, Mack LA, Patten RM, Thomas CR, Elliott S. MR Imaging with IV superparamagnetic ironoxide: efficacy in the detection of focal hepatic lesions. *AJR* 1993;161:1191-1198
- 9 Bluemke DA, Paulson EK, Choti MA, DeSena S, Clavien PA. Detection of hepatic lesions in candidates for surgery: comparison of Ferumoxides-enhanced MR imaging and dual-phase helical CT. *AJR* 2000;175:1653-1658
- 10 Bellin NB, Zaim S, Auberton E, Sarfati G, Duron VJ, Khayat D, Grellet J. Liver metastases: Safety and efficacy of detection with superparamagnetic iron oxide in MR imaging. *Radiology* 1994;193:657-663
- 11 Grangier C, Tourniaire J, Mentha G, Schiau R, Howarth N, Chachuat A, Grossholz M, Terrier F. Enhancement of liver hemangiomas on T1-weighted MR SE images by superparamagnetic iron oxide particles. *J Comput Assist Tomogr* 1994;18:888-896
- 12 Hahn RF, Stark DD, Weissleder R, Elizondo G, Saini S Ferrucci JT. Superparamagnetic iron oxide: Clinical application to imaging tissue perfusion in vascular liver tumors. *Radiology* 1990;174:361-366
- 13 Grandin C, Van Beers BE, Robert A, Gigot JF, Geubel A, Pringot J. Benign hepatocellular tumors: MRI after superparamagnetic iron oxide administration. *J Comput Assist Tomogr* 1995;19:412-418
- 14 Parley MR, Mergo PJ, Torres GM, Ros PR. Characterization of focal hepatic lesions with Ferumoxides-enhanced T2-weighted MR imaging. *AJR* 2000;175:159-163
- 15 Clement O, Frija G, Chambon C, Schouman-Clayes E, Mosnier JF, Poupon MF, Balkau B. Liver tumors in cirrhosis: experimental study with SPIO-enhanced MR imaging. *Radiology* 1991;180:31-36
- 16 Krinsky GA, Lee VS, Theise ND, Weinreb JC, Rofsky NM, Diflo T, Teperman LW. Hepatocellular carcinoma and dysplastic nodules in patients with cirrhosis: prospective diagnosis with MR imaging and explantation correlation. *Radiology* 2001;219:445-454
- 17 Fernandez MDP, Redvanly R. Primary hepatic malignant neoplasms. *Radiol Clin North Am* 1998;36:333-348
- 18 Reimer P, Jahnke N, Fiebich M, Schima W, Deckers F, Marx C, Holzknecht N, Saini S. Hepatic lesion detection and characterization value of nonenhanced MR imaging, superparamagnetic iron oxide-enhanced MR imaging, and spiral CT -ROC analysis. *Radiology* 2000;217:152-158
- 19 Arbab AS, Ichikawa T, Araki T, Toyama K, Nambu A, Ohsawa S, Kumagai H, Aikawa Y. Detection of hepatocellular carcinoma and its metastases with various pulse sequences using superparamagnetic iron oxide (SHU-555-A). *Abdom Imaging* 2000;25:151-158
- 20 Kondo H, Kanematsu M, Hoshi H, Murakami T, Kim T, Hori M, Matsuo M, Nakamura H. Preoperative detection of malignant hepatic tumors: comparison of combined methods of MR imaging with combined methods of CT. *AJR* 2000;174:947-954
- 21 Mori K, Yoshioka H, Itai Y, Okamoto Y, Takahashi N, Saida Y. Arterioportal shunts in cirrhotic patients: Evaluation of the difference between tumorous and nontumorous arterioportal shunts on MR imaging with superparamagnetic iron oxide. *AJR* 2000;175:1659-1664
- 22 Hahn PF, Stark DD, Weissleder R, Elizondo G, Saini S, Ferrucci JT. Clinical Application of superparamagnetic iron oxide of MR imaging of tissue perfusion in vascular liver tumors. *Radiology* 1991;174:361-366
- 23 Paley MR, Ros PR. Hepatic metastases. *Radiol Clin North Am* 1998;36:349-368
- 24 Mergo PJ, Ros PR. Benign lesions of the liver. *Radiol Clin North Am* 1998;36:319-332
- 25 Mortelet KJ, Praet M, Van Vlierberghe H, et al. CT and MR imaging findings in focal nodular hyperplasia of the liver: radiologic-pathologic correlation. *AJR* 2000;175:687-692
- 26 Carlson SK, Daniel JC, Bender CE, Welth TJ. CT of focal nodular hyperplasia of the liver. *AJR* 2000;174:705-712
- 27 Ji Y, Zhu XZ, Tan YS, Zeng HY, Ye QH, Tang ZY. A clinicopathological study of hepatic focal nodular hyperplasia. *Zhonghua Binglixue Zazhi* 2000;29:334-336
- 28 Yi Y, Zhu XZ, Sun HC, Tan YS, Ma ZC, Ye QH, Sujie A, Tang ZY. Hepatocellular adenoma and focal nodular hyperplasia: a series of 24 patients with clinicopathological and radiological correlation. *Chinese Medical Journal* 2000;113:852-857
- 29 Ruppert-Kohlmayr AJ, Uggowitz MM, Kugler C, Zebedin D, Schaffler G, Ruppert GS. Focal nodular hyperplasia and hepatocellular adenoma of the liver: differentiation with multiphasic helical CT. *AJR* 2001;176:1493-1498
- 30 Yan FH, Zhou KR, Jiang YP, Shi WB. Inflammatory pseudotumor of the liver: 13 cases of MRI findings. *World J Gastroenterol* 2001;7:422-424
- 31 Ye HY, Xie ZF, Gao YG, Liang Y, Ji XL, Yu G. Hepatic angiomyolipoma: correlation of MRI and pathologic findings. *Zhonghua Fangshexue Zazhi* 2001;35:679-681
- 32 Braga HJ, Imam K, Bluemke DA. MR imaging of intrahepatic cholangiocarcinoma: use of Ferumoxides for lesion localization and extension. *AJR* 2001;177:111-114
- 33 Ahmadi T, Itai Y, Takahashi M, Onaya H, Kobayashi T, Tanaka YO, Matsuzake Y, Tanaka N, Okada Y. Angiomyolipoma of the liver: significance of CT and MR dynamic study. *Abdom Imaging* 1998;23:520-526

• LIVER CANCER •

# Antitumor activities of human dendritic cells derived from peripheral and cord blood

Jin-Kun Zhang, Jun Li, Hai-Bin Chen, Jin-Lun Sun, Yao-Juan Qu, Juan-Juan Lu

Jin-Kun Zhang, Jun Li, Hai-Bin Chen, Jin-Lun Sun, Yao-Juan Qu, Juan-Juan Lu, Cancer Pathology Laboratory, Shantou University Medical College, Shantou 515031, Guangdong Province, China  
Supported by Natural Science Foundation of the Higher Education Office of Guangdong Province, No. 9501 and No.9816

Correspondence to: Prof. Jin Kun Zhang, Cancer Pathology Laboratory, Shantou University Medical College, 22 Xinlinglu, Shantou 515031, Guangdong Province, China. Jkzhang@stu.edu.cn

Telephone: +86-754-8900443 Fax: +86-754-8557562

Received 2001-07-19 Accepted 2001-12-29

## Abstract

**AIM:** To observe the biological specialization of human peripheral blood dendritic cells (DC) and cord blood derived DC and its effects on effector cells killing human hepatocarcinoma cell line BEL-7402 *in vitro*.

**METHODS:** The DC biological characteristics were detected with immunohistochemical and MTT assay. Two antitumor experimental groups are: peripheral blood DC and cord blood DC groups. Peripheral blood DC groups used LAK cells as the effector cells and BEL-7402 as target cells, while cord blood DC groups used CTL induced by tumor antigen twice pulsed DC as effector cells and BEL-7402 as target cells, additional peripheral blood DC and cord blood DC are added to observe its stimulating activities to effector cells. The effector's cytotoxicity to tumor cells were detected with neutral red colorimetric assay at two effector/target ratios of 5:1 and 10:1.

**RESULTS:** Peripheral blood DC and cord blood DC highly expressed HLA-ABC, HLA-DR, HLA-DQ, CD54 and S-100 protein. The stimulating activities to lymphocyte proliferation were compared between experimental groups (DC added) and control group (no DC added), in six experiment subgroups, the DC/lymphocyte ratio was sequentially 0.25:100, 0.5:100, 1:100, 2:100, 4:100 and 8:100, A values ( $\bar{x} \pm s$ ) were 0.75396 $\pm$ 0.009, 0.84916 $\pm$ 0.010, 0.90894 $\pm$ 0.012, 0.98371 $\pm$ 0.007, 1.01299 $\pm$ 0.006 and 1.20384 $\pm$ 0.006 in peripheral blood DC groups and 0.77650 $\pm$ 0.005, 0.83008 $\pm$ 0.007, 0.92725 $\pm$ 0.007, 1.05990 $\pm$ 0.010, 1.15583 $\pm$ 0.011, 1.22983 $\pm$ 0.011 in cord blood DC groups. A value was 0.59517 $\pm$ 0.005 in control group. The stimulating activities were higher in experimental groups than in control group ( $P < 0.01$ ), which were increased when the DC concentration was enlarged ( $P < 0.01$ ). Two differently derived DCs had the same phenotypes and similar stimulating activities ( $P > 0.05$ ). In peripheral blood DC groups, the cytotoxicity ( $\bar{x} \pm s$ ) of the LD groups (experimental groups) and L groups (control group) was 58.16% $\pm$ 2.03% (5:1), 46.18% $\pm$ 2.25% (10:1) and 38.13% $\pm$ 1.29% (5:1) and 65.40% $\pm$ 1.56% (10:1) respectively; in cord blood DC groups, TD groups (experimental groups) and T groups (control groups) were 69.71% $\pm$ 2.33% (5:1), 77.64% $\pm$ 1.94% (10:1) and 56.89% $\pm$ 1.82% (5:1) and 60.99% $\pm$ 1.42% (10:1) respectively. The cytotoxicity activities were enhanced with increased effector/target ratio ( $P < 0.01$ ). At the same

**effector/target ratio, the cytotoxicity of experimental groups were bigger than that of control groups ( $P < 0.01$ ). The cytotoxicity activities of cord blood DC groups were higher than that of peripheral blood DC groups ( $P < 0.01$ ).**

**CONCLUSION:** Peripheral blood DC and cord blood DC are mature DC in morphology and function, both can enhance the effector cell killing activities to hepatocarcinoma cells. DC pulsed with tumor antigen can induce higher specific CTL activity than unpulsed DC.

Zhang JK, Li J, Chen HB, Sun JL, Qu YJ, Lu JJ. Antitumor activities of human dendritic cells derived from peripheral and cord blood. *World J Gastroenterol* 2002;8(1):87-90

## INTRODUCTION

Dendritic cells (DC) is a potent professional antigen presenting cell, the only one that can stimulate the naive T cell<sup>[1-4]</sup>. DC can present exogenous antigen to CD4<sup>+</sup> cell by MHC-II antigen presenting pathways as well as to CD8<sup>+</sup> cell by MHC-I pathways. It also provides plenty of costimulating signals, so that it plays a key role in antitumor immunity<sup>[5-9]</sup>. Although the peripheral blood DC is easily separated, DC was able to enhance the killing activity of Lymphokine and PHA activated killer (LAK) cells *in vitro*<sup>[10-12]</sup>, but in some patients with tumors, especially some patients with advanced tumors, autogenous DC may be defective. In this article, two differently derived DCs are studied on their induction of anti-hepatocarcinoma cell activity. It provides experimental evidence for clinical application of DC directed tumor immunotherapy.

## MATERIAL AND METHODS

### Blood

Human peripheral blood provided by young volunteers, and cord blood provided by Shantou University Medical College First Affiliated Hospital.

### Tumor cell line

BEL-7402 tumor cell line was bought from Experimental Animal Center, Sun Yat-Sen University of Medical Sciences.

### Main reagents

Percoll was purchased from Pharmacia. Mini-MACS (magnetic activated cell sorter) and CD34 cell separation kit were purchased from Miltenyi GmbH Biotec, a kit including the following reagents: A1-human Ig (FcR), A2-haptin coupled CD34 monoclonal antibody, B-colloid anti-haptin antibody and microbead. rhSCF, rhGM-CSF and rh TNF- $\alpha$  were obtained from Pepro Tech Ltd or Institute of Basic Medicine Sciences, Chinese Military Medical Academy. Mouse anti-human antibody CD54, HLA-ABC, HLA-DR, HLA-DQ, S-100 protein and SABC immunohistochemical kit were obtained from Biotec, Boehringer Mannheim and Boster, respectively. MTT was from Amresco.

### Isolation of human blood DC

**Isolation of Human Peripheral blood DC<sup>[9]</sup>** Four step method of our laboratory was used. Peripheral blood mononuclear cells from

healthy volunteers were prepared using Ficoll-Hypaque ( $\rho=1077 \text{ g}\cdot\text{L}^{-1}$ ) centrifugation method. Interface cells were collected and washed three times to remove platelets. Discontinuous Percoll density gradient centrifugation was employed, and interface cells between 35% and 50% called preliminary enrichment of DC were collected, cultured in PRMI 1640 with  $100\text{mL}\cdot\text{L}^{-1}$  inactivated fetal calf serum ( $100 \text{ mL}\cdot\text{L}^{-1}$  FCS PRMI 1640) at  $37^\circ\text{C}$ , in a saturation humidity, atmosphere of  $50\text{mL}\cdot\text{L}^{-1} \text{ CO}_2$  for 36 hours, then panned on Ig coated petri dish for further purification, nonadhesive cells were collected as the mature DC.

**Isolation of human cord blood DC** The  $\text{CD}34^+$  stem cells, were separated using  $\text{CD}34^+$  stem cell separation kit and microbead, Mini-MACS cell sorter, cultured with rhGM-CSF, rhTNF- $\alpha$  and rhSCF for 14 d, mature DC was acquired.

#### Immunohistochemistry method for DC phenotypes

Peripheral blood DC smear and cord blood DC smear were prepared and incubated with mouse anti human HLA-ABC, CD54, HLA-DQ, HLA-DR and S-100 protein primary antibody. ABC staining and DAB were used to display the result.

#### DC stimulating activity to homogenous lymphocyte

**DC stimulating activity to homogenous lymphocyte proliferation** Human peripheral blood lymphocytes were obtained by Ficoll separation method. Two groups of peripheral blood DC and cord blood DC were divided. In each group, six subgroups were divided according to the DC/lymphocyte ratio of 0.25:100, 0.5:100, 1:100, 2:100, 4:100 and 8:100 respectively. Lymphocyte concentration was  $8\times 10^8\cdot\text{L}^{-1}$ , PHA was  $50\text{mg}\cdot\text{L}^{-1}$ . Control group as DC+PHA served as control in each subgroup. Additional lymphocyte+PHA and PHA also served as control groups. Each subgroup set three wells on 96 multiwell culture plates. Each experiment repeated 4 times.

**MTT colorimetric method detecting the lymphocyte proliferation** Add  $20 \mu\text{L}$  MTT ( $5\text{g}\cdot\text{L}^{-1}$ ) to each well of multiwell culture plate, incubate for 4 hours, then add  $150\mu\text{L}$  DMSO, mixed about 10 min until the crystal completely dissolved. The absorption value (A value) of each well was immediately read by Bio-Rad 3550-UV type automatic enzyme linked detector at 490nm wavelength. The minus of A value in experimental group and A in DC+PHA shows the proliferative response. The minus of A value in lymphocyte + PHA group and A in PHA shows the lymphocyte proliferation of control group. SPSS software was applied for analysis of variation.

#### Effector cells induced

**LAK cell induced** The human peripheral blood mononuclear cells were prepared by the same procedure above, cultured at  $2\times 10^9\cdot\text{L}^{-1}$  population with the final concentration of rhIL-2  $1000\text{kU}\cdot\text{L}^{-1}$  and PHA  $20\text{mg}\cdot\text{L}^{-1}$  in  $100\text{mL}\cdot\text{L}^{-1}$  FCS PRMI-1640 at  $37^\circ\text{C}$  in a full humidified  $50\text{mL}\cdot\text{L}^{-1} \text{ CO}_2$  atmosphere for 7 d. Half volume of solution was replaced by fresh culture medium at d4.

**CTL induced twice by antigen pulsed DC** The whole culture system included human peripheral mononuclear cells  $1\times 10^8\cdot\text{L}^{-1}$ , cord blood DC  $5\times 10^6\cdot\text{L}^{-1}$ , ultrasonic disrupted BEL-7402 cells  $1\times 10^9\cdot\text{L}^{-1}$ , IL-2  $80 \text{ kU}\cdot\text{L}^{-1}$ . They were cultured for 5 d and pulsed again at d3. Control culture system (no DC added) was set.

#### Antitumor experiment

**DC induced CTL killing activity to hepatocarcinoma cells** The experiment was conducted two groups: peripheral blood DC group and cord blood DC group, each group being divided into two subgroups. Peripheral blood DC groups: BEL-7402+LAK (L group) as control

group, BEL-7402 +LAK +DC (LD group) as experiment group. BEL-7402 cell concentration was  $8\times 10^8\cdot\text{L}^{-1}$ , DC was  $8\times 10^6\cdot\text{L}^{-1}$ , two LAK /BEL-7402 ratio of 5:1 and 10:1 were applied. Cord blood DC groups: BEL7402+CTL (T group) as control group, BEL7402+DC-CTL (TD group) as experimental group. Cell concentration and ratio were the same as above. Additional BEL-7402 culture media was set as control group. Each group set three paralleled wells, cultured in 96 multiwell culture plate for 48 hours, the effector cell killing activities were detected. The procedure above was repeated for 4 times.

**Neutral red uptake method** Neutral red uptake method was applied to detect the cytotoxicity activities of effector cells,  $0.1 \text{ mL}$  neutral red solution  $0.3\text{g}\cdot\text{L}^{-1}$  was added to each well, incubated at  $37^\circ\text{C}$  for 1 h, rinsed with PBS, solution of hydrochloride ethanol  $0.1 \text{ mL}$  was added, and absorbance was detected at 570 nm by Bio-Rad automatic enzyme linked detector. Formula for cytotoxicity calculation is below:

$$(1 - \frac{\text{A value of experiment group} - \text{A value of medium control group}}{\text{A value of control group} - \text{A value of medium control group}}) \times 100\%$$

SPSS for windows statistic software are used for data variation analysis.

## RESULTS

#### DC phenotypes analysis

Immunohistochemical ABC method showed that human peripheral blood DC and human cord blood DC had high expression of HLA-ABC, HLA-DR, HLA-DQ and CD54. S-100 protein was also positive. Positive cells were big and irregular in shaped and filled with diffuse brown-yellow particles in cytoplasm, the neucleus was also big and irregular. However, the phenotype difference between peripheral blood DC and cord blood DC was not distinct.

#### DC stimulating activity to lymphocyte

In human peripheral blood DC and human cord blood DC groups, lymphocyte proliferation activities were significantly higher than control groups ( $P<0.01$ ), which was increased when DC concentration was enlarged ( $P<0.01$ ). Human peripheral blood DC and human cord blood derived DC had no significant difference in lymphocyte stimulation ( $P>0.05$ , Figure 1).

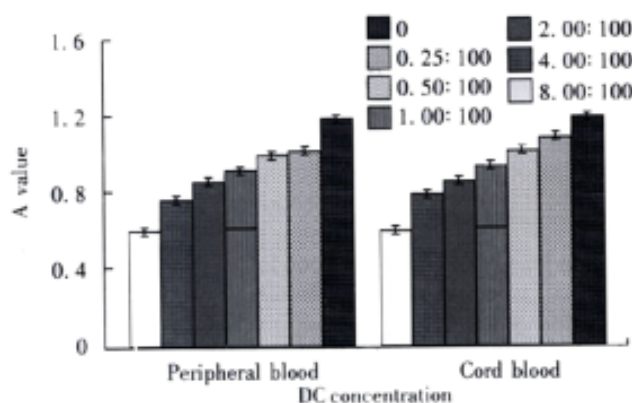


Figure 1 Lymphocyte proliferation response by different DC concentrations.

#### DC induced effector's cytotoxicity activities

In groups of human peripheral blood DC and human cord blood DC, cytotoxicity activities enhanced with the increased effector/target ratio ( $P<0.01$ ). Within the same ratio, cytotoxicity activities of experimental groups were higher than control groups ( $P<0.01$ ). Cytotoxicity activities of human cord blood DC groups were bigger

than human peripheral blood DC groups ( $P < 0.01$ , Figure 2)

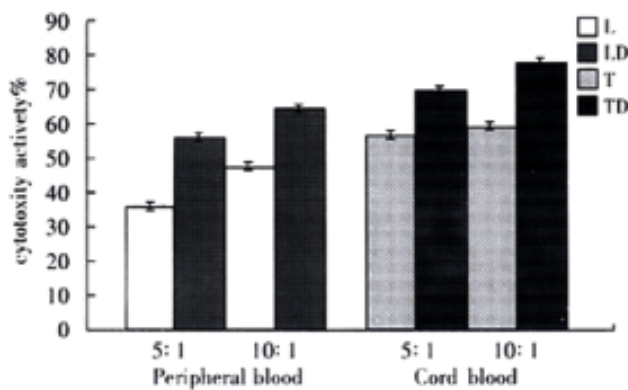


Figure 2 DC's effect to cytotoxicity activity of effector against BEL7402.

## DISCUSSION

DC is a potent antigen presenting cells, mainly takes part in cell immunity and T cell dependent humoral immunity, and plays a key role in antitumor immunity<sup>[13-21]</sup>. Recently, with the construction of DC isolation method and expanding culture *in vitro*, research has transfer red from the relationship between tumor infiltrating DC and the prognosis to DC application in tumor immunotherapy, especially how to improve the tumor cell immunogenicity and enhance the DC antigen presenting efficacy and stimulating activity to CTL<sup>[22-30]</sup>. In this experiment, DC of human peripheral blood and cord blood were studied on its potential in clinical application.

Human peripheral blood DC isolation was made according to four step method modified in this laboratory. This method is easy to operate, low in cost and reliable, and has been used in this laboratory for many years, and high purity of DC can be obtained by this method<sup>[31,32]</sup>. Another method is used in cord blood DC isolation: CD34<sup>+</sup> cell isolation kit combined with cell factor expanding culture for preparation of cord blood derived DC. This is an advancing method. The principle of CD34<sup>+</sup> cell isolation kit is as follows: CD34<sup>+</sup> monoclonal antibody recognizes the specific antigen of stem cell membrane, by which the antibody coupled magnetic microbead binds to cells, when the cells pass through column in the magnetic field, the CD34<sup>+</sup> can be acquired by positive selection. Three reagents comprises in CD34<sup>+</sup> isolation kit: A1, human Ig, used as blocking reagent to FcR for preventive non specific binding of CD34<sup>+</sup> monoclonal antibody to CD34<sup>+</sup> cells. A2, hapten coupled CD34 monoclonal antibody, can specifically bind with CD34 molecule. B, anti-hapten antibody linked with microbead, can link the microbead with CD34<sup>+</sup> cells. When the cells pass through MACS (magnetic cell sorter) column in magnetic field, negative cells can pass through the column, while positive cells were absorbed to column. When the column was taken away from magnetic field, the elution from column included the positive cells. MACS cell isolation has been verified by immunofluorescent PCR, FISH and FACS method. It has the characteristics of high purity (93%-99.9%)<sup>[14]</sup>, large number of cells processing ability in a single time, and easy operating, simple procedure. When cell factors such as rhGM-CSF, rhTNF- $\alpha$  and SCF are added to stem cell culture media, most of CD34<sup>+</sup> cells differentiate to DC<sup>[33]</sup>. Though the GM-CSF can stimulate cell growth of both the DC progenitor and monocyte or macrophage, for high purity of CD34<sup>+</sup> cell in initiate culture system, clearance most of monocyte and macrophage by its adherence to flask by replacing media and culture plate. Cell factor secreted by monocyte and macrophage also benefits DC development.

In this article, a series of antibodies were used for immunohistochemical staining of DC, results showed that human peripheral blood DC had and CD34<sup>+</sup> derived cord blood DC high

expression of CD54, HLA-ABC, HLA-DR, HLA-DQ, and S-100 protein. The positive cells accounted for above 95% and 90% respectively, demonstrating that DC here is mature<sup>[34,35]</sup>.

For DC functional analysis, MTT assay was used to detect the DC activity of stimulating the allogeneous lymphocyte. The principle of MTT assay is that the living proliferating cells can deoxidize the MTT (thiazoyl blue tetrazolium bromide) to purple crystal formazan and deposit in cytoplasm, so we can use the colorimetric method to detect the cell proliferation. With continuous modification, it has become a very consummate method with characteristics of sensitivity, simple procedure, safety and no radioactivity. In this experiment, DC can clearly stimulate the lymphocyte response to PHA. It shows that the DC has potent MLR stimulating activity which contributes to DC expression of adherence and MHC- II molecule. Phenotype and functionally mature DC of high purity provided primitive condition for DC application in antitumor.

Tumor cells expressed low level antigen and has antigen modulation, so tumor antigen can not be efficiently presented and the T cell mediated immune response can not be activated, by which tumor can escape the surveillance of immune system. As a nonprofessional APC, tumor cells with no expression of costimulator often leads to T cell anergy. Special attention has been paid to DC for its present exogenous antigen to CD8<sup>+</sup> cell by MHC- I antigen presenting pathway as well as its expression of costimulating signal<sup>[36-40]</sup>. In this article, peripheral and human cord blood DC can significantly improve effector's cytotoxicity, due to a large quantity of dendrites, and many kinds of surface molecules and receptors and cytokine secreted<sup>[41,42]</sup>. LAK cells induced for 7 days chiefly demonstrated CTL's characteristic of CD16<sup>+</sup>, CD8<sup>+</sup> and CD3<sup>+</sup>, which can efficiently kill the target cells<sup>[43-46]</sup>. It has been found recently that DC secretion of exosome can present antigen and induce immune response. This is another path for effector activation<sup>[47]</sup>. In general, from patients in well condition, autogenous peripheral blood DC and LAK cells can be acquired, for it is low in cost; while in patient in bad condition, cord blood DC can be used as an alternative.

Cord blood DC can more efficiently induce effector's cytotoxicity than peripheral blood DC, due to the following factors: ① Cord blood DC comprises some immature DC, the coexistence of mature and immature DC can be synergetic, immature DC can ingest and process antigen, while mature DC can present antigen and activate T cells, therefore, coexistence of mature and immature DC is better than single mature DC<sup>[48]</sup>. ② Both cord DC and CTL were pulse twice with tumor antigen, and specific antitumor activity improved. LAK cells induced 7 days can secrete perforin and granular particles nonspecific to ally kill target cells while human cord blood DC pulsed *in vitro* by tumor antigen can efficiently present tumor antigen to effector which occupy the TCR of CTL, and activate the specific CTL, with the help of costimulator such as CD80, CD86 and CD40. Furthermore, DC can secrete nave T specific chemotactic factor DC-CKK. Some other cell factors such as MCP-1, RANTES and IL-8 also can also play a chemotactic role in DC emigrant. DC can form a cluster of cells and secrete a large number of IL-12 which bind with IL-12R of CTL and enhance CTL proliferating response and cytotoxicity. IL-12 mediates T<sub>H</sub>1 immune response and inclines to tumor killing activity<sup>[42,49-51]</sup>. If permitted, twice antigen pulsed DC should be used.

Summary, human blood DC and cord blood DC have a potential application in the clinical therapy of hepatocarcinoma, especially late hepatocarcinoma.

## REFERENCES

- 1 Rissoan MC, Soumelis V, Kadowaki N, Grouard G, Briere F, Malefyt MDW, Liu YJ. Reciprocal control of T helper cell and



- dendritic cell differentiation. *Science* 1999;283:1183-1186
- 2 Steinman RM, Inaba K. Myeloid dendritic cells. *J Leukocyte Bio* 1999; 66:205-208
  - 3 Bottomly K. T cells and dendritic cells get intimate. *Science* 1999;283: 1124-1125
  - 4 Cao X, Zhang W, Wang J, Zhang M, Huang X, Hamada H, Chen W. Therapy of established tumor with a hybrid cellular vaccine generated by using granulocyte-macrophage colony-stimulating factor genetically modified dendritic cells. *Immunology* 1999;97:616-625
  - 5 Hu JY, Wang S, Zhu JG, Zhou GH, Sun QB. Expression of B7 costimulation molecules by colorectal cancer cells reduces tumorigenicity and induces anti tumor immunity. *World J Gastroenterol* 1999;5: 147-151
  - 6 De VM, Heirman C, Van MS, Devos S, Corthals J, Moser M, Thielemans K. Retrovirally transduced bone marrow-derived dendritic cells require CD4<sup>+</sup> T cell help to elicit protective and therapeutic antitumor immunity. *J Immunology* 1999;162:144-151
  - 7 Albert ML, Sauter B, Bhardwaj N. Dendritic cells acquire antigen from apoptotic cells and induce class I-restricted CTLs. *Nature* 1998; 392: 86-89
  - 8 Banchereau J, Steinman RM. Dendritic cells and the control of immunity. *Nature* 1998; 392:245-252
  - 9 Luft T, Pang KC, Thomas E, Hertzog P, Hart DN, Trapani J, Cebon J. Type I IFNs enhance the terminal differentiation of dendritic cells. *J Immunol* 1998;161:1947-1953
  - 10 Zhang JK, Chen HB, Sun JL, Zhou YQ. Effect of dendritic cells on LPAK cells induced at different time in killing hepatoma cells. *Shijie Huaren Xiaohua Zazhi* 1999;7:673-675
  - 11 Sun JL, Zhang JK, Chen HB, Cheng JD, Qiu YQ. Promoting effects of dendritic cells on LPAK cells killing human hepatoma cells. *Zhongguo Zhongliu Linchuang yu Kangfu* 1998;5:16-18
  - 12 Chen HB, Zhang JK, Huang ZL, Sun JL, Zhou YQ. Effects of cytokines on dendritic cells against human hepatoma cell line. *Shijie Huaren Xiaohua Zazhi* 1999;7:191-193
  - 13 Shimizu Y, Guidotti LG, Fowler P, Chisari FV. Dendritic cell immunization breaks cytotoxic T lymphocyte tolerance in hepatitis B virus transgenic mice. *J Immunol* 1998;161:4520-4529
  - 14 Mackensen A, Krause T, Blum U, Uhrmeister P, Mertelsmann R, Lindemann A. Homing of intravenously and intralymphatically injected human dendritic cells generated *in vitro* from CD34<sup>+</sup> hematopoietic progenitor cells. *Cancer Immunol Immunother* 1999; 48: 118-122
  - 15 Salgaller ML, Tjoa BA, Lodge PA, Ragde H, Kenny G, Boynton A, Murphy GP. Dendritic cell-based immunotherapy of prostate cancer. *Crit Rev Immunol* 1998;18:109-119
  - 16 Lim SH, Bailey Wood R. Idiotypic protein-plused dendritic cell vaccination in multiple myeloma. *Int J Cancer* 1999;83:215-222
  - 17 Greden TF, Jaffee EM. Cancer vaccines. *J Clin Oncol* 1999; 17: 1047-1060
  - 18 Chen CH, Wu TC. Experimental vaccine strategies for cancer immunotherapy. *J Biomed Sci* 1998; 5: 231-252
  - 19 Wang RF. Human tumor antigens: implications for cancer vaccine development. *J Mol Med* 1999; 77: 640-655
  - 20 Li MS, Yuan AL, Zhang WD, Liu SD, Lu AM, Zhou DY. Dendritic cells *in vitro* induce efficient and special anti tumor immune response. *Shijie Huaren Xiaohua Zazhi* 1999;7:161-163
  - 21 Li MS, Yuan AL, Zhang WD, Chen XQ, Tian XH, Piao YJ. Immune response induced by dendritic cells induce apoptosis and inhibit proliferation of tumor cells. *Shijie Huaren Xiaohua Zazhi* 2000;8:56-58
  - 22 Xiao LF, Luo LQ, Zhou Y, Huang SL. Study of the phenotype of PBLs activated by CD28/CD80 and CD2/CD58 and acting with hepatoma cells and the restricted usage of TCR V $\alpha$  gene subfamily. *Shijie Huaren Xiaohua Zazhi* 1999;7:1044-1046
  - 23 Gilboa E, Nair SK, Lysterly HK. Immunotherapy of cancer with dendritic cell based vaccines. *Cancer Immunol* 1998;46:82-87
  - 24 Morse MA, Coleman RE, Akabani G, Niehaus N, Coleman D, Lysterly HK. Migration of human dendritic cells after injection in patients with metastatic malignancies. *Cancer Res* 1999;59:56-58
  - 25 Marriott I, Bost KL, Inscho EW. Extracellular uridine nucleotides initiate cytokine production by murine dendritic cells. *Cellular Immunology* 1999;195:147-156
  - 26 Sun JL, Zhang JK, Chen HB, Zhou YQ. Morphology of cultured human peripheral blood dendritic cells and their antitumor activity. *Zhongguo Zuzhihuaxue yu Xibaoxue Zazhi* 1999; 8: 28-31
  - 27 Nunez R, Grob P, Baumann S, Zuniga A, Ackermann M, Suter M. Immortalized cell lines derived from mice lacking both type I and type II IFN receptors unify some functions of immature and mature dendritic cells. *Immunol and Cell Bio* 1999;77:153-163
  - 28 Wu MC. Progress in surgical treatment of primary hepatocellular carcinoma. *Huaren Xiaohua Zazhi* 1998;6:921-923
  - 29 Zou QY, Li RB, Zheng PL, Yang LP, Chen YZ, Kong XP. Effect of embryohepatic extracts on proliferation and differentiation of hepatoma BEL-7402 cells. *Shijie Huaren Xiaohua Zazhi* 1999;7:243-245
  - 30 Kanto T, Hayashi N, Takehara T, Tatsumi T, Kuzushita N, Ito A, Sasaki Kasahara A, Hori M. Impaired allostimulatory capacity of peripheral blood dendritic cells recovered from hepatitis C virus infected individuals. *J Immunol* 1999;162: 5584-5591
  - 31 Zhang JK, Sun JL, Chen HB, Zang Y, Qu YJ. Influence of granulocyte-macrophage colony-stimulating factor and tumor necrosis factor upon the anti-hepatoma activities of human dendritic cells. *World J Gastroenterol* 2000; 6:718-720
  - 32 Sun JL, Zhang JK, Chen JD, Chen HB, Chew YQ, Chen JX. *in vitro* study on the morphology of human blood dendritic cells and LPAK cells inducing apoptosis of the hepatoma cell line. *Chinese medical journal* 2001; 114: 600-605
  - 33 Herlyn D, Birebent B. Advances in cancer vaccine development. *Ann Med* 1999; 31: 66-78
  - 34 Austyn JM. Dendritic cells. *Curr Opin Hematol* 1998;5:3-15
  - 35 Zhai SH, Liu JB, Zhu P, Wang YH. CD54, CD80, CD86 and HLA-ABC expressions in liver cirrhosis and hepatocarcinoma. *Shijie Huaren Xiaohua Zazhi* 2000;8:292-295
  - 36 Reid SD, Penna G, Adorini L. The control of T cell responses by dendritic cell subsets. *Curr Opin Immunol* 2000; 12:114-121
  - 37 Macpherson G, Kushnir N, Wykes M. Dendritic cells, B cells and the regulation of antibody synthesis. *Immun Rev* 1999;172:325-334
  - 38 Lanzavecchia A, Sallusto F. From synapses to immunological memory: the role of sustained T cell stimulation. *Curr Opin Immunol* 2000; 12: 92-98
  - 39 Dubois B, Bridon JM, Fayette J, Barthelemy C, Banchereau J, Caux C, Briere F. Dendritic cells directly modulate B cell growth and differentiation. *J Leuk Biol* 1999; 66: 224-229
  - 40 Mailliard RB, Dallal RM, Son YI, Lotze MT. Dendritic cells promote T-cell survival or death depending upon their maturation state and presentation of antigen. *Immunol Invest* 2000; 29: 177-185
  - 41 Stockwin LH, McGonagle D, Martin IG, Blair GE. Dendritic cells: immunological sentinels with a central role in health and disease. *Immunol and Cell Biol* 2000; 78: 91-102
  - 42 Macpherson G, Wykes M. Dendritic cell-B cell interaction: dendritic cells provide B cells with CD40-independent proliferation signals and CD40-dependent survival signals. *Immunology* 2000; 100:1-3
  - 43 Huang SL, Xiao LF, Luo LQ, Chen HQ. Phenotype analysis and restricted usage of TCR V $\alpha$  genes subfamily in mAb-costimulated T cells after incubated with hepatocellular carcinoma cell line. *Shijie Huaren Xiaohua Zazhi* 1998;6:1033-1035
  - 44 Tang ZY. Advances in clinical research of hepatocellular carcinoma in China. *Shijie Huaren Xiaohua Zazhi* 1998; 6:1013-1016
  - 45 Chen Q, Ye YB, Chen Z. Activation of killer cells with soluble gastric cancer antigen combined with anti CD3 McAb. *World J Gastroenterol* 1999;5:179-180
  - 46 Zhang JK, Sun JL, Chen HB, Zhou YQ. Ultrastructural comparison of apoptosis of human hepatoma cells and LAK cells. *Shijie Huaren Xiaohua Zazhi* 1998;6:877-879
  - 47 Zitvogel L, Regnault A, Lozier J, Wolfers J, Flament C, Tenza D, Ricciardi Castagnoli P, Paposo G, Amigorena S. Eradication of established murine tumors using a novel cell-free vaccine: dendritic cell-derived exosomes. *Nat Med* 1998;4: 594-600
  - 48 Fujii S, Fujimoto K, Shimizu K, Ezaki T, Kawano F, Takatsuki K, Kawakita M, Matsuno K. Presentation of tumor antigens by phagocytic dendritic cell clusters generated from human CD34<sup>+</sup> hematopoietic progenitor cells: induction of autologous cytotoxic T lymphocytes against leukemic cells in acute myelogenous leukemia patient. *Cancer Res* 1999;59:2150-2158
  - 49 Chiodoni C, Paglia P, Stoppacciaro A, Rodolfo M, Parenza M, Colombo MP. Dendritic cells infiltrating tumors cotransduced with granulocyte/macrophage colony-stimulating factor (GM-CSF) and CD40 ligand genes take up and present endogenous tumor-associated antigens, and prime naive mice for a cytotoxic T lymphocyte response. *J Exp Med* 1999;190:125-133
  - 50 Rosenzweig M, Camus S, Guigon M, Gluckman JC. The influence of interleukin (IL)-4, IL-13, and Flt3 ligand on human dendritic cell differentiation from cord blood CD34<sup>+</sup> progenitor cells. *EXP Hematol* 1998;26:63-72
  - 51 Holtl L, Rieser C, Papesh C, Ramoner R, Herold M, Klocker H, Radmayr C, Stenzl A, Bartsch G, Thurnher M. Cellular and humoral immune responses in patients with metastatic renal cell carcinoma after vaccination with antigen pulsed dendritic cells. *J Urol* 1999; 161: 777-782

• VIRAL LIVER DISEASES •

# Anti-HBV hairpin ribozyme-mediated cleavage of target RNA in vitro

Yu-Hu Song, Ju-Sheng Lin, Nan-Zhi Liu, Xin-Juan Kong, Na Xie, Nan-Xia Wang, You-Xin Jin, Kuo-Huan Liang

Ju-Sheng Lin, Nan-Zhi Liu, Xin-Juan Kong, Na Xie, Nan-Xia Wang, Kuo-Huan Liang, Institute of Liver Diseases, Tongji Hospital, Tongji Medical College, Huazhong University of Science and Technology, Wuhan 430030, Hubei Province, China

Yu-Hu Song, You-Xin Jin, State Key Laboratory of Molecular Biology, Shanghai Institute of Biochemistry, Chinese Academy of Science, Shanghai 200031, China

Supported by Ministry of Health (No 98-1-140) and Chinese Academy of Sciences (No KJ951-B1-610)

Correspondence to: Dr. JIN You-Xin, State Key Laboratory of Molecular Biology, Shanghai Institute of Biochemistry, Chinese Academy of Science, Shanghai 200031, China. yxjin@sunm.shnc.ac.cn  
Telephone: +86-21-64374430-221

Received 2001-07-19 Accepted 2001-10-28

## Abstract

**AIM:** To study the preparation and cleavage activity of HpRz directed against the transcript of HBV core gene *in vitro*.

**METHODS:** HpRz gene designed by computer targeting the transcript of HBV core gene was cloned into the vector p1.5 between 5'-cis-Rz and 3'-cis-Rz. <sup>32</sup>p-labeled HpRz transcript proved whether the vector fit for the preparation of hairpin ribozyme *in vitro*. <sup>32</sup>p-labeled pKC transcript containing HBV core region as target-RNA was transcribed using T<sub>7</sub> RNA polymerase and purified by denaturing PAGE. Cold HpRz transcript was incubated with <sup>32</sup>p-labeled target-RNAs under different conditions and radio autographed after denaturing polyacrylamide gel electrophoresis.

**RESULTS:** HpRz has the specific ability of cleavage of target RNA at 37°C and 12 mM MgCl<sub>2</sub>. K<sub>m</sub>=26.31nmol/L, K<sub>cat</sub>=0.18/min. These results revealed that the design of HpRz was correct.

**CONCLUSION:** HpRz prepared in this study possesses specific catalytic activity from the identification of cleavage activity. These results indicate that hairpin ribozyme may intracellularly inhibit the replication of HBV, therefore it may become a novel potent weapon for the treatment of hepatitis B.

Song YH, Lin JS, Liu NZ, Kong XJ, Xie N, Wang NX, Jin YX, Liang KH. Anti-HBV hairpin ribozyme-mediated cleavage of target RNA *in vitro*. *World J Gastroenterol* 2002;8(1):91-94

## INTRODUCTION

Hepatitis B is a major worldwide health problem<sup>[1-5]</sup>. Hepatitis B virus is a small hepatotropic DNA virus, causing acute and chronic B-type hepatitis in man. Chronic infection is associated with a high risk of liver cirrhosis and primary liver carcinoma<sup>[6-14]</sup>. Currently available therapies are of limited efficacy<sup>[15-33]</sup>. Ribozyme is a kind of catalytic RNA which can catalyze the cleavage of sequence-specific RNA. Compared with antisense RNA, ribozyme may be a more effective experimental tool to suppress the gene expression. Possessing both antisense and RNA cleavage activity, the enzymatic nature of

ribozyme may facilitate effectiveness even at low level of expression<sup>[34]</sup>. Hepatitis B virus is a DNA virus that replicates through reverse transcription of a RNA intermediate (pregenic RNA). So engineered anti-HBV ribozyme can potentially be multifunctional, targeting pregenomic RNA and viral mRNA to suppress the replication of hepatitis B virus. Since previous attempt to use hammerhead ribozyme for the intracellular inhibition of HBV replication have been largely unsuccessful in intact cell<sup>[35,36]</sup>, however engineered hairpin ribozymes have been shown to inhibit replication of human immunodeficiency virus, hepatitis C virus and human papilloma virus *in vivo*<sup>[37-44]</sup>. So we designed hairpin ribozyme to inhibit HBV replication. It is well known that HBV C region is associated with viral replication. In this report we have designed hairpin ribozyme targeting core gene of HBV by computer, prepared hairpin ribozyme by transcription of recombinant plasmid *in vitro*, and proved its ability to cleave HBV *in vitro* from identification of activity of anti-HBV hairpin ribozyme.

## MATERIALS AND METHODS

### Materials

E. coli DH5α has been maintained in our laboratory. The ribozyme vector p1.5 (kind gift of Qi GR, Shanghai Institute of Biochemistry), Plasmid pKC<sup>[45]</sup> for target-RNAs (constructed by Dr Lian JQ, the Forth Military Medical University) has been maintained in our laboratory. DNA sequence Kit, *in vitro* transcription kit, restriction endonucleases, T4 DNA ligase, RNase A free DNase I were purchased from Promega Company; and RNase inhibitor, T4 DNA polymerase from Takara Company, α<sup>32</sup>p dATP and α<sup>32</sup> UTP from Beijing Yahui Company. Materials were used all of analytical purification.

Oligonucleotides of HpRz: R1 5'-CTA GAT CCG GAA GAA CTA AAC CAG AGA AAC AGA TCT CTT CGG AGA TCG TAC ATT ACC TGG TAG GTA C-3'; R2 5'-CTA CCA GGT AAT GTA CGA TCT CCG AAG AGA TCT GTT TCT CTG GTT TAG TTC TTC CGG AT-3'. They were chemically synthesized in Beckman Oligo-1000 DNA synthesizer.

### Methods

**In vitro transcription and purification of target RNA** The template pKC was linearized with BstXI, the 3'-overhangs of linearized pKC was blunted with T4 DNA polymerase. *in vitro* transcription was carried out at 37°C for 90 min in a 20 μL final volume containing 40 mmol·L<sup>-1</sup> Tris·HCl (pH 7.5), 50 mmol·L<sup>-1</sup> DTT, 2 mmol·L<sup>-1</sup> spermidine, 8 mmol·L<sup>-1</sup> MgCl<sub>2</sub>, 0.25 mmol·L<sup>-1</sup> ATP, GTP, CTP, 0.05 mmol·L<sup>-1</sup> UTP, 370 KBq alpha <sup>32</sup>p-UTP, 80 U T<sub>7</sub> RNA polymerase and 4 μg linearized template. Target RNA was purified by 60g·L<sup>-1</sup> denaturing gel electrophoresis by cutting off the autoradiograph bands. Labeled target RNA was dissolved in DEPC H<sub>2</sub>O and reserved under -20°C.

**Construction of recombinant plasmid for ribozyme and preparation of ribozyme *in vitro*** The hairpin ribozyme HpRz for HBV was designed according to the computer software pcFOLD compiled by Professor Zuker (Canadian Academy of Science). The

homologous possibility with the gene of human being was excluded by consulting with RNA sequence of human cell from NCBI Genbank. Synthesized ribozyme fragments were cloned into XbaI/KpnI sites of p1.5 as pHpRz. Recombinant plasmid was identified by being digested with EcoRI and HindIII, then the DNA sequence of recombinant plasmid was analyzed through the dideoxy method developed by Sanger (Figure 1). The template pHpRz was linearized with EcoRI and *in vitro* transcription and purification of ribozyme were the same as those of target RNA. To get a large amount of transcribed HpRz without isotope, the transcription of HpRz was set up according to manufacture's instruction, then template was digested with RNase A free DNase I, the RNA was dissolved in DEPC H<sub>2</sub>O and measured by spectrophotometer containing 3'-cis-Rz and 5'-cis-Rz.

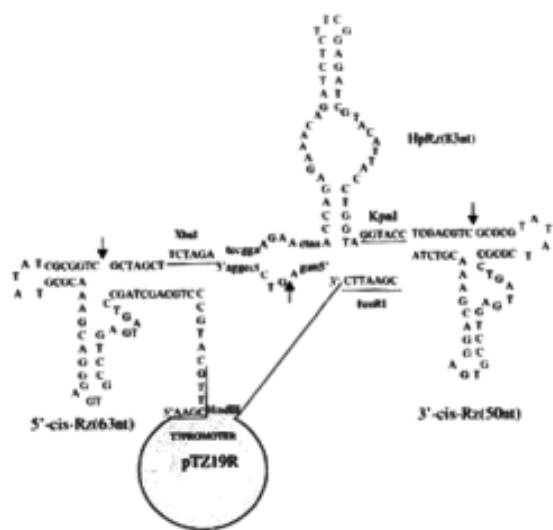


Figure 1 Structure of HpRz plus 5'-cis-Rz and 3'-cis-Rz.

***In vitro* cleavage reaction of HpRz** The cold hairpin ribozyme and target RNA labeled by alpha-<sup>32</sup>P UTP were quantified. The cleavage reaction of ribozyme was performed in ribozyme buffer (40 mmol·L<sup>-1</sup> Tris·HCl pH7.5/ 12 mmol·L<sup>-1</sup> MgCl<sub>2</sub>) at 37°C with 10 nmol·L<sup>-1</sup> <sup>32</sup>P-labeled substrate and 10 n mol·L<sup>-1</sup> cold ribozyme. In this condition the cleavage mixture was incubated at different time points. The volume of the reaction is 5 μL. One μL loading buffer (2.5g·L<sup>-1</sup> Bromophenol Blue, 2.5g·L<sup>-1</sup> Xylene cyanol FF, 20 mmol·L<sup>-1</sup> EDTA and saturated Urea) was added to stop the reaction. The result could be analyzed after running a 60g·L<sup>-1</sup> denaturing polyacrylamide gel electrophoresis. The cleavage efficiency was calculated from Bq values of the bands of substrate (S) and products (P)  $CE = [P/(P+S)] \cdot 100\%$ .

**Kinetics of the cleavage reaction** The procedure was described by Uhlenbeck<sup>[46]</sup>. The cleavage reactions were done and the results were analyzed as above.  $K_m$  and  $K_{cat}$  were calculated by Lineweaver-Burk method (double- reciprocal plot).

## RESULTS

### Identification of recombinant plasmid pHpRz

The result of digested recombinant plasmid by EcoRI and HindIII was analyzed by running 20g·L<sup>-1</sup> agarose gel electrophoresis (Figure 2). This result and the DNA sequence analysis showed that the clone was correct.

### Identification of transcription of ribozyme

The transcription of ribozyme from EcoRI-linearized template should include three bands: 50nt, 63nt and 83nt. The result showed our design was correct (Figure 3).

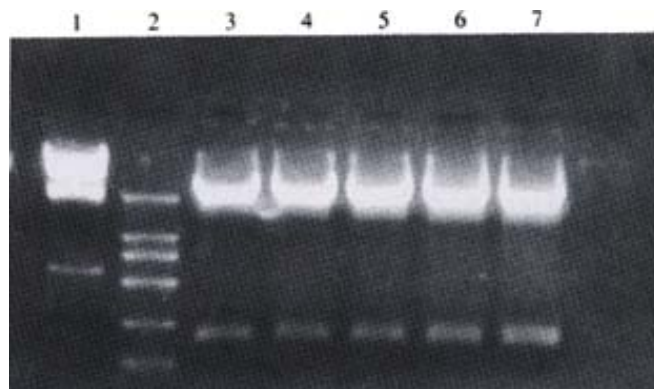


Figure 2 The analysis of HpRz digested by EcoRI and HindIII (20g·L<sup>-1</sup> agarose gel). lane 1: λ DNA/HindIII marker; lane 2: DL2000 DNA marker; lane 3-7: HpRz digested by EcoRI and HindIII.

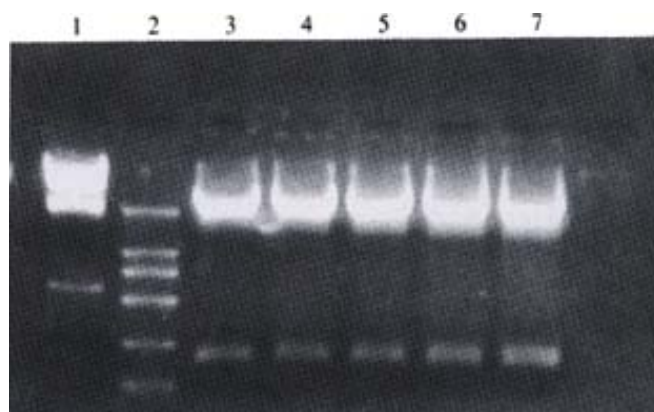


Figure 3 *in vitro* transcript of pHpRz. HpRz is 83nt. 5'-cis-Rz is 63nt, 3'-cis-Rz is 50nt.

### *In vitro* cleavage reaction of ribozyme and kinetics of the cleavage reaction

**Time course** The cleavage mixture (Rz : substrate = 1:1 mol·L<sup>-1</sup>) were incubated at 37°C for different time points, it was shown that the reaction product increased with the increase in incubation time and within 60 min it was linear,  $CE = 32.67\%$  (Figures 4 and 5).

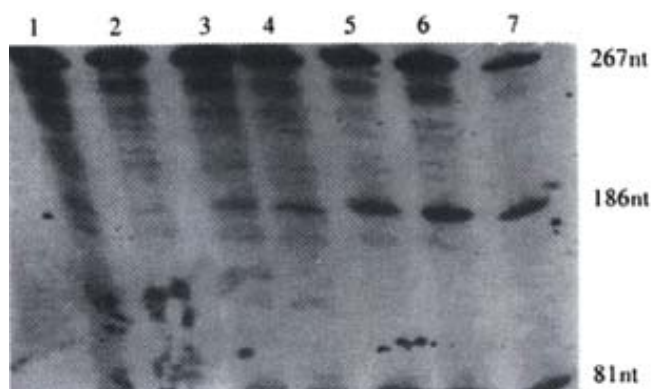


Figure 4 Time course. Specific cleavage of HBV RNA target molecules by HpRz *in vitro*. Lane 1: substrate control; lane 2: incubated for 6 min; lane 3: 10 min; lane 4: 20 min; lane 5: 40 min; lane 6: 60 min; lane 7: 90 min.

**The kinetics of cleavage reaction** Under the condition of 37°C and 40-minute reaction time, the cleavage efficiency was calculated at Rz:S = 1:1, 1:2, 1:4, 1:8 and 1:16 (mol/L) ratio.  $K_m$  and  $K_{cat}$  were obtained by the Lineweaver-Burke method (Figure 6)  $K_m = 26.31 \text{ nmol} \cdot \text{L}^{-1}$ ,  $K_{cat} = 0.18 \cdot \text{min}^{-1}$ .

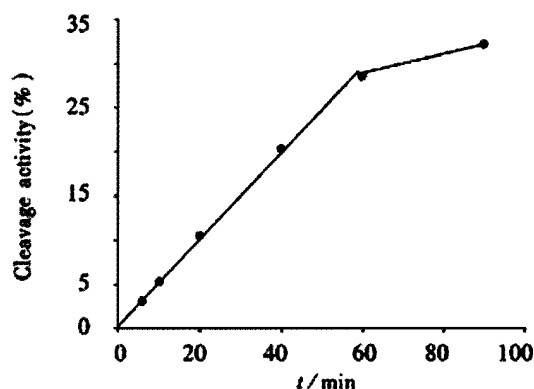


Figure 5 Time curves of cleavage reactions of HpRz prepared *in vitro*.

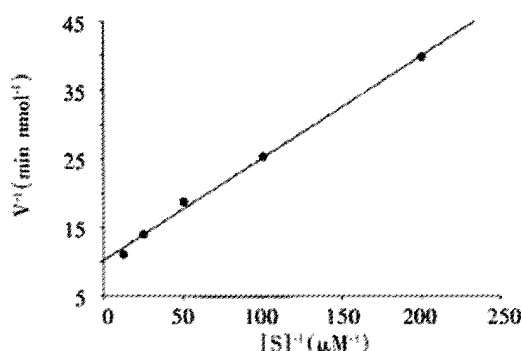


Figure 6 Lineweaver-burk kinetic plots of the specific cleavage of HBV RNA target molecules by HpRz prepared *in vitro*. HpRz concentration is 5 nmol·L<sup>-1</sup>, substrate concentration is 80,40,20,10 5nmol·L<sup>-1</sup>. Reaction is at 37°C for 40 min.

## DISCUSSION

Ribozyme is classified into six kinds. Hammerhead ribozyme and hairpin ribozyme have been studied extensively as experimental tools for trans suppression of gene expression and possible therapeutic application. Hammerhead ribozyme is small and easy to design and there is less restriction of selection of target site, so its application is extensive. Although hammerhead ribozyme was used to suppress HBV replication, and hammerhead ribozyme-mediated cleavage of target RNA could be achieved *in vitro* and in cell extract, they showed poor effect in intact cells<sup>[35, 36]</sup>. Cellular protein and low Mg<sup>2+</sup> concentration limited intracellular ribozyme activity. It will be difficult to raise the intracellular Mg<sup>2+</sup> level. Protein can influence the ribozyme intracellular performance. However, cellular protein may also have positive effect on ribozyme-mediated catalysis. Because of limited knowledge on mechanisms of protein modulation of catalytic RNA activity and the complex formed by ribozyme and ribonucleoprotein are frequently large, poorly defined and difficult to study, it is hard for us to use protein to enhance ribozyme activity. Compared with hammerhead ribozyme, hairpin ribozyme has complex structure, hard to design and there is too much restriction of target site and its application is limited. It possesses the better cleavage activity under physiological condition from *in vitro* assays done under standard condition at 37°C and low Mg<sup>2+</sup> concentration. PJ Welch<sup>[47]</sup> designed three hairpin ribozymes against the pgRNA (pregenic RNA) encoding HBV surface antigen, the polymerase and the X protein and demonstrated that two of them can cleave target RNA *in vitro* and reduced the level of HBV expression and suppressed HBV replication *in vivo*. Zu *et al.*<sup>[48]</sup> used hairpin ribozyme library to identify accessible target sites within HBV pregenomic RNA, four hairpin ribozyme targeting conserved region in subtypes of HBV can inhibit HBV replication in intact cell. Until now no report on hairpin

ribozyme directed against core gene of HBV has available. In this report we have designed and constructed hairpin ribozyme to cleave transcripts of HBV core gene *in vitro*. Our experiment was the study of preparation and cleavage activity of hairpin ribozyme-HpRz by means of the computer design, cloning the ribozyme gene into the vector that possessed cis-cleavage ribozymes and labeled it with isotope. The *in vitro* transcription effect of ribozyme was satisfactory, 5'-cis-Rz and 3'-cis-Rz cut themselves and released the purposed ribozyme. The ribozyme flanking sequences could be shortened and ribozyme structure induced by the secondary structure of long flanking sequences would be eliminated. That would affect ribozyme turnover ratio/binding activity in the result of an accurate hybridization and better cleavage for ribozyme. Moreover isolation of ribozyme is very convenient by cutting off autoradiograph bands. Ribozyme is quantified more accurately. In this paper the number of nucleotide of hairpin ribozyme was similar to that of the cleavage product, so we can not use transcribed HpRz labeled by isotope. The ribozyme vector was proved to fit for preparation of hammerhead ribozyme<sup>[49-51]</sup>. In our study we also used the preparation of hairpin ribozyme and its efficacy is similar to that of hammerhead ribozyme. So the vector possesses wide applicability in the study of preparation of ribozyme *in vitro*, not only hammerhead ribozyme, but also hairpin ribozyme.

HBV is a double-stranded DNA virus replicates through pregenomic RNA intermediate, which provides a therapeutic opportunity for a novel antiviral gene therapy based on ribozyme RNA cleavage. In our experiment, we have designed and constructed hairpin ribozyme directed against HBV core region. The kinetics of hairpin ribozyme showed that HpRz possessed specific ability of cleaving the HBV transcripts *in vitro*. These results indicated that HpRz is worthy of being further studied in intact cells and developed as a nucleic acid drug in the future. However the *in vitro* result can not completely reflect *in vivo* performance. The total HBV mRNA transcript in cell forms the secondary and tertiary structure which affect ribozyme combination with the substrate and cleavage activity. The subcellular compartment where the ribozyme is located, degradation of ribozyme, the complexes which are formed by ribozyme and ribonucleoprotein within cell and gene delivery system, affect the combination with substrate and cleavage of ribozyme. So *in vivo* effect of the ribozyme should be investigated as soon as possible. The ribozyme fragments would be cloned into eucaryotic vectors and transfected into HepG2 cell or Huh7 cell. Experimental analysis of the anti-HBV ribozyme activity *in vivo* is in progress and should help determine its potential use as antiviral agents against HBV.

## REFERENCES

- Shi H, Wang FS. Host factors in chronicity of hepatitis B virus infection and their significances in clinic. *Shijie Huaren Xiaohua Zaizhi* 2001;9:66-69
- Befeler AS, Di Bisceglie AM. Hepatitis B. *Infect Dis Clin North Am* 2000; 14:617-632
- Maddrey WC. Hepatitis B: an important public health issue. *J Med Virol* 2000; 61:362-366
- Lau GK. Hepatitis B infection in China. *Clin Liver Dis* 2001;5:361-379
- Merican I, Guan R, Amarapuka D, Alexander MJ, Chutaputti A, Chien RN, Hasnain SS, Leung N, Lesmana L, Phiet PH, Sjalfoellah Noer HM, Sollano J, Sun HS, Xu DZ. Chronic hepatitis B virus infection in Asian countries. *J Gastroenterol Hepatol* 2000;15:1356-1361
- Guo SP, Wang WL, Zhai YQ, Zhao YL. Expression of nuclear factor-κB in hepatocellular carcinoma and its relation with the X protein of hepatitis B virus. *World J Gastroenterol* 2001;7:340-344
- Shi DR, Lu L, Wang JH, Dong CL, Cong WT. HBV DNA distribution of hepatitis B virus in pancreas and liver of patients with cirrhosis. *Shijie Huaren Xiaohua Zazhi* 2000;8:751-754
- Wu C, Cheng ML, Ding YS, Liu RC, Li J, Wang WL, Hu L. A five-year follow up survey of risk factor of viral hepatic cirrhosis. *Shijie Huaren Xiaohua Zazhi* 2000; 8:1365-1367
- Wang HY, Yan RQ, Long JB, Wu QL. Cyclin D1 amplification is associated with HBV DNA intergration and pathology in human hepatocellular carcinoma. *Shijie Huaren Xiaohua Zazhi* 1999;7:98-100
- Fang ZR, Yang DH, Qin HR, Hua CZ, Xu Z, Qiu HL. Expression of

- IGF-I, IGF-I receptor mRNA in hepatocellular carcinomas and adjacent nontumor tissue. *Shijie Huaren Xiaohua Zazhi* 1999;7:848-850
- 11 Yan JC, Ma Y, Chen WB, Shun XH. Pathological significance of expression intrahepatic smooth muscle fiber in hepatitis B. *Shijie Huaren Xiaohua Zazhi* 2000;8:1242-1246
- 12 Zhai SH, Liu JB, Liu YM, Zhang LL, Du ZH. Expression of HBsAg, HCV-Ag and AFP in liver cirrhosis and hepatocarcinoma. *Shijie Huaren Xiaohua Zazhi* 2000;8:524-527
- 13 Feitelson MA. Hepatitis B virus in hepatocarcinogenesis. *J Cell Physiol* 1999;181:188-202
- 14 Arbuthnot P, Kew M. Hepatitis B virus and hepatocellular carcinoma. *Int J Exp Pathol* 2001;82:77-100
- 15 Zhuang L, You J, Tang BZ, Ding SY, Yan KH, Peng D, Zhang YM, Zhang L. Preliminary results of Thymosin- $\alpha$ 1 versus interferon- $\alpha$  treatment in patient with HBeAg negative and serum HBV DNA positive chronic hepatitis B. *World J Gastroenterol* 2001;7:407-410
- 16 Xie Q, Guo Q, Zhou XQ, Gu RY. Effect of adenine arabinoside monophosphate coupled to lactosaminated human serum albumin on duck hepatitis B virus. *Shijie Huaren Xiaohua Zazhi* 1999;7:125-126
- 17 Li J, Tang B. Effect on replication of hepatitis B virus by Chinese traditional medicine. *Shijie Huaren Xiaohua Zazhi* 2000; 8:945-946
- 18 Zhu Y, Wang YL, Shi L. Clinical analysis of the efficacy of interferon alpha treatment of hepatitis. *World J Gastroenterol* 1998; 4:85-86
- 19 Xu KC, Wei BH, Yao XX, Zhang WD. Recently therapy for chronic hepatitis B virus by combined traditional Chinese and Western medicine. *Shijie Huaren Xiaohua Zazhi* 1999; 7:970-974
- 20 Zoulim F, Trepo C. New antiviral agents for the therapy of chronic hepatitis B virus infection. *Intervirology* 1999; 42:125-144
- 21 Lau GK. Use of immunomodulatory therapy (other than interferon) for the treatment of chronic hepatitis B virus infection. *J Gastroenterol Hepatol* 2000;15 Suppl:E46-52
- 22 Guan R. Interferon monotherapy in chronic hepatitis B. *J Gastroenterol Hepatol* 2000;15 Suppl:E34-40
- 23 Torresi J, Locarnini S. Antiviral chemotherapy for the treatment of hepatitis B virus infections. *Gastroenterology* 2000;118:S83-103
- 24 Schiff ER. Lamivudine for hepatitis B in clinical practice. *J Med Virol* 2000;61:386-391
- 25 Farrell G. Hepatitis B e antigen seroconversion: effects of lamivudine alone or in combination with interferon alpha. *J Med Virol* 2000;61: 374-379
- 26 Lai CL, Yuen MF. Profound suppression of hepatitis B virus replication with lamivudine. *J Med Virol* 2000;61:367-373
- 27 Jarvis B, Faulds D. Lamivudine. A review of its therapeutic potential in chronic hepatitis B. *Drugs* 1999;58:101-141
- 28 Malik AH, Lee WM. Chronic hepatitis B virus infection: treatment strategies for the next millennium. *Ann Intern Med* 2000;132:723-731
- 29 Lok AS. Hepatitis B infection: pathogenesis and management. *J Hepatol* 2000;32(1 Suppl):89-97
- 30 Liu J, McIntosh H, Lin H. Chinese medicinal herbs for chronic hepatitis B: a systematic review. *Liver* 2001;21:280-286
- 31 Doo E, Liang TJ. Molecular anatomy and pathophysiologic implications of drug resistance in hepatitis B virus infection. *Gastroenterology* 2001;120:1000-1008
- 32 Farrell GC. Clinical potential of emerging new agents in hepatitis B. *Drugs* 2000;60:701-710
- 33 Shaw T, Locarnini S. Combination chemotherapy for hepatitis B virus: the path forward? *Drugs* 2000;60:517-531
- 34 Muotri AR, da Veiga Pereira L, dos Reis Vasques L, Menck CF. Ribozymes and the anti-gene therapy: how a catalytic RNA can be used to inhibit gene function. *Gene* 1999;237:303-310
- 35 von Weizsacker F, Blum HE, Wands JR. Cleavage of hepatitis B virus RNA by three ribozymes transcribed from a single DNA template. *Biochem Biophys Res Commun* 1992; 189:743-748
- 36 Beck J, Nassal M. Efficient hammerhead ribozyme-mediated cleavage of the structured hepatitis B virus encapsidation signal *in vitro* and in cell extracts, but not in intact cells. *Nucleic Acids Res* 1995; 23:4954-4962
- 37 Feng Y, Leavitt M, Tritz R, Duarte E, Kang D, Mamounas M, Gilles P, Wong-Staal F, Kennedy S, Merson J, Yu M, Barber JR. Inhibition of CCR5-dependent HIV-1 infection by hairpin ribozyme gene therapy against CC-chemokine receptor 5. *Virology* 2000;276:271-278
- 38 Klebba C, Ottmann OG, Scherr M, Pape M, Engels JW, Grez M, Hoelzer D, Klein SA. Retrovirally expressed anti-HIV ribozymes confer a selective survival advantage on CD4<sup>+</sup> T cells *in vitro*. *Gene Ther* 2000; 7:408-416
- 39 Andang M, Hinkula J, Hotchkiss G, Larsson S, Britton S, Wong-Staal F, Wahren B, Ahrlund-Richter L. Dose-response resistance to HIV-1/MuLV pseudotype virus *ex vivo* in a hairpin ribozyme transgenic mouse model. *Proc Natl Acad Sci* 1999;96:12749-12753
- 40 Perez-Ruiz M, Sievers D, Garcia-Lopez PA, Berzal-Herranz A. The antisense sequence of the HIV-1 TAR stem-loop structure covalently linked to the hairpin ribozyme enhances its catalytic activity against two artificial substrates. *Antisense Nucleic Acid Drug Dev* 1999; 9:33-42
- 41 Koizumi M, Ozawa Y, Yagi R, Nishigaki T, Kaneko M, Oka S, Kimura S, Iwamoto A, Komatsu Y, Ohtsuka E. Design and anti-HIV-1 activity of hammerhead and hairpin ribozymes containing a stable loop. *Nucleosides Nucleotides* 1998;17:207-218
- 42 Li X, Gervais A, Kang D, Law P, Spector SA, Ho AD, Wong-Staal F. Gene therapy targeting cord blood-derived CD34<sup>+</sup> cells from HIV-exposed infants: preclinical studies. *Gene Ther* 1998; 5:233-239
- 43 Welch PJ, Tritz R, Yei S, Leavitt M, Yu M, Barber J. A potential therapeutic application of hairpin ribozymes: *in vitro* and *in vivo* studies of gene therapy for hepatitis C virus infection. *Gene Ther* 1996;3:994-1001
- 44 Alvarez-Salas LM, Cullinan AE, Siwkowski A, Hampel A, DiPaolo JA. Inhibition of HPV-16 E6/E7 immortalization of normal keratinocytes by hairpin ribozymes. *Proc Natl Acad Sci* 1998; 95:1189-1194
- 45 Lian JQ, Zhou YX and Jin YX. Effect of specific connected ribozyme-mediated cleave on anti-HBV *in vitro*. *Disi Junyi Daxue Xuebao* 1999; 20: 97-101
- 46 Uhlenbeck OC. A small catalytic oligoribonucleotide. *Nature* 1987; 328:596-600
- 47 Welch PJ, Tritz R, Yei S, Barber J, Yu M. Intracellular application of hairpin ribozyme genes against hepatitis B virus. *Gene Ther* 1997;4:736-743
- 48 zu Putlitz J, Yu Q, Burke JM, Wands JR. Combinatorial screening and intracellular antiviral activity of hairpin ribozymes directed against hepatitis B virus. *J Virol* 1999;73:5381-5387
- 49 Liu DZ, Jin YX, Hou H, Huang YZ, Yang GC, Xu Q. Preparation and identification of activity of anti-HPV-6b/11E1 universal ribozyme-Rz1198 *in vitro*. *Asian J Androl* 1999;1:195-201
- 50 Xu R, Zhou X, Xie Q, Jin Y, Liao D. Preparation and identification of hammerhead ribozyme *in vitro* against rat caspase-3 mRNA fragment *Zhonghua Gan Zang Bing Za Zhi* 2000;8:361-363
- 51 Xu RH, Liu J, Zhou XQ, Xie Q, Jin YX, Yu H, Liao D. Activity identification of anti-caspase-3 mRNA hammerhead ribozyme in both cell-free condition and BRL-3A cells. *Chinese Medical Journal* 2001;114:606-611



• VIRAL LIVER DISEASES •

# Seek protein which can interact with hepatitis B virus X protein from human liver cDNA library by yeast two-hybrid system

Xiao-Zhong Wang, Xiang-Rong Jiang, Xiao-Chun Chen, Zhi-Xing Chen, Dan Li, Jian-Yin Lin, Qi-Min Tao

Xiao-Zhong Wang, Xiang-Rong Jiang, Xiao-Chun Chen, Zhi-Xing Chen, Dan Li, Department of Gastroenterology, Union Hospital of Fujian Medical University, Fuzhou 350001, Fujian Province, China  
Jian-Yin Lin, Laboratory of molecular biology, Fujian Medical University, Fuzhou 350004, Fujian Province, China  
Qi-Min Tao, Liver Disease Institute, Beijing University, Beijing 100044, China

Correspondence to: Dr. Xiao-Zhong Wang, Department of Gastroenterology, Union Hospital of Fujian Medical University, Fuzhou 350001, Fujian Province, China. drwangxz@pub6.fz.fj.cn  
Telephone: +86-591-3357896 ext 8482

Received 2001-05-31 Accepted 2001-07-15

## Abstract

**AIM:** To seek the X associated protein (XAP) with the constructed bait vector pAS2-1X from normal human liver cDNA library.

**METHODS:** The X region of the HBV gene was amplified by PCR and cloned into the eukaryotic expression vector pAS2-1. The reconstituted plasmid pAS2-1X was transformed into the yeast cells and the expression of X protein (pX) was confirmed by Western blot analysis. Yeast cells were cotransformed with pAS2-1X and the normal human liver cDNA library and were grown in selective SC/-trp-leu-his-ade medium, the second screen was performed with the LacZ report gene. Furthermore, segregation analysis and mating experiment were performed to eliminate the false positive and the true positive clones were selected for PCR and sequencing.

**RESULTS:** Reconstituted plasmid pAS2-1X including the anticipated fragment of X gene was proved by auto-sequencing assay. Western blot analysis showed that reconstituted plasmid pAS2-1X expressed BD:X fusion protein in yeast cells. Of  $5 \times 10^6$  transformed colonies screened, 65 grew in the selective SC/-trp-leu-his-ade medium, 5 scored positive for  $\beta$ -gal activity, and only 2 remaining clones passed through the segregation analysis and mating experiment. Sequence analysis identified that two clones contained similar cDNA fragment: GAAGTTGCG.

**CONCLUSION:** The short peptide (glutacid-leucine-alanine) is a possible required site for XAP binding to pX. Normal human liver cDNA library has difficulties in expressing the integrated XAP on yeast cells.

Wang XZ, Jiang XR, Chen XC, Chen ZX, Li D, Lin JY, Tao QM. Seek protein which can interact with hepatitis B virus X protein from human liver cDNA library by yeast two-hybrid system. *World J Gastroenterol* 2002;8(1):95-98

## INTRODUCTION

Modern biological investigations indicate many proteins have relationship with the development of hepatocellular carcinoma<sup>[1-8]</sup>. More and more evidences have demonstrated hepatitis B virus (HBV)

X protein which encoded by the smallest open reading frame (ORF) of the HBV genome plays an important role in the carcinogenesis<sup>[9-13]</sup>. At a molecular level, several endogenous genes critical for cell proliferation or apoptosis and the inflammatory response seemed interacted with HBx, such as c-Fos, c-Jun, CREB, CD44, TNF- $\alpha$ , p21 and p53<sup>[14-21]</sup>. In addition, DNA transfection approaches have clearly demonstrated that pX is a transactivator of a wide variety of viral and cellular promoters<sup>[22-24]</sup>, but the underlying mechanism of transactivation is currently obscure. Since HBx has no ability to bind DNA, protein-protein interaction seems to be crucial for HBx transactivation<sup>[25-28]</sup>. One most direct way to identify the mechanism of HBx transactivation is to find out host proteins that interact specifically with HBx. We use the yeast two-hybrid system, a genetic approach to search the clone genes that interact with a protein of interest by *in vivo* complementation in yeast cells, to seek XAP from normal human liver cDNA library.

## MATERIALS AND METHODS

### Plasmid Construction

To make the bait plasmid, the X region of the HBV gene was amplified by PCR using as forward and reverse primers XF and XR, which contain an EcoRI and Pst I site respectively for ease of cloning. The sequence of the primers, with the restriction enzyme site underlined are: XF: ACGGAATTCATGGCTGCTAGGCTGTG, XR: ATCCTGCAGAGGTGAAAAAGTTGCAT. These bind to nucleotide positions 1374 and 1838 on HBV genome. The templates for this reaction were sera of HBV DNA positive patients. The 464bp product was cloned into the respective restriction enzyme sites of plasmid pAS2-1 (Clontech) and this plasmid was subsequently named pAS2-1X.

### Western Blot analysis

*Saccharomyces cerevisiae* AH109 (Clontech) was grown in YPD medium (10g·L<sup>-1</sup> yeast extract, 20 g·L<sup>-1</sup> peptone, 20 g·L<sup>-1</sup> dextrose). This yeast strain carries LacZ, HIS3 and ADE2 reporter genes under the control of Gal4-binding sites was used to screen the liver cDNA library. Yeast cells were transformed with pAS2-1X using lithium acetate method previously published by Gietz *et al*<sup>[29]</sup> and were grown in selective SC/-trp medium. Cells were collected by centrifugation and lysates were prepared according to Urea/SDS method. A part of protein extract were resolved on a 120g·L<sup>-1</sup> SDS-polyacrylamide gel and transferred onto polyvinylidene difluoride membrane. After blocking with nonfat dried milk, the membrane was treated with 1:3000 diluted Gal4 DNA-BD monoclonal antibody (Clontech) followed by 1:1000 diluted alkaline phosphatase-conjugated goat anti-mouse IgG. Subsequently the blot was developed by 5-bromo-4-chloro-3-indolyl phosphate and nitro blue tetrazolium. The untransformed yeast cells were used for negative control.

### Screening of the liver cell cDNA library by the yeast two-hybrid system

The screening procedure used was a modification of the method

described by Gietz *et al*<sup>[29]</sup>. Yeast cells AH109 were transformed with pAS2-1X and pACT2-cDNA library (Clontech) by Liac-mediated transformation and were grown in selective SC/-trp-leu-his-ade medium for 7 days. After about 3 days at 30°C, the growing colonies were assayed for  $\alpha$ -gal activity by replica plating the yeast transformants onto Whatman filter papers, the filters were snap frozen in liquid nitrogen for 10s twice and incubated for 1-8h at 30°C in a buffer containing 5-bromo-4-chloro-3-indolyl- $\alpha$ -D-galactopyranoside(X-gal) solution. Positive interactions were detected by the appearance of blue colonies. Segregation analysis and mating experiment were done to exclude the type I, II, III false positive and true positive colonies were obtained.

### Sequence analysis of pACT2-cDNA

The pACT2-cDNA plasmid genome was isolated following the standard protocol. Briefly, the true positive clones were grown in SC/-leu medium, cells were collected by centrifugation and resuspended in lysis buffer (20g·L<sup>-1</sup> Triton 100, 10g·L<sup>-1</sup> SDS, 10mmol L<sup>-1</sup> NaCl, 10mmol·L<sup>-1</sup> Tris-HCl pH8.0, 1mmol·L<sup>-1</sup> Na<sub>2</sub>EDTA) and phenol, chloroform and isoamyl alcohol(volume fraction 25:24:1). After addition of acid-washed glass beads (Sigma), samples were centrifugated and plamid DNA recovered. The pACT2-cDNA plasmid DNA was purified by CsCl gradient centrifugation to permit PCR using the Matchmaker AD LD-Insert Screening Amplimers (Clontech) which anneals to GAL4-AD. Auto-sequencing assay was performed in Shanghai Shengong Biological Corporation.

## RESULTS

### Plasmid construction

The HBV X fragment was successfully generated by PCR(figure 1) and cloned into plasmid pAS2-1. Reconstituted plasmid pAS2-1X including the anticipated fragment of X gene was proved by digesting with restricted endonuclease and auto-sequencing assay as follows: GACTGTATCGCCGGTATTGCAATACCCAGCTTTGACTCATATGGCCATGGAGGCCGAATTCATGGCTGCTAGGCTGTGCTGCCAACTGGATCCTGCGCGGGACGTCCTTTGTGTACGTCCCGTCACGCGTGAATCCCGCGGACGACCCCTCCCGGGGCGCTTGGGGCTCTACCGCCCCTTCTCCGCTGTGTGATCCGACCGACACGGGGCGCACCTCTCTTTACGCGGACTCCCCGTCTGTGCCTTCTCATCTGCCGGACCGTGTGCACTTCGCTTCACCTCTGCACGTCGCATGGAAACCACCGTGAACGCCCCACCGGAACCTGCCCCAAGGCCTTGCAAGAGGACTCTTGGAATTGCAGCAATGTCAACGACCGACCTTGAGGCATACTCAAAGACTGTGTGTTTAAACGAGTGGGAGGAGTTGGGGAGGAGATTAGGTTAAAGGTCTTTGTACTAGGAGGCTGTAGGCATAAATTGGTGTGTTTACACAGCACCATTGCAATTTTACCTCTGCAGCCAAGCTAATTCGGGCGAATTTCTTATGATTTATGATTTTATTATTAATAAGTTATAAAAAAATAAGTGTATACAAATTTTAAAGGTGACTTTTANGTTTTAAACGAAAATNTTATNTTGAGTAACTNTTTCCTGGAGGTCAAGGTTGCTT (underlined fractions are restriction enzyme site).

### Western Blot analysis

Western Blot Analysis proved that yeast cells transformed with pAS2-1X have positive signal which can not be seen in the control, pAS2-1X can express BD:X fusion protein yeast cells(figure 2). Besides, The colony-lift assay showed that the reconstruted plasmid could not active LacZ reporter gene in yeast. pAS2-1X can be used as bait vector in yeast two-hybrid system.

### Screening of the liver cell cDNA library

Of 5×10<sup>6</sup> transformed colonies screened, 65 grew in the selective SC/-trp-leu-his-ade medium. Out of these HIS<sup>+</sup> ADE<sup>+</sup>

prototrophs, 5 scored positive for  $\beta$ -gal activity, only 2 remaining clones passed through the segregation analysis and mating experiment.

### Sequence analysis

PCR (Figure 3) and sequence analysis identified that two clones contained the same cDNA sequence: GAACTTGCG, which encodes glutacid-leucine -alanine.

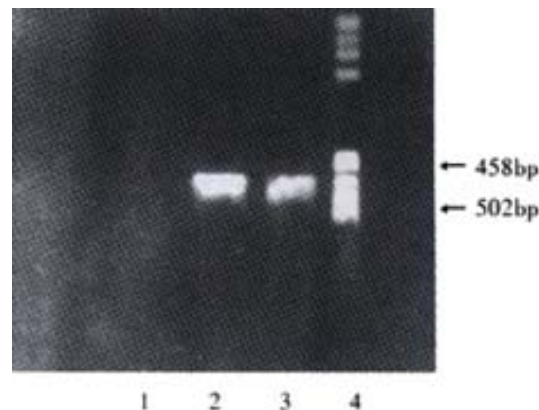


**Figure 1** Electrophoresis of X gene PCR products  
1: Negative control; 2:Positive control; 3:Sample; 4: Marker

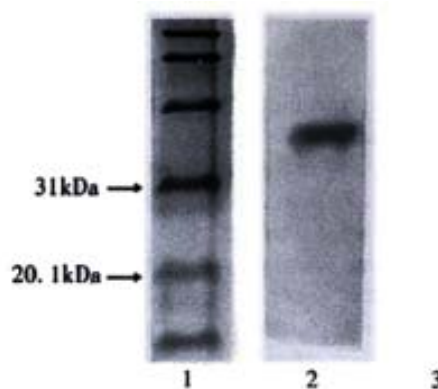


**Figure 2** Western blot of yeast after being transformed with pAS2-1X  
1:Marker; 2: pX; 3: Negative control



**Figure 3** Library cDNA amplified from positive yeast clones  
1:100bp DNA ladder; 2. 3: positive cloned

## DISCUSSION

Persistent Hepatitis B virus infection is strongly associated with the development of hepatocellular carcinoma(HCC). The viral X gene encodes a 17-kd protein, termed pX, fuctions a transcriptional activator of a variety of viral and cellular genes, it is capable of interacting with a wide variety of cellular protein, including cell-cycle control and apoptosis protein. There are well documented that pX acts through apoptosis pathway involving Fas and caspase 3<sup>[30-33]</sup>, it also

interacts with p53, a wellknown tumor suppressor gene<sup>[34-36]</sup> and inhibits nucleotide excision repair<sup>[37-39]</sup>. However, ample evidences showed that pX may function by additional profound mechanisms in HCC<sup>[40-43]</sup>.

Identification and characterization of proteins in a cell with which a given protein interacts is often helpful for understanding the function and mechanisms of action of that protein. The yeast two-hybrid system is a molecular genetic test for protein interaction, which is firstly established by Fileds *et al* in 1989<sup>[44]</sup>. It's a powerful and sensitive technique for the identification of genes that code for proteins which interact in a biologically significant fashion with a protein of interest. The assay is performed in the yeast cells so as to reflect the real situations *in vivo* and has the potential to identify the weak and transient interaction between two protein. In addition, since the cDNA library can be constructed according to various type of tissues, organs and cells, many proteins interact with transcription factors, protein kinases, phosphatases, receptors, cytoskeletal proteins as well as proteins involved in cell cycle regulation and apoptosis can be study by this elegant approach. Although the yeast two-hybrid system has become a standard procedure for molecular biologists, it remains some deficiency. The most important problem is different types of false positives, fortunately, they can be eliminated by other method such as segregation analysis and mating experiment<sup>[29,45]</sup>.

Our study successfully constructed the bait vector pAS2-1X, HIS and ADE independent growth and blue -colony formation in the  $\alpha$ -gal assay by yeast cells harboring both pAS2-1X and pACT2-cDNA recombinant plasmids and the behaviors of cells in false-positive elimination tests suggested the isolated clones can specifically interact with pX and the results were reliable.

It should be greatly concerned that XAPs studied by the yeast two-hybrid system in the past were different in size, structure and biological functions<sup>[46]</sup>. Lee *et al*<sup>[47]</sup> indentified an XAP1 that is a human homolog of the monkey UV-damaged DNA-binding protein in 1995; Kuzhandaivelu *et al*<sup>[48]</sup> discovered an XAP2 which is known as the p38 subunit of the aryl hydrocarbon receptor complex (ARA9) in 1996; Huang *et al*<sup>[49]</sup> reported an XAPC7 contained a polypeptide with high sequence homology to the PROS-28.1 subunit of proteasome of *Drosophila melanogaster* and the  $\alpha$  proteasome subunit of *Arabidopsis thaliana* in 1996; Cong *et al*<sup>[50]</sup> isolated an XAP3 which is a human homolog of the rat protein kinase C-binding protein in 1997; Melegari *et al*<sup>[51]</sup> proved an XIP including two consensus phosphorylation sites for protein kinase C and Casein kinase II in 1998; Sun *et al*<sup>[52]</sup> demonstrated a p55sen appeared to be related to the family of EGF-like protein in gengeral in 1998; Rahmani *et al*<sup>[53,54]</sup> identified an HVDVC3 which is a third member of the family of human genes that encode the voltage-dependent anion channel. The reasonable explantation for these distinct results has not been obtained yet. Whether there exists different kinds of XAP or funtional fragment interacting with pX or the repetitive results depend on the high transformation efficiency remains obscure. One of the possible mechanism may be a specific fragment can interact with pX specially and the proteins containing this fragment thus can bind to pX. Sequence analysis shown that both two true positive clones we isolated contained the sequence encodes glutacid-leucine -alanine, therefore, it's rational to deduce this short peptide is a required site for XAP binding to pX.

The interaction of proteins shall locate at nucleus in yeast two-hybrid system. However, some proteins require modification such as glycosylation outside the necleus after the expression, and others are only correctly folded and actived in the cooperation of some particular proteins which don't exist in yeast cells, so not all proteins can obtain normal structure and biological function in yeast cells. The cDNA library used for seeking XAP in the past research including Epstein-Barr virus transformed human peripheral lymphocyte cDNA library,

Hela  $\lambda$  gt11 cDNA library or senescent human liver cDNA library, were all library consititued from abnormal cells. Our study had not isolated integrated cDNA sequence of XAP partly owing to the difference between normal human liver cDNA library and abnormal cells cDNA library in protein's expression, modification and activation.

In conclusion, the short peptide (glutacid-leucine-alanine) is a possibly required site for XAP binding to pX. Normal human liver cDNA library has difficulties in expressing the integrated XAP on yeast cells.

## REFERENCES

- Kong XB, Yang ZK, Liang LJ, Huang JF, Lin HL. Overexpression of P-glycoprotein in hepatocellular carcinoma and its clinical implication. *World J Gastroenterol* 2000;6:134-135
- Sun JJ, Zhou XD, Liu YK, Zhou G. Phase tissue intercellular adhesion molecule-1 expression in nude mice human liver cancer metastasis model. *World J Gastroenterol* 1998;4:314-316
- Xiao CZ, Dai YM, Yu HY, Wang JJ, Ni CR. Relationship between expression of CD44v6 and nm23-H1 and tumor invasion and metastasis in hepatocellular carcinoma. *World J Gastroenterol* 1998;4:412-414
- Feng T, Zeng ZC, Zhou L, Chen WY, Zuo YP. Detection of human liver-specific F antigen in serum and its preliminary application. *World J Gastroenterol* 1999;5:175-176
- Lin GY, Chen ZL, Lu CM, Li Y, Ping XJ, Huang R. Immunohistochemical study on p53, H-rasp21, c-erbB-2 protein and PCNA expression in HCC tissues of Han and minority ethnic patients. *World J Gastroenterol* 2000;6:234-238
- Huang XF, Wang CM, Dai XW, Li ZJ, Pan BR, Y LB, Qian B, Fan L. Expressions of chromograninA and cathepsinD in human primary hepatocellular carcinoma. *World J Gastroenterol* 2000;6:693-698
- Mei MH, Xu J, Shi QF, Yang JH, Chen Q, Qin LL. Clinical significance of serum intercellular adhesion molecule-1 detection in patients with hepatocellular carcinoma. *World J Gastroenterol* 2000;6:408-410
- Zhao CY, Li YL, Liu SX, Feng ZJ. Changes of IL-6 and relevant cytokines in patients with hepatocellular carcinoma and their clinical significance. *World J Gastroenterol* 2000;6(Suppl 3):33
- Yu DY, Moon HB, Son JK. Incidence of hepatocellular carcinoma in transgenic mice expressing the hepatitis B virus X-protein. *J Hepatol* 1999;31:123-132
- Zhu HZ, Cheng GX, Chen JQ, Kuang SY, Cheng Y, Zhang XL, Li HD, Xu SF, Shi JQ, Qian GS, Gu JR. Preliminary study on the production of transgenic mice harboring hepatitis B virus X gene. *World J Gastroenterol* 1998;4:536-539
- Wang XZ, Tao QM. The relationship between HBV x gene and hepatocellular carcinoma. *Shijie Huaren Xiaohua Zazhi* 1999;7:1063-1064
- Yu DY, Moon HB, Son JK, Jeong S, Yu SL, Yoon H, Han YM, Lee CS, Park JS, Lee CH, Hyun BH, Murakami S, Lee KK. Incidence of hepatocellular carcinoma in transgenic mice expressing the hepatitis B virus X-protein. *J Hepatol* 1999; 31: 123-132
- Gao FG, Sun WS, Cao YL, Zhang LN, Song J, Li HF, Yan SK. HBx-DNA probe preparation and its application in study of hepatocarcinogenesis. *World J Gastroenterol* 1998;4:320-322
- Feitelson MA. Hepatitis B X antigen and P53 in the development of hepatocellular carcinoma. *J Hepatobiliary Pancreat Surg* 1998; 5:367-374
- Qin LL, Su JJ, Li Y, Yang C, Ban KC, Yian RQ. Expression of IGF-c $\alpha$ , p53, p21 and HBxAg in precancerous events of hepatocarcinogenesis induced by AFB1 and /or HBV in tree shrews. *World J Gastroenterol* 2000;6:138-139
- Lara-Pezzi E, Serrador JM, Montoya MC, Zamora D, Yanez-Mo M, Carretero M, Furthmayr H, Sanchez-Madrid R, Lopez-Cabrera M. The hepatitis B virus x protein induces a migratory phenotype in a CD44-dependent manner: possible role of HBx in invasion and metastasis. *Hepatology* 2001;33:1271-1281
- Lin GY, Chen ZL, Lu CM, Li Y, Ping XJ, Huang R. Immunohistochemical study on p53, H-rasp21, c-erbB-2 protein and PCNA expression in HCC tissues of Han and minority ethnic patients. *World J Gastroenterol* 2000;6:234-238
- Sun BH, Zhang J, Wang BJ, Zhao XP, Wang YK, Yu ZQ, Yang DL, Hao LJ. Analysis of *in vivo* patterns of caspase 3 gene expression in primary hepatocellular carcinoma and its relationship to p21<sup>WAF1</sup> expression and hepatic apoptosis. *World J Gastroenterol* 2000;6:356-360
- Feng DY, Zheng H, Tan Y, Cheng RX. Effect of phosphorylation of MAPK and Stat3 and expression of ca2fos and ca2jun proteins on

- hepatocarcinogenesis and their clinical significance. *World J Gastroenterol* 2001;7:33-36
- 20 Natoli G, Avantaggiati ML, Chirillo P, Puri PL, Ianni A, Balsano C, Levrero M. Ras- and raf-dependent activation of c-jun transactivational activity by the hepatitis B virus transactivator pX. *Oncogene* 1994; 9: 2837-2843
- 21 Lara PE, Majano PL, Gomez GM, Garcia MC, Moreno OR, Levrero M, Lopez CM. The hepatitis B virus X protein up-regulates tumor necrosis factor alpha gene expression in hepatocytes. *Hepatology* 1998; 28: 1013-1021
- 22 Caselmann WH. Trans-activation of cellular genes by hepatitis B virus proteins: a possible mechanism of hepatocarcinogenesis. *Adv Virus Res* 1996; 47:253-302
- 23 Hildt E, Hofschneider PH, Urban S. The role of hepatitis B virus (HBV) in the development of hepatocellular carcinoma. *Semin Virol* 1999; 7:333-337
- 24 Nomura T; Lin Y, Dorjsuren D, Ohno S, Yamashita T, Murakami S. Human hepatitis B virus X protein is detectable in nuclei of transfected cells, and is active for transactivation. *Biochem Biophys Acta* 1999; 1453: 330-340
- 25 Hu Z, Zhang Z, Doo E, Coux O, Goldberg AL, Liang TJ. Hepatitis B virus X protein is both a substrate and a potential inhibitor of the proteasome complex. *J Virol* 1999; 73: 7231-7240
- 26 Shintani Y, Yotsuyanagi H, Moriya K, Fujie H, Tsutsumi T, Kanegae Y, Kimura S, Saito I, Koike K. Induction of apoptosis after switch-on of the hepatitis B virus X gene mediated by the Cre/loxP recombination system. *J Gen Virol* 1999; 80(Pt 12): 3257-3265
- 27 Maguire H F, J P Hoeffler, A Siddiqui. HBV X protein alter the DNA binding specificity of CREB and ATF-2 by protein-protein interaction. *Science* 1991;252:842-844
- 28 Lara PE, Armesilla AL, Majano PL, Redondo JM, Lopez CM. The hepatitis B virus X protein activates nuclear factor of activated T cells (NF-AT) by a cyclosporin A-sensitive pathway. *EMBO J* 1998; 17: 7066-7077
- 29 Gietz RD, Raine BT, Robbins A, Graham KC, Woods RA. Identification of proteins that interact with a protein of interest: applications of the yeast two-hybrid system. *Molecular Cellular Biochemistry* 1997; 172:67-69
- 30 Sun BH, Zhao XP, Wang BJ, Yang DL, Hao LJ. FADD and TRADD Expression and apoptosis in primary hepatocellular carcinoma. *World J Gastroenterol* 2000;6:223-227
- 31 Wang XZ, Chen XC, Yang YH, Chen ZX, Huang YH, Tao QM. Relationship between HBxAg and Fas/FasL in patients with hepatocellular carcinoma. *World J Gastroenterol* 2000;6(suppl 3):17
- 32 Shin EC, Shin JS, Park JH, Kim H, Kim SJ. Expression of fas ligand in human hepatoma cell lines: role of hepatitis-B virus X (HBx) in induction of Fas ligand. *Int J Cancer* 1999; 82: 587-591
- 33 Gottlob K, Fulco M, Levrero M, Graessmann A. The hepatitis B virus HBx protein inhibits caspase 3 activity. *J Biol Chem* 1998; 273: 33347-33353
- 34 Lee SG, Rho HM. Transcriptional repression of the human p53 gene by hepatitis B viral X protein. *Oncogene* 2000; 19: 468-471
- 35 Lee H, Kim HT, Yun Y. Liver-specific enhancer II is the target for the p53-mediated inhibition of hepatitis B viral gene expression. *J Biol Chem* 1998; 273: 19786-19791
- 36 Prost S, Ford JM, Taylor C, Doig J, Harrison DJ. Hepatitis B x protein inhibits p53-dependent DNA repair in primary mouse hepatocytes. *J Biol Chem* 1998; 273: 33327-33332
- 37 Groisman IJ, Koshy R, Henkler F, Groopman JD, Alaoui-Jamali MA. Downregulation of DNA excision repair by the hepatitis B virus-x protein occurs in p53-proficient and p53-deficient cells. *Carcinogenesis* 1999; 20: 479-483
- 38 Jia L, Wang XW, Harris CC. Hepatitis B virus X protein inhibits nucleotide excision repair. *Int J Cancer* 1999; 80: 875-879
- 39 Becker SA, Lee TH, Butel JS, Slagle BL. Hepatitis B virus X protein interferes with cellular DNA repair. *J Virol* 1998; 72: 266-272
- 40 Lin GY, Chen ZL, Lu CM, Li Y, Wang J, Ping XJ, Huang R. Immunohistochemical study on p53, H-rasp21, c-erbB-2 protein and PCNA expression in tumor tissues of Han and minority ethnic patients with primary hepatic carcinoma in Xinjiang. *World J Gastroenterol* 2000;6 (suppl):53
- 41 Lee SW, Lee YM, Bae SK, Murakami S, Yun Y, Kim KW. Human hepatitis B virus X protein is a possible mediator of hypoxia-induced angiogenesis in hepatocarcinogenesis. *Biochem Biophys Res Commun* 2000; 268: 456-461
- 42 Lian Z, Liu J, Pan J, Satioglu Tufan NL, Zhu M, Arbuthnot P, Kew M, Clayton MM, Feitelson MA. A cellular gene up-regulated by hepatitis B virus-encoded X antigen promotes hepatocellular growth and survival. *Hepatology* 2001;34:146-157
- 43 Qin LL, Su JJ, Li Y, Yang C, Ban KC, Yian RQ. Expression of IGF- $\alpha$ , p53, p21 and HBxAg in precancerous events of hepatocarcinogenesis induced by AFB1 and/or HBV in tree shrews. *World J Gastroenterol* 2000;6:138-139
- 44 Fields S, Song OK. A novel genetic system to detect protein-protein interactions. *Nature* 1989; 340:245-246
- 45 Bartel P, Chien CT, Sternglanz R. Elimination of false positives that arise in using the two hybrid system. *Biotechniques* 1993;14: 920-924
- 46 Wang XZ, Tao QM. Advances on research of hepatitis B virus pX associated Protein. *GanZang* 2000;5:55-56
- 47 Lee TH, Elledge SJ, Butel JS. Hepatitis B virus X protein interacts with a probable cellular DNA repair protein. *J Virol* 1995; 69:1107-1114
- 48 Kuzhandaivelu N, Cong YS, Inouye C, Yang W M, Seto E. XAP2, a novel hepatitis B virus X-associated protein that inhibits X transactivation. *Nucleic Acids Res* 1996; 24:4741-4750
- 49 Huang J, Kwong J, Sun ECY, Liang TJ. Proteasome complex as a potential cellular target of hepatitis B virus X protein. *J Virol* 1996; 70:5582-5591
- 50 Cong YS, Yao YL, Yang WM, Kuzhandaivelu N, Seto. The hepatitis B virus X-associated protein, XAP3, is a protein kinase C-binding protein. *J Biological Chemistry* 1997;272:16482-16489
- 51 Melegari M, Scaglioni PP, Wands JR. Cloning and characterization of a novel hepatitis B virus X binding protein that inhibit viral replication. *J Virol* 1998; 72:1737-1743
- 52 Sun BS, Zhu X, Clayton MM, Pan J, Feitelson MA. Identification of a protein isolated from senescent human cells that binds to hepatitis B virus X antigen. *Hepatology* 1998; 27:228-239
- 53 Rahmani Z, C. Maunoury, A. Siddiqui. Isolation of a novel human voltage-dependent anion channel gene. *Eur J Hum Genet* 1998; 6:337-340
- 54 Rahmani Z, K Huh, R Lasher. Hepatitis virus x protein colocalizes to mitochondria with a human voltage-dependent anion channel HVDAC3 and alter its transmembrane potential. *J Virol* 2000; 74:2840-2846

Edited by Wang JH and Xu XQ

• BASIC RESEARCH •

# Expression and bioactivity identification of soluble MG7 scFv

Zhao-Cai Yu, Jie Ding, Bo-Rong Pan, Dai-Ming Fanm, Xue-Yong Zhang

Zhao-Cai Yu, Jie Ding, Dai-Ming Fan, Xue-Yong Zhang, Department of Gastroenterology, Xijing Hospital, Fourth Military Medical University, Xi'an 710032, Shaanxi Province, China  
Bo-Rong Pan, Oncological Center, Xijing Hospital, Fourth Military Medical University, Xi'an 710032, Shaanxi Province, China  
Supported by the Foundation for Medical Science Research of PLA (No. 962047)

Correspondence to: Prof. Xue-Yong Zhang, Department of Gastroenterology, Xijing Hospital, Fourth Military Medical University, Xi'an 710033, Shaanxi Province, China. xyzhang@fmmu.edu.cn.  
Telephone: +86-029-3374576

Received 2001-09-25 Accepted 2001-10-29

## Abstract

**AIM:** To examine the molecular mass and identify the bioactivity of MG<sub>7</sub> scFv for its application as a targeting mediator in gene therapy of gastric cancer.

**METHODS:** Two strongly positive recombinant phage clones screened from MG<sub>7</sub> recombinant phage antibody library were separately transfected into *E.coli* TG1. Plasmid was isolated from the transfected *E.coli* TG1 and digested by EcoR I and Hind III to examine the length of exogenous scFv gene. Then, the positive recombinant phage clones were individually transfected into *E.coli* HB2151. The transfectant was cultured and induced by IPTG. Perplasmic extracts was prepared from the induced transfectant by osmotic shock. ELISA was used to examine the antigen-binding affinity of the soluble MG<sub>7</sub> scFv. Immunodotting assay was adopted to evaluate the yield of soluble MG<sub>7</sub> scFv produced by transfected *E.coli* HB2151. Western blot was used to examine the molecular mass of MG<sub>7</sub> scFv. Finally, the nucleotide sequence of MG<sub>7</sub> scFv was examined by DNA sequencing.

**RESULTS:** two positive recombinant phage clones were found to contain the exogenous scFv gene. ELISA showed that MG<sub>7</sub> scFv had strong antigen-binding affinity. Immunodotting assay showed that transfected *E.coli* HB2151 could successfully produce the soluble MG<sub>7</sub> scFv with high yield via induction by IPTG. The molecular mass of MG<sub>7</sub> scFv was 30 kDa by western blot. DNA sequencing demonstrated that the V<sub>H</sub> and V<sub>L</sub> genes of MG<sub>7</sub> scFv were 363bp and 321bp, respectively.

**CONCLUSION:** We have successfully developed the soluble MG<sub>7</sub> scFv which possessed strong antigen-binding affinity.

Yu ZC, Ding J, Pan BR, Fan DM, Zhang XY. Expression and bioactivity identification of soluble MG<sub>7</sub> scFv. *World J Gastroenterol* 2002;8(1):99-102

## INTRODUCTION

Gastric cancer takes the leading place in the incidence of various tumors in china<sup>[1]</sup>. Many conventional approaches, including surgical, chemical and physical treatments, appear palliative in most advanced cases. Because these conventional approaches cannot selectively target at the tumor cells and completely eradicate them,

and recurrence and metastasis of tumor may develop due to the existence of residual tumor cells. Therefore, targeting therapy for tumor is badly needed to achieve a greater curative effect and overcome the obstacle existing in the conventional approaches<sup>[2-13]</sup>. Recent studies showed that the targeting therapy had a promise in the treatment of gastric cancer<sup>[14-29]</sup>. In the present study, we produced the soluble MG<sub>7</sub> scFv and evidenced that MG<sub>7</sub> scFv is a favorable mediator for targeting therapy of gastric cancer.

## MATERIALS AND METHODS

### Restriction analysis of the strong recombinant phage clones

The strong positive recombinant phage clones (3  $\mu$ L containing  $2 \times 10^9$  pfu) were separately added into 5mL log-phase *E.coli* TG1 and incubated for 1 h at 37°C with shaking at 250 r·min<sup>-1</sup>. Plasmid was isolated from the culture product and digested by EcoR I and Hind III. Electrophoresis was performed to check the digested product.

### Production and antigen-binding affinity test of the soluble MG<sub>7</sub> scFv

The strongly positive recombinant phage clones (3  $\mu$ L containing  $2 \times 10^9$  pfu) were separately added into 5mL log-phase *E.coli* HB2151 and incubated for 1 h at 37°C with shaking at 250 r·min<sup>-1</sup>. 10  $\mu$ L IPTG (isopropyl  $\beta$ -D-thiogalactopyranoside) were added and incubated overnight at 37°C with shaking at 250 r·min<sup>-1</sup>. Cells were precipitated by centrifugation and supernatant was also collected. The precipitated cells were subjected to osmotic shock for preparation of soluble MG<sub>7</sub> scFvs. KATOIII cells in log phase were transferred into a 96 wells-plate and immobilized on the wall by centrifugation at 1000g for 10min, and finally fixed in 0.25mL·L<sup>-1</sup> glutaraldehyde. 0.2 mL perplasmic extracts and supernatant were applied to each well and incubated at 4°C overnight. 0.2 mL anti-E tag antibody were applied to each well and incubated at 37°C for 2 h. 0.1 ml HRP-labeled goat anti-mouse (HRP-GAM) Ig solution was added into each well. The absorbance value (A) at 450nm of reactant in each well was measured after incubation for 1 h at 37°C and staining with TMB.

### Immunodotting test of the yield of soluble MG<sub>7</sub> scFv

40  $\mu$ L of perplasmic extracts and supernatant were separately dotted on the Hybond-C super membrane and dried at 60°C for 30 min. After being blocked by 50 mL·L<sup>-1</sup> nonfat milk for 2 h, the Hybond-C super membrane was incubated in 5mL diluted anti-E tag antibody solution at 37°C for 2 h. 5 mL HRP- labeled goat anti-mouse (HRP-GAM) Ig solution were added for another incubation at 37°C for 1 h and eventually stained by DAB.

### Western blot test of the molecular mass of soluble MG<sub>7</sub> scFv

40  $\mu$ L of perplasmic extracts and supernatant were firstly analyzed by SDS-PAGE and then transferred onto the Hybond-C super membrane. After being blocked by 50 mL·L<sup>-1</sup> nonfat milk, the Hybond-C super membrane was incubated in 5mL diluted anti-E tag antibody solution at 37°C for 2 h. 5 mL of HRP- labeled goat anti-mouse (HRP-GAM) Ig solution were added for another incubation at 37°C for 1 h and



eventually stained by DAB.

### DNA sequencing of MG<sub>7</sub> scFv

DNA sequencing was performed by ABI PRISM™ 377 DNA sequencer.

## RESULTS

### Restriction analysis of the strong positive recombinant phage clones

Two strongly positive clones were found to be recombinant clones which contained the exogenous gene. One of the two strongly positive clones contained a 450bp fragment of exogenous gene (Lane 1) and the other one contained a 750bp fragment of exogenous gene (Lane 2, Figure 1).

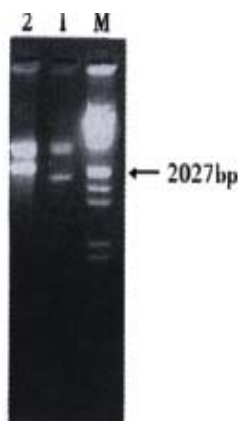


**Figure 1** Restriction analysis of the strong positive recombinant phage clones. M:  $\lambda$ /EcoR I and Hind II; 1,2: Recombinant clones

### Antigen-binding affinity of the soluble MG<sub>7</sub> scFv by ELISA

One of the strong positive clones was shown to produce soluble form of MG<sub>7</sub> scFv with Antigen-binding activity (Table 1). This clone was confirmed to contain a 750bp fragment of exogenous gene by restriction analysis above and chosen for later use.

**Table 1** ELISA of the soluble MG<sub>7</sub> scFv for binding with KATOIII cells (A value)

| ELISA        | Number of strong positive clones |       | Neg. ctrl |
|--------------|----------------------------------|-------|-----------|
|              | 1                                | 2     |           |
| First round  | 0.287                            | 0.776 | 0.201     |
| Second round | 0.346                            | 0.802 | 0.223     |

### The yield of soluble MG<sub>7</sub> scFv

The positive signal displayed on the dotting site with perplasmic

extracts from induced *E.coli* HB2151 was significantly stronger than that from non-induced *E.coli* HB2151 (Figure 2). It implied that *E.coli* HB2151 had successfully produced the soluble MG<sub>7</sub> scFv via induction by IPTG.



**Figure 2** Immunodotting of soluble MG<sub>7</sub> scFv. 1: Periplasmic extracts from induced *E.coli* HB2151; 2: Supernatant from induced *E.coli* HB2151; 3: Periplasmic extracts from non-induced *E.coli* HB2151

### The molecular mass of MG<sub>7</sub> scFv

A protein band with positive signal was found at Mr 30 indicating that the soluble MG<sub>7</sub> scFv was a protein of Mr 30 (Figure 3).

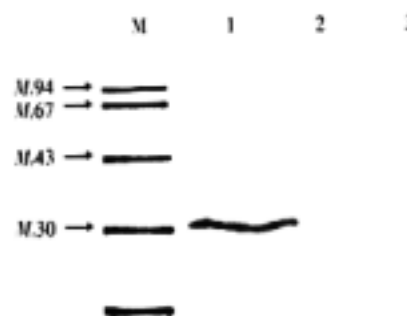


**Figure 3** Western blot of the molecular mass of soluble MG<sub>7</sub> scFv. M: Protein marker; 1: Periplasmic extracts from induced *E.coli* HB2151; 2: Supernatant from induced *E.coli* HB2151; 3: Periplasmic extracts from non-induced *E.coli* HB2151

### DNA sequence of MG<sub>7</sub> scFv

The V<sub>H</sub> and V<sub>L</sub> genes of MG<sub>7</sub> scFv were respectively 363 bp and 321 bp in length. The V<sub>H</sub> gene has two conserved codon for cysteine at 67-69bp and 289-291bp. The V<sub>L</sub> gene has two conserved codon for cysteine at 472-474bp and 664-666bp. Both of the V<sub>H</sub> and V<sub>L</sub> genes are highly homologous with the variable fragment of some known antibodies (Figure 4).

ATG GCC CAG GTG AAG CTG CAG CAG TCT GGG CCT GAA GTG GTA AAG CCT GGG GCT TCA GTG AAG TTG TCC TGC  
AAG GCT TCT GGC TAC ATC TTC ACA AGT TAT GAT ATA GAC TGG GTG AGG CAG ACG CCT GAA CAG GGA CTT GAG  
TGG ATT GGA TGG ATT TTT CCT GGA GAG GGG AGT ACT GAA TAC AAT GAG AAG TTC AAG GGC AGG GCC ACA CTG

VH

AGT GTA GAC AAG TCC TCC AGC ACA GCC TAT ATG GAG CTC ACT AGG CTG ACA TCT GAG GAC TCT GCT GTC TAT  
TTC TGT GCT AGA GGG GAC TAC TAT AGG CGC TAC TTT GAC TTG TGG GGC CAA GGG ACC ACG GTC ACC GTC TCC  
TCA GGT GGA GGC GGT TCA GGC GGA GGT GGC TCT GGC GGT GGC GGA TCG GAC ATC GAG CTC ACT CAG

Linker

TCT CCA GCA ATC ATG TCT GCA TCT CCA GGG GAG AGG GTC ACC ATG ACC TGC AGT GCC AGC TCA AGT ATA CGT  
TAC ATA TAT TGG TAC CAA CAG AAG CCT GGA TCC TCC CCC AGA CTC CTG ATT TAT GAC ACA TCC AAC GTG GCT

VL

CCT GGA GTC CCT TTT CGC TTC AGT GGC AGT GGG TCT GGG ACC TCT TAT TCT CTC ACA ATC AAC CGA ATG GAG  
GCT GAG GAT GCT GCC ACT TAT TAC TGC CAG GAG TGG AGT GGT TAT CCG TAC ACG TTC GGA GGG GCA CCA AGC  
TGG GAA ATC AAA CGG

**Figure 4** Nucleotide sequence of MG<sub>7</sub> scFv

## DISCUSSION

MG<sub>7</sub>, a monoclonal antibody against human gastric cancer, was proved to possess quite high specificity and sensitivity to gastric cancer associated antigen. It was successfully used in experimental targeting therapy in nude mice bearing transplanted human gastric cancer<sup>[30]</sup>. But owing to its murine origin, like many other similar antibodies, MG<sub>7</sub> antibody can elicit anti-mouse immunoreaction in man and thus its use in clinical practice is restricted<sup>[31,32]</sup>. One of the efficient strategies to this problem is to remove the constant region of antibody which makes main contribution to the immunogenicity of the murine antibody to human being<sup>[33-38]</sup>. On the other hand, antibody without constant region, termed scFv, is less antigenic and induces weaker repulsive reaction. In addition, it is a smaller molecule and comprises 1/6 of its original antibody in molecular mass which ensure that scFv can more readily penetrate into the tumor tissue *in vivo* and be easily cleared up from the normal tissue<sup>[39,40]</sup>. Besides, the scFv is more available than its original antibody by gene engineering technology which can provide an economical means for diagnosis of gastric cancer<sup>[41-47]</sup>.

As mentioned above, the scFv is advantageous to its original antibody in clinical practice. Therefore, developing the MG<sub>7</sub> scFv is of great significance in both early diagnosis and therapy of gastric cancer. For example, MG<sub>7</sub> scFv fused with avidin can be used as a reagent in immuno-PCR for early diagnosis of gastric cancer. Additionally, a new immunotoxin for treatment of gastric cancer can be developed by fusing the MG<sub>7</sub> ScFv and A subunit of ricin together. MG<sub>7</sub> ScFv can direct the A subunit of ricin to MG<sub>7</sub> positive gastric cancer cells<sup>[48-50]</sup>. In our previous study, the MG<sub>7</sub> recombinant phage antibody derived from MG<sub>7</sub> hybridoma was constructed and subsequently two strong positive phage antibody clones were screened out from this library<sup>[51]</sup>.

Targeting therapy for tumors in the last decade has become a highlight in the field of tumor therapy<sup>[52-57]</sup>. In past, the discoveries of many tumor specific antigen (TSA) and tumor associated antigen (TAA) assured the practicability of antibody as a tool in tumor targeting therapy<sup>[58-69]</sup>. Ascribed to its high specificity and sensitivity in recognizing associated antigen, antibody is the optimal candidate for targeting mediator. Therefore, targeting therapy mediated by antibody still remains as a promising curative modality among the ways of tumor therapy and attracts worldwide attention<sup>[70]</sup>.

This study was conducted with the purpose to produce the soluble MG<sub>7</sub> scFv, identify its antigen-binding affinity, determine its molecular mass and get an understanding of its nucleotide sequence. We first examined the length of exogenous MG<sub>7</sub> scFv gene harbored in the two strong positive phage antibody clones by restriction analysis and found that one of the phage antibody clones contained a 750bp fragment of exogenous gene which was identical to many discovered scFvs in length. Secondly, we prepared the periplasmic extracts (containing majority of the soluble scFv) from IPTG-induced *E.coli* HB2151 and detected the antigen-binding affinity of MG<sub>7</sub> scFv by ELISA. One of the soluble MG<sub>7</sub> scFvs was shown to possess apparent antigen-binding activity. Subsequently, immunodotting test exhibited that *E.coli* HB2151 had successfully produced the soluble MG<sub>7</sub> scFv with high yields via induction by IPTG. Meanwhile, western blot suggested that the molecular mass of soluble MG<sub>7</sub> scFv was Mr 30. Finally, DNA sequencing unraveled that the MG<sub>7</sub> scFv had the common characteristics shared by other known scFvs in nucleotide sequence. Collectively, we have successfully developed the soluble MG<sub>7</sub> scFv and created an opportunity to study its application in targeting therapy of gastric cancer.

## REFERENCE

- Niu WX, Qin XY, Liu H, Wang CP. Clinicopathological analysis of patients with gastric cancer in 1200 cases. *World J Gastroenterol* 2001; 7: 281-284
- Wang SH, Wang HT, Jiang SC. Selection of human anti-HAV McAb from a phage antibody library. *Zhongguo shengwu jishu Zazi* 1998; 14: 173-

- 178
- Lu XP, Li BJ, Chen SL, Lu B and Jiang NY. Effect of chemotherapy or targeting chemotherapy on apoptosis of colorectal carcinoma. *Shijie Huaren Xiaohua Zazhi* 1999; 7:3332-334
- Liu HF, Liu WW, Fang DC. Induction of apoptosis in human gastric carcinoma cell line SGC7901 by anti-Fas monoclonal antibody. *Shijie Huaren Xiaohua Zazhi* 1999; 7: 476-487
- Ning XY, Yang DH. Research and progress is *in vivo* gene therapy for primary liver cancer. *Shijie Huaren Xiaohua Zazhi* 2000; 8:89-90
- Chen JP, Lin C, Xu CP, Zhang XY, Fu M, Deng YP, Wei Y and Wu M. Transduction efficiency, biologic effect and mechanism of recombinant RA538, antisense C-myc adenovirus on different cell lines. *Shijie Huaren Xiaohua Zazhi* 2000;8:266-270
- Guo SY, Gu QL, Liu BY, Zhu ZG, Yin HR and Lin YZ. Experimental study on the treatment of gastric cancer by TK gene combined with mL-2 gene. *Shijie Huaren Xiaohua Zazhi* 2000;8:974-978
- Pan X, Pan W, Ni CR, Ke CW, Cao GW and Qi ZT. Killing effect of tetracycline-controlled expression of DT/VEGF system on liver cell cancer. *Shijie Huaren Xiaohua Zazhi* 2000; 8:867-873
- Leng JJ, Chen YQ, Leng XS. Genetic therapy for pancreatic neoplasms. *Shijie Huaren Xiaohua Zazhi* 2000; 8: 916-918
- Pan X, Pan W, Ke CW, Zhang B, Cao GW, Qi ZT. Tetracycline controlled DT/VEGF system gene therapy mediated by adenovirus vector. *Shijie Huaren Xiaohua Zazhi* 2000;8:1121-1126
- Wang FS, Wu ZZ. Current situation in studies of gene therapy for liver cirrhosis and liver fibrosis. *Shijie Huaren Xiaohua Zazhi* 2000;8:371-396
- Pan X, Ke CW, Pan W, He X, Cao GW, Qi ZT. Killing effect of DT/VEGF system on gastric carcinoma cell. *Shijie Huaren Xiaohua Zazhi* 2000; 8: 393-396
- Cao GW, Qi ZT, Pan X, Pan W, He X, Ke CW. Gene therapy for human colorectal carcinoma using promoter controlled bacterial ADP-ribosylating toxin genes human CEA, PEA and DTA gene transfer. *World J Gastroenterol* 1998;4:388-391
- Lu XP, Li BJ, Chen SL, Lu B, Jiang NY. Anti-CEA monoclonal antibody targeting therapy for colorectal carcinoma. *Shijie Huaren Xiaohua Zazhi* 1999;7:329-331
- Engelstadter M, Bobkova M, Baier M, Stitz J, Holtkamp N, Chu TH, Kurth R, Dornburg R, Buchholz CJ, Cichutek K. Targeting human T cells by retroviral vectors displaying antibody domains selected from a phage display library. *Hum Gene Ther* 2000;11:293-303
- Wu YD, Song XQ, Zhou DN, Hu XH, Gan YQ, Li ZG, Liao P. Experimental and clinical study on targeting treatment of liver cancer using radionuclide- anti-AFP antibody -MMC doublet. *Shijie Huaren Xiaohua Zazhi* 1999; 7: 387-390
- Zhang J, Liu YF, Yang SJ, Sun ZW, Qiao Q and Zhang SZ. Construction and expression of mouse/humanized ScFv and their fusion to humanized mutant TNF- $\alpha$  against hepatocellular carcinoma. *Shijie Huaren Xiaohua Zazhi* 2000; 8: 616-620
- Chen ZN, Bian HJ, Jiang JL. Recent progress in anti-hepatoma monoclonal antibody and its application. *Shijie Huaren Xiaohua Zazhi* 1998; 6: 461-462
- Romanczuk H, Galer CE, Zabner J, Barsomian G, Wadsworth SC, O'Riordan CR. Modification of an adenoviral vector with biologically selected peptides: a novel strategy for gene delivery to cells of choice. *Hum Gene Ther* 1999; 10: 2615-2626
- Wang W, Zhou J, Xu L and Zhen Y. Antineoplastic effect of intracellular expression of a single-chain antibody directed against type IV collagenase. *J Environ Pathol Toxicol Oncol* 2000; 19: 61-68
- Li J, Wang Y, Li Q. Construction and expression of ScFv from anti-human gastric cancer McAb 3H11. *Zhonghua Zhongliu Zazhi* 1998; 20: 85-87
- Wei XC, Wang XJ, Chen K, Zhang L, Liang Y, Lin XL. Killing effect of TNF-related apoptosis inducing ligand regulated by tetracycline on gastric cancer cell line NCI-N87. *World J Gastroenterol* 2001; 7: 559-562
- Liu DH, Zhang W, Su YP, Zhang XY, Huang YX. Construction of eukaryotic expression vector of sense and antisense VEGF165 and its expression regulation. *Shijie Huaren Xiaohua Zazhi* 2001; 9: 886-891
- Liu WC, Mu HX, Ren J, Zhang XY, Pan BR. Anti-tumor activity of defensin on gastric cancer cell line *in vitro*. *Shijie Huaren Xiaohua Zazhi* 2001; 9: 622-626
- Yang JT, Fang DC, Yang SM, Luo YH, Lu R, Luo KL, Liu WW. Construction of sense and antisense hTR eukaryotic expression vector. *Shijie Huaren Xiaohua Zazhi* 2000; 8: 491-493
- Huang ZH, Qian WF, Chi DB, Jiang ZS. Apoptosis in human colorectal cancer Lovo cells induced by HSVtk/GCV system *in vitro*. *Shijie Huaren Xiaohua Zazhi* 2001;9:194-197
- Qian WF, Huang ZH, Chi DB. Herpes simplex virus thymidine kinase/ganciclovir system combined with 5-FU for the treatment of experimental colorectal cancer. *Shijie Huaren Xiaohua Zazhi* 2001;9: 190-193
- Xu DX, Chen WS, Ye ZJ. The antisense gene of growth factor receptor

- reversing the malignant phenotype of human hepatoma cells. *Shijie Huaren Xiaohua Zazhi* 2001; 9: 175-179
- 29 Tang YC, Li Y, Qian GX. Reduction of tumorigenicity of SMMC-7721 hepatoma cells by vascular endothelial growth factor antisense gene therapy. *World J Gastroenterol* 2001; 7: 22-27
- 30 Fan DM, Zhang XY, Chen XT, Qiao TD, Chen BJ. Preparation and immunohistologic identification of mAbs against a poor differentiated gastric cancer line MKN-46-9. *Jiefangjun Yixue Zhazhi* 1988; 13: 12-15
- 31 Klimka A, Matthey B, Roovers RC, Barth S, Arends JW, Engert A, Hoogenboom HR. Human anti-CD30 recombinant antibodies by guided phage antibody selection using cell panning. *Br J Cancer* 2000; 83: 252-260
- 32 Watkins NA, Ouwehand WH. Introduction to antibody engineering and phage display. *Vox Sang* 2000; 78: 72-79
- 33 Zhai W, Davies J, Shang DZ, Chan SW, Allain JP. Human recombinant single-chain antibody fragments, specific for the hypervariable region 1 of hepatitis C virus, from immune phage-display libraries. *J Viral Hepat* 1999; 6: 115-124
- 34 De Greeff A, van Alphen L, Smith HE. Selection of recombinant antibodies specific for pathogenic *Streptococcus suis* by subtractive phage display. *Infect Immun* 2000; 68: 3949-3955
- 35 Long MC, Jager S, Mah DC, Jebailey L, Mah MA, Masri SA, Nagata LP. Construction and characterization of a novel recombinant single-chain variable fragment antibody against Western equine encephalitis virus. *Hybridoma* 2000; 19: 1-13
- 36 Johns M, George AJ, Ritter MA. In vivo selection of ScFv from phage display libraries. *J Immunol Methods* 2000; 239: 137-151
- 37 Mao S, Gao C, Lo CH, Wirsching P, Wong CH, Janda KD. Phage-display library selection of high-affinity human single-chain antibodies to tumor-associated carbohydrate antigens sialyl Lewisx and Lewisx. *Proc Natl Acad Sci U S A* 1999; 96: 6953-6958
- 38 Kupsch JM, Tidman NH, Kang NV, Truman H, Hamilton S, Patel N, Newton Bishop JA, Leigh IM, Crowe JS. Isolation of human tumor-specific antibodies by selection of an antibody phage library on melanoma cells. *Clin Cancer Res* 1999; 5: 925-931
- 39 Franconi R, Roggero P, Pirazzi P, Arias FJ, Desiderio A, Bitti O, Pashkoulou D, Mattei B, Bracci L, Masenga V, Milne RG, Benvenuto E. Functional expression in bacteria and plants of an ScFv antibody fragment against tospoviruses. *Immunotechnology* 1999; 4: 189-201
- 40 Yi K, Chung J, Kim H, Kim I, Jung H, Kim J, Choi I, Suh P, Chung H. Expression and characterization of anti-NCA-95 ScFv (CEA 79 ScFv) in a prokaryotic expression vector modified to contain a Sfi I and Not I site. *Hybridoma* 1999; 18: 243-249
- 41 McCall AM, Adams GP, Amoroso AR, Nielsen UB, Zhang L, Horak E, Simmons H, Schier R, Marks JD, Weiner LM. Isolation and characterization of an anti-CD16 single-chain Fv fragment and construction of an anti-HER2/neu/anti-CD16 bispecific scFv that triggers CD16-dependent tumor cytotoxicity. *Mol Immunol* 1999; 36: 433-445
- 42 Winthrop MD, DeNardo SJ, DeNardo GL. Development of a hyperimmune anti-MUC-1 single chain antibody fragments phage display library for targeting breast cancer. *Clin Cancer Res* 1999; 5(10 Suppl): 3088s-3094s
- 43 Stadler BM. Antibody production without animals. *Dev Biol Stand* 1999; 101: 45-48
- 44 Topping KP, Hough VC, Monson JR, Greenman J. Isolation of human colorectal tumour reactive antibodies using phage display technology. *Int J Oncol* 2000; 16: 187-195
- 45 Adams GP, Schier R. Generating improved single-chain Fv molecules for tumor targeting. *J Immunol Methods* 1999; 231: 249-260
- 46 Lekkerkerker A, Logtenberg T. Phage antibodies against human dendritic cell subpopulations obtained by flow cytometry-based selection on freshly isolated cells. *J Immunol Methods* 1999; 231: 53-63
- 47 van Kuppevelt TH, Dennissen MA, van Venrooij WJ, Hoet RM, Veerkamp JH. Generation and application of type-specific anti-heparan sulfate antibodies using phage display technology. Further evidence for heparan sulfate heterogeneity in the kidney. *J Biol Chem* 1998; 273: 12960-12966
- 48 Yang LJ, Sui YF, Chen ZN. Preparation and activity of conjugate of monoclonal antibody HAB18 against hepatoma F(ab')<sub>2</sub> fragment and staphylococcal enterotoxin A. *World J Gastroenterol* 2001; 7: 216-221
- 49 Cheng H, Liu YF, Zhang HZ, Shen WA, Zhang SZ. Construction and expression of anti-HCC immunotoxin of sFv-TNF- $\alpha$  and GFP fusion proteins. *Shijie Huaren Xiaohua Zazhi* 2001; 9: 640-644
- 50 Rodenburg CM, Mernaugh R, Bilbao G, Khazaeli MB. Production of a single chain anti-CEA antibody from the hybridoma cell line T84.66 using a modified colony-lift selection procedure to detect antigen-positive ScFv bacterial clones. *Hybridoma* 1998; 17: 1-8
- 51 Yu ZC, Ding J, Nie YZ, Fan DM and Zhang XY. Preparation of single chain variable fragment of MG<sub>7</sub> mAb by phage display technology. *World J Gastroenterol* 2001; 7: 510-514
- 52 Darimont BD. The Hsp90 chaperone complex-A potential target for cancer therapy *World J Gastroenterol* 1999; 5: 195-198
- 53 Bi WX, Xu SD, Zhang PH, Kong F. Antitumoral activity of low density lipoprotein acilacinomycin complex in mice bearing H22 tumor. *World J Gastroenterol* 2000; 6: 140-142
- 54 Yang CQ, Wang JY, Fang JT, Liu JJ, Guo JS. A comparison between intravenous and peritoneal route on liver targeted uptake and expression of plasmid delivered by Glyco poly L-lysine. *World J Gastroenterol* 2000; 6: 508-512
- 55 Chen YP, Zhang L, Lu QS, Feng XR, Luo KX. Lactosamination of liposomes and hepatotropic targeting research. *World J Gastroenterol* 2000; 6: 593-596
- 56 He Y, Zhou J, Wu JS, Dou KF. Inhibitory effects of EGFR antisense oligodeoxynucleotide in human colorectal cancer cell line. *World J Gastroenterol* 2000; 6: 747-749
- 57 Wang XW, Yuan JH, Zhang RG, Guo LX, Xie Y, Xie H. Antihepatoma effect of alpha fetoprotein antisense phosphorothioate oligodeoxyribonucleotides *in vitro* and in mice. *World J Gastroenterol* 2001; 7: 345-351
- 58 Wang L, Lu W, Chen YG, Zhou XM, Gu JR. Comparison of gene expression between normal colon mucosa and colon carcinoma by means of messenger RNA differential display. *World J Gastroenterol* 1999; 5: 533-534
- 59 Kong XB, Yang ZK, Liang LJ, Huang JF, Lin HL. Overexpression of P-glycoprotein in hepatocellular carcinoma and its clinical implication. *World J Gastroenterol* 2000; 6: 134-135
- 60 Qin LL, Su JJ, Li Y, Yang C, Ban KC, Yian RQ. Expression of IGF-c $\alpha$ , p53, p21 and HBxAg in precancerous events of hepatocarcinogenesis induced by AFB1 and/or HBV in tree shrews. *World J Gastroenterol* 2000; 6: 138-139
- 61 Li J, Feng CW, Zhao ZG, Zhou Q, Wang LD. A preliminary study on ras protein expression in human esophageal cancer and precancerous lesions. *World J Gastroenterol* 2000; 6: 278-280
- 62 Tian XJ, Wu J, Meng L, Dong ZW, Shou CC. Expression of VEGF121 in gastric carcinoma MGC803 cell line. *World J Gastroenterol* 2000; 6: 281-283
- 63 Xu AG, Li SG, Liu JH, Gan AH. The function of apoptosis and protein expression of bcl2, p53 and C-myc in the development of gastric cancer. *World J Gastroenterol* 2000; 6(Suppl 3): 27-33
- 64 Li JY, Huang Y, Lin MF. Clinical evaluation of several tumor markers in the diagnosis of primary hepatic cancer. *World J Gastroenterol* 2000; 6(Suppl 3): 39-41
- 65 Lin GY, Chen ZL, Lu CM, Li Y, Wang J, Ping XJ, Huang R. Immunohistochemical study on p53, Hrasp21, cerbB2 protein and PCNA expression in tumor tissues of Han and minority ethnic patients with primary hepatic carcinoma in Xinjiang. *World J Gastroenterol* 2000; 6(Suppl 3): 53-58
- 66 Fan ZR, Yang DH, Cui J, Qin HR, Huang CC. Expression of insulin like growth factor and its receptor in hepatocellular carcinogenesis. *World J Gastroenterol* 2001; 7: 285-288
- 67 Zheng CX, Zhan WH, Zhao JZ, Zheng D, Wang DP, He YL, Zheng ZQ. The prognostic value of preoperative serum levels of CEA, CA19-9 and CA72-4 in patients with colorectal cancer. *World J Gastroenterol* 2001; 7: 431-434
- 68 Xu AG, Li SG, Liu JH, Gan AH. Function of apoptosis and expression of the proteins Bcl-2, p53 and C-myc in the development of gastric cancer. *World J Gastroenterol* 2001; 7: 403-406
- 69 Li XG, Song JD, Wang YQ. Differential expression of a novel colorectal cancer differentiation-related gene in colorectal cancer. *World J Gastroenterol* 2001; 7: 551-554
- 70 Chen QK, Yuan SZ, Zeng ZY, Huang ZQ. Tumoricidal activation of murine resident peritoneal macrophages on pancreatic carcinoma by interleukin2 and monoclonal antibodies. *World J Gastroenterol* 2000; 6: 287-289